

Molecular targets for the treatment of metastatic colorectal cancer

Edited by

Alessandro Passardi and David Gibbons

Published in

Frontiers in Oncology



FRONTIERS EBOOK COPYRIGHT STATEMENT

The copyright in the text of individual articles in this ebook is the property of their respective authors or their respective institutions or funders. The copyright in graphics and images within each article may be subject to copyright of other parties. In both cases this is subject to a license granted to Frontiers.

The compilation of articles constituting this ebook is the property of Frontiers.

Each article within this ebook, and the ebook itself, are published under the most recent version of the Creative Commons CC-BY licence. The version current at the date of publication of this ebook is CC-BY 4.0. If the CC-BY licence is updated, the licence granted by Frontiers is automatically updated to the new version.

When exercising any right under the CC-BY licence, Frontiers must be attributed as the original publisher of the article or ebook, as applicable.

Authors have the responsibility of ensuring that any graphics or other materials which are the property of others may be included in the CC-BY licence, but this should be checked before relying on the CC-BY licence to reproduce those materials. Any copyright notices relating to those materials must be complied with.

Copyright and source acknowledgement notices may not be removed and must be displayed in any copy, derivative work or partial copy which includes the elements in question.

All copyright, and all rights therein, are protected by national and international copyright laws. The above represents a summary only. For further information please read Frontiers' Conditions for Website Use and Copyright Statement, and the applicable CC-BY licence.

ISSN 1664-8714
ISBN 978-2-8325-4206-4
DOI 10.3389/978-2-8325-4206-4

About Frontiers

Frontiers is more than just an open access publisher of scholarly articles: it is a pioneering approach to the world of academia, radically improving the way scholarly research is managed. The grand vision of Frontiers is a world where all people have an equal opportunity to seek, share and generate knowledge. Frontiers provides immediate and permanent online open access to all its publications, but this alone is not enough to realize our grand goals.

Frontiers journal series

The Frontiers journal series is a multi-tier and interdisciplinary set of open-access, online journals, promising a paradigm shift from the current review, selection and dissemination processes in academic publishing. All Frontiers journals are driven by researchers for researchers; therefore, they constitute a service to the scholarly community. At the same time, the *Frontiers journal series* operates on a revolutionary invention, the tiered publishing system, initially addressing specific communities of scholars, and gradually climbing up to broader public understanding, thus serving the interests of the lay society, too.

Dedication to quality

Each Frontiers article is a landmark of the highest quality, thanks to genuinely collaborative interactions between authors and review editors, who include some of the world's best academicians. Research must be certified by peers before entering a stream of knowledge that may eventually reach the public - and shape society; therefore, Frontiers only applies the most rigorous and unbiased reviews. Frontiers revolutionizes research publishing by freely delivering the most outstanding research, evaluated with no bias from both the academic and social point of view. By applying the most advanced information technologies, Frontiers is catapulting scholarly publishing into a new generation.

What are Frontiers Research Topics?

Frontiers Research Topics are very popular trademarks of the *Frontiers journals series*: they are collections of at least ten articles, all centered on a particular subject. With their unique mix of varied contributions from Original Research to Review Articles, Frontiers Research Topics unify the most influential researchers, the latest key findings and historical advances in a hot research area.

Find out more on how to host your own Frontiers Research Topic or contribute to one as an author by contacting the Frontiers editorial office: frontiersin.org/about/contact

Molecular targets for the treatment of metastatic colorectal cancer

Topic editors

Alessandro Passardi — Department of Medical Oncology, Scientific Institute of Romagna for the Study and Treatment of Tumors (IRCCS), Italy
David Gibbons — St. Vincent's University Hospital, Ireland

Citation

Passardi, A., Gibbons, D., eds. (2024). *Molecular targets for the treatment of metastatic colorectal cancer*. Lausanne: Frontiers Media SA.
doi: 10.3389/978-2-8325-4206-4

Table of contents

- 05 **Editorial: Molecular targets for the treatment of metastatic colorectal cancer**
Alessandro Passardi and David Gibbons
- 08 **MXRA8 is an immune-relative prognostic biomarker associated with metastasis and CD8⁺ T cell infiltration in colorectal cancer**
Lulu Tan, Daan Fu, Feng Liu, Jia Liu, Yang Zhang, Xin Li, Jinbo Gao, Kaixiong Tao, Guobin Wang, Lin Wang and Zheng Wang
- 21 **Case report: Preclinical efficacy of NEDD8 and proteasome inhibitors in patient-derived models of signet ring high-grade mucinous colorectal cancer from a Lynch syndrome patient**
Erica Torchiano, Consalvo Petti, Sabrina Arena, Francesco Sassi, Giorgia Migliardi, Alfredo Mellano, Roberta Porporato, Marco Basiricò, Loretta Gammaitoni, Enrico Berrino, Monica Montone, Giorgio Corti, Giovanni Crisafulli, Caterina Marchiò, Alberto Bardelli and Enzo Medico
- 29 **Efficacy and safety of a biomarker-driven cetuximab-based treatment regimen over 3 treatment lines in mCRC patients with *RAS/BRAF* wild type tumors at start of first line: The CAPRI 2 GOIM trial**
Giulia Martini, Davide Ciardiello, Stefania Napolitano, Erika Martinelli, Teresa Troiani, Tiziana Pia Latiano, Antonio Avallone, Nicola Normanno, Massimo Di Maio, Evaristo Maiello and Fortunato Ciardiello
- 35 **Efficacy of third-line anti-EGFR-based treatment versus regorafenib or trifluridine/tipiracil according to primary tumor site in *RAS/BRAF* wild-type metastatic colorectal cancer patients**
Lisa Salvatore, Maria Bensi, Raffaella Vivolo, Ina Valeria Zurlo, Emanuela Dell'Aquila, Roberta Grande, Annunziato Anghelone, Alessandra Emiliani, Fabrizio Citarella, Maria Alessandra Calegari, Marta Ribelli, Michele Basso, Carmelo Pozzo and Giampaolo Tortora
- 43 **Notch-Jagged1 signaling and response to bevacizumab therapy in advanced colorectal cancer: A glance to radiomics or back to physiopathology?**
Francesca Negri, Lorena Bottarelli, Giuseppe Pedrazzi, Michele Maddalo, Ludovica Leo, Gianluca Milanese, Roberto Sala, Michele Lecchini, Nicoletta Campanini, Cecilia Bozzetti, Andrea Zavani, Gianluca Di Rienzo, Cinzia Azzoni, Enrico Maria Silini, Nicola Sverzellati, Federica Gaiani, Gian Luigi de' Angelis and Letizia Gnetti
- 53 **Predictive potential of angiopoietin-2 in a mCRC subpopulation treated with vanucizumab in the McCAVE trial**
Cláudia S. Ferreira, Galina Babitzki, Irina Klamann, Oliver Krieter, Katharina Lechner, Johanna Bendell, Suzana Vega Harring and Florian Heil

- 66 **Ongoing complete response after treatment cessation with dabrafenib, trametinib, and cetuximab as third-line treatment in a patient with advanced BRAF^{V600E} mutated, microsatellite-stable colon cancer: A case report and literature review**
Gudrun Piringer, Jörn Decker, Vera Trommet, Thomas Kühr, Sonja Heibl, Konrad Dörfler and Josef Thaler
- 74 **Efficacy and safety of third-line or later-line targeted treatment for patients with metastatic colorectal cancer: a meta-analysis**
Wen-Hui Xue, Xue-Wei Li, Ya-Qian Ding, Na Wu, Bei-Bei Pei, Xiao-Yan Ma, Jun Xie and Wen-Hui Yang
- 85 **The crosstalk between anoikis and epithelial-mesenchymal transition and their synergistic roles in predicting prognosis in colon adenocarcinoma**
Jiahui Zhou, Sheng Yang, Dawei Zhu, Hao Li, Xinsheng Miao, Menghui Gu, Wei Xu, Yan Zhang, Wei Tang, Renbin Shen, Jianhua Zha, Jianhua Zhu, Zheng Yuan and Xinhua Gu
- 103 **Recent advances in nanomedicine preparative methods and their therapeutic potential for colorectal cancer: a critical review**
Arinjay Jain and Sankha Bhattacharya
- 130 **LM02 trial Perioperative treatment with panitumumab and FOLFIRI in patients with wild-type RAS, potentially resectable colorectal cancer liver metastases—a phase II study**
Gudrun Piringer, Thomas Gruenberger, Josef Thaler, Irene Kührer, Klaus Kaczirek, Friedrich Längle, Istvan Viragos-Toth, Arno Amann, Wolfgang Eisterer, Reinhold Függer, Johannes Andel, Angelika Pichler, Judith Stift, Lidija Sölkner, Michael Gnant and Dietmar Öfner on behalf of the Austrian Breast Colorectal Cancer Study Group (ABCSG)
- 141 **Targeted splicing therapy: new strategies for colorectal cancer**
Yifeng Zheng, Guoqiang Zhong, Chengcheng He and Mingsong Li



OPEN ACCESS

EDITED AND REVIEWED BY

Liang Qiao,
Westmead Institute for Medical Research,
Australia

*CORRESPONDENCE

Alessandro Passardi

✉ alessandro.passardi@irst.emr.it

David Gibbons

✉ davidgibbons47@gmail.com

RECEIVED 20 November 2023

ACCEPTED 21 November 2023

PUBLISHED 12 December 2023

CITATION

Passardi A and Gibbons D (2023) Editorial:
Molecular targets for the treatment of
metastatic colorectal cancer.
Front. Oncol. 13:1341594.
doi: 10.3389/fonc.2023.1341594

COPYRIGHT

© 2023 Passardi and Gibbons. This is an
open-access article distributed under the
terms of the [Creative Commons Attribution
License \(CC BY\)](#). The use, distribution or
reproduction in other forums is permitted,
provided the original author(s) and the
copyright owner(s) are credited and that
the original publication in this journal is
cited, in accordance with accepted
academic practice. No use, distribution or
reproduction is permitted which does not
comply with these terms.

Editorial: Molecular targets for the treatment of metastatic colorectal cancer

Alessandro Passardi^{1*} and David Gibbons^{2,3*}

¹Department of Medical Oncology, IRCCS Istituto Romagnolo per lo Studio dei Tumori (IRST) "Dino Amadori", Meldola, Italy, ²Department of Pathology, St Vincent's University Hospital, Dublin, Ireland, ³School of Medicine and Medical Sciences, University College Dublin, Dublin, Ireland

KEYWORDS

colorectal cancer, molecular targets, metastatic colon cancer, angiogenesis, EGFR inhibitors, immunocheck point inhibitors, refractory colorectal cancer, BRAF V600E

Editorial on the Research Topic

Molecular targets for the treatment of metastatic colorectal cancer

Colorectal cancer (CRC) accounts for approximately 10% of all cancer cases and represents the third most common cancer worldwide. Most importantly, it is the second leading cause of cancer-related deaths worldwide. The disease is often diagnosed at an advanced stage, when treatment options are limited (1, 2).

From the 1990s on, fluorouracil-based chemotherapy was used to treat metastatic CRC (mCRC), improving overall survival (OS) to 14 months. Later, the combination regimens with oxaliplatin (FOLFOX) or irinotecan (FOLFIRI) prolonged the OS to about 20 months (3). From the early 2000s targeted drugs, like anti-epidermal growth factor receptor [EGFR] or anti-vascular endothelial growth factor [VEGF] antibodies, have entered clinical practice, significantly increasing patients' OS to approximately 36 months (4).

Antiangiogenic agents, such as Bevacizumab and Aflibercept, are widely used in combination with first and second line chemotherapy for mCRC (4). Despite several years of translational research in this field, no validated predictive markers have been found to select patients more likely to benefit from these agents. A multidisciplinary group from University Hospital of Parma, Italy, performed an interesting trial to investigate the role of the Notch intracellular domain (NICD) and its ligand Jagged-1 expression, as well as radiomics in the prediction of the efficacy of bevacizumab in treatment-naïve metastatic CRC patients. Study results, presented in this Research Topic, suggested that high NICD and Jagged-1 expression levels were associated with early disease progression (Negri et al.). Moreover, the integration of quantitative information combined with clinical and histologic characteristics helped predict patient outcomes. This seems to be a promising field of research, which needs validation in larger cohorts of patients. Vanucizumab (RO5520985), a humanised immunoglobulin G-1-like bispecific monoclonal antibody targeting both VEGF-A and Angiopoietin-2, has been recently evaluated in the phase II McCAVE trial in combination with FOLFOX first line chemotherapy, showing similar efficacy in terms of PFS and OS compared to bevacizumab. In the attempt to find new predictors for outcome related to the anti-angiogenic treatment, Ferreira et al. explored the potential predictive and prognostic role of baseline tissue and plasma levels of Angiopoietin-2 in a subgroup of patients enrolled into the Mc Cave trial. Overall, low

tissue baseline levels of Angiopoietin-2 were associated with longer PFS. Moreover, patients with KRAS wild-type mCRC and high levels of Angiopoietin-2 had higher PFS when treated with vanucizumab with respect to bevacizumab.

EGFR plays a key role in colorectal tumorigenesis, and acts to activate several intracellular signalling pathways, such as the RAS-RAF-MAP kinase and the PI3K-PTEN-Akt pathway, thus favouring cell proliferation, migration and differentiation. Anti-EGFR antibodies, cetuximab and panitumumab, are widely used for mCRC patients, in particular in combination with first line chemotherapy in patients with left sided RAS/BRAF WT tumors (4). In this subgroup of patients, in addition to significantly increasing OS, these combination therapies may allow conversion of unresectable to resectable liver metastases, thus expanding the possibilities of cure in mCRC. The LM02 trial, presented in this Research Topic, evaluated FOLFIRI plus panitumumab regimen as perioperative therapy in untreated RAS WT mCRC patients with liver limited disease [Piringer et al.]. Among the 36 patients included, 91.4% completed the preoperative therapy. The objective response rate and R0 resection rate were 65.7% and 82.7%, respectively. Noteworthy, The OS rates at 12 and 24 months were 85.6% and 73.3%, respectively. Unfortunately, despite great efforts to select patients addicted to anti-EGFR blockade, treatment efficacy suffers from either innate or acquired mechanisms of resistance, largely driven by RAS or BRAF mutations. Liquid biopsy analysis with the detection of such and other mutations might help monitor tumour spatial and temporal heterogeneity and predict resistance to anti EGFR agents. It has recently been recommended to select patients for the use of anti-EGFR drugs beyond progression or as rechallenge strategy. The phase II CAPRI 2 GOIM trial, a proposal, presented in this Research Topic by Martini et al., is a clinical trial designed to follow RAS/BRAF wild type mCRC cases, as determined on initial FFPE diagnostic tissue, through three lines of therapy to include FOLFIRI, Cetuximab, Folfex and bevacizumab in various combinations, depending on dynamic mutation changes with time, as measured by Liquid Biopsy analyses, after each line of treatment. Endpoints will include Response rate (RR), PFS and OS.

More recent acquisitions include the use of immuncheckpoint inhibitors (ICIs), i.e. Pembrolizumab or Nivolumab/Ipilimumab combination, in mCRC patients with Microsatellite instability or deficient Mismatch Repair. However, approximately 95% of mCRC are microsatellite-stable/mismatch-repair-proficient, and this condition involves resistance to ICIs (5). The molecular mechanism of ICI resistance is largely unknown and clinical research is addressing the complex issue of transforming tumors from the immune “cold” state to the immune “hot” state. Insufficient CD8+ T cell infiltration or loss of CD8+ T cell function might restrict the efficiency of immunotherapy in CRC. In this context, Tan et al. found that matrix remodelling associated protein 8 (MXRA8) was over expressed in CRC, significantly affecting tumor malignancy, metastasis and recurrence. Moreover, MXRA8 seemed to correlate with CRC immunity, reflecting an abnormal immune status, characterized by less infiltration or dysfunction of CD8+ T cells. Therefore, MXRA8 might be implemented as a potential immunotherapeutic and prognostic biomarker for CRC.

An increasing number of patients with mCRC are able to receive 3 or more lines of therapy and in recent years the therapeutic armamentarium in this setting has significantly expanded. In particular, regorafenib, an oral multikinase inhibitor, and trifluridine/tipiracil, an oral fluoropyrimidine, represent the standard treatment options for chemorefractory mCRC patients. In the Correct and Recourse trials, Regorafenib and trifluridine/tipiracil showed a significant OS improvement in comparison to best supportive care [HR 0.77 (IC 95% 0.64-0.94), p 0.0052; HR 0.66 (IC 95% 0.56-0.78), p <0.001, respectively] (6, 7). Another option in this setting includes (even if with evidence from only phase 2 trials), the rechallenge with EGFR inhibitors in RAS/BRAF WT tumors. Salvatore et al. present here a retrospective trial to assess the efficacy, according to tumor site, of the different treatment regimens (anti-EGFR-based therapy versus regorafenib or trifluridine/tipiracil) in refractory RAS/BRAF wt mCRC patients. They found a significant benefit in terms of OS in favour of anti-EGFR therapy in the left sided tumor group, whereas no differences were observed in the right sided tumor group. These results suggest an opportunity, to be confirmed in randomized trials, to select left side tumors for antiEGFR treatment in later lines. Therapeutic options in refractory disease will further increase in the coming years, thanks to the introduction of Fruquintinib and the combination of trifluridine/tipiracil with bevacizumab, the efficacy of which has recently been demonstrated in phase III studies. Furthermore, combination therapies of these drugs are underway, especially with ICIs, which could take a further step forward in the fight against CRC. Xue et al. carried out a meta-analysis of 22 studies including 1,866 patients with refractory mCRC treated with targeted therapies as third or later line of treatment. The pooled ORRs for VEGF and EGFR inhibitors were 4% and 19%, respectively. More favourable objective response and disease control rates were reported for patients treated with combined treatments with respect to monotherapy. Larger well-designed clinical trials are expected to better analyze efficacy and safety of VEGF and EGFR inhibitors, as well as combined strategies (in particular with ICIs), in the treatment of refractory mCRC.

Another key molecular target in CRC is BRAF. In particular, BRAF^{V600E} mutations are present in about 12% of mCRC and are associated with right sidedness, poor differentiation, and mucinous-type tumors, but above all with a poor disease prognosis and a poor response to standard therapies. The European Medicines Agency (EMA) has recently approved doublet therapy with encorafenib, a kinase inhibitor of BRAF, and cetuximab as second or third line treatment for BRAF^{V600E} mCRC, according to the results of the phase III Beacon trial. This targeted treatment is under investigation in combination with both first line chemotherapy and ICIs in MSI mCRC patients. Moreover, other BRAF inhibitors, such as vemurafenib and dabrafenib are being evaluated in clinical trials. Piringer et al. report, in this Research Topic a patient case with an impressive therapeutic result (i.e. a complete remission still persisting after several years) in a 52-year-old woman with advanced BRAF^{V600E} mutated, MSS mCRC, treated with dabrafenib, trametinib, and cetuximab as later-line therapy.

There is a growing need for clinical and preclinical research aimed at identifying new targets for the selective treatment of mCRC. Among the new tumor targets under development, abnormal gene splicing is emerging as a process able to promote tumor cell proliferation and

invasion, resistance to apoptosis and probably resistance or sensitivity to chemotherapy. Numerous splicing isoforms have been identified, that are appropriate candidates for targeted treatment, even in mCRC (Zheng et al.). Zhou et al. deeply investigated the role of Anoikis and epithelial-mesenchymal transition (EMT) in the occurrence of distant metastasis of CRC. In particular, they focused on the understanding of their crosstalk and the identification of key genes. Besides the prognostic role, these findings could help in developing novel therapeutic targets for patients with mCRC. A further new frontier in the selective treatment of solid tumors, including mCRC, is nanomedicine. Nanoparticles are able to maximize treatment efficacy, by directly targeting cancer cells and regulating drug release [Jain and Bhattacharya]. The review by Jain and Bhattacharya carefully describes the nanomaterials that can be employed, as well as the preparation techniques and targeting mechanisms. Even though this field of research seems promising, more data from preclinical and clinical studies are eagerly awaited to bring this technology to the market.

Author contributions

AP: Writing – original draft, Writing – review & editing. DG: Writing – original draft, Writing – review & editing.

References

1. Siegel RL, Wagle NS, Cercak A, Smith RA, Jemal A. Colorectal cancer statistics, 2023. *CA Cancer J Clin* (2023) 73(3):233–54. doi: 10.3322/caac.21772
2. Sung H, Ferlay J, Siegel RL, Laversanne M, Soerjomataram I, Jemal A, et al. Global cancer statistics 2020: GLOBOCAN estimates of incidence and mortality worldwide for 36 cancers in 185 countries. *CA Cancer J Clin* (2021) 71:209–49. doi: 10.3322/caac.21660
3. Tournigand C, André T, Achille E, Lledo G, Flesh M, Mery-Mignard D, et al. FOLFIRI followed by FOLFOX6 or the reverse sequence in advanced colorectal cancer: a randomized GERCOR study. *J Clin Oncol* (2004) 22(2):229–37. doi: 10.1200/JCO.2004.05.113
4. Cervantes A, Adam R, Roselló S, Arnold D, Normanno N, Taïeb J, et al. Metastatic colorectal cancer: ESMO clinical practice guideline for diagnosis, treatment and follow-up. *Ann Oncol* (2022) 34:10–32. doi: 10.1016/j.annonc.2022.10.003
5. Matteucci L, Bittoni A, Gallo G, Ridolfi L, Passardi A. Immunocheckpoint inhibitors in microsatellite-stable or proficient mismatch repair metastatic colorectal cancer: are we entering a new era? *Cancers (Basel)* (2023) 15(21):5189. doi: 10.3390/cancers15215189
6. Grothey A, Van Cutsem E, Sobrero A, Siena S, Falcone A, Ychou M, et al. regorafenib monotherapy for previously treated metastatic colorectal cancer (CORRECT): An international, multicentre, randomised, placebo-controlled, phase 3 trial. *Lancet* (2013) 381:303–12. doi: 10.1016/S0140-6736(12)61900-X
7. Mayer RJ, Van Cutsem E, Falcone ARECOURSE Study Group. Randomized trial of TAS-102 for refractory metastatic colorectal cancer. *N Engl J Med* (2015) 372:1909–19. doi: 10.1056/NEJMoa1414325

Funding

The author(s) declare that no financial support was received for the research, authorship, and/or publication of this article.

Conflict of interest

The authors declare that the research was conducted in the absence of any commercial or financial relationships that could be construed as a potential conflict of interest.

The author(s) declare that author AP was a guest editor and author DG was an associate editor. They were both members of the Frontiers editorial board, at the time of submission. This had no impact on the peer review process and the final decision.

Publisher's note

All claims expressed in this article are solely those of the authors and do not necessarily represent those of their affiliated organizations, or those of the publisher, the editors and the reviewers. Any product that may be evaluated in this article, or claim that may be made by its manufacturer, is not guaranteed or endorsed by the publisher.



OPEN ACCESS

EDITED BY

Alessandro Passardi,
Department of Medical Oncology
(IRCCS), Italy

REVIEWED BY

Zhen Wang,
Zhejiang University, China
Kai Zhang,
Zhengzhou University, China

*CORRESPONDENCE

Lin Wang
✉ lin_wang@hust.edu.cn
Zheng Wang
✉ zhengwang@hust.edu.cn

[†]These authors have contributed
equally to this work

SPECIALTY SECTION

This article was submitted to
Gastrointestinal Cancers:
Colorectal Cancer,
a section of the journal
Frontiers in Oncology

RECEIVED 10 November 2022

ACCEPTED 22 December 2022

PUBLISHED 10 January 2023

CITATION

Tan L, Fu D, Liu F, Liu J, Zhang Y, Li X,
Gao J, Tao K, Wang G, Wang L and
Wang Z (2023) MXRA8 is an immune-
relative prognostic biomarker
associated with metastasis and CD8⁺
T cell infiltration in colorectal cancer.
Front. Oncol. 12:1094612.
doi: 10.3389/fonc.2022.1094612

COPYRIGHT

© 2023 Tan, Fu, Liu, Liu, Zhang, Li, Gao,
Tao, Wang, Wang and Wang. This is an
open-access article distributed under
the terms of the [Creative Commons
Attribution License \(CC BY\)](https://creativecommons.org/licenses/by/4.0/). The use,
distribution or reproduction in other
forums is permitted, provided the
original author(s) and the copyright
owner(s) are credited and that the
original publication in this journal is
cited, in accordance with accepted
academic practice. No use,
distribution or reproduction is
permitted which does not comply
with these terms.

MXRA8 is an immune-relative prognostic biomarker associated with metastasis and CD8⁺ T cell infiltration in colorectal cancer

Lulu Tan^{1†}, Daan Fu^{2†}, Feng Liu³, Jia Liu³, Yang Zhang⁴, Xin Li⁴,
Jinbo Gao¹, Kaixiong Tao¹, Guobin Wang¹, Lin Wang^{4*}
and Zheng Wang^{1*}

¹Department of Gastrointestinal Surgery, Union Hospital, Tongji Medical College, Huazhong
University of Science and Technology, Wuhan, China, ²Department of Anesthesiology, Union
Hospital, Tongji Medical College, Huazhong University of Science and Technology, Wuhan, China,

³Research Center for Tissue Engineering and Regenerative Medicine, Union Hospital, Tongji
Medical College, Huazhong University of Science and Technology, Wuhan, China, ⁴Department of
Clinical Laboratory, Union Hospital, Tongji Medical College, Huazhong University of Science and
Technology, Wuhan, China

Background: Colorectal cancer (CRC) is the second most common cause of
cancer-related deaths worldwide. Tumor metastasis and CD8⁺ T cell infiltration
play a crucial role in CRC patient survival. It is important to determine the
etiology and mechanism of the malignant progression of CRC to develop more
effective treatment strategies.

Methods: We conducted weighted gene co-expression network analysis
(WGCNA) to explore vital modules of tumor metastasis and CD8⁺ T cell
infiltration, then with hub gene selection and survival analysis. Multi-omics
analysis is used to explore the expression pattern, immunity, and prognostic
effect of MXRA8. The molecular and immune characteristics of MXRA8 are
analyzed in independent cohorts, clinical specimens, and *in vitro*.

Results: MXRA8 expression was strongly correlated with tumor malignancy,
metastasis, recurrence, and immunosuppressive microenvironment.
Furthermore, MXRA8 expression predicts poor prognosis and is an
independent prognostic factor for OS in CRC.

Conclusion: MXRA8 may be a potential immunotherapeutic and prognostic
biomarker for CRC.

KEYWORDS

MXRA8, metastasis, CD8⁺ T cell, immune infiltration, colorectal cancer

Introduction

Colorectal cancer (CRC) is the third most common cancer and the second most common cause of cancer-related deaths worldwide (1). Approximately 20% of CRC patients have been reported to have progressed to a metastatic state at presentation, and up to 50% of localized CRC patients eventually present with metastatic disease (2, 3). The prognosis of metastatic CRC (mCRC) patients remains poor, with a three-year survival rate of less than 30% (4). Therefore, it is important to determine the etiology and mechanism of the malignant progression of CRC to develop more effective treatment strategies.

Immunotherapy, especially immune checkpoint inhibitors (ICIs), has become one of the effective therapeutic options for mCRC (5). ICIs have shown promising success in non-small cell lung cancer, metastatic melanoma, metastatic bladder cancer and prostate cancer (6, 7). However, ICIs demonstrated very limited clinical activity in mCRC. An important molecular mechanism of ICIs resistance is insufficient CD8⁺ T cell infiltration or loss of CD8⁺ T cell function (8). Studies have shown that the extent and activity of CD8⁺ T cells can affect tumor prognosis and immunotherapy response rates (9, 10). Less infiltration of CD8⁺ T cells in the center of tumor focus, has restricted the efficiency of immunotherapy in CRC (11). Therefore, identifying biomarkers and mechanisms of reduced infiltration and dysfunction of CD8⁺ T cells in CRC is critical for mCRC immunotherapy.

This study explored potential prognostic biomarkers and their biological functions in CRC, identifying matrix remodeling associated protein 8 (MXRA8) as a target gene. MXRA8 is a receptor for various articular viruses (12), but its role in cancer development and progression remains unsolved. Studies have demonstrated that MXRA8 is highly expressed in most solid tumor tissues compared to adjacent normal tumors (13), and it can modulate iron death and promote glioma progression (14). High MXRA8 expression is associated with poorer overall survival in clear cell renal cell carcinoma (15), but the potential function of MXRA8 in CRC has not been elucidated. In current study, highly expressed of MXRA8 was first determined in CRC tissues, and verified to promote invasion and metastasis in CRC cell. Furthermore, the expression level of MXRA8 reflects abnormal immune status in CRC, including infiltration and dysfunction of CD8⁺ T cells. Therefore, MXRA8 can be used a potential immunotherapeutic and prognostic biomarker for CRC.

Materials and methods

Data preprocessing

The expression profile of CRC tissues in GSE87211, GSE39582, GSE38832, GSE16158 and GSE16537 datasets were

downloaded from GEO database (<http://www.ncbi.nlm.nih.gov/geo/>). GSE87211 dataset was used for module and gene selection significantly associated with CRC metastasis and weighted gene co-expression networks analysis (WGCNA) establishment. GSE39582 dataset was used as the training cohort to construct the prognostic prediction model. TCGA-COAD normalized data and clinical information were downloaded from UCSC Xena website (<https://xenabrowser.net>). GSE38832, GSE16158 and GSE16537 dataset were used as validation cohort. All gene expression profiles were normalized by R software.

Weighted gene co-expression networks analysis

The top 25% of genes with the largest variance in GSE87211 were selected for further co-expression network construction. To ensure the reliability of the results, an outlier was removed. Module identification was accomplished with the dynamic tree cut method. This study aims to set soft-thresholding power to 4 (scale-free $R^2 = 0.93$). Each module contains at least 30 genes, and Pearson correlation analysis was conducted to identify the module with the strongest association with metastasis CRC and examine the relationship among gene modules.

Differentially expressed genes analysis and enrichment analysis

DEGs in CRC and normal tissue in GSE87211 were screened by the “limma” package in R, with an adjusted p -value < 0.05 and $|\log_2FC| > 1$ considered statistically significant. Gene ontology (GO) and Kyoto encyclopedia of genes and genomes (KEGG) enrichment analyses were performed on the overlapping genes of DEGs and metastasis-related modules.

Nomogram construction

Univariate Cox analysis was performed to determine the association between the expression of metastasis-related DEGs and patients' recurrence-free survival (RFS). Lasso penalized Cox regression analysis was used to select metastasis-related genes associated with prognosis. Based on prognostic importance, MXRA8 was identified as an important prognostic molecule, so MXRA8 expression and relevant clinical parameters were used to construct a nomogram. Calibration curves and a receiver operating characteristic (ROC) curve were used to estimate the accuracy and efficiency of the nomogram in a time-dependent manner.

Gene set variation analysis and gene set enrichment analysis

GSE39582 and TGA datasets were divided into high and low groups according to the median MXRA8 expression level. Hallmark gene sets were used as a reference gene set. The GSVA package in R was used for GSVA analysis of MXRA8 high and low groups to identify common activation/inhibition pathways. All samples in GSE39582 were divided into two groups according to their risk score. GSEA was conducted to analyze the difference between groups using an adjusted *p*-value < 0.05 and a false discovery rate < 0.25.

Immune cell infiltration

The enrichment levels of 64 immune signatures in tumor tissues were evaluated by xCell algorithm in GSE87211 dataset. The relative proportions of 22 immune cell types in tumor tissues were evaluated by CIBERSORT algorithm in GSE87211 dataset (16). Correlation analysis of MXRA8 expression levels and immune cells was performed using the Pearson correlation coefficient.

Plasmid and siRNA

Plasmids overexpressing MXRA8 and an empty vector were purchased from Qinda (Wuhan, China). MXRA8 siRNA and negative siRNA controls were constructed by Qinda (Wuhan, China). The target sequences for MXRA8 siRNAs were AGGACATCCAGCTAGATTA (MXRA8 si1) and CGGGAAAGTCAAAGGGGAA (MXRA8 si2). CRC cells (SW48 and LoVo, purchased from ATCC) were transfected with siRNA or plasmid using Lipofectamine 3000 reagent (Invitrogen, MA, USA) according to manufacturer's instructions. The knockdown efficiency was validated by qRT-PCR and western blot.

Cell migration assay

Cell migration was measured using transwell chambers (Beaverbio, Jiangsu, China). Suspensions of 10×10^4 cells in 200 μ L of serum-free medium were added to the upper chamber, and a medium containing 10% FBS was added to the lower chamber. After culturing for 12 h, the migrating cells were fixed with 4% paraformaldehyde and stained with crystal violet. The cells were counted in four random fields under a light microscope. The control group was used as the standard and the statistical results of the treatment group were standardized.

Wound-healing assay

The cells were seeded in 6-well plates and grown to 90% confluence in a complete medium. The artificial wound was made by scraping the confluent cell monolayer with a 200- μ L pipette tip, then washed with PBS to remove the detached cells. The remaining cells were grown in a serum-free medium, and cell migration was observed by microscopy and analyzed objectively using Image J. Wound closure (%) was calculated using the following formula: $(1 - [72\text{-hour area}/0\text{-hour area}]) \times 100$.

Quantitative real-time PCR

Total RNA from cultured cells was extracted using a Trizol reagent kit (Takara, Dalian, China), and qRT-PCR was performed as described previously (17). GAPDH was used as an internal control. The primer sequences were as follows: 5'-GCGGAGGCTACGAATACTCG-3' (forward), 5'-TCTAGGTCGATGTACTTGGCAG-3' (reverse), GAPDH: 5'-GGAGCGAGATCCCTCCAAAAT-3' (forward), 5'-GGCTGTTGTCATACTTCTCATGG-3' (reverse).

Western blot

CRC cells transfected with siRNA were collected for protein extraction by using a RIPA buffer (Sigma-Aldrich, Darmstadt, Germany) containing proteinase and phosphatase inhibitors on ice. With the protein concentration being determined, the collected proteins were separated by SDS-PAGE and transferred onto a nitrocellulose membrane (Bio-Rad, Richmond, CA, USA). Post milk blocking, the membranes were incubated with specific primary antibodies (Abcam, ab185444), secondary antibodies and ECL detection reagents (Millipore, USA), for the visualization by chemiluminescence system (UVP, San Gabriel, CA). Image J software was used for protein band quantification.

Immunohistochemistry

Paraffin-embedded specimens were prepared from tissue samples (35 CRC tissues and 35 paired adjacent normal tissues) collected from 35 patients who had been diagnosed with CRC at the Union Hospital (Wuhan, China) according to the original histopathological reports (Supplementary Table 1). All samples were collected with the informed consent of patients. All tissue specimens were collected immediately after surgical excision and quickly fixed in 4% paraformaldehyde solution for 24h. The tissues removed from the fixative were then

dehydrated, transparent, waxed, and embedded. The paraffin section was 3 μ m thick. IHC analysis of tissue was performed using anti-MXRA8 (Abcam, ab185444, 1: 100) and anti-CD8 (Abcam, ab209775, 1:2000 dilution) antibodies and overnight incubation at 4°C. After epitope retrieval, H₂O₂ treatment and non-specific antigens blocking, chips were next incubated with secondary antibody as described previously (18). The IHC results were scored by two independent observers.

Statistical analysis

All statistical analyses were performed using R software 4.0.3. The Student's *t*-test was used to determine the significance of DEGs, the cell migration assay, and the wound-healing assay. The Wilcoxon test was applied to determine the significance of the difference between the risk score and clinicopathological characteristics. GraphPad Prism 8.00 software was used to calculate the area under the curve. *****p*<0.0001; ****p*<0.001; ***p*<0.01; **p*<0.05; ns, not significant.

Results

The turquoise/yellow module was identified as the pivotal module associated with metastasis and CD8⁺ by WGCNA

Considering the significance of metastasis in determining the prognosis of CRC patients, WGCNA was used to analyze the co-expression patterns between metastasis and whole-transcriptome profiling data (Figure S1A). The optimal soft threshold was set to 4 to construct a scale-free network (Figure S1B) to identify 12 modules (Figures 1A, S1C). The turquoise and yellow module highly correlated with metastasis were chosen for further analysis (Figure 1B). Gene expression profiles from GSE87211 identified 2901 upregulated DEGs in CRC samples compared to normal control tissues (Figure 1C). In current study, 699 genes with the highest connectivity in the turquoise/yellow module were intersected with the 2901 DEGs, outputting 306 candidate genes (Figure 1D). GO functions and KEGG pathways enriched analysis indicated that the genes were related to metastasis functions (Figures 1E, F).

MXRA8 was selected as a hub gene associated with metastasis

The metastasis-related gene signature (MGS) was constructed by using LASSO Cox regression analysis to screen the most significant prognostic markers within the module (Figures 2A–C), consisting of six genes (SIX4, PRRX2,

MXRA8, SLC11A1, ADAMTS6, and FLT1). The MGS score of each patient was calculated based on the expression levels of the six genes. The median MGS score was regarded as the cutoff, with all patients being classified as MGS-high or MGS-low, and dead CRC patients having a higher risk score than live patients (Figure 2D). A shorter survival time was found in CRC patients with MGS-high by survival analysis (Figure 2E), which was consistent with the Kaplan-Meier analysis results (*p*<0.0001) (Figure 2F).

TNM stage and risk score were independent risk factors for RFS by Multivariate Cox regression analysis (Figures S2A, B). The expression of risk score-high group genes was related with metastasis pathways (EMT, angiogenesis, hedgehog signaling, and notch signaling pathway) (*p*< 0.0001) by GSEA (Figure S2C). A nomogram for forecasting the CRC patients' survival probability was established by combining the risk score and clinicopathological characteristics (age, sex, and stage) of the patients (Figure S3A). The probabilities for 3-, 5-, and 10-year survival predicted by the nomogram highly accorded with the observed values (Figure S3B). The area under the ROC curves for 3-, 5-, and 10-year OS were 0.700, 0.692, and 0.763, respectively (Figure S3C). Moreover, the AUC values presented that the risk score combined with tumor stage showed the best ability to predict OS among the factors analyzed (Figure S3D).

MXRA8 has been scarcely any report in most cancers, but being of great importance for CRC prognostic (Figure 2C). Higher expression of MXRA8 was found in tumors (compared to normal), in CRC patients with positive lymphatic metastasis (compared to negative lymphatic metastasis), in CRC patients with more advanced stage (Figures 2G; S3E, F), and patients with recurrence and metastasis (compared to no recurrence and metastasis) (Figure 2H).

Construction of an MXRA8-based prognostic prediction model

MXRA8 expression was statistically significant by univariate Cox regression analysis (Figure 3A) and identified as an independent prognostic biomarker in the multivariate Cox proportional hazards regression model using GSE39582 data (HR = 1.25, 95% confidence interval (CI) = 1.03–1.50, *p* = 0.02, Figure 3B). A nomogram for forecasting the CRC patients' survival probability was established by combining MXRA8 and clinicopathological characteristics (age, sex, and stage) (Figure 3C). The probabilities for 1-, 3-, and 5-year survival predicted by the nomogram highly accorded with the observed values (Figure 3D). The area under the ROC curves for 3-, 5-, and 10-year OS were 0.843, 0.779, and 0.754, respectively (Figure 3E). Moreover, the AUC values presented that MXRA8 combined with tumor stage showed the best ability to predict OS among the factors analyzed (Figure 3F).

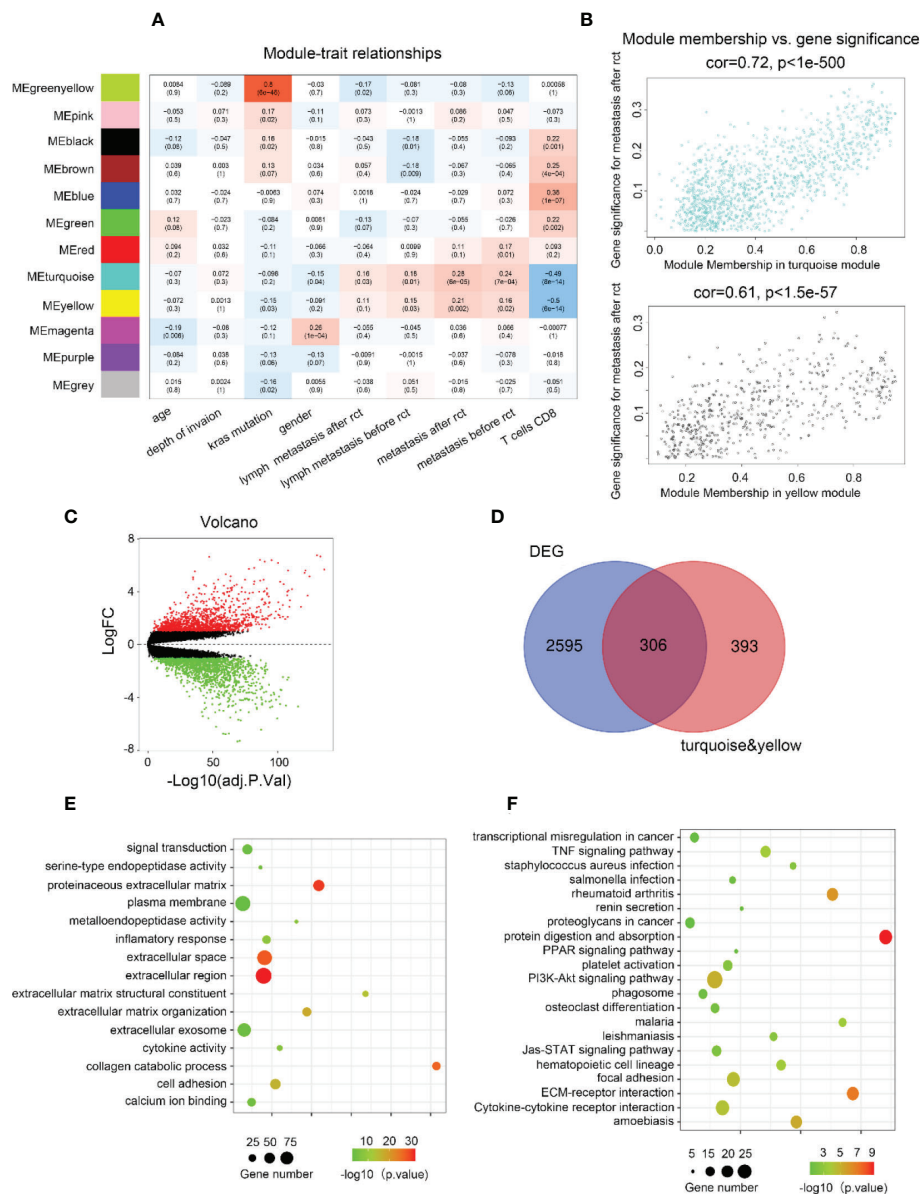


FIGURE 1
Biological function and pathway annotation. **(A)** Heatmap of the correlation between modules and cancer hallmarks. **(B)** Correlation between turquoise/yellow module and metastasis. **(C)** The volcano plot of differentially expressed genes (DEGs) between colorectal carcinoma samples and normal colorectal tissue samples ($\log_{2}FC > 2$ and adjusted p -value < 0.05). The horizontal axis represents the adjusted p -value, and the vertical axis represents the fold change. Red and green circles indicate up- and down-regulated genes, respectively. **(D)** Venn plot of the intersection of upregulated differentially expressed genes and selected genes from WGCNA. **(E)** The top 15 GO functions enriched for the upregulated 306 genes. **(F)** The top of 21 KEGG pathways enriched for the up-related 306 genes.

MXRA8 is involved in cancer-related signaling pathways in CRC

KEGG pathway gene sets and GSVA analysis of hallmark in MXR8 high and low expression samples from GSE39582 and TCGA datasets revealed that tumor metastasis-related pathways enrichment in the MXR8 high group (Figure 4A). MXR8 was highly negatively associated with microsatellite instability but

positively associated with immune checkpoint molecule expression, chemokines, and chemokine receptor expression (Figure 4B). In IHC staining, MXRA8 protein expression increased in tumor tissue (Figures 4C, D and S4A). Furthermore, MXRA8 and CD8 negatively correlated with CRC expression (Figure 4E). MXRA8 expression is positively associated with Tumor Immune Dysfunction and Exclusion (TIDE) and negatively associated with microsatellite instability

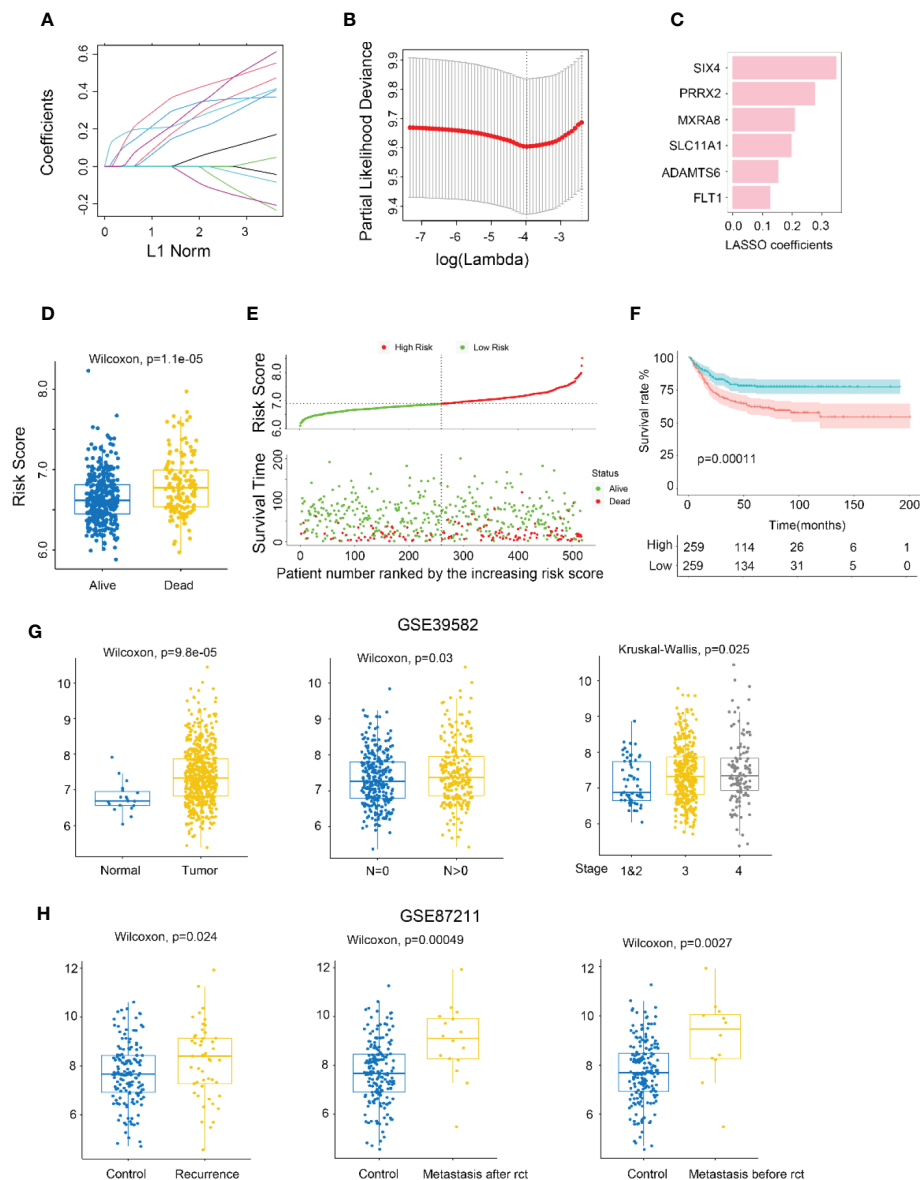


FIGURE 2

Identifying MXRA8 as a hub gene. (A) LASSO coefficient profiles of metastasis-related prognostic differential expressed genes. (B) 10-fold cross-validation for penalty parameter λ selection in LASSO model. (C) LASSO coefficients of six metastasis-related genes. (D) Comparison of risk scores in alive and dead patients. (E) The distribution of risk score, patients' status, and RFS time. (F) Kaplan-Meier RFS curves for patients in high- and low-risk groups. (G) Boxplot indicating MXRA8 expression in normal/tumor (left), lymph metastasis or not (middle), and different stages (right) from GSE39582 database. (H) Boxplot indicating MXRA8 expression in normal/recurrence (left), normal/metastasis after resection (middle), normal/metastasis before resection (right) from TCGA database.

(MSI), the immunophenoscore (IPS), and checkpoint (CP) (Figures 4F, G and S4B).

MXRA8 promotes CRC cell invasion and migration *in vitro*

In vitro, the ability of invasion and migration was assessed by MXRA8 knockdown in SW48 or plasmid transfection in LoVo

(Figures 5A, E). The protein expression of MXRA8 in SW48 cells was decreased followed by MXRA8 knockdown (Figure 5B). The migratory and invasive abilities were reduced with MXRA8 knockdown by transwell assays in SW48 (Figure 5C). Cell migratory ability was repressed with MXRA8 knockdown by wound-healing assays in SW48 (Figure 5D). Furthermore, transwell assays showed that the invasive and migratory abilities were enhanced with MXRA8 plasmid transfection in LoVo (Figure 5F). A wound-healing assay illustrated that the cell

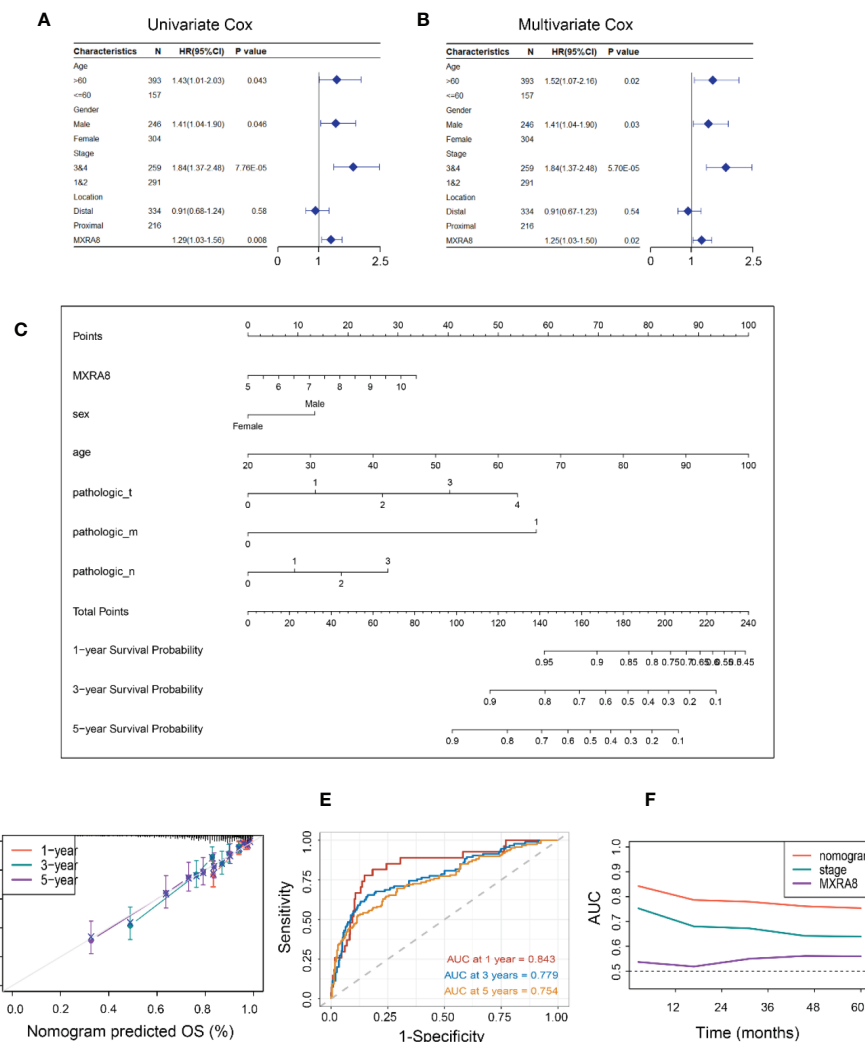


FIGURE 3

Constructing an MXRA8-based prognostic prediction model. (A) Univariate Cox regression analysis of MXRA8 and clinicopathological characteristics (B) Multivariate Cox regression analysis of MXRA8 and clinicopathological characteristics. (C) Nomogram developed based on MXRA8 and clinicopathological characteristics. (D) Plots depict the calibration of the model regarding the agreement between predicted and observed OS. Model performance is shown by the plot relative to the 45-degree line, representing perfect prediction. Calibration analysis of the agreement between nomogram predicted 1-, 3-, and 5-year survival and observed outcomes. (E) Time-dependent ROC curves at 1, 3, and 5 years of the nomogram. (F) AUC plotted for different durations of OS for nomogram-based signature, tumor stage, and MXRA8 in TCGA datasets.

migratory ability was upregulated when MXRA8 was overexpressed in LoVo (Figure 5G). These results corroborated that MXRA8 played a pivotal role in CRC migration and invasion *in vitro*.

High expression of MXRA8 correlates with low CD8⁺ T cell infiltration

Several algorithms were used to conduct the following study in CRC, and the expression of MXRA8 was negatively correlated with CD8⁺ T cell levels in GSE87211 and TCGA datasets (Figures 6A, B). The protein expression of MXRA8 is

negatively correlated with the stromal and immune scores but positively with tumor purity (Figure 6C). A correlation matrix between MXRA8 and immune cells/stromal cells revealed that MXRA8 is negatively correlated with CD8⁺ T cells but positively with multiple types of stromal cells (skeletal muscle, pericytes, mv endothelial cells, ly endothelial cells, fibroblasts, endothelial cells, chondrocytes, and adipocytes), suggesting its potential role mediated by CD8⁺ and the stromal cells in tumor progression (Figures 6D, E). The prognostic value of MXRA8 was validated using TCGA cohorts. In the univariate Cox regression analysis, MXRA8 expression was statistically significant (left of Figure S5A). Furthermore, multivariate Cox regression analysis indicated that MXRA8 was an independent risk factor for

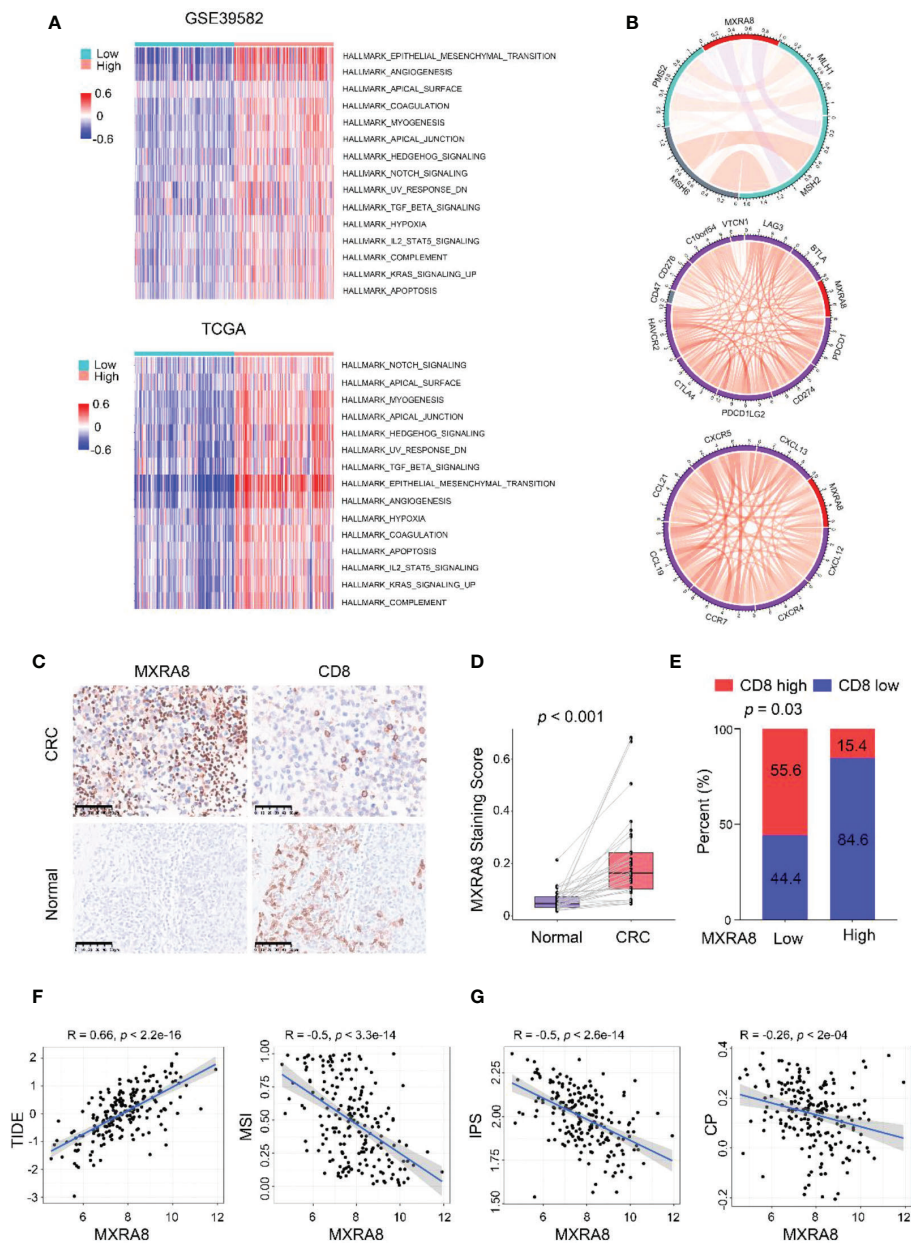


FIGURE 4

MXRA8 promotes CRC migration and immunosuppression. (A) GSEA analysis of hallmark and KEGG pathway gene sets in MXRA8 high and low expression samples from GSE39582 and TCGA datasets. (B) In TCGA, MXRA8 expression is negatively associated with microsatellite instability but positively associated with immune checkpoint molecule expression, chemokines, and chemokine receptors expression. (C) IHC images of MXRA8 protein expression in normal and tumor tissue. Scale bars, 50 μ m. (D) Statistical analysis of MXRA8 expression in CRC and adjacent normal tissues. (E) Statistical analysis of the correlation between MXRA8 and CD8 expression in CRC tissues. (F, G) MXRA8 expression is positively linked to tumor immune dysfunction and exclusion (TIDE) and negatively associated with microsatellite instability (MSI), immunophenoscore (IPS), and checkpoint (CP).

overall survival in CRC (HR = 1.61, 95% CI = 1.01–2.67, right of Figure S5A). Furthermore, higher expression of MXRA8 was associated with a poorer survival rate (Figures S5B–D), indicating that high MXRA8 expression is an unfavorable prognostic biomarker for CRC (Figure S5).

Discussion

Tumor metastasis and CD8⁺ T cell infiltration play a crucial role in CRC patient survival. In this study, we conducted WGCNA to explore vital modules of tumor metastasis and

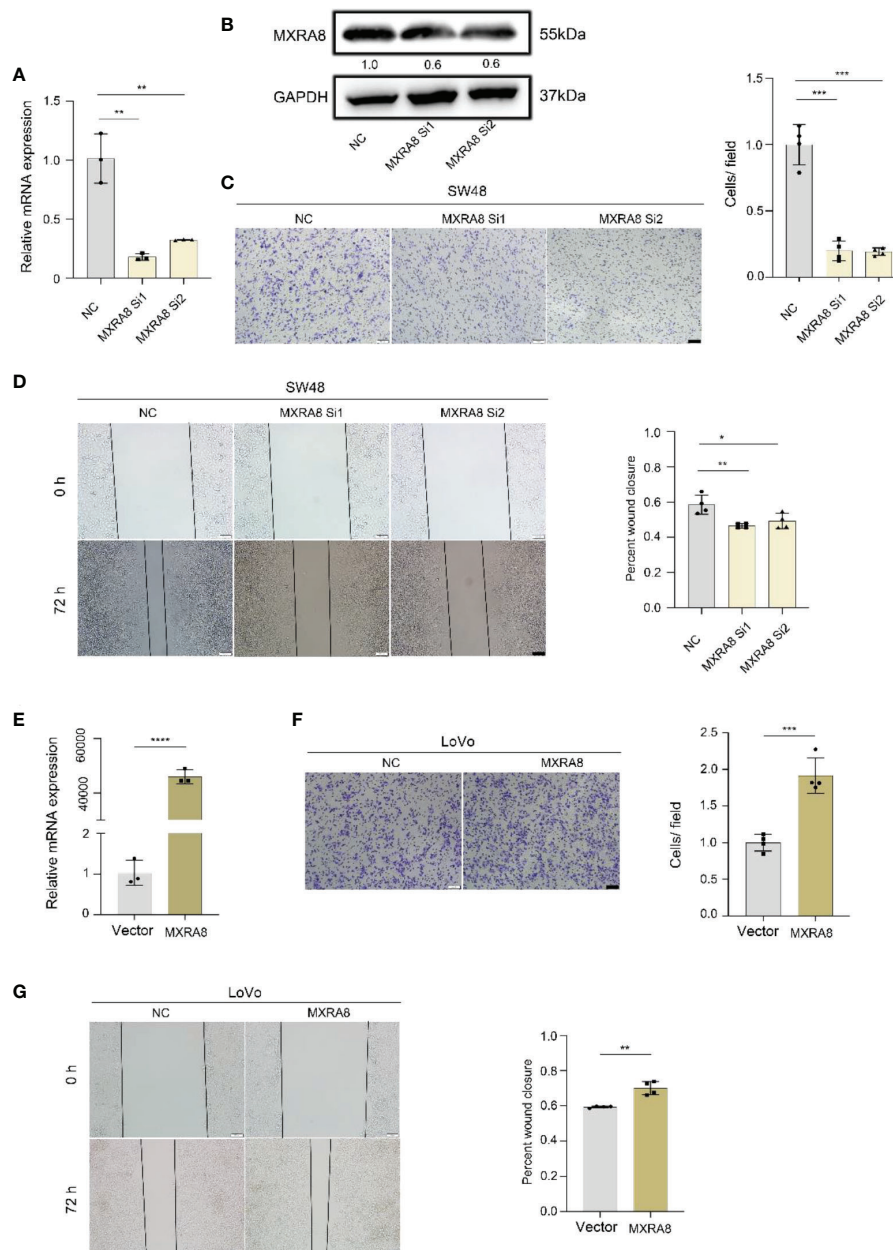


FIGURE 5

MXRA8 promotes CRC cell invasion and migration *in vitro*. (A–D) Levels of MXRA8 mRNA, MXRA8 protein, images of transwell assay for migration, and wound healing assay in SW48 transfected with MXRA8 siRNA. (E–G) Levels of MXRA8 mRNA, images of transwell assay for migration, and wound healing assay in LoVo with MXRA8 plasmid transfection. **** $p < 0.0001$; *** $p < 0.001$; ** $p < 0.01$; * $p < 0.05$.

CD8⁺ T cell infiltration, then with hub gene selection and survival analysis. A CRC prognosis prediction model based on six related genes was constructed, of which one gene, MXRA8, shows potential as a biomarker for survival and CD8⁺ T cell infiltration in CRC.

The comprehensive evaluation of MXRA8 in four independent CRC cohorts demonstrated high expression of MXRA8 in tumors (compared to normal), in CRC patients with positive lymphatic metastasis (compared to negative

lymphatic metastasis), advanced stage, recurrence, and metastasis. The nomogram, including MXRA8 and tumor stage, also showed good prognostic, predictive performance. To further clarify the role of MXRA8 in cancer, we conducted GSEA analysis of hallmark and KEGG pathways, showing that high expression of MXRA8 was positively associated with migration and immunosuppression.

MXRA8 is highly expressed in CRC and associated with CRC metastasis. MXRA8 is a transmembrane protein that can

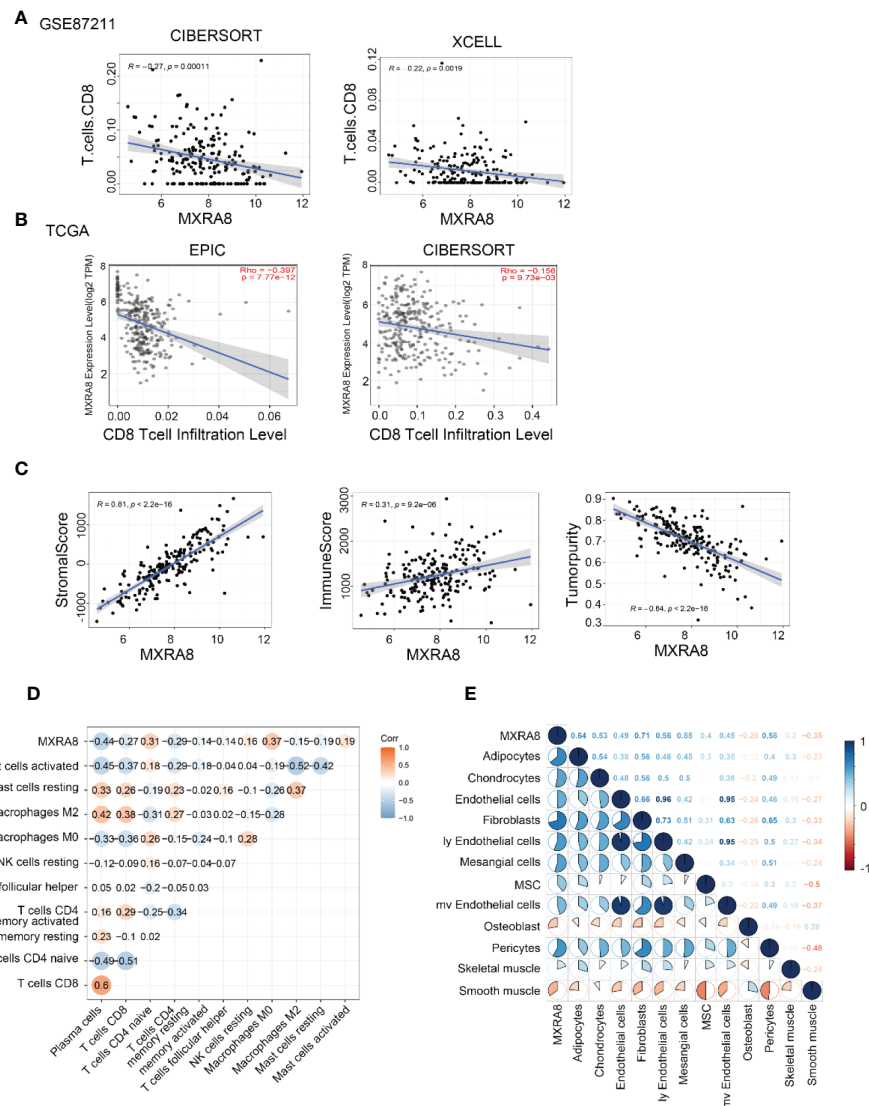


FIGURE 6

High MXRA8 expression correlates with low CD8⁺ T cell infiltration level. (A) The protein expression of MXRA8 is negatively correlated with CD8⁺ T cell infiltration level in GSE87211 with CIBERSORT and XCELL algorithm. (B) The mRNA expression of MXRA8 is negatively correlated with CD8⁺ T cell infiltration level in TCGA with EPIC and CIBERSORT algorithm. (C) The protein expression of MXRA8 is positively correlated with a stromal score and immune score but negatively associated with tumor purity. (D) Correlation analysis between MXRA8 expression levels and immune cells (E) Correlation analysis between MXRA8 expression levels and stromal cells infiltration.

influence integrin signaling and regulate cell-cell interactions (19, 20). MXRA8 also serves as a receptor for multiple arthritogenic alphaviruses (21). The function of MXRA8 in cancer development and progression has not been addressed, but it has been reported to be highly expressed in thyroid cancer (22), kidney cancer (15), esophageal cancer (23), and pancreatic cancer (24). Therefore, this study is the first report on the high expression of MXRA8 in CRC. Additionally, MXRA8 is associated with CRC metastasis, and increased MXRA8 promotes CRC invasion and metastasis *in vitro*. This is similar to the results of a recent study by Roger et al., which found that MXRA8 is highly expressed in lung metastasis of breast cancer,

and miR-200s can down-regulate MXRA8 expression to inhibit the growth and metastasis of breast tumor cells *in vivo* (25).

MXRA8 promotes CRC invasion and metastasis through multiple mechanisms and is involved in tumor invasion and metastasis. EMT-like changes in tumor cells not only loosen cell-cell adhesion complexes, enhancing cell migration and invasive properties but are also associated with enhanced stem cell properties and drug resistance (26, 27). The present study depicted that the MXRA8 high expression group revealed significant enrichment of EMT and angiogenesis. MXRA8 was confirmed to be an adhesion molecular protein expressed in epithelial and mesenchymal cells (28). These results suggest that

MXRA8 may be involved in cell adhesion and migration. Hypoxia and TGF- β signaling can promote tumor EMT and angiogenesis in multiple ways and are thought to contribute to tumor invasion and metastasis (29, 30). In our study, the high MXRA8 group showed significant enrichment of hypoxia and TGF- β signaling pathways. In addition, our study revealed that MXRA8 expression correlated with the expression of multiple metastasis-associated chemokines (CXCL12, CXCL13, CCL9, CCL21, CXCR4, CXCR5, and CCR7) (31–37), suggesting that MXRA8 may be involved in tumor invasion and metastasis by regulating the secretion of chemokines. Numerous studies have reported that chemokines can regulate tumor invasiveness and metastasis and play a crucial role in establishing the composition of the “pre-metastatic niche” (38). For example, the CXCL12/CXCR4 axis is involved in tumor growth, invasion, angiogenesis, and metastasis in CRC, breast and pancreatic cancers (39–42). Nonetheless, the role of MXRA8 in tumor metastasis still requires further study.

MXRA8 levels are associated with cancer immunity, and ICI is changing the treatment paradigm for many cancers (43), with adequate infiltration of tumor-reactive CD8⁺ T cells a prerequisite for the ICI response (44). In colorectal cancer, IL-2 activates TPH1-5-HTP-AhR signaling in the tumor microenvironment to induce CD8⁺ T cell exhaustion in tumor tissues (45). In addition, significant enrichment of immunosuppressive cytokines TGFB1 and IL10 have been found in the Epithelial-mesenchymal transition-high group of almost all cancer types, forming an immunosuppressive microenvironment and leading to decreased infiltration of CD8⁺ T cells (46). Inefficient antigen presentation due to immune escape is also an important factor leading to poor infiltration of CD8⁺ T cells. T cell suppressor receptors such as CTLA-4, PD-1, and TIGIT are essential for T cell activation, antigen recognition, and recruitment, and can inhibit effective anti-tumor immune responses (47). These signaling pathways (TGF- β , EMT, Hypoxia), participating in limiting CD8⁺ T cell infiltration, have been preliminary demonstrated to be associated with high expression of MXRA8 in this work. Furthermore, MXRA8 was linked to the expression of several immune checkpoints in our work, including PD-1, PD-L1, PD-L2, CTLA-4, TIM-3, and LAG-3; thus, MXRA8 may be involved in tumor immune escape. While more in-depth studies between MXRA8 and CD8⁺ T cell infiltration are needed, we propose some ideas about it.

MXRA8 mRNA levels were inversely related to the abundance of most of the immune cell types, especially plasma cells, M2 macrophages, and CD4 memory cells. Correlation analysis showed that the expression of MXRA8 correlated with the expression of many stromal cells, including endothelial cells, fibroblasts, and adipocytes. In many previous studies, fibroblasts and endothelial cells play key roles in cancer progression by promoting extracellular matrix deposition and remodeling, EMT, invasion, metastasis, and therapy resistance (48, 49).

These results demonstrate that MXRA8 may affect the development and prognosis of cancers by shaping the tumor microenvironment.

TIDE was recently evaluated as a potential biomarker to predict the response to ICI therapy in prospective clinical trials and many tumor types (50). TIDE prediction scores correlated with T cell dysfunction in Cytotoxic T Lymphocyte (CTL)-high tumors and T cell exclusion in CTL-low tumors (51). In our study, patients with high MXRA8 expression had less CTL infiltration and higher TIDE and T cell exclusion scores so that MXRA8 may be involved in tumor immune escape through T cell exclusion. The IPS function was used to measure the immune state of the samples (52), and the higher the composite score of IPS, the stronger the immunogenicity of the sample. Our study showed that patients with high MXRA8 expression had lower IPS scores and antigen immunogenicity, indicating poor responsiveness to immunotherapy, which is consistent with the TIDE predictions. Overall, these results suggest that patients with low MXRA8 expression may have a better response to immunotherapy and that MXRA8 may be a potential biomarker for predicting the efficacy of CRC immunotherapy.

Conclusion

This study first found that MXRA8 was overexpressed in CRC. Meanwhile, MXRA8 expression was strongly correlated with tumor malignancy, metastasis, recurrence, and immunosuppressive microenvironment. Furthermore, MXRA8 expression predicts poor prognosis and is an independent prognostic factor for OS in CRC. MXRA8 can also serve as a potential biomarker for immunotherapy. In the future, the role of MXRA8 in CRC prognosis and immunotherapy should be validated in prospective, multicenter, and randomized clinical trials that include follow-up data and receive immunotherapy.

Data availability statement

The datasets presented in this study can be found in online repositories. The names of the repository/repositories and accession number(s) can be found in the article/Supplementary Material.

Author contributions

LT: Data curation, Formal analysis, Methodology, Software, Validation, Visualization, Writing - original draft. DF: Methodology, Investigation, Validation, Software, Formal analysis. FL: Methodology, Validation, Writing - review & editing. JL: Validation, Writing - review & editing. YZ: Funding acquisition, Writing - review & editing. JG: Methodology, Resources, Supervision. KT: Resources, Supervision. GW: Resources, Supervision. LW: Resources, Writing - review & editing, Supervision. ZW: Conceptualization, Writing - review &

editing, Supervision, Funding acquisition. All authors contributed to the article and approved the submitted version.

Funding

This work was supported by the National Natural Science Foundation of China (81974382, 81902135).

Acknowledgments

We thank all the participants in this study.

Conflict of interest

The authors declare that the research was conducted in the absence of any commercial or financial relationships that could be construed as a potential conflict of interest.

References

- Sung H, Ferlay J, Siegel RL, Laversanne M, Soerjomataram I, Jemal A, et al. Global cancer statistics 2020: GLOBOCAN estimates of incidence and mortality worldwide for 36 cancers in 185 countries. *CA Cancer J Clin* (2021) 71(3):209–49. doi: 10.3322/caac.21660
- Schmoll HJ, Van Cutsem E, Stein A, Valentini V, Glimelius B, Haustermans K, et al. ESMO consensus guidelines for management of patients with colon and rectal cancer. a personalized approach to clinical decision making. *Ann Oncol* (2012) 23(10):2479–516. doi: 10.1093/annonc/mds236
- Bockelman C, Engelmann BE, Kaprio T, Hansen TF, Glimelius B. Risk of recurrence in patients with colon cancer stage II and III: A systematic review and meta-analysis of recent literature. *Acta Oncol* (2015) 54(1):5–16. doi: 10.3109/0284186x.2014.975839
- Rahbari NN, Carr PR, Jansen L, Chang-Claude J, Weitz J, Hoffmeister M, et al. Time of metastasis and outcome in colorectal cancer. *Ann Surg* (2019) 269(3):494–502. doi: 10.1097/sla.0000000000002564
- Kishore C, Bhadra P. Current advancements and future perspectives of immunotherapy in colorectal cancer research. *Eur J Pharmacol* (2021) 893:173819. doi: 10.1016/j.ejphar.2020.173819
- Chen X, Xu R, He D, Zhang Y, Chen H, Zhu Y, et al. CD8⁺ T effector and immune checkpoint signatures predict prognosis and responsiveness to immunotherapy in bladder cancer. *Oncogene* (2021) 40(43):6223–34. doi: 10.1038/s41388-021-02019-6
- Bagchi S, Yuan R, Engleman EG. Immune checkpoint inhibitors for the treatment of cancer: Clinical impact and mechanisms of response and resistance. *Annu Rev Pathol* (2021) 16:223–49. doi: 10.1146/annurev-pathol-042020-042741
- Eugene J, Jouand N, Ducoin K, Dansette D, Oger R, Deleine C, et al. The inhibitory receptor CD94/NKG2A on CD8⁺ tumor-infiltrating lymphocytes in colorectal cancer: a promising new druggable immune checkpoint in the context of HLA-E/beta 2m overexpression. *Mod Pathol* (2020) 33(3):468–82. doi: 10.1038/s41379-019-0322-9
- Cabrita R, Lauss M, Sanna A, Donia M, Skaarup Larsen M, Mitra S, et al. Tertiary lymphoid structures improve immunotherapy and survival in melanoma. *Nature* (2020) 577(7791):561–5. doi: 10.1038/s41586-019-1914-8
- Jin Y, Tan A, Feng J, Xu Z, Wang P, Ruan P, et al. Prognostic impact of memory CD8⁺ T cells on immunotherapy in human cancers: A systematic review and meta-analysis. *Front Oncol* (2021) 11:698076. doi: 10.3389/fonc.2021.698076
- Zhang S, Zhong M, Wang C, Xu Y, Gao W-Q, Zhang Y. CCL5-deficiency enhances intratumoral infiltration of CD8⁺ T cells in colorectal cancer. *Cell Death Dis* (2018) 9:766. doi: 10.1038/s41419-018-0796-2
- Zhang R, Kim AS, Fox JM, Nair S, Basore K, Klimstra WB, et al. Mxra8 is a receptor for multiple arthropod-borne alphaviruses. *Nature* (2018) 557(7706):570–4. doi: 10.1038/s41586-018-0121-3
- Song D, Jia X, Liu X, Hu L, Lin K, Xiao T, et al. Identification of the receptor of oncolytic virus M1 as a therapeutic predictor for multiple solid tumors. *Signal Transd Target Ther* (2022) 7(1):100. doi: 10.1038/s41392-022-00921-3
- Xu Z, Chen X, Song L, Yuan F, Yan Y. Matrix remodeling-associated protein 8 as a novel indicator contributing to glioma immune response by regulating ferroptosis. *Front Immunol* (2022) 13:834595. doi: 10.3389/fimmu.2022.834595
- Li S, Xu W. Mining TCGA database for screening and identification of hub genes in kidney renal clear cell carcinoma microenvironment. *J Cell Biochem* (2020) 121(8-9):3952–60. doi: 10.1002/jcb.29511
- Chen B, Khodadoust MS, Liu CL, Newman AM, Alizadeh AA. Profiling tumor infiltrating immune cells with CIBERSORT. *Methods Mol Biol* (2018) 1711:243–59. doi: 10.1007/978-1-4939-7493-1_12
- Yuan J, Tan L, Yin Z, Zhu W, Tao K, Wang G, et al. MIR17HG-miR-18a/19a axis, regulated by interferon regulatory factor-1, promotes gastric cancer metastasis via wnt/beta-catenin signalling. *Cell Death Dis* (2019) 10:454. doi: 10.1038/s41419-019-1685-z
- Tan L, Yuan J, Zhu W, Tao K, Wang G, Gao J. Interferon regulatory factor-1 suppresses DNA damage response and reverses chemotherapy resistance by downregulating the expression of RAD51 in gastric cancer. *Am J Cancer Res* (2020) 10(4):1255–70.
- Han S-W, Jung Y-K, Lee E-J, Park H-R, Kim G-W, Jeong J-H, et al. DICAM inhibits angiogenesis via suppression of AKT and p38 MAP kinase signalling. *Cardiovasc Res* (2013) 98(1):73–82. doi: 10.1093/cvr/cvt019
- Jung Y-K, Han S-W, Kim G-W, Jeong J-H, Kim H-J, Choi J-Y. DICAM inhibits osteoclast differentiation through attenuation of the integrin alpha V beta 3 pathway. *J Bone Miner Res* (2012) 27(9):2024–34. doi: 10.1002/jbmr.1632
- Zhang R, Earnest JT, Kim AS, Winkler ES, Desai P, Adams LJ, et al. Expression of the Mxra8 receptor promotes alphavirus infection and pathogenesis in mice and drosophila. *Cell Rep* (2019) 28(10):2647–58. doi: 10.1016/j.celrep.2019.07.105
- Wu L, Zhou Y, Guan Y, Xiao R, Cai J, Chen W, et al. Seven genes associated with lymphatic metastasis in thyroid cancer that is linked to tumor immune cell infiltration. *Front Oncol* (2022) 11:756246. doi: 10.3389/fonc.2021.756246
- Zhang D, Qian C, Wei H, Qian X. Identification of the prognostic value of tumor microenvironment-related genes in esophageal squamous cell carcinoma. *Front Mol Biosci* (2020) 7:599475. doi: 10.3389/fmolb.2020.599475
- Ichihara R, Shiraki Y, Mizutani Y, Iida T, Miyai Y, Esaki N, et al. Matrix remodeling-associated protein 8 is a marker of a subset of cancer-associated fibroblasts in pancreatic cancer. *Pathol Int* (2022) 72(3):161–75. doi: 10.1111/pin.13198
- Simpson KE, Watson KI, Moorehead RA. Elevated expression of miR-200c/141 in MDA-MB-231 cells suppresses MXRA8 levels and impairs breast cancer growth and metastasis in vivo. *Genes* (2022) 13(4):691. doi: 10.3390/genes13040691
- Aiello NM, Kang Y. Context-dependent EMT programs in cancer metastasis. *J Exp Med* (2019) 216(5):1016–26. doi: 10.1084/jem.20181827
- Wu HT, Zhong HT, Li GW, Shen JX, Ye QQ, Zhang ML, et al. Oncogenic functions of the EMT-related transcription factor ZEB1 in breast cancer. *J Transl Med* (2020) 18(1):51. doi: 10.1186/s12967-020-02240-z

Publisher's note

All claims expressed in this article are solely those of the authors and do not necessarily represent those of their affiliated organizations, or those of the publisher, the editors and the reviewers. Any product that may be evaluated in this article, or claim that may be made by its manufacturer, is not guaranteed or endorsed by the publisher.

Supplementary material

The Supplementary Material for this article can be found online at: <https://www.frontiersin.org/articles/10.3389/fonc.2022.1094612/full#supplementary-material>

28. Song H, Zhao Z, Chai Y, Jin X, Li C, Yuan F, et al. Molecular basis of arthritogenic alphavirus receptor MXRA8 binding to chikungunya virus envelope protein. *Cell* (2019) 177(7):1714–1724.e12. doi: 10.1016/j.cell.2019.04.008
29. Lin Y-T, Wu K-J. Epigenetic regulation of epithelial-mesenchymal transition: focusing on hypoxia and TGF-beta signaling. *J BioMed Sci* (2020) 27(1):39. doi: 10.1186/s12929-020-00632-3
30. Li L, Yu R, Cai T, Chen Z, Lan M, Zou T, et al. Effects of immune cells and cytokines on inflammation and immunosuppression in the tumor microenvironment. *Int Immunophar* (2020) 88:106939. doi: 10.1016/j.intimp.2020.106939
31. Shi Y, Riese DJ II, Shen J. The role of the CXCL12/CXCR4/CXCR7 chemokine axis in cancer. *Front Pharmacol* (2020) 11:574667. doi: 10.3389/fphar.2020.574667
32. Benedicto A, Hernandez-Unzueta I, Sanz E, Márquez J. Ocoxin increases the antitumor effect of BRAF inhibition and reduces cancer associated fibroblast-mediated chemoresistance and protumoral activity in metastatic melanoma. *Nutrients* (2021) 13(2):686. doi: 10.3390/nut13020686
33. Korbecki J, Grochans S, Gutowska I, Barczak K, Baranowska-Bosiacka I. CC chemokines in a tumor: A review of pro-cancer and anti-cancer properties of receptors CCR5, CCR6, CCR7, CCR8, CCR9, and CCR10 ligands. *Int J Mol Sci* (2020) 21(20):7619. doi: 10.3390/ijms21207619
34. Chao C-C, Lee W-F, Wang S-W, Chen P-C, Yamamoto A, Chang T-M, et al. CXCL12/CXCR4 axis promotes metastasis via CXCR4-dependent signaling pathway in non-small cell lung cancer. *J Cell Mol Med* (2021) 25(19):9128–40. doi: 10.1111/jcmm.16743
35. Gao L, Xu J, He G, Huang J, Xu W, Qin J, et al. CCR7 high expression leads to cetuximab resistance by cross-talking with EGFR pathway in PI3K/AKT signals in colorectal cancer. *Am J Cancer Res* (2019) 9(11):2531–43.
36. Fu Q, Tan X, Tang H, Liu J. CCL21 activation of the MALAT1/SRSF1/mTOR axis underpins the development of gastric carcinoma. *J Transl Med* (2021) 19(1):210. doi: 10.1186/s12967-021-02806-5
37. Tian C, Li C, Zeng Y, Liang J, Yang Q, Gu F, et al. Identification of CXCL13/CXCR5 axis's crucial and complex effect in human lung adenocarcinoma. *Int Immunophar* (2021) 94:107416. doi: 10.1016/j.intimp.2021.107416
38. Vilgelm AE, Richmond A. Chemokines modulate immune surveillance in tumorigenesis, metastasis, and response to immunotherapy. *Front Immunol* (2019) 10:333. doi: 10.3389/fimmu.2019.00333
39. Wang D, Wang X, Si M, Yang J, Sun S, Wu H, et al. Exosome-encapsulated miRNAs contribute to CXCL12/CXCR4-induced liver metastasis of colorectal cancer by enhancing M2 polarization of macrophages. *Cancer Lett* (2020) 474:36–52. doi: 10.1016/j.canlet.2020.01.005
40. Santagata S, Ieranò C, Trotta AM, Capiluongo A, Auletta F, Guardascione G, et al. CXCR4 and CXCR7 signaling pathways: A focus on the cross-talk between cancer cells and tumor microenvironment. *Front Oncol* (2021) 11:591386. doi: 10.3389/fonc.2021.591386
41. Daniel SK, Seo YD, Pillarisetty VG. The CXCL12-CXCR4/CXCR7 axis as a mechanism of immune resistance in gastrointestinal malignancies. *Semin Cancer Biol* (2020) 65:176–88. doi: 10.1016/j.semcancer.2019.12.007
42. Zielińska KA, Katanaev VL. The signaling duo CXCL12 and CXCR4: Chemokine fuel for breast cancer tumorigenesis. *Cancers (Basel)* (2020) 12(10):3071. doi: 10.3390/cancers12103071
43. Topalian SL, Drake CG, Pardoll DM. Immune checkpoint blockade: A common denominator approach to cancer therapy. *Cancer Cell* (2015) 27(4):450–61. doi: 10.1016/j.ccell.2015.03.001
44. Farhood B, Najafi M, Mortezaee K. CD8⁺ cytotoxic T lymphocytes in cancer immunotherapy: A review. *J Cell Physiol* (2019) 234(6):8509–21. doi: 10.1002/jcp.27782
45. Liu Y, Zhou N, Zhou L, Wang J, Zhou Y, Zhang T, et al. IL-2 regulates tumor-reactive CD8⁺ T cell exhaustion by activating the aryl hydrocarbon receptor. *Nat Immunol* (2021) 22(3):358–69. doi: 10.1038/s41590-020-00850-9
46. Tiwari JK, Negi S, Kashyap M, Nizamuddin S, Singh A, Khattri A. Pan-cancer analysis shows enrichment of macrophages, overexpression of checkpoint molecules, inhibitory cytokines, and immune exhaustion signatures in EMT-high tumors. *Front Oncol* (2022) 11:793881. doi: 10.3389/fonc.2021.793881
47. Banta KL, Xu X, Chitre AS, Au-Yeung A, Takahashi C, O'Gorman WE, et al. Mechanistic convergence of the TIGIT and PD-1 inhibitory pathways necessitates co-blockade to optimize anti-tumor CD8⁺ T cell responses. *Immunity* (2022) 55(3):512–526.e9. doi: 10.1016/j.immuni.2022.02.005
48. Asif PJ, Longobardi C, Hahne M, Medema JP. The role of cancer-associated fibroblasts in cancer invasion and metastasis. *Cancers* (2021) 13(18):4720. doi: 10.3390/cancers13184720
49. Chen W-Z, Jiang J-X, Yu X-Y, Xia W-J, Yu P-X, Wang K, et al. Endothelial cells in colorectal cancer. *World J Gastroint Oncol* (2019) 11(11):946–56. doi: 10.4251/wjgo.v11.i11.946
50. Chen Y, Li Z-Y, Zhou G-Q, Sun Y. An immune-related gene prognostic index for head and neck squamous cell carcinoma. *Clin Cancer Res* (2021) 27(1):330–41. doi: 10.1158/1078-0432.Ccr-20-2166
51. Jiang P, Gu S, Pan D, Fu J, Sahu A, Hu X, et al. Signatures of T cell dysfunction and exclusion predict cancer immunotherapy response. *Nat Med* (2018) 24(10):1550–8. doi: 10.1038/s41591-018-0136-1
52. Garcia-Mulero S, Alonso MH, Pardo J, Santos C, Sanjuan X, Salazar R, et al. Lung metastases share common immune features regardless of primary tumor origin. *J Immunother Cancer* (2020) 8(1):e000491. doi: 10.1136/jitc-2019-000491



OPEN ACCESS

EDITED BY

Alessandro Passardi,
Department of Medical Oncology (IRCCS),
Italy

REVIEWED BY

Guozhong Jiang,
First Affiliated Hospital of Zhengzhou
University, China
Krishna Sinha,
University of Texas MD Anderson Cancer
Center, United States

*CORRESPONDENCE

Erica Torchiario
✉ erica.torchiario@ircc.it
Enzo Medico
✉ enzo.medico@ircc.it

†PRESENT ADDRESS

Alberto Bardelli,
Department of Oncology, University of
Torino, Italy and IFOM ETS – The AIRC
Institute of Molecular Oncology, Milan, Italy

SPECIALTY SECTION

This article was submitted to
Gastrointestinal Cancers:
Colorectal Cancer,
a section of the journal
Frontiers in Oncology

RECEIVED 23 December 2022

ACCEPTED 12 January 2023

PUBLISHED 02 February 2023

CITATION

Torchiario E, Petti C, Arena S, Sassi F,
Migliardi G, Mellano A, Porporato R,
Basiricò M, Gammaitoni L, Berrino E,
Montone M, Corti G, Crisafulli G,
Marchiò C, Bardelli A and Medico E (2023)
Case report: Preclinical efficacy of NEDD8
and proteasome inhibitors in patient-
derived models of signet ring high-grade
mucinous colorectal cancer from a Lynch
syndrome patient.
Front. Oncol. 13:1130852.
doi: 10.3389/fonc.2023.1130852

COPYRIGHT

© 2023 Torchiario, Petti, Arena, Sassi,
Migliardi, Mellano, Porporato, Basiricò,
Gammaitoni, Berrino, Montone, Corti,
Crisafulli, Marchiò, Bardelli and Medico. This
is an open-access article distributed under
the terms of the [Creative Commons
Attribution License \(CC BY\)](https://creativecommons.org/licenses/by/4.0/). The use,
distribution or reproduction in other
forums is permitted, provided the original
author(s) and the copyright owner(s) are
credited and that the original publication in
this journal is cited, in accordance with
accepted academic practice. No use,
distribution or reproduction is permitted
which does not comply with these terms.

Case report: Preclinical efficacy of NEDD8 and proteasome inhibitors in patient-derived models of signet ring high-grade mucinous colorectal cancer from a Lynch syndrome patient

Erica Torchiario^{1*}, Consalvo Petti¹, Sabrina Arena^{1,2},
Francesco Sassi¹, Giorgia Migliardi¹, Alfredo Mellano¹,
Roberta Porporato¹, Marco Basiricò¹, Loretta Gammaitoni¹,
Enrico Berrino^{1,3}, Monica Montone¹, Giorgio Corti²,
Giovanni Crisafulli⁴, Caterina Marchiò^{1,3},
Alberto Bardelli^{1,2†} and Enzo Medico^{1,2*}

¹Candiolo Cancer Institute, Fondazione del Piemonte per l'Oncologia (FPO) - IRCCS, Candiolo, Italy,

²Department of Oncology, University of Torino, Candiolo, Italy, ³Department of Medical Sciences,
University of Turin, Torino, Italy, ⁴IFOM ETS, The AIRC Institute of Molecular Oncology, Milano, Italy

High-grade mucinous colorectal cancer (HGM CRC) is particularly aggressive, prone to metastasis and treatment resistance, frequently accompanied by "signet ring" cancer cells. A sizeable fraction of HGM CRCs (20-40%) arises in the context of the Lynch Syndrome, an autosomal hereditary syndrome that predisposes to microsatellite instable (MSI) CRC. Development of patient-derived preclinical models for this challenging subtype of colorectal cancer represents an unmet need in oncology. We describe here successful propagation of preclinical models from a case of early-onset, MSI-positive metastatic colorectal cancer in a male Lynch syndrome patient, refractory to standard care (FOLFOX6, FOLFIRI-Panitumumab) and, surprisingly, also to immunotherapy. Surgical material from a debulking operation was implanted in NOD/SCID mice, successfully yielding one patient-derived xenograft (PDX). PDX explants were subsequently used to generate 2D and 3D cell cultures. Histologically, all models resembled the tumor of origin, displaying a high-grade mucinous phenotype with signet ring cells. For preclinical exploration of alternative treatments, in light of recent findings, we considered inhibition of the proteasome by bortezomib and of the related NEDD8 pathway by pevonedistat. Indeed, sensitivity to bortezomib was observed in mucinous adenocarcinoma of the lung, and we previously found that HGM CRC is preferentially sensitive to pevonedistat in models with low or absent expression of cadherin 17 (CDH17), a differentiation marker. We therefore performed IHC on the tumor and models, and observed no CDH17 expression, suggesting sensitivity to pevonedistat. Both bortezomib and pevonedistat showed strong activity on 2D cells at 72 hours and on 3D organoids at 7 days, thus providing valid options for *in vivo* testing. Accordingly, three PDX cohorts were treated for four weeks, respectively with vehicle, bortezomib and pevonedistat. Both drugs significantly reduced tumor growth, as compared to the

vehicle group. Interestingly, while bortezomib was more effective *in vitro*, pevonedistat was more effective *in vivo*. Drug efficacy was further substantiated by a reduction of cellularity and of Ki67-positive cells in the treated tumors. These results highlight proteasome and NEDD8 inhibition as potentially effective therapeutic approaches against Lynch syndrome-associated HGM CRC, also when the disease is refractory to all available treatment options.

KEYWORDS

Lynch syndrome, mucinous colorectal cancer, signet ring cells, NEDD8 pathway inhibition, proteasome inhibition, preclinical study

Introduction

Colorectal cancer (CRC) is one of the most common causes of cancer-related death in the world (1). High-grade mucinous (HGM) CRC occurs in about 10-20% of cases (2) and is characterized by abundant extracellular mucin that accounts for at least 50% of the tumor volume. Although actively secreting mucins, HGM CRC cells are poorly differentiated, and indicate worse prognosis (3). This counterintuitive property is further exacerbated by the presence of “signet ring” cells, that do not interact with each other and contain a large vacuole filled with mucus (4). Signet ring CRC (SR-CRC) is more frequent in young patients (5) (6), and is endowed with marked metastatic propensity (7). HGM/SR-CRC is more frequently found in the proximal colon (8) and typically diagnosed in advanced stage.

HGM/SR-CRC frequently displays microsatellite instability (MSI) and the consequent propensity to accumulate mutations, leading to genetic evolution. Interestingly, 20-40% of mucinous CRCs arise at young age in the context of the Lynch Syndrome (9), an autosomal hereditary syndrome that predisposes to MSI CRC (2). Additional molecular features of HGM/SR-CRC include mutations in key genes of the RAS/MAPK (10) and PI3K/AKT/mTOR pathways (11), and overexpression of specific mucin genes, like *MUC2* and *MUC5AC* (11).

Until now no specific clinical guidelines have been developed for mucinous CRC patients, therefore they undergo standard CRC treatments including FOLFOX (leucovorin, fluorouracil, oxaliplatin), XELOX (capecitabine and oxaliplatin), and FOLFIRI (folic acid, fluorouracil and irinotecan) (12). Checkpoint blockade immunotherapy is an additional option for patients with MSI-positive disease (13). Typically, SR-CRC patients are less responsive to treatment, with shorter overall survival (3, 14). Consequently, new therapeutic options represent a still unmet clinical need.

The most effective way to explore alternative antineoplastic therapies relies on derivation and testing of patient-derived models, such as cell lines, organoids (PDOs) and xenografts (PDXs) (15, 16). However, an extensive internet and literature search for SR-CRC patient-derived models was unsuccessful, reflecting the need to obtain such models for preclinical explorations. We therefore propagated and extensively characterized 2D and 3D cell cultures and patient-derived xenografts (PDXs) from a case of early onset, MSI-positive metastatic SR-CRC in a Lynch syndrome patient, unresponsive to standard care (FOLFOX6, FOLFIRI-Panitumumab) and, surprisingly, also to immunotherapy with nivolumab.

We have previously found that inhibition of the NEDD8 pathway by the small molecule pevonedistat, also known as MLN4924 (17) is effective on mucinous CRC *in vitro* and *in vivo*, in cell lines and PDXs (18). NEDD8 is an ubiquitin-like peptide that, when conjugated to target proteins, modulates their activity. Major targets of neddylation are the ubiquitin ligases of the cullin-ring family, that in turn ubiquitinate and direct to the proteasome specific subsets of target proteins (19). Interestingly, the proteasome inhibitor bortezomib displayed efficacy in invasive lung adenocarcinoma patients only in the case of mucinous tumors (20). We therefore considered pevonedistat and bortezomib as promising candidate drugs to be tested in the newly derived SR-CRC cells and PDXs.

Case description

The clinical history of this case is summarized in Figure 1A. A 26-year-old male patient presented with abdominal pain and underwent cholecystectomy. After one month, a CT scan highlighted a neoplastic lesion in the right colon with multiple mesenteric lymphadenopathies and nodules of peritoneal carcinosis. Histological analysis of a colonoscopy biopsy revealed SR-CRC. The patient immediately underwent right hemicolectomy, lymphadenectomy and exeresis of carcinosis nodes. Histological evaluation of the surgical specimens confirmed the diagnosis of SR-CRC in all samples. The molecular pathology report described a positive MSI status with negativity of tumor tissue for PMS2 and MLH1, no mutations in *KRAS*, *NRAS* and *BRAF* and p.His1047Arg mutation in exon 20 of the *PIK3CA* gene. Germline analysis revealed heterozygous frameshift mutation of *MLH1*, consistent with a Lynch syndrome diagnosis. Four weeks after surgery, new solid tissue formations and suspect lymph nodes were detected by CT scan, while blood levels of CEA were still low (1.1 mg/ml). After 5 cycles of FOLFOX6, a CT scan showed minimal dimensional increase in different lesions, and CEA increased to 3.2 mg/ml. Considering the *KRAS* wild type status, FOLFIRI plus panitumumab was chosen as second line treatment. After 4 cycles, a CT showed new peritoneal lesions and enlargement of old formations, with CEA = 3.9 mg/ml, which led to further treatment change to nivolumab. After an initial disease stabilization, by the 11th nivolumab cycle a drastic increment of CEA (26.4 mg/ml) was observed, with PET and CT detecting substantial increment of lesions size. An explorative laparotomy was performed together with Pressurized Intraperitoneal Aerosol Chemotherapy

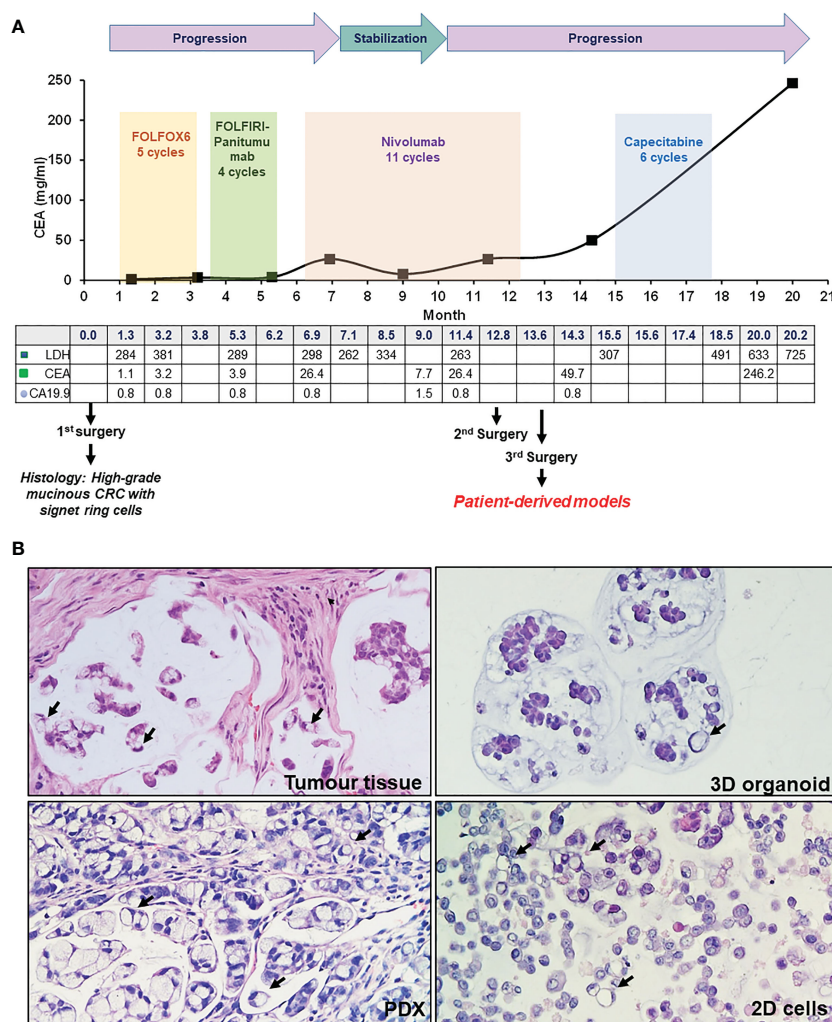


FIGURE 1

Patient case history and tumor histology. (A) Case history, outlining clinical progression, therapy and surgery history, and blood marker profiles. (B) H&E staining of patient tumor tissue (third surgery), PDX, organoid and 2D cells culture, as indicated. Signet ring cells are highlighted by black arrows (20X magnification).

(PIPAC) with oxaliplatin. After this, a third cytoreductive surgery was performed. Patient-derived models were obtained from this surgery. Subsequently, the patient underwent adjuvant chemotherapy with capecitabine. Due to further disease progression, a palliative cytoreductive surgery was performed and eventually the patient passed away. In summary, this case of SR-CRC did not display clinical response to any line of treatment.

Results

Derivation and characterization of PDX and *in vitro* models

To analyze tumor tissue morphology, hematoxylin/eosin staining (H&E) was performed, highlighting a highly mucinous tumor with abundant signet ring cells and conspicuous stromal infiltration (Figure 1B). A PDX line was generated from a colon lesion

obtained from the third surgery. Subsequently, a 3D organoid line and a 2D adherent cell line were derived from the PDX (see Methods). Both 2D and 3D cultures survived more than one freeze/thaw cycles, and displayed massive mucus production in the culture medium. H&E staining of cell and organoid cytoclots showed abundant signet ring cells and mucus, similar to the tumor of origin (Figure 1B). All patient derived models, together with the tumor of origin, stained negative for cadherin 17 (CDH17, from Abnova), indicating a poorly differentiated tumor and potential sensitivity to pevonedistat (18) (Figure 2). To verify if the models maintained the molecular profile of the tumor of origin, and to search for actionable molecular alterations, deep sequencing of a 161-gene panel (ThermoFisher Oncomine Comprehensive Assay v.3) was performed on germline (DNA from white blood cells), tumor (from third surgery) and models, setting the variant allele frequency (VAF) for somatic mutation detection at 0.02. Germline analysis confirmed the MLH1 p Glu23Glyfs*8 frameshift mutation due to the insertion of an additional G in a stretch of five Gs. We observed strong

concordance between the tumor tissue and all derived models, unfortunately with no targetable alteration. All samples (tumor tissue, 2D cells, 3D organoids and PDX) carried KRAS p.Gly13Asp mutation, most probably selected during the panitumumab treatment (21), CTNNB1 p.Ser45Phe and GNAS p.Arg201His. The PDX also showed a subclonal ERBB2 variant (p.Arg896His) and a frameshift deletion of *ARID1A* gene (p.Ile1816fs). Interestingly, no PIK3CA

mutations were detected, highlighting heterogeneity or molecular evolution of the disease after the first surgery. The observed beta-catenin gain-of-function mutation, CTNNB1 Ser45Phe, is quite common in CRC patients (22), and could possibly be exploited in the future for combined treatments (data here described are reported in Table 1 in Supplementary). To further search for possible targets, whole exome sequencing was performed on tumor and germline DNA. All previously found mutations, including the germline MLH1 variant, were confirmed, but again no targetable mutations were found. A copy number gain was found in the long arm of chromosome 1, frequently observed in CRC (23), but with no current clinical implications.

Preclinical evaluation of drug response

Considering the observed clinical resistance to standard and targeted treatments, and the absence of any therapeutic indication emerging from deep sequencing, the newly derived SR-CRC models were evaluated for sensitivity to the proteasome inhibitor bortezomib and to the NEDD8 inhibitor pevonedistat. Initial assessments on the 2D cell line *in vitro* revealed marked sensitivity to bortezomib, with an IC₅₀ of 4.06 nM (Figure 3A) and significant but lower sensitivity to pevonedistat (IC₅₀ = 910 nM, Figure 3B). Efficacy of both drugs was confirmed on 3D organoids at one week of treatment, again with higher sensitivity to bortezomib (Figures 3C, D). Subsequently, both drugs were tested for efficacy *in vivo*, in the PDX model. Three PDX cohorts were treated for four weeks respectively with vehicle, bortezomib and pevonedistat (see Methods). As showed in Figure 4A, both drugs markedly reduced tumor growth compared to the vehicle group, with better efficacy and higher statistical significance for pevonedistat (Figure 4B). Kaplan-Meier analysis revealed significantly longer survival of bortezomib and pevonedistat-treated cohorts (log rank *p*-value of 0.009 and 0.002 respectively; Figures 4C, D). Intriguingly, while bortezomib seemed more effective *in vitro*, pevonedistat efficacy was slightly more pronounced *in vivo*. Histological analysis of PDX explants at the end of treatment revealed that vehicle-treated tumors not only were larger, but also displayed higher cellularity, while the smaller, bortezomib- and pevonedistat-treated tumors were richer in mucus and necrosis, with lower absolute amounts of Ki67-positive cells (Figure 4E). Mucus and necrosis could be at the basis of the oscillations in tumor volume observed in the treated cohorts (Figure 3A). Altogether, these results provide preclinical evidence for both drugs as potentially viable therapeutic options for SR-CRC.

Discussion

Over the last 25 years, the incidence of early onset CRC has been steadily increasing (24). Indeed, substantial increment of CRC incidence in 20–34 year old men and women is estimated to take place by 2030 (25). Early onset CRC is typically diagnosed at an advanced stage and characterized by rapid progression, mucinous or signet ring histology (HGM/SR-CRC) and lower differentiation

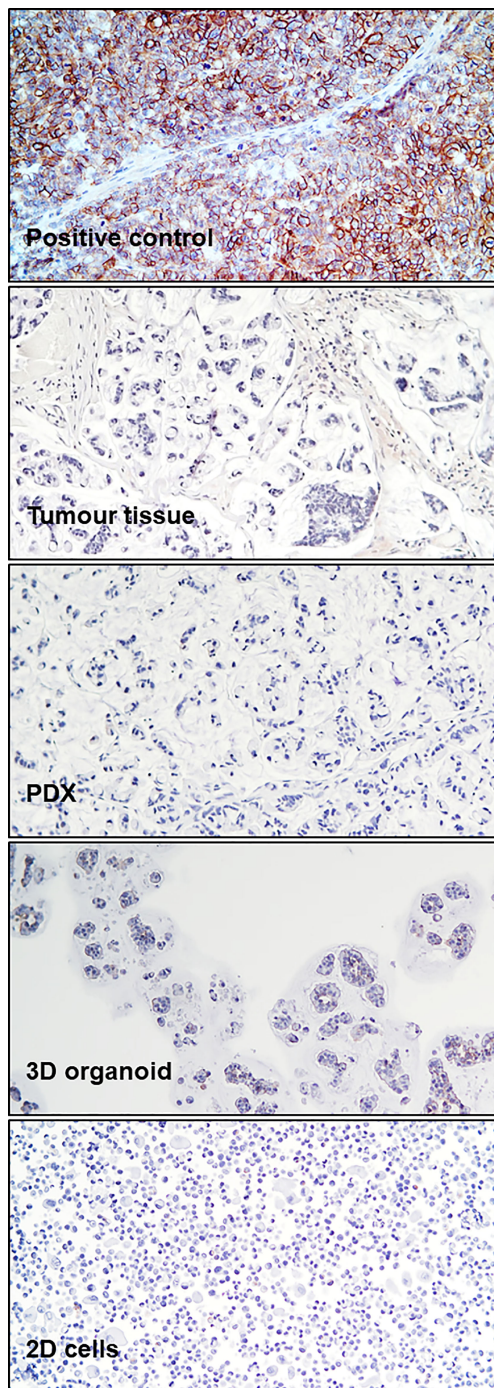


FIGURE 2
CDH17 Immunohistochemistry. Immunohistochemical staining for CDH17 in a positive control (xenograft SNU1746 cell line) and in patient tumor tissue (third surgery), PDX, 3D organoids, and 2D cells, as indicated.

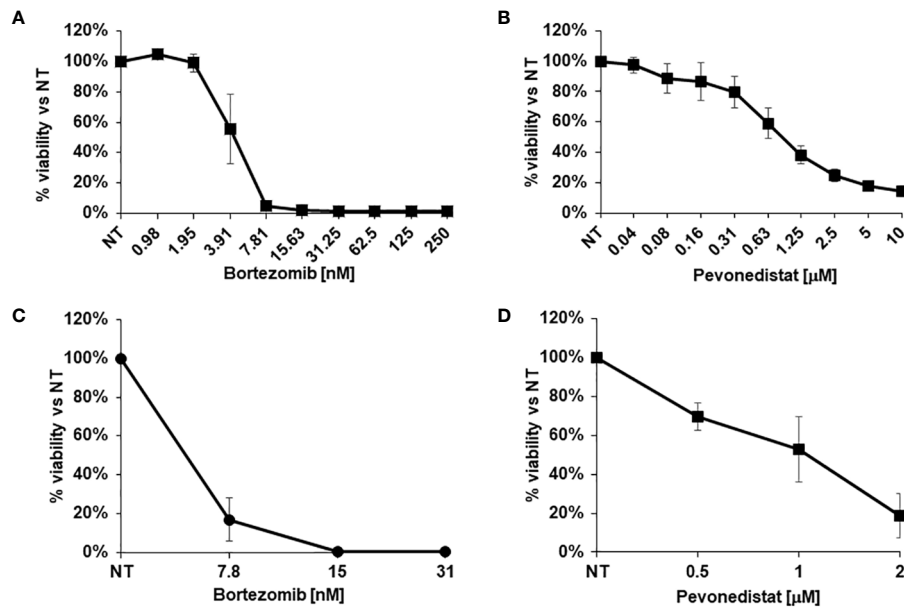


FIGURE 3

In vitro drug response assays. (A, B) Viability of 2D cells after *in vitro* treatment with increasing concentrations of Bortezomib (A) or Pevonedistat (B) for 72h. C, (D) Viability of 3D organoids after *in vitro* treatment with increasing concentrations of Bortezomib (C) or Pevonedistat (D) for 1 week. Cell viability was evaluated using the CellTiter-Glo[®] assay.

(26). About 20% of early-onset CRC is hereditary, mostly in the context of the Lynch syndrome, i.e. germline mutations in mismatch repair genes (27). HGM/SR-CRC is associated with higher rate of MSI positivity, a positive predictor of response to checkpoint inhibition-based immunotherapy (28). However, both the mucinous phenotype and Lynch syndrome context are negatively associated with PD-L1 expression by cancer cells in MSI tumors (29). In line with these observations, the patient described here displayed only transient disease stabilization by checkpoint blockade.

Preclinical models like organoids and PDXs are widely recognized as the best possible ways to recapitulate tumor biology and to discover and test new therapeutic strategies (15, 30). This is particularly true when actionable molecular alterations are found, leading to hypothesis-based precision medicine approaches. Unfortunately, the case described here displayed no such alterations, leading to an alternative search for candidate treatments based on previous literature. Accordingly, we tested for sensitivity to proteasome and NEDD8 inhibition in three patient-derived models of increasing complexity: 2D cells, 3D organoids, and *in vivo* PDXs. In this way, drug efficacy could be assessed in multiple experimental conditions, to yield more reliable results. Indeed, the *in vitro* results were highly concordant, with an extremely high efficacy of bortezomib, while the PDX experiments highlighted a therapeutic advantage of pevonedistat. This could be explained by the known limitations of bortezomib efficacy *in vivo* due to high toxicity, poor pharmacokinetics, and low tumor penetration (31, 32). Moreover, the presence of residual mucin is known to form a barrier to drug delivery (33), potentially affecting efficacy of both drugs.

Overall, the preclinical results provided here highlight pevonedistat and bortezomib as potentially effective therapeutic

approaches against HGM/SR-CRC. Although limited to a single case, negativity for CDH17 of the tumor and all models further confirmed its potential value as a marker of poor differentiation and pevonedistat sensitivity (18). However, for both drugs, more studies are needed to further improve penetration and response in the context of HGM/SR-CRC. Along this line, a number of studies showed efficacy of combinations of bortezomib or pevonedistat with other drugs. Examples include combination of bortezomib with vorinostat and dexamethasone in relapsed multiple myeloma [NCT01720875 (34)]. Pevonedistat was found to synergize with EGFR pathway inhibition, leading to tumor regression, in CRC xenograft models (35). Bortezomib and pevonedistat could also increase the efficacy of immunotherapy, because both drugs have been shown to induce immunogenic cell death, potentially enhancing antitumor immunity and allowing more durable responses to immunotherapy (36, 37). Additional possibilities for pevonedistat combinations can be derived from its mechanism of action, that ultimately drives stabilization of the replication initiation protein CDT1 at the end of the S-phase. This leads to DNA re-replication, aneuploidy and DNA damage, which in turn results in S and G2/M arrest, causing apoptosis and senescence. For this reason pevonedistat has successfully been tested as a radiosensitizer, in head and neck squamous carcinoma (38), pancreatic and breast cancer (39, 40). Moreover, pevonedistat combination with PARP inhibitors has been described as a possible new strategy for non-small cell lung cancer treatment (41). All the above considerations, together with the better *in vivo* profile, highlight pevonedistat as the preferred candidate for further explorations.

A limitation of this study is that it includes a single case: validation of treatment efficacy and prediction in an adequate cohort of preclinical models is required to move these therapeutic

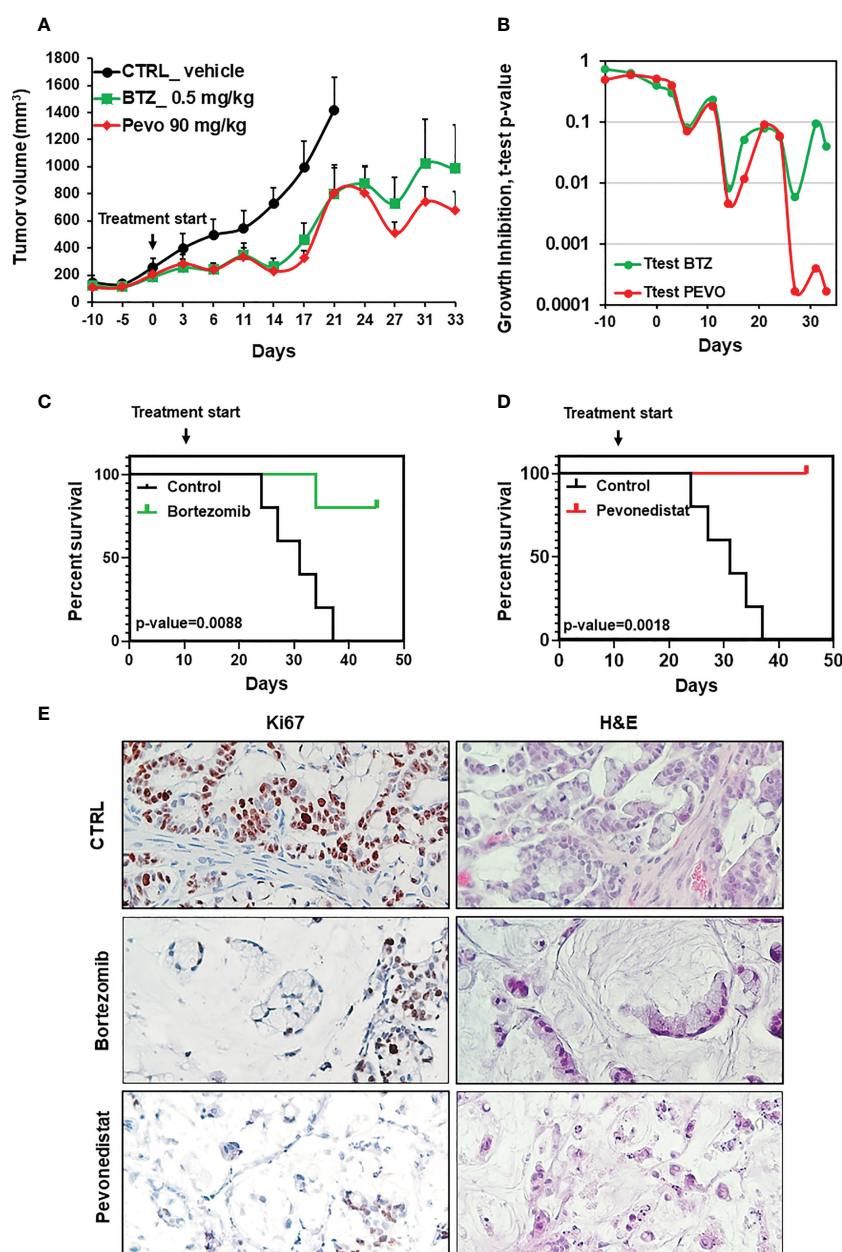


FIGURE 4

In vivo efficacy of pevonedistat and bortezomib. (A) *In vivo* growth of three PDX cohorts (n=5), treated for four weeks respectively with vehicle, bortezomib (0.5mg/kg) and pevonedistat (90mg/kg). (B) T-test p-values comparing tumor size in the vehicle cohort vs. the bortezomib or pevonedistat cohort, at different treatment times. (C, D) Kaplan-Meier survival plots comparing the vehicle cohort vs the bortezomib (C) or pevonedistat (D) cohorts. P-values are from Logrank test analysis. (E) Representative pictures of IHC staining for Ki67 after PDX treatment with vehicle, bortezomib and pevonedistat, at the end of the experiment.

strategies towards clinical assessment in patients. However, this case proves the feasibility and informativeness of the preclinical research strategy in the context of HGM/SR-CRC in early onset patients, where standard therapy frequently fails.

conclusions of this article will be made available by the authors, without undue reservation. Further inquiries can be directed to the corresponding authors.

Data availability statement

The original contributions presented in the study are included in the article and [Supplementary Material](#). The raw data supporting the

Ethics statement

The studies involving human participants were reviewed and approved by Ethics Committee of the Candiolo Cancer Institute. The patients/participants provided their written informed consent to

participate in this study. The animal study was reviewed and approved by Istituto Superiore di Sanità. Written informed consent was obtained from the individual(s) for the publication of any potentially identifiable images or data included in this article.

Author contributions

Conceptualization: EM and ET; experimental design: EM and ET; experimental procedures: ET, CP, FS, RP, MB, MM, EB, and LG; bioinformatic analyses: GCo, GCr, and EB; procurement of models and patient material: EM, SA, and AM; data curation: ET, CP, and EM; writing-original draft preparation: ET and EM; writing-review and editing: EM, ET, CP, CM, SA, and AM; overall supervision and funding acquisition: EM. All authors contributed to the article and approved the submitted version.

Funding

This research was funded by: AIRC under 5 per Mille 2018 - ID. 21091 program – P.I. Bardelli Alberto - G.L. Medico Enzo (EM, AB); AIRC Accelerator Award Project n. 24285 (EM); MAECI PGR00815 (EM); Ministero della Salute, “Progetto di Rete ACC 2019”-RC 2020 (EM); H2020 INFRAIA grant agreement no. 731105 EDiReX (EM); and Fondazione Piemontese per la Ricerca sul Cancro-ONLUS, 5x1000 Ministero della Salute 2017 “See-HER” (EM).

References

- Rawla P, Sunkara T, Barsouk A. Epidemiology of colorectal cancer: incidence, mortality, survival, and risk factors. *Prz Gastroenterol* (2019) 14(2):89–103. doi: 10.5114/pg.2018.81072
- Hugen N, van Beek JJ, de Wilt JH, Nagtegaal ID. Insight into mucinous colorectal carcinoma: clues from etiology. *Ann Surg Oncol* (2014) 21(9):2963–70. doi: 10.1245/s10434-014-3706-6
- Park JS, Huh JW, Park YA, Cho YB, Yun SH, Kim HC, et al. Prognostic comparison between mucinous and nonmucinous adenocarcinoma in colorectal cancer. *Med (Baltimore)* (2015) 94(15):e658. doi: 10.1097/MD.0000000000000658
- Börger ME, Gosens MJ, Jeuken JW, van Kempen LC, van de Velde CJ, van Krieken JH, et al. Signet ring cell differentiation in mucinous colorectal carcinoma. *J Pathol* (2007) 212(3):278–86. doi: 10.1002/path.2181
- An Y, Zhou J, Lin G, Wu H, Cong L, Li Y, et al. Clinicopathological and molecular characteristics of colorectal signet ring cell carcinoma: A review. *Pathol Oncol Res* (2021) 27:1609859. doi: 10.3389/pore.2021.1609859
- Hyngstrom JR, Hu CY, Xing Y, You YN, Feig BW, Skibber JM, et al. Clinicopathology and outcomes for mucinous and signet ring colorectal adenocarcinoma: analysis from the national cancer data base. *Ann Surg Oncol* (2012) 19(9):2814–21. doi: 10.1245/s10434-012-2321-7
- Yun SO, Cho YB, Lee WY, Kim HC, Yun SH, Park YA, et al. Clinical significance of signet-Ring-Cell colorectal cancer as a prognostic factor. *Ann Coloproctol* (2017) 33(6):232–8. doi: 10.3393/ac.2017.33.6.232
- Hugen N, Verhoeven RH, Radema SA, de Hingh IH, Pruijt JF, Nagtegaal ID, et al. Prognosis and value of adjuvant chemotherapy in stage III mucinous colorectal carcinoma. *Ann Oncol* (2013) 24(11):2819–24. doi: 10.1093/annonc/mdt378
- Lynch HT, Lynch JF. The lynch syndromes. *Curr Opin Oncol* (1993) 5(4):687–96. doi: 10.1097/00001622-199307000-00013
- Kakar S, Deng G, Smyrk TC, Cun L, Sahai V, Kim YS. Loss of heterozygosity, aberrant methylation, BRAF mutation and KRAS mutation in colorectal signet ring cell carcinoma. *Mod Pathol* (2012) 25(7):1040–7. doi: 10.1038/modpathol.2012.44
- Hugen N, Simons M, Halilović A, van der Post RS, Bogers AJ, Marijnissen-van Zanten MA, et al. The molecular background of mucinous carcinoma beyond MUC2. *J Pathol Clin Res* (2015) 1(1):3–17. doi: 10.1002/cjp2.1
- Luo C, Cen S, Ding G, Wu W. Mucinous colorectal adenocarcinoma: clinical pathology and treatment options. *Cancer Commun (Lond)* (2019) 39(1):13. doi: 10.1186/s40880-019-0361-0
- Cohen R, Colle R, Pudlitz T, Heran M, Duval A, Svrcek M, et al. Immune checkpoint inhibition in metastatic colorectal cancer harboring microsatellite instability or mismatch repair deficiency. *Cancers (Basel)* (2021) 13(5):1149. doi: 10.3390/cancers13051149
- Kim SH, Shin SJ, Lee KY, Kim H, Kim TI, Kang DR, et al. Prognostic value of mucinous histology depends on microsatellite instability status in patients with stage III colon cancer treated with adjuvant FOLFOX chemotherapy: a retrospective cohort study. *Ann Surg Oncol* (2013) 20(11):3407–13. doi: 10.1245/s10434-013-3169-1
- Invrea F, Rovito R, Torchiaro E, Petti C, Isella C, Medico E. Patient-derived xenografts (PDXs) as model systems for human cancer. *Curr Opin Biotechnol* (2020) 63:151–6. doi: 10.1016/j.copbio.2020.01.003
- Byrne AT, Alferez DG, Amant F, Annibaldi D, Arribas J, Biankin AV, et al. Interrogating open issues in cancer precision medicine with patient-derived xenografts. *Nat Rev Cancer* (2017) 17(4):254–68. doi: 10.1038/nrc.2016.140
- Soucy TA, Smith PG, Milhollen MA, Berger AJ, Gavin JM, Adhikari S, et al. An inhibitor of NEDD8-activating enzyme as a new approach to treat cancer. *Nat* (2009) 458(7239):732–6. doi: 10.1038/nature07884
- Picco G, Petti C, Sassi F, Grillone K, Migliardi G, Rossi T, et al. Efficacy of NEDD8 pathway inhibition in preclinical models of poorly differentiated, clinically aggressive colorectal cancer. *J Natl Cancer Inst* (2017) 109(2):djw209. doi: 10.1093/jnci/djw209
- Watson IR, Irwin MS, Ohh M. NEDD8 pathways in cancer, sine quibus non. *Cancer Cell* (2011) 15:168–76. doi: 10.1016/j.ccr.2011.01.002
- Drilon A, Schoenfeld AJ, Arbour KC, Litvak A, Ni A, Montecalvo J, et al. Exceptional responders with invasive mucinous adenocarcinomas: A phase 2 trial of bortezomib in patients with. *Cold Spring Harb Mol Case Stud* (2019) 5(2):a003665. doi: 10.1101/mcs.a003665

Acknowledgments

The authors thank Daniela Cantarella, Barbara Martinoglio, Benedetta Mussolin and Stefania Giove for technical assistance, Simona Destefanis for secretarial assistance. We also thank Livio Trusolino and Andrea Bertotti for suggestions and discussions.

Conflict of interest

The authors declare that the research was conducted in the absence of any commercial or financial relationships that could be construed as a potential conflict of interest.

Publisher's note

All claims expressed in this article are solely those of the authors and do not necessarily represent those of their affiliated organizations, or those of the publisher, the editors and the reviewers. Any product that may be evaluated in this article, or claim that may be made by its manufacturer, is not guaranteed or endorsed by the publisher.

Supplementary material

The Supplementary Material for this article can be found online at: <https://www.frontiersin.org/articles/10.3389/fonc.2023.1130852/full#supplementary-material>

21. Misale S, Yaeger R, Hobor S, Scala E, Janakiraman M, Liska D, et al. Emergence of KRAS mutations and acquired resistance to anti-EGFR therapy in colorectal cancer. *Nat* (2012) 486(7404):532–6. doi: 10.1038/nature11156
22. Willauer AN, Liu Y, Pereira AAL, Lam M, Morris JS, Raghav KPS, et al. Clinical and molecular characterization of early-onset colorectal cancer. *Cancer* (2019) 125(12):2002–10. doi: 10.1002/cnrc.31994
23. Woo XY, Giordano J, Srivastava A, Zhao ZM, Lloyd MW, de Bruijn R, et al. Conservation of copy number profiles during engraftment and passaging of patient-derived cancer xenografts. *Nat Genet* (2021) 53(1):86–99. doi: 10.1038/s41588-020-00750-6
24. Vuik FE, Nieuwenburg SA, Bardou M, Lansdorp-Vogelaar I, Dinis-Ribeiro M, Bento MJ, et al. Increasing incidence of colorectal cancer in young adults in Europe over the last 25 years. *Gut* (2019) 68(10):1820–6. doi: 10.1136/gutjnl-2018-317592
25. Rogers JE, Johnson B. The reality of early-onset colorectal cancer: highlighting the needs in a unique but emerging population. *Dig Med Res* (2021) 4:63. doi: 10.21037/dmr-21-77
26. Vuik FER, Nieuwenburg SAV, Nagtegaal ID, Kuipers EJ, Spaander MCW. Clinicopathological characteristics of early onset colorectal cancer. *Aliment Pharmacol Ther* (2021) 54(11–12):1463–71. doi: 10.1111/apt.16638
27. Mauri G, Sartore-Bianchi A, Russo AG, Marsoni S, Bardelli A, Siena S. Early-onset colorectal cancer in young individuals. *Mol Oncol* (2019) 13(2):109–31. doi: 10.1002/1878-0261.12417
28. Dudley JC, Lin MT, Le DT, Eshleman JR. Microsatellite instability as a biomarker for PD-1 blockade. *Clin Cancer Res* (2016) 22(4):813–20. doi: 10.1158/1078-0432.CCR-15-1678
29. Kim JH, Park HE, Cho NY, Lee HS, Kang GH. Characterisation of PD-L1-positive subsets of microsatellite-unstable colorectal cancers. *Br J Cancer* (2016) 115(4):490–6. doi: 10.1038/bjc.2016.211
30. Durinikova E, Buzo K, Arena S. Preclinical models as patients' avatars for precision medicine in colorectal cancer: past and future challenges. *J Exp Clin Cancer Res* (2021) 40(1):185. doi: 10.1186/s13046-021-01981-z
31. Williamson MJ, Silva MD, Terkelsen J, Robertson R, Yu L, Xia C, et al. The relationship among tumor architecture, pharmacokinetics, pharmacodynamics, and efficacy of bortezomib in mouse xenograft models. *Mol Cancer Ther* (2009) 8(12):3234–43. doi: 10.1158/1535-7163.MCT-09-0239
32. Yan W, Wu Z, Zhang Y, Hong D, Dong X, Liu L, et al. The molecular and cellular insight into the toxicology of bortezomib-induced peripheral neuropathy. *BioMed Pharmacother* (2021) 142:112068. doi: 10.1016/j.biopha.2021.112068
33. Boegh M, Nielsen HM. Mucus as a barrier to drug delivery – understanding and mimicking the barrier properties. *Basic Clin Pharmacol Toxicol* (2015) 116(3):179–86. doi: 10.1111/bcpt.12342
34. Brown S, Pawlyn C, Tillotson AL, Sherratt D, Flanagan L, Low E, et al. Bortezomib, vorinostat, and dexamethasone combination therapy in relapsed myeloma: Results of the phase 2 MUK four trial. *Clin Lymphoma Myeloma Leuk* (2021) 21(3):154–61.e3. doi: 10.1016/j.clml.2020.11.019
35. Invrea F, Punzi S, Petti C, Minelli R, Peoples MD, Bristow CA, et al. Synthetic lethality screening highlights colorectal cancer vulnerability to concomitant blockade of NEDD8 and EGFR pathways. *Cancers (Basel)* (2021) 13(15):3805. doi: 10.3390/cancers13153805
36. Gulla A, Morelli E, Samur MK, Botta C, Hideshima T, Bianchi G, et al. Bortezomib induces anti-multiple myeloma immune response mediated by cGAS/STING pathway activation. *Blood Cancer Discov* (2021) 2(5):468–83. doi: 10.1158/2643-3230.BCD-21-0047
37. McGrail DJ, Garnett J, Yin J, Dai H, Shih DJH, Lam TNA, et al. Proteome instability is a therapeutic vulnerability in mismatch repair-deficient cancer. *Cancer Cell* (2020) 37(3):371–86.e12. doi: 10.1016/j.ccell.2020.01.011
38. Vanderdys V, Allak A, Guessous F, Benamar M, Read PW, Jameson MJ, et al. The neddylation inhibitor pevonedistat (MLN4924) suppresses and radiosensitizes head and neck squamous carcinoma cells and tumors. *Mol Cancer Ther* (2018) 17(2):368–80. doi: 10.1158/1535-7163.MCT-17-0083
39. Wei D, Li H, Yu J, Sebolt JT, Zhao L, Lawrence TS, et al. Radiosensitization of human pancreatic cancer cells by MLN4924, an investigational NEDD8-activating enzyme inhibitor. *Cancer Res* (2012) 72(1):282–93. doi: 10.1158/0008-5472.CAN-11-2866
40. Yang D, Tan M, Wang G, Sun Y. The p21-dependent radiosensitization of human breast cancer cells by MLN4924, an investigational inhibitor of NEDD8 activating enzyme. *PLoS One* (2012) 7(3):e34079. doi: 10.1371/journal.pone.0034079
41. Guo ZP, Hu YC, Xie Y, Jin F, Song ZQ, Liu XD, et al. MLN4924 suppresses the BRCA1 complex and synergizes with PARP inhibition in NSCLC cells. *Biochem Biophys Res Commun* (2017) 483(1):223–9. doi: 10.1016/j.bbrc.2016.12.162



OPEN ACCESS

EDITED BY

David Gibbons,
St. Vincent's University Hospital, Ireland

REVIEWED BY

Gianluca Russo,
University of Naples Federico II, Italy
Khalil Saleh,
Gustave Roussy Cancer Campus, France

*CORRESPONDENCE

Giulia Martini
✉ giulia.martini@unicampania.it

SPECIALTY SECTION

This article was submitted to
Molecular and Cellular Oncology,
a section of the journal
Frontiers in Oncology

RECEIVED 07 November 2022

ACCEPTED 20 January 2023

PUBLISHED 13 February 2023

CITATION

Martini G, Ciardiello D, Napolitano S,
Martinelli E, Troiani T, Latiano TP,
Avallone A, Normanno N, Di Maio M,
Maiello E and Ciardiello F (2023) Efficacy
and safety of a biomarker-driven
cetuximab-based treatment regimen over
3 treatment lines in mCRC patients with
RAS/BRAF wild type tumors at start of first
line: The CAPRI 2 GOIM trial.
Front. Oncol. 13:1069370.
doi: 10.3389/fonc.2023.1069370

COPYRIGHT

© 2023 Martini, Ciardiello, Napolitano,
Martinelli, Troiani, Latiano, Avallone,
Normanno, Di Maio, Maiello and Ciardiello.
This is an open-access article distributed
under the terms of the [Creative Commons
Attribution License \(CC BY\)](https://creativecommons.org/licenses/by/4.0/). The use,
distribution or reproduction in other
forums is permitted, provided the original
author(s) and the copyright owner(s) are
credited and that the original publication in
this journal is cited, in accordance with
accepted academic practice. No use,
distribution or reproduction is permitted
which does not comply with these terms.

Efficacy and safety of a biomarker-driven cetuximab-based treatment regimen over 3 treatment lines in mCRC patients with *RAS/BRAF* wild type tumors at start of first line: The CAPRI 2 GOIM trial

Giulia Martini^{1*}, Davide Ciardiello^{1,2}, Stefania Napolitano¹,
Erika Martinelli¹, Teresa Troiani¹, Tiziana Pia Latiano²,
Antonio Avallone³, Nicola Normanno⁴, Massimo Di Maio⁵,
Evaristo Maiello² and Fortunato Ciardiello¹

¹Dipartimento di Medicina di Precisione, Oncologia Medica, Università degli Studi della Campania "Luigi Vanvitelli", Napoli, Italy, ²Oncologia Medica, Fondazione Istituto di Ricovero e Cura a Carattere Scientifico (IRCCS) Casa Sollievo della Sofferenza, San Giovanni Rotondo, Italy, ³Istituto Nazionale per lo Studio e la Cura dei Tumori "Fondazione Giovanni Pascale" – Istituto di Ricovero e Cura a Carattere Scientifico (IRCCS), Oncologia Clinica Sperimentale Addome, Napoli, Italy, ⁴Biologia Cellulare e Bioterapie, Istituto Nazionale per lo Studio e la Cura dei Tumori "Fondazione Giovanni Pascale" – Istituto di Ricovero e Cura a Carattere Scientifico, Napoli, Italy, ⁵Dipartimento di Oncologia, Università di Torino, Azienda Ospedaliera Mauriziana, Torino, Italy

Background: Monoclonal antibodies targeting EGFR such as cetuximab or panitumumab represent a major step forward in the treatment of *RAS* wild type (WT) metastatic colorectal cancer (mCRC). Unfortunately, primary and acquired resistance mechanisms occur, with a huge percentage of patients succumbing to the disease. In the last years, *RAS* mutation has been identified as the main molecular driver that determine resistance to anti-EGFR monoclonal antibodies. Liquid biopsy analysis allows to a dynamic and longitudinal assessment of mutational status during mCRC disease and has provided important information on the use of anti-EGFR drugs beyond progression or as rechallenge strategy in patients with *RAS* WT tumors.

Methods: The phase II CAPRI 2 GOIM trial investigates the efficacy and safety of a bio-marker-driven cetuximab-based treatment regimen over 3 treatment lines in mCRC patients with *RAS/BRAF* WT tumors at start of first line.

Discussion: The aim of the study is to identify patients with *RAS/BRAF* WT tumors defined as "addicted" to an-anti EGFR based treatment along three lines of therapy. Moreover, the trial will evaluate the activity of cetuximab re-introduction in combination with irinotecan as 3rd line therapy as rechallenge for patients that will be treated in second line with FOLFOX plus bevacizumab, having a *RAS/BRAF* mutant disease at progression after FOLFIRI plus cetuximab first line. A novel characteristic of this program is that the therapeutic algorithm will be defined at each treatment decision (*first line, second line and third line*) in a prospective

fashion in each patient by a liquid biopsy assessment of *RAS/BRAF* status by a comprehensive 324 genes Foundation One Liquid assay (Foundation/Roche).

Trial registration: EudraCT Number: 2020-003008-15, [ClinicalTrials.gov](https://clinicaltrials.gov/ct2/show/study/NCT05312398) identifier: NCT05312398.

KEYWORDS

colorectal cancer, EGFR, liquid biopsy, biomarker, cetuximab

Introduction

Metastatic colorectal cancer

Colorectal cancer (CRC) is one of the most diagnosed cancers worldwide, with 1.8 million new cases per year (1). In the last years, the use of standard chemotherapy and targeted agents has considerably increased the prognosis of metastatic colorectal cancer (mCRC) patients, with an improvement in median overall survival (OS) to approximately 36 months (2). Several clinical trials have explored the use of cetuximab or panitumumab monoclonal antibodies (mAbs) to target the Epidermal Growth Factor Receptor (EGFR) in the treatment of *RAS* wild type (WT) metastatic colorectal cancer (mCRC) among different lines of treatment (3). However, despite the huge improvement of patient responses, the response is impaired due to the presence of innate or acquired mechanisms of resistance to anti-EGFR blockade (4). In the past years, several molecular biomarkers have been identified in retrospective preclinical and clinical analyses to predict resistance to cetuximab and panitumumab. Among these, *RAS* mutational status is today the principal biomarker of poor response to an anti-EGFR drugs and patients with *RAS*-mutated mCRC are excluded by their treatment (5). In addition, other components of the EGFR signalling pathway determine intrinsic or acquired resistance to EGFR inhibitor including mutation of *BRAF* and *PI3KCA*; amplification of *HER2*, *MET* and *KRAS*; and loss of *PTEN* expression (6, 7). All these alterations seem converge to the MAPK-ERK intracellular driver, which is over-activated and is responsible of tumor survival even when EGFR inhibitors are used (8). The molecular scenario is complicated by the presence of inter-tumor and intratumor heterogeneity of resistance mechanisms, with different molecular clones present at the same time in a patient and even in the same organ (9). In recent years, we have assisted to a widespread use of circulating tumor DNA (ctDNA) testing over the tissue biopsy for the detection in blood of mutations that characterize resistance to target therapy in mCRC (10, 11). Morelli et al. have previously demonstrated how *RAS* and *EGFR* mutant alleles exponentially decline when treatment with EGFR inhibitors is interrupted, with a half-life of nearly 4 months (12, 13). These data provide strong support for the so called rechallenge strategy with anti-EGFR monoclonal antibodies, in a subset of patients treated in front line with chemotherapy plus cetuximab or panitumumab followed by an EGFR free interval of at least 4 months after progression. Different

trials are underway, to prospectively study rechallenge treatment with cetuximab and panitumumab. Phase II clinical trials have been published to date as the CAVE mCRC trial, in which rechallenge strategy in refractory patients with *RAS* WT mCRC with cetuximab plus avelumab, an anti-programmed death ligand 1 (PD-L1) monoclonal antibody has demonstrated clinical evidence of improved overall survival, with the highest benefit obtained in those patients with baseline *RAS/BRAF/EGFR* WT circulating tumor DNA (ctDNA) (14).

Rationale of the study

The rationale of anti-EGFR treatment beyond progression of disease comes from our previous CAPRI GOIM Study, performed in 25 Italian centres in which 340 patients with *KRAS* exon 2 WT mCRC received a first line treatment with FOLFIRI plus cetuximab; of these, 153 mCRC patients, at progression after responding to FOLFIRI plus cetuximab, were treated with FOLFOX or with FOLFOX plus cetuximab in a randomized phase II study (15). In addition, the CAPRI GOIM clinical program has performed extensive translational research with the establishment of a selected 22 multigene next generation sequencing (NGS) test for DNA extracted from tumor tissue and of a selected *RAS* gene. Beaming technology has been used for circulating free tumor DNA extracted from plasma. The main findings of the CAPRI GOIM clinical research project can be summarized as follows: FOLFIRI plus cetuximab is an effective front line treatment in molecularly selected patients with mCRC. Efficacy is similar in fit elderly patients. Efficacy is higher in patients with *KRAS/NRAS/BRAF/PIK3CA* WT tumors. *RAS* testing by liquid biopsy is feasible and predicts efficacy of FOLFIRI plus cetuximab. Second line FOLFOX plus cetuximab is a promising therapeutic approach in patients with *KRAS/NRAS/BRAF/PIK3CA* WT tumors that benefited from first line FOLFIRI plus cetuximab (16). Extended and comprehensive multigene assessment by NGS allows the identification of potential rare gene alterations that could be responsible for resistance to cetuximab in *KRAS/NRAS/BRAF/PIK3CA* WT tumors.

Based on the findings of the CAPRI GOIM trial, the CAPRI 2 GOIM trial has the purpose of investigate the efficacy and safety of a biomarker-driven cetuximab-based treatment regimen over 3 treatment lines in mCRC patients with *RAS/BRAF* WT tumors at start of first line.

In the present paper we describe and discuss the scientific and clinical rationale, the design and treatment lines of the CAPRI 2 GOIM clinical trial (Figure 1).

Materials and methods

Based on dynamic and longitudinal liquid biopsy assessment of RAS/BRAF status, that will be prospectively performed before each line of treatment, 200 mCRC patients will be treated with cetuximab in combination with chemotherapy throughout three lines of therapy, as follows: FOLFIRI plus cetuximab (first line); FOLFOX plus cetuximab (second line); irinotecan plus cetuximab (third line) in case of RAS/BRAF WT at each time point of progression. If after the first line progression, the liquid biopsy assessment indicates *RAS* and/or *BRAF* mutant status, patients will receive FOLFOX plus bevacizumab as the second line of therapy. If after the second line progression, the liquid biopsy assessment indicates *RAS* and/or *BRAF* mutant status, patients will be treated with regorafenib or trifluridine-tipiracil (investigator's choice), as third line of therapy (Figure 1). Each treatment will be administered using standard doses and schedules until progression of disease or unacceptable toxicity (Figure 2).

Technical procedures to manage diagnostic samples from enrolled patients:

Liquid biopsy: Two blood samples will be obtained before each line of treatment (total of 29 mL): one will be shipped to Foundation Roche Germany for extended RAS/BRAF molecular analysis, the second will be processed for additional translational analyses. Liquid biopsy assessment will be performed with a comprehensive 324 genes Foundation One Liquid NGS assay (Foundation/Roche). Briefly, blood samples will be collected before each line of treatment and will be shipped to Foundation Roche Germany for extended RAS/BRAF molecular analysis. Circulating cell-free DNA will be isolated from plasma and analyzed with the Foundation One Liquid assay (Foundation/Roche). This assay assesses SNVs, indels, CNVs and

fusions in 324 cancer related genes (<https://www.foundationmedicine.com/genomic-testing/foundation-one-liquid>).

Tissue analysis: Baseline Formalin-fixed-paraffin-embedded (FFPE) of primary tumor or metastasis will be analyzed by local laboratory for the determination of RAS/BRAF mutational status.

Moreover, a baseline FFPE sample will be shipped to Foundation Roche Germany for molecular analysis. FFPE samples will be analyzed with the Foundation One CDx assay (Foundation/Roche), which covers single nucleotide variants (SNVs), indels, copy number variations (CNV) and fusions in 324 cancer-related genes (<https://www.foundationmedicine.com>). An additional baseline FFPE sample will be shipped to the Cell Biology and Biotherapy Unit, Istituto Nazionale Tumori "Fondazione Giovanni Pascale" IRCCS, Napoli for further translational analyses.

Translational analyses: additional 12 mL of whole blood will be collected. Plasma and peripheral blood mononuclear cells (PBMC) will be collected, stored at -70/-80 °C (preferred) until shipment on dry ice to the Cell Biology and Biotherapy Unit, Istituto Nazionale Tumori "Fondazione Giovanni Pascale" IRCCS, Napoli.

Patients

Patients eligible for inclusion in the CAPRI 2 GOIM trial have to meet all of the following criteria at the start of first line treatment: - Histologically proven diagnosis of colorectal adenocarcinoma - Diagnosis of metastatic disease - *RAS* and *BRAF* WT status of FFPE analysis of primary CRC and/or distant metastasis - Measurable disease.

Other eligible criteria are described in Tables 1, 2.

Study endpoints

Primary endpoint

The primary endpoint of the study is the Response rate (RR) for each line of treatment according to Response Evaluation Criteria in Solid Tumors (RECIST) v1.1.

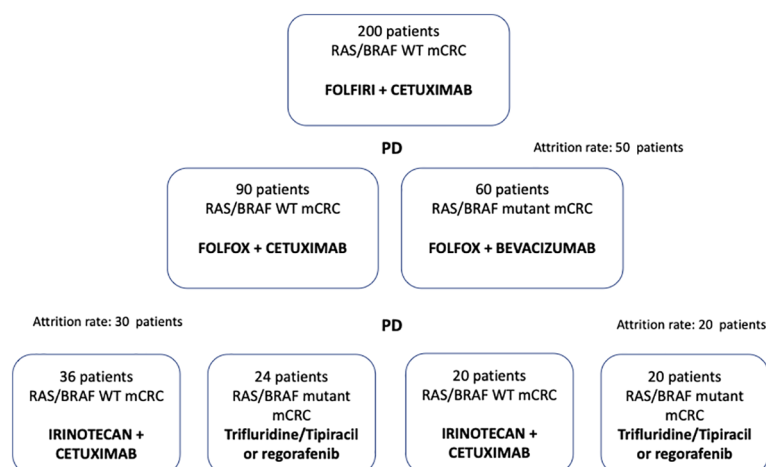
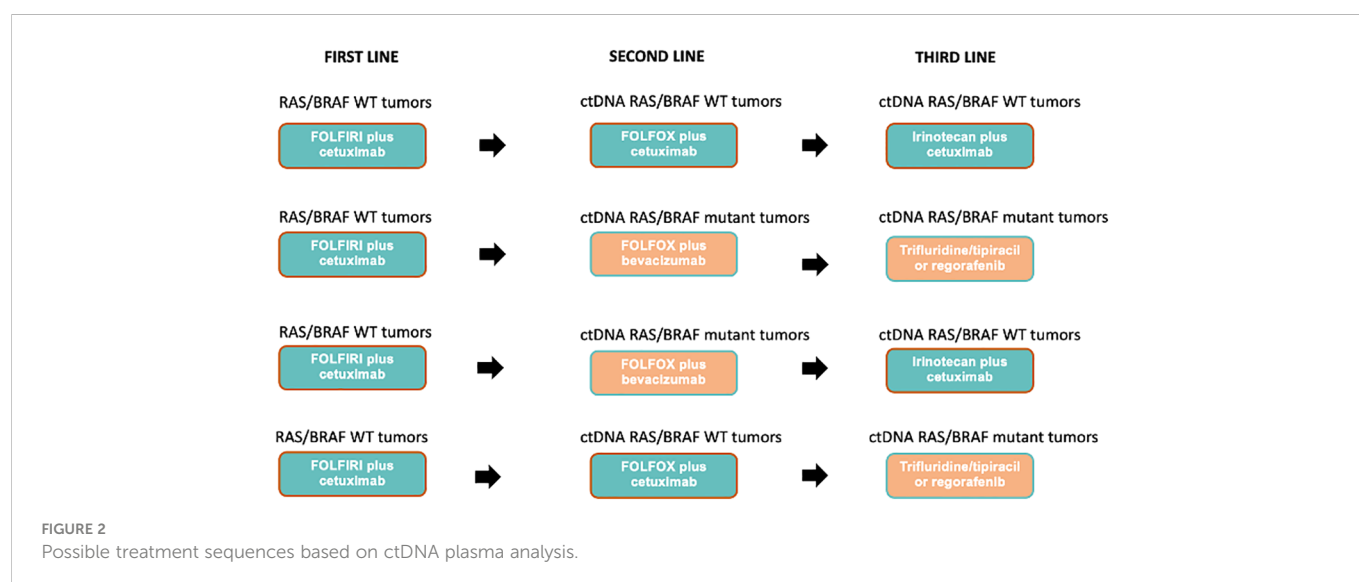


FIGURE 1
Capri 2 GOIM clinical trial consort diagram.



Secondary endpoints

- Progression Free Survival (PFS): measured from the start of therapy until the first observation of disease progression or death due to any cause.
- Overall Survival (OS): calculated from the start of the study treatment until death.
- Safety: Adverse events graded according to NCI CTCAE v 5.0.
- Molecular profiles of tumor tissue and liquid biopsy: molecular analysis of formalin fixed paraffin embedded (FFPE) tumor tissue, which is representative of the primary tumor or of a metastatic site at the diagnosis of mCRC, will be performed before the first line, whilst blood samples for liquid biopsy will be collected before each line of treatment.

Exploratory endpoints

An additional aliquot of the blood/plasma/fecal samples will be stored for further translational studies. The analysis on tissue and plasma samples will be performed by Foundation Roche laboratories in Germany using a comprehensive 324 genes Foundation One Liquid assay (Foundation/Roche).

The analysis of fecal samples for gut microbioma study will be performed by the gastroenterology unit, Casa Sollievo della Sofferenza, Via padre Pio 7d 70013, San Giovanni Rotondo (FG).

Statistical analysis

The primary analysis of response will be performed in a modified intention-to-treat population (mITT), defined as all enrolled patients

TABLE 1 Patients eligible for inclusion in this study have to meet all of the following criteria at the start of first line treatment.

1. Histologically proven diagnosis of colorectal adenocarcinoma
2. Diagnosis of metastatic disease
3. RAS and BRAF wild-type status of FFPE analysis of primary colorectal cancer and/or related metastasis
4. Measurable disease according to Response Evaluation Criteria in Solid Tumors (RECIST criteria, vers.1.1)
5. Male or female patients ≥ 18 years of age
6. ECOG Performance Status 0,1
7. Adequate bone marrow, liver and renal function assessed within 14 days before starting study treatment as defined by the following parameters: Bone marrow: Absolute Neutrophil Count (ANC) $\geq 1.5 \times 10^9/L$ Hemoglobin (Hgb) ≥ 9 g/dL Platelets $\geq 100 \times 10^9/L$ Liver function: Serum total bilirubin $\leq 1.5 \times$ upper limit of normal (ULN) Aspartate aminotransferase (AST) (serum glutamic oxaloacetic transaminase [SGOT]) and ALT (SGPT) $\leq 2.5 \times$ ULN, except in patients with tumor involvement of the liver who must have AST and ALT $\leq 5 \times$ ULN Renal function: Serum creatinine $\leq 1.5 \times$ ULN or 24-hour clearance ≥ 50 mL/min
8. If female and of childbearing potential, have a negative result on a pregnancy test performed a maximum of 7 days before initiation of study treatment
9. If female and of childbearing potential, or if male, agreement to use adequate contraception (e.g., abstinence, intrauterine device, oral contraceptive, or double-barrier method), during the study and until at least 3 months after last dose of study treatment administration, based on the judgment of the Investigator or a designated associate
10. Signed informed consent obtained before screening.

TABLE 2 Patients eligible for this study must not meet any of the following criteria at the start of first line treatment.

11. Any contraindication to the use of cetuximab, Irinotecan, 5-FU, oxaliplatin, folinic acid, bevacizumab, trifluridine-tipiracil, regorafenib
12. Active uncontrolled infections, active disseminated intravascular coagulation or history of interstitial lung disease
13. Past or current history of malignancies other than colorectal carcinoma, except for curatively treated basal and squamous cell carcinoma of the skin cancer or <i>in situ</i> carcinoma of the cervix
14. Pregnancy (exclusion to be ascertained by a beta hCG test)
15. Breastfeeding
16. Fertile women (<2 years after last menstruation) and men of childbearing potential not willing to use effective means of contraception•
17. Myocardial infarction, unstable angina pectoris, balloon angioplasty (PTCA) with or without stenting within the past 12 months before inclusion in the study, Grade III or IV heart failure (NYHA classification)
18. Cardiac arrhythmias requiring anti-arrhythmic therapy, with the exception of beta blockers or digoxin
19. Medical or psychological impairments associated with restricted ability to give consent or not allowing conduct of the study
20. Previous chemotherapy for the colorectal cancer with the exception of adjuvant treatment, completed at least 6 months before entering the study
21. Participation in a clinical study or experimental drug treatment within 30 days prior to study inclusion or during participation in the study
22. Known or clinically suspected brain metastases
23. History of acute or subacute intestinal occlusion or chronic inflammatory bowel disease or chronic diarrhoea
24. Severe, non-healing wounds, ulcers or bone fractures
25. Uncontrolled hypertension
26. Marked proteinuria (nephrotic syndrome)
27. Known DPD deficiency (specific screening not required)
28. Known history of alcohol or drug abuse
29. A significant concomitant disease which, in the investigating physician's opinion, rules out the patient's participation in the study
30. Absent or restricted legal capacity

with RAS/BRAF wild-type tumors who received at least one dose of study treatment. No reliable prospective data for defining the percentage of WT and mutated patients according to liquid biopsy after FOLFIRI plus Cetuximab as first line and any second line FOLFOX plus bevacizumab are available at the time of the trial design. However, we assume that acquired RAS or BRAF mutations detectable in the plasma occur as often as 40% at the beginning of the second line. Moreover, at the beginning of the third line we assume that 40% of patients who received a continuous EGFR inhibition in second line will acquire a mutation in RAS or BRAF genes; on the other hand, in about half of patients who received FOLFOX plus bevacizumab as second line, RAS or BRAF WT status will be restored. On the basis of this assumption, we calculated that 200 patients will receive a first line with FOLFIRI plus cetuximab. In addition, FOLFOX plus cetuximab as second line for patients WT on liquid biopsy would provide the trial with a power of 80% to detect a significantly higher response rate of 35% compared to historical control of 20%. $P_0 = 0.20$ $P_t = 0.35$; the study requires a sample size of 56, achieves 81% power to detect a difference ($P_1 - P_0$) of 0.15 using a one-sided binomial test. The target significance level is 0.05. The actual significance level achieved by this test is 0.0432. These results assume that the population proportion under the null hypothesis is 0.2000. If the number of responses is 12 or less, the

null hypothesis that $P \leq 0.20$ is accepted with a target error rate of 0.19 (1-power=1-0.81). The expected response rate increase in the third line will be as follow: $P_0 = 0.02$ $P_t = 0.15$. The study requires a sample size of 28; achieves 81% power to detect a difference ($P_1 - P_0$) of 0.13 using a one- sided binomial test. The target significance level is 0.025. The actual significance level achieved by this test is 0.018. These results assume that the population proportion under the null hypothesis is 0.02. If the number of responses is 8 or less, the hypothesis that $P \leq 0.02$ is accepted with a target error rate of 0.19. We will determine PFS and OS using the Kaplan-Meier method and the median survival estimate of the OS and PFS and the related confidence interval (CI) will be compared to the lower bound of the CI observed in the historical control. This comparison will be made only for descriptive purposes.

Discussion

The CAPRI 2 GOIM clinical trial is the first trial to explore the use of anti-EGFR treatment for three subsequent treatment lines in those patients defined as addicted to anti-EGFR blockade. Moreover, the study will also evaluate the activity and efficacy of cetuximab plus irinotecan rechallenge for those patients treated in second line with

chemotherapy plus anti-angiogenic drugs (FOLFOX plus bevacizumab), having a RAS or BRAF mutant disease at the time of progression after FOLFIRI plus cetuximab first line treatment. Although exclusion criteria of the CAPRI 2 GOIM clinical trial do not refer to patients with microsatellite instable (MSI) tumors, these should be treated with pembrolizumab in first line setting, as international guidelines recommend according to the results of KEYNOTE-177 trial (17). Therefore, these patients are not the right candidates for CAPRI 2 GOIM trial, for which the principal objective is to investigate how three lines of EGFR-based treatment could be effective in patients with RAS/BRAF WT tumors. Moreover, at the time of trial initiation in Italy pembrolizumab was not yet reimbursed for first line treatment in patients with MSI mCRC. For this reason, if a patient enrolled in the trial shows microsatellite instability at the molecular analysis, investigators should discuss with the patient the best treatment option, as in this case pembrolizumab, and therefore evaluate to exit from the trial.

Liquid biopsy assessment with a comprehensive 324 genes Foundation One Liquid NGS assay (Foundation/Roche) will provide not only an integrated analysis of RAS and BRAF genes mutational status along all the duration of the trial, but also an extensive study of potential biomarkers of response to cetuximab based treatment that, together with the analysis of the influence of gut microbiome on anti-tumor activity will allow to a better tailored anti-cancer treatment in mCRC.

The CAPRI 2 GOIM clinical trial will enroll 200 patients from 25 Italian centers. The first patient has been enrolled in July 2021. We estimate the end of enrollment in September 2023 and the end of the study on July 2026.

References

1. Siegel RL, Miller KD, Fuchs HE. Cancer statistics, 2022. *CA Cancer J Clin* (2022) 72(1):7–33. doi: 10.3322/caac.21708
2. Cervantes A, Adam R, Roselló S, Arnold D, Normanno N, Taïeb J, et al. ESMO Guidelines Committee. Metastatic colorectal cancer: ESMO Clinical Practice Guideline for diagnosis, treatment and follow-up. *Ann Oncol* (2023) 34(1):10–32 doi: . doi: 10.1016/j.annonc.2022.10.003
3. Ciardiello F, Tortora G. EGFR antagonists in cancer treatment. *N Engl J Med* (2008) 358(11):1160–74. doi: 10.1056/NEJMra0707704. [published correction appears in *N Engl J Med*. 2009 Apr 9;360(15):1579].
4. Martini G, Ciardiello D, Vitiello PP, Napolitano S, Cardone C, Cuomo A, et al. Resistance to anti-epidermal growth factor receptor in metastatic colorectal cancer: What does still need to be addressed? *Cancer Treat Rev* (2020) 86:102023. doi: 10.1016/j.ctrv.2020.102023
5. Simanshu DK, Nissley DV, McCormick F. RAS proteins and their regulators in human disease. *Cell* (2017) 170(1):17–33. doi: 10.1016/j.cell.2017.06.009
6. Sartore-Bianchi A, Amatu A, Porcu L, Ghezzi S, Lonardi S, Leone F, et al. HER2 positivity predicts unresponsiveness to EGFR-targeted treatment in metastatic colorectal cancer. *Oncologist* (2019) 24(10):1395–402. doi: 10.1634/theoncologist.2018-0785
7. Tol J, Nagtegaal ID, Punt CJ. BRAF mutation in metastatic colorectal cancer. *N Engl J Med* (2009) 361(1):98–9. doi: 10.1056/NEJMc0904160. [published correction appears in *N Engl J Med*. 2011 Sep 1;365(9):869].
8. Troiani T, Napolitano S, Vitagliano D, Morgillo F, Capasso A, Sforza V, et al. Primary and acquired resistance of colorectal cancer cells to anti-EGFR antibodies converge on MEK/ERK pathway activation and can be overcome by combined MEK/EGFR inhibition. *Clin Cancer Res* (2014) 14(20):3775–86. doi: 10.1158/1078-0432.CCR-13-2181
9. Martini G, Dienstmann R, Ros J, Baraibar I, Cuadra-Urteaga JL, Salva F, et al. Molecular subtypes and the evolution of treatment management in metastatic colorectal cancer. *Ther Adv Med Oncol* (2020) 12:1758835920936089. doi: 10.1177/1758835920936089
10. Normanno N, Esposito Abate R, Lambiasi M, Forgione L, Cardone C, Iannaccone A, et al. RAS testing of liquid biopsy correlates with the outcome of metastatic colorectal cancer patients treated with first-line FOLFIRI plus cetuximab in the CAPRI-GOIM trial. *Ann Oncol* (2018) 29(1):112–8. doi: 10.1093/annonc/mdx417
11. Khan KH, Cunningham D, Werner B, Vlachogiannis G, Spiteri I, Heide T, et al. Longitudinal liquid biopsy and mathematical modeling of clonal evolution forecast time to treatment failure in the PROSPECT-c phase II colorectal cancer clinical trial. *Cancer Discov* (2018) 8(10):1270–85. doi: 10.1158/2159-8290.CD-17-0891
12. Morelli MP, Overman MJ, Dasari A, Kazmi SMA, Mazard T, Vilar E, et al. Characterizing the patterns of clonal selection in circulating tumor DNA from patients with colorectal cancer refractory to anti-EGFR treatment. *Ann Oncol* (2015) 26:731–6. doi: 10.1093/annonc/mdv005
13. Parseghian CM, Loree JM, Morris VK, Liu X, Clifton KK, Napolitano S, et al. Anti-EGFR-resistant clones decay exponentially after progression: Implications for anti-EGFR re-challenge. *Ann Oncol* (2019) 30(2):243–9. doi: 10.1093/annonc/mdy509
14. Martinelli E, Martini G, Familietti V, Troiani T, Napolitano S, Pietrantonio F, et al. Cetuximab rechallenge plus avelumab in pretreated patients with RAS wild-type metastatic colorectal cancer: The phase 2 single-arm clinical CAVE trial. *JAMA Oncol* (2021) 7(10):1529–35. doi: 10.1001/jamaoncol.2021.2915
15. Ciardiello F, Normanno N, Maiello E, Martinelli E, Troiani T, Piconti S, et al. Clinical activity of FOLFIRI plus cetuximab according to extended gene mutation status by next-generation sequencing: findings from the CAPRI-GOIM trial. *Ann Oncol* (2014) 25(9):1756–61. doi: 10.1093/annonc/mdu230
16. Ciardiello F, Normanno N, Martinelli E, Troiani T, Piconti S, Cardone C, et al. CAPRI-GOIM investigators. Cetuximab continuation after first progression in metastatic colorectal cancer (CAPRI-GOIM): A randomized phase II trial of FOLFOX plus cetuximab versus FOLFOX. *Ann Oncol* (2016) 27(6):1055–61. doi: 10.1093/annonc/mdw136
17. André T, Shiu KK, Kim TW, Jensen BV, Jensen LH, Punt C, et al. Pembrolizumab in microsatellite-instability-high advanced colorectal cancer. *N Engl J Med* (2020) 383(23):2207–18. doi: 10.1056/NEJMoa2017699

Author contributions

GM, DC, EvM, FC: clinical trial and protocol development. GM, SN, DC, EM, and TT have written the manuscript for the study protocol with the support of MM, NN and AA. All authors contributed to the article and approved the submitted version.

Funding

All the costs for the study implementation will be in charge of the sponsor Gruppo Oncologico dell'Italia Meridionale (GOIM), that will receive from Merck Serono S.p.A. a partial economical support and the study Investigational Medicinal Product (IMP) provision.

Conflict of interest

The authors declare that the research was conducted in the absence of any commercial or financial relationships that could be construed as a potential conflict of interest.

Publisher's note

All claims expressed in this article are solely those of the authors and do not necessarily represent those of their affiliated organizations, or those of the publisher, the editors and the reviewers. Any product that may be evaluated in this article, or claim that may be made by its manufacturer, is not guaranteed or endorsed by the publisher.



OPEN ACCESS

EDITED BY

Alessandro Passardi,
Scientific Institute of Romagna for the
Study and Treatment of Tumors (IRCCS),
Italy

REVIEWED BY

Alfonso De Stefano,
G. Pascale National Cancer Institute
Foundation (IRCCS), Italy
Kathrin Heinrich,
Ludwig Maximilian University of Munich,
Germany

*CORRESPONDENCE

Lisa Salvatore
✉ lisa.salvatore@policlinicogemelli.it

[†]These authors share first authorship

SPECIALTY SECTION

This article was submitted to
Gastrointestinal Cancers:
Colorectal Cancer,
a section of the journal
Frontiers in Oncology

RECEIVED 15 December 2022

ACCEPTED 03 February 2023

PUBLISHED 21 February 2023

CITATION

Salvatore L, Bensi M, Vivolo R, Zurlo IV,
Dell'Aquila E, Grande R, Anghelone A,
Emiliani A, Citarella F, Calegari MA,
Ribelli M, Basso M, Pozzo C and Tortora G
(2023) Efficacy of third-line anti-EGFR-
based treatment versus regorafenib or
trifluridine/tipiracil according to primary
tumor site in RAS/BRAF wild-type
metastatic colorectal cancer patients.
Front. Oncol. 13:1125013.
doi: 10.3389/fonc.2023.1125013

COPYRIGHT

© 2023 Salvatore, Bensi, Vivolo, Zurlo,
Dell'Aquila, Grande, Anghelone, Emiliani,
Citarella, Calegari, Ribelli, Basso, Pozzo and
Tortora. This is an open-access article
distributed under the terms of the [Creative Commons Attribution License \(CC BY\)](https://creativecommons.org/licenses/by/4.0/). The
use, distribution or reproduction in other
forums is permitted, provided the original
author(s) and the copyright owner(s) are
credited and that the original publication in
this journal is cited, in accordance with
accepted academic practice. No use,
distribution or reproduction is permitted
which does not comply with these terms.

Efficacy of third-line anti-EGFR-based treatment versus regorafenib or trifluridine/tipiracil according to primary tumor site in RAS/BRAF wild-type metastatic colorectal cancer patients

Lisa Salvatore^{1,2*}, Maria Bensi^{1,2†}, Raffaella Vivolo^{1,2},
Ina Valeria Zurlo^{1,3}, Emanuela Dell'Aquila^{4,5}, Roberta Grande^{6,7},
Annunziato Anghelone^{1,2}, Alessandra Emiliani³,
Fabrizio Citarella⁴, Maria Alessandra Calegari¹, Marta Ribelli³,
Michele Basso¹, Carmelo Pozzo¹ and Giampaolo Tortora^{1,2}

¹Oncologia Medica, Comprehensive Cancer Center, Fondazione Policlinico Universitario Agostino Gemelli, IRCCS, Rome, Italy, ²Oncologia Medica, Università Cattolica del Sacro Cuore, Rome, Italy, ³Oncologia Medica, Ospedale Fatebenefratelli Isola Tiberina - Gemelli Isola, Rome, Italy, ⁴Department of Medical Oncology, Campus Bio-Medico University of Rome, Rome, Italy, ⁵Medical Oncology 1, IRCCS Regina Elena National Cancer Institute, Rome, Italy, ⁶UOSD Coordinamento Screening Oncologici, ASL Frosinone, Frosinone, Italy, ⁷DH Oncologico, Ospedale F. Spaziani - ASL, Frosinone, Italy

Background: Right- (R) and left-sided (L) metastatic colorectal cancer (mCRC) exhibit different clinical and molecular features. Several retrospective analyses showed that survival benefit of anti-EGFR-based therapy is limited to RAS/BRAF wt L-sided mCRC patients. Few data are available about third-line anti-EGFR efficacy according to primary tumor site.

Methods: RAS/BRAF wt patients mCRC treated with third-line anti-EGFR-based therapy versus regorafenib or trifluridine/tipiracil (R/T) were retrospectively collected. The objective of the analysis was to compare treatment efficacy according to tumor site. The primary endpoint was progression-free survival (PFS); secondary endpoints were overall survival (OS), response rate (RR) and toxicity.

Results: A total of 76 RAS/BRAF wt mCRC patients, treated with third-line anti-EGFR-based therapy or R/T, were enrolled. Of those, 19 (25%) patients had a R-sided tumor (9 patients received anti-EGFR treatment and 10 patients R/T) and 57 (75%) patients had a L-sided tumor (30 patients received anti-EGFR treatment and 27 patients R/T). A significant PFS [7.2 vs 3.6 months, HR 0.43 (95% CI 0.2-0.76), $p=0.004$] and OS benefit [14.9 vs 10.9 months, HR 0.52 (95% CI 0.28-0.98), $p=0.045$] in favor of anti-EGFR therapy vs R/T was observed in the L-sided tumor group. No difference in PFS and OS was observed in the R-sided tumor group. A significant interaction according to primary tumor site and third-line regimen was observed for PFS ($p=0.05$). RR was significantly higher in L-sided patients treated with anti-EGFR vs R/T (43% vs. 0%; $p<0.0001$), no difference was observed in R-sided

patients. At the multivariate analysis, third-line regimen was independently associated with PFS in L-sided patients.

Conclusions: Our results demonstrated a different benefit from third-line anti-EGFR-based therapy according to primary tumor site, confirming the role of L-sided tumor in predicting benefit from third-line anti-EGFR vs R/T. At the same time, no difference was observed in R-sided tumor.

KEYWORDS

colorectal cancer, primary tumor site, third-line therapy, RAS/BRAF wild-type, anti-egfr ab, Regorafenib, trifluridine/tipiracil

1 Introduction

The primary tumor site of metastatic colorectal cancer (mCRC) is associated with specific clinical-pathological and molecular features (1). From an anatomical point of view, differential characteristics between left- (L) and right- (R) sided tumors are based on embryological origin, physiological function, food transit, and gut microbiome (2). From a genetic and molecular point of view, R-sided colon cancer is associated with RAS and BRAF mutations and DNA mismatch-repair enzyme deficiency, while L-sided colon cancer is associated with EGFR, HER2-neu, APC, and TP53 mutations (3). Several studies demonstrated that the primary tumor site has both a prognostic and predictive role. Regarding the prognostic role, a metaanalysis of 66 studies, including 1437846 mCRC patients, showed that L-sided tumor site was associated with longer OS in comparison to R-sided tumor site [HR 0.82 (95% CI 0.79-0.84), $p < 0.001$] (4). Regarding the predictive role, a metaanalysis of 13 randomized controlled trials, investigated the correlation between efficacy of first-line therapy (bevacizumab vs anti-EGFR-based treatment) in mCRC patients and primary tumor location. In patients with RAS/BRAF wild-type (wt) L-sided mCRC, an anti-EGFR based first-line therapy showed an improved PFS and OS in comparison to bevacizumab-based treatment [PFS: HR 0.86 (95% CI 0.73-1.02); OS: HR 0.71 (95%CI 0.58-0.85)]. By contrast, in R-sided mCRC patients, the benefit from bevacizumab plus chemotherapy was higher as compared to anti-EGFR-based treatment [PFS: HR 0.65 (95%CI 0.50-0.86); OS: HR 0.77 (95%CI 0.57- 1.03)] (5). Accordingly, international and national guidelines (6, 7) recommend anti-EGFR plus chemotherapy for the first-line treatment of all wt L-sided mCRC patients as preferred option.

However, besides first-line treatment, few clinical data is available on the prognostic and/or predictive role of the primary tumor site for subsequent lines of therapy. With respect to anti-EGFR therapy efficacy for pretreated mCRC patients, Brule í et al., reanalyzed the results of NCIC CO.17 trial (cetuximab vs best supportive care) according to primary tumor site. In this study, primary tumor location was not prognostic, but strongly predictive: KRAS wt L-sided mCRC patients had significantly longer PFS when treated with cetuximab compared to best supportive care [5.4 vs 1.8 months, HR 0.28 (95% CI 0.18-0.45), $p < 0.0001$], while no difference was observed in R-sided mCRC patients [1.9 vs 1.9 months, HR 0.73 (95%CI 0.42-

1.27), $p = 0.26$] (interaction $p = 0.002$) (8). Boeckx et al., in a retrospective analysis of study 20050181 (FOLFIRI-Panitumumab vs FOLFIRI) and study 20020408 (panitumumab vs best supportive care), investigated the efficacy of anti-EGFR-based therapy, after first-line, according to primary tumor location. RAS wt L-sided tumor had better outcomes with panitumumab than with the comparator treatment [study 20050181 PFS: 8.0 vs 5.8 months, HR 0.88 (95% CI 0.69-1.12), $p = 0.31$, study 20020408 PFS: 5.5 vs 1.6 months, HR 0.50 (95% CI 0.22-1.15), $p < 0.0001$] (9).

To date, regorafenib (R) and trifluridine/tipiracil (T) represent two standard treatment options for chemorefractory mCRC patients. In the CORRECT (10) and RECURSE (11) trials, R and T showed a significant OS improvement in comparison to best supportive care [HR 0.77 (IC 95% 0.64-0.94) $p = 0.0052$] [HR 0.66 (IC 95% 0.56-0.78), $p < 0.001$], respectively. Despite the statistically significant OS improvements, the absolute benefit appeared limited, and it was independent from both RAS status and primary tumor site.

Based on this limited evidence, we retrospectively compared the efficacy of third-line therapy with anti-EGFR-based treatment versus R/T in RAS/BRAF wt mCRC patients, according to the primary tumor site.

2 Materials and methods

2.1 Study population

Patients with RAS and BRAF wt mCRC, treated with R or T versus anti-EGFR-based treatment in third-line, were retrospectively included in the study. Patients were enrolled by four Italian Medical Oncology Units (Comprehensive Cancer Center, Fondazione Policlinico Universitario Agostino Gemelli-IRCCS, Università Cattolica del Sacro Cuore, Rome; Ospedale Fatebenefratelli Isola Tiberina - Gemelli Isola, Rome; Department of Medical Oncology, Campus Bio-Medico University, Rome; Ospedale F. Spaziani - ASL Frosinone)

Patients had to have received two prior regimens of standard chemotherapy (oxaliplatin, irinotecan, fluoropyrimidine) for metastatic disease. Previous treatments could include bevacizumab. Patients who received cetuximab and/or panitumumab in first- or second-line were excluded from the anti-EGFR group; on the

contrary, they could be enrolled in the R/T group. Prior therapy with R or T was not allowed.

The R-sided tumor was defined as cancer from the cecum to the transverse colon, L-sided tumor was defined as cancer from the splenic flexure to the rectum. For each patient we collected the following available variables: baseline ECOG performance status (PS), gender, age, synchronous vs metachronous disease, previous anticancer treatments, and number of metastatic sites (single vs multiple).

2.2 Study outcomes

This is a retrospective, multicenter, observational study aiming to investigate the predictive role of primary tumor site in RAS/BRAF wt mCRC patients receiving anti-EGFR or R/T as third-line treatment. The primary endpoint was progression-free survival (PFS); the secondary endpoints were overall survival (OS), response rate (RR), and toxicity. PFS was defined as the time from the start of third-line treatment to disease progression or death from any cause, whichever occurred first. OS was defined as the time from treatment start to the date of death for any reasons. RR was the percentage of patients achieving an objective response (complete response or partial response) according to RECIST criteria (version 1.1). Disease evaluation was performed with a computed tomography (CT) scan of chest and abdomen every 8–12 weeks, according to clinical practice. Toxicity rate was defined as the percentage of patients experiencing a specific adverse event (AE) during the treatment, according to NCTCAE version 5.0.

2.3 Statistical analysis

Chi-square test was performed to compare patient characteristics and RR between R- and L- tumor groups, and incidence of AEs according to treatment group. PFS and OS analyses were carried out using the Kaplan-Meier method. Cox proportional regression was used for univariate and multivariate analyses of PFS and OS. Statistical significance was established at $p = 0.05$. Hazard ratios (HR) with 95% confidence interval (CI) were estimated using a logistic regression model. All analyses were conducted using MedCalc statistical software version 18.11.3 (MedCalc Software, Ostend, Belgium; <http://www.medcalc.org;2019>).

3 Results

3.1 Patients characteristics

A total of 76 RAS/BRAF wt mCRC patients, receiving, as third-line treatment, R or T or anti-EGFR based-therapy, were enrolled in the study. Fifty-seven (75%) patients had a L-sided tumor, 19 (25%) patients had a R-sided tumor. Thirty-nine (51%) patients received anti-EGFR-based therapy (16 patients panitumumab and 23 irinotecan plus cetuximab), 37 (49%) patients received R or T. Among patients with L-sided tumor, 30 (53%) were treated with

anti-EGFR-based therapy and 27 (47%) with R/T. Among patients with R-sided tumor, 9 (47%) were treated with anti-EGFR-based therapy and 10 (53%) with R/T.

Baseline clinical characteristics were well-balanced between the two groups. The median age was 64 years (range 38–81) in the L-sided tumor group, and 63 years (range 38–78) in the R-sided tumor group. Males were 51% and 53% in the L- and R-sided tumor group, respectively; ECOG PS was 0 in 28% and 26%; metastases were synchronous in 72% and 79%; sites of metastases were multiple in 72 and 74% of L- and R-sided tumor group, respectively. Clinical baseline patients characteristics and treatment information are summarized in Table 1.

3.2 Efficacy and activity of third-line treatment according to primary tumor site

In the L-sided tumor group, median PFS and OS were significantly longer in patients treated with anti-EGFR in comparison to patients treated with R/T [median PFS: 7.2 (95% CI 6.5–7.8) vs 3.6 months (95% CI 3.2–3.9), HR 0.43 (95% CI 0.2–0.76), $p=0.004$; median OS: 14.9 (95% CI 7.2–22.7) vs 10.9 months (95% CI 6.0–15.9), HR 0.52 (95% CI 0.28–0.98), $p=0.045$]. By contrast, in the R-sided tumor group, no significant difference in both PFS and OS according to treatment was observed [median PFS: 3.5 (95% CI 0–7.0) vs 3.3 months (95% CI 1.3–5.3), HR 1.40 (95% CI 0.52–3.79), $p=0.50$; median OS: 9.3 (95% CI 4.2–14.4) vs 4.8 months (95% CI 0–16.0), HR 0.82 (95% CI 0.29–2.30), $p=0.70$] (Figures 1, 2). A significant interaction according to primary tumor site and third-line regimen was observed for PFS ($p=0.05$), but not for OS ($p=0.38$) (Figure 1, 2).

In the L-sided tumor group, RR was 43% in patients treated with anti-EGFR and 0% in patients treated with R/T ($p < 0.0001$). No difference in RR was observed in patients with R-sided colon cancer according to treatment (RR 11% in patients treated with anti-EGFR vs RR 10% in patients treated with R/T, $p=0.99$) (Figure 3).

At the multivariate analysis, in the L-sided tumor group, third line regimen (anti-EGFR vs R/T) was independently associated with PFS [HR 0.45 (95% CI 0.25–0.80), $p=0.006$], but not with OS. By contrast, in the R-sided tumor group, at the multivariate analysis no association between third-line regimen and survival outcomes was observed. Univariate and multivariate analyses for PFS and OS are showed in Table 2.

3.3 Toxicity

The incidence of any grade and grade 3/4 AEs was significantly higher in patients treated with R/T in comparison to patients treated with anti-EGFR (any grade: 88% vs 64%, $p=0.018$; grade 3/4: 47% vs 20%, $p=0.017$).

The most frequent AE in patients treated with anti-EGFR was folliculitis (any grade 49%, grade 3/4 13%), while the most frequent AEs in patients treated with R/T were hand-foot syndrome (any grade 35%, grade 3/4 6%), hypertension (any grade 24%, grade 3/4 6%), neutropenia (any grade 21%, grade 3/4 15%) and anemia (any grade 12%, grade 3/4 6%). The incidence of AEs was reported in Table 3.

TABLE 1 Patients characteristics.

Characteristics, N (%)	Right-sided (N = 19)	Left-sided (N = 57)	p-value
Age (years), median (range)	63 (38-78)	64 (38-81)	
≤65 years	13 (68.4)	30 (52.6)	0.11
>65 years	6 (31.6)	27 (47.4)	
Sex			
Male	10 (52.6)	29 (50.9)	0.89
Female	9 (47.4)	28 (49.1)	
ECOG PS at the beginning of 3 rd line			
0	5 (26.3)	16 (28)	0.88
1-2	12 (63.2)	35 (61.4)	
NA	2 (10.5)	6 (10.6)	
Time between diagnosis of PT and metastases			
Synchronous (≤ 6 months)	15 (78.9)	41 (72)	0.55
Metachronous (> 6 months)	4 (21.1)	16 (28)	
3 rd line therapy			
Anti-EGFR	9 (47.4)	30 (52.6)	0.69
R/T	10 (52.6)	27 (47.4)	
N metastatic sites at the beginning of 3 rd line			
1	5 (26.3)	16 (28.1)	0.88
≥2	14 (73.7)	41 (71.9)	
Prior systemic anticancer agents			
fluoropyrimidine	19 (100)	57 (100)	1
oxaliplatin	15 (78.9)	53 (92.9)	0.08
irinotecan	18 (94.7)	56 (98.2)	0.41
bevacizumab	14 (73.7)	40 (70.2)	0.77
Anti-EGFR	10 (52.6)	26 (45.6)	0.59

N, number; ECOG PS, Eastern Cooperative Group Performance Status; PT, primary tumor; NA, not applicable; R/T, Regorafenib or Trifluridine/Tipiracil.

4 Discussion

To the best of our knowledge, this study was the first investigating the efficacy of a third-line therapy with anti-EGFR-based treatment versus R/T in RAS/BRAF wt mCRC patients, according to the primary tumor site. Our results confirm the benefit of third-line anti-EGFR treatment in L-sided tumors, supporting the predictive role of primary tumor location also in pretreated mCRC patients.

The benefit of first-line chemotherapy plus cetuximab or panitumumab in L-sided mCRC has been clearly demonstrated (5), while clinical evidence on the role of primary tumor site in predicting benefit from EGFR inhibitors in pretreated mCRC patients is still limited. Chen et al., in a cohort study of 969 KRAS wt mCRC patients treated with third-line cetuximab, demonstrated a significant longer time to treatment discontinuation ($p=0.0005$) and OS ($p<0.0001$) in L-sided vs R-sided tumor patients, confirming the prognostic role of primary tumor site (12). Moretto et al., analyzing 75 RAS/BRAF wt mCRC patients treated with cetuximab +/- irinotecan or

panitumumab as first-line or subsequent lines, demonstrated a lack of activity of anti-EGFR in R-sided vs L-sided tumors. Specifically, RR was 0% and 41% in R-sided and L-sided tumor patients ($p=0.0032$), respectively (13). The main limitations of these studies are the retrospective nature and the lack of a control arm.

Concerning treatment with R/T, the impact of the primary tumor site was not well defined. Subgroup analyses of both CORRECT and RECURSE trials demonstrated a survival benefit regardless of primary tumor site (10, 11). In a multicenter retrospective study of 505 mCRC patients treated with R or T, R-sided patients had a shorter OS in comparison to L-sided patients ($p=0.041$), but at the multivariate analysis for OS, primary tumor location was not an independent prognostic factor ($p=0.64$) (14).

The strength of our study was stringent inclusion criteria for patients: we selected only RAS/BRAF wt mCRC patients, also in the R/T group, in order to evaluate a homogeneous population; previous treatment with cetuximab or panitumumab was not allowed in the anti-EGFR group, thus avoiding potentially resistant patients.

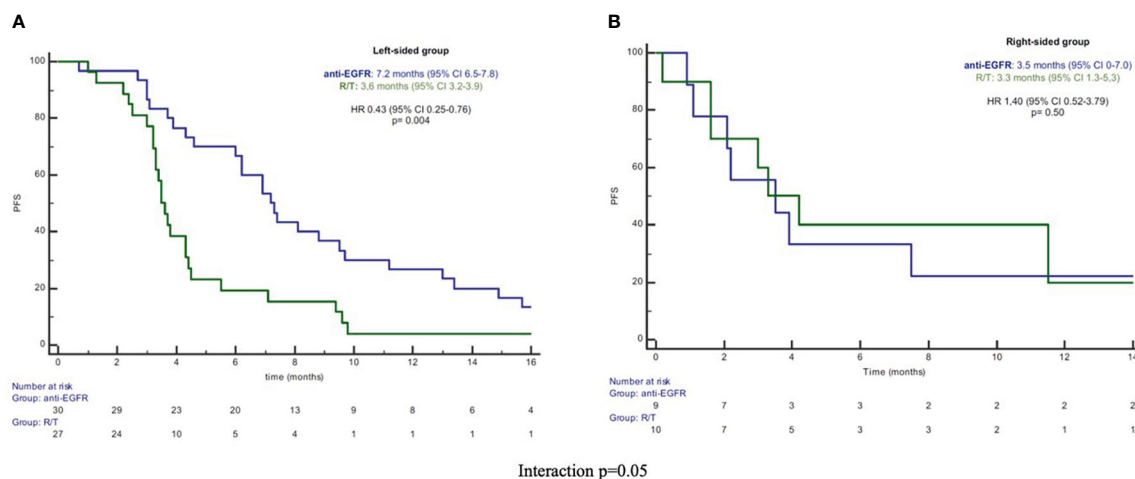


FIGURE 1

(A) Kaplan-Meier PFS curves in left-sided group. (B) Kaplan-Meier PFS curves in right-sided group. PFS, progression-free survival; R/T, Regorafenib or Trifluridine/Tipiracil; HR, hazard ratio; CI, confidence interval.

Furthermore, our retrospective study, compared third-line anti-EGFR therapy with R/T, a standard treatment option in pretreated mCRC patients.

Our study population was characterized by an imbalance in the primary tumor site (75% L-sided side vs 25% R-sided), that could be explained by the different molecular profiling between L- and R-sided tumors. Our analysis showed a significant longer PFS and OS for patients treated with anti-EGFR vs R/T in the L-sided tumor group [median PFS 7.2 vs 3.6 months, HR 0.43 (95% CI 0.2-0.76), $p=0.004$; median OS 14.9 vs 10.9 months, HR 0.52 (95% CI 0.28-0.98), $p=0.045$]. By contrast, no significant difference in survival outcomes was observed between anti-EGFR vs R/T in the R-sided tumor group [median PFS 3.5 vs 3.3 months, HR 1.40 (95% CI 0.52-3.79), $p=0.50$; median OS 9.3 vs 4.8 months, HR 0.82 (95% CI 0.29-2.30), $p=0.70$]. A significant interaction according to primary tumor site and third-line treatment was observed for PFS ($p=0.05$). In the multivariate analysis, the third-line regimen was independently associated with PFS [HR

0.45 (95% CI 0.25–0.80), $p=0.006$] in the L-sided tumor group. Also, regarding the activity, we observed a different RR according to third-line regimen and primary tumor site: in particular, in the L-sided tumor group, RR was 43% in patients treated with anti-EGFR and 0% in patients treated with R/T ($p<0.0001$), while no difference was observed in the R-sided tumor group. Our results confirmed the predictive role of the primary tumor site for third-line anti-EGFR-based treatment in RAS/BRAF wt patients.

The different distribution of consensus molecular subtypes (CMS) between L- and R-sided tumors may explain the different sensitivity to anti-EGFR according to primary tumor site. L-sided tumors are more representative of CMS2, enriched for epithelial signature, and CMS4, associated to epithelial-mesenchymal transition (3, 15, 16). CMS2 is an over-activated epithelial growth factor pathway with higher expression of EGFR and the EGFR-ligands amphiregulin and epiregulin, that are correlated to an increased response to EGFR inhibitor therapy in RAS/BRAF wt CRC (17). Stintzing et al.,

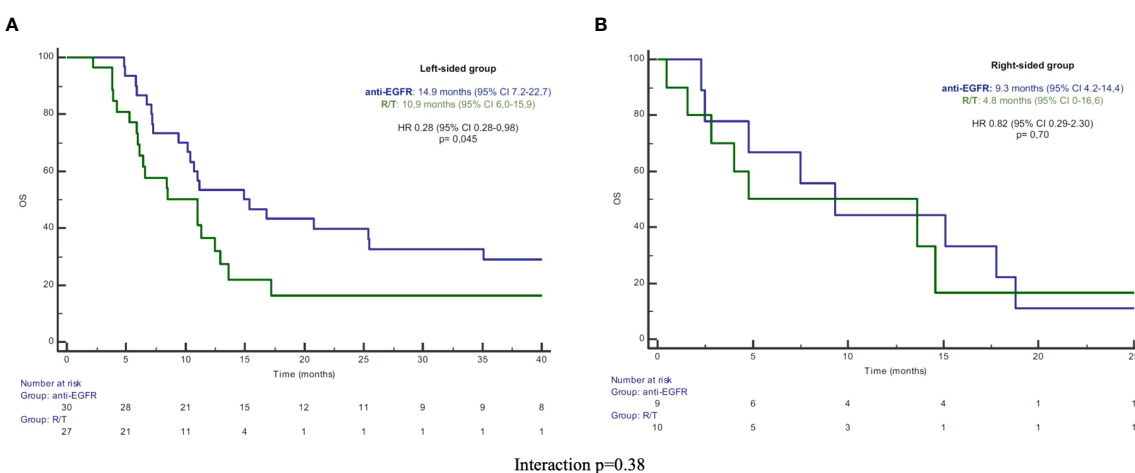


FIGURE 2

(A) Kaplan-Meier OS curves in left-sided group. (B) Kaplan-Meier OS curves in right-sided group. PFS, progression-free survival; R/T, Regorafenib or Trifluridine/Tipiracil; HR, hazard ratio; CI, confidence interval.

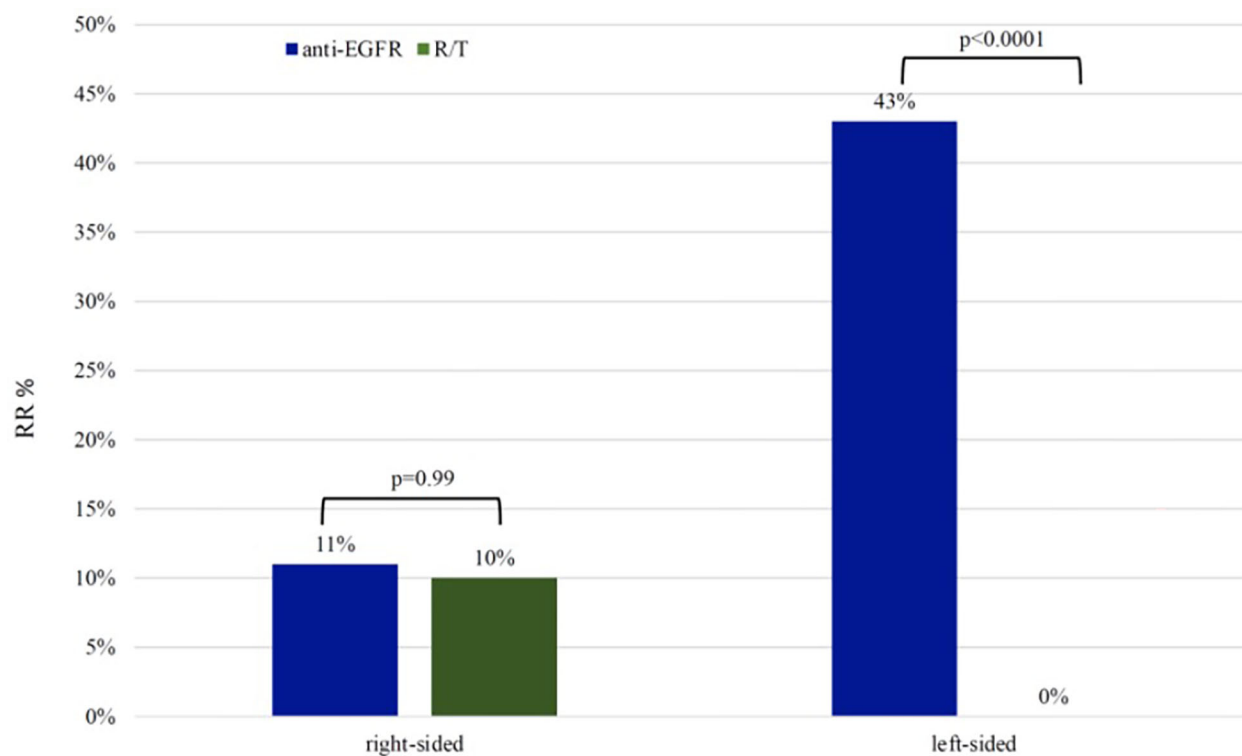


FIGURE 3

Response rate in left-sided group and right-sided group RR, response rate; R/T, Regorafenib or Trifluridine/tipiracil.

analyzing gene signature of 514 samples of patients enrolled in the FIRE-3 study, demonstrated that patients with CMS4 tumors had a longer OS when treated with cetuximab vs bevacizumab (18). In another molecular analysis of RAS/BRAF wt patients from the COIN and PICCOLO study, patients with CMS4 tumors showed a longer OS and PFS when treated with anti-EGFR-based treatment vs chemotherapy alone (19).

The different benefit from anti-EGFR according to primary tumor site in RAS/BRAF wt mCRC patients may be also explained by a heterogeneity of primary resistance profile. Not only the well-known mutations in RAS and BRAF genes, but also the less common alterations such as HER2 and MET amplification, deregulation of the PI3K/PEN/AKT axis, NTRK/ROS/ALK/RET rearrangements, may represent negative predictive factors for response to anti-EGFR

TABLE 2 Univariate and multivariate analyses for PFS and OS.

Variables	PFS				OS			
	Univariate Analysis HR (95% CI); p-value		Multivariate Analysis HR (95% CI); p-value		Univariate Analysis HR (95% CI); p-value		Multivariate Analysis HR (95% CI); p-value	
	Right-sided	Left-sided	Right-sided	Left-sided	Right-sided	Left-sided	Right-sided	Left-sided
Median age ≤65 vs >65 years	0.92 (0.32–2.60); p = 0.87	0.98 (0.58–1.68); p = 0.95	–	–	1.28 (0.44–3.67); p=0.65	1.26 (0.70–2.26); p = 0.44	–	–
N metastatic sites at the beginning of 3 rd line 1 vs ≥2	0.07 (0.01–0.55); p = 0.01	0.46 (0.25–0.86); p = 0.01	0.07 (0.01–0.55); p = 0.01	0.48 (0.26–0.90); p = 0.02	0.10 (0.01–0.80); p=0.03	0.25 (0.11–0.56); p = 0.001	–	0.25 (0.11–0.56); p = 0.001
Time between diagnosis of PT and metastases Synchronous vs metachronous	8.36 (1.07–65.36); p = 0.043	1.02 (0.56–1.87); p = 0.95	–	–	10.93 (1.37–87.31); p = 0.02	1.20 (0.63–2.29); p = 0.58	10.93 (1.37–87.31); p = 0.02	–
3 rd line therapy Anti-EGFR vs R/T	1.40 (0.52–3.79); p = 0.50	0.43 (0.25–0.76); p = 0.004	–	0.45 (0.25–0.80); p = 0.006	0.82 (0.29–2.30); p = 0.70	0.52 (0.28–0.98); p = 0.045	–	–

PFS, progression-free survival; OS, overall survival; N, number; HR, hazard ratio; CI, confidence interval; PT primary tumor R/T, Regorafenib or Trifluridine/Tipiracil.

TABLE 3 Adverse Events.

Adverse events	Anti-EGFR (N=39)	R/T (N=34)	p- value	Anti-EGFR (N=39)	R/T (N=34)	p- value
	Any grade N (%)	Any Grade N (%)		Grade 3-4 N (%)	Grade 3-4 N (%)	
Any adverse events	25 (64)	30 (88)	0.018	8 (20%)	16 (47)	0.017
Fatigue	10 (26)	16 (47)	0.06	1 (3%)	3 (9)	0.24
Nausea	1 (3)	3 (9)	0.24	0 (0)	0 (0)	1
Diarrhea	5 (13)	5 (15)	0.89	0 (0)	1 (3)	0.86
Stomatitis	5 (13)	3 (9)	0.59	0 (0)	0 (0)	1
Dermatitis acneiform	19 (49)	0 (0)	<0.00001	5 (13)	0 (0)	0.02
Hand-foot syndrome	2 (5)	12 (35)	0.001	0 (0)	6 (18)	0.02
Hypertension	0 (0)	8 (24)	0.005	0 (0)	2 (6)	0.03
Neutropenia	4 (10)	7 (21)	0.22	2 (5)	5 (15)	0.16
Anemia	0 (0)	4 (12)	0.12	0 (0)	3 (9)	0.24
Trombocytopenia	2 (5)	0 (0)	0.46	0 (0)	0 (0)	1
Transaminases increase	0 (0)	2 (6)	0.461	0 (0)	0 (0)	1

N, number; R/T, Regorafenib or Trifluridine/tipiracil.

(20). Morano et al., analyzing RAS/BRAF wt mCRC patients receiving panitumumab-based maintenance therapy in the Valentino trial, demonstrated that the combined assessment of sidedness and molecular alterations of primary resistance to anti-EGFR according to PRESSING panel (21) identified a subpopulation with inferior benefit from anti-EGFR-based therapy (22).

Concerning the safety profile, our study, showed a significant higher incidence of AEs in the group of patients treated with R/T in comparison to anti-EGFR-based therapy (p 0.018), and a drug-specific toxicities (hand-foot syndrome and hypertension for R, neutropenia and anemia for T, folliculitis for anti-EGFR), as previously reported.

Our study presented several limitations, such as the retrospective design, the lack of randomization, the lack of a negative hyperselection, such as with the PRESSING panel, and the small sample size, especially for the R-sided group. We did not explore the optimal therapeutic sequence, as investigated by the REVERCE trial, which reported a longer OS for patients receiving regorafenib followed by cetuximab vs the reverse sequence [17.4 vs 11.6 months, HR 0.61 (95% CI 0.39–0.96), p 0.0293] (23). Furthermore, our study excluded patients receiving anti-EGFR rechallenge according to CRICKET (24) and CHRONOS trials (25). The ongoing randomized PARERE study (26), investigating rechallenge with panitumumab followed by regorafenib versus the reverse sequence in chemorefractory RAS/BRAF wt patients selected by liquid biopsy, could further clarify the role of anti-EGFR according to primary tumor site.

5 Conclusion

In conclusion, our results demonstrated a different benefit from third-line anti-EGFR therapy according to primary tumor site,

confirming the role of L-sided tumor in predicting benefit from third-line anti-EGFR vs R/T. At the same time, no difference was observed in R-sided tumors. Despite several limitations, our study confirmed previous evidence and, waiting for results from the PARERE trial, we can conclude that the preferred third-line option for RAS-BRAF wt L-sided mCRC patients, not yet treated with panitumumab or cetuximab, is still anti-EGFR. By contrast, in R-sided mCRC patients, the choice between anti-EGFR and R/T should be based on previous treatment toxicity and patient clinical conditions.

Data availability statement

The raw data supporting the conclusions of this article will be made available by the authors, without undue reservation.

Author contributions

LS and MBe contributed to conception, design of the study, organized the database, performed the statistical analysis and wrote the manuscript. RV, IZ, ED, RG, AA, AE, FC, MC, MR, MBa, CP involved in the data collection. GT contributed to manuscript revision, read, and approved the submitted version. All authors contributed to the article and approved the submitted version.

Acknowledgments

We acknowledge the support of: - Ministero della Salute – Ricerca Corrente 2022 to GT - My first AIRC grant number 27367 to LS.

Conflict of interest

The authors declare the following financial interests/personal relationships which may be considered as potential competing interests: LS received speakers' and consultant's fee from MSD, Astra-Zeneca, Servier, Bayer, Merck, Amgen, Pierre-Fabre. GT received speakers' and consultant's fee from BMS, Astra-Zeneca, MSD, Merck, Servier.

The remaining authors declare that the research was conducted in the absence of any commercial or financial

relationships that could be constructed as a potential conflict of interest.

Publisher's note

All claims expressed in this article are solely those of the authors and do not necessarily represent those of their affiliated organizations, or those of the publisher, the editors and the reviewers. Any product that may be evaluated in this article, or claim that may be made by its manufacturer, is not guaranteed or endorsed by the publisher.

References

1. Buflin JA. Colorectal cancer: evidence for distinct genetic categories based on proximal or distal tumor location. *Ann Intern Med* (1990) 113:779–88. doi: 10.7326/0003-4819-113-10-779
2. Yamauchi M, Lochhead P, Morikawa T, Huttenhower C, Chan AT, Giovannucci E, et al. Colorectal cancer: A tale of two sides or a continuum? *Gut* (2012) 61:794–7. doi: 10.1136/gutjnl-2012-302014
3. Lee MS, Menter DG, Kopetz S. Right versus left colon cancer biology: Integrating the consensus molecular subtypes. *J Natl Compr Canc Netw* (2017) 15:411–9. doi: 10.6004/jnccn.2017.0038
4. Petrelli F, Tomasello G, Borronovo K, Ghidini M, Turati L, Dalleria P, et al. Prognostic survival associated with left-sided vs. right-sided colon cancer: A systematic review and meta-analysis. *JAMA Oncol* (2017) 3:211–9. doi: 10.1001/jamaoncol.2016.4227
5. Holch JW, Ricard I, Stintzing S, Modest DP, Heinemann V. The relevance of primary tumor location in patients with metastatic colorectal cancer: A meta-analysis of first-line clinical trials. *Eur J Cancer* (2017) 70:87–98. doi: 10.1016/j.ejca.2016.10.007
6. NCCN Guidelines. *Colon rectal (Version: 2.2022)*. Available at: <https://www.nccn.org/guidelines/guidelines-detail?category=1&id=1428> (Accessed November 2022).
7. Linee Guida AIOM. *Tumori del colon* (2021). Available at: <https://www.aiom.it/linee-guida-aiom-2021-tumori-del-colon/> (Accessed November 2022).
8. Brulé SY, Jonker DJ, Karapetis CS, O'Callaghan CJ, Moore MJ, Wong R, et al. Location of colon cancer (right-sided versus left-sided) as a prognostic factor and a predictor of benefit from cetuximab in NCIC CO.17. *Eur J Cancer* (2015) 51:1405–14. doi: 10.1016/j.ejca.2015.03.015
9. Boeckx N, Koukakis R, Op de Beeck K, Rolfo C, Van Camp G, Siena S, et al. Effect of primary tumor location on second- or later-line treatment outcomes in patients with RAS wild-type metastatic colorectal cancer and all treatment lines in patients with RAS mutations in four randomized panitumumab studies. *Clin Colorectal Cancer* (2018) 17:170–178.e3. doi: 10.1016/j.clcc.2018.03.005
10. Grothey A, Van Cutsem E, Sobrero A, Siena S, Falcone A, Ychou M, et al. CORRECT study group. regorafenib monotherapy for previously treated metastatic colorectal cancer (CORRECT): An international, multicentre, randomised, placebo-controlled, phase 3 trial. *Lancet* (2013) 381:303–12. doi: 10.1016/S0140-6736(12)61900-X
11. Mayer RJ, Van Cutsem E, Falcone ARECOURSE Study Group. Randomized trial of TAS-102 for refractory metastatic colorectal cancer. *N Engl J Med* (2015) 372:1909–19. doi: 10.1056/NEJMoa1414325
12. Chen KH, Shao YY, Chen HM, Lin YL, Lin ZZ, Lai MS, et al. Primary tumor site is a useful predictor of cetuximab efficacy in the third-line or salvage treatment of KRAS wild-type (exon 2 non-mutant) metastatic colorectal cancer: a nationwide cohort study. *BMC Cancer* (2016) 16:327. doi: 10.1186/s12885-016-2358-2
13. Moretto R, Cremolini C, Rossini D, Pietrantonio F, Battaglin F, Mennitto A, et al. Location of primary tumor and benefit from anti-epidermal growth factor receptor monoclonal antibodies in patients with RAS and BRAF wild-type metastatic colorectal cancer. *Oncologist* (2016) 21:988–94. doi: 10.1634/theoncologist.2016-0084
14. Nakajima H, Fukuoka S, Masuishi T, Nakajima H, Fukuoka S, Masuishi T, et al. Clinical impact of primary tumor location in metastatic colorectal cancer patients under later-line regorafenib or Trifluridine/Tipiracil treatment. *Front Oncol* (2021) 11:688709. doi: 10.3389/fonc.2021.688709
15. Loree JM, Pereira AAL, Lam M, Willauer AN, Raghav K, Dasari A, et al. Classifying colorectal cancer by tumor location rather than sidedness highlights a continuum in mutation profiles and consensus molecular subtypes. *Clin Cancer Res* (2018) 24:1062–72. doi: 10.1158/1078-0432.CCR-17-2484
16. Guinney J, Dienstmann R, Wang X, de Reyniès A, Schlicker A, Soneson C, et al. The consensus molecular subtypes of colorectal cancer. *Nat Med* (2015) 21:1350–6. doi: 10.1038/nm.396
17. Jacobs B, De Roock W, Piessevaux H, Van Oirbeek R, Biesmans B, De Schutter J, et al. Amphiregulin and epiregulin mRNA expression in primary tumors predicts outcome in metastatic colorectal cancer treated with cetuximab. *J Clin Oncol* (2009) 27:5068–74. doi: 10.1200/JCO.2008.21.3744
18. Stintzing S, Wirapati P, Lenz HJ, Neureiter D, Fischer von Weikersthal L, Decker T, et al. Consensus molecular subgroups (CMS) of colorectal cancer (CRC) and first-line efficacy of FOLFIRI plus cetuximab or bevacizumab in the FIRE3 (AIO KRK-0306) trial. *Ann Oncol* (2019) 30:1796–803. doi: 10.1093/annonc/mdz387
19. Ten Hoorn S, Sommeijer DW, Elliott F, Fisher D, de Back TR, Trinh A, et al. Molecular subtype-specific efficacy of anti-EGFR therapy in colorectal cancer is dependent on the chemotherapy backbone. *Br J Cancer* (2021) 125:1080–8. doi: 10.1038/s41416-021-01477-9
20. Zhao B, Wang L, Qiu H, Zhang M, Sun L, Peng P, et al. Mechanisms of resistance to anti-EGFR therapy in colorectal cancer. *Oncotarget* (2017) 8:3980–4000. doi: 10.18632/oncotarget.14012
21. Cremolini C, Morano F, Moretto R, Berenato R, Tamborini E, Perrone F, et al. Negative hyper-selection of metastatic colorectal cancer patients for anti-EGFR monoclonal antibodies: the PRESSING case-control study. *Ann Oncol* (2017) 28:3009–14. doi: 10.1093/annonc/mdx546
22. Morano F, Corallo S, Lonardi S, Raimondi A, Cremolini C, Rimassa L, et al. Negative hyperselection of patients with RAS and BRAF wild-type metastatic colorectal cancer who received panitumumab-based maintenance therapy. *J Clin Oncol* (2019) 37:3099–110. doi: 10.1200/JCO.19.01254
23. Shitara K, Yamanaka T, Denda T, Tsuji Y, Shinozaki K, Komatsu Y, et al. REVERCE: a randomized phase II study of regorafenib followed by cetuximab versus the reverse sequence for previously treated metastatic colorectal cancer patients. *Ann Oncol* (2019) 30:259–65. doi: 10.1093/annonc/mdy52
24. Cremolini C, Rossini D, Dell'Aquila E, Lonardi S, Conca E, Del Re M, et al. Rechallenge for patients with RAS and BRAF wild-type metastatic colorectal cancer with acquired resistance to first-line cetuximab and irinotecan: A phase 2 single-arm clinical trial. *JAMA Oncol* (2019) 5:343–50. doi: 10.1001/jamaoncol.2018.5080
25. Sartore-Bianchi A, Pietrantonio F, Lonardi S, Mussolin B, Rua F, Crisafulli G, et al. Circulating tumor DNA to guide rechallenge with panitumumab in metastatic colorectal cancer: the phase 2 CHRONOS trial. *Nat Med* (2022) 28:1612–8. doi: 10.1038/s41591-022-01886-0
26. Moretto R, Rossini D, Capone I, Boccaccino A, Perrone F, Tamborini E, et al. Rationale and study design of the PARERE trial: Randomized phase II study of panitumumab re-treatment followed by regorafenib versus the reverse sequence in RAS and BRAF wild-type chemo-refractory metastatic colorectal cancer patients. *Clin Colorectal Cancer* (2021) 20:314–7. doi: 10.1016/j.clcc.2021.07.001



OPEN ACCESS

EDITED BY

Alessandro Passardi,
Romagnolo Scientific Institute for
the Study and Treatment of Tumors
(IRCCS), Italy

REVIEWED BY

Nicholas Pavlidis,
University of Ioannina, Greece
Antonella Argentiero,
National Cancer Institute Foundation
(IRCCS), Italy

*CORRESPONDENCE

Francesca Negri
✉ fnegri@aio.pr.it

SPECIALTY SECTION

This article was submitted to
Gastrointestinal Cancers:
Colorectal Cancer,
a section of the journal
Frontiers in Oncology

RECEIVED 27 December 2022

ACCEPTED 10 February 2023

PUBLISHED 28 February 2023

CITATION

Negri F, Bottarelli L, Pedrazzi G,
Maddalo M, Leo L, Milanese G, Sala R,
Lecchini M, Campanini N, Bozzetti C,
Zavani A, Di Rienzo G, Azzoni C, Silini EM,
Sverzellati N, Gaiani F, de' Angelis GL and
Gnetti L (2023) Notch-Jagged1 signaling
and response to bevacizumab therapy in
advanced colorectal cancer: A glance to
radiomics or back to physiopathology?
Front. Oncol. 13:1132564.
doi: 10.3389/fonc.2023.1132564

COPYRIGHT

© 2023 Negri, Bottarelli, Pedrazzi, Maddalo,
Leo, Milanese, Sala, Lecchini, Campanini,
Bozzetti, Zavani, Di Rienzo, Azzoni, Silini,
Sverzellati, Gaiani, de' Angelis and Gnetti.
This is an open-access article distributed
under the terms of the [Creative Commons
Attribution License \(CC BY\)](#). The use,
distribution or reproduction in other
forums is permitted, provided the original
author(s) and the copyright owner(s) are
credited and that the original publication in
this journal is cited, in accordance with
accepted academic practice. No use,
distribution or reproduction is permitted
which does not comply with these terms.

Notch-Jagged1 signaling and response to bevacizumab therapy in advanced colorectal cancer: A glance to radiomics or back to physiopathology?

Francesca Negri^{1*}, Lorena Bottarelli², Giuseppe Pedrazzi³,
Michele Maddalo⁴, Ludovica Leo³, Gianluca Milanese⁵,
Roberto Sala³, Michele Lecchini⁵, Nicoletta Campanini²,
Cecilia Bozzetti⁶, Andrea Zavani³, Gianluca Di Rienzo³,
Cinzia Azzoni², Enrico Maria Silini^{2,7}, Nicola Sverzellati⁵,
Federica Gaiani^{1,3}, Gian Luigi de' Angelis^{1,3} and Letizia Gnetti⁷

¹Gastroenterology and Endoscopy Unit, University Hospital of Parma, Parma, Italy, ²Pathology Unit, Department of Medicine and Surgery, University of Parma, Parma, Italy, ³Department of Medicine and Surgery, University of Parma, Parma, Italy, ⁴Medical Physics Department, University Hospital of Parma, Parma, Italy, ⁵Radiology, Department of Medicine and Surgery, University of Parma, Parma, Italy, ⁶Oncology Unit, University Hospital of Parma, Parma, Italy, ⁷Pathology Unit, University Hospital of Parma, Parma, Italy

Introduction: The Notch intracellular domain (NICD) and its ligands Jagged-1 (Jag1), Delta-like ligand (DLL-3) and DLL4 play an important role in neoangiogenesis. Previous studies suggest a correlation between the tissue levels of NICD and response to therapy with bevacizumab in colorectal cancer (CRC). Another marker that may predict outcome in CRC is radiomics of liver metastases. The aim of this study was to investigate the expression of NICD and its ligands and the role of radiomics in the selection of treatment-naïve metastatic CRC patients receiving bevacizumab.

Methods: Immunohistochemistry (IHC) for NICD, Jag1 and E-cadherin was performed on the tissue microarrays (TMAs) of 111 patients with metastatic CRC treated with bevacizumab and chemotherapy. Both the intensity and the percentage of stained cells were evaluated. The absolute number of CD4+ and CD8+ lymphocytes was counted in three different high-power fields and the mean values obtained were used to determine the CD4/CD8 ratio. The positivity of tumor cells to DLL3 and DLL4 was studied. The microvascular density (MVD) was assessed in fifteen cases by counting the microvessels at 20x magnification and expressed as MVD score. Abdominal CT scans were retrieved and imported into a dedicated workstation for radiomic analysis. Manually drawn regions of interest (ROI) allowed the extraction of radiomic features (RFs) from the tumor.

Results: A positive association was found between NICD and Jag1 expression ($p < 0.001$). Median PFS was significantly shorter in patients whose tumors expressed high NICD and Jag1 (6.43 months vs 11.53 months for negative cases; $p = 0.001$). Those with an MVD score ≥ 5 (CD31-high, NICD/Jag1

positive) experienced significantly poorer survival. The radiomic model developed to predict short and long-term survival and PFS yielded a ROC-AUC of 0.709; when integrated with clinical and histopathological data, the integrated model improved the predictive score (ROC-AUC of 0.823).

Discussion: These results show that high NICD and Jag1 expression are associated with progressive disease and early disease progression to anti VEGF-based therapy; the preliminary radiomic analyses show that the integration of quantitative information with clinical and histological data display the highest performance in predicting the outcome of CRC patients.

KEYWORDS

Notch signaling pathway, bevacizumab, colorectal cancer, Jagged-1, therapy resistance

Introduction

Notch signaling is an evolutionary conserved pathway that plays a critical role in regulating cell-fate differentiation during embryonic development (1, 2). This pathway also affects angiogenesis (3), is aberrantly activated in several cancers and influences malignant proliferation and progression (4). The activation of the Notch pathway arises when specific ligands, such as Jagged-1 (Jag1) or Delta-like ligand (DLL)-3 or DLL4, bind to the Notch transmembrane receptor (1). Jag1 or DLL ligand binding to Notch receptor leads to the separation of the Notch extracellular domain by proteases of the ADAM family. Subsequently, the Notch intracellular domain (NICD) is released by a gamma-secretase processing and transits to the nucleus where it regulates downstream gene expression (1).

Notch signaling triggered *via* Jag1 and DLLs plays a double role (5, 6): it inhibits DLLs (5) while it activates Jag1 (6). Previous studies have revealed that Notch signaling can be triggered by soluble forms of DLLs and Jag1 (7–9), which have different consequences on tumor progression: while soluble DLLs hinder tumor growth (10), soluble Jag1 greatly exacerbates the malignant development of cancer. Jag1 plays a key role in promoting epithelial to mesenchymal transition (EMT) as well as fostering cancer stem cell (CSC) phenotypes (8). Our previous data suggested an association between high tissue levels of NICD and poorer response to anti-vascular endothelial growth factor (VEGF) bevacizumab as first-line therapy in metastatic colorectal cancer (CRC) patients, but not to chemotherapy alone (11). No association was found between NICD and DLL4 expression within the same tumor (11). Jag1 might reduce Notch signaling, thereby enhancing responses to VEGF; such tumors could therefore be more susceptible to VEGF inhibition or different anti-angiogenic treatments.

The role of imaging in CRC staging has been recently expanded by the implementation of non-invasive biomarkers extrapolated from medical images (12). Radiomics of liver metastases in patients with CRC showed to predict outcome in patients treated with FOLFIRI and bevacizumab (13). Recent attention has been given

to a multiomics strategy for comprehensive genotype–phenotype characterization of several oncological diseases (14, 15). Proteomics analysis can uncover new therapeutic choices, thus reducing the emergence of drug resistance and potentially improving patient outcomes (16). However, research mostly focused on radiomics alone, without attempting to integrate the radiomic signature with reliable clinical predictors and molecular data (KRAS mutation status or microsatellite instability) (17). Therefore, predictive models in CRC patients might be further improved by multidisciplinary approaches encompassing quantitative metrics derived from diagnostic studies, which have been more widely used for other cancer types, instead.

These data prompted us to investigate the expression of NICD, Jag1, DLL3 and DLL4 and a series of markers potentially involved in angiogenesis and immune response to bevacizumab therapy.

We also tested whether radiomics could select treatment-naïve metastatic CRC patients responding to bevacizumab, beyond clinical and NICD/Jag1/DLL expression parameters.

Materials and methods

We characterized a series of tumors by using immunohistochemistry (IHC) in tissue microarrays (TMAs) from 111 pre-treatment surgical specimens from patients with metastatic CRC treated with anti VEGF-therapy bevacizumab in combination with chemotherapy between 2008 and 2017 at the University Hospital of Parma (Parma, Italy). Cases were selected based on the availability of retrospective archival-FFPE (formalin-fixed, paraffin-embedded) tissue specimens. The study protocol was approved by the local Ethics Committee (AVEN: Comitato Etico dell'Area Vasta Emilia Nord). The procedures used in this study adhere to the tenets of the Declaration of Helsinki. Response to bevacizumab was assessed by using time point RECIST version 1.1 (i.e. best response at time point).

NICD staining and other parameters were collected; patients' demographics, primary tumor characteristics and therapy details are listed in Table 1.

TABLE 1 Patients’ characteristics and tissue microarray expression data.

Characteristics	N = 111 (%)
Age (years)	66
Range	32-84
Sex	
Male	60 (54)
Female	51 (46)
CEA	
<30	57 (51)
>30	41(37)
Unknown	13 (12)
Primary tumor side	
Right side	47 (43)
Left side	63 (57)
Unknown	1
Number of metastatic sites	
1	51 (46)
≥2	60 (54)
Subsequent chemotherapy	
Yes	87 (79)
Received aflibercept	9/87 (10)
KRAS	
Mutant	61 (68)
Wild type	29 (32)
Unknown	21
NICD	
High	42 (38)
Low	69 (62)
Jag1	
Positive	68 (62)
Negative	42 (38)
DLL4	
Positive	90 (86)
Negative	14 (14)
Not evaluable	7
DLL3	
Positive	79 (81)
Negative	18 (19)
Not evaluable	14
CD4/CD8	

(Continued)

TABLE 1 Continued

Characteristics	N = 111 (%)
2/1-3/1	84 (92)
1/1	6 (7)
1/2	1 (1)
Not evaluable	20
CD3	
Positive	94 (100)
Negative	0
Not evaluable	17
Cyclin D1	
High	71 (75)
Low	23 (25)
Not evaluable	17
CD44	
High	22 (24)
Low	70 (76)
Not evaluable	19
Mismatch repair protein	
MSI	7 (8)
MSS	76 (92)
Not evaluable	28

DLL, Delta-like ligand; Jag1, Jagged-1; MSI, Microsatellite instability; MSS, microsatellite stable; NICD, Notch intracellular domain.

Tissue microarray construction

The following method was used to construct TMAs. Hematoxylin and eosin slides were reviewed to select tumor foci for each patient. A TMA instrument (3DHISTECH) was used to obtain cylindrical tissue cores from the selected areas of each donor block. Cores were assembled and embedded in the recipient block. Each core was 0.6 mm in diameter and its surface measured 0.282 mm² (2 or 3 high-power fields). The distance from one core to the other was 0.7 or 0.8 mm. 5 μm thick sections were cut from the recipient block to perform immunohistochemistry (Figure 1).

Immunohistochemistry

Firstly, the expression of Notch Intracellular Domain (NICD VAL 1744 clone D3B8, dilution 1:100, Cell Signaling Technology), Jag1 (JAG1 clone D4Y1R, dilution 1:100 Cell Signaling Technology) and E-cadherin (clone 36, Ventana Roche, ready-to-use) was studied and only certain staining patterns were considered positive. NICD, Jag1 and E-cadherin staining were considered positive when they showed cytoplasmic and/or nuclear reactivity, cytoplasmic and/or membrane reactivity and membrane reactivity,

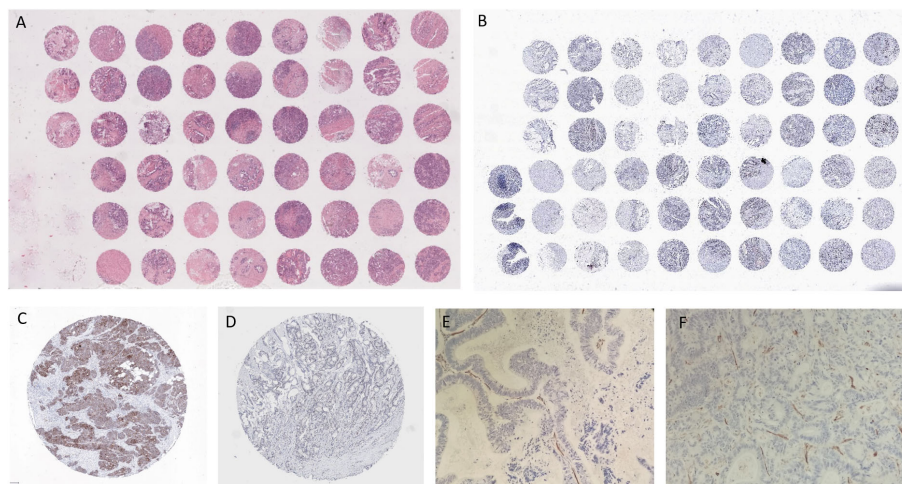


FIGURE 1

(A) TMA, Hematoxylin and Eosin; (B) TMA, NICD; (C) NICD; (D) Jag1; (E) CD31 non responder patient; (F) CD31 responder patient with NICD and Jag1+.

respectively. Both the intensity and the percentage of stained cells were evaluated. The intensity was assessed as 0 = negative, 1 = weak, 2 = moderate and 3 = strong.

Secondly, the absolute number of CD4+ (clone SP35) and CD8+ (clone SP57) lymphocytes was counted in three different high-power fields and the mean values obtained were used to determine the CD4/CD8 ratio. A CD4/CD8 ratio of 2.0 was considered normal. The assessment of CD3+ (clone 2GLV6), CD44+ (clone SP37) and CyclinD1+ (clone SP4-R) was given as a percentage of positive cells (Ventana Roche, ready-to-use).

Thirdly, the expression of DLL3 (clone SP347, Ventana Roche, ready-to-use) and DLL4 (clone 4A11F8 dilution 1:100 Biorbyt) was studied. Positivity was defined as $\geq 25\%$ tumor cells, high expression of DLL3/DLL4 was defined as $\geq 75\%$ tumor cells. The intensity was assessed as 0 = negative, 1 = weak, 2 = moderate and 3 = strong.

Lastly, mismatch repair proteins (MLH1 - clone M1, PMS2 - clone A16-4, MSH2 - clone G219-1129, MSH6 - clone SP93; Ventana Roche, ready-to-use) were studied. Negative expression of one of them was considered proof of microsatellite instability. In fifteen cases we assessed angiogenesis by counting the microvessels at 20x magnification (Nikon, Eclipse E400).

The immunostained sections for CD31 (Ventana, ready-to-use solution) were examined at low power to select the three areas with the highest vascularity (hotspots).

Two pathologists separately assessed each case without any clinical information.

Radiomic data

Patients that underwent abdominal Computed Tomography (CT) at the University Hospital of Parma for CRC staging were included in the study. CT scans were performed with different CT scanners and imaging protocols; images were retrieved from Picture Archive and Communication System (PACS) and were subsequently imported into a dedicated software (3D Slicer) for tumor segmentation.

One radiologist (ML) evaluated all CT scans visually and identified the target lesion on portal venous phase. The reader was instructed to draw manually multiple regions of interest (ROI) at different levels by tracing the boundaries of the lesions: subsequently, a dedicated tool (SlicerRadiomics) software interpolated the ROIs to obtain the volume of interest (VOI) which allowed the extraction of 852 radiomic features (RF). The VOI was manually modified by the reader in case of inaccurate segmentation. Image preprocessing based on wavelet decomposition was performed by SlicerRadiomic before feature calculation to generate independent radiomic predictors.

The radiomic dataset included shape, first-order, Gray-Level-Cocurrence-Matrix (GLCM), Gray-Level-Run-Length-Matrix (GLRLM), Gray-Level-Size-Zone-Matrix (GLSZM), Neighboring-Gray-Tone-Difference-Matrix (NGTDM), Gray-Level-Dependence-Matrix (GLDM).

Statistical analysis and classification model

Classical statistics

The chi-square test and Fisher's exact test were used to perform univariate comparisons between categorical variables.

The Kaplan-Meier method was used to estimate the mean and median time for progression free survival (PFS) followed by a Cox regression analysis to evaluate the relationship between survival and covariates in a multivariable framework. The model was evaluated by making use of model diagnostics. This included checking for the overall goodness of fit, model adherence to key assumptions, influential observations and nonlinearity. The variables considered in the Cox regression were KRAS, type of chemotherapy protocol, site of primary tumor, NICD, CD44, Jag1, CD3, DLL4 expression; only NICD expression resulted statistically significant and was maintained in the final model. The regression coefficients were reported as hazard

ratios (HRs). The 95% confidence intervals (CIs) were also estimated from the analysis.

The commercial package IBM-SPSS v.28 and the open-source statistical system Jamovi version 2.3.0, which is based on the widely used open-source system R, were used to perform survival analysis. A p-value less than 0.05 was considered statistically significant ($p < 0.05$).

Multimic models

Classification models were developed to predict time to disease progression. With this aim in mind, PFS at 9 months was used to stratify patients in two groups, namely short and long-term survivals. We considered PFS at 9 months as a target variable because a comprehensive meta-analysis has recently showed that PFS ranges between 7 and 10.8 months for CRC patients treated with bevacizumab (18). Therefore, we acquired the central value of that interval from the meta-analysis to further stratify the prognosis of our patients according to the integrated profile. Three models were developed: radiomic (R), clinical/Notch signaling (C/N) and the comprehensive integrated model (I). In the R model, we removed redundant highly correlated features by calculating their Spearman Rho correlation coefficient: RFs with a coefficient greater than 0.99 were excluded from the successive analyses. Subsequently, feature standardization by z-score was applied. In the C/N model, the same variables considered in the Cox regression were added as predictors (Table 1). In both R and C/N models, a L2 penalized logistic regression algorithm was implemented for features selection and validation. Most predictive features were selected by means of a wrapper approach, i.e. the sequential forward feature selection algorithm with 20 Monte-Carlo cross-validation (MCCV) splits. We chose the area under the receiver operating characteristic (ROC) curve (ROC-AUC) as performance metric. We iterated the selection process 50 times, using 50 different random states and, subsequently, we selected the features that had higher frequency of occurrence for both R and C/N models. Through 5000 MCCV splits (train:0.7, test:0.3), different numbers of clinical/genomic and radiomic features were selected and used respectively for R and C/N model training and validation. Likelihood ratio test was applied to verify if the addition of another feature significantly improved the model performance. The selected C/N and R features were used together to build the I model.

For all models, the ROC-AUC and accuracy scores for each MCCV were calculated and averaged over these iterations. Mean ROC curve and mean learning curve were also plotted. Recall and precision metrics were also calculated

Survival analysis was performed in radiomic dataset. Kaplan–Meier survival curves PFS for two risk groups were calculated and then compared using log-rank test. The risk groups were assessed by using continuous RFs, previously selected by the machine-learning model. Risk groups based on RFs were developed using ROC analysis to determine the cutoff value of each RF for optimal stratification into two classes: Youden index was chosen as optimal threshold. Subsequently, we combined the selected features in a single variable and we performed Kaplan–Meier analysis again. Finally, we calculated the probability to predict longer-term class in each risk group of combined features. Probabilities derived from the R model were averaged over MCCV splits.

Machine-learning model, analysis and plots were performed by means of Python v. 3.8.5; scikit-learn and MLextend machine learning libraries were used for features selection and model development.

Results

Classical statistics

A total of 111 patients have been included in the analysis. The cohort is shown in Table 1. A positive association was found in univariate analysis between NICD and Jag1 expression ($p < 0.001$; Table 2). No significant association was found for the other analyzed markers and KRAS mutation (data not shown). All main clinical characteristics were comparable among the subgroups of patients (data not shown). Specifically, no significant associations of NICD and Jag1 immunostaining scores with age, baseline CEA levels, number of metastatic sites and subsequent chemotherapy were observed.

Compared with patients who had NICD and/or Jag1 low tumors, patients whose pre-treatment tumors expressed high NICD and Jag1 levels showed poor RECIST 1.1 categories with higher rates of stable disease (SD) or progressive disease (PD) as best response, and lower frequencies of complete response (CR) or partial response (PR); $p = 0.002$ (Table 3). Associations between NICD and Jag1 and therapy response were further evaluated using PFS and Kaplan–Meier and Cox proportional hazard modeling. Median PFS was significantly shorter in patients whose tumors expressed high NICD and Jag1 (6.43 months vs 11.53 months for negative cases; $p = 0.001$, Figure 2). Cox regression following univariate analysis confirmed NICD as the only independent predictor for PFS (HR = 1.820 [1.165 – 2.844]; $p = 0.009$).

TABLE 2 Association between NICD and Jag1 expression in CRC.

	Low Jag1	High Jag1	
Low NICD	38 (56%)	30 (44%)	
High NICD	4 (10%)	38 (90%)	
			χ^2 continuity correction $p < 0.001$
			Fisher's exact test $p < 0.001$

Jag1, Jagged-1; NICD, Notch intracellular domain.

TABLE 3 Response according to NICD and Jag1 protein expression.

NICD-Jag1	Response rate		Total
	SD + PD	CR + PR	
Low NICD_Low Jag1	13 (34%)	25 (66%)	38
Low NICD_High Jag1	21 (70%)	9 (30%)	30
High NICD_Low Jag1	3 (75%)	1 (25%)	4
High NICD_High Jag1	28 (74%)	10 (26%)	30
			χ^2 continuity correction $p = 0.002$
			Fisher's exact test $p < 0.001$

CR, complete response; Jag1, Jagged-1; NICD, Notch intracellular domain; PD, progressive disease; PR, partial response; SD, stable disease.

Quite surprisingly, 5 patients with high NICD tumors showed long PFS. Each case was evaluated for the following features: inflammation, staging, grading and microvascular density. The last one was the only noteworthy characteristic. For this reason, we assessed the microvascular density according to Chalkey's methods: microvessels were counted manually for each hotspot at 20x magnification (high power field) and expressed as MVD score. This assessment was carried out for 15 patients based on response to therapy: 5 were non responder (NICD/Jag1 positive), 10 were responder (5 NICD/Jag1 positive and 5 NICD/Jag1 negative). Those with an MVD score ≥ 5 (CD31-high, NICD/Jag1 positive) were associated with significantly poorer survival. Low CD31 was seen in all 10 responder patients (both 5 NICD/Jag1 positive and NICD/Jag1 negative) and associated with a better prognosis.

Multimomics

The retrospectively collected 111 CRC cases were decreased due to inclusion criteria that comprised the availability of (i) CT data and (ii) PFS information. Thus, the ensuing results based on the multimomic approach refer to a restricted population of 76 subjects. Regarding feature preprocessing, the Spearman correlation matrix for RFs is reported in Figure S1. Redundant features were removed, thereby reducing the number of RFs by about 33.6%.

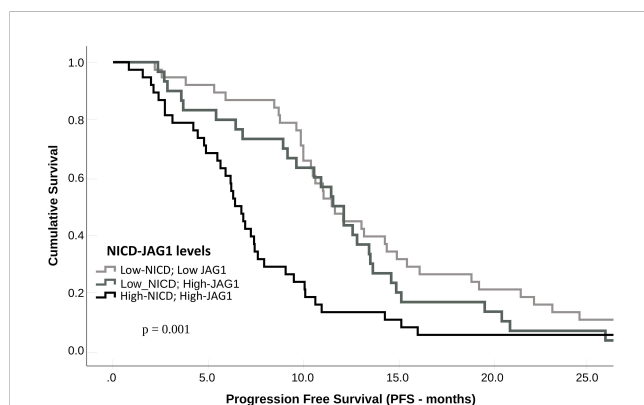


FIGURE 2
Progression-free survival (PFS) according to NICD and Jag1 expression levels in metastatic CRC patients treated with bevacizumab.

In the R model, the best performance in differentiating short and long survival was obtained by selecting two RFs: Strength (NGTDM) and Skewness (first order) with a ROC-AUC of 0.709 and an accuracy of 0.671. Likelihood ratio showed that the performance of the model would not significantly improve by adding further RFs (Table 4).

In the C/N Model, the most predictive features were Jag1 and NICD, whereas the addition of a third feature was not significantly relevant: the ROC-AUC was higher as compared to the R model alone, with a ROC-AUC of 0.743, while accuracy was slightly lower (0.649) (Table 4).

The I Model included the previously selected R and C/N features, that had a negative effect on the likelihood of predicting long survivors, as shown by odds ratios (Table S1). The I model yielded the highest ROC-AUC (0.823) and accuracy (0.751) values. The mean ROC curves are displayed in Figure 3.

Learning curves show the ROC-AUC score (Figure S2A) and accuracy (Figure S2B) as a function of the number of training samples. We plotted performance scores obtained by predictions for both training (blue line) and validation (green line) datasets and averaged over all iterations of the MCCV. For each model, we also calculated and averaged over 5000 MCCV splits the recall metric representing the true predictions of longer survival class: 0.794 [95% CI : 0.790, 0.797] for R model, 0.660 [95% CI: 0.654, 0.666] for C model and 0.767 [95% CI : 0.763, 0.770] for I model. In addition, we calculated precision metrics (i.e. positive predictive value), representing the fraction of true positive cases among the total positive predicted instances: 0.642 [95% CI : 0.641, 0.645] for R model, 0.673 [95% CI: 0.669, 0.676] for C model and 0.751 [95% CI : 0.749, 0.754] for I model.

Kaplan Meier curves of PFS (Figure S3) showed significantly different risk strata for Strength, whereas none for skewness. The combined RF (strength-skewness) created 3 risk groups which significantly stratified in PFS curve (Figure 4). Probabilities of longer-term class prediction are listed in Table 5.

Discussion

The diagnosis of CRC is based on the integration of multiple features (histopathology, immunohistochemistry and molecular findings) and its management is of the utmost importance.

TABLE 4 Performances of the R, C/N and I models.

Model name	ROC AUC	ROC AUC 95%CI	Accuracy	Accuracy 95%CI
R	0.709	0.706-0.711	0.671	0.668-0.673
C/N	0.743	0.741-0.745	0.649	0.647-0.651
I	0.823	0.824-0.828	0.751	0.749-0.753

Although immunohistochemistry has been widely used to detect microsatellite instability in CRC screening for defective DNA mismatch repair, unexpectedly negative results have been reported probably due to somatic mutations. This implies that the analysis should be completed with microsatellite instability-polymerase chain reaction test to have reliable results (19).

In this study, we investigated NICD expression and a series of other correlated markers that have been previously associated with angiogenesis to predict tumor progression-free in advanced stage CRC treated with bevacizumab and first-line chemotherapy. Our results show that high NICD and Jag1 expression are associated with PD and early disease progression to anti VEGF-based therapy.

Notch signaling may regulate both the initiation and the cessation of angiogenesis through different mechanisms (20). The potentiality of Notch signaling to rule angiogenic processes becomes crucial in the context of aberrant angiogenesis. Furthermore, neoangiogenesis in CRC may differ in distinct tumor subtypes (21).

Angiogenesis is the expansion of emergent vascular sprouts from preexisting blood vessels. Luminal endothelial cells switch into tip cells that lead to the outgrowth of a multicellular stalk. Notch signaling involves cell fate determination as a mechanism to determine tip and stalk cells (21). The distribution of vascular sprouts depends on Notch triggering; moreover, the formation of a new sprout or the alteration of the original vessel relies upon Notch-DLL4 expression in endothelial tip cells (20). VEGF signaling can be downregulated in cells with activated Notch signaling by decreasing VEGF receptor transcription levels (22–24). In these cases, the

uncontrolled dysfunctional tumor vessels proliferation under Notch signaling is not inhibited by VEGFR. The uncontrolled angiogenesis increases tumor hypoxia which is detrimental to chemotherapy as well. VEGF regulates blood vessel function by inducing tumor cell growth and suppressing immune activation (25).

Unlike DLL4, Jag1 is overexpressed in tumor cells. It is supposed to work as a communication element between tumor cells and tumor-associated endothelial cells to trigger Notch signaling, enhance cell proliferation and stabilize vessels (26). Jag1 is a critical regulator of tip cell formation and sprouting because of its ability to modulate DLL4-Notch signaling in the angiogenic endothelium (20). Notch and VEGF induce the expression of DLL4 (27, 28); on the contrary, Jag1 is not upregulated by Notch and is induced by inflammatory cytokines, such as TNF- α , which reduces DLL4 transcription. These signals might modulate angiogenesis by changing the ratio of DLL4 and Jag1 expression, allowing the integration of different pro or antiangiogenic signals. The intricate interaction of the ligands DLL4 and Jag1 traces the pathway of tip cell selection (20).

Although the detailed mechanisms behind Notch activation have not been fully discovered, it is known that the related soluble ligands influence several contexts. They regulate the proliferation of regulatory T cells (7, 9), influence tumor microenvironment, promote adipocyte differentiation (29), mediate hematopoietic cell differentiation (30) and neurogenesis (31). Moreover, Jag1 overexpression in cancer cells can activate Notch signaling in adjacent endothelial cells (32). Our study focused on NICD expression, however did not underestimate the role of tumor microenvironment. In fact, the assessment of CD3 and CD4/CD8

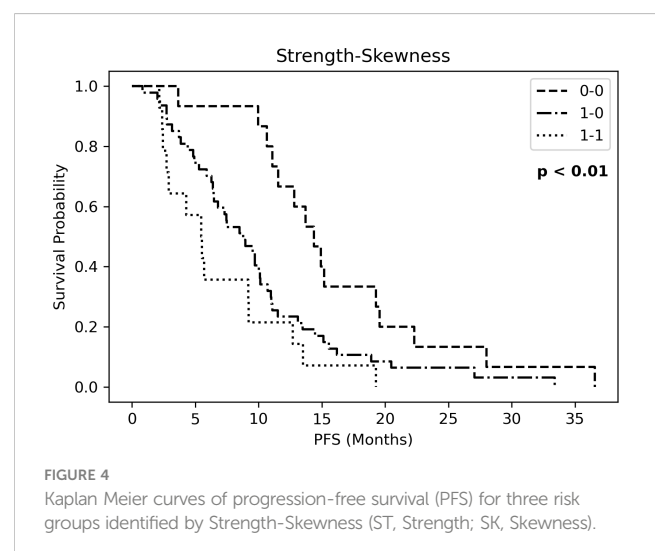
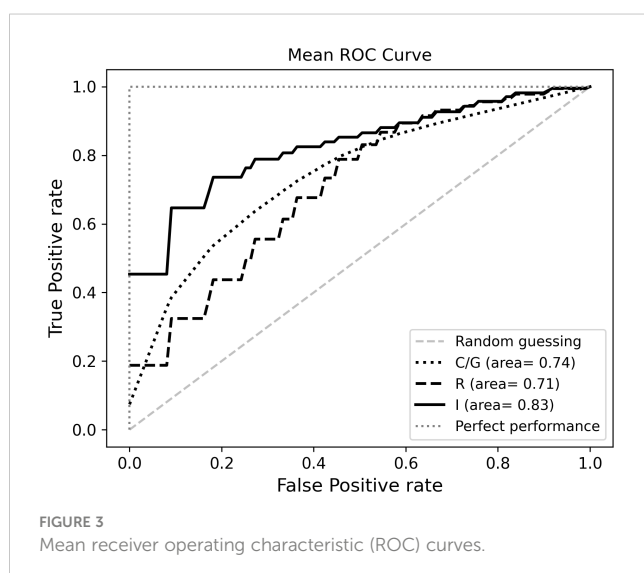


TABLE 5 Probabilities of longer-term class prediction.

R MODEL			
Strength	Skewness	Probability	Standard deviation
0	0	0.692	0.024
1	1	0.300	0.029
0	1	0.498	0.028

ratio did not show a correlation with tumor aggressiveness or survival. Although we have restricted our analysis to lymphocytes, we know that Notch signaling can also affect other factors such as tumor associated fibroblasts, endothelial cells and the expression of CTLA4 in tumor infiltrating lymphocytes. Further studies are necessary to assess the interaction of Notch with other stromal cells (33, 34).

This study did not prove that DLL4 was relevant to define the biological behavior of tumors. Patients with a highly vascular tumor microenvironment went worse in comparison to those with a poor tumor vascularization. However, the expression of Notch and Jag1 was associated with a better outcome only in those patients with a poor tumor vascularization.

We developed an integrated model which included clinical, genomic and radiomic variables to explore its potential role in the prediction of survival. The model was designed to predict 9-months PFS in CRC patients and included a first-order (skewness) and a second-order (NGTDM strength), along with NICD and Jag1 expression levels. Results showed that each additional increase of one point of NGTDM strength - which accounts for tumor heterogeneity - was associated with approximately 50% decrease in the odds of survival.

Regarding prognostic performance, our radiomic model agreed with other CT-based radiomic models that have been proposed, which yielded ROC-AUCs between 0.66 and 0.74 (18, 35). The integration of radiomics with clinical (36) and genomic predictors have led to increased model performances (17, 37, 38); this study has confirmed this finding. Cao et al. tested a radiomic signature in 381 patients with CRC and showed that a radiomic-derived score was able to stratify their outcome and enrich the TNM staging (39). In our study, we differentiated three groups of patients based on binarization of the values of RFs: those individuals with lower RF “skewness” were those with longer survival; similarly, when patients displayed lower RF “strength” values their outcome was better. Lower “skewness” and “strength” values might potentially be related to more homogeneous lesions, which could be related to a more favorable outcome. Radiomics might represent a step forward into personalized and tailored medicine, helping to identify patients that might benefit most from therapy.

Our research has some limitations. Firstly, we enrolled a single center retrospective cohort and no external validation was considered: performances of our multiomic models derived from cross-validation analyses. Therefore, further studies based on datasets from other centers are needed to evaluate model generalizability. Secondly, the repeatability and robustness of

radiomic features with respect to CT acquisition parameters and to manual segmentation were not addressed. We recognize the reproducibility of manual segmentations of CRC to be a potential source of variability potentially affecting the results, given the potential challenges in the identification of the boundaries of such lesions with an impact on the generalization of our model. Therefore, we look forward to future studies on larger populations with multiple readers to be involved in the segmentation process. However, the purpose of the radiomic analysis of this study was to produce preliminary results to be compared with the histopathological data.

In conclusion, this study provides the first evidence that high NICD and Jag1 expression predict early disease progression in CRC patients treated with anti-VEGF-based therapy.

Although the data must be confirmed in a larger series, the increase in intratumoral microvascular density could predict a lower response to treatment.

Further studies will be necessary to demonstrate our hypothesis that newly formed vessels in tumors expressing elevated NICD do not benefit from bevacizumab and expand our preliminary results on the potential role of radiomics to improve the prediction of outcome of CRC patients.

Data availability statement

The data that support the findings of this study are available on request from the corresponding author, [FN].

Ethics statement

The studies involving human participants were reviewed and approved by AVEN: Comitato Etico dell’Area Vasta Emilia Nord. The patients/participants provided their written informed consent to participate in this study.

Author contributions

FN, LG, RS and LB conceived the study. LG, NC, ES, GM, LL, MM, CB, AZ and GP performed the analyses. FN, LG, LB, GP, LL, GM, MM, RS, ES, CA, GLdA interpreted the data, and wrote the manuscript. GDR and FG helped to review the manuscript. All authors contributed to the article and approved the submitted version.

Funding

We acknowledge the financial donation by SNUPI Onlus.

Acknowledgment

We acknowledge the technical assistance of Debora Esposito and Katuscia Barbieri.

Conflict of interest

The authors declare that the research was conducted in the absence of any commercial or financial relationships that could be construed as a potential conflict of interest.

References

- Andersson ER, Sandberg R, Lendahl U. Notch signaling: simplicity in design, versatility in function. *Development* (2011) 138(17):3593–612. doi: 10.1242/dev.063610
- Bray SJ. Notch signalling: a simple pathway becomes complex. *Nat Rev Mol Cell Biol* (2006) 7(9):678–89. doi: 10.1038/nrm2009
- Li JL, Harris AL. Crosstalk of VEGF and notch pathways in tumour angiogenesis: therapeutic implications. *FBL* (2009) 14(8):3094–110. doi: 10.2741/3438
- Bolós V, Grego-Bessa J, de la Pompa JL. Notch signaling in development and cancer. *Endocr Rev* (2007) 28(3):339–63. doi: 10.1210/er.2006-0046
- Shimojo H, Ohtsuka T, Kageyama R. Dynamic expression of notch signaling genes in neural Stem/Progenitor cells. *Front Neurosci* (2011) 5:78. doi: 10.3389/fnins.2011.00078
- Manderfield LJ, High FA, Engleka KA, Liu F, Li L, Rentschler S, et al. Notch activation of Jagged1 contributes to the assembly of the arterial wall. *Circulation* (2012) 125(2):314–23. doi: 10.1161/CIRCULATIONAHA.111.047159
- Urs S, Roudabush A, O'Neill CF, Pinz I, Prudovsky I, Kacer D, et al. Soluble forms of the notch ligands Delta1 and Jagged1 promote in vivo tumorigenicity in NIH3T3 fibroblasts with distinct phenotypes. *Am J Pathol* (2008) 173(3):865–78. doi: 10.2353/ajpath.2008.080006
- Lu J, Ye X, Fan F, Xia L, Bhattacharya R, Bellister S, et al. Endothelial cells promote the colorectal cancer stem cell phenotype through a soluble form of jagged-1. *Cancer Cell* (2013) 23(2):171–85. doi: 10.1016/j.ccr.2012.12.021
- Campese AF, Grazioli P, de Cesaris P, Riccioli A, Bellavia D, Pelullo M, et al. Mouse sertoli cells sustain *De novo* generation of regulatory T cells by triggering the notch pathway through soluble JAGGED1. *Biol Reprod* (2014) 90(3):53, 1–10. doi: 10.1095/biolreprod.113.113803
- Huang Y, Lin L, Shanker A, Malhotra A, Yang L, Dikov MM, et al. Resuscitating cancer immunosurveillance: Selective stimulation of DLL1-notch signaling in T cells rescues T-cell function and inhibits tumor growth. *Cancer Res* (2011) 71(19):6122–31. doi: 10.1158/0008-5472.CAN-10-4366
- Negri FV, Crafa P, Pedrazzi G, Bozzetti C, Lagrasta C, Gardini G, et al. Strong notch activation hinders bevacizumab efficacy in advanced colorectal cancer. *Future Oncol* (2015) 11(23):3167–74. doi: 10.2217/fon.15.218
- Staal FCR, van der Reijdt DJ, Taghavi M, Lambregts DMJ, Beets-Tan RG, Maas M. Radiomics for the prediction of treatment outcome and survival in patients with colorectal cancer: A systematic review. *Clin Colorectal Cancer* (2021) 20(1):52–71. doi: 10.1016/j.clcc.2020.11.001
- Dohan A, Gallix B, Guieu B, le Malicot K, Reinhold C, Soyer P, et al. Early evaluation using a radiomic signature of unresectable hepatic metastases to predict outcome in patients with colorectal cancer treated with FOLFIRI and bevacizumab. *Gut* (2020) 69(3):531–539. doi: 10.1136/gutjnl-2018-316407
- Zanfardino M, Franzese M, Pane K, Cavaliere C, Monti S, Esposito G, et al. Bringing radiomics into a multi-omics framework for a comprehensive genotype-phenotype characterization of oncological diseases. *J Transl Med* (2019) 17(1):337. doi: 10.1186/s12967-019-2073-2
- Lu M, Zhan X. The crucial role of multiomic approach in cancer research and clinically relevant outcomes. *EPMA J* (2018) 9(1):77–102. doi: 10.1007/s13167-018-0128-8
- Chauvin A, Boisvert F-M. Clinical proteomics in colorectal cancer, a promising tool for improving personalised medicine. *Proteomes* (2018) 6(4):49. doi: 10.3390/proteomes6040049

Publisher's note

All claims expressed in this article are solely those of the authors and do not necessarily represent those of their affiliated organizations, or those of the publisher, the editors and the reviewers. Any product that may be evaluated in this article, or claim that may be made by its manufacturer, is not guaranteed or endorsed by the publisher.

Supplementary material

The Supplementary Material for this article can be found online at: <https://www.frontiersin.org/articles/10.3389/fonc.2023.1132564/full#supplementary-material>

- Badic B, Tixier F, Cheze Le Rest C, Hatt M, Visvikis D. Radiogenomics in colorectal cancer. *Cancers (Basel)* (2021) 13(5). doi: 10.3390/cancers13050973
- Cao D, Zheng Y, Xu H, Ge W, Xu X. Bevacizumab improves survival in metastatic colorectal cancer patients with primary tumor resection: A meta-analysis. *Sci Rep* (2019) 9(1):20326. doi: 10.1038/s41598-019-56528-2
- Adeleke S, Haslam A, Choy A, Diaz-Cano S, Galante JR, Mikropoulos C, et al. Microsatellite instability testing in colorectal patients with lynch syndrome: lessons learned from a case report and how to avoid such pitfalls. *Per Med* (2022) 19(4):277–86. doi: 10.2217/pme-2021-0128
- Benedito R, Roca C, Sörensen I, Adams S, Gossler A, Fruttiger M, et al. The notch ligands Dll4 and Jagged1 have opposing effects on angiogenesis. *Cell* (2009) 137(6):1124–35. doi: 10.1016/j.cell.2009.03.025
- Sugiyama M, Oki E, Nakaji Y, Tsutsumi S, Ono N, Nakanishi R, et al. High expression of the notch ligand jagged-1 is associated with poor prognosis after surgery for colorectal cancer. *Cancer Sci* (2016) 107(11):1705–1716. doi: 10.1111/cas.13075
- Hellström M, Phng LK, Hofmann JJ, Wallgard E, Coultas L, Lindblom P, et al. Dll4 signalling through Notch1 regulates formation of tip cells during angiogenesis. *Nature* (2007) 445(7129):776–780. doi: 10.1038/nature05571
- Tammela T, Zarkada G, Wallgard E, Murtomäki A, Suchting S, Wirzenius M, et al. Blocking VEGFR-3 suppresses angiogenic sprouting and vascular network formation. *Nature* (2008) 454(7204):656–60. doi: 10.1038/nature07083
- Siekman AF, Lawson ND. Notch signalling limits angiogenic cell behaviour in developing zebrafish arteries. *Nature* (2007) 445(7129):781–4. doi: 10.1038/nature05577
- Ellis LM, Hicklin DJ. VEGF-targeted therapy: mechanisms of anti-tumour activity. *Nat Rev Cancer* (2008) 8(8):579–91. doi: 10.1038/nrc2403
- Dufraigne J, Funahashi Y, Kitajewski J. Notch signaling regulates tumor angiogenesis by diverse mechanisms. *Oncogene* (2008) 27(38):5132–7. doi: 10.1038/onc.2008.227
- Lobov IB, Renard RA, Papadopoulos N, Gale NW, Thurston G, Yancopoulos GD, et al. Delta-like ligand 4 (Dll4) is induced by VEGF as a negative regulator of angiogenic sprouting. *Proc Natl Acad Sci* (2007) 104(9):3219–24. doi: 10.1073/pnas.0611206104
- Noguera-Troise I, Daly C, Papadopoulos NJ, Coetsee S, Boland P, Gale NW, et al. Blockade of Dll4 inhibits tumour growth by promoting non-productive angiogenesis. *Nature* (2006) 444(7122):1032–7. doi: 10.1038/nature05355
- Urs S, Turner B, Tang Y, Rostama B, Small D, Liaw L. Effect of soluble Jagged1-mediated inhibition of notch signaling on proliferation and differentiation of an adipocyte progenitor cell model. *Adipocyte* (2012) 1(1):46–57. doi: 10.4161/adip.19186
- Han W, Ye Q, Moore MAS. A soluble form of human delta-like-1 inhibits differentiation of hematopoietic progenitor cells. *Blood* (2000) 95(5):1616–25. doi: 10.1182/blood.V95.5.1616.005k31_1616_1625
- Morrison SJ, Perez SE, Qiao Z, Verdi JM, Hicks C, Weinmaster G, et al. Transient notch activation initiates an irreversible switch from neurogenesis to gliogenesis by neural crest stem cells. *Cell* (2000) 101(5):499–510. doi: 10.1016/S0092-8674(00)80860-0
- Tiemeijer LA, Ristori T, Stassen OMJA, Ahlberg JJ, de Bijl JJJ, Chen CS, et al. Engineered patterns of notch ligands Jag1 and Dll4 elicit differential spatial control of endothelial sprouting. *iScience* (2022) 25(5):104306. doi: 10.1016/j.isci.2022.104306

33. D'Assoro AB, Leon-Ferre R, Braune EB, Lendahl U. Roles of notch signaling in the tumor microenvironment. *Int J Mol Sci* (2022) 23(11):6241. doi: 10.3390/ijms23116241
34. Derakhshani A, Hashemzadeh S, Asadzadeh Z, Shadbad MA, Rasibonab F, Safarpour H, et al. Cytotoxic T-lymphocyte antigen-4 in colorectal cancer: Another therapeutic side of capecitabine. *Cancers (Basel)* (2021) 13(10):2414. doi: 10.3390/cancers13102414
35. Vandendorpe B, Durot C, Lebellec L, le Deley MC, Sylla D, Bimbai AM, et al. Prognostic value of the texture analysis parameters of the initial computed tomographic scan for response to neoadjuvant chemoradiation therapy in patients with locally advanced rectal cancer. *Radiother Oncol* (2019) 135:153–60. doi: 10.1016/j.radonc.2019.03.011
36. Wang J, Shen L, Zhong H, Zhou Z, Hu P, Gan J, et al. Radiomics features on radiotherapy treatment planning CT can predict patient survival in locally advanced rectal cancer patients. *Sci Rep* (2019) 9(1):15346. doi: 10.1038/s41598-019-51629-4
37. Dai W, Mo S, Han L, Xiang W, Li M, Wang R, et al. Prognostic and predictive value of radiomics signatures in stage I-III colon cancer. *Clin Transl Med* (2020) 10(1):288–93. doi: 10.1002/ctm2.31
38. Chu Y, Li J, Zeng Z, Huang B, Zhao J, Liu Q, et al. A novel model based on CXCL8-derived radiomics for prognosis prediction in colorectal cancer. *Front Oncol* (2020) 10:575422. doi: 10.3389/fonc.2020.575422
39. Cai D, Duan X, Wang W, Huang ZP, Zhu Q, Zhong ME, et al. A metabolism-related radiomics signature for predicting the prognosis of colorectal cancer. *Front Mol Biosci* (2021) 7:613918. doi: 10.3389/fmolb.2020.613918



OPEN ACCESS

EDITED BY

Gianluca Russo,
University of Naples Federico II, Italy

REVIEWED BY

Andrea Moreno Manuel,
Fundación de Investigación del Hospital
General Universitario de Valencia, Spain
Alessandro Passardi,
Scientific Institute of Romagna for the
Study and Treatment of Tumors (IRCCS),
Italy
David Lau,
Olivia Newton-John Cancer Research
Institute,
Australia

*CORRESPONDENCE

Cláudia S. Ferreira
✉ claudia.ferreira.cf1@roche.com
Galina Babitzki
✉ galina.babitzki@roche.com

†PRESENT ADDRESS

Johanna Bendell,
Roche Pharma Research and Early
Development, Roche Innovation Center
Basel, Basel, Switzerland

†These authors share first authorship

‡No longer employees of Roche
Diagnostics GmbH

RECEIVED 06 February 2023

ACCEPTED 31 March 2023

PUBLISHED 03 May 2023

CITATION

Ferreira CS, Babitzki G, Klamann I, Krieter O,
Lechner K, Bendell J, Vega Harring S and
Heil F (2023) Predictive potential of
angiopoietin-2 in a mCRC
subpopulation treated with
vanucizumab in the McCaVE trial.
Front. Oncol. 13:1157596.
doi: 10.3389/fonc.2023.1157596

COPYRIGHT

© 2023 Ferreira, Babitzki, Klamann, Krieter,
Lechner, Bendell, Vega Harring and Heil. This
is an open-access article distributed under
the terms of the [Creative Commons
Attribution License \(CC BY\)](https://creativecommons.org/licenses/by/4.0/). The use,
distribution or reproduction in other
forums is permitted, provided the original
author(s) and the copyright owner(s) are
credited and that the original publication in
this journal is cited, in accordance with
accepted academic practice. No use,
distribution or reproduction is permitted
which does not comply with these terms.

Predictive potential of angiopoietin-2 in a mCRC subpopulation treated with vanucizumab in the McCaVE trial

Cláudia S. Ferreira^{1*†}, Galina Babitzki^{2*†}, Irina Klamann^{1‡},
Oliver Krieter¹, Katharina Lechner¹, Johanna Bendell^{3†},
Suzana Vega Harring^{1‡} and Florian Heil¹

¹Roche Pharma Research and Early Development, Roche Innovation Center Munich,
Penzberg, Germany, ²PHCS Biostatistics & Data Management, Roche Innovation Center Munich,
Penzberg, Germany, ³Sarah Cannon Research Institute and Tennessee Oncology, Nashville,
TN, United States

Introduction: Angiopoietin-2 (Ang-2) is a key mediator of tumour angiogenesis. When upregulated it is associated with tumour progression and poor prognosis. Anti-vascular endothelial growth factor (VEGF) therapy has been widely used in the treatment of metastatic colorectal cancer (mCRC). The potential benefit of combined inhibition of Ang-2 and VEGF-A in previously untreated patients with mCRC was evaluated in the phase II McCaVE study (NCT02141295), assessing vanucizumab versus bevacizumab (VEGF-A inhibitor), both in combination with mFOLFOX-6 (modified folinic acid [leucovorin], fluorouracil and oxaliplatin) chemotherapy. To date, there are no known predictors of outcome of anti-angiogenic treatment in patients with mCRC. In this exploratory analysis, we investigate potential predictive biomarkers in baseline samples from McCaVE participants.

Methods: Tumour tissue samples underwent immunohistochemistry staining for different biomarkers, including Ang-2. Biomarker densities were scored on the tissue images using dedicated machine learning algorithms. Ang-2 levels were additionally assessed in plasma. Patients were stratified by KRAS mutation status determined using next generation sequencing. Median progression-free survival (PFS) for each treatment group by biomarker and KRAS mutation was estimated using Kaplan–Meier plots. PFS hazard ratios (and 95% confidence intervals) were compared using Cox regression.

Results: Overall low tissue baseline levels of Ang-2 were associated with longer PFS, especially in patients with wild-type KRAS status. In addition, our analysis identified a new subgroup of patients with KRAS wild-type mCRC and high levels of Ang-2 in whom vanucizumab/mFOLFOX-6 prolonged PFS significantly (log-rank $p=0.01$) by ~5.5 months versus bevacizumab/mFOLFOX-6. Similar findings were seen in plasma samples.

Discussion: This analysis demonstrates that additional Ang-2 inhibition provided by vanucizumab shows a greater effect than single VEGF-A inhibition in this subpopulation. These data suggest that Ang-2 may be both a prognostic

biomarker in mCRC and a predictive biomarker for vanucizumab in KRAS wild-type mCRC. Thus, this evidence can potentially support the establishment of more tailored treatment approaches for patients with mCRC.

KEYWORDS

angiopoietin-2, predictive biomarkers, VEGF, KRAS mutation status, phase II clinical trial, colorectal cancer, vanucizumab, bevacizumab

1 Introduction

Vascular endothelial growth factor (VEGF) is a key mediator of angiogenesis, a pivotal process in tumour growth and metastasis (1, 2), and a regulator of vascular permeability (3). Regimens based on anti-VEGF agents, such as bevacizumab, have led to improvements in outcomes for some patients with colorectal cancer (CRC) (4–8). However, the efficacy of these agents can be limited by the activation of compensatory alternative angiogenic pathways that provide the tumour with an escape mechanism(s) allowing angiogenesis to continue (9). One suggested option for obtaining further control of angiogenesis would be to combine anti-VEGF agents with other compounds that are directed towards these angiogenic escape pathways and have complementary modes of action (10, 11).

Resistance to VEGF-targeted therapies may be partly mediated by angiopoietin-2 (Ang-2), a Tie2 receptor ligand and a key regulator of angiogenesis (11, 12). Ang-2 is upregulated in several tumour types, including metastatic CRC (mCRC), and is associated with poor prognosis (13–16). Like VEGF, Ang-2 is a driver of vascular destabilisation (17), and high levels have been found to counteract the vascular-normalising effects of anti-VEGF therapy (18). In patients with mCRC receiving bevacizumab-containing therapy, those with elevated serum levels of Ang-2 had worse survival outcomes than patients with low Ang-2 levels (19). These findings suggest that Ang-2 may be a useful biomarker in patients receiving anti-angiogenic/anti-VEGF treatment and may provide a rationale for a treatment strategy involving dual inhibition of both VEGF and Ang-2.

Vanucizumab (RO5520985) is a humanised immunoglobulin (Ig)G-1-like bispecific monoclonal antibody targeting both VEGF-A and Ang-2 that has shown anti-tumour, anti-angiogenic and anti-metastatic effects in preclinical studies (20). In phase I studies, vanucizumab has been associated with marked post-infusion reductions in circulating unbound VEGF-A and Ang-2 in plasma, tumour and wound-healing biopsies, thus confirming its mechanism of action (21). It has also demonstrated an acceptable safety profile and favourable pharmacokinetic/pharmacodynamic effects in patients with advanced cancer (22). In the phase II McCaVE (Vanucizumab plus mFOLFOX-6 Versus Bevacizumab plus mFOLFOX-6 in Patients with Previously Untreated Metastatic Colorectal Carcinoma) study, conducted in previously untreated patients with mCRC, vanucizumab and bevacizumab (both plus modified [m] folinic acid [leucovorin], 5-fluorouracil and oxaliplatin [FOLFOX-6]) showed similar clinical efficacy in terms

of progression-free survival (PFS) and overall response rates (23). Hence, the efficacy seen with both agents appeared to be mediated mainly *via* VEGF-blockade. Of note, overall outcomes were worse in both treatment arms in patients with higher than median baseline Ang-2 plasma levels versus those with low/equal Ang-2 levels in the total study population (23).

There is strong evidence that Kirsten rat sarcoma virus oncogene (*KRAS*) mutation status is a predictive biomarker in mCRC in anti-epidermal growth factor receptor (EGFR) therapy (24). The *KRAS* protein acts as a regulator of downstream signalling pathways, such as cell proliferation and survival, and ultimately tumorigenesis (25). Mutations in this protein therefore promote angiogenesis, and impact the prognosis and treatment of CRC (26). *KRAS* mutations have been reported in up to ~50% of patients with CRC (26, 27) and in 36% of those with mCRC (28). Shorter survival outcomes have been reported for patients with CRC and *KRAS* mutations than for those with wild-type *KRAS* CRC (26, 28). Bevacizumab combined with chemotherapy is the recommended first-line treatment for patients with mCRC (29) as it prolongs PFS by 2–6 months, irrespective of *KRAS* mutation status (30, 31). However, limited data are available on the impact of *KRAS* mutation status on clinical outcomes in patients with mCRC treated with other anti-angiogenic agents, such as the bispecific antibody vanucizumab, which targets both VEGF-A and Ang-2.

There are currently no known predictors for the outcome of anti-angiogenic treatment. Different trials have shown mixed data on some biomarkers (e.g. VEGF-A, endothelial nitric oxide synthase, VEGFR1/R2, *KRAS* mutation status) (24, 32–35), but no clear predictors have been identified in patients with mCRC receiving anti-angiogenic/anti-VEGF treatment. The aim of this exploratory analysis was to investigate the predictive potential of biomarkers, including Ang-2, in patients with mCRC treated with vanucizumab or bevacizumab, both plus mFOLFOX-6, in the McCaVE study. We examined biomarker levels in tumour tissue and plasma (Ang-2 only) samples, and given the importance of *KRAS* mutations on survival in patients with mCRC, we stratified patients by *KRAS* mutation status.

2 Methods

In the phase II McCaVE study (NCT02141295), previously untreated patients with mCRC were randomised to receive either vanucizumab/mFOLFOX-6 or bevacizumab/mFOLFOX-6.

The study design, patient characteristics and treatment details have been published (23). All patients provided written informed consent as approved by local institutional review boards.

2.1 Tissue biomarker sampling and analysis

Tumour tissue (from surgical specimens or biopsies) were collected from all participating patients before treatment and analysed separately by treatment arm.

Archival tumour tissue samples were obtained, embedded in paraffin blocks and sectioned (HistogeneX, now CellCarta, Antwerp, Belgium). Eight 2.5–4.0 µm thick sections per tumour block were processed according to routine histology and immunohistochemistry (IHC) protocols. Sections were stained with haematoxylin and eosin (H&E) or subjected to chromogenic brightfield simplex, duplex or triplex assays developed and validated at the Roche Innovation Center Munich (Penzberg, Germany). Tumour samples were assessed histologically and only those determined to be from a primary CRC were included in the biomarker and mutational status exploratory analysis presented here.

Details on IHC assays used for staining for the various biomarkers analysed in tumour tissue samples are given in Table 1. Ang-2 (biomarker of angiogenesis) and CD34 (biomarker of vessels in the total tumour vasculature) were assessed using duplex staining for Ang-2 (ANGPT2)/CD34. Perforin (PRF1, cytolytic protein expressed by CD8+ T-cells)/CD3 (total T-cell marker), MKi67 (proliferating T-cell marker)/

CD8 (cytotoxic T-cell marker) and Forkhead box P3 (FOXP3, regulatory T-cell marker) staining was used to assess densities of lymphocyte subpopulations. CD163+ CD68+ staining was used to assess the percentage of area coverage of M2 macrophages in the tumour area, the cleaved form of caspase 3 (CLEAVED CASP3 [CC3]) was used as a marker for apoptosis and carbonic anhydrase isoform 9 (CA9) was used as a marker of hypoxia.

2.2 Automated tissue image analyses and visual slide assessments

Tissue slides were scanned at 20× magnification using a high-throughput whole-slide scanner (Ventana iScan HT, Ventana Medical Systems, Inc., Tucson, AZ, USA). Tissue sample quality and consistency of staining were assessed at the Roche Innovation Center Munich, Germany. A digital pathology algorithm was used to detect the tissue area on the slide. Tumour, necrotic and exclusion areas were annotated manually by a certified pathologist according to internal guidelines. Digital whole-slide scans were subjected to automated image analysis using the in-house developed IRIS digital pathology platform, where the images were scored using dedicated whole-slide automated image analysis algorithms written in Matlab (www.mathworks.com).

The digital pathology algorithms included a colour deconvolution step for stain unmixing (36), followed by a candidate extraction step. Machine learning classification (random forest, logistic regression with L1 regularisation or support vector

TABLE 1 Staining details for biomarkers analysed in tumour tissue samples.

Biomarker	Antibody clone	Detection system	Staining instrument
Ang-2 (ANGPT2)/CD34 duplex staining	Ang2 clone K-20H6 (Roche Diagnostics GmbH) (monoclonal rabbit Ab) self-prepared dispenser CD34 clone QBEnd/10 (Ventana Medical Systems) (monoclonal mouse Ab) ready to use dispenser	Ultraview AP Red (CD34) (Ventana 760-501) Optiview DAB (Ang-2) (Ventana 760-099)	Ventana Discovery XT
Perforin/CD3 duplex staining	Anti-PRF1 clone 5B10 (Abcam) (monoclonal mouse Ab) self-prepared dispenser Anti-CD3E clone 2GV6 (Ventana Medical Systems) (monoclonal rabbit Ab) ready to use dispenser	Ultraview AP Red (CD3) (Ventana 760-501) Optiview DAB (perforin) (Ventana 760-099)	Ventana Discovery Ultra
MKi67/CD8 duplex staining	MKi67 clone 30-9 (Ventana Medical Systems) (monoclonal rabbit Ab) ready to use dispenser CD8 clone SP239 (Spring bioscience) (monoclonal rabbit Ab) self-prepared dispenser	Ultraview AP Red (CD8) (Ventana 760-501) Optiview DAB (MKi68) (Ventana 760-099)	Ventana Discovery Ultra
FOXP3	236A/E7 (CNIO, Madrid) (monoclonal mouse Ab) self-prepared dispenser	Optiview DAB (Ventana 760-099)	Ventana Benchmark XT
CD163/CD68 duplex staining	Anti-CD163 clone MRQ-26 (Cell Marque) (monoclonal mouse Ab) ready to use dispenser Anti-CD68 clone PG-M1 (DAKO) (monoclonal mouse Ab) ready to use dispenser	Ultraview AP Red (CD68) (Ventana 760-501) Optiview DAB (CD163) (Ventana 760-099)	Ventana Discovery XT
CC3/CA9/MKi67 triplex staining	CASP3 clone J20H1L1 (Spring Bioscience) (monoclonal rabbit Ab) self-prepared dispenser CA9 clone 1G7 (Origene Technologies) (monoclonal mouse Ab) self-prepared dispenser MKi67 clone 30-9 (Ventana Medical Systems) (monoclonal rabbit Ab) ready to use dispenser	Iview Blue (CC3) (Ventana 760-097) Optiview DAB (CA9) (Ventana 760-700) Ultraview Red (MKi67) (Ventana 760 501)	Benchmark XT

Ab, antibody.

All chromogenic simplex, duplex or triplex assays are brightfield and were developed and validated at the Roche Innovation Center Munich.

machine) was used to classify different phenotypes based on a set of features and to remove non-specific stained structures. The x and y coordinates of the detected objects were recorded and displayed in the IRIS viewer in the form of polygons or seeds (cell centroid).

Algorithm results overlaid on the tissue images were visually checked for accuracy by a pathologist who also manually annotated and excluded image artefacts. Tissue annotations and algorithm results (x,y coordinates and respective labels) were stored in a spatial database for further data analysis.

The reports generated were cell densities (number of cells per mm^2) for the phenotypes total CD3+, PRF1+ CD3E+, PRF1+ CD3E-, total CD8+, MKi67+ CD8A+, MKi67- CD8A+, FOXP3+, MKi67+, CC3+, and CA9+, vessel densities (number of vessels per mm^2) for the phenotypes ANGPT2+ CD34+ (Ang-2) and CD34+ (total), and ratios for (ANGPT2+ CD34+)/CD34+ (relative amount of Ang-2+ vessels to total number of vessels), (PRF1+ CD3E+)/total CD3+ (relative amount of natural killer T cells to total CD3), (MKi67+ CD8A+)/total CD8+ (relative amount of proliferating CD8 to total CD8) and CD163+ CD68+ (percentage of area coverage of M2 macrophages in tumour area).

All digital pathology scoring algorithms were verified for performance during a development phase before use on clinical trial data. Detailed descriptions can be found in the [Supplementary Material](#).

2.3 Plasma sampling and analysis

Blood (approximately 6 mL) samples were taken prior to the receipt of treatment for the determination of free and total Ang-2 circulating levels. Samples were stabilised in K3-EDTA. Free Ang-2 levels were assessed using an enzyme-linked immunosorbent assay (Quantikine®). Analytical methods have been reported in more detail (21, 37).

2.4 Determination of KRAS mutation status

Specimens with >50% tumour content were macro-dissected from archival formalin-fixed paraffin-embedded tumour samples, and the DNA was extracted. Only samples meeting the minimum amplifiable DNA copy number for sequence enrichment (quantified using Asuragen's QuantideX® DNA QC assay) (38) were processed further. Sequence enrichment and library preparation were carried out using the QuantideX® Pan Cancer kit, followed by next generation sequencing (NGS) (Illumina MiSeq® system) (39). Target median amplicon coverage was 1000-fold. The QuantideX® NGS Pan Cancer panel interrogates 46 gene regions (amplicons) within 21 oncogenes, including *KRAS* (codon regions 4–15, 55–65, 104–118 and 137–148; for a full list of oncogenes see Kelnar et al. (40)). Patients were classified as having mutated or wild-type *KRAS*.

2.5 Statistical analysis

All patients randomised to treatment with either vanucizumab/mFOLFOX-6 or bevacizumab/mFOLFOX-6 for whom data on *KRAS*

mutation status were available were included in this exploratory analysis. To assess the predictive potential of biomarkers, the association between PFS and the density of various biomarkers in tissue samples and circulating levels of free Ang-2 in patient plasma samples was explored. PFS was the primary endpoint of the McCAVE clinical trial and was defined as the time from randomisation to the date of first documented occurrence of progression based on Response Evaluation Criteria In Solid Tumors (RECIST) version 1.1 criteria (41), as determined by the investigator, or death from any cause on study, whichever occurred first.

All analyses were performed separately in tissue and plasma samples from each of the two study arms, stratified by *KRAS* mutation status (wild-type vs mutated). Biomarker density in tumour samples and baseline Ang-2 levels in plasma were classified as higher than (high) or lower/equal (low) to the median value. Median PFS for each treatment group by biomarker level (high or low) and by *KRAS* mutation status (wild-type or mutated) was estimated using Kaplan–Meier plots. Between-group differences in PFS were compared statistically using univariate Cox models. For each of the specified subgroups, hazard ratios (HRs) and 95% confidence intervals (CIs) were calculated for the vanucizumab/mFOLFOX-6 arm relative to the bevacizumab/mFOLFOX-6 arm using Cox regression. Statistical analyses were conducted using JMP®, Version 15.2.0. SAS Institute Inc., Cary, NC, USA, 1989–2021.

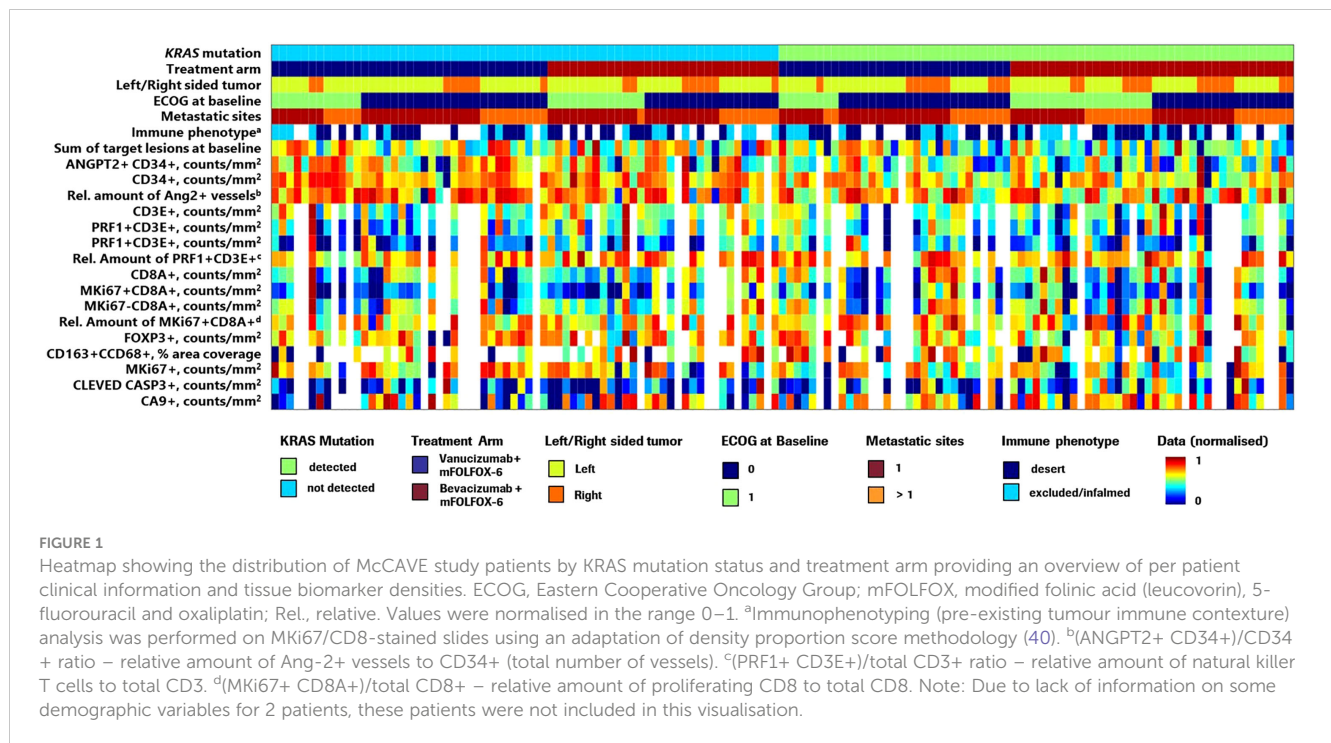
3 Results

3.1 Patient population

Of 189 patients enrolled in the McCAVE phase II study, 94 were randomised to the vanucizumab/mFOLFOX-6 arm and 95 were randomised to the bevacizumab/mFOLFOX-6 arm. Baseline median age (64.0/63.0 years), and proportion of patients with left-sided tumours (75.3%/61.1%) or >1 metastatic site (63.8%/63.2%) were broadly comparable for the two groups; however, greater proportions of participants receiving vanucizumab/mFOLFOX-6 were male (59.6%/40.0%) and had an ECOG performance 0 (63.8%/49.5%) ([Supplementary Table 1](#)). *KRAS* mutation status data were available for 80 patients receiving vanucizumab/mFOLFOX-6 and 81 receiving bevacizumab/mFOLFOX-6; 37 (46.3%) and 45 (55.6%), respectively, carried a *KRAS* mutation. A breakdown of the *KRAS* mutation landscape ([Supplementary Figure 1](#)) shows that the *KRAS* mutations primarily occurred at codons 12 and 13 of exon 2. A heatmap of the McCAVE study cohort at baseline by known *KRAS* mutation status and treatment arm is presented in [Figure 1](#). This provides a descriptive overview of baseline patient population information and associated per-patient tissue biomarker densities. There is no clear relationship between Ang-2 expression and the listed patient demographics.

3.2 Biomarker analyses

[Figure 2](#) presents the Forest plots of PFS HRs (95% CI) of vanucizumab/FOLFOX-6 versus bevacizumab/FOLFOX-6 stratified for each tissue biomarker dichotomised by its median value (see [Supplementary Table 2](#)) and by *KRAS* mutations status. In patients



with wild-type *KRAS* and high baseline densities of Ang-2+ vessels (ANGPT2+ CD34+), there was a PFS benefit with vanucizumab-based treatment over bevacizumab/mFOLFOX-6, as demonstrated by the 95% CIs of the HR below 1. A similar finding was observed for the subgroup of *KRAS* wild-type patients with a high relative amount of Ang-2+ vessels to the total number of vessels.

An analogous observation (95% CIs of the HR below 1) was also seen in patients with wild-type *KRAS* and high levels of CC3, again indicating a PFS benefit with vanucizumab/FOLFOX-6 over bevacizumab/mFOLFOX-6. Higher than median baseline levels of MKi67 and CA9 showed a trend towards a PFS benefit (upper 95% CI of the HR just over 1) in patients with wild-type *KRAS* treated with vanucizumab/mFOLFOX-6 versus bevacizumab/mFOLFOX-6.

In patients with mutant *KRAS* and high baseline densities of Ang-2, the PFS benefit favoured bevacizumab/FOLFOX-6 (95% CIs of the HRs above 1). In this sub-population, the relative amount of Ang-2+ vessels also correlated with a favourable clinical outcome. Likewise, high median baseline levels of MKi67 showed a trend towards a PFS benefit (lower 95% CI of the HR just below 1) in patients with mutant *KRAS* treated with bevacizumab/mFOLFOX-6 versus vanucizumab/mFOLFOX-6.

As a clear PFS benefit (i.e. 95% CIs of the HRs above or below 1) for either bevacizumab/mFOLFOX-6 or vanucizumab/mFOLFOX-6 was observed for higher than median baseline levels of Ang-2, and as the additional blockade of this angiopoietin represents the main difference in mode of action between bevacizumab and vanucizumab, we decided to focus on the Ang-2 analysis in more detail.

3.3 Ang-2 tissue analysis

Data on *KRAS* mutation status and Ang-2 in tissue samples were available for 139 patients (68 receiving vanucizumab/

mFOLFOX-6 and 71 bevacizumab/mFOLFOX-6) (Table 2A); 71 (51%) of whom had mutant *KRAS*.

High densities of Ang-2+ vessels were associated with a significantly longer PFS in patients with wild-type *KRAS* treated with vanucizumab when compared with those who received bevacizumab (median 386 vs 223 days, difference: 163 days in favour of vanucizumab, $p=0.01$; see Kaplan–Meier curves Figure 3A and Table 2A). This trend was not seen in *KRAS* wild-type patients with low Ang-2+ vessel densities or in *KRAS* mutant patients with high or low Ang-2+ vessel densities (Figure 3B). Indeed, in *KRAS* mutant patients, high densities of Ang-2+ vessels were associated with a significantly longer PFS in patients treated with bevacizumab when compared with those who received vanucizumab (median 394 vs 219 days, difference: 175 days in favour of bevacizumab, $p=0.01$; Table 2A).

Representative IHC images of higher than median and lower than median Ang-2+ CD34+ tissue staining are shown in Figure 4.

Information on response to treatment was available for 134 patients (64 receiving vanucizumab/mFOLFOX-6 and 70 bevacizumab/mFOLFOX-6). Best overall response according to median tissue density of Ang-2+ and stratified by *KRAS* mutation status is shown in Table 3.

3.4 Ang-2 plasma analysis

To confirm the results obtained in tissue samples, we also investigated the association between higher and lower than median plasma levels of Ang-2 and PFS in patients with and without mutant *KRAS* tumours.

Data on *KRAS* mutation status and Ang-2 in plasma were available for 156 patients (77 receiving vanucizumab/mFOLFOX-6 and 79

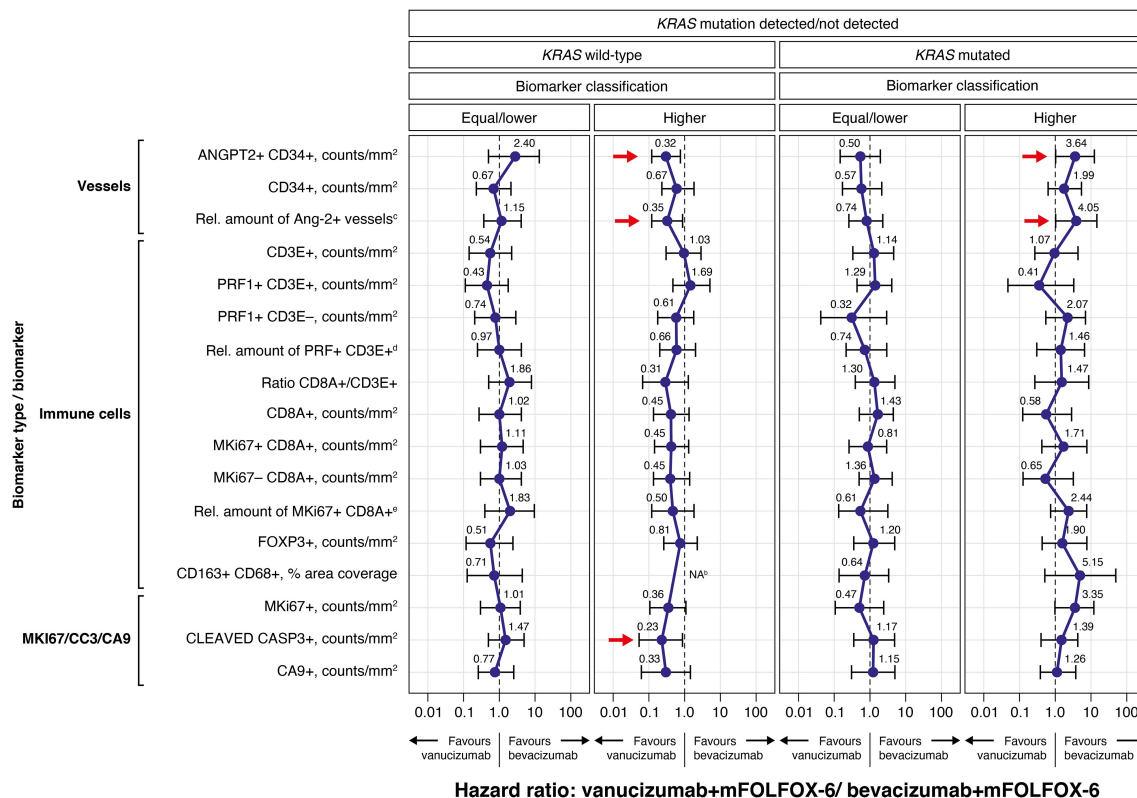


FIGURE 2

Forest plots of progression-free survival (PFS) hazard ratios (95% CI) for the vanucizumab/mFOLFOX-6 arm relative to the bevacizumab/mFOLFOX-6 arm for each tissue biomarker, dichotomised by the median value^a, and by *KRAS* mutation status (wild-type vs. mutated), calculated using Cox regression. Each error bar is constructed using the minimum and maximum of the data. mFOLFOX, modified folinic acid (leucovorin), 5-fluorouracil and oxaliplatin; Rel., relative. ^aMedian values for each biomarker can be found in [Supplementary Table 2](#). ^bThe hazard ratio estimation for CD163+ CD68+ macrophages not shown as the upper confidence interval could not be reliably estimated (however, the point estimate was close to zero). ^c(ANGPT2+ CD34+)/CD34+ ratio – relative amount of Ang-2+ vessels to CD34+ (total number of vessels). ^d(PRF1+ CD3E+)/total CD3+ – relative amount of natural killer T cells to total CD3. ^e(MKi67+ CD8A+)/total CD8+ – relative amount of proliferating CD8 to total CD8.

receiving bevacizumab/mFOLFOX-6); 78 (50%) of whom had mutant *KRAS* tumours ([Table 2B](#)). In patients with wild-type *KRAS* and higher than median baseline Ang-2 levels (see [Supplementary Table 2](#)), median PFS estimated from the Kaplan–Meier curves was significantly longer (median PFS 361 vs 224 days; difference: 137 days, $p=0.048$) in patients who received vanucizumab/mFOLFOX-6 than in those treated with bevacizumab/mFOLFOX-6 ([Figure 5A](#); [Table 2B](#)).

No similar trend was seen in *KRAS* wild-type patients with low Ang-2 levels or in *KRAS* mutant patients with high or low Ang-2 levels ([Figure 5B](#)). The above-reported benefit of bevacizumab in *KRAS* mutant patients with high tissue densities of Ang-2+ was not confirmed in plasma sample analyses.

4 Discussion

The aim of this exploratory analysis, conducted in patients with mCRC, was to identify potential predictive biomarkers for a survival benefit with anti-angiogenic treatment. Given its reported impact on patient survival ([26](#), [28](#)), patients were stratified by *KRAS* mutation status. Identifying predictors for the outcome of anti-

angiogenic treatment in patients with mCRC could eventually guide the development of patient enrichment strategies.

In this study, in mCRC patients with wild-type *KRAS*, higher than median tissue baseline densities of Ang-2 positive vessels were associated with a significant PFS benefit of 163 days (~5.5 months) in patients treated with vanucizumab/mFOLFOX-6 versus those treated with bevacizumab/mFOLFOX-6. Similar findings were seen in plasma samples from wild-type *KRAS* patients, with high baseline Ang-2 levels associated with a PFS benefit of 137 days in those treated with vanucizumab/mFOLFOX-6 versus bevacizumab/mFOLFOX-6.

Previous research has suggested that Ang-2 is a useful prognostic factor in mCRC patients, with high baseline levels associated with shorter overall survival in a number of studies (e.g. Jary et al. ([15](#)), Goede et al. ([19](#)), Chung et al. ([42](#))). Previously reported results from the McCaVE study found that baseline plasma Ang-2 levels were prognostic for PFS in patients receiving vanucizumab or bevacizumab plus chemotherapy; high Ang-2 plasma levels at baseline were associated with a shorter PFS compared with low levels ([23](#)).

Consistent with these findings, the current exploratory analysis shows that, overall, low baseline levels of Ang-2 were associated

TABLE 2 Median progression-free survival, estimated using Kaplan-Meier methodology, stratified by *KRAS* mutation status and treatment arm.

(A) Tissue samples										
KRAS wild-type (n=68)										
		Vanucizumab/mFOLFOX-6 (n=38)			Bevacizumab/mFOLFOX-6 (n=30)			Difference in PFS** (days)	HR (95% CI) ^a	Log-rank p-value
		n	PFS (days)	Lower–upper 95% (days)	n	PFS (days)	Lower–upper 95% (days)			
Ang-2+	Higher***	24	386	320–559	17	223	170–338	163	0.32 (0.13; 0.82)	p=0.01 ^b
	Lower***	14	304	304–337	13	445	200–NA	-141	2.40 (0.46; 12.46)	p=0.17
KRAS mutation (n=71)										
		Vanucizumab/mFOLFOX-6 (n=30)			Bevacizumab/mFOLFOX-6 (n=41)			Difference in PFS** (days)	HR (95% CI) ^a	Log-rank p-value
		n	PFS (days)	Lower–upper 95% (days)	n	PFS (days)	Lower–upper 95% (days)			
Ang-2+	Higher***	12	219	56–343	17	394	225–459	-175	3.64 (1.05; 12.60)	p=0.01 ^b
	Lower***	18	381	237–NA	24	309	222–515	72	0.50 (0.14; 1.80)	p=0.16
(B) Plasma samples										
KRAS wild-type (n=78)										
		Vanucizumab/mFOLFOX-6 (n=42)			Bevacizumab/mFOLFOX-6 (n=36)			Difference in PFS** (days)	HR (95% CI) ^a	Log-rank p-value
		n	PFS (days)	Lower–upper 95% (days)	n	PFS (days)	Lower–upper 95% (days)			
Ang-2	Higher***	21	361	304–386	17	224	200–282	137	0.39 (0.14; 1.02)	p=0.048 ^b
	Lower***	21	394	337–NA	19	486	284–NA	-92	0.84 (0.26; 3.03)	p=0.83
KRAS mutation (n=78)										
		Vanucizumab/mFOLFOX-6 (n=35)			Bevacizumab/mFOLFOX-6 (n=43)			Difference in PFS** (days)	HR (95% CI) ^a	Log-rank p-value
		n	PFS (days)	Lower–upper 95% (days)	n	PFS (days)	Lower–upper 95% (days)			
Ang-2	Higher***	16	343	62–NA	17	292	175–459	51	0.97 (0.32; 2.96)	p=0.96
	Lower***	19	265	219–NA	26	338	222–444	-73	0.99 (0.33; 2.96)	p=0.99

(A) By baseline Ang-2 densities in tissue samples (n=139)*; (B) by baseline plasma angiopoietin-2 concentration (n=156)*.

*Patients for whom sufficient tumour tissue was available or for whom DNA extraction was successful.

**PFS (vanucizumab/mFOLFOX-6) – PFS (bevacizumab/mFOLFOX-6).

***Baseline Ang-2+ densities/Ang-2 levels were classed as higher or lower than the median value: 85.2 and 22.0 counts/mm² in biopsies and surgical specimens, respectively/3.0 ng/mL in plasma samples.

^aHRs and 95% CIs calculated using univariate Cox regression.

^bValue is significant.

Ang-2, angiopoietin-2; CI, confidence interval; HR, hazard ratio; NA, not available; PFS, progression-free survival.

with longer PFS than high Ang-2 levels, especially in patients with wild-type *KRAS* status. Although wild-type *KRAS* is generally associated with a better prognosis than mutated *KRAS* in patients with CRC (26, 28, 43), the results of our study demonstrate additionally, for the first time, that those wild-type *KRAS* patients who were at risk of a poorer outcome (i.e. those with high Ang-2 levels) had a significant PFS benefit if they received vanucizumab treatment instead of bevacizumab. The likely mechanism underlying this observation is that the additional blocking of Ang-2 signalling pathways with vanucizumab counteracts the Ang-2 upregulation escape mechanism that has previously been described (11). None of the above-mentioned studies reporting on the prognostic significance of Ang-2 in mCRC examined patients by *KRAS* mutation status (15, 19, 23, 42). A study by Peeters et al. (44), which found no association between baseline Ang-2 levels and PFS

in patients with mCRC receiving trebananib, an investigational peptide-Fc fusion protein that neutralises the interaction between angiopoietins-1/-2 and the Tie2 receptor, with or without chemotherapy, did examine patients by *KRAS* mutation status, but found no evidence that this impacted results. However, Peeters et al. (44) did not report any subgroup analysis of biomarkers (e.g. Ang-2) according to *KRAS* mutation status.

The observed significant PFS benefit for high density of Ang-2 positive vessels in *KRAS* wild-type patients treated with vanucizumab was accompanied by a parallel result for high levels of CC3. This biomarker of apoptosis showed a PFS benefit for vanucizumab over bevacizumab when present at baseline in higher than median levels in the *KRAS* wild-type subpopulation (Figure 2). Also of note is a similar trend shown by CA9 (hypoxia) and MKi67 (proliferation), which could be indicative that the fast growth of the

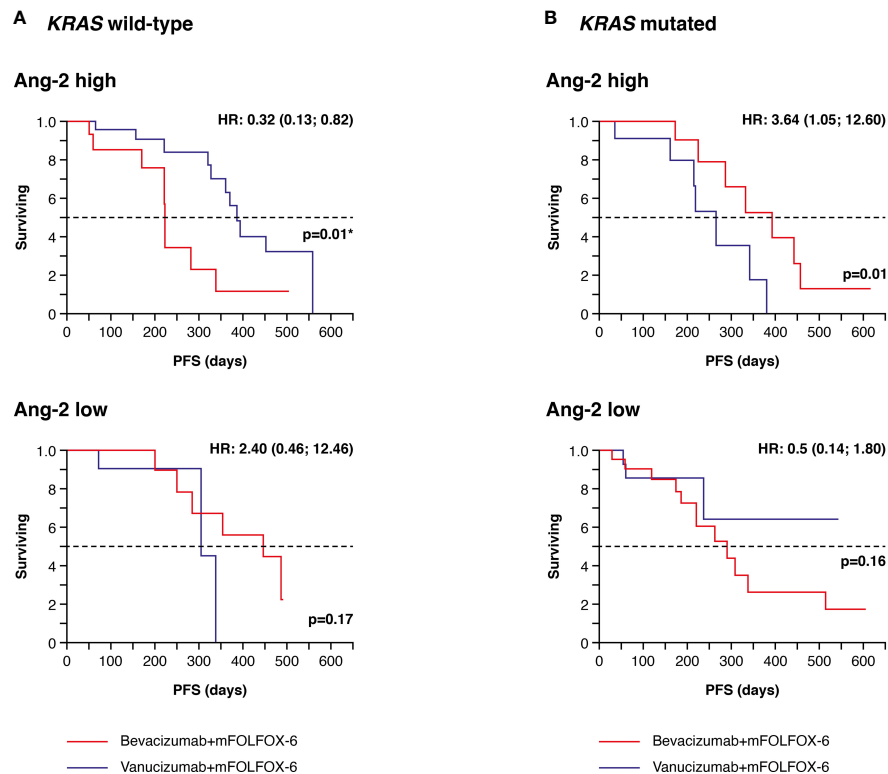


FIGURE 3

Kaplan–Meier plots of progression-free survival (PFS) in tumour tissue samples. (A) Patients with wild-type *KRAS* and higher (high) or lower/equal (low) median levels of baseline angiopoietin-2 (Ang-2)^a treated with vanucizumab/mFOLFOX-6 or bevacizumab/mFOLFOX-6. (B) Patients with mutant *KRAS* and high or low baseline angiopoietin-2 (Ang-2) treated with vanucizumab/mFOLFOX-6 or bevacizumab/mFOLFOX-6. Numbers of patients at risk at each time point are shown in Supplementary Table 3. mFOLFOX, modified folinic acid (leucovorin), 5-fluorouracil and oxaliplatin. ^aMedian values for Ang-2 can be found in Supplementary Table 2. Hazard ratios (HRs) and 95 confidence intervals (CIs) were calculated using univariate Cox regression. p-values are from the log-rank test. *Value is significant.

tumour in these previously untreated patients is not being supported at the same rate by the formation of new tumour neo-vascularisation, resulting in apoptosis triggered by hypoxia (45), and for CD8-related phenotypes.

Altogether our data highlight the interplay between these biomarkers in the underlying tumour growth mechanism. The increased need for oxygen and nutrients by growing tumours, added to the immature and inefficient tumour-associated vasculature, leads to a hypoxic microenvironment (46) that activates the Ang-2 signalling pathway, providing further vessel sprouting and, hence, potentiating angiogenesis (47, 48). Indeed, Ang-2 has been shown to be present in higher concentrations only at sites undergoing vascular remodelling and in a hypoxic tumour microenvironment (48). With our data showing that *KRAS* wild-type patients with high densities at baseline of Ang-2, CC3 and CA9 benefit from vanucizumab treatment, we hypothesise that in this ‘Ang-2-rich’ group of patients the added inhibition of Ang-2 is more effective in slowing tumour growth and metastasis than VEGF inhibition alone, counteracting tumour escape mechanisms, thus allowing increased levels of vessel normalisation and immune cell infiltration, by upregulation of the expression of adhesion molecules to which T-cells bind in order to cross the endothelial cells layer (49, 50). The normalisation of the tumour vasculature, and more generally of the tumour microenvironment, stimulates T-cell

activation (49) and contributes to a more efficient reach of the combined FOLFOX chemotherapy.

We additionally investigated the association of the different patient sub-populations, given by the Ang-2 and *KRAS* patient stratification, with best overall response (assessed according to Response Evaluation Criteria in Solid Tumours [RECIST] 1.1 criteria) and observed that a greater number of patients responded to vanucizumab than to bevacizumab in the *KRAS* wild-type high Ang-2 population, which also suggests that this subpopulation benefits more from the dual inhibition of Ang-2 and VEGF-A.

No association was observed between PFS and high/low baseline tissue densities of CD34 (used as a biomarker of vessels), which suggests that the prolongation of PFS observed with vanucizumab versus bevacizumab in patients with wild-type *KRAS* and high levels of Ang-2 is an effect that cannot be extended to the general vessels, and can be considered a result of the additional Ang-2 blockade seen with vanucizumab.

Overall, our current analysis suggests that, although high Ang-2 levels remain a negative prognostic biomarker in mCRC, vanucizumab treatment has the potential to turn this negative prognostic into a positive predictive biomarker in the *KRAS* wild type mCRC subpopulation. It also underscores the importance of investigating biomarker combinations for patient stratification rather than looking at biomarkers, gene mutations, etc., in

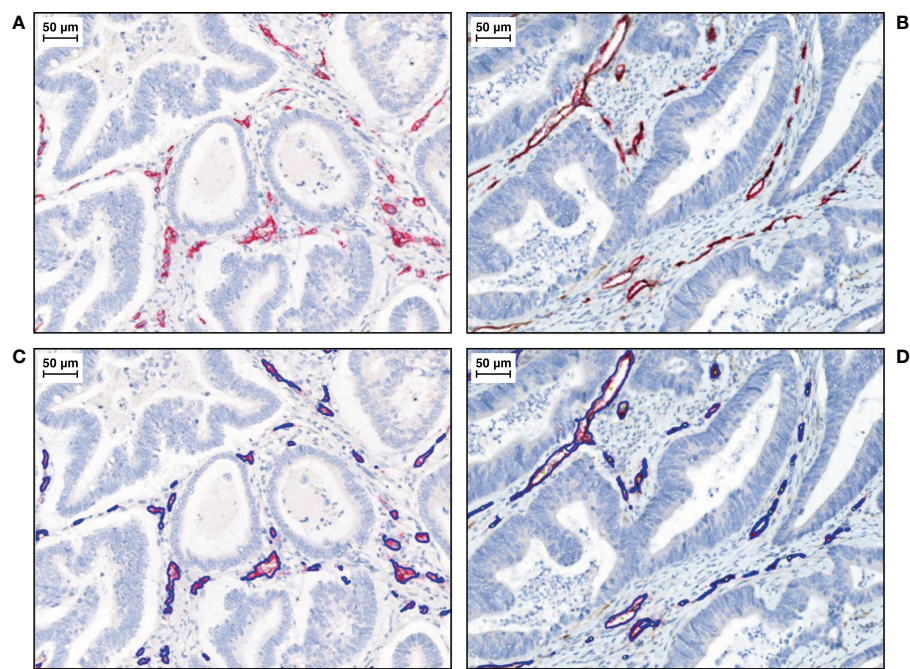


FIGURE 4
Representative IHC images of duplex Ang-2+ CD34+ tissue staining, with CD34+ endothelial cells stained in red (total vessel population) and Ang-2 + endothelial cells stained in DAB (brown). Haematoxylin is stained in blue. **(A)** Lower than median and **(B)** higher than median.^aWith algorithm results overlays on **(C)** lower than median and **(D)** higher than median. IHC, immunohistochemistry.

isolation. In this analysis’s cohort, ~30% of the patients have at baseline both Ang-2 high levels (dichotomised according to the median) and *KRAS* wild-type status (Table 2).

In contrast to our above findings, the Forest plot of PFS HRs for vanucizumab/FOLFOX-6 versus bevacizumab/FOLFOX-6 showed that patients with *KRAS* mutations and high tissue Ang-2 positive vessels responded better to bevacizumab than to vanucizumab. This was seen in the analyses of Ang-2 levels in tissue (Ang-2 presence in vessels’ endothelial cells only) but not in plasma. It should be borne in mind that *KRAS* mutations are heterogeneous, and that *KRAS*

mutations in different codons dictate a distinct angiogenic profile (51–53), which could impact the efficacy of different administered therapies (51, 52). Hence, targeting Ang-2 may be less effective in a *KRAS*-mutated population. Our *KRAS* mutated mCRC cohort exhibited typical heterogeneity regarding mutation subtypes, with most *KRAS* mutations occurring at codons 12 and 13 of exon 2 (Supplementary Figure 1) (53). G12D, the most common subtype identified, has been reported to be significantly associated with poor PFS (43). However, the low patient numbers in each *KRAS* mutation/treatment/Ang-2 subgroup in our dataset precluded further

TABLE 3 Best overall response according to median Ang-2+ density.

<i>KRAS</i> mutation status	Treatment arm	Ang-2+ median density	Best overall response*			
			Progressive disease	Stable disease	Partial response	Complete response
KRAS wild-type	Vanucizumab/mFOLFOX-6	Higher**	0	7	17	0
		Lower**	0	8	6	0
	Bevacizumab/mFOLFOX-6	Higher**	2	5	8	1
		Lower**	0	3	9	1
KRAS mutation	Vanucizumab/mFOLFOX-6	Higher**	2	9	1	0
		Lower**	1	5	7	1
	Bevacizumab/mFOLFOX-6	Higher**	0	8	10	0
		Lower**	2	11	10	0

*Assessed according to Response Evaluation Criteria in Solid Tumours (RECIST) 1.1 criteria.
**Baseline Ang-2+ densities/Ang-2 levels were classed as higher or lower than the median value: 85.2 and 22.0 counts/mm² in biopsies and surgical specimens, respectively/3.0 ng/mL in plasma samples.

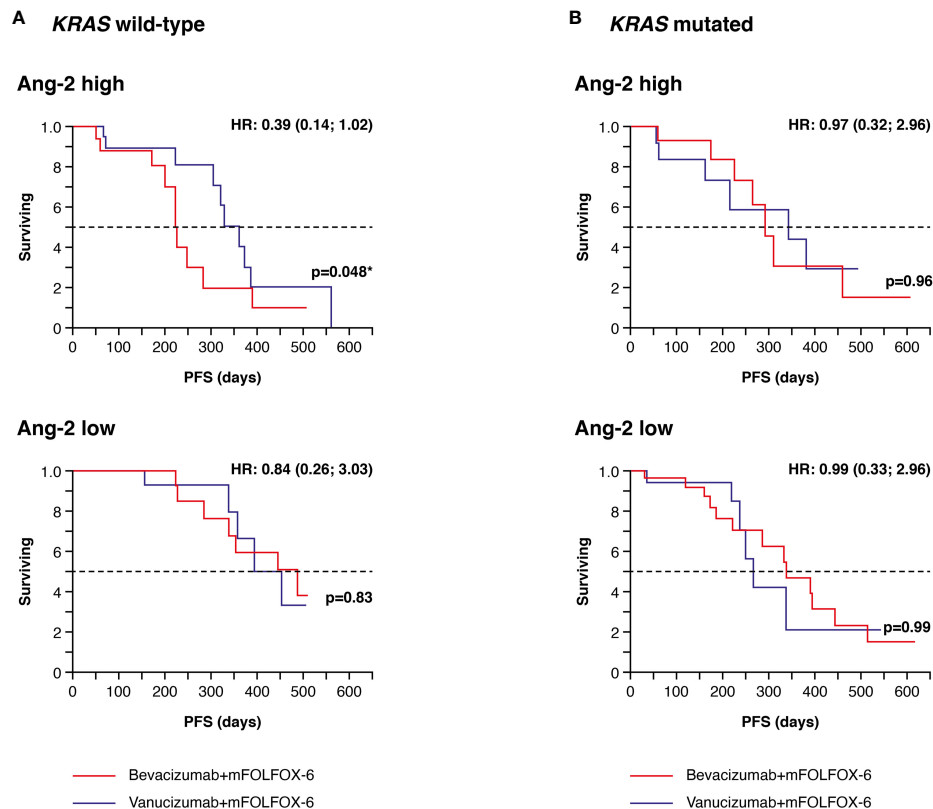


FIGURE 5

Kaplan–Meier plots of progression-free survival (PFS) in plasma samples. (A) Patients with wild-type *KRAS* and higher (high) or lower/equal (low) median levels of baseline angiopoietin-2 (Ang-2)^a treated with vanucizumab/mFOLFOX-6 or bevacizumab/mFOLFOX-6. (B) Patients with mutant *KRAS* and high or low baseline Ang-2 treated with vanucizumab/mFOLFOX-6 or bevacizumab/mFOLFOX-6. Numbers of patients at risk at each time point are shown in [Supplementary Table 3](#). mFOLFOX, modified folinic acid (leucovorin), 5-fluorouracil and oxaliplatin. ^aMedian values for Ang-2 can be found in [Supplementary Table 2](#). Hazard ratios (HRs) and 95 confidence intervals (CIs) were calculated using univariate Cox regression. p-values are from the log-rank test. *Value is significant.

stratification by *KRAS* mutation subtype and, hence, exploration of their association with clinical outcome and potential mechanisms of effect.

Overall, these findings suggest that although Ang-2 status seems to have a potential predictive value in *KRAS*-wild type patients, favouring vanucizumab over bevacizumab, it has no impact on treatment choice and outcome in the *KRAS*-mutated population. Recent advances have been made in the field of *KRAS*-directed therapy with several registered trials targeting different *KRAS* mutation variants (54, 55). As our understanding evolves on both angiogenesis and the influence of *KRAS*, the search for treatment options for these patients with an unmet need for therapies that account for their a priori disadvantage might lead to the investigation of novel combination therapies, similar to previous studies assessing anti-angiogenic and immunotherapy combination treatment (56).

Strengths of our study include that our finding of an association between high levels of Ang-2 and improved PFS in vanucizumab-treated patients with wild-type *KRAS* was seen in tumour tissue data and confirmed in plasma data in separate analyses. The patient subgroups derived from this cohort after stratification were relatively balanced, both in terms of *KRAS* mutation status and tissue biomarker and plasma Ang-2 levels, which precluded the over- or under-representation of specific patient subpopulations.

Limitations include that this analysis of McCAVE study data was exploratory, hypothesis-generating, and McCAVE was an early phase clinical trial in which typically the number of enrolled patients is small; hence, the low sample sizes of the patient groups analysed, resulting from the stratification of patients by *KRAS* status and baseline biomarker levels, limit the statistical power of the analysis. An additional limitation is that no post-treatment biomarker or gene mutation status data are available to determine changes over time or in response to treatment. Since this work is an exploratory *post-hoc* analysis, further studies are required for hypothesis confirmation.

Other bispecific antibodies targeting VEGF/Ang-2 have shown promising antitumour activity in preclinical studies and in patients with solid tumours (57, 58). Although the clinical development of vanucizumab for cancer treatment was discontinued following the finding of a similar PFS benefit with vanucizumab and bevacizumab in the overall McCAVE study population (i.e. the primary endpoint of the study was not met), the vessel stabilisation benefit provided by dual inhibition of Ang-2 and VEGF-A was further leveraged in ophthalmology in the treatment of neovascular age-related macular degeneration and visual impairment due to diabetic macular oedema, resulting in the development of the bispecific antibody faricimab (59).

In summary, exploratory analyses of biomarker levels in baseline tumour tissue and plasma samples from patients with

previously untreated mCRC stratified for *KRAS* mutation status, suggest a subgroup of patients with *KRAS* wild-type and higher than median levels of baseline Ang-2 in whom vanucizumab/mFOLFOX-6 was associated with a significant survival benefit of ~5.5 months over patients treated with bevacizumab/mFOLFOX-6. Our results indicate that both Ang-2 and *KRAS* mutation status, separately and in combination, are relevant biomarkers in mCRC. This evidence potentially supports the goal of developing more tailored anti-angiogenic treatments for patients with mCRC.

Data availability statement

The original contributions presented in the analysis are included in the article/Supplementary Material. Further inquiries can be directed to the corresponding authors. Details on the commitment of Roche to Data Sharing and the Roche Global Policy on Sharing of Clinical Study Information can be found at https://go.roche.com/data_sharing, where access to the clinical study documents can also be requested.

Author contributions

CF, GB and FH contributed to conception and design of the presented work. CF, GB, IK, FH, SVH, OK, KL and JB performed data acquisition/processing, data analysis and/or interpretation of data. CF developed dedicated digital pathology software for tissue data analysis and performed data harmonization. GB performed the statistical analysis. CF, GB, IK, FH, SVH, OK, KL and JB contributed to drafting and/or revision of the manuscript. All authors contributed to the article and approved the submitted version.

Funding

This research was funded by F. Hoffmann-La Roche, who also funded medical writing assistance with the preparation of the manuscript.

Acknowledgments

The authors would like to thank the patients and their families, Martin Emmert and Otto Huber from quattro research GmbH for their database technical support, Gabriele Dietmann for the contract management support and Christian Klein for the meaningful discussions. The authors would like to acknowledge Gill Gummer and Deirdre Elmhirst (Rx Communications, Mold, UK) for medical writing assistance with the preparation of this manuscript, funded by F. Hoffmann-La Roche.

Conflict of interest

This study was sponsored by Roche. CF, GB, IK, FH, SVH, OK and KL were employees of Roche Diagnostics GmbH at the date of

study conduct. CF, FH, OK, KL, JB declare sponsor stock ownership. JB declares research funding all to institution: Gilead, Genentech/Roche, BMS, Five Prime, Lilly, Merck, MedImmune, Celgene, EMD Serono, Taiho, MacroGenics, GSK, Novartis, OncoMed, LEAP, TG Therapeutics, AstraZeneca, BI, Daiichi Sankyo, Bayer, Incyte, Apexigen, Koltan, SynDevRex, Forty Seven, AbbVie, Array, Onyx, Sanofi, Takeda, Eisai, Celldex, Agios, Cytomx, Nektar, ARMO, Boston Biomedical, Ipsen, Merrimack, Tarveda, Tyrogenex, Oncogenex, Marshall Edwards, Pieris, Mersana, Calithera, Blueprint, Evelo, FORMA, Merus, Jacobio, Effector, Novocare, Arrys, Tracoon, Sierra, Innate, Arch Oncology, Prelude Oncology, Unum Therapeutics, Vyriad, Harpoon, ADC, Amgen, Pfizer, Millennium, Imclone, Acerta Pharma, Rgenix, Bellicum, Gossamer Bio, Arcus Bio, Seattle Genetics, TempestTx, Shattuck Labs, Synthorx, Inc., Revolution Medicines, Inc., Bicycle Therapeutics, Zymeworks, Relay Therapeutics, Scholar Rock, NGM Biopharma, Stemcentrx, Beigene, CALGB, Cyteir Therapeutics, Foundation Bio, Innate Pharma, Morphotex, OncXerna, NuMab, AtlasMedx, Treadwell Therapeutics, IGM Biosciences, Mabspace, Hutchinson MediPharma, REPARE Therapeutics, NeoImmune Tech, Regeneron, PureTech Health; Consulting/Advisory Role all to institution: Gilead, Genentech/Roche, BMS, Five Prime, Lilly, Merck, MedImmune, Celgene, Taiho, MacroGenics, GSK, Novartis, OncoMed, LEAP, TG Therapeutics, AstraZeneca, BI, Daiichi Sankyo, Bayer, Incyte, Apexigen, Array, Sanofi, ARMO, Ipsen, Merrimack, Oncogenex, FORMA, Arch Oncology, Prelude Therapeutics, Phoenix Bio, Cyteir, Molecular Partners, Innate, Torque, Tizona, Janssen, Tolero, Amgen, Seattle Genetics, Moderna Therapeutics, Tanabe Research Laboratories, Beigene, Continuum Clinical, Agios, Bicycle Therapeutics, Relay Therapeutics, Evelo, Pfizer, Samsung Bioepis, Fusion Therapeutics; Food/Beverage/Travel: Gilead, Genentech/Roche, BMS, Lilly, Merck, MedImmune, Celgene, Taiho, Novartis, OncoMed, BI, ARMO, Ipsen, Oncogenex, FORMA. JB declares current employment by F. Hoffmann-La Roche Ltd. SVH is a shareholder of Exact Sciences Corporation.

The remaining authors declare that the research was conducted in the absence of any commercial or financial relationships that could be constructed as a potential conflict of interest.

Publisher's note

All claims expressed in this article are solely those of the authors and do not necessarily represent those of their affiliated organizations, or those of the publisher, the editors and the reviewers. Any product that may be evaluated in this article, or claim that may be made by its manufacturer, is not guaranteed or endorsed by the publisher.

Supplementary material

The Supplementary Material for this article can be found online at: <https://www.frontiersin.org/articles/10.3389/fonc.2023.1157596/full#supplementary-material>

References

- Folkman J. Role of angiogenesis in tumor growth and metastasis. *Sem Oncol* (2002) 29(6 Suppl. 16):15–8. doi: 10.1053/sonc.2002.37263
- Kong DH, Kim MR, Jang JH, Na H-J, Lee S. A review of anti-angiogenic targets for monoclonal antibody cancer therapy. *Int J Mol Sci* (2017) 18:1786. doi: 10.3390/ijms18081786
- Ferrara N, Kerbel RS. Angiogenesis as a therapeutic target. *Nature* (2005) 438:967–74. doi: 10.1038/nature04483
- Hurwitz H, Fehrenbacher L, Novotny W, Cartwright T, Hainsworth J, Heim W, et al. Bevacizumab plus irinotecan, fluorouracil, and leucovorin for metastatic colorectal cancer. *N Eng J Med* (2004) 350:2335–42. doi: 10.1056/NEJMoa032691
- Kabbinavar FF, Hambleton J, Mass RD, Hurwitz H, Bergsland E, Sarkar S. Combined analysis of efficacy: the addition of bevacizumab to fluorouracil/leucovorin improves survival for patients with metastatic colorectal cancer. *J Clin Oncol* (2005) 23:3706–12. doi: 10.1200/JCO.2005.00.232
- Tebbutt NC, Wilson K, Gebbski VJ, Cummins MM, Zannino D, van Hazel GA, et al. Capecitabine, bevacizumab, and mitomycin in first-line treatment of metastatic colorectal cancer: results of the Australasian gastrointestinal trials group randomized phase III MAX study. *J Clin Oncol* (2010) 28:3191–8. doi: 10.1200/JCO.2009.27.7723
- Giantonio BJ, Catalano PJ, Meropol NJ, O'Dwyer PJ, Mitchell EP, Alberts EA, et al. Bevacizumab in combination with oxaliplatin, fluorouracil, and leucovorin (FOLFOX4) for previously treated metastatic colorectal cancer: results from the Eastern cooperative oncology group study E3200. *J Clin Oncol* (2007) 25:1539–44. doi: 10.1200/JCO.2006.09.6305
- Saltz LB, Clarke S, Diaz-Rubio E, Scheithauer W, Figer A, Wong R, et al. Bevacizumab in combination with oxaliplatin-based chemotherapy as first-line therapy in metastatic colorectal cancer: a randomized phase III study. *J Clin Oncol* (2008) 26:2013–19. doi: 10.1200/JCO.2007.14.9930
- Bergers G, Hanahan D. Modes of resistance to anti-angiogenic therapy. *Nat Rev Cancer* (2008) 8:592–603. doi: 10.1038/nrc2442
- Carmeliet P, Jain RK. Molecular mechanisms and clinical applications of angiogenesis. *Nature* (2011) 473:298–307. doi: 10.1038/nature10144
- Haibe Y, Kreidieh M, El Hajj H, Khalifeh I, Mukherji D, Temraz S, et al. Resistance mechanisms to anti-angiogenic therapies in cancer. *Front Oncol* (2020) 10:221. doi: 10.3389/fonc.2020.00221
- Felcht M, Luck R, Schering A, Seidel P, Srivastava K, Hu J, et al. Angiopoietin-2 differentially regulates angiogenesis through TIE2 and integrin signalling. *J Clin Invest* (2012) 122:1991–2005. doi: 10.1172/JCI58832
- Etoh T, Inoue H, Tanaka S, Barnard GF, Kitano S, Mori M. Angiopoietin-2 is related to tumor angiogenesis in gastric carcinoma: possible *in vivo* regulation via induction of proteases. *Canc Res* (2001) 61:2145–53.
- Sfiligoi C, de Luca A, Cascone I, Sorbello V, Fuso L, Ponzone R, et al. Angiopoietin-2 expression in breast cancer correlates with lymph node invasion and short survival. *Int J Canc* (2003) 103:466–74. doi: 10.1002/ijc.10851
- Jary M, Vernerey D, Lecomte T, Dobi E, Ghiringhelli F, Monnien F, et al. Prognostic value of angiopoietin-2 for death risk stratification in patients with metastatic colorectal carcinoma. *Canc Epidemiol Biomarkers Prev* (2015) 24:603–12. doi: 10.1158/1055-9965.EPI-14-1059
- Munakata S, Ueyama T, Ishihara H, Komiyama H, Tsukamoto R, Kawai M, et al. Angiopoietin-2 as a prognostic factor in patients with incurable stage IV colorectal cancer. *J Gastrointest Canc* (2021) 52:237–42. doi: 10.1007/s12029-020-00392-1
- Leong A, Kim M. The angiopoietin-2 and TIE pathway as a therapeutic target for enhancing antiangiogenic therapy and immunotherapy in patients with advanced cancer. *Int J Mol Sci* (2020) 21:8689. doi: 10.3390/ijms21228689
- Chae SS, Kamoun WS, Farrar CT, Kirkpatrick ND, Niemeyer E, de Graaf AMA, et al. Angiopoietin-2 interferes with anti-VEGFR2-induced vessel normalization and survival benefit in mice bearing gliomas. *Clin Canc Res* (2010) 16:3618–27. doi: 10.1158/1078-0432.CCR-09-3073
- Goede V, Coutelle O, Neuneier J, Reinacher-Schick A, Schnell R, Koslowsky TC, et al. Identification of serum angiopoietin-2 as a biomarker for clinical outcome of colorectal cancer patients treated with bevacizumab-containing therapy. *Br J Canc* (2010) 103:1407–14. doi: 10.1038/sj.bjc.6605925
- Kienast Y, Klein C, Scheuer W, Raemisch R, Lorenzon E, Bernicke D, et al. Ang-2-VEGF-A crossMab, a novel bispecific human IgG1 antibody blocking VEGF-a and ang-2 functions simultaneously, mediates potent antitumor antiangiogenic and antimetastatic efficacy. *Clin Canc Res* (2013) 19:6730–40. doi: 10.1158/1078-0432.CCR-13-0081
- Heil F, Babitzki G, Julien-Laferrriere A, Ooi C-H, Hidalgo M, Massard C, et al. Vanucizumab mode of action: serial biomarkers in plasma, tumor and skin-wound-healing biopsies. *Sci Transl Med* (2021) 14:100984. doi: 10.1016/j.tran.2020.100984
- Hidalgo M, Martinez-Garcia M, Le Tourneau C, Le Tourneau C, Massard C, Garralda E, et al. First-in-human phase I study of single-agent vanucizumab, a first-in-class bi-specific antiAng-2/anti-VEGF antibody, in adult patients with advanced solid tumors. *Clin Canc Res* (2018) 24:1536–45. doi: 10.1158/1078-0432.CCR-17-1588
- Bendell JC, Sauri T, Cubillo A, Gracián LC, Alvarez R, López-López C, et al. The McCaVE trial: Vanucizumab plus mFOLFOX-6 versus bevacizumab plus mFOLFOX-6 in patients with previously untreated metastatic colorectal carcinoma (mCRC). *Oncologist* (2020) 25:e451–9. doi: 10.1634/theoncologist.2019-0291
- Taieb J, Jung A, Sartori-Bianchi A, Peeters M, Seligmann M, Zaanen A, et al. The evolving biomarker landscape for treatment selection in metastatic colorectal cancer. *Drugs* (2019) 79:1375–94. doi: 10.1007/s40265-019-01165-2
- Zhu G, Pei L, Xia H, Tang Q, Bi F. Role of oncogenic KRAS in the prognosis, diagnosis and treatment of colorectal cancer. *Mol Canc* (2021) 20:143. doi: 10.1186/s12943-021-01441-4
- Meng M, Zhong K, Jiang T, Liu Z, Kwan HY, Su T. The current understanding on the impact of KRAS on colorectal cancer. *BioMed Pharmacother* (2021) 140:111717. doi: 10.1016/j.biopha.2021.111717
- Ye J, Lin M, Zhang Z, Zhu X, Li S, Liu H, et al. Tissue gene mutation profiles in patients with colorectal cancer and their clinical implications. *BioMed Rep* (2020) 13:43–8. doi: 10.3892/br.2020.1303
- Levin-Sparenberg E, Bylsma LC, Lowe K, Sangare L, Fryzek JP, Alexander DD. A systematic literature review and meta-analysis describing the prevalence of KRAS, NRAS, and BRAF gene mutations in metastatic colorectal cancer. *Gastroenterol Res* (2020) 13:184–98. doi: 10.14740/gr1167
- Van Cutsem E, Cervantes A, Adam R, Sobrero A, Van Krieken JH, Aderka D, et al. ESMO consensus guidelines for the management of patients with metastatic colorectal cancer. *Ann Oncol* (2016) 27:1386–422. doi: 10.1093/annonc/mdw235
- Hurwitz H, Yi J, Ince W, Novotny WF, Rosen O. The clinical benefit of bevacizumab in metastatic colorectal cancer is independent of K-ras mutation status: analysis of a phase III study of bevacizumab with chemotherapy in previously untreated metastatic colorectal cancer. *Oncologist* (2009) 14:22–8. doi: 10.1634/theoncologist.2008-0213
- Price TJ, Hardingham JE, Lee CK, Weickhardt A, Townsend AR, Wrin JW, et al. Impact of KRAS and BRAF gene mutation status on outcomes from the phase III AGITG MAX trial of capecitabine alone or in combination with bevacizumab and mitomycin in advanced colorectal cancer. *J Clin Oncol* (2011) 29:2675–82. doi: 10.1200/JCO.2010.34.5520
- Ortiz-Morales MJ, Toledano-Fonseca M, Mena-Osuna R, Cano MT, Gómez-España A, De la Haba-Rodríguez, et al. Basal VEGF-a and ACE plasma levels of metastatic colorectal cancer patients have prognostic value for first-line treatment with chemotherapy plus bevacizumab. *Cancers (Basel)* (2022) 14:3054. doi: 10.3390/cancers14133054
- de Rauglaudre B, Sibertin-Blanc C, Fabre A, Le Maricot K, Bennouna J, Ghiringhelli F, et al. Predictive value of vascular endothelial growth factor polymorphisms for maintenance bevacizumab efficacy in metastatic colorectal cancer: an ancillary study of the PRODIGE 9 phase III trial. *Ther Adv Med Oncol* (2022) 14:17588359221141307. doi: 10.1177/17588359221141307
- Chionh F, Gebbski V, Al-Obaidi SJ, Mooi JK, Bruhn JA, Lee CK, et al. VEGF-a, VEGFR1 and VEGFR2 single nucleotide polymorphisms and outcomes from the AGITG MAX trial of capecitabine, bevacizumab and mitomycin c in metastatic colorectal cancer. *Sci Rep* (2022) 12:1238. doi: 10.1038/s41598-021-03952-y
- Marisi G, Scarpi E, Passardi A, Nanni O, Ragazzini A, Valgiusti A, et al. Circulating VEGF and eNOS variations as predictors of outcome in metastatic colorectal cancer patients receiving bevacizumab. *Sci Rep* (2017) 7:1293. doi: 10.1038/s41598-017-01420-0
- Ruifrok AC, Johnston DA. Quantification of histochemical staining by color deconvolution. *Anal Quant Cytol Histol* (2001) 23:291–9.
- Stubenrauch K, Wessels U, Essig U, Vogel R, Waltenberger A, Hansbauer A, et al. An immunodepletion procedure advances free angiopoietin-2 determination in human plasma samples during anti-cancer therapy with bispecific anti-Ang2/VEGF CrossMab. *J Pharm BioMed Anal* (2015) 102:459–67. doi: 10.1016/j.jpba.2014.10.005
- Asuragen Inc. (2016). Available at: https://asuragen.com/wp-content/uploads/2016/05/Quantidex-DNA-Assay_Protocol_Guide-v1.pdf.
- Asuragen Inc. (2016). Available at: <https://asuragen.com/wp-content/uploads/2016/05/49612v1-Quantidex-NGS-Pan-Cancer-Kit-Protocol.pdf>.
- Kelnar K, Church M, Pickens W, Kaplan J, Shelton J, Popowski M, et al. Analytical validation of the Quantidex NGS DNA hotspot 21 kit, a diagnostic NGS system for the detection of actionable mutations in FFPE tumors. poster presented at association for molecular pathology (AMP) annual meeting (2018). Available at: https://www.researchgate.net/publication/339177831_Analytical_Validation_of_the_Quantidex_NGS_DNA_Hotspot_21_Kit_a_Diagnostic_NGS_System_for_the_Detection_of_Actionable_Mutations_in_FFPE_Tumors/link/5e42b8e0a6fdcc9659a55cc/download.
- Eisenhauer EA, Therasse P, Bogaerts J, Schwartz LH, Sargent D, Ford R, et al. New response evaluation criteria in solid tumours: revised RECIST guideline (version 1.1). *Eur J Canc* (2009) 45:228–47. doi: 10.1016/j.ejca.2008.10.026
- Chung YC, Hou YC, Chang CN, Hsueh T-H. Expression and prognostic significance of angiopoietin in colorectal carcinoma. *J Surg Oncol* (2006) 94:631–8. doi: 10.1002/jso.20423
- Zocche DM, Ramirez C, Fontao FM, Costa LD, Redal MA. Global impact of KRAS mutation patterns in FOLFOX treated metastatic colorectal cancer. *Front Genet* (2015) 6:116. doi: 10.3389/fgene.2015.00116

44. Peeters M, Strickland AH, Lichinitser M, Suresh AVS, Manikhas G, Shapiro J, et al. A randomised, double-blind, placebo-controlled phase 2 study of trebananib (AMG 386) in combination with FOLFIRI in patients with previously treated metastatic colorectal carcinoma. *Br J Canc* (2013) 108:503–11. doi: 10.1038/bjc.2012.594
45. Elmore S. Apoptosis: a review of programmed cell death. *Toxicol Pathol* (2007) 35:495–516. doi: 10.1080/01926230701320337
46. Viillard C, Larrivée B. Tumor angiogenesis and vascular normalization: alternative therapeutic targets. *Angiogenesis* (2017) 20:409–26. doi: 10.1007/s10456-017-9562-9
47. Abou Khouzam R, Brodaczewska M, Filipiak A, Zeinelabdin NA, Buart A, Szczylik C, et al. Tumor hypoxia regulates immune escape/invasion: influence on angiogenesis and potential impact of hypoxic biomarkers on cancer therapies. *Front Immunol* (2021) 11:613114. doi: 10.3389/fimmu.2020.613114
48. Huang H, Bhat A, Woodnutt G, Lappe R. Targeting the ANGPT-TIE2 pathway in malignancy. *Nat Rev Canc* (2010) 10:575–85. doi: 10.1038/nrc2894
49. Schmittnaegel M, Rigamonti N, Kadioglu E, Cassará A, Wyser Rimli C, Kiialainen A, et al. Dual angiopoietin-2 and VEGFA inhibition elicits antitumor immunity that is enhanced by PD-1 checkpoint blockade. *Sci Transl Med* (2017) 9 (385):eaak9670. doi: 10.1126/scitranslmed.aak9670
50. Fukumura D, Kloepper J, Amoozgar Z, Duda DG, Jain RK. Enhancing cancer immunotherapy using antiangiogenics: opportunities and challenges. *Nat Rev Clin Oncol* (2018) 15:325–40. doi: 10.1038/nrclinonc.2018.29
51. Figueras A, Arbos MA, Quiles MT, Viñals F, Germà JR, Capellà G. The impact of KRAS mutations on VEGF-a production and tumour vascular network. *BMC Canc* (2013) 13:125. doi: 10.1186/1471-2407-13-125
52. Shen M, Qi R, Ren J, Lv D, Yang H. Characterization with KRAS mutant is a critical determinant in immunotherapy and other multiple therapies for non-small cell lung cancer. *Front Oncol* (2022) 11:780655. doi: 10.3389/fonc.2021.780655
53. Li ZN, Zhao L, Yu LF, Wei M-J. BRAF and KRAS mutations in metastatic colorectal cancer: future perspectives for personalized therapy. *Gastroenterol Rep (Oxf)* (2020) 8:192–205. doi: 10.1093/gastro/goaa022
54. Rahman S, Garrel S, Gerber M, Maitra R, Goel S. Therapeutic targets of KRAS in colorectal cancer. *Cancers (Basel)* (2021) 13:6233. doi: 10.3390/cancers13246233
55. Ledford H. Cancer drugs are closing in on some of the deadliest mutations. *Nature* (2022) 610:620–2. doi: 10.1038/d41586-022-03392-2
56. Wallin JJ, Bendell J, Funke R, Sznol M, Korski K, Jones S, et al. Atezolizumab in combination with bevacizumab enhances antigen-specific T-cell migration in metastatic renal cell carcinoma. *Nat Commun* (2016) 7:1–8. doi: 10.1038/ncomms12624
57. Girard N, Wermke M, Barlesi F, Kim D-W, Ghiringhelli F, Bennouna J, et al. Phase Ib study of BI 836880 (VEGF/Ang2 nanobody) plus ezabenzimab (BI 754091; anti-PD-1 antibody) in patients (pts) with solid tumors. *J Clin Oncol* (2021) 39(15 Suppl.):Abstract 2579. doi: 10.1200/JCO.2021.39.15_suppl.2579
58. Kovalchuk B, Berghoff A, Karreman MA, Frey K, Piechutta M, Fischer M, et al. Nintedanib and a bi-specific anti-VEGF/Ang2 nanobody selectively prevent brain metastases of lung adenocarcinoma cells. *Clin Exp Metastasis* (2020) 37:637–48. doi: 10.1007/s10585-020-10055-x
59. Heier JS, Khanani AM, Ruiz CQ, Basu K, Ferrone PJ, Brittain C, et al. TENAYA and LUCERNE investigators. efficacy, durability, and safety of intravitreal faricimab up to every 16 weeks for neovascular age-related macular degeneration (TENAYA and LUCERNE): two randomised, double-masked, phase 3, non-inferiority trials. *Lancet* (2022) 399:729–40. doi: 10.1016/S0140-6736(22)00010-1



OPEN ACCESS

EDITED BY

Alessandro Passardi,
Scientific Institute of Romagna for the
Study and Treatment of Tumors (IRCCS),
Italy

REVIEWED BY

Hossein Taghizadeh,
Medical University of Vienna, Austria
Reetu Mukherji,
MedStar Georgetown University Hospital,
United States

*CORRESPONDENCE

Gudrun Piringer

✉ gudrun.piringer@kepleruniklinikum.at

SPECIALTY SECTION

This article was submitted to
Gastrointestinal Cancers:
Colorectal Cancer,
a section of the journal
Frontiers in Oncology

RECEIVED 15 February 2023

ACCEPTED 28 March 2023

PUBLISHED 05 May 2023

CITATION

Piringer G, Decker J, Trommet V, Kühr T,
Heibl S, Dörfler K and Thaler J (2023)
Ongoing complete response after
treatment cessation with dabrafenib,
trametinib, and cetuximab as third-line
treatment in a patient with advanced
BRAF^{V600E} mutated, microsatellite-stable
colon cancer:
A case report and literature review.
Front. Oncol. 13:1166545.
doi: 10.3389/fonc.2023.1166545

COPYRIGHT

© 2023 Piringer, Decker, Trommet, Kühr,
Heibl, Dörfler and Thaler. This is an open-
access article distributed under the terms of
the [Creative Commons Attribution License](https://creativecommons.org/licenses/by/4.0/)
(CC BY). The use, distribution or
reproduction in other forums is permitted,
provided the original author(s) and the
copyright owner(s) are credited and that
the original publication in this journal is
cited, in accordance with accepted
academic practice. No use, distribution or
reproduction is permitted which does not
comply with these terms.

Ongoing complete response after treatment cessation with dabrafenib, trametinib, and cetuximab as third-line treatment in a patient with advanced BRAF^{V600E} mutated, microsatellite-stable colon cancer: A case report and literature review

Gudrun Piringer^{1,2,3*}, Jörn Decker⁴, Vera Trommet¹,
Thomas Kühr^{1,3}, Sonja Heibl^{1,3}, Konrad Dörfler³
and Josef Thaler^{1,3}

¹Department of Internal Medicine IV, Wels-Grieskirchen Medical Hospital, Wels, Austria, ²Department of Hematology and Oncology, Kepler University Hospital, Linz, Austria, ³Medical Faculty, Johannes Kepler University Linz, Linz, Austria, ⁴Department of Internal Medicine, Klinikum Rohrbach, Rohrbach, Austria

Metastatic BRAF^{V600E} mutated colorectal cancer is associated with poor overall survival and modest effectiveness to standard therapies. Furthermore, survival is influenced by the microsatellite status. Patients with microsatellite-stable and BRAF^{V600E} mutated colorectal cancer have the worst prognosis under the wide range of genetic subgroups in colorectal cancer. Herein, we present a patient case of an impressive therapeutic efficacy of dabrafenib, trametinib, and cetuximab as later-line therapy in a 52-year-old woman with advanced BRAF^{V600E} mutated, microsatellite-stable colon cancer. This patient achieved a complete response after 1 year of triple therapy. Due to skin toxicity grade 3 and recurrent urinary tract infections due to mucosal toxicity, a therapy de-escalation to dabrafenib and trametinib was performed, and the double therapy was administered for further 41 months with ongoing complete response. For 1 year, the patient was off therapy and is still in complete remission.

KEYWORDS

combination targeted therapy, dabrafenib, trametinib, MSS, BRAF-V600 mutation

Introduction

BRAF is a component of the RAS-RAF-MAPK signaling pathway (1). Eight to 12% of metastatic colorectal cancer (CRC) and approximately half of the patients with melanoma have a BRAF mutation (2). BRAF^{V600E} mutation is the most frequent BRAF mutation (90%) and leads to constitutive, RAS-independent activation of BRAF kinase activity and MAPK pathway signaling through downstream activation of MEK (MEK 1 and MEK 2) and ERK (ERK1 and ERK2) kinases and promotes tumor cell migration, proliferation, and survival (2, 3). In metastatic CRC, BRAF^{V600E} mutation is associated with right-side, poorly differentiated, and mucinous-type tumors and is a negative prognostic factor (4). Its mortality is a nearly twofold increase compared to that of BRAF wild-type tumors (5) due to poor response to standard therapies (5–7).

Several studies investigated the effect of targeted therapies in BRAF^{V600E} mutated tumors to improve the outcome. Encorafenib, dabrafenib, and vemurafenib are potent tyrosine kinase inhibitors of the BRAF^{V600E} kinase, and trametinib and binimetinib potentially inhibit the MEK kinase, although BRAF or MEK inhibitor monotherapy showed dramatic response rates in >50% of patients with metastatic BRAF^{V600E} mutated melanoma (8, 9), and only 5% of metastatic CRC patients with the same BRAF^{V600E} mutation responded to monotherapy (10, 11). In contrast to melanoma, it is hypothesized that a major factor underlying the lack of clinical response with single-agent BRAF or MEK inhibitor in CRC is a robust adaptive feedback signaling that leads to reactivation of MAPK signaling, often mediated by epidermal growth factor receptor (EGFR) following BRAF-inhibitor treatment (12, 13).

In this case report, we report a patient who had progressive disease after failure of standard chemotherapies in 2017. At this timepoint, the currently approved doublet targeted therapy with encorafenib plus cetuximab, which was approved by the European Medicines Agency (EMA) in 2020, was still under investigation in the BEACON trial, and an off-label use was not possible (14). Due to a lack of therapy alternatives, the patient was offered an off-label use of cetuximab plus dabrafenib plus trametinib based on a few clinical trial reports, which are summarized in the following.

Combined inhibition of BRAF and MEK with dabrafenib and trametinib showed improved response and survival rates compared with dabrafenib alone in metastatic BRAF^{V600E} mutated melanoma, which resulted in its approval in 2014 (15). However, this combination was only evaluated in a small sample size in metastatic BRAF^{V600E} mutated CRC. In a pharmacodynamic cohort study, a total of 43 patients with BRAF^{V600E} mutated CRC were treated with dabrafenib plus trametinib and showed an overall response rate (ORR) of 12% including a complete response (CR) in one patient and stable disease in further 56% of patients (16). The median progression-free survival (PFS) was 3.5 months. One patient had a CR by week 32 of the study treatment with a duration of response >36 months. Mutational analysis revealed that the patient achieving a CR and two of three evaluable patients achieving a partial response had PIK3CA mutations. Further, the tumor of the patient with CR was microsatellite instable (MSI). To achieve greater MAPK suppression and improved efficacy in

patients with metastatic BRAF^{V600E} mutated CRC, a clinical phase I study with three arms evaluated dabrafenib plus trametinib plus panitumumab versus dabrafenib plus panitumumab versus trametinib plus panitumumab in 142 patients and demonstrated ORR in 21%, 10%, and 0% (17). Median PFS was 4.2, 3.5, and 2.6 months, and median overall survival (OS) was 9.1, 13.2, and 8.2 months. One patient in the triplet and doublet treatment groups (dabrafenib plus panitumumab) had a CR. Analysis of the microsatellite status showed a trend toward a statistically significant increase in PFS in MSI versus microsatellite stable (MSS) tumors. None of the MSS patients remained in the study longer than 1 year with this combination therapy. In the MSI cohort, one patient achieved a partial response lasting >24 months, and another patient had a CR over 26 months. Nevertheless, one patient treated with dabrafenib plus panitumumab was MSS and achieved a CR. Due to the small sample size and a limited number of studies, this targeted combination is not approved in BRAF^{V600E} mutated CRC. Currently, doublet therapy with encorafenib plus cetuximab is the only approved targeted therapy in this patient population from second-line therapy based on the results from the phase III BEACON trial (14).

We want to highlight in this case the potential of targeted therapies in some patients with pretreated, advanced colon cancer and that treatment can be discontinued as an ongoing response. Furthermore, in the Discussion section, EMA-approved standard treatments for metastatic BRAF^{V600E} mutated CRC are summarized, and current areas of research to enhance efficacy and to individualize therapy in different subgroups of metastatic BRAF^{V600E} mutated CRC will be discussed.

Case description

A 52-year-old woman without a significant medical history presented to the hospital due to a 3-day history of obstipation, abdominal pain, and nausea in February 2017. On examination, her abdomen was distended and mildly tender on the left side. Blood tests revealed anemia. On the computer tomography scan (CT scan), one suspicious lesion in the liver with a diameter of 3 cm and a suspicious mass in the colon descendens were described (Figure 1). In the diagnostic colonoscopy, a 5-cm non-obstructive tumor in the colon descendens was found. Biopsies of the primary tumor confirmed the diagnosis of adenocarcinoma of the colon. In the magnetic resonance imaging of the liver, two suspicious lesions in segments VII and VI were described. The liver metastases were classified by the liver surgeon as primary resectable. An initial hemicolectomy with simultaneous atypical liver resection was performed in February 2017. The histology of the primary tumor revealed a poorly differentiated, MSS, Her2-negative, and BRAF^{V600E} mutated adenocarcinoma of the colon with a lymphatic vessel and perineural involvement as well as lymph node involvement in eight of 14 removed lymph nodes. The liver metastases were completely resected, and the liver lesions were confirmed histologically to be metastatic lesions. FoundationONE[®] analysis of the primary tumor showed BRAF^{V600E} mutation, PTEN-loss, DDR1 R514C alteration, KDM5A R782Q alteration, TP53

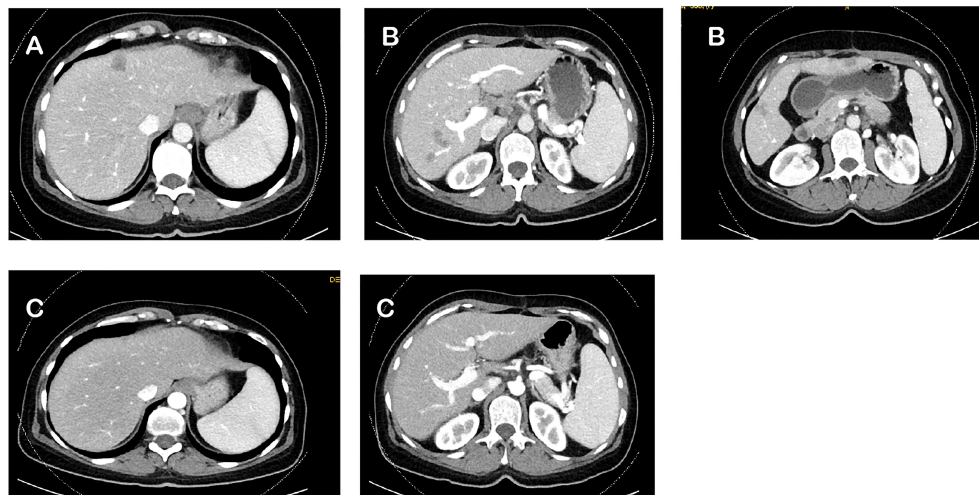


FIGURE 1

Computed tomography scan (CT scan) regarding the clinical response during whole course of treatment. (A) Baseline CT scan in February 2017. (B) CT scan after adjuvant CAPOX in June 2017. (C) CT scan after 1 year of dabrafenib, trametinib, and cetuximab in October 2018.

Y234 alteration, and MSS status. The tumor mutational burden was 0 Muts/Mb.

A 6-month course of postoperative, pseudoadjuvant chemotherapy with capecitabine and oxaliplatin (CAPOX) was planned. The rationale for pseudoadjuvant chemotherapy with CAPOX was to reduce the risk of recurrences, which occur in approximately 50% of patients with resectable liver metastases. However, the best postoperative strategy for primary resected colorectal liver metastases is uncertain—both pseudoadjuvant chemotherapy and perioperative chemotherapy tend to show a favorable effect in PFS, but not in OS (18–20). Further, the patient preferred an oral regimen. After 3 months of CAPOX therapy, an interim CT scan was performed in June 2017. The CT scan showed five new liver metastases without further metastases in other organs (Figure 1), and the tumor marker carcinoembryonic antigen (CEA) was elevated. A first-line palliative chemotherapy regimen with FOLFIRI and bevacizumab was administered from June until September 2017. After 3 months, the CT scan showed further progress in the liver, and tumor markers were further increasing. Resectability of the liver metastases was excluded. For second-line therapy, the patient was randomized in the control arm of the BEACON study, and FOLFIRI plus cetuximab was administered for 2 months in this trial. The interim CT scan in November 2017 showed progression of the liver metastases and detection of new metastases in the lung, and retroperitoneal lymph nodes metastases and tumor makers further increased. According to the study, the patient went off protocol due to progressive disease. A cross-over to one of the targeted-treatment arms in the BEACON study or off-label use of this targeted therapy was not possible.

The performance status was reduced to Eastern Cooperative Oncology Group (ECOG) performance status 2 due to the progressive disease, but the patient was willing to receive further therapy. Because of the lack of promising third-line therapy in BRAF^{V600E} mutated CRC, the patient received an off-label use of dabrafenib, trametinib, and cetuximab based on reports of a few

clinical phase I–II trials, which was mentioned above (16, 17). The therapy was started in December 2017. Two months after the beginning of the third-line palliative therapy, the CT scan showed partial response in the liver, lung, and retroperitoneal lymph nodes. After another 2 months of therapy, the lung metastases and retroperitoneal lymph node metastases could no longer be detected on the CT scan. The liver metastases had almost disappeared. Due to skin toxicity with papulopustular eruption grade 3 (Figure 2), steroid-containing cream and 100 mg of minocycline per day were prescribed, and cetuximab therapy was temporarily stopped. Furthermore, the patient suffered from recurrent urinary tract infections due to mucosal toxicity requiring antibiotic therapy in the early stages to prevent urosepsis. In August 2018, no further progression was detected on the CT scan (Figure 1), and in October 2018, a PET/CT showed a CR. Since October 2018, cetuximab was terminated due to persistent severe skin toxicity and recurrent urinary tract infections, and double therapy with dabrafenib and



FIGURE 2

Pronounced skin toxicity due to cetuximab therapy.

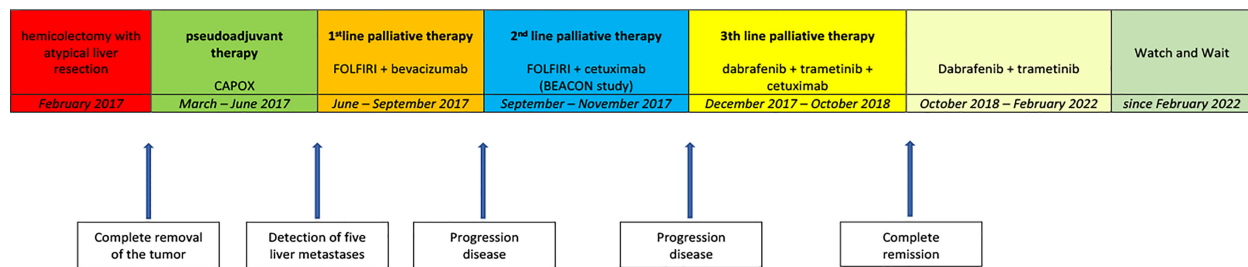


FIGURE 3
Flowchart of the whole course of treatment.

trametinib was continued with better tolerance. The urinary tract infections were fewer, and the skin recovered. Therapy with dabrafenib and trametinib was terminated on February 2022 at the request of the patient, and a watch-and-wait strategy with CT scan and blood tests including CEA every 3 months was recommended. Until January 2023, the patient is still in CR and in excellent general condition. Figure 3 shows an overview of the whole course of treatment in this patient, and Figure 4 shows the changes in the tumor marker during the therapy. The patient consented to the publication of her medical history.

Discussion

To the best of our knowledge, achieving an ongoing CR after treatment cessation with dabrafenib, trametinib, and intermittent cetuximab as third-line treatment in a patient with an advanced BRAF^{V600E} mutated, MSS colon cancer is unique.

State-of-the-art therapy

The first-line recommendations for patients with metastatic BRAF^{V600E} mutated CRC are FOLFOXIRI or doublet

chemotherapy regimen plus bevacizumab based on the subgroup analysis of the TRIBE study (21) and TRIBE 2 study (22, 23). The decision to use triplet or doublet chemotherapy regimens plus bevacizumab should be based on a risk/benefit discussion with the patient. In 2020, EMA approved doublet therapy with encorafenib + cetuximab for the treatment of patients with BRAF^{V600E} mutated metastatic CRC (mCRC) who have received prior systemic therapy, according to the results of the phase III BEACON trial (14). In this trial, 665 patients were randomized to receive triplet therapy with encorafenib plus binimetinib plus cetuximab or doublet therapy with encorafenib plus cetuximab or standard therapy with FOLFIRI/irinotecan plus cetuximab. The median PFS and the median OS for triplet and doublet therapies were superior compared to those of the standard group (median PFS 4.3 vs. 4.2 vs. 1.5 months; median OS 9.0 vs. 8.4 vs. 5.3 months). The ORR was 26% vs. 20% vs. 2%. However, the study was not powered to compare the two experimental groups directly. However, descriptive analyses comparing triplet and doublet arms showed similar efficacy in the overall population across endpoints including PFS and OS, and adverse events were higher with triplet compared to doublet therapies. The results suggested that the doublet regimen is sufficient to maximize the OS benefit with better tolerability, and doublet therapy was approved by EMA.

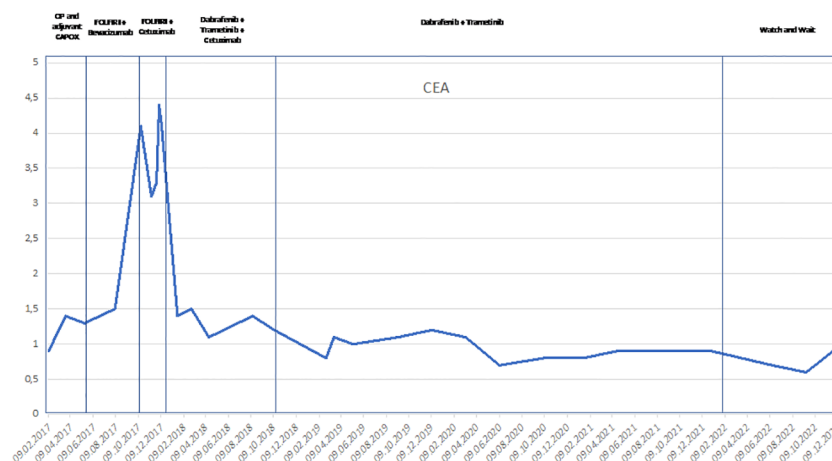


FIGURE 4
Line chart of the changes of the tumor marker CEA during the process of the treatment since February 2017. CEA, carcinoembryonic antigen.

Later-line therapies include other chemotherapy combinations, TAS-102, and/or regorafenib with modest effectiveness (24).

For metastatic BRAF^{V600E} mutated CRC with MSI-h, the therapeutic approach is different, and microsatellite status should be tested up-front. In a pooled analysis of four studies, the incidence of BRAF^{V600E} mutated CRC was 34.6% in patients with mismatch repair deficiency and 6.8% in patients with microsatellite-stable CRC (25). The molecular relationship between BRAF mutation and MSI is through high-level CpG island methylator phenotype and MLH1 promoter methylation. Pembrolizumab is approved by the EMA for patients with metastatic MSI-h CRC in the first-line setting and after fluoropyrimidine-based combination therapy based on the results from the Keynote-177 study (26) and Keynote-164 study (27). The Keynote-177 study showed that pembrolizumab was superior in terms of PFS and OS compared with chemotherapy in the overall MSI-h population as well as in patients with BRAF^{V600E} mutated CRC and MSI-h (26).

In second-line and third-line settings, pembrolizumab showed highly promising outcomes with ORR of 20% and 55% in patients with BRAF^{V600E} mutated CRC and MSI-h (27). Furthermore, in the CheckMate-142 trial, the combination of nivolumab plus ipilimumab in MSI-h-patients who received prior chemotherapy showed an ORR of 55% and a 12-month OS rate of 85%, irrespective of BRAF status (28).

BRAF^{V600E} mutated CRC is not a homogenous disease, and up-front treatment decision is currently made by microsatellite status. From the second line of therapy, targeted therapy represents the standard of care and significantly improved outcomes. Nevertheless, the prognosis of metastatic BRAF^{V600E} mutated CRC remains poor, and further investigations are needed to improve survival.

Areas of research

The current objectives of the research are a) the implementation of targeted therapies in the first-line setting and b) combining targeted therapies with chemotherapy or c) immunotherapy or d) other targeted therapies based on molecular analyses. Further, there is a great need to predict the outcomes by identification of e) different molecular subgroups.

- a. The ANCHOR study evaluated in a single-arm phase II study encorafenib plus binimetinib plus cetuximab in previously untreated metastatic BRAF^{V600E} mutated CRC, and the results were recently published (29). Among 95 patients, the ORR was 47.4% with all partial responses. The median PFS was 5.8 months, and the median OS was 18.3 months. The primary endpoint was met. However, these results showed that the combination therapy in the first-line setting is quite similar to the recommended chemotherapy-based regimens in the first-line setting of metastatic BRAF^{V600E} mutated CRC. The results signal that there is a need to evaluate mechanisms of acquired resistance, as the short PFS interval is likely due to resistance that arises despite inhibiting BRAF, MEK, and EGFR.
- b. To improve the outcome, the phase III BREAKWATER study explores in three arms the combination of encorafenib plus cetuximab with or without chemotherapy (mFOLFOX or FOLFIRI) versus control (mFOLFOX, FOLFIRI, and FOLFIRINOX ± bevacizumab) in the first-line setting in 765 patients (ClinicalTrials.gov Identifier: NCT04607421). Updated safety and anti-tumor activity data from the BREAKWATER safety lead-in demonstrated that the addition of chemotherapy to encorafenib plus cetuximab was generally tolerable with preliminary promising antitumor activity (30). The final results are eagerly awaited.
- c. A further interesting approach is the combination of immunotherapy and targeted therapy in metastatic BRAF^{V600E} mutated CRC. Currently, immunotherapy is only approved in patients with MSI-h. However, in metastatic BRAF^{V600E} mutated CRC, the addition of immunotherapy is evaluated in not only MSI-h patients but also MSS patients based on data from preclinical studies that suggest that combining MAPK inhibition and immunotherapy could enhance antitumor efficacy in BRAF and KRAS mutant cancers (31–33). A recent proof-of-concept single-arm phase II study evaluated the addition of a PDL-1 inhibitor spartalizumab to dabrafenib and trametinib in patients with BRAF^{V600E} mutated CRC (34). Of the 37 included patients, most of them were MSS (n = 32). In these patients with MSS BRAF^{V600E} mutated CRC, the ORR was 25%, and the disease control rate was 75%. Median PFS was 5 months with 18% of patients remaining on therapy for over 1 year. The authors of the study suggest a potential tumor cell-intrinsic mechanism of synergy between MAPK inhibition and immunotherapy, and additional studies are needed to more fully understand the benefits of MAPK inhibition combined with immunotherapy in MSS BRAF^{V600E} mutated CRC. A phase II study evaluates the addition of nivolumab to encorafenib plus cetuximab versus doublet therapy with encorafenib plus cetuximab in BRAF^{V600E} mutated, MSS CRC after the failure of at least one prior treatment. The primary endpoint is PFS (ClinicalTrials.gov Identifier: NCT05308446). The SEAMARK trial investigates in a phase II clinical trial the efficacy of encorafenib plus cetuximab plus pembrolizumab versus pembrolizumab alone in patients with untreated metastatic BRAF^{V600E} mutated CRC and MSI-h (ClinicalTrials.gov Identifier: NCT05217446).
- d. The mechanism of resistance to targeted therapies is not completely understood. Unlike other tumors with BRAF^{V600E} mutations, like melanoma, non-small cell lung cancer, and papillary thyroid cancer, BRAF mono-inhibition in CRC resulted only in marginal clinical activity. BRAF inhibition causes a rapid feedback activation of EGFR because of the missing negative feedback mechanism driven by ERK1/2 activation and leads to MEK1/2 activation through several escape mechanisms. Various mechanisms of resistance have been discovered, from activation of various receptor tyrosine kinases to activation of other cell signaling pathways such as

the PI3K/AKT pathway (35, 36). Receptor tyrosine kinases have multiple pathways by which they can promote cell signaling, and reactivation of receptor tyrosine kinases following inhibition of the MAPK pathway stimulates cellular growth through various pathways. The majority of resistances are centered around the reactivation of the MAPK pathway. Several analyses of mutational profiles and preclinical studies suggested activations of the phosphoinositide 3-kinase (PI3K) pathway as a potential mechanism of resistance to BRAF inhibitors (37). To overcome the potential mechanism of resistance, the combination PI3K inhibitor alpelisib was investigated (38) in 28 refractory BRAF^{V600E} mutated CRC in a phase Ib study and showed good tolerability of the triplet therapy but with quite similar efficacy compared with dual therapy. The ORR was 18%, and the disease control rate was 93% in the triplet arm. However, this was a small study. In a subsequent phase II study, 52 patients received the same regimens and demonstrated a PFS of 5.4 versus 4.2 months in the triplet versus doublet therapy (39). PTEN loss or the signaling pathway STAT has also been associated with intrinsic resistance to BRAF/MEK targeted therapies. Targeting the Wnt/ β -catenin signaling pathway represents another potential future treatment option, as Wnt was shown to activate signaling through RAF-MEK-ERK targeting (40). With further understanding of the complex mechanism of resistance, the therapeutic landscape will be changing to individualize therapy strategies based on molecular subtypes, and studies are needed to investigate multi-targeted combination treatments to overcome resistance.

- e. A recently published study evaluating whole-exome sequencing identified inactivating mutations in RNF43, a negative regulator of WNT, to predict improved response rates and survival in patients with BRAF^{V600E} mutated CRC and MSS tumors treated with anti-BRAF/EGFR combination therapies (41). The RNF43 mutation frequency was approximately 43%–44% (92%–100% in the MSI cohort and 28%–30% in the MSS cohort) in the discovery and validation cohort. The ORR in the RNF43^{mutated} subgroup was 63% compared with 31% in the RNF43^{wild-type} subgroup. Patients with the MSS-RNF43^{mutated} subtype achieved the highest ORR with 54% compared to the MSS-RNF43^{wild-type} subtype (21%) and MSI-RNF43^{mutated} subtypes (18%). Evaluation of circulating tumor DNA (ctDNA) is a further area of research. In an exploratory analysis of the BEACON trial, ctDNA was measured at baseline and the end of treatment. Variant allele frequency (VAF) of BRAF^{V600E} was measured, and patients were grouped in high and low categories (BRAF^{V600E} or ctDNA was not detected). Over 90% of patients had detectable BRAF^{V600E} mutations in the ctDNA. Patients with a higher VAF for BRAF^{V600E} had a worse prognosis. Compared with the control group of the BEACON trial, patients with triplet or doublet therapy had increased response rates, independent of VAF. CtDNA

VAF was found to be prognostic but not predictive of drug response (42). Biomarker analysis of the VELOUR (43) and RAISE studies (44) indicated a non-significant benefit of the addition of aflibercept in the VELOUR study and ramucirumab in the RAISE study to chemotherapy in BRAF^{V600E} mutated mCRC compared with wild-type BRAF mCRC. Prognostic and predictive biomarkers are of great interest to further individualize therapy in this rare subgroup of metastatic CRC.

Conclusion

Patients with BRAF^{V600E} mutated, MSS tumors have the worst prognosis among the variety of subgroups of CRC patients. The treatment options for patients with BRAF^{V600E} mutated CRC are limited. Our patient case showed that even in later lines, a targeted therapy combination could achieve an ongoing complete remission. Even a de-escalation from triplet to doublet therapy and subsequent discontinuation of therapy showed ongoing CR in this impressive patient case.

Data availability statement

The original contributions presented in the study are included in the article/supplementary material. Further inquiries can be directed to the corresponding author.

Ethics statement

Written informed consent was obtained from the individual(s) for the publication of any potentially identifiable images or data included in this article.

Author contributions

All authors listed have made a substantial, direct, and intellectual contribution to the work and approved it for publication.

Funding

Funded by the Johannes Kepler Open Access Publishing Fund.

Conflict of interest

The authors declare that the research was conducted in the absence of any commercial or financial relationships that could be construed as a potential conflict of interest.

Publisher's note

All claims expressed in this article are solely those of the authors and do not necessarily represent those of their affiliated

organizations, or those of the publisher, the editors and the reviewers. Any product that may be evaluated in this article, or claim that may be made by its manufacturer, is not guaranteed or endorsed by the publisher.

References

- Wan PT, Garnett MJ, Roe SM, Lee S, Niculescu-Duvaz D, Good VM, et al. Mechanism of activation of the RAF/ERK signaling pathway by oncogenic mutations of b-RAF. *Cell* (2004) 116:855–67. doi: 10.1016/S0092-8674(04)00215-6
- Barras D. BRAF mutation in colorectal cancer: an update. *Biomark Cancer* (2015) 7:9–12. doi: 10.4137/BIC.S25248
- Davies H, Birnrell GR, Cox C, Stephens C, Edkins S, Clegg S, et al. Mutations of the BRAF gene in human cancer. *Nature* (2002) 417:949–54. doi: 10.1038/nature00766
- Chu JE, Johnson B, Kugathasan L, Morris VK, Raghav K, Swanson L, et al. Populations-based screening for BRAF V600E in metastatic colorectal cancer reveals increased prevalence and poor prognosis. *Clin Cancer Res* (2020) 26:4599. doi: 10.1158/1078-0432.CCR-20-1024
- Morris V, Overmann JM, Jiang ZQ, Garrett C, Agarwal S, Eng C, et al. Progression-free survival remains poor over sequential lines of systemic therapy in patients with BRAF-mutated colorectal cancer. *Clin Colorectal Cancer* (2014) 13:164–71. doi: 10.1016/j.clcc.2014.06.001
- Samowitz WS, Sweeney C, Herrich J, Albertsen H, Levin TR, Murtaugh M, et al. Poor survival associated with the BRAF V600E mutation in microsatellite-stable colon cancers. *Cancer Res* (2005) 65(14):6063–9. doi: 10.1158/0008-5472.CAN-05-0404
- Bokemeyer C, Van Cutsem E, Rougier P, Ciardiello F, Heeger S, Schlichting M, et al. Addition of cetuximab to chemotherapy as first-line treatment for KRAS wild-type metastatic colorectal cancer: pooled analysis of the CRYSTAL and OPUS randomised clinical trials. *Eur J Cancer* (2012) 48:1466–75. doi: 10.1016/j.ejca.2012.02.057
- Flaherty KT, Puzanov I, Kim KB, Ribas A, McArthur GA, Sosman JA, et al. Inhibition of mutated, activated BRAF in metastatic melanoma. *N Engl J Med* (2010) 363:809–19. doi: 10.1056/NEJMoa1002011
- Flaherty KT, Robert C, Hersey P, Nathan P, Garbe C, Milhem M, et al. Improved survival with MEK inhibition in BRAF-mutated melanoma. *N Engl J Med* (2012) 367:107–14. doi: 10.1056/NEJMoa1203421
- Hyman DM, Puzanov I, Subbiah V, Faris JE, Chau I, Blay JY, et al. Vemurafenib in multiple nonmelanoma cancers with BRAF V600 mutations. *N Engl J Med* (2015) 373:726–36. doi: 10.1056/NEJMoa1502309
- Infante JR, Fecher LA, Falchook GS, Nallapareddy S, Gordon MS, Becerra C, et al. Safety, pharmacodynamic, and efficacy data for the oral MEK-inhibitor trametinib: a phase 1 dose-escalation trial. *Lancet Oncol* (2012) 13:773. doi: 10.1016/S1470-2045(12)70270-X
- Corcoran RB, Ehi H, Turke AB, Coffee EM, Nishino M, Cogdill AP, et al. EGFR-mediated re-activation of MAPK signaling contributes to insensitivity of BRAF mutant colorectal cancers to RAF inhibition with vemurafenib. *Cancer Discovery* (2012) 2:227–35. doi: 10.1158/2159-8290.CD-11-0341
- Prahalad A, Sun C, Huang S, Nicolantonio FD, Salazar R, Zecchin D, et al. Unresponsiveness of colon cancer to BRAF(V600E) inhibition through feedback activation of EGFR. *Nature* (2012) 483:100–3. doi: 10.1038/nature10868
- Kopetz S, Grothey A, Yaeger R, Van Cutsem E, Desai J, Yoshino T, et al. Encorafenib plus cetuximab with or without binimetinib for BRAF V600E metastatic colorectal cancer. *NEJM* (2019) 381:1632–43. doi: 10.1056/NEJMoa1908075
- Flaherty KT, Infante JR, Daud A, Gonzalez R, Kefford RF, Sosman J, et al. Combined BRAF and MEK inhibition in melanoma with BRAF V600E mutations. *N Engl J Med* (2012) 367:1694–703. doi: 10.1056/NEJMoa1210093
- Corcoran RB, Atreya CE, Falchook GS, Kwak EL, Ryan DP, Bendell JC, et al. Combined BRAF and MEK inhibition with dabrafenib and trametinib in BRAF V600E mutant colorectal cancer. *J Clin Oncol* (2015) 33:4023–31. doi: 10.1200/JCO.2015.63.2471
- Corcoran RB, André T, Atreya CE, Schellens JHM, Yoshino T, Bendell JC, et al. EGFR and MEK inhibition in patients with BRAF V600E mutant colorectal cancer. *Cancer Discovery* (2018) 8:428–43. doi: 10.1158/2159-8290.CD-17-1226
- Mity E, Fields AL, Bleiberg H, Labianca R, Portier G, Tu D, et al. Adjuvant chemotherapy after potentially curative resection of metastases from colorectal cancer: a pooled analysis of two randomized trials. *J Clin Oncol* (2008) 26:4906–11. doi: 10.1200/JCO.2008.17.3781
- Kanemitsu Y, Kato T, Shimizu Y, Inaba Y, Shimada Y, Nakamura K, et al. A randomized phase II/III trial comparing hepatectomy followed by mFOLFOX6 with hepatectomy alone as treatment for liver metastasis from colorectal cancer: japan clinical oncology group study JCOG0603. *Jpn J Clin Oncol* (2009) 39:406–9. doi: 10.1093/jco/hyp035
- Sonbol MB, Siddiqui R, Usón RLS, Pathak S, Firwana B, Botrus G, et al. The role of systemic therapy in resectable colorectal liver metastases: systematic review and network meta-analysis. *Oncologist* (2022) 27:1034–40. doi: 10.1093/oncolo/oyac212
- Cremolini C, Loupakis F, Antoniotti C, Lupi C, Sensi E, Lonardi S, et al. FOLFOXIRI plus bevacizumab versus FOLFIRI plus bevacizumab as first-line treatment of patients with metastatic colorectal cancer: updated overall survival and molecular subgroup analyses of the open-label, phase 3 TRIBE study. *Lancet Oncol* (2015) 16:1306–15. doi: 10.1016/S1470-2045(15)00122-9
- Cremolini A, Antoniotti C, Rossini D, Lonardi S, Loupakis F, Pietrantonio F, et al. Upfront FOLFOXIRI plus bevacizumab and reintroduction after progression versus mFOLFOX6 plus bevacizumab in the treatment of patients with metastatic colorectal cancer (TRIBE 2): a multicentre, open-label, phase 3, randomised, controlled trial. *Lancet Oncol* (2020) 21:497–507. doi: 10.1016/S1470-2045(19)30862-9
- Cremolini C, Antoniotti C, Stein A, Stein A, Bendell J, Gruenberger T, et al. Individual patient data meta-analysis of FOLFOXIRI plus bevacizumab versus doublets plus bevacizumab as initial therapy of unresectable metastatic colorectal cancer. *J Clin Oncol* (2020) 38:3314–24. doi: 10.1200/JCO.20.01225
- Grassi E, Corbelli J, Papiani G, Barera MA, Gazzaneo F, Tambari S. Current therapeutic strategies in BRAF-mutated metastatic colorectal cancer. *Front Oncol* (2021) 11:601–722. doi: 10.3389/fonc.2021.601722
- Venderbosch S, Nagtegaal ID, Maughan TS, Smith CG, Cheadle JP, Fisher D, et al. Mismatch repair status and BRAF mutation status in metastatic colorectal cancer patients: a pooled analysis of the CAIRO, CAIRO2, COIN, and FOCUS studies. *Clin Cancer Res* (2014) 20:5322–30. doi: 10.1158/1078-0432.CCR-14-0332
- André T, Shiu KK, Kim TW, Jensen BV, Jensen LH, Punt C, et al. Pembrolizumab in microsatellite-instability-high advanced colorectal cancer. *N Engl J Med* (2020) 383:2207–18. doi: 10.1056/NEJMoa2017699
- Le DT, Kim TW, Van Cutsem E, Geva R, Jäger D, Hara H, et al. Phase II open-label study of pembrolizumab in treatment-refractory, microsatellite instability-high/mismatch repair-deficient metastatic colorectal cancer: keynote-164. *J Clin Oncol* (2020) 38:11–9. doi: 10.1200/JCO.19.02107
- Overman MJ, Lonardi S, Wong KYM, Lenz HJ, Gelsomino F, Aglietta M, et al. Durable clinical benefit with nivolumab plus ipilimumab in DNA mismatch repair-deficient/microsatellite instability-high metastatic colorectal cancer. *J Clin Oncol* (2018) 36:773–9. doi: 10.1200/JCO.2017.76.9901
- Van Cutsem E, Taieb J, Yaeger R, Yoshino T, Grothey A, Maiello E, et al. ANCHOR CRC: results from a single-arm, phase II study of encorafenib plus binimetinib and cetuximab in previously untreated BRAF V600E-mutant metastatic colorectal cancer. *J Clin Oncol* (2023). doi: 10.1200/JCO.22.01693
- Tabernero J, Yoshino T, Kim TW, et al. BREAKWATER safety lead-in (SLI): encorafenib + cetuximab + chemotherapy for BRAF V600E metastatic colorectal cancer. *Ann Oncol* (2022) 33:1392–3. doi: 10.1016/j.annonc.2022.08.022
- Ebert PJR, Cheung J, Yang Y, McNamara E, Hong R, Moskalenk M, et al. MAP kinase inhibition promotes T cell anti-tumor activity in combination with PD-L1 checkpoint blockade. *Immunity* (2016) 44:609–21. doi: 10.1016/j.immuni.2016.01.024
- Liu L, Mayes PA, Eastman S, Shi H, Yadavilli S, Zhang T, et al. The BRAF and MEK inhibitors dabrafenib and trametinib: effects on immune function and in combination with immunomodulatory antibodies targeting PD-1, PD-L1, and CTLA-4. *Clin Cancer Res* (2015) 21:1639–51. doi: 10.1158/1078-0432.CCR-14-2339
- Hong A, Piva M, Liu S, Hugo W, Lomeli SH, Zoete V, et al. Durable suppression of acquired MEK inhibitor resistance in cancer by sequestering MEK from ERK and promoting antitumor T-cell immunity. *Cancer Discovery* (2021) 11:714–35. doi: 10.1158/2159-8290.CD-20-0873
- Tian J, Chen JH, Chao SX, Pelka K, Giannakis M, Hess J, et al. Combined PD-1, BRAF and MEK inhibition in BRAF^{V600E} colorectal cancer: a phase 2 trial. *Nat Med* (2023) 29(2):458–66. doi: 10.1038/s41591-022-021181-8
- Yaeger R, Yao Z, Hyman DM, Hechtman JF, Vakiani E, Zhao HY, et al. Mechanisms of acquired resistance to BRAF V600E inhibition in colon cancers converge on RAF dimerization and are sensitive to its inhibition. *Cancer Res* (2017) 77:6513–23. doi: 10.1158/0008-5472.CAN-17-0768
- Xu T, Wang X, Wang Z, Deng T, Qi C, Liu D, et al. Molecular mechanisms underlying the resistance of BRAF V600E-mutant metastatic colorectal cancer to EGFR/BRAF inhibitors. *Ther Adv Med Oncol* (2022) 14:1–12. doi: 10.1177/17588359221105022
- Mao M, Tian F, Mariadason JM, Tsao CC, Lemos R, Dayyani F, et al. Resistance to BRAF inhibition in BRAF-mutant colon cancer can be overcome with PI3K inhibition or demethylating agents. *Clin Cancer Res* (2013) 19:657–67. doi: 10.1158/1078-0432.CCR-11-1446

38. van Geel R, Tabernero J, Elez E, Bendell JC, Spreafico A, Schuler M, et al. A phase Ib dose-escalation study of encorafenib and cetuximab with or without alpelisib in metastatic BRAF-mutant colorectal cancer. *Cancer Discovery* (2017) 7:610–9. doi: 10.1158/2159-8290.CD-16-0795
39. Tabernero J, Van Geel R, Guren TK, Yaeger R, Spreafico A, Faris J, et al. Phase 2 results: encorafenib and cetuximab with or without alpelisib in patients with advanced BRAF-mutated colorectal cancer. *J Clin Oncol* (2016) 34 (suppl 15):3544.
40. Jeong WJ, Ro EJ, Choi KY. Interaction between wnt/ β -catenin and RAS-ERK pathways and an anti-cancer strategy via degradations of β -catenin and RAS by targeting the wnt/ β -catenin pathway. *Oncol* (2018) 2:1–10. doi: 10.1038/s41698-018-0049-y
41. Elez E, Ros J, Fernández J, Villacampa G, Moreno-Cárdenas AB, Arenillas C, et al. RNF43 mutations predict response to anti-BRAF/EGFR combinatory therapies in BRAFV600E metastatic colorectal cancer. *Nature Medicine* (2022) 28:2162–217. doi: 10.1038/s41591-022-01976-z
42. Kopetz S, Murphy DA, Pu J, Yaeger R, Ciardiello F, Desai J, et al. Evaluation of baseline BRAF V600E mutation in circulating tumor DNA and efficacy response from the BEACON study. *J Clin Oncol* (2022) 40(4_suppl 162):162. doi: 10.1200/JCO.2022.40.4_suppl.162
43. Wirapati P, Pomella V, Vandenbosch B, Kerr P, Maiello E, Jeffery GM, et al. Velour trial biomarkers update: impact of RAS, BRAF, and sidedness on aflibercept activity. *J Clin Oncol* (2017) 35:3538. doi: 10.1200/JCO.2017.35.15_suppl.3538
44. Yoshino T, Portnoy DC, Obermannová R, Bodoky G, Prausová J, García-Carbonero R, et al. Biomarker analysis beyond angiogenesis: RAS/RAF mutation status, tumour sidedness, and second-line ramucirumab efficacy in patients with metastatic colorectal carcinoma from RAISE—a global phase III study. *Ann Oncol* (2018) 30:124–31. doi: 10.1093/annonc/mdy461



OPEN ACCESS

EDITED BY

Alessandro Passardi,
Scientific Institute of Romagna for the
Study and Treatment of Tumors (IRCCS),
Italy

REVIEWED BY

Eleonora Lai,
University Hospital and University of
Cagliari, Italy
Alfonso De Stefano,
G. Pascale National Cancer Institute
Foundation (IRCCS), Italy

*CORRESPONDENCE

Wen-Hui Yang

✉ yangwenhui-10012@163.com

Jun Xie

✉ junxie@sxmu.edu.cn

[†]These authors have contributed equally to
this work

RECEIVED 20 February 2023

ACCEPTED 17 May 2023

PUBLISHED 31 May 2023

CITATION

Xue W-H, Li X-W, Ding Y-Q, Wu N,
Pei B-B, Ma X-Y, Xie J and Yang W-H
(2023) Efficacy and safety of third-line
or later-line targeted treatment for
patients with metastatic colorectal
cancer: a meta-analysis.
Front. Oncol. 13:1165040.
doi: 10.3389/fonc.2023.1165040

COPYRIGHT

© 2023 Xue, Li, Ding, Wu, Pei, Ma, Xie and
Yang. This is an open-access article
distributed under the terms of the [Creative
Commons Attribution License \(CC BY\)](#). The
use, distribution or reproduction in other
forums is permitted, provided the original
author(s) and the copyright owner(s) are
credited and that the original publication in
this journal is cited, in accordance with
accepted academic practice. No use,
distribution or reproduction is permitted
which does not comply with these terms.

Efficacy and safety of third-line or later-line targeted treatment for patients with metastatic colorectal cancer: a meta-analysis

Wen-Hui Xue^{1†}, Xue-Wei Li^{2†}, Ya-Qian Ding¹, Na Wu¹,
Bei-Bei Pei¹, Xiao-Yan Ma¹, Jun Xie^{2*} and Wen-Hui Yang^{3*}

¹Department of Digestive Oncology, Cancer Center, Shanxi Bethune Hospital, Shanxi Academy of Medical Sciences, Tongji Shanxi Hospital, Third Hospital of Shanxi Medical University, Taiyuan, Shanxi, China, ²Department of Biochemistry and Molecular Biology, Shanxi Key Laboratory of Birth Defect and Cell Regeneration, Shanxi Medical University, Taiyuan, Shanxi, China, ³Department of Gastroenterology, Shanxi Province Cancer Hospital/Shanxi Hospital Affiliated to Cancer Hospital, Chinese Academy of Medical Sciences/Cancer Hospital Affiliated to Shanxi Medical University, Taiyuan, Shanxi, China

Targeted therapy has been standardized in front-line therapies for metastatic colorectal cancer (mCRC), while explicit recommendations for third- or later-line are still lacking. This study evaluated the efficacy and safety of combining targeted therapy with chemotherapy in the third- or later-line treatment for mCRC *via* meta-analysis, providing evidence-based guidance for clinical or research practice. Comprehensive retrieval of related studies was conducted according to the PRISMA guideline. Studies were stratified with patient characteristics and pharmacological classification of the drugs. For the data available for quantitative analysis, pooled overall response rate, disease control rate, hazard ratios (HRs) for overall survival (OS) and progression-free survival (PFS), and adverse events rate with respective 95% confidence intervals (CIs) were calculated. A total of 22 studies (1,866 patients) were included in this meta-analysis. Data from 17 studies (1,769 patients) involving targets of epidermal growth factor receptor (EGFR) and vascular endothelial growth factor (VEGF) were extracted for meta-analyses. The overall response rates for monotherapy and combined therapy were 4% (95% CI: 3%, 5%) and 20% (95% CI: 11%, 29%). The pooled HRs (combined therapy vs. mono) for OS and PFS were 0.72 (95% CI: 0.53, 0.99) and 0.34 (95% CI: 0.26, 0.45). Another five studies were included in narrative depiction, involving targets of BRAF, HER-2, ROS1, and NTRK. The findings of this meta-analysis indicate that VEGF and EGFR inhibitors manifest promising clinical response rates and prolonged survival in the treatment of mCRC with acceptable adverse events.

KEYWORDS

efficacy, safety, metastatic colorectal cancer, meta-analysis, targeted therapy

Introduction

Colorectal cancer (CRC) is one of the most common malignancies worldwide; the estimated annual incidence and mortality are 19.7/100,000 and 8.9/100,000 (1, 2). Among patients diagnosed with CRC, 20% had metastatic colorectal cancer (mCRC) and 40% had recurrence after previous treatment of localized diseases (3, 4). Furthermore, prognosis remains poor after standard treatment for patients with mCRC, with a median 5-year survival rate of less than 20% (4).

At present, the standard first-line and second-line therapies for mCRC are a combination of doublet or cytotoxic triplet chemotherapy and targeted therapies, including anti-epidermal growth factor receptor (EGFR) or anti-vascular endothelial growth factor (VEGF) antibody, the choice of treatment is influenced by patient features, cancer characteristics, and molecular profiles (5–8). In addition, RAS and BRAF tests are recommended by the European Society for Medical Oncology (ESMO) and the United States (US) National Comprehensive Cancer Network (NCCN) guidelines before the initiation of first-line therapy (9, 10). The choice of second-line regimen depends on the first-line systemic treatment, and approximately two-thirds of mCRC patients received second-line treatment (11). Fluorouracil, folinic acid, and irinotecan (FOLFIRI) and fluorouracil, folinic acid, and oxaliplatin (FOLFOX) are typical second-line chemotherapy options for mCRC patients (12). However, the efficacy of chemotherapy is very low in the third-line treatment of CRC, and tumor shrinkage is rarely observed (13). Immunotherapy revolutionized the oncology landscape in the past 10 years, pembrolizumab or nivolumab are recommended as treatment options in second-line and beyond for patients with deficient MMR/MSI-high mCRC (11, 12). For CRC patients receiving third-line treatment, considering molecular cancer characteristics and clinical trial registration is an important aspect of management (12). Cetuximab or panitumumab is particularly effective for KRAS/NRAS wild-type mCRC patients not previously treated with EGFR antibodies and is recommended as the standard treatment for the third-line or later-line follow-up treatment (14, 15). Regorafenib is recommended in RAS wild-type patients previously treated with EGFR antibodies (10). Furthermore, receptor tyrosine kinase inhibitor (rTKI) has been shown to prolong progression-free survival (PFS) in refractory mCRC patients with acceptable tolerability (16). Agents targeting human epidermal growth factor receptor-2 (HER2), neurotrophic tyrosine receptor kinase (NTRK),

and c-ros oncogene 1, receptor tyrosine kinase (ROS1) were used in the treatment of mCRC (17–19). Nevertheless, EGFR inhibitors are associated with toxicity, including rash and diarrhea in tissues expressing EGFR. Multi-kinase inhibitors can cause hand-foot skin reactions, rash, fatigue, diarrhea, and hypertension (20). Therefore, when the quality of life gains importance as a therapeutic goal, the difference in the mechanism of action and, more importantly, the safety of available third-line/late-line mCRC therapy may guide the treatment choices of individual patients.

Targeted therapy has been standardized in front-line therapies for mCRC, but explicit recommendations for third- or later-line are still lacking. As far as it is concerned, several studies reported the efficacy and safety of targeted treatment alone or combined chemotherapy (16, 21–28). This study aimed to conduct a meta-analysis through a synthesis of the evidence to generate a comprehensive assessment of efficacy and safety of third-line or later-line targeted treatment for patients with mCRC and subsequently to provide evidence and clues for clinical research and practice.

Materials and methods

Statements

This meta-analysis was conducted based on published citations that had declared ethical approvals, and no original clinical raw data of the published results were collected or utilized, thereby ethical approval was not warranted for this study. This study was based on the Preferred Reporting Items for Systematic Reviews and Meta-analysis (PRISMA) (29).

Search strategy and selection criteria

We systematically searched the online electronic databases, PubMed, Scopus, and Embase, from the databases' inception to June 16, 2022, with articles in English all considered. The following keywords and terms were used for the online database search: third-line, later-line, fruquintinib, famitinib, bevacizumab, ramucirumab, cetuximab, panitumumab, trastuzumab, pertuzumab, tucatinib, lapatinib, larotrectinib, entrectinib, encorafenib, vemurafenib, targeted therapy, VEGF, ALK, ROS1, EGFR, HER2, NTKR, BRAF, metastatic colorectal cancer, and mCRC. The search strategy was (((((((((((((((((((third-line[Title/Abstract]) OR (later-line[Title/Abstract]) OR (fruquintinib[Title/Abstract]) OR (famininib[Title/Abstract]) OR (bevacizumab[Title/Abstract]) OR (ramucirumab [Title/Abstract]) OR (cetuximab[Title/Abstract]) OR (panitumumab[Title/Abstract]) OR (trastuzumab[Title/Abstract]) OR (pertuzumab[Title/Abstract]) OR (tucatinib[Title/Abstract]) OR (lapatinib[Title/Abstract]) OR (larotrectinib[Title/Abstract]) OR (entrectinib[Title/Abstract]) OR (encorafenib[Title/Abstract]) OR (vemurafenib[Title/Abstract]) OR (targeted therapy[Title/Abstract]) OR (VEGF[Title/Abstract]) OR (ALK[Title/Abstract]) OR (ROS1[Title/Abstract]) OR (EGFR[Title/Abstract]) OR (HER2 [Title/Abstract]) OR (NTKR[Title/Abstract]) OR (BRAF[Title/Abstract]) AND ((metastatic colorectal cancer[Title/Abstract]) OR

Abbreviations: mCRC, metastatic colorectal cancer; HRs, hazard ratios; OS, overall survival; CIs, confidence intervals; CRC, colorectal cancer; EGFR, epidermal growth factor receptor; ESMO, European Society for Medical Oncology; US, United States; NCCN, National Comprehensive Cancer Network; FOLFIRI, fluorouracil, folinic acid, and irinotecan; FOLFOX, fluorouracil, folinic acid, and oxaliplatin; rTKI, receptor tyrosine kinase inhibitor; PFS, progression-free survival; HER2, human epidermal growth factor receptor-2; NTRK, neurotrophic tyrosine receptor kinase; ROS1, receptor tyrosine kinase; PRISMA, Preferred Reporting Items for Systematic Reviews and Meta-analysis.

(mCRC[Title/Abstract])) AND (english[Filter]). The references of related reviews and included articles were also searched to retrieve additional studies not previously identified in the initial literature search. Inclusion criteria were as follows: clinical trials or cohort studies evaluating the efficacy and safety of third-line or later-line targeted treatment of patients with mCRC and relevant outcomes regarding treatment effects and adverse events were reported or could be calculated from the available data in the citation. Exclusion criteria included conference abstracts, case reports or case series, reviews, news, and editorials.

Two independent investigators (Wen-Hui Xue and Xue-Wei Li) accomplished the literature search and conducted the process of study selection. A third author (Wen-Hui Yang) was involved if no consensus was achieved.

Data extraction and quality assessments

The following information was extracted from each study: name of the first author, year of publication, country, study design, number of patients, age of patients, percentage of females, patient performance, targeted molecule, lines of current treatment, therapy schedule, response rate, complete response rate (ORR), partial response rate, stable disease rate, disease progression rate, disease control rate, hazard ratios (HRs) for overall survival (OS) and progression-free survival (PFS), and adverse events rate. Clinical response and disease progression were assessed according to Response Evaluation Criteria in Solid Tumors (RECIST version 1.1) (30). The Cochrane Collaboration tool was used to evaluate the risk of bias in randomized trials enrolled in this meta-analysis (31). The methodological index for non-randomized studies (MINORS) was used for single-arm studies (32).

Statistical analysis

The R (A language and environment for statistical computing, Version 3.6.1) was used for statistical analyses. Pooled rates and HRs with their respective 95% confidence intervals (CIs) were synthesized with a random or fixed-effects model. A random-effects model was used if the I^2 value was $> 50\%$; otherwise, a fixed-effects model was used. The Cochran Q test was used to assess heterogeneity between studies, and the I^2 statistic was used to test the magnitude of the heterogeneity. Egger's tests were performed to evaluate the publication bias in this meta-analysis. A p -value less than 0.05 was considered to be of statistical significance.

Results

Study selection and characteristics

A total of 620 articles were identified from the databases searched. Sixty-one duplicates were eliminated, and 537 studies were excluded through an initial screening. After a full-text assessment for eligibility of the remaining 22 articles, 17 studies

were eligible for inclusion in this meta-analysis, and five studies were narratively depicted. No additional studies were identified through reference screening of the included papers and relevant reviews. Figure 1 shows details on the literature search and study selection. The enrolled 22 citations contained 1,866 patients with confirmed mCRC and reported relevant eligible outcomes for data synthesis. Twenty studies were clinical trials, and two studies were cohort studies. These studies were conducted in China, the United States, Italy, South Korea, Vietnam, France, Spain, and Japan. Table 1 shows detailed characteristics of the included studies. The quality of included studies was rated as high based on the Cochrane Collaboration tool and the MINORS scale (Tables 1, 2).

Treatment response

Nine studies assessed the efficacy of EGFR inhibitors monotherapy or combining chemotherapy as third-line or later-line treatment for mCRC. The other eight studies evaluated the efficacy of VEGF antibodies in treating mCRC. The pooled ORRs for monotherapy and combined therapy were 4% (95% CI: 3%, 5%) and 20% (95% CI: 11%, 29%). In the subgroup analysis of molecule targets, the pooled ORRs for VEGF and EGFR inhibitors were 4% (95% CI: 2%, 5%) and 19% (95% CI: 10%, 27%). The pooled disease progression rates for monotherapy and combined therapy were 53% (95% CI: 25%, 80%) and 34% (95% CI: 28%, 40%), respectively. The respective pooled disease progression rates for VEGF and EGFR inhibitors were 46% (95% CI: 20%, 72%) and 36% (95% CI: 29%, 43%). Concerning stable disease rates, the pooled rates for monotherapy and combined therapy were 49% (95% CI: 34%, 64%) and 43% (95% CI: 34%, 51%), and the pooled rates for VEGF and EGFR inhibitors were 57% (95% CI: 44%, 69%) and 37% (95% CI: 31%, 42%). The pooled disease control rates for monotherapy and combined therapy were 62% (95% CI: 50%, 74%) and 61% (95% CI: 54%, 68%), respectively. The pooled disease control rates for VEGF and EGFR inhibitors were 59% (95% CI: 50%, 68%) and 62% (95% CI: 54%, 71%) (Table 3).

The efficacy of BRAF inhibitor monotherapy for mCRC is not promising, with 0% to 5% ORRs (37). The anti-HER2 antibody trastuzumab and the dual EGFR/HER2 kinase inhibitor lapatinib were used in a phase 2 trial performed at four Italian academic cancer centers; the results were as follows: ORR of 30%, DCR of 74%, with 22% of Grade 3 toxicity (41). In addition, results of the MyPathway Study revealed that trastuzumab plus pertuzumab showed an ORR of 38% (95% CI: 23% to 55%) in 37 mCRC patients (19). In the study of Hong et al., four in eight patients with TRK fusion-positive colon cancer demonstrated a response to larotrectinib with a median response duration of 3.7 months (18). Doebele et al. reported that one in four patients with CRC responded to entrectinib, an ROS1 and NTRK inhibitor (17).

Survival

A total of four studies reported the Kaplan–Meier estimates of overall survival in the treatment and control groups. The pooled HR

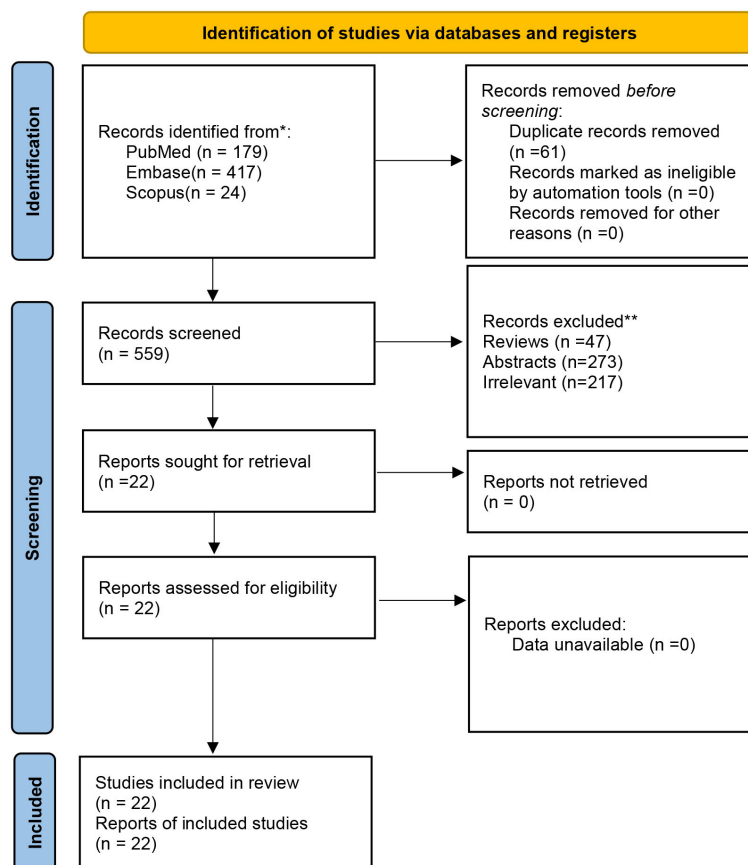


FIGURE 1
Search results and flow chart of the meta-analysis.

was 0.72 (95% CI: 0.53, 0.99) (Figure 2). For PFS, the pooled HR of five trials was 0.34 (95% CI: 0.26, 0.45) (Figure 3).

Adverse events

Hematological adverse events were the most frequently reported in included studies. The occurrence rates of anemia for VEGF and EGFR inhibitors were 26% (95% CI: 7%, 44%) and 42% (95% CI: 3%, 87%). The pooled occurrence rates of leucopenia for VEGF and EGFR inhibitors were 36% (95% CI: 9%, 63%) and 33% (95% CI: 6%, 60%). With regard to neutropenia, pooled occurrence rates for VEGF and EGFR inhibitors were 34% (95% CI: 9%, 60%) and 47% (95% CI: 24%, 71%). The occurrence rates of thrombocytopenia for VEGF and EGFR inhibitors were 25% (95% CI: 14%, 36%) and 18% (95% CI: 12%, 23%).

Publication bias

P-values of Egger's tests for publication bias were < 0.001, 0.129, 0.001, 0.052, 0.588, 0.622, 0.078 in the pooled analyses of overall response, stable disease, disease progression, disease control, HR for OS, HR for PFS, and adverse events, respectively.

Discussion

CRC is one of the most important tumors, with high incidence and mortality rates worldwide (43). Many patients are diagnosed at the metastatic stage of the disease; for these patients, treatment is mainly based on chemotherapy (44). Maintaining the quality of life is the primary goal and urgent need of mCRC patients undergoing third-line or later-line treatment (8). However, few insights are gained to guide the selection and sequencing of treatments for these patients (10, 14). Recently, prolonged OS in patients with mCRC has been observed through targeted therapies, such as antibodies against EGFR and VEGF (44).

In the meta-analysis, 17 published articles containing 1,769 patients with diagnosed mCRC and treated with targeted therapies were included. This meta-analysis showed that the pooled ORRs for VEGF and EGFR inhibitors were 4% and 19% in the third-line or later-line treatment of mCRC. Targeted therapy combined with chemotherapy demonstrated favorable ORR and disease control rate with less disease progression than target monotherapy. The results corroborated the findings from previous clinical trials. Furthermore, targeted therapy revealed increased OS and PFS; the goal of the third-line or later-line treatment is to prolong survival and prevent tumor progression without affecting the quality of life. The molecular type of mCRC in included studies was not specified.

TABLE 1 Characteristics of included studies.

Author	Year	Country	Study design	No. of patient	Age (yrs)	Female (%)	ECOG-PS	Targets	Lines of treatment	Treatment schedule	Control	Tumor molecular pathology	MINORS scores
Akiyoshi (28)	2017	Japan	Phase 2	43	62 (32 - 75)	42	0 or 1	EGFR	Third	Panitumumab was administered at a dose of 6 mg/kg and irinotecan at a dose of either 150 mg/m ² or the tolerated irinotecan dose during prior treatment.	NA	KRAS wild type	14
Andre (23)	2012	France	Single-arm, multi-centered phase 2 study	65	62 (34 - 84)	40	0 or 1 or 2	EGFR	Third	Panitumumab at a dose of 6 mg/kg on day 1 was administered as a 60-min intravenous infusion, just before the administration of irinotecan 180 mg/m ² in 90 min on day 1 of each fortnightly cycle (cycles are every 14 days).	NA	KRAS wild type	15
Bai (24)	2015	China	Cohort study	19	59 (48 - 72)	47	0 or 1 or 2	EGFR	Third	Cetuximab was infused at a first dose of 400 mg/m ² and then at 250 mg/m ² every week.	NA	NR	14
Chen (33)	2019	China	Single-arm phase 2 study	26	57 (28 - 75)	63	0 or 1 or 2	VEGF	Third or later	Apatinib-500 milligrams (mg) per flat dose, 28-day cycle	NA	NR	15
Chi (34)	2021	China	A Double-Blinded, Placebo-Controlled, Randomized Phase 3 Trial	419	56	36	0 or 1	EGFR	Third or later	oral anlotinib (12 mg/day; days 1–14; 21 days per cycle)	Placebo	NR	NA
Cremolini (35)	2019	Italy	Phase 2 Single-Arm	28	69 (45 - 79)	32	0 or 1	EGFR	Third	Biweekly cetuximab, 500 mg/m ² , plus irinotecan, 180 mg/m ² .	NA	RAS and BRAF wild type	14
Doebele (17)	2020	South Korea, Spain, USA	Phase 1	4	NR	NR	0 or 1 or 2	ROS1 and NTRK	NR	Entrectinib orally at a dose of at least 600 mg once per day	NA	NR	13
Eng (36)	2019	USA	Phase 3	75	59 (52 - 66)	57	0 or 1	VEGF	Third	Regorafenib 160 mg (group C) was given orally once daily on days 1–21 of a 28-day cycle.	NA	NR	14
Gebbia (21)	2006	Italy	Retrospective study	60	62 (37 - 81)	42	1 or 2	EGFR	Third or later	Weekly irinotecan 120 mg/m ² as a 1h intravenous infusion and cetuximab 400 mg/m ² infused over 2h as the initial dose and 250 mg/m ² infused over 1h for the subsequent administrations	NA	NR	13
Hong (18)	2020	USA	Phase 1	8	NR	NR	NR	NTRK	NR	Larotrectinib was administered orally (capsule or liquid formulation), continuously, on a 28-day schedule	NA	TRK fusion-positive	14

(Continued)

TABLE 1 Continued

Author	Year	Country	Study design	No. of patient	Age (yrs)	Female (%)	ECOG-PS	Targets	Lines of treatment	Treatment schedule	Control	Tumor molecular pathology	MINORS scores
Hainsworth (19)	2018	USA	Phase 2a	37	NR	NR	0, 1, or 2	HER2	NR	Trastuzumab (8 mg/kg IV loading dose, then 6 mg/kg IV every 3 weeks) plus pertuzumab (840 mg IV loading dose, then 420 mg IV every 3 weeks)	NA	NR	14
Kopetz (37)	2015	NR	Phase 2	21	65 (38 - 91)	48	0 or 1	BRAF	Third or later	Vemurafenib was provided in microprecipitated bulk powder formulation as 240-mg film-coated tablets, dosed at the previously determined maximum-tolerated dose of 960 mg orally twice a day, and administered continuously in 28-day cycles.	NA	BRAF-mutated	13
Li (38)	2015	China, South Korea, Taiwan, and Vietnam	Randomised, double-blind, placebo-controlled, phase 3 trial	204	58 (50 - 66)	42	0 or 1	VEGF	Third or later	Patients received regorafenib 160 mg orally once daily on days 1–21 of each 28-day cycle	Placebo	NR	NA
Li (25)	2018	China	Randomised, double-blind, placebo-controlled, phase 3 trial	416	55 (23 - 75)	39	0 or 1	VEGF	Third or later	Fruquintinib, 5 mg orally, once daily for 21 days, followed by 7 days off in 28-day cycles	Placebo	NR	NA
Masuishi (39)	2020	Japan	Phase 2	34	65 (41 - 80)	32	0 or 1	EGFR	Third	Patients received 150 mg/m ² irinotecan intravenously every 2 weeks. Cetuximab was administered as a 2h intravenous infusion at a loading dose of 400 mg/m ² , followed by weekly 1h infusions of 250 mg/m ² .	NA	KRAS wild type	14
Osumi (40)	2018	Japan	Phase 2	40	59 (31 - 72)	65	0 or 1	EGFR	Third	C-mab was initially given at a dose of 500 mg/m ² as a 2h infusion followed by biweekly dose of 500 mg/m ² as a 1h infusion. CPT-11 was given at a dose of 150 mg/m ² biweekly.	NA	NR	14
Sartore-Bianchi (41)	2016	Italy	Phase 2	27	62 (50 - 68)	15	0 or 1	HER2	Third or later	Trastuzumab was given intravenously at a 4 mg/kg loading dose, then at 2 mg/kg once per week, and lapatinib was given orally at 1000 mg per day in 21-day treatment cycles.	NA	KRAS codon 12/13 wild type	14
Vincenzi (22)	2006	Italy	Phase 2	55	63 (27 - 79)	53	0 or 1 or 2	EGFR	Third	Cetuximab was given at an initial dose of 400 mg/m ² , followed by weekly infusions of 250 mg/m ² . Irinotecan was administered weekly at the dose of 90 mg/m ² .	NA	NR	15

(Continued)

TABLE 1 Continued

Author	Year	Country	Study design	No. of patient	Age (yrs)	Female (%)	ECOG-PS	Targets	Lines of treatment	Treatment schedule	Control	Tumor molecular pathology	MINORS scores
Xu (27)	2017a	China	Phase 2	71	50 (25 - 69)	40	0 or 1	VEGF	Third or later	Fruquintinib plus best supportive care	Placebo plus best supportive care	NR	NA
Xu (16)	2017b	China	double-blinded, placebo-controlled, phase 2	154	55 (24 - 71)	42	0 or 1	VEGF	Third or later	Patients were treated with 25-mg oral famitinib	Placebo	NR	NA
Yoshida (26)	2016	Japan	Phase 2	28	68 (38 - 78)	32	0 or 1 or 2	VEGF	Third	Bevacizumab was given intravenously every 2 weeks, and S-1 was administered orally on days 1–28 of a 42-day cycle.	NA	mutated KRAS	14
Yoshida (42)	2020	Japan	Single-arm, multi-centered phase 2 study	32	67 (45 - 78)	37.5	0 or 1	VEGF	Third or later	TAS-102 (35 mg/m ²) was given orally twice daily on days 1–5 and 8–12 in a 4-week cycle, and bevacizumab (5 mg/kg) was administered by intravenous infusion every 2 weeks.	NA	NR	16

It is reported that the benefit in PFS and OS was observed only in the KRAS wild-type patients for both cetuximab and panitumumab (45, 46). Moreover, the NCCN clinical practice guideline recommended that regorafenib could be utilized in fit patients with the refractory disease after standard chemotherapy including fluoropyrimidine, oxaliplatin, and irinotecan and anti-VEGF or anti-EGFR therapies (RAS wild type) (47).

However, hematological adverse events, including anemia, neutropenia, leucopenia, and thrombocytopenia, were commonly observed in included studies. In addition, the evidence on clinical trials of other targeted therapies, namely, BRAF inhibitors, HER2 inhibitors, anti-NTRK agents, and ROS1 inhibitors, was limited, so we could not pool these outcomes. Therapies with HER2, NTRK, and ROS1 blockade have shown significant antitumor activity, and more well-designed clinical trials are needed to verify the efficacy and safety of these agents. It is recommended in HER2-positive patients with mCRC, treatment with HER2 dual blockade is optionally recommended, especially in RAS WT tumors (48).

This meta-analysis was conducted at the population level, because individual patient data cannot be obtained. In the current study, a comprehensive literature search in English was performed to increase the probability of obtaining all relevant included studies. Data extraction was conducted by two independent reviewers using a pre-designed form. In addition, we assessed the quality of enrolled studies using the Cochrane Collaboration tool and the MINORS scale. The quality of included studies was rated as high. We assessed the heterogeneity between the studies. Results showed significant heterogeneities in the analyses of OS and PFS. The heterogeneity may be attributed to differences in patient characteristics, study design, drug compliance, prior lines of therapy in each study, and other relevant factors. Due to heterogeneity between third-line or later-line treatment regimens, it is difficult for us to determine the specific subgroups, and therefore subgroup analysis based on regimens was not performed. Meta-regression was not performed due to a limited number of studies in each subgroup. Furthermore, the findings of Egger's tests indicated that publication bias might not be neglected in analyzing several indicators. Albeit with the heterogeneity and publication bias in included studies and limitations of this meta-analysis, the results may provide evidence-based information on the efficacy and safety of third-line or later-line target therapy for patients with mCRC.

Based on the outcomes of this meta-analysis, we may conclude that targeted therapies, including VEGF and EGFR inhibitors, showed promising clinical response rates and prolonged survival in the treatment of mCRC patients with progression after first- and second-line therapy. Targeted therapy for mCRC patients with biomarker selection may improve marginal prognosis but is unlikely to change the treatment pattern of most patients significantly. Incidences of hematological adverse events were durable and acceptable. However, the pathogenesis of these adverse events remains poorly understood (49). Personalized treatment or combined therapy was recommended based on the feature of mCRC. It is expected that well-designed clinical trials, as well as real-world studies, should be conducted to address issues on the evaluation of efficacy and safety of VEGF and EGFR inhibitors and other targets in the treatment of mCRC. Very preliminary

TABLE 2 Quality evaluation for Cochrane tool.

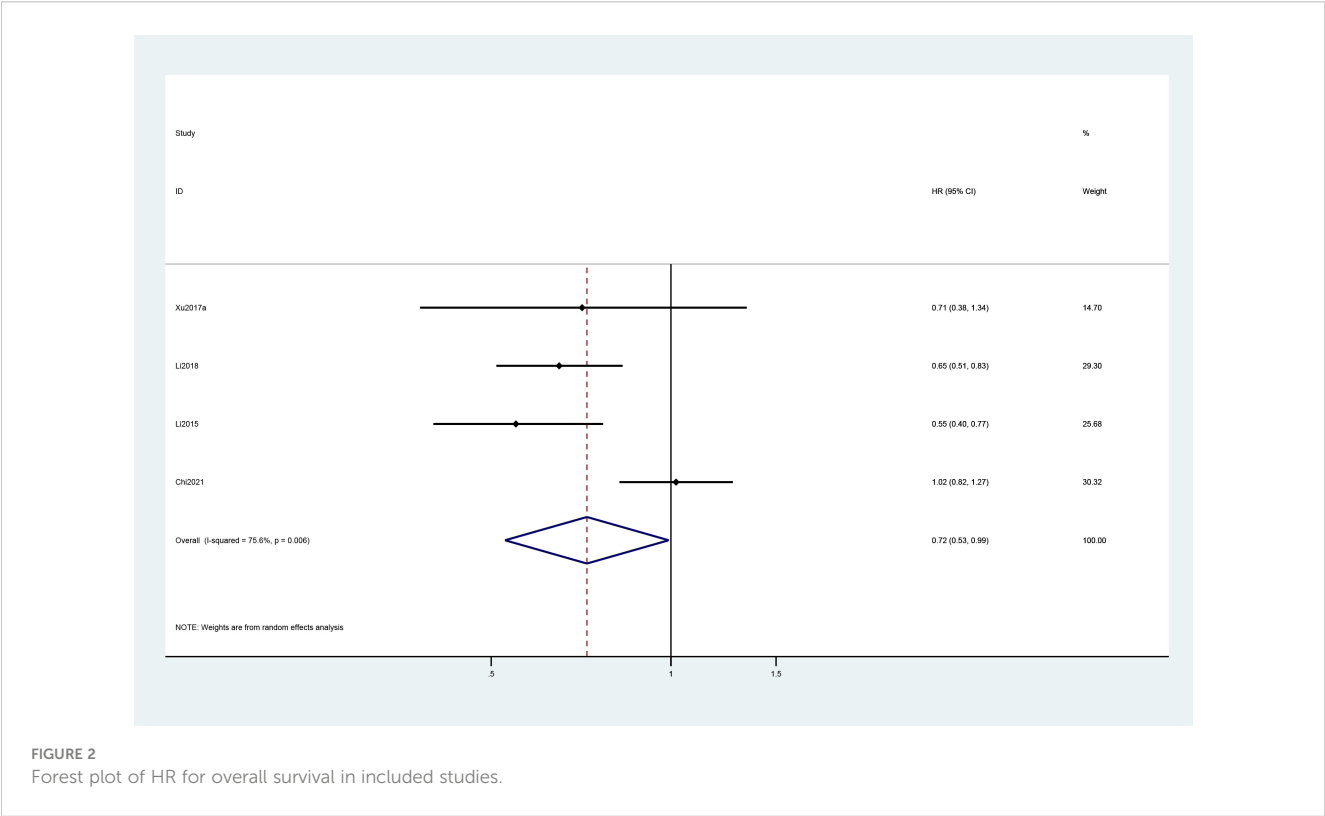
Study	Random sequence generation (selection bias)	Allocation concealment (selection bias)	Blinding of participants and personnel (performance bias)	Blinding of outcome assessment (detection bias)	Incomplete outcome data (attrition bias)	Selective reporting (reporting bias)	Other bias	Total quality scores
Chi, 2021 (34)	*	*	*	*	*	*	*	7
Li, 2015 (25)	*	*	*	*	*	*	*	7
Li, 2018 (38)	*	*	*	*	*	*	*	7
Xu, 2017a (27)	*	*	*	*	*	*	*	7
Xu, 2017b (16)	*	*	*	*	*	*	*	7

Each * equals 1 point.

TABLE 3 Subgroup analysis of treatment responses.

Treatment responses	VEGF inhibitors		EGFR inhibitors		Monotherapy		Combined therapy	
	Pooled rate	95% CI	Pooled rate	95% CI	Pooled rate	95% CI	Pooled rate	95% CI
Overall response	4%	(2%, 5%)	19%	(10%, 27%)	4%	(3%, 5%)	20%	(11%, 29%)
Disease progression	46%	(20%, 72%)	36%	(29%, 43%)	53%	(25%, 80%)	34%	(28%, 40%)
Stable disease	57%	(44%, 69%)	37%	(31%, 42%)	49%	(34%, 64%)	43%	(34%, 51%)
Disease control	59%	(50%, 68%)	62%	(54%, 71%)	62%	(50%, 74%)	61%	(54%, 68%)

EGFR, epidermal growth factor receptor; VEGF, vascular endothelial growth factor; CI, confidence interval.



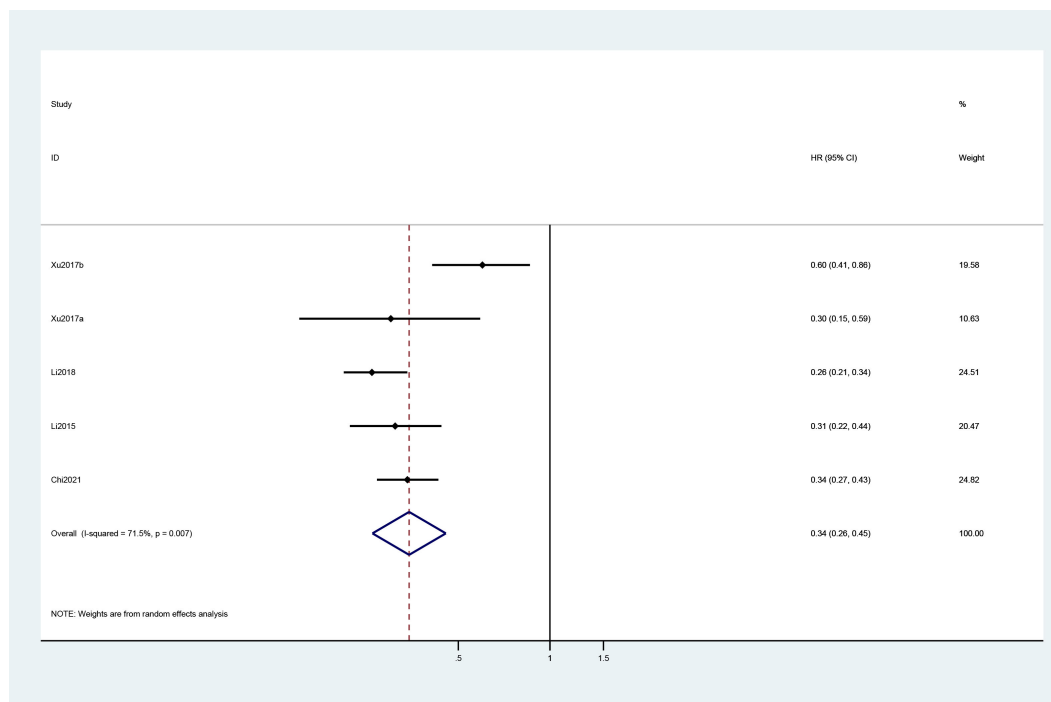


FIGURE 3
Forest plot of HR for progression-free survival in included studies.

evidence was found regarding the targets of HER2, NTRK, and BRAF. Further studies are needed to investigate if such targets may perform an essential role as VEGF and EGFR in the later line management of mCRC.

Data availability statement

The original contributions presented in the study are included in the article/supplementary material. Further inquiries can be directed to the corresponding authors.

Author contributions

W-HY and JX conceived and designed this study. W-HX, X-WL, Y-QD, NW, B-BP, and X-YM were responsible for the collection, extraction, and analysis of the data. W-HX were responsible for writing the paper. W-HY and JX performed the quality evaluation and completed data analysis. W-HY polished the English language. All authors and participants reviewed the paper. All authors contributed to the article and approved the submitted version.

Funding

This work was supported by grants from the National Natural Science Foundation of China (No. 82002619), Key Medical Research Projects of Shanxi Province (No. 2020XM55), Talent introduction scientific research start-up fund of Shanxi Bethune Hospital (No. 2020RC006).

Conflict of interest

The authors declare that the research was conducted in the absence of any commercial or financial relationships that could be construed as a potential conflict of interest.

Publisher's note

All claims expressed in this article are solely those of the authors and do not necessarily represent those of their affiliated organizations, or those of the publisher, the editors and the reviewers. Any product that may be evaluated in this article, or claim that may be made by its manufacturer, is not guaranteed or endorsed by the publisher.

References

- Kreidieh M, Mukherji D, Temraz S, Shamseddine A. Expanding the scope of immunotherapy in colorectal cancer: current clinical approaches and future directions. *BioMed Res Int* (2020) 2020:9037217. doi: 10.1155/2020/9037217
- Keum N, Giovannucci E. Global burden of colorectal cancer: emerging trends, risk factors and prevention strategies. *nature reviews. Gastroenterol Hepatol* (2019) 16:713–32. doi: 10.1038/s41575-019-0189-8
- Kahi CJ, Boland CR, Dominitz JA, Giardiello FM, Johnson DA, Kaltenbach T, et al. Colonoscopy surveillance after colorectal cancer resection: recommendations of the US multi-society task force on colorectal cancer. *Gastroenterology* (2016) 150:758–768.e711. doi: 10.1053/j.gastro.2016.01.001
- Biller LH, Schrag D. Diagnosis and treatment of metastatic colorectal cancer: a review. *Jama* (2021) 325:669–85. doi: 10.1001/jama.2021.0106
- Wróbel P, Ahmed S. Current status of immunotherapy in metastatic colorectal cancer. *Int J Colorectal Dis* (2019) 34:13–25. doi: 10.1007/s00384-018-3202-8
- Morse MA, Hochster H, Benson A. Perspectives on treatment of metastatic colorectal cancer with immune checkpoint inhibitor therapy. *Oncologist* (2020) 25:33–45. doi: 10.1634/theoncologist.2019-0176
- Yiu AJ, Yiu CY. Biomarkers in colorectal cancer. *Anticancer Res* (2016) 36:1093–102.
- Bekaii-Saab T, Kim R, Kim TW, O'Connor JM, Strickler JH, Malka D, et al. Third- or later-line therapy for metastatic colorectal cancer: reviewing best practice. *Clin Colorectal Cancer* (2019) 18:e117–29. doi: 10.1016/j.clcc.2018.11.002
- Van Cutsem E, Cervantes A, Adam R, Sobrero A, Van Krieken JH, Aderka D, et al. ESMO consensus guidelines for the management of patients with metastatic colorectal cancer. *Ann Oncol* (2016) 27:1386–422. doi: 10.1093/annonc/mdw235
- Benson AB, Venook AP, Al-Hawary MM, Cederquist L, Chen YJ, Ciombor KK, et al. Rectal cancer, version 2.2018, NCCN clinical practice guidelines in oncology. *J Natl Compr Cancer Network JNCCN* (2018) 16:874–901. doi: 10.6004/jnccn.2018.0061
- De Falco V, Napolitano S, Roselló S, Huerta M, Cervantes A, Ciardiello F, et al. How we treat metastatic colorectal cancer. *ESMO Open* (2020) 4:e000813. doi: 10.1136/esmoopen-2020-000813
- Modest DP, Pant S, Sartore-Bianchi A. Treatment sequencing in metastatic colorectal cancer. *Eur J Cancer (Oxford Engl 1990)* (2019) 109:70–83. doi: 10.1016/j.ejca.2018.12.019
- Nielsen DL, Palshof JA, Larsen FO, Jensen BV, Pfeiffer P. A systematic review of salvage therapy to patients with metastatic colorectal cancer previously treated with fluorouracil, oxaliplatin and irinotecan +/- targeted therapy. *Cancer Treat Rev* (2014) 40:701–15. doi: 10.1016/j.ctrv.2014.02.006
- Van Cutsem E, Peeters M, Siena S, Humblet Y, Hendlisz A, Neyns B, et al. Open-label phase III trial of panitumumab plus best supportive care compared with best supportive care alone in patients with chemotherapy-refractory metastatic colorectal cancer. *J Clin Oncol* (2007) 25:1658–64. doi: 10.1200/JCO.2006.08.1620
- Jonker DJ, O'Callaghan CJ, Karapetis CS, Zalcberg JR, Tu D, Au HJ, et al. Cetuximab for the treatment of colorectal cancer. *N Engl J Med* (2007) 357:2040–8. doi: 10.1056/NEJMoa071834
- Xu RH, Shen L, Wang KM, Wu G, Shi CM, Ding KF, et al. Farnitinib versus placebo in the treatment of refractory metastatic colorectal cancer: a multicenter, randomized, double-blinded, placebo-controlled, phase II clinical trial. *Chin J Cancer* (2017) 36:97. doi: 10.1186/s40880-017-0263-y
- Doebele RC, Drilon A, Paz-Ares L, Siena S, Shaw AT, Farago AF, et al. Entrectinib in patients with advanced or metastatic NTRK fusion-positive solid tumours: integrated analysis of three phase 1-2 trials. *Lancet Oncol* (2020) 21:271–82. doi: 10.1016/S1470-2045(19)30691-6
- Hong DS, DuBois SG, Kummar S, Farago AF, Albert CM, Rohrberg KS, et al. Larotrectinib in patients with TRK fusion-positive solid tumours: a pooled analysis of three phase 1/2 clinical trials. *Lancet Oncol* (2020) 21:531–40. doi: 10.1016/S1470-2045(19)30856-3
- Hainsworth JD, Meric-Bernstam F, Swanton C, Hurwitz H, Spigel DR, Sweeney C, et al. Targeted therapy for advanced solid tumors on the basis of molecular profiles: results from MyPathway, an open-label, phase IIa multiple basket study. *J Clin Oncol* (2018) 36:536–42. doi: 10.1200/JCO.2017.75.3780
- Piawah S, Venook AP. Targeted therapy for colorectal cancer metastases: a review of current methods of molecularly targeted therapy and the use of tumor biomarkers in the treatment of metastatic colorectal cancer. *Cancer* (2019) 125:4139–47. doi: 10.1002/cnrc.32163
- Gebbia V, Del Prete S, Borsellino N, Ferrai F, Tralongo P, Verderame F, et al. Efficacy and safety of cetuximab/irinotecan in chemotherapy-refractory metastatic colorectal adenocarcinomas: a clinical practice setting, multicenter experience. *Clin Colorectal Cancer* (2006) 5:422–8. doi: 10.3816/CCC.2006.n.013
- Vincenzi B, Santini D, Rabitti C, Coppola R, Zobel BB, Trodella L, et al. Cetuximab and irinotecan as third-line therapy in advanced colorectal cancer patients: a single centre phase II trial. *Br J Cancer* (2006) 94:792–7. doi: 10.1038/sj.bjc.6603018
- André T, Blons H, Mabro M, Chibaudel B, Bachet JB, Tournigand C, et al. Panitumumab combined with irinotecan for patients with KRAS wild-type metastatic colorectal cancer refractory to standard chemotherapy: a GERCOR efficacy, tolerance, and translational molecular study. *Ann Oncol* (2013) 24:412–9. doi: 10.1093/annonc/mds465
- Bai M, Deng T, Han R, Zhou L, Ba Y. Gemcitabine plus s-1 versus cetuximab as a third-line therapy in metastatic colorectal cancer: an observational trial. *Int J Clin Exp Med* (2015) 8:2159–65.
- Li J, Qin S, Xu R, Yau TC, Ma B, Pan H, et al. Regorafenib plus best supportive care versus placebo plus best supportive care in Asian patients with previously treated metastatic colorectal cancer (CONCUR): a randomised, double-blind, placebo-controlled, phase 3 trial. *Lancet Oncol* (2015) 16:619–29. doi: 10.1016/S1470-2045(15)70156-7
- Yoshida M, Takagane A, Miyake Y, Shimada K, Nagata N, Sato A, et al. A phase II study of third-line combination chemotherapy with bevacizumab plus s-1 for metastatic colorectal cancer with mutated KRAS (SAVIO study). *Oncology* (2016) 91:24–30. doi: 10.1159/000446372
- Xu RH, Li J, Bai Y, Xu J, Liu T, Shen L, et al. Safety and efficacy of fruquintinib in patients with previously treated metastatic colorectal cancer: a phase Ib study and a randomized double-blind phase II study. *J Hematol Oncol* (2017) 10:22. doi: 10.1186/s13045-016-0384-9
- Akiyoshi K, Hamaguchi T, Yoshimura K, Takahashi N, Honma Y, Iwasa S, et al. A prospective, multicenter phase II study of the efficacy and feasibility of 15-minute panitumumab infusion plus irinotecan for oxaliplatin- and irinotecan-refractory, KRAS wild-type metastatic colorectal cancer (Short infusion of panitumumab trial). *Clin Colorectal Cancer* (2018) 17:e83–9. doi: 10.1016/j.clcc.2017.10.004
- Moher D, Liberati A, Tetzlaff J, Altman DG. Preferred reporting items for systematic reviews and meta-analyses: the PRISMA statement. *Int J Surg (London England)* (2010) 8:336–41. doi: 10.1016/j.ijsu.2010.02.007
- Eisenhauer EA, Therasse P, Bogaerts J, Schwartz LH, Sargent D, Ford R, et al. New response evaluation criteria in solid tumours: revised RECIST guideline (version 1.1). *Eur J Cancer* (2009) 45:228–47. doi: 10.1016/j.ejca.2008.10.026
- Higgins JP, Altman DG, Gøtzsche PC, Jüni P, Moher D, Oxman AD, et al. The cochrane collaboration's tool for assessing risk of bias in randomised trials. *BMJ (Clinical Res ed)* (2011) 343:d5928. doi: 10.1136/bmj.d5928
- Slim K, Nini E, Forestier D, Kwiatkowski F, Panis Y, Chipponi J. Methodological index for non-randomized studies (minors): development and validation of a new instrument. *ANZ J surgery* (2003) 73:712–6. doi: 10.1046/j.1445-2197.2003.02748.x
- Chen X, Qiu T, Zhu Y, Sun J, Li P, Wang B, et al. A single-arm, phase II study of apatinib in refractory metastatic colorectal cancer. *Oncologist* (2019) 24:883–e407. doi: 10.1634/theoncologist.2019-0164
- Chi Y, Shu Y, Ba Y, Bai Y, Qin B, Wang X, et al. Anlotinib monotherapy for refractory metastatic colorectal cancer: a double-blinded, placebo-controlled, randomized phase III trial (ALTER0703). *Oncologist* (2021) 26:e1693–703. doi: 10.1002/onco.13857
- Cremolini C, Rossini D, Dell'Aquila E, Lonardi S, Conca E, Del Re M, et al. Rechallenge for patients with RAS and BRAF wild-type metastatic colorectal cancer with acquired resistance to first-line cetuximab and irinotecan: a phase 2 single-arm clinical trial. *JAMA Oncol* (2019) 5:343–50. doi: 10.1001/jamaoncol.2018.5080
- Eng C, Kim TW, Bendell J, Argilès G, Tebbutt NC, Di Bartolomeo M, et al. Atezolizumab with or without cobimetinib versus regorafenib in previously treated metastatic colorectal cancer (IMblaze370): a multicentre, open-label, phase 3, randomised, controlled trial. *Lancet Oncol* (2019) 20:849–61. doi: 10.1016/S1470-2045(19)30027-0
- Kopetz S, Desai J, Chan E, Hecht JR, O'Dwyer PJ, Maru D, et al. Phase II pilot study of vemurafenib in patients with metastatic BRAF-mutated colorectal cancer. *J Clin Oncol* (2015) 33:4032–8. doi: 10.1200/JCO.2015.63.2497
- Li J, Qin S, Xu RH, Shen L, Xu J, Bai Y, et al. Effect of fruquintinib vs placebo on overall survival in patients with previously treated metastatic colorectal cancer: the FRESCO randomized clinical trial. *Jama* (2018) 319:2486–96. doi: 10.1001/jama.2018.7855
- Masuishi T, Tsuji A, Kotaka M, Nakamura M, Kochi M, Takagane A, et al. Phase 2 study of irinotecan plus cetuximab rechallenge as third-line treatment in KRAS wild-type metastatic colorectal cancer: JACCRO CC-08. *Br J Cancer* (2020) 123:1490–5. doi: 10.1038/s41416-020-01042-w
- Osumi H, Shinozaki E, Mashima T, Wakatsuki T, Suenaga M, Ichimura T, et al. Phase II trial of biweekly cetuximab and irinotecan as third-line therapy for pretreated KRAS exon 2 wild-type colorectal cancer. *Cancer science* (2018) 109:2567–75. doi: 10.1111/cas.13698
- Sartore-Bianchi A, Trusolino L, Martino C, Bencardino K, Lonardi S, Bergamo F, et al. Dual-targeted therapy with trastuzumab and lapatinib in treatment-refractory, KRAS codon 12/13 wild-type, HER2-positive metastatic colorectal cancer (HERACLES): a proof-of-concept, multicentre, open-label, phase 2 trial. *Lancet Oncol* (2016) 17:738–46. doi: 10.1016/S1470-2045(16)00150-9
- Yoshida Y, Yamada T, Kamiyama H, Kosugi C, Ishibashi K, Yoshida H, et al. Combination of TAS-102 and bevacizumab as third-line treatment for metastatic colorectal cancer: TAS-CC3 study. *Int J Clin Oncol* (2021) 26:111–7. doi: 10.1007/s10147-020-01794-8

43. Bray F, Ferlay J, Soerjomataram I, Siegel RL, Torre LA, Jemal A. Global cancer statistics 2018: GLOBOCAN estimates of incidence and mortality worldwide for 36 cancers in 185 countries. *CA: Cancer J Clin* (2018) 68:394–424. doi: 10.3322/caac.21492
44. Grothey A, Fakhri M, Tabernero J. Management of BRAF-mutant metastatic colorectal cancer: a review of treatment options and evidence-based guidelines. *Ann Oncol* (2021) 32:959–67. doi: 10.1016/j.annonc.2021.03.206
45. Amado RG, Wolf M, Peeters M, Van Cutsem E, Siena S, Freeman DJ, et al. Wild-type KRAS is required for panitumumab efficacy in patients with metastatic colorectal cancer. *J Clin Oncol* (2008) 26:1626–34. doi: 10.1200/JCO.2007.14.7116
46. Karapetis CS, Khambata-Ford S, Jonker DJ, O'Callaghan CJ, Tu D, Tebbutt NC, et al. K-Ras mutations and benefit from cetuximab in advanced colorectal cancer. *New Engl J Med* (2008) 359:1757–65. doi: 10.1056/NEJMoa0804385
47. Benson AB, Venook AP, Al-Hawary MM, Cederquist L, Chen YJ, Ciombor KK, et al. NCCN guidelines insights: colon cancer, version 2.2018. *J Natl Compr Cancer Network JNCCN* (2018) 16:359–69. doi: 10.6004/jnccn.2018.0021
48. Cervantes A, Adam R, Roselló S, Arnold D, Normanno N, Taïeb J, et al. Metastatic colorectal cancer: ESMO clinical practice guideline for diagnosis, treatment and follow-up. *Ann Oncol* (2023) 34:10–32. doi: 10.1016/j.annonc.2022.10.003
49. Smith KM, Desai J. Nivolumab for the treatment of colorectal cancer. *Expert Rev Anticancer Ther* (2018) 18:611–8. doi: 10.1080/14737140.2018.1480942



OPEN ACCESS

EDITED BY

Alessandro Passardi,
Scientific Institute of Romagna for the
Study and Treatment of Tumors (IRCCS),
Italy

REVIEWED BY

Yingkun Xu,
Chongqing Medical University, China
Rongzhang Dou,
University of Texas MD Anderson Cancer
Center, United States

*CORRESPONDENCE

Jianhua Zhu
✉ yaoli78@163.com
Zheng Yuan
✉ linzi80_80@126.com
Xinhua Gu
✉ 1173421755@qq.com

[†]These authors have contributed equally to
this work

RECEIVED 11 March 2023

ACCEPTED 17 May 2023

PUBLISHED 07 June 2023

CITATION

Zhou J, Yang S, Zhu D, Li H, Miao X, Gu M,
Xu W, Zhang Y, Tang W, Shen R, Zha J,
Zhu J, Yuan Z and Gu X (2023) The
crosstalk between anoikis and epithelial-
mesenchymal transition and their
synergistic roles in predicting prognosis in
colon adenocarcinoma.
Front. Oncol. 13:1184215.
doi: 10.3389/fonc.2023.1184215

COPYRIGHT

© 2023 Zhou, Yang, Zhu, Li, Miao, Gu, Xu,
Zhang, Tang, Shen, Zha, Zhu, Yuan and Gu.
This is an open-access article distributed
under the terms of the [Creative Commons
Attribution License \(CC BY\)](https://creativecommons.org/licenses/by/4.0/). The use,
distribution or reproduction in other
forums is permitted, provided the original
author(s) and the copyright owner(s) are
credited and that the original publication in
this journal is cited, in accordance with
accepted academic practice. No use,
distribution or reproduction is permitted
which does not comply with these terms.

The crosstalk between anoikis and epithelial-mesenchymal transition and their synergistic roles in predicting prognosis in colon adenocarcinoma

Jiahui Zhou^{1†}, Sheng Yang^{2,3†}, Dawei Zhu^{1†}, Hao Li^{1†},
Xinsheng Miao¹, Menghui Gu¹, Wei Xu¹, Yan Zhang¹, Wei Tang¹,
Renbin Shen¹, Jianhua Zha¹, Jianhua Zhu^{1*}, Zheng Yuan^{1*}
and Xinhua Gu^{1*}

¹Department of Gastrointestinal Surgery, The Affiliated Suzhou Hospital of Nanjing Medical University, Suzhou Municipal Hospital, Gusu School, Nanjing Medical University, Suzhou, China, ²Department of Colorectal Surgery, The First Affiliated Hospital of Nanjing Medical University, Nanjing, China,

³Colorectal Institute of Nanjing Medical University, Nanjing, China

Anoikis and epithelial-mesenchymal transition (EMT) are significant phenomena occurring in distant metastasis of colon adenocarcinoma (COAD). A comprehensive understanding of their crosstalk and the identification of key genes are vital for treating the distant metastasis of COAD. The objective of this study was to design and validate accurate prognostic predictors for COAD patients based on the anoikis and EMT processes. We obtained gene signatures from various databases and performed univariate and multivariate Cox regression analyses, principal component analysis (PCA). The COAD patients were categorized into the worst prognosis group, the Anoikis Potential Index (API) Low + EMT Potential Index (EPI) High group and the others group. Then we utilized gene set enrichment analysis (GSEA) to identify differentially expressed genes and to establish a prognostic risk model. The model classified patients into high- or low-risk groups, with patients in the high-risk group displaying worse survival status. A nomogram was established to predict overall survival rates, demonstrating high specificity and sensitivity. Additionally, we connected the risk model to the tumor microenvironment (TME) using single-sample GSEA and the MCP counter tool, as well as evaluated the sensitivity to common chemotherapeutic drugs, such as Gefitinib and Gemcitabine. Lastly, cell and tissue experiments suggested a positive correlation among anoikis resistance, EMT, and liver/lung metastasis of COAD. This is the first study to comprehensively analyze the crosstalk between anoikis and EMT and offers new therapeutic targets for COAD metastasis patients.

KEYWORDS

colon adenocarcinoma, anoikis, EMT, crosstalk, risk model

Introduction

According to the statistics presented by the American Cancer Society (2023), COAD ranks third in terms of the incidence and mortality rate of all cancers, irrespective of gender. It affects young individuals and poses a serious health risk to the public (1). It has been reported that Stage I patients can attain a 5-year survival rate (after surgical resection) of $\geq 90\%$, while the patients with distant metastasis showed a 5-year survival rate of only 11%, despite the application of adjuvant chemotherapy, targeted drugs, or immunotherapy (2, 3). This has necessitated the need to thoroughly understand and urgently address the problem of COAD metastasis.

EMT is a phenomenon where epithelial cells can acquire a mesenchymal phenotype, which is first observed in embryonic development. Once EMT is activated, tumor cells undergo many changes, such as their dissociation with tight junctions, disruption of apical-basal polarity, and remodeling of cytoskeletal structures, all of which contribute to the movement of cells from their primary location, invasion of neighboring tissues, survival during the circulation process, and the eventual formation of metastatic foci at distant sites (4, 5). Several studies have reported an association between EMT and COAD metastasis. Wang et al. revealed that the THZ1 could promote EMT by inhibiting the degradation of Snail, which in turn increased colorectal cancer liver metastasis (6). Xiang et al. demonstrated that Snail could facilitate the formation of M2-macrophages by secreting CXCL2, which finally promoted the lung metastasis of colorectal cancer (7).

Epithelial cells increase their survival rate by attaching to the ECM. In addition, they undergo apoptosis after they get detached from the ECM, which is defined as the anoikis phenomenon (8). It was noted that the tumor cells acquire resistance to anoikis, where even when they get detached from the ECM they cannot undergo apoptosis easily, invade the surrounding tissues, and subsequently metastasize distantly (9). Many recent studies have highlighted the correlation between anoikis and COAD metastasis. Wei et al. reported that simultaneous inhibition of PDK1 and STAS3-Y705

enhanced the anoikis process, which further inhibited colorectal cancer liver metastasis (10). Xu et al. demonstrated that CPT1A-mediated FAO activation promoted anoikis resistance in colorectal cancer cells and improved lung metastasis (11).

Both the EMT and anoikis phenomena occur during the invasive stage of primary tumors and undergo a few crosstalks (12). It was observed that up-regulated Claudin-1 reduced E-cadherin expression *via* ZEB-1 modulation, attenuating the invasive ability, and anoikis of COAD cells (13). Up-regulated miR-450a was reported to inhibit EMT, promote anoikis, and thus inhibit the migration and invasion capacities of ovarian cancer cells (14). The deletion of 4.1N facilitated EMT, anoikis resistance, and consequently the metastasis of epithelial ovarian cancer cells (15). Therefore, the co-analysis of EMT and anoikis could help to identify the genes that play key roles in COAD metastasis.

This study comprehensively and substantively described the interaction between anoikis and EMT. We divided COAD patients into the worst prognosis group and the others groups by univariate and multivariate Cox regression analysis and PCA. We then used GSEA to identify differentially expressed genes and to establish a prognostic risk model containing NAT1, CDKN2A, and PCOLCE2 with high specificity and sensitivity. In addition, we linked the risk model to the TME and assessed the sensitivity to common chemotherapeutic drugs. Finally, cell and tissue experiments further demonstrated the correlation between anoikis, EMT and COAD metastasis. Figure 1 depicts the flowchart used in this study.

Materials and methods

Data sources and analysis

A total of 338 ARGs (anoikis-linked genes) were obtained from GeneCards (<https://www.genecards.org/>), and the genes showing a relevance score of >1 were chosen in the study. The EMT signature containing 198 genes (EMT-related genes, i.e., ERGs) was derived from the MSigDB portal in GSEA (<http://software.broadinstitute.org/gsea/msigdb>). The genetic information and clinically-relevant data from The Cancer Genome Atlas (TCGA) database (<https://portal.gdc.cancer.gov/repository>) was acquired for 459 COAD patients. Meanwhile, gene expression matrices containing 317 ARGs and 195 ERGs were extracted independently using R language software, and the 'limma' software was used to analyze the variations between the two. Thereafter, 152 DEGs for ARGs (diff-ARGs) and 125 DEGs for ERGs (diff-ERGs) were selected based on the following screening criteria: $|FC| > 1.5$ and $p < 0.05$. The 'Rcircos' software was applied to map the location of anoikis and EMT-related genes on human chromosomes. The data associated with the somatic mutations, genome mutations, and Copy number variations (CNV) in COAD were also derived from TCGA.

Survival analysis

In this study, univariate and multivariate Cox regression analyses were carried out with the help of the 'survival' package. The Kaplan Meier (KM) curves were plotted to compare the

Abbreviations: EMT: epithelial-mesenchymal transition, COAD: Colon adenocarcinoma, qPCR: quantitative polymerase chain reaction, IHC: Immunohistochemistry, PCA: principal component analysis, ECM: extracellular matrix, CTC: circulating tumor cells, ARGs: anoikis-related genes, ERGs: EMT-related genes, GSEA: Gene Set Enrichment Analysis, TCGA: The Cancer Genome Atlas, CNV: copy number variation, OS: overall survival, ROC: receiver operating characteristic, AUC: area under the ROC curve, API: Anoikis Potential Index, EPI: EMT Potential Index, GO: gene ontology, FDR: False discovery rate, DEGs: differentially expressed genes, KEGG: Kyoto Encyclopedia of Genes And Genomes, LASSO: least absolute shrinkage and selection operator, PAEGs: prognostic anoikis-related genes and EMT-related genes, KM: Kaplan Meier, DCA: decision curve analysis, ssGSEA: single sample GSEA, HLA: human leukocyte antigen, H&E: Hematoxylin-eosin, MF: molecular functions, BP: biological process, COAD: cellular components, NAT1: Arylamine N-acetyltransferase 1, PCOLCE2: Procollagen C-endopeptidase enhancer 2, CDKN2A: Cyclin-dependent kinase inhibitor 2A, TME: The tumor microenvironment, CAF: cancer-associated fibroblasts, CTL: Cytotoxic T lymphocyte, MHC: major histocompatibility complex.

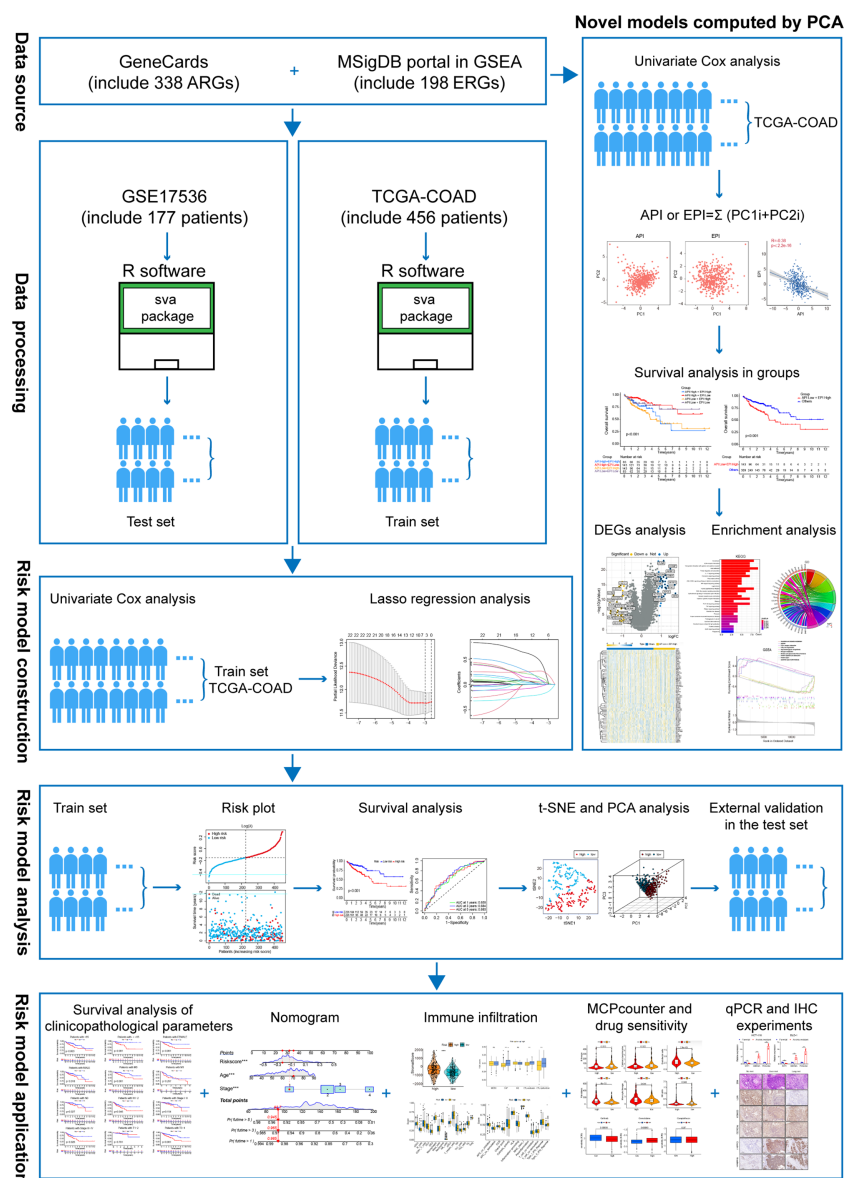


FIGURE 1
The flowchart of overall study methods and results.

differences (variations) in overall survival (OS) between different groups. The logarithmic rank test was employed to determine the P-value between different groups. Furthermore, the time-dependent receiver operating characteristic (ROC) curves were assessed using the 'survivalROC' packets. The area under the ROC curve (AUC) value was used to evaluate the prognostic performance of the ROC curve.

Computational models of anoikis and EMT levels in COAD

In this study, Principal component analysis (PCA) was conducted for determining the anoikis and EMT scores for understanding the degree of anoikis and EMT in each sample.

Then, univariate Cox regression analysis was conducted for analyzing the survival of anoikis and EMT-related genes. Then, the gene expression matrix ($P < 0.05$) for PCA was extracted, and the principal components 1 and 2 were determined as the main subjects. Based on a few earlier reports (16–18), the Anoikis Potential Index (API) and EMT Potential Index (EPI) were defined, respectively: $API \text{ or } EPI = \sum (PC1i + PC2i)$, where i denotes the expression of related genes.

Gene set enrichment analysis

GSEA was utilized to study the relationship between both groups after dividing the TCGA samples into the API Low + EPI High group and the others group. For each analysis, 1000 genome

permutations were carried out. The enrichment function was selected using the below-mentioned criteria: the ‘clusterProfiler’ software was used to enrich and evaluate the gene set with the false discovery rate (FDR) of 0.25 and 0.05 NOM p-value. The first five up- and down-regulated functions of the two enrichment sets were visualized by multiple GSEA maps. Then, the DEGs were identified using the differential expression analysis. Thereafter, the ‘ClusterProfiler’ was employed for carrying out Gene ontology (GO) and Kyoto Encyclopedia of Genes and Genomes (KEGG) enrichment analyses for enriching and analyzing the DEGs. Finally, the ‘Enrichplot’ and ‘ggplot2’ software were used for presenting the enrichment results as a bar graph, bubble graph, chord graph, and cluster circle graph.

Construction of an anoikis-related and EMT-related prognostic model

In this study, univariate Cox regression analysis was conducted for identifying 12 anoikis-linked genes and 11 EMT-related genes. The ‘glmnet’ software was utilized for determining the optimal value of the penalty parameter, lambda, through 1000 times of cross-validation with the Least absolute shrinkage and selection operator (LASSO) regression technique. The risk scores for every COAD patient were estimated using the coefficient and expression of the candidate prognostic anoikis-related genes and EMT-related genes (PAEG), with the following risk scoring formula: $\sum_{i=1}^n \text{Coef}_i * \text{Expri}$; where Coef_i denotes the coefficient of gene *i*, and Expri denotes the expression of every gene in patient *i* (18).

Validating the PAEG risk model

The expression levels of 3 mRNAs, risk score, survival duration, and risk level for each TCGA sample were integrated into a table and used as a training set. The GSE17536 dataset was used as the test set to validate the training set’s accuracy. The risk prognosis was examined using the KM chart and a log-rank test. Also, the ROC curve was plotted using the ‘timeROC’ tool. Then, the risk heat map, survival state diagram, and risk curve were generated using the ‘pheatmap’ program. PCA and t-SNE analysis were carried out using the ‘Rtsne’ and ‘ggplot2’ packages, respectively. Lastly, the risk score values were combined with clinical parameters (such as age, sex, grade, and TNM stage) and visualized using the forest map.

Nomogram construction and calibration

In this study, clinical characteristics such as age, TNM stage, and risk scores were used as research subjects for univariate Cox analysis. The survival rates of COAD patients after one, three, and five years were anticipated by a nomograph using the ‘RMS’ tool. Here, calibration curves were used to evaluate the nomogram’s accuracy. Lastly, the ‘ggDCA’ software was used for plotting the decision curve analysis (DCA) curve for predicting the clinical values of various objects.

Immune infiltration levels in the high- and low-risk groups

Firstly, the ‘ESTIMATE’ software was employed for assessing the stromal score, immune score, and tumor purity between both groups. Then, the differences in immune function, the activity of immune cells, and the immune pathways between the two groups in the training set and test set were examined using the single sample GSEA (ssGSEA) test, and the data were visualized using the box graph. Based on the COAD expression matrix, the ‘MCP counter’ web tool was used for estimating the abundance of various non-immune and immune stromal cells. The data were then observed using violin plots. Then, the human leukocyte antigen (HLA) gene expression and the expression levels of various immune checkpoint genes in both groups were estimated.

Prediction of chemosensitivity

In this study, the half maximal inhibitory concentration (IC₅₀) of three commonly used chemotherapeutic drugs, such as Gefitinib, Gemcitabine, and Camptothecin, was determined in colorectal cancer using the ‘pRRophic’ package. Thereafter, the difference in the sensitivity levels of the above chemotherapy drugs between the high- and low-risk groups was assessed by comparing the variations in the IC₅₀ values between both groups.

Patient tissue specimens and cell lines

Herein, the tissue specimens of COAD patients without distant metastasis, with liver metastasis, and with lung metastasis were extracted from the patients after surgical resection in the Department of Gastrointestinal Surgery, Suzhou Municipal Hospital, Jiangsu, China. The patients had not undergone preoperative chemoradiotherapy, and all specimens were sampled within 10 mins after resection and subsequently fixed in 10% formalin. The Ethics Committee in the hospital approved the experimental procedures used in the study, and the patients were also asked to sign a consent form.

The HCT-116 and DLD-1 colon cancer cell lines were supplied by the Shanghai Cell Bank, Chinese Academy of Sciences (China). These cells were cultured in the DMEM medium (Hyclone, USA) containing 10% (v/v) fetal bovine serum (Hyclone, USA), and 1% (v/v) penicillin/streptomycin solution (Beyotime, China), at 37°C, under 5% CO₂ and 95% humidity conditions. The anoikis-resistance model was developed based on published literature (19, 20). Herein, the above-mentioned COAD cell lines were continually cultivated in ultra-low-attachment 6-well cell culture plates (Corning, USA) for 7 days and were transferred to the normal culture plates for 24 h. The re-adhered cells were defined as anoikis-resistant cells. All the experiments were conducted using mycoplasma-free cells. The Shanghai Cell Bank of the Chinese Academy of Sciences (China) validated all the cell lines used in the past three years.

RNA extraction and qRT-PCR analyses

The TRIzol reagent (Takara, Japan) was used for isolating the total RNA samples from the normal and anoikis-resistant cells. These RNA samples were reverse-transcribed into cDNA using the HiScript II RT SuperMix qPCR kit (Vazyme, China). The qRT-PCR experiments were carried out with the aid of the SYBR Premix Ex Taq Kit (Takara, Japan) on an RT-PCR instrument (7500 Sequence Detection System, Applied Biosystems, USA). The primers were designed and acquired from RiboBio (China). In this study, GAPDH was employed as the internal control for all experiments. The gene expression was represented using the $2^{-\Delta\Delta CT}$ technique. Table S1 lists the primer sequences used in the study.

Hematoxylin-eosin staining and immunohistochemistry

Herein, H&E staining and IHC experiments were conducted as mentioned in an earlier study (21). Table S2 lists the antibodies used in this study.

Statistical analysis

All data were statistically analyzed using the R language (ver. 4.1.2) and GraphPad Prism software (ver. 8.0.1). The Kolmogorov-Smirnov normality test was carried out for determining if the data followed the Gaussian distribution, and the data were compared for every sample. If the data conformed to a non-Gaussian distribution, a non-parametric test (Wilcoxon rank test or Spearman correlation) was carried out. On the other hand, when the data conformed to a Gaussian distribution, the parametric test was conducted (unpaired Student's test, one-way ANOVA, or Pearson correlation). Values with $P < 0.05$ were deemed statistically significant.

Results

Identifying the differentially expressed ARGs and ERGs associated with prognosis

Initially, the ARGs and ERGs were downloaded from GeneCards and GSEA, and subsequently, the diff-ARGs and diff-ERGs were selected, respectively. The locations of diff-ARGs and diff-ERGs on human chromosomes were mapped separately in Supplementary Figure 1A, B. Then, the clinical prognostic data of COAD patients were acquired from TCGA, and subsequently, 152 diff-ARGs and 125 diff-ERGs were combined with the clinical data using univariate Cox analysis ($P < 0.05$), to eventually obtain 12 prognosis-related ARGs (TIMP1, BDNF, IGF1, CDKN2A, MTA1, NAT1, INHBB, CD24, CD36, TRAF2, NOTCH3, PPP2R2A) and 11 prognosis-related ERGs (BGN, CXCL1, FSTL3, GPC1, MMP3, OXTR, PCOLCE2, SCG2, SERPINE1, SERPINH11, TPM2) (Figure 2A, B). Thereafter, the expression levels of the 23 genes in

521 COAD samples (41 normal samples and 480 tumor samples) from TCGA were determined, and box plots were generated independently, which indicated that the genes were differentially expressed between healthy and malignant tissues (Figures 2C, D). Meanwhile, the correlations between these 12 ARGs and 11 ERGs associated with prognosis were further analyzed and plotted using the 'corrplot' package (Figure 2E). Then, the pairs of genes for the Sankey diagram ($P < 0.05$, $|cor| > 0.3$) were selected, where the positive value represented the positive relationship, whereas the negative value indicated a negative correlation (Figure 2F).

Construction of API and EPI with negative correlation

To further investigate the crosstalk between ARGs and ERGs, the anoikis and EMT levels in each tumor tissue were calculated and quantified based on the 12 prognosis-related ARGs and 11 prognosis-related ERGs with PCA, and the API and EPI were separately defined (Figure 3A, B). A negative correlation was detected between API and EPI in COAD patients (Figure 3C). Subsequently, the COAD patients were classified into four molecular subtype groups based on their API and EPI scores, namely API High + EPI High; API High + EPI Low; API Low + EPI High; and API Low + EPI Low. The results of the prognosis analysis indicated that patients in the API Low + EPI High group exhibited the shortest survival time compared to the other three groups (Figure 3D). Then, the data from the other groups of COAD patients were combined and compared with the API Low + EPI High group for prognostic analysis, and the corresponding p -value < 0.001 was obtained (Figure 3E). Both analysis results indicated that high anoikis resistance and high EMT levels were associated with an unfavorable prognosis.

Enrichment analysis of DEGs in the 'API Low + EPI high' and 'the others' group

Subsequently, the DEGs in the API Low + EPI High group were analyzed and compared to the others groups. Based on the criterion of $|FC| > 1.8$, 70 DEGs were screened, and a volcano map was plotted (Figure 4A) using the clustering heat map (Figure 4B). KEGG analysis that was drawn using the barplot indicated that the DEGs in the two groups were primarily enriched in "Focal adhesion", "Viral protein interaction with cytokine and cytokine receptor", "ECM-receptor interaction", "NF- κ B signaling pathway", "IL-17 signaling pathway", "Chemokine signaling pathway", "Cytokine-cytokine receptor interaction", and "PI3K-Akt signaling pathway" (Figure 4C). GO analysis plotted by chord diagram suggested a major difference in molecular functions (MF), biological process (BP), or cellular components (CC) in both groups. The DEGs were mainly enriched in "collagen fibril organization", "extracellular matrix organization", "extracellular structure organization", "antimicrobial peptide-mediated antimicrobial humoral immune response", "external

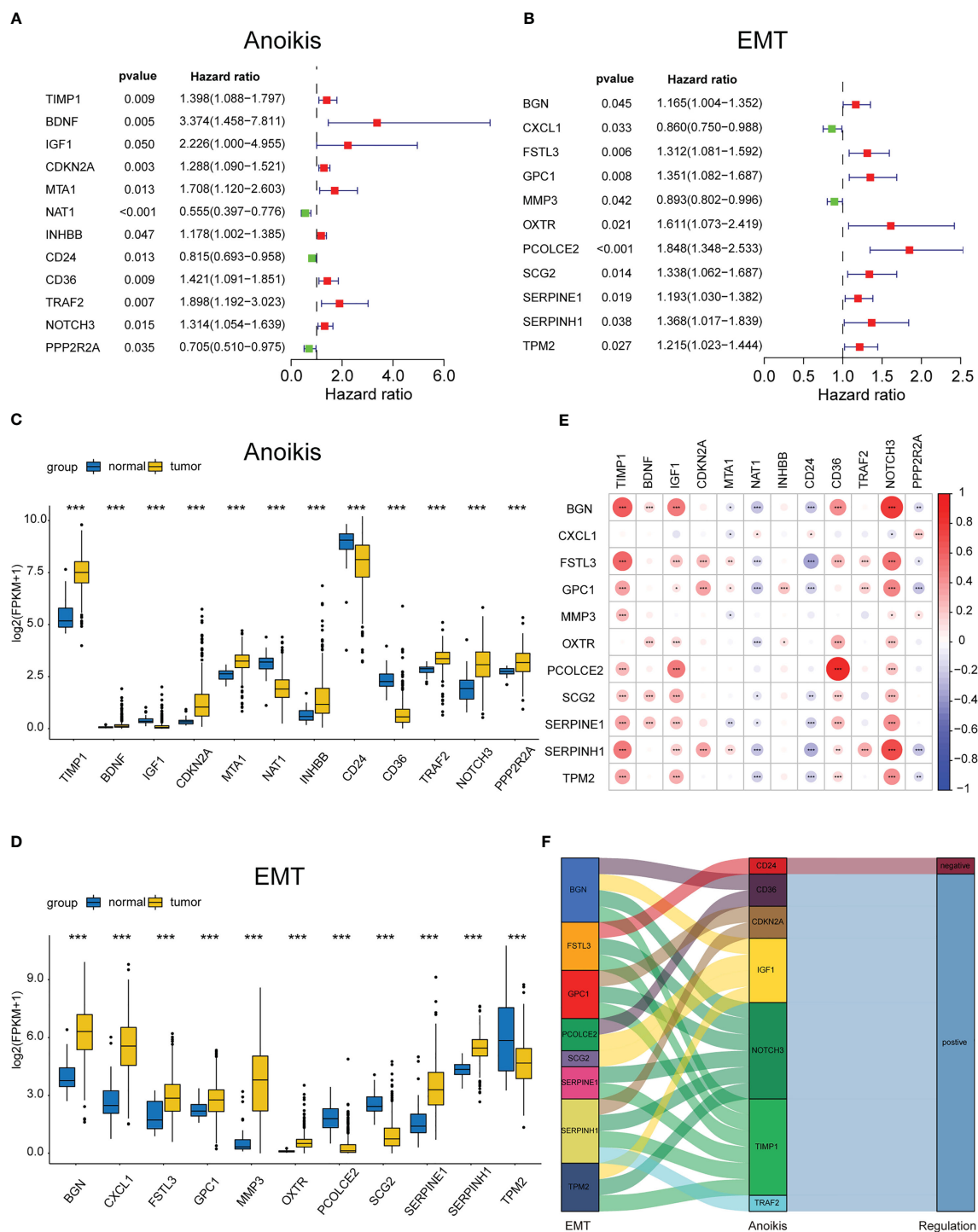


FIGURE 2

Identifying the differentially expressed ARGs and ERGs associated with prognosis. Forest map of 11 prognostic anoikis-related genes (A) and 12 prognostic EMT-related genes (B) by univariate Cox analysis ($P < 0.05$). The differential expression box plot of 11 prognostic anoikis-related genes (C) and 12 prognostic EMT-related genes (D) in COAD. (E) Pearson correlation analysis of 11 prognostic anoikis-related genes and 12 prognostic EMT-related genes. The red color represents a positive correlation; the blue color represents a negative correlation. (F) The Sankey diagram displayed the relationship between 11 prognostic anoikis-related genes and 12 prognostic EMT-related genes. * $p < 0.05$, ** $p < 0.01$, and *** $p < 0.001$.

encapsulating structure organization”, “humoral immune response”, “antimicrobial humoral response”, and “wound healing” (Figure 4D). The GSEA enrichment analysis between the two groups was described using multiple GSEA diagrams based on the following filtering criteria: $FDR < 0.25$ and $NOM P < 0.05$

(Figure 4E). The top five functions that were enriched in the API Low+EPI High group were “Asthma”, “ECM-receptor interaction”, “Glycosaminoglycan biosynthesis”, “Protein digestion and absorption” and “Systemic lupus erythematosus”. The five leading functions enriched in the others group were recorded to be

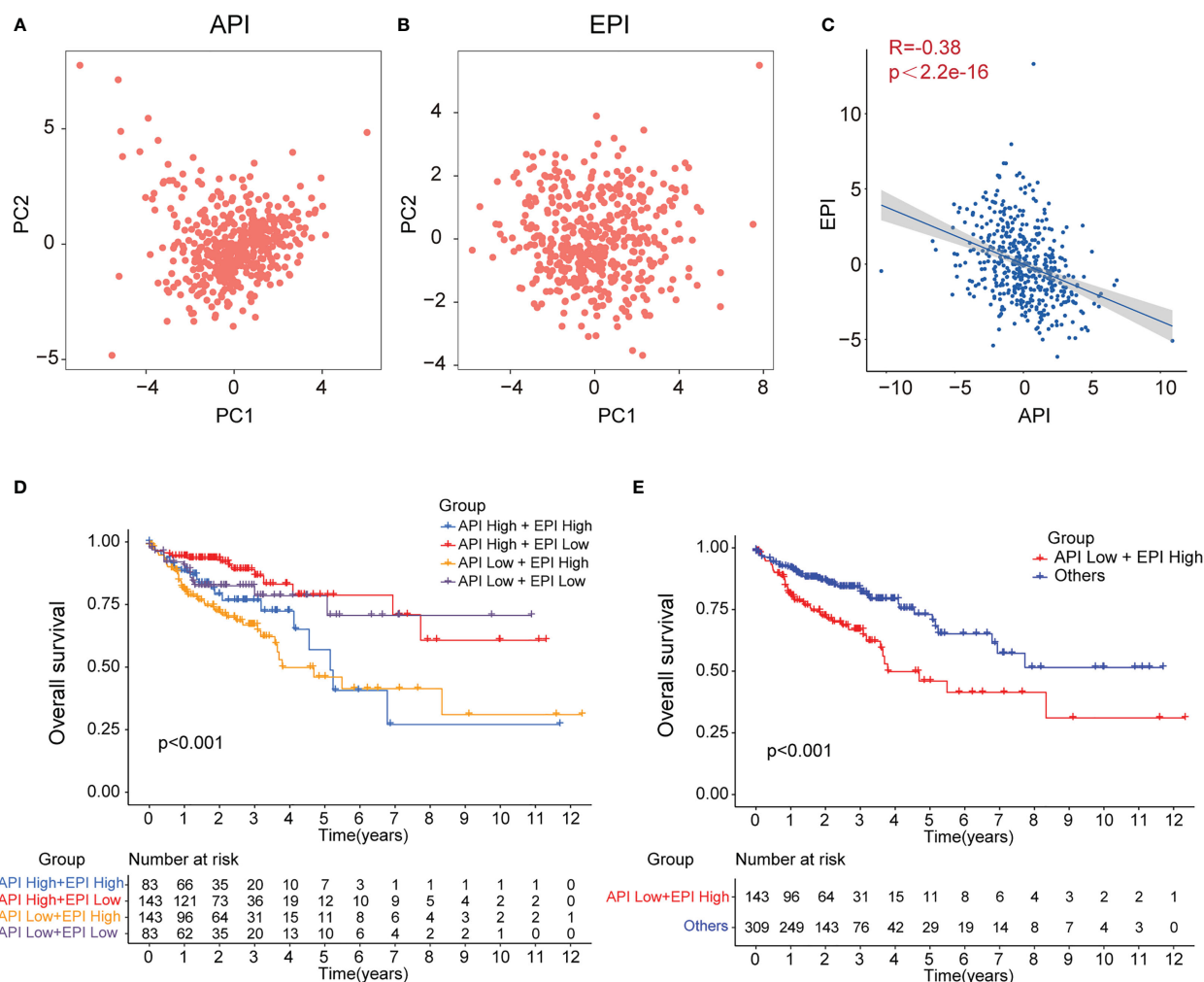


FIGURE 3

Construction of API and EPI with negative correlation. PCA analysis of 11 prognostic anoikis-related genes (A) and 12 prognostic EMT-related genes (B). (C) Scatter plot showing the spearman correlation of API and EPI. The KM plot showing overall survival in 4 groups (D) and two newly defined groups (E).

“Ascorbate and alternate metabolism”, “Fatty acid degradation”, “Nitrogen metabolism”, “Pentose and glucuronate interconversions”, and “Protein export”.

Construction of the prognostic ARGs and ERGs (PAEG) risk model, PCA analysis, and survival analysis of clinicopathological parameters

To construct a risk model for COAD patients based on anoikis and EMT, the 12 prognosis-associated ARGs and 11 prognosis-associated ERGs were combined, and the 23 genes were then subjected to Lasso regression analysis (Figure 5A, B). The corresponding coefficient criterion was evaluated by 1,000-fold cross-validation. the optimal penalty parameter lambda was determined, and the corresponding coefficient criterion was calculated depending on a minimum criterion. Lastly, a three-mRNA (NAT1, PCOLCE2, CDKN2A) prognostic risk model was constructed. The risk score was calculated using the following formula: risk score = $(-0.135312062940216 \times \text{NAT1}$

expression) + $(0.178733977096469 \times \text{PCOLCE2 expression}) + (0.0267778987311829 \times \text{CDKN2A expression})$. The COAD patients were classified into high-risk or low-risk groups depending on risk score values. Then, the GSE17536 data set was selected as the test set for verification, whereas the TCGA data set ($n = 452$) was chosen as a training set. The risk curve, scatter plot, and risk heat maps were used for highlighting the relationship between the survival time, risk score, and abundance of three genes in COAD patients, determined using the training (Figure 5C) and test sets (Figure 5D). The results of the prognostic analysis revealed that high-risk patients exhibited a short survival duration compared to the low-risk patients in the training ($p < 0.001$) (Figure 5E) and test sets ($p = 0.006$) (Figure 5F). Furthermore, ROC curves were used for characterizing the specificity and sensitivity of the risk model. For the 1-, 3-, and 5-year risk scores, the area under the ROC curve (AUC) values in the training set were 0.658, 0.684, and 0.680 (Figure 6A), respectively, whereas the test set's corresponding values were 0.655, 0.633, and 0.634 (Figure 6D). Also, the Rtsne package and ggplot2 packages were employed for plotting the t-SNE analysis images from the training set (Figure 6B) and test set (Figure 6E), independently. The scatterplot3d program was utilized

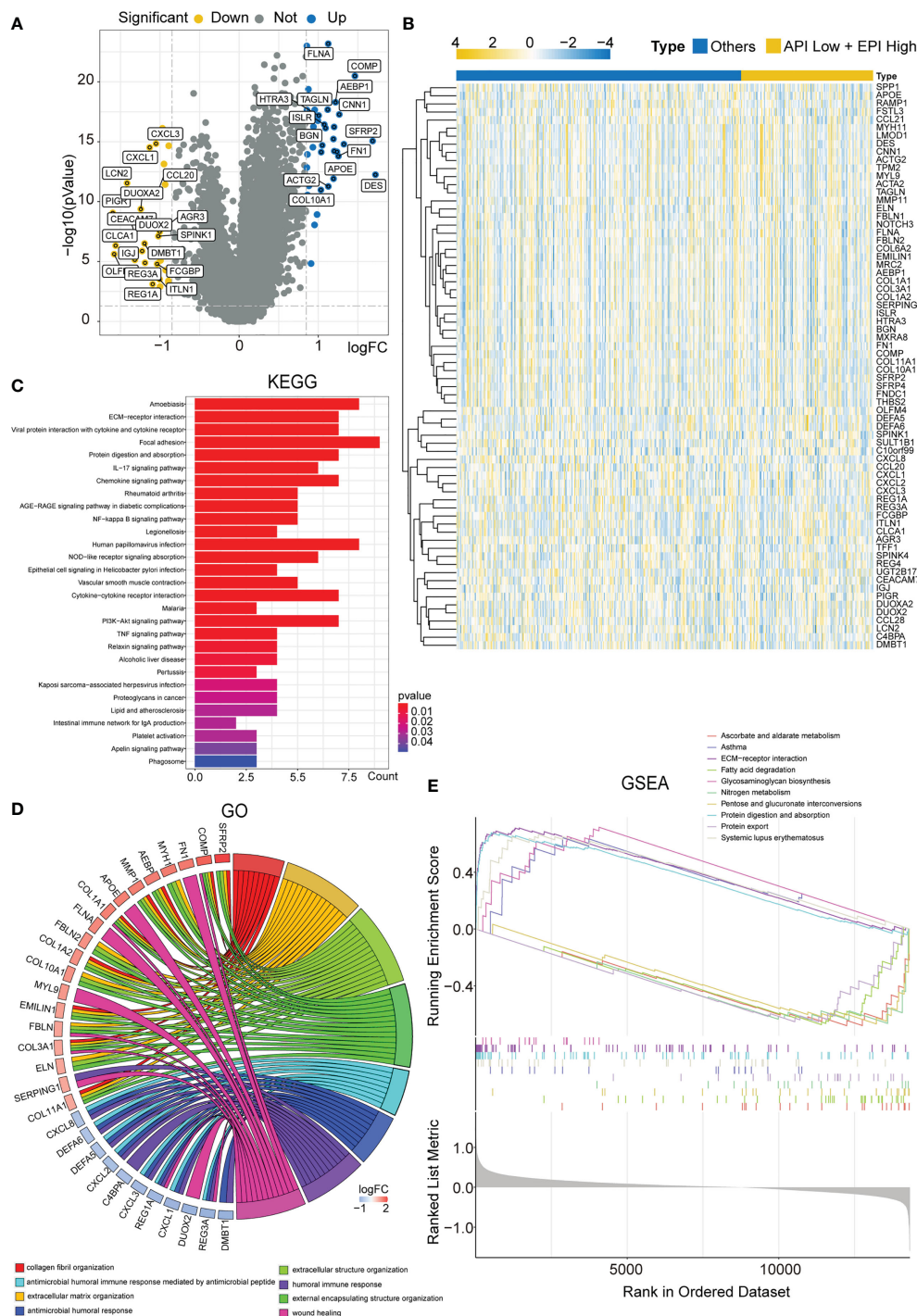


FIGURE 4

Enrichment analysis of DEGs in the 'API Low + EPI high' and 'others' group. (A) Volcano plots displaying the DEGs between two groups. (B) Heatmap created by the DEGs between two groups. The results of KEGG and GO enrichment analysis of the DEGs between two groups showing by barplot (C) and chord diagram (D). GSEA results illustrating ten significant enrichments of KEGG in two groups.

to capture the 3D images of the PCA analysis of the training (Figure 6C) and test sets (Figure 6F). The above findings highlighted the fact that the high- and low-risk patients showed a favorable heterogeneity in the training and test sets. Finally, the COAD patients were sub-classified in the training set depending on their clinical traits (such as gender, Stage, age, and TNM stage), and the

survival durations of high- and low-risk patients were compared after subclassification. The KM curves revealed that a few of the subgroups such as age (both ≤ 65 and >65), gender (male and female), M0 (patients with no distant metastasis), N0 or N 1-2 (patients with or without lymph nodes metastasis), stage III-IV, and T 3-4 (Figure 6G) showed a significant survival duration ($P < 0.05$).

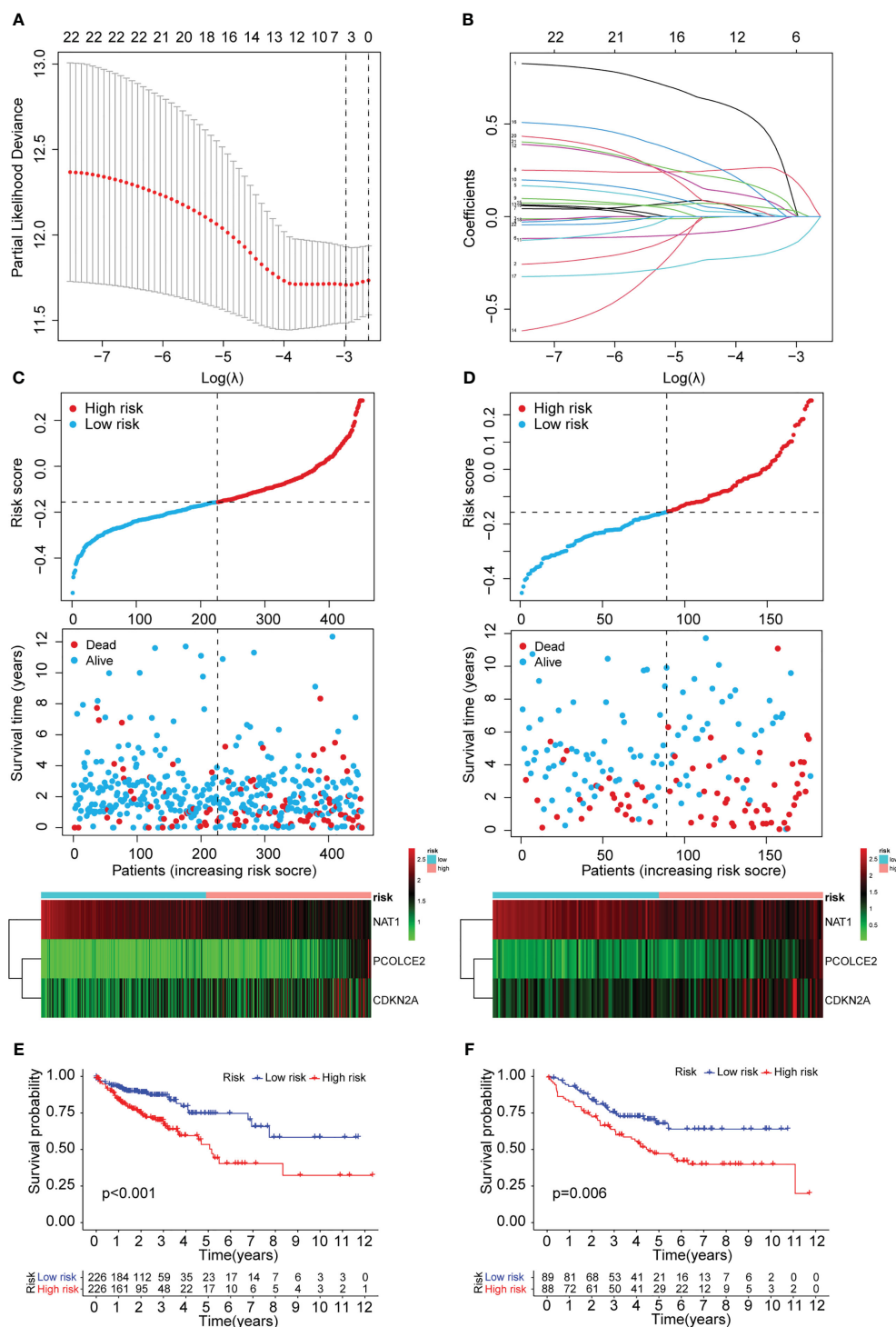


FIGURE 5

Construction of the prognostic ARGs and ERGs (PAEG) risk model. (A) 1000 cross-validation to determine the optimal penalty parameters λ . (B) Lasso regression of the 11 prognostic anoikis-related genes and 12 prognostic EMT-related genes. Scatter plot showing risk score distribution of high-risk and low-risk and the relationship between survival time and risk score based on the training set (C) and test set (D). KM plot showing overall survival in training set (E) and test set (F).

Cox regression analysis and nomogram development

In this study, univariate and multivariate Cox regression analyses were carried out to determine if the risk model could serve as an

outstanding independent prognostic signature. The findings of the univariate Cox regression analysis implied that some factors like age, T stage, M stage, N stage, and risk score were significantly and positively related to OS in the training set (Figure 7A). Furthermore, a strong and positive relationship was observed between the risk score, grade, and

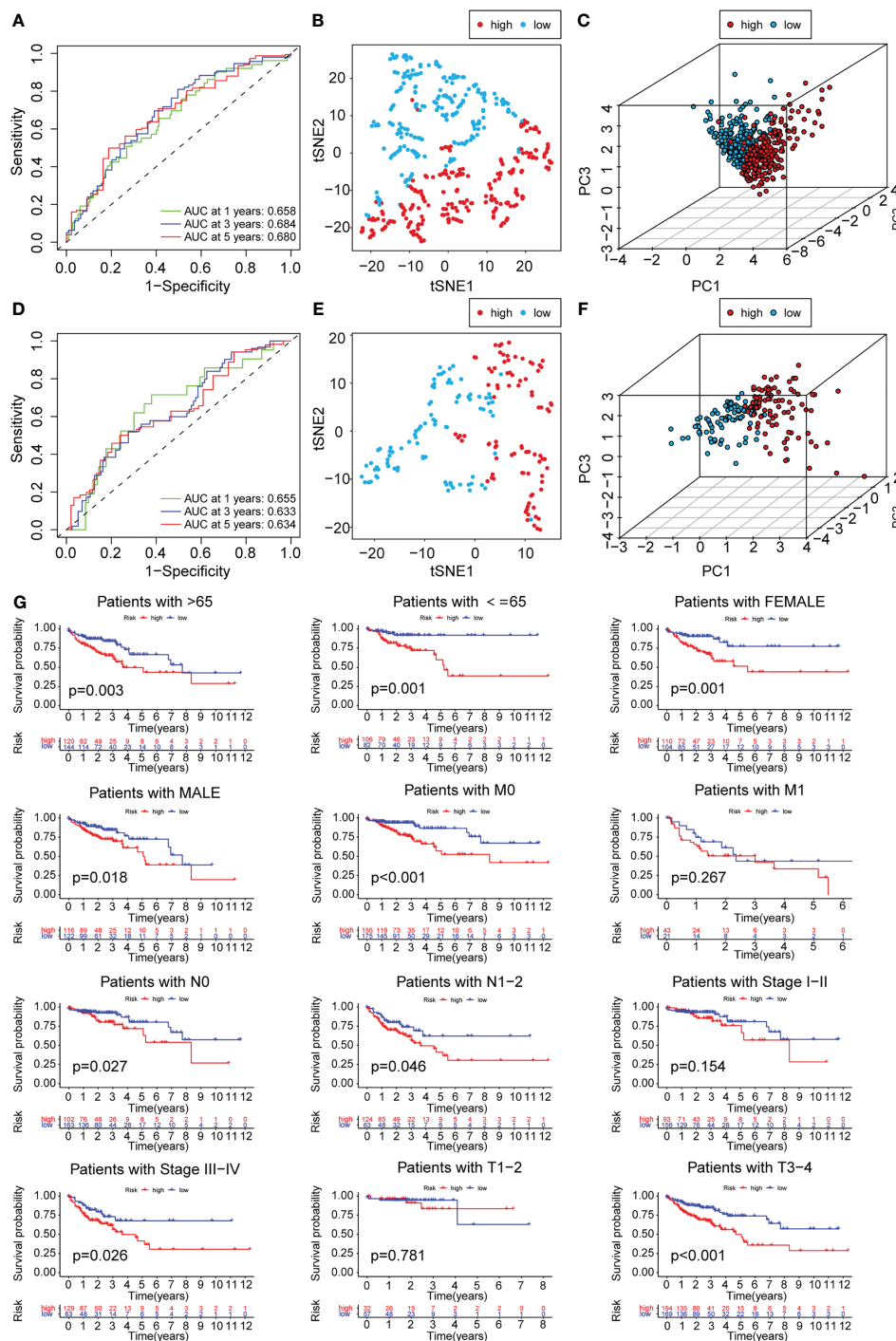


FIGURE 6

PCA analysis and survival analysis of clinicopathological parameters. The 1-, 3- and 5-year ROC curve of risk score in training set (A) and test set (D). The t-SNE analysis of training set (B) and test set (E). The 3D scatter plot of PCA results of training set (C) and test set (F). (G) KM plot in subgroups including gender, age and tumor stages.

OS in the test set (Figure 7C). On the other hand, the multivariate regression analysis of the significant factors involved in the univariate analysis indicated that characteristics such as age, M stage, T stage, and risk score in the training set were significantly linked to OS (Figure 7B), while risk score and grade in the test set were significantly and positively related to OS (Figure 7D). The aforementioned findings demonstrated that the risk prediction model was an effective and

independent predictor that outperformed clinical factors such as age and TNM stage.

Thereafter, based on the above findings, a nomogram was developed in this study, which included factors like stage, age, and risk score (Figure 7E). Also, calibration curves were plotted for the nomogram, where the results indicated that all three calibration curves (1-, 3-, and 5-year) were close to the standard curve, thus

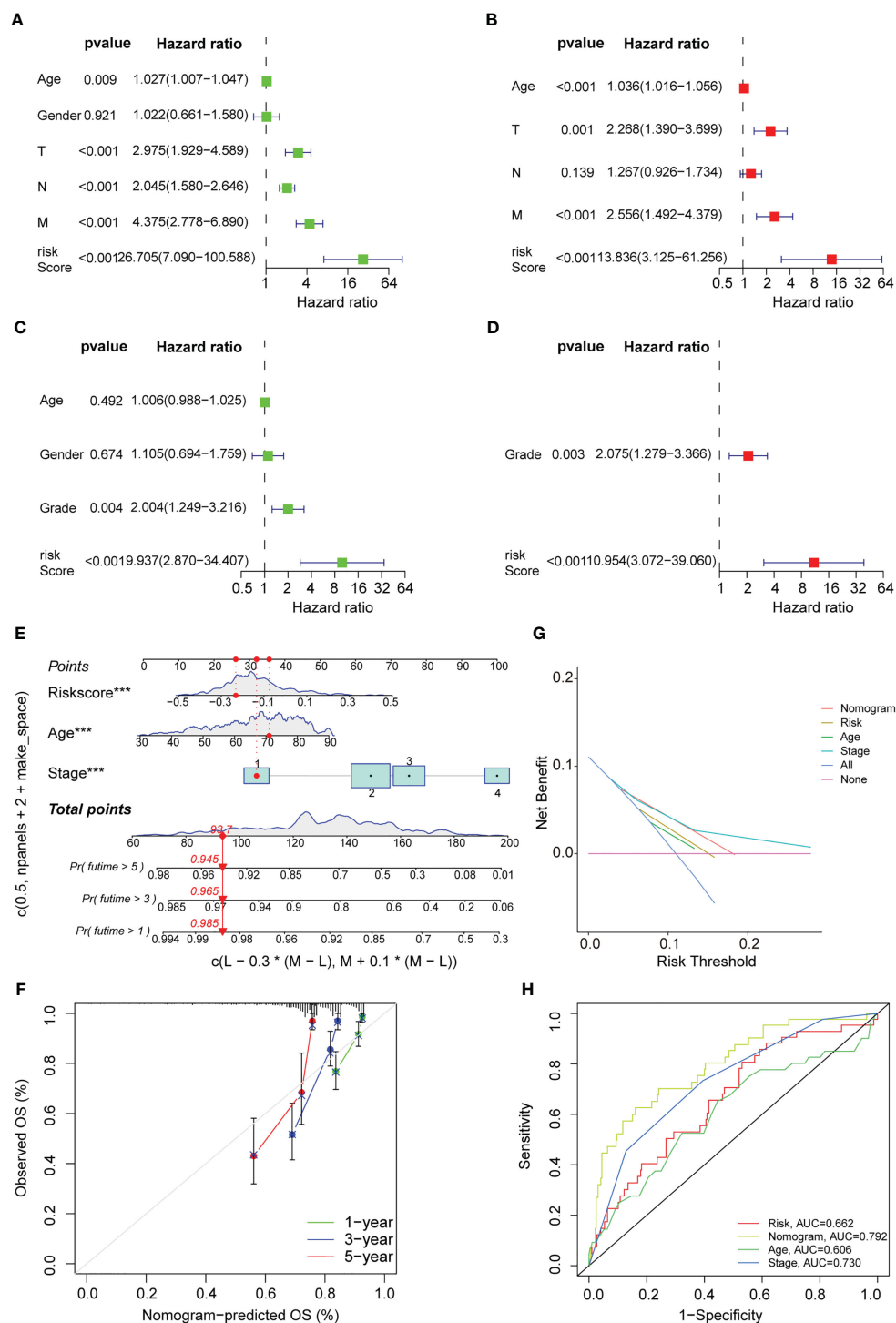


FIGURE 7

Cox regression analysis and nomogram development. Univariate Cox regression analysis displaying the association between patients' overall survival and clinicopathological parameters along with the PAEG risk score in training set (A) and test set (C). Multivariate Cox regression analysis revealing independent prognostic factors in training set (B) and test set (D). (E) Nomogram depending on the PAEG risk score and other clinicopathologic feature predicting the 1-, 3- and 5-year overall survival for COAD patients. (F) Calibration curves uncovering the consistency between predicted and observed 1-, 3- and 5-year overall survival rates in COAD patients based on the nomogram. DCA curve (G) and ROC curve (H) of nomogram, risk and other clinicopathologic feature in COAD.

demonstrating an acceptable predictive effect (Figure 7F). The DCA curve indicated that the nomogram was much more beneficial than the extreme curves (Figure 7G). The ROC curves indicated that AUC values for the nomogram, age, risk, and stage were 0.792, 0.662, 0.606,

and 0.730, respectively (Figure 7H). The nomogram curve exhibited a greater AUC value compared to the risk score curve, age curve, and stage curve, suggesting that the nomogram was a better predictor of prognosis.

Immune infiltration analysis, MCP counter, and drug sensitivity of the PAEG risk model

Earlier studies have shown that the TME was linked to COAD distant metastasis, immunotherapy response, and drug sensitivity (22–24). The content of stromal cells present in the TME is indicated by the stromal score. The immune score indicates the content of immune cells in the TME. The high-risk patients showed higher stromal cell levels (Figure 8A), however, no remarkable difference was observed in the proportion of immune cells between the low- and high-risk groups (Supplementary Figure 2A). A higher tumor purity is linked to a better prognosis as it indicates the proportion of tumor cells present in the tissue. The tumor purity was higher in the low-risk group (Figure 8B). TIDE scores were used to assess the potential of tumor immune infiltration in the gene expression profile of the malignant samples and could anticipate the response to the immune checkpoint blockade therapy. The high-risk patients showed enhanced expression of the cytotoxic T lymphocyte (CTL) exclusion, cancer-associated fibroblasts (CAF), and CTL dysfunction (Figure 8C). The ssGSEA technique was then used to investigate the infiltration status of 16 immune cells and derive the scores of 13 immunological functions to further assess the relationship between immune infiltration and the risk model. The low-risk patients displayed a higher infiltration of CD8⁺ T cells, Th1 cells, B cells, Th2 cells, and Treg cells as well as higher immunological functions like APC_co_inhibition and Cytolytic_activity. On the other hand, the high-risk patients displayed a higher infiltration level of macrophages and immunological functions like Type_II_IFN_response in the training set (Figures 8D, E). In the test set, the low-risk group displayed higher immunological functions such as Check-point, Cytolytic_activity, APC_co_inhibition, HLA, T_cell_co_inhibition, Inflammation-promoting, and T_cell_co_stimulation. They also showed a higher infiltration level of aDCs, B cells, Neutrophils, TILs, iDCs, Th2 cells, Th1 cells, CD8⁺ T cells, and Treg cells (Figure 8F, G). Then, the MCPcounter software was used for comparing the contents of 10 immune and stromal cells in the two groups. The high-risk group contained a higher number of endothelial cells and fibroblasts, whereas the low-risk group contained more B lineage, cytotoxic lymphocytes, and NK cells (Figure 9A, Supplementary Figure 2B). Also, 10 common immune checkpoint molecules and 24 major histocompatibility complex (MHC) molecules in the high- and low-risk groups were evaluated, and no remarkable differences were noted (Supplementary Figure 2C, D).

Finally, the sensitivity of the high- and low-risk patients to the common therapeutic drugs used in COAD was evaluated, and the findings implied that the high-risk patients showed a higher sensitivity to gemcitabine, while the low-risk patients showed a higher sensitivity to gefitinib. Both groups showed no difference in their sensitivity to camptothecin (Figure 9B).

Validation of PAEG in the risk model in cell and tissue experiments

In this study, the anoikis-resistant COAD cell lines such as HCT-116 and DLD-1 were constructed. Then, the mRNA expression levels

of NAT1, CDKN2A, and PCOLCE2 in the parental and anoikis-resistant groups were detected separately by means of qPCR. The findings of this experiment indicated that the NAT1 mRNA expression level was decreased, whereas the CDKN2A and PCOLCE2 mRNA expression levels were elevated in the anoikis-resistant group, which led to the conclusion that NAT1 could facilitate anoikis, while CDKN2A and PCOLCE2 were responsible for anoikis resistance (Figure 10A). Considering the significant role of PAEGs in the distant metastasis of COAD, four cases of primary COAD tissues without distant metastasis, with liver metastasis, and with lung metastasis were selected, respectively, to detect the protein expression levels of the above-mentioned three genes by IHC. An earlier study showed that Claudin-1 could attenuate E-cadherin expression in colorectal cancer by upregulating ZEB-1, which, in turn, promoted EMT and reduced anoikis (13). Also N-cadherin is one of the key markers of EMT. Hence, Claudin-1 and N-cadherin were used as references and compared to the three PAEGs. The results implied that the NAT1 protein expression level was elevated in the tissues without distant metastasis compared to the tissues with liver and lung metastasis, whereas the CDKN2A and PCOLCE2 protein expression levels were increased in the tissues with liver and lung metastasis. The above findings indicated a positive correlation between high anoikis resistance, high EMT, and more distant metastasis of COAD (Figure 10B).

Discussion

Distant metastases severely limit the prognosis of COAD patients. Although current therapeutic approaches are more mature, a recent meta-analysis suggested that median recurrence-free survival was 1.3 years after resection of colorectal liver metastases (25). A high recurrence rate is an important cause of death for COAD patients. Most patients with distant metastases are not detected during the initial diagnosis and suffer a worse prognosis. Therefore, it is essential to investigate techniques that help in preventing distant metastasis of COAD. According to existing research (26, 27), the first step of distant metastases of COAD involves the invasion of tumor cells into the stromal environment. Both anoikis and EMT play important roles in inhibiting and promoting invasion during this phase; therefore, an in-depth study of the crosstalk between anoikis and EMT can help uncover key genes involved in distant metastasis.

In this study, API and EPI were quantified for determining the anoikis and EMT levels in COAD, using the PCA technique, and the group that showed the worst survival curve (i.e., the API Low + EPI High group) was isolated. This was in agreement with an earlier finding that anoikis repressed metastasis and EMT promoted metastasis (28, 29). This is the first study that used this technique for clustering COAD patients, and a favorable prognostic difference presents the rationality and effectiveness of this type of grouping technique, which needs to be further analyzed and experimentally validated.

Next, a risk model was developed using three genes: NAT1, CDKN2A, and PCOLCE2. Arylamine N-acetyltransferase 1

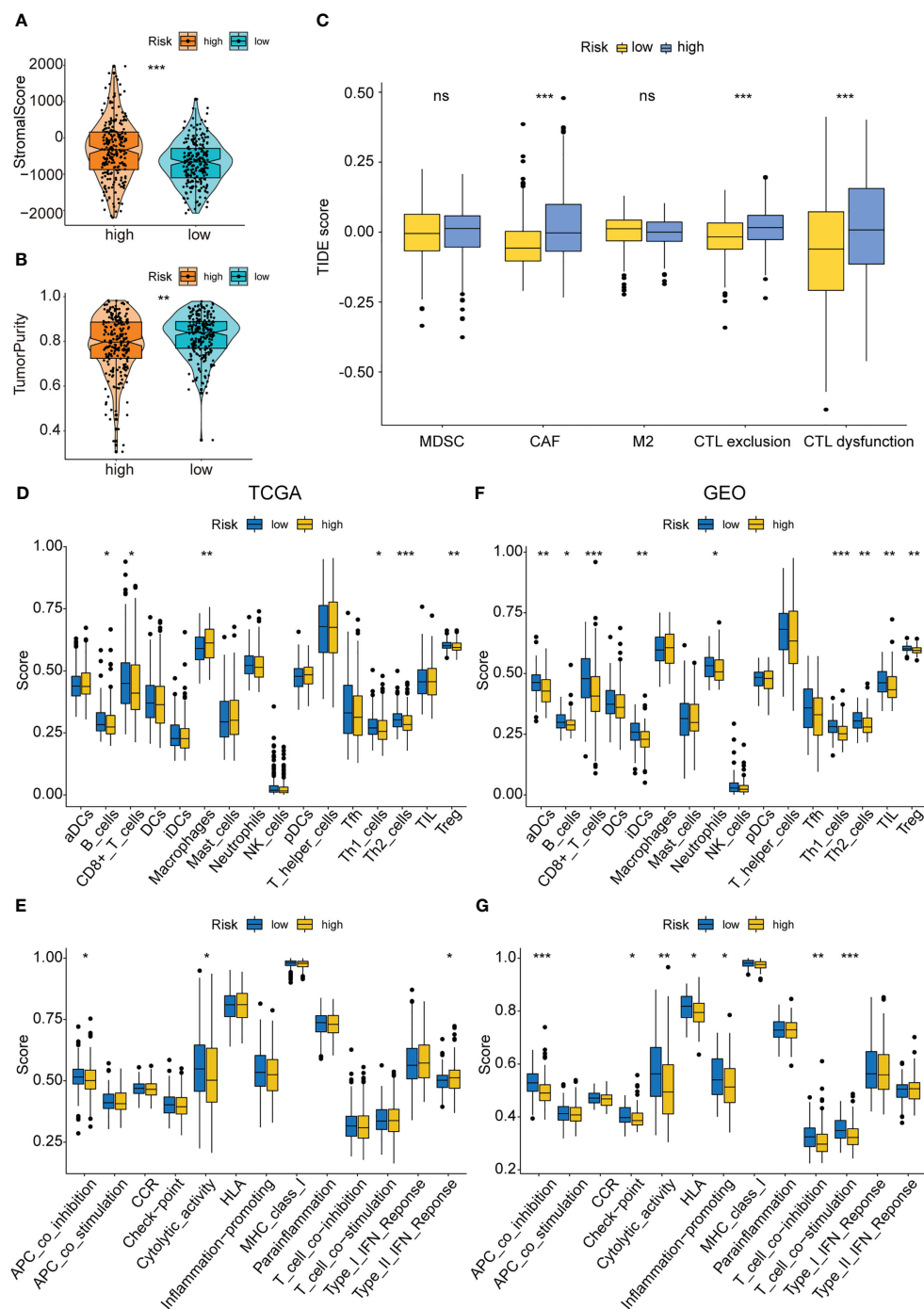
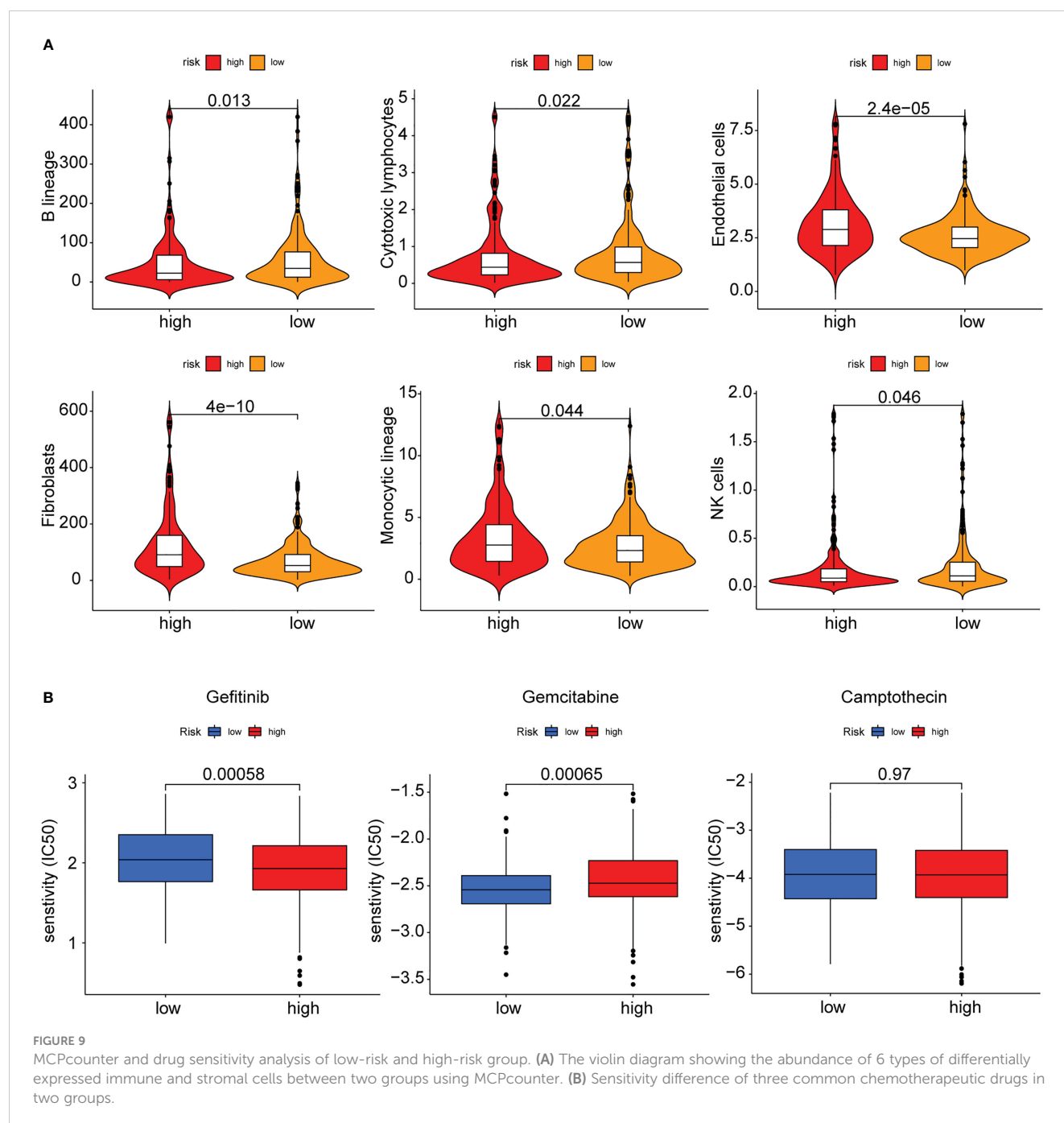


FIGURE 8

Immune infiltration analysis of the PAEG risk model. (A, B) The violin and box plot displaying the difference of the stromal score and tumor purity in two groups. (C) TIDE analysis showing the difference of tumor immune dysfunction and exclusion in two groups. The infiltrating levels of 16 immune cell types in training set (D) and test set (F) estimated by ssGSEA. The infiltrating levels of 13 immune functions in training set (E) and test set (G) estimated by ssGSEA. ns means $p > 0.05$, * $p < 0.05$, ** $p < 0.01$, and *** $p < 0.001$.

(NAT1) was shown to catalyze the N- or O-acetylation of different arylamine and heterocyclic amine substrates and was observed to be involved in tumor progression and chemotherapy resistance (30). MicroRNA-6744-5p facilitated anoikis and targeted NAT1 in breast cancer cells (31). NAT1 expression levels also correlated with EMT status and metastatic behavior in breast cancer patients (32). Moreover, by interacting significantly with CDK4 and CDK6, the

cyclin-dependent kinase inhibitor 2A (CDKN2A) functioned as a negative regulator of the proliferation of normal cells (33). CDKN2A also played a vital role in regulating the anoikis in hepatocellular carcinoma cells (34) and pancreatic cancer cells (35–38) and hence could serve as an anoikis-related signature gene to predict the prognosis of endometrial carcinoma patients (39). Meanwhile, CDKN2A may facilitate colorectal cancer cell



metastasis through the induction of EMT and may be associated with the infiltration status of multiple immune cells (40, 41). Procollagen C-endopeptidase enhancer 2 (PCOLCE2) refers to a collagen-binding protein that binds to the C-terminal pro-peptide of types I and II procollagens and could enhance the cleavage of the pro-peptide by BMP1 (42). PCOLCE2 can be considered as an EMT-linked gene for anticipating the prognosis of gastric cancer patients (43, 44) and the metastasis ability of COAD (45). However, none of the studies determined the role of PCOLCE2 in anoikis. The risk model was used for categorizing the COAD patients into the high- and low-risk categories, and the OS duration of the patients with different clinicopathological parameters like gender, age, and

stage was seen to be significantly different between both categories. The nomogram curve that was developed using the risk model was more sensitive and specific in reflecting the prognosis of COAD patients than age, stage, and risk model.

Furthermore, the stromal and immune infiltration analysis was carried out based on the risk model. The findings revealed that this risk model was associated with a few acquired immune cells like Th1 cells, Th2 cells, B cells, and Treg cells, and with the innate immune cells like lymphocytes, monocytes, and NK cells, but not with numerous MHC molecules and immune checkpoint genes. However, it showed a stronger correlation with stromal infiltrates such as CAF and endothelial cells. Anoikis resistance and EMT are

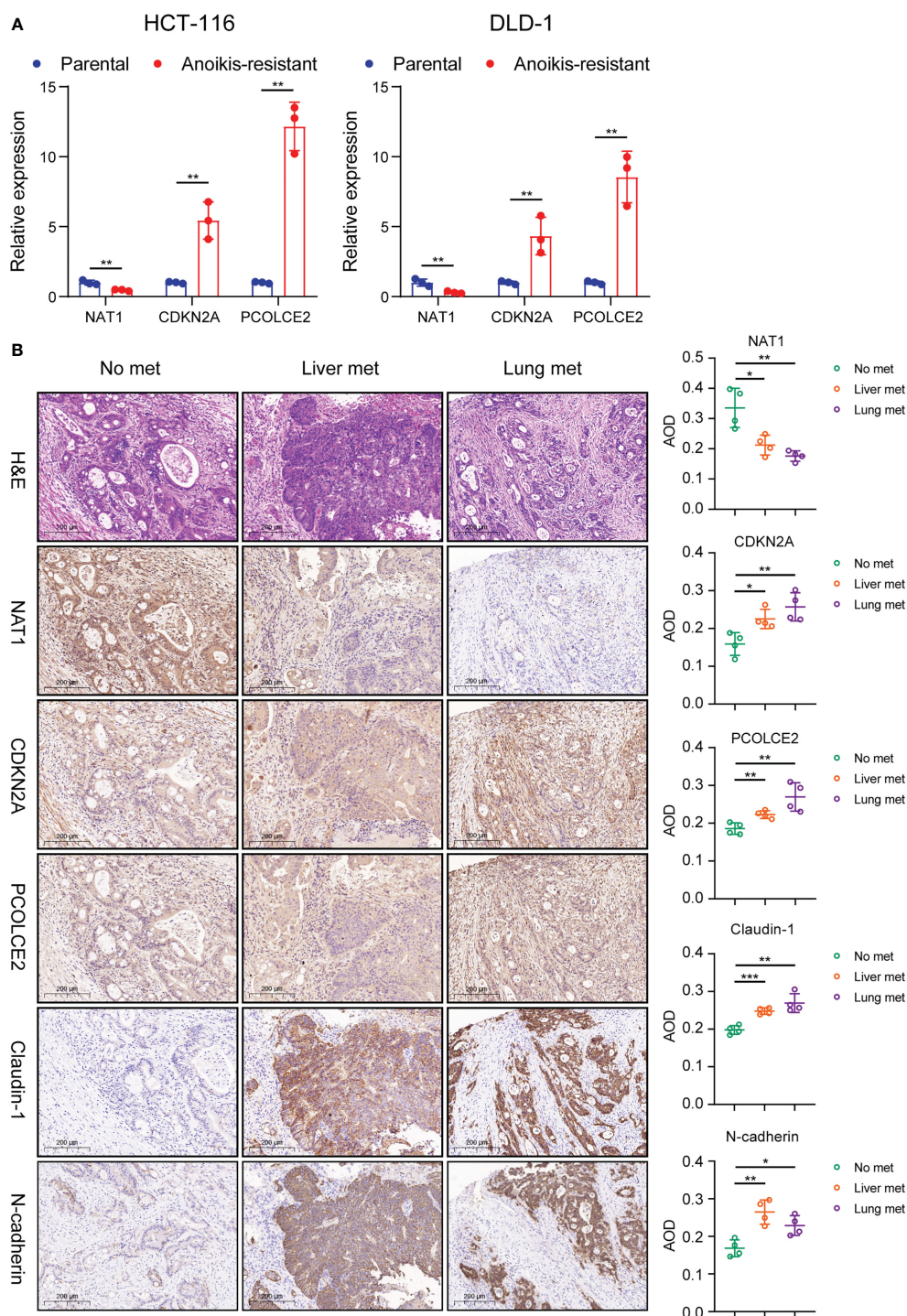


FIGURE 10

Validation of PAEG in the risk model in cell and tissue experiments. **(A)** Relative expression of NAT1, CDKN2A and PCOLCE2 in the parental and anoikis-resistant groups by qPCR. **(B)** The protein expression of NAT1, CDKN2A, PCOLCE2, Claudin-1 and N-cadherin in the primary tumor in the no distant metastasis group (n=4), liver metastasis group (n=4) and lung metastasis group (n=4) were detected by IHC (scale bars, 200 μ m.) and the AOD values were expressed as scatter plots. * p < 0.05, ** p < 0.01, and *** p < 0.001.

related to cell adhesion and ECM remodeling, while stromal cells are involved in the composition and remodeling of ECM (46–49). Hence, the risk model can better reflect the differences in stromal cell distribution, and the specific molecular mechanisms deserve further investigation.

Lastly, our cell experiments confirmed the relationship between the expression of NAT1, CDKN2A, PCOLCE2, and anoikis, suggesting that NAT1 promoted anoikis while CDKN2A and PCOLCE2 contributed to anoikis resistance in COAD cells. IHC was used for verifying the link between these PAEGs and distant

metastasis of COAD, and the results also suggested that the high NAT1 expression level was associated with no distant metastasis while the high CDKN2A or PCOLCE2 expression levels were related to hepatopulmonary metastasis. The above findings were in agreement with the findings of the univariate Cox analysis of these genes in TCGA.

This study has some limitations despite its superiorities. Firstly, we obtained the EMT signature containing 198 genes from the MSigDB portal in where some important genes of EMT such as ZEB1, ZEB2, SNAI1 are not included. This may bring some uncertainties, and a more complete database may yield better analysis results. Secondly, the ROC curves for the 1-year, 3-year, and 5-year risk scores were <0.7 in the training and test sets, indicating that the prediction rate was less accurate, and the risk model needs further improvement. Thirdly, after classifying the patients into the API Low + EPI High and the others group, the immune infiltration, stromal infiltration, and drug sensitivity rates in the two groups were determined by means of gene enrichment and DEG analyses. The ESTIMATE tool indicated no significant difference in the immune cell proportion between the low- and high-risk groups, it should be noted that the analysis did not include some important immune cells such as dendritic cells or NK cells. Fourthly, the study found no significant difference in the expression of 10 immune checkpoint molecules and 24 MHC molecules between the low- and high-risk groups, suggesting that the immune checkpoint blockade therapy response may not be affected by the risk model. Finally, the molecular mechanisms of the three PAEGs in anoikis and EMT need to be explored and validated by further *in vivo* and *in vitro* experiments. Additionally, the univariate Cox analysis of PCOLCE2 revealed that it is a poor predictive gene, although its expression is low in tumor tissues relative to normal tissue, which is an intriguing and paradoxical finding. More research is needed to determine its role and mechanism in colorectal cancer, as very few studies have investigated the role played by this gene. Hence, more research needs to be conducted to determine its role and mechanism in the future.

This is the first study that combines the anoikis and EMT analysis based on distant metastasis of COAD. Herein, a favorable molecular group and prognostic risk model was constructed, which can help to establish biomarkers and drug intervention targets for patients with distant metastasis. Moreover, drug sensitivity analyses were conducted in this study, which can provide some clinical drug references for these patients.

Conclusions

Collectively, based on the anoikis and EMT gene sets, the prognosis-related ARGs and ERGs were identified using univariate Cox analysis, and then PCA stratified analysis was used for categorizing the patients into two groups based on the greatest prognostic differences. A prognostic risk model was constructed, which showed good predictive sensitivity and specificity. This risk model was linked to the tumor microenvironment, especially stromal infiltration. Finally, the findings in this study could help in developing novel molecular biomarkers, therapeutic targets, and clinical medicines for treating patients with COAD metastasis.

Data availability statement

The original contributions presented in the study are included in the article/[Supplementary Material](#). Further inquiries can be directed to the corresponding authors.

Ethics statement

The studies involving human participants were reviewed and approved by the Ethical Committee of The Affiliated Suzhou Hospital of Nanjing Medical University. The patients/participants provided their written informed consent to participate in this study.

Author contributions

JZhou, SYang, DZhu and HLi for the acquisition of data, analysis and interpretation of data, statistical analysis and drafting of the manuscript. XMiao, MGu, WXu, YZhang, WTang, JZha, RShen and JZhu for technical and material support. JZhou, ZYuan, and XGu for study concept and design, obtained funding and study supervision. All authors read and approved the final manuscript.

Funding

This work was supported by the Clinical study of the accurate laparoscopic surgical treatment of rectal cancer (Grant No. LCZX202111); the Key Medical Discipline Gastrointestinal Surgery of Suzhou (Grant No. SZXK202109).

Acknowledgments

We thank Bullet Edits Limited for the linguistic editing and proofreading of the manuscript.

Conflict of interest

The authors declare that the research was conducted in the absence of any commercial or financial relationships that could be construed as a potential conflict of interest.

Publisher's note

All claims expressed in this article are solely those of the authors and do not necessarily represent those of their affiliated organizations, or those of the publisher, the editors and the reviewers. Any product that may be evaluated in this article, or claim that may be made by its manufacturer, is not guaranteed or endorsed by the publisher.

Supplementary material

The Supplementary Material for this article can be found online at: <https://www.frontiersin.org/articles/10.3389/fonc.2023.1184215/full#supplementary-material>

References

- Siegel RL, Miller KD, Wagle NS, Jemal A. Cancer statistics, 2023. *CA Cancer J Clin* (2023) 73:17–48. doi: 10.3322/caac.21763
- Miller KD, Nogueira L, Devasia T, Mariotto AB, Yabroff KR, Jemal A, et al. Cancer treatment and survivorship statistics, 2022. *CA Cancer J Clin* (2022) 72:409–36. doi: 10.3322/caac.21731
- Siegel RL, Wagle NS, Cercek A, Smith RA, Jemal A. Colorectal cancer statistics, 2023. *CA Cancer J Clin* (2023) 73:233–54. doi: 10.3322/caac.21772
- Nieto MA, Huang RY, Jackson RA, Thiery JP. EMT: 2016. *Cell* (2016) 166:21–45. doi: 10.1016/j.cell.2016.06.028
- Zhang N, Ng AS, Cai S, Li Q, Yang L, Kerr D. Novel therapeutic strategies: targeting epithelial-mesenchymal transition in colorectal cancer. *Lancet Oncol* (2021) 22:e358–68. doi: 10.1016/s1470-2045(21)00343-0
- Zhou Y, Lu L, Jiang G, Chen Z, Li J, An P, et al. Targeting CDK7 increases the stability of snail to promote the dissemination of colorectal cancer. *Cell Death Differ* (2019) 26:1442–52. doi: 10.1038/s41418-018-0222-4
- Bao Z, Zeng W, Zhang D, Wang L, Deng X, Lai J, et al. SNAIL induces EMT and lung metastasis of tumours secreting CXCL2 to promote the invasion of M2-type immunosuppressed macrophages in colorectal cancer. *Int J Biol Sci* (2022) 18:2867–81. doi: 10.7150/ijbs.66854
- Taddei ML, Giannoni E, Fiaschi T, Chiarugi P. Anoikis: an emerging hallmark in health and diseases. *J Pathol* (2012) 226:380–93. doi: 10.1002/path.3000
- Buchheit CL, Weigel KJ, Schafer ZT. Cancer cell survival during detachment from the ECM: multiple barriers to tumour progression. *Nat Rev Cancer* (2014) 14:632–41. doi: 10.1038/nrc3789
- Qin W, Tian Y, Zhang J, Liu W, Zhou Q, Hu S, et al. The double inhibition of PDK1 and STAT3-Y705 prevents liver metastasis in colorectal cancer. *Sci Rep* (2019) 9:12973. doi: 10.1038/s41598-019-49480-8
- Wang YN, Zeng ZL, Lu J, Wang Y, Liu ZX, He MM, et al. CPT1A-mediated fatty acid oxidation promotes colorectal cancer cell metastasis by inhibiting anoikis. *Oncogene* (2018) 37:6025–40. doi: 10.1038/s41388-018-0384-z
- Tiwari N, Gheldof A, Tatari M, Christofori G. EMT as the ultimate survival mechanism of cancer cells. *Semin Cancer Biol* (2012) 22:194–207. doi: 10.1016/j.semcancer.2012.02.013
- Singh AB, Sharma A, Smith JJ, Krishnan M, Chen X, Eschrich S, et al. Claudin-1 up-regulates the repressor ZEB-1 to inhibit E-cadherin expression in colon cancer cells. *Gastroenterology* (2011) 141:2140–53. doi: 10.1053/j.gastro.2011.08.038
- Muys BR, Sousa JF, Praça JR, de Araújo LF, Sarshad AA, Anastasakis DG, et al. miR-450a acts as a tumor suppressor in ovarian cancer by regulating energy metabolism. *Cancer Res* (2019) 79:3294–305. doi: 10.1158/0008-5472.Can-19-0490
- Wang D, Zhang L, Hu A, Wang Y, Liu Y, Yang J, et al. Loss of 4.1N in epithelial ovarian cancer results in EMT and matrix-detached cell death resistance. *Protein Cell* (2021) 12:107–27. doi: 10.1007/s13238-020-00723-9
- Zhang B, Wu Q, Li B, Wang D, Wang L, Zhou YL. m(6)A regulator-mediated methylation modification patterns and tumor microenvironment infiltration characterization in gastric cancer. *Mol Cancer* (2020) 19:53. doi: 10.1186/s12943-020-01170-0
- Wilkerson MD, Hayes DN. ConsensusClusterPlus: a class discovery tool with confidence assessments and item tracking. *Bioinformatics* (2010) 26:1572–3. doi: 10.1093/bioinformatics/btq170
- Chen L, Niu X, Qiao X, Liu S, Ma H, Shi X, et al. Characterization of interplay between autophagy and ferroptosis and their synergistical roles on manipulating immunological tumor microenvironment in squamous cell carcinomas. *Front Immunol* (2021) 12:739039. doi: 10.3389/fimmu.2021.739039
- Yu Y, Song Y, Cheng L, Chen L, Liu B, Lu D, et al. CircCEMIP promotes anoikis-resistance by enhancing protective autophagy in prostate cancer cells. *J Exp Clin Cancer Res* (2022) 41:188. doi: 10.1186/s13046-022-02381-7
- Yu Y, Liu B, Li X, Lu D, Yang L, Chen L, et al. ATF4/CEMIP/PKC α promotes anoikis resistance by enhancing protective autophagy in prostate cancer cells. *Cell Death Dis* (2022) 13:46. doi: 10.1038/s41419-021-04494-x
- Zhang C, Wang L, Jin C, Zhou J, Peng C, Wang Y, et al. Long non-coding RNA lnc-LALC facilitates colorectal cancer liver metastasis via epigenetically silencing LZTS1. *Cell Death Dis* (2021) 12:224. doi: 10.1038/s41419-021-03461-w
- Liu Y, Zhang Q, Xing B, Luo N, Gao R, Yu K, et al. Immune phenotypic linkage between colorectal cancer and liver metastasis. *Cancer Cell* (2022) 40:424–437.e425. doi: 10.1016/j.ccell.2022.02.013
- Chandra R, Karalis JD, Liu C, Murimwa GZ, Voth Park J, Heid CA, et al. The colorectal cancer tumor microenvironment and its impact on liver and lung metastasis. *Cancers (Basel)* (2021) 13:6206. doi: 10.3390/cancers13246206
- Zhu X, Tian X, Ji L, Zhang X, Cao Y, Shen C, et al. A tumor microenvironment-specific gene expression signature predicts chemotherapy resistance in colorectal cancer patients. *NPJ Precis Oncol* (2021) 5:7. doi: 10.1038/s41698-021-00142-x
- Ecker BL, Lee J, Saadat LV, Aparicio T, Buisman FE, Balachandran VP, et al. Recurrence-free survival versus overall survival as a primary endpoint for studies of resected colorectal liver metastasis: a retrospective study and meta-analysis. *Lancet Oncol* (2022) 23:1332–42. doi: 10.1016/s1470-2045(22)00506-x
- Tsilimigras DI, Brodt P, Clavien PA, Muschel RJ, D'Angelica MI, Endo I, et al. Liver metastases. *Nat Rev Dis Primers* (2021) 7:27. doi: 10.1038/s41572-021-00261-6
- Achrol AS, Rennert RC, Anders C, Soffietti R, Ahluwalia MS, Nayak L, et al. Brain metastases. *Nat Rev Dis Primers* (2019) 5:5. doi: 10.1038/s41572-018-0055-y
- Jin L, Chun J, Pan C, Kumar A, Zhang G, Ha Y, et al. The PLG1-GDH1 axis promotes anoikis resistance and tumor metastasis through CamKK2-AMPK signaling in LKB1-deficient lung cancer. *Mol Cell* (2018) 69:87–99.e87. doi: 10.1016/j.molcel.2017.11.025
- Huang Y, Hong W, Wei X. The molecular mechanisms and therapeutic strategies of EMT in tumor progression and metastasis. *J Hematol Oncol* (2022) 15:129. doi: 10.1186/s13045-022-01347-8
- Butcher NJ, Minchin RF. Arylamine n-acetyltransferase 1: a novel drug target in cancer development. *Pharmacol Rev* (2012) 64:147–65. doi: 10.1124/pr.110.004275
- Malagobadan S, Ho CS, Nagoor NH. MicroRNA-6744-5p promotes anoikis in breast cancer and directly targets NAT1 enzyme. *Cancer Biol Med* (2020) 17:101–11. doi: 10.20892/j.issn.2095-3941.2019.0010
- Savci-Heijink CD, Halfwerk H, Hooijer GJ, Koster J, Horlings HM, Meijer SL, et al. Epithelial-to-mesenchymal transition status of primary breast carcinomas and its correlation with metastatic behavior. *Breast Cancer Res Treat* (2019) 174:649–59. doi: 10.1007/s10549-018-05089-5
- Okamoto A, Demetrick DJ, Spillare EA, Hagiwara K, Hussain SP, Bennett WP, et al. Mutations and altered expression of p16INK4 in human cancer. *Proc Natl Acad Sci U.S.A.* (1994) 91:11045–9. doi: 10.1073/pnas.91.23.11045
- Hu H, Li Z, Chen J, Wang D, Ma J, Wang W, et al. P16 reactivation induces anoikis and exhibits antitumor potency by downregulating akt/survivin signalling in hepatocellular carcinoma cells. *Gut* (2011) 60:710–21. doi: 10.1136/gut.2010.220020
- Amano M, Eriksson H, Manning JC, Detjen KM, André S, Nishimura S, et al. Tumour suppressor p16(INK4a) - anoikis-favouring decrease in N/O-glycan/cell surface sialylation by down-regulation of enzymes in sialic acid biosynthesis in tandem in a pancreatic carcinoma model. *FEBS J* (2012) 279:4062–80. doi: 10.1111/febs.12001
- Rabien A, Sanchez-Ruderisch H, Schulz P, Otto N, Wimmel A, Wiedenmann B, et al. Tumor suppressor p16INK4a controls oncogenic K-ras function in human pancreatic cancer cells. *Cancer Sci* (2012) 103:169–75. doi: 10.1111/j.1349-7006.2011.02140.x
- Kemmer W, Kessel P, Sanchez-Ruderisch H, Möller H, Hinderlich S, Schlag PM, et al. Loss of UDP-N-acetylglucosamine 2-epimerase/N-acetylmannosamine kinase (GNE) induces apoptotic processes in pancreatic carcinoma cells. *FASEB J* (2012) 26:938–46. doi: 10.1096/fj.11-186700
- André S, Sanchez-Ruderisch H, Nakagawa H, Buchholz M, Kopitz J, Forberich P, et al. Tumor suppressor p16INK4a-modulator of glycomic profile and galectin-1 expression to increase susceptibility to carbohydrate-dependent induction of anoikis in pancreatic carcinoma cells. *FEBS J* (2007) 274:3233–56. doi: 10.1111/j.1742-4658.2007.05851.x
- Chen S, Gu J, Zhang Q, Hu Y, Ge Y. Development of biomarker signatures associated with anoikis to predict prognosis in endometrial carcinoma patients. *J Oncol* (2021) 2021:3375297. doi: 10.1155/2021/3375297
- Shi WK, Li YH, Bai XS, Lin GL. The cell cycle-associated protein CDKN2A may promotes colorectal cancer cell metastasis by inducing epithelial-mesenchymal transition. *Front Oncol* (2022) 12:834235. doi: 10.3389/fonc.2022.834235
- Kang N, Xie X, Zhou X, Wang Y, Chen S, Qi R, et al. Identification and validation of EMT-immune-related prognostic biomarkers CDKN2A, CMTM8 and ILK in colon cancer. *BMC Gastroenterol* (2022) 22:190. doi: 10.1186/s12876-022-02257-2
- Steiglitz BM, Keene DR, Greenspan DS. PCOLCE2 encodes a functional procollagen C-proteinase enhancer (PCPE2) that is a collagen-binding protein differing in distribution of expression and post-translational modification from the previously described PCPE1. *J Biol Chem* (2002) 277:49820–30. doi: 10.1074/jbc.M209891200
- Zhang M, Cao C, Li X, Gu Q, Xu Y, Zhu Z, et al. Five EMT-related genes signature predicts overall survival and immune environment in microsatellite instability-high gastric cancer. *Cancer Med* (2022) 12:2075–88. doi: 10.1002/cam4.4975
- Xu H, Wan H, Zhu M, Feng L, Zhang H, Su F. Discovery and validation of an epithelial-mesenchymal transition-based signature in gastric cancer by genomics and prognosis analysis. *BioMed Res Int* (2021) 2021:9026918. doi: 10.1155/2021/9026918

45. Shi C, Xie Y, Li X, Li G, Liu W, Pei W, et al. Identification of ferroptosis-related genes signature predicting the efficiency of invasion and metastasis ability in colon adenocarcinoma. *Front Cell Dev Biol* (2021) 9:815104. doi: 10.3389/fcell.2021.815104
46. Grünwald BT, Devisme A, Andrieux G, Vyas F, Aliar K, McCloskey CW, et al. Spatially confined sub-tumor microenvironments in pancreatic cancer. *Cell* (2021) 184:5577–5592.e5518. doi: 10.1016/j.cell.2021.09.022
47. Zhang HF, Hughes CS, Li W, He JZ, Surdez D, El-Naggar AM, et al. Proteomic screens for suppressors of anoikis identify IL1RAP as a promising surface target in Ewing sarcoma. *Cancer Discovery* (2021) 11:2884–903. doi: 10.1158/2159-8290.Cd-20-1690
48. Yuan JW, Zhang YN, Liu YR, Li W, Dou SX, Wei Y, et al. Diffusion behaviors of integrins in single cells altered by epithelial to mesenchymal transition. *Small* (2022) 18: e2106498. doi: 10.1002/sml.202106498
49. Papanicolaou M, Parker AL, Yam M, Filipe EC, Wu SZ, Chitty JL, et al. Temporal profiling of the breast tumour microenvironment reveals collagen XII as a driver of metastasis. *Nat Commun* (2022) 13:4587. doi: 10.1038/s41467-022-32255-7



OPEN ACCESS

EDITED BY

Alessandro Passardi,
Scientific Institute of Romagna for the
Study and Treatment of Tumors (IRCCS),
Italy

REVIEWED BY

Rani Mata,
Pondicherry University, India
Gamze Varan,
Vaccine Institute of Hacettepe University,
Türkiye

*CORRESPONDENCE

Sankha Bhattacharya
✉ sankhabhatt@gmail.com

RECEIVED 25 April 2023

ACCEPTED 05 June 2023

PUBLISHED 22 June 2023

CITATION

Jain A and Bhattacharya S (2023) Recent
advances in nanomedicine preparative
methods and their therapeutic potential for
colorectal cancer: a critical review.
Front. Oncol. 13:1211603.
doi: 10.3389/fonc.2023.1211603

COPYRIGHT

© 2023 Jain and Bhattacharya. This is an
open-access article distributed under the
terms of the [Creative Commons Attribution
License \(CC BY\)](https://creativecommons.org/licenses/by/4.0/). The use, distribution or
reproduction in other forums is permitted,
provided the original author(s) and the
copyright owner(s) are credited and that
the original publication in this journal is
cited, in accordance with accepted
academic practice. No use, distribution or
reproduction is permitted which does not
comply with these terms.

Recent advances in nanomedicine preparative methods and their therapeutic potential for colorectal cancer: a critical review

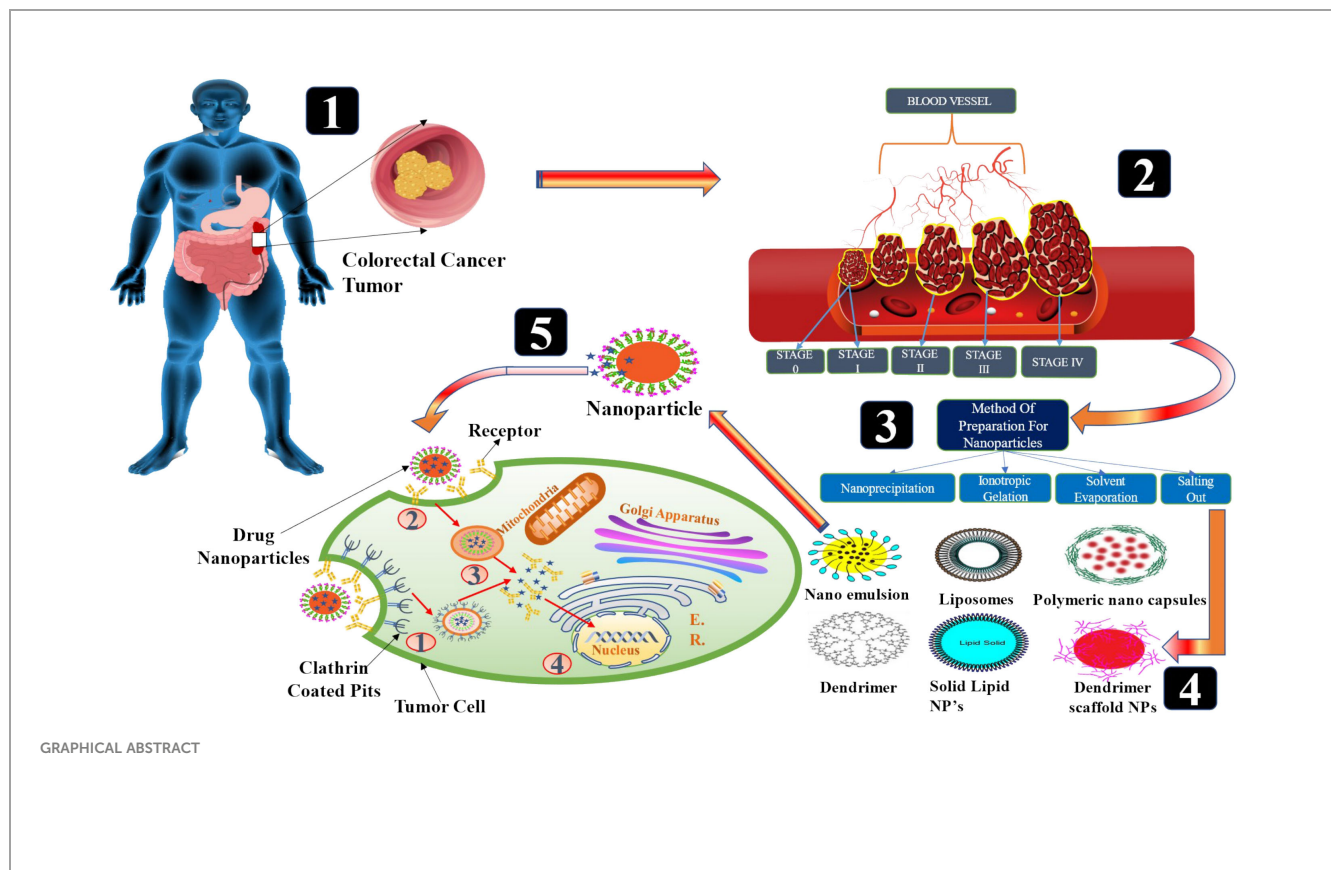
Arinjay Jain and Sankha Bhattacharya *

Department of Pharmaceutics, School of Pharmacy & Technology Management Shirpur, SVKM'S
NMIMS Deemed-to-be University, Shirpur, Maharashtra, India

Colorectal cancer (CRC) is a prevalent malignancy that affects a large percentage of the global population. The conventional treatments for CRC have a number of limitations. Nanoparticles have emerged as a promising cancer treatment method due to their ability to directly target cancer cells and regulate drug release, thereby enhancing therapeutic efficacy and minimizing side effects. This compilation examines the use of nanoparticles as drug delivery systems for CRC treatment. Different nanomaterials can be used to administer anticancer drugs, including polymeric nanoparticles, gold nanoparticles, liposomes, and solid lipid nanoparticles. In addition, we discuss recent developments in nanoparticle preparation techniques, such as solvent evaporation, salting-out, ion gelation, and nanoprecipitation. These methods have demonstrated high efficacy in penetrating epithelial cells, a prerequisite for effective drug delivery. This article focuses on the various targeting mechanisms utilized by CRC-targeted nanoparticles and their recent advancements in this field. In addition, the review offers descriptive information regarding numerous nano-preparative procedures for colorectal cancer treatments. We also discuss the outlook for innovative therapeutic techniques in the management of CRC, including the potential application of nanoparticles for targeted drug delivery. The review concludes with a discussion of current nanotechnology patents and clinical studies used to target and diagnose CRC. The results of this investigation suggest that nanoparticles have great potential as a method of drug delivery for the treatment of colorectal cancer.

KEYWORDS

colorectal cancer, nanomaterials, anticancer drug, tumor microenvironment, enhanced permeability and retention



Introduction

In many cases, a cancerous growth called colorectal cancer (CRC) can be found in the gastrointestinal tract. Currently, CRC is the third leading cause of death in the globe (1). Around a quarter of all cancer cases are due to CRC, making it one of the most common malignancies. Younger patients are increasingly more likely to have colon cancer (2). Economic and living conditions have steadily improved over the past few decades, which has led to an increase in CRC (3). Colorectal cancer (CRC) can be caused by genetic mutations, just like other types of cancer. These mutations affect oncogenes, tumor suppressors, and genes involved in DNA repair processes (4). Depending on the source of the mutation, CRC can be classified as sporadic, hereditary, or familial. Sporadic CRC refers to cancers that occur during a person's lifetime and are caused by

mutations that are not related to genetic diseases. These mutations affect people's brains and their offspring and account for 70 percent of all colon cancers. The molecular mechanisms behind cancer are diverse and target many genes (5). However, approximately 70% of CRC patients follow a specific mutation pattern that results in characteristic mutations. The system usually starts with a mutation in the adenomatous polyposis coli (APC) gene, a tumor that causes benign adenoma or polyp formation. Subsequent mutations in genes such as KRAS, TP53 and DCC contribute to the disease. Inherited cancers represent a small fraction, comprising only 5% of all colorectal cancer cases. These cancers arise from inherited mutations affecting one allele of the mutated gene. When a point mutation occurs in the other allele, it initiates the formation of tumor cells and eventually carcinoma development (6, 7). On the other hand, familial CRC comprises around 25% of all cases and is also caused by inherited mutations. However, it is not classified as an inherited cancer in the strict sense, as it does not fit into any specific inherited cancer syndrome variant (8).

In addition to genetic mutations, various personal traits and habits are recognized as risk factors for the development of CRC or polyps. Advancing age is a significant risk factor, with the chances of developing CRC notably increasing after the age of fifty, while occurrences before this age are rare except in cases of inherited cancers (9). Recent research indicates that individuals diagnosed with bowel diseases tend to have a heightened awareness of colorectal cancer compared to others (10–14). Conditions such as inflammatory bowel disease, chronic ulcerative colitis, and Crohn's

Abbreviations: CRC, Colorectal cancer; CDC, Center for disease control and prevention; EPR, Enhanced permeability and retention; 5-FU, 5-Fluorouracil; TME, Tumor microenvironment; HDW, Hedyotis diffusa Willid; EMT, Epithelial-mesenchymal transition; RES, Reticuloendothelial system; NPs, Nanoparticles; CEA, Carcinoembryonic antigen; CHEK2, Checkpoint kinase 2; TPP, Triphosphosphate; DDS, Drug Delivery Systems; CS, Chitosan; CCSNPs, Cromolyn chitosan nanoparticles; Doc, Docetaxel; EC, Ethyl Cellulose; CAP, Cellulose Acetate Phthalate; ICD, Immunogenic cell death; IMT-PNPs, Imatinib polymeric nanoparticles; SLNs, Solid lipid nanoparticles; FA, Folic acid; FER, Ferulic acid; ROS, Reactive oxygen species; GNPs, Gold nanoparticles; SC, Subcutaneous.

disease, particularly when accompanied by adenomatous polyps, are considered primary lesions that elevate the risk of developing CRC (15–18). Family history also plays a significant role, as numerous studies have demonstrated a 2.5 to 3 times greater risk of colorectal cancer among relatives of affected individuals (19).

Other risk factors, such as leading a sedentary lifestyle, can elevate the likelihood of developing colorectal cancer (20). A sedentary lifestyle is often associated with obesity, another major risk factor for colon cancer. More importantly, this increased risk has been attributed to dietary choices and the accumulation of adipose tissue (VAT), the metabolic equivalent of total body fat. VAT promotes colon cancer development by causing inflammation in the colon and rectum by releasing proinflammatory cytokines. This process also causes insulin resistance and affects metabolic enzymes such as adiponectin and lectins (21). Smoking and alcohol increase the risk of colon cancer. Alcohol, especially its metabolite acetaldehyde, is considered carcinogenic and increases the risk of cancer, especially in individuals with specific enzymes that metabolize alcohol. Smoking, on the other hand, was associated with a 10.8 percent increased risk of lung cancer, mainly due to the presence of carcinogens such as nicotine, which can reach the stomach and cause polyps (22).

CRC is cured with a variety of surgical, radiation, chemotherapy, and other modalities, including immunotherapy and targeted therapy (23). Because CRC is difficult to detect in its earliest stages, people who present with symptoms are almost always in the middle or later stages of the illness. Drug resistance and recurrence of CRC may result from the presence of tumor stem cells (24). Recent advances in pharmaceutical colloidal system preparation have made it possible to develop drug carriers that are both safe and effective. Liposomes, niosomes, polymeric, nanoparticles, micelles, gold nanoparticles, and other colloidal carriers are examples of drug delivery systems. NPs have risen to the top for the drug delivery due to an increase in their therapeutic efficacy over the last decade. NPs are solid colloidal particles with a diameter ranging from 10 nm to 1000 nm used in pharmaceuticals (25). There are three ways to deliver medication or biologically active ingredient: dissolving, encapsulating, or attaching to the surface of macromolecular molecules. To make nanoparticles of one type or the other, a variety of different preparation methods and starting materials are required. The morphology and structure of these two kinds are vastly different. A dense polymeric matrix makes up nanospheres, whereas a polymeric membrane encloses the core of nano capsules (1).. By acting as a unique carrier for biomacromolecules, nanoparticles can enhance ingestion and absorption of insoluble medications and targeted release pharmaceuticals, as well as achieve precisely focused therapy (26).. Antitumor medications can be delivered to specific tumours using this method in a variety of ways, including passive and active targeting (27). Passive targeting indicates that the nano DDS can efficiently accumulate in the tumor depending on the physiological and pathological properties of the tumor location and the nature of the nano delivery system (23). Tumours have a distinct microenvironment compared to healthy tissue. Because the microvascular structure of solid tumours differs from that of normal tissue, macromolecules and massive particles are unable

to permeate the capillary wall because the endothelial space is dense and complete. Solid tumor tissue has many new blood vessels, the vascular wall space is broad, the structural integrity is poor, and lymphatic reflux is absent (28). Macromolecular drugs or particles with diameters of 100 nm are more likely to accumulate in tumor tissue because of this difference; additionally, specific pH, enzyme environment, and reduction environment in tumor site can be used to achieve the release of drugs at specific sites in order to achieve the goal of targeted drug delivery (29). Tumor cells proliferate rapidly, resulting in a lack of blood vessels and lymphatics in the tumor tissue, which results in a high rate of leakage of substances from blood vessels into the tumor tissue, which can't easily return to the lymphatic vessels, increasing the retention and infiltration of the tumor (30). To distribute macromolecules or nanoparticles by tumor extravasation, the retention effect of solid tumours is unique. Tumor vascular endothelium has huge gaps that allow macromolecule medicines to selectively extravasate into tumor tissue as a result of increased vascular density brought on by angiogenesis in solid tumours (31). For example, EPR-based cancer therapy for macromolecular cancers could be used to treat more tumours. Nitroglycerin has been shown to boost the EPR impact of tumours by increasing the transfer of medications to tumours by 2-3-fold and thereby improving the therapeutic effect (32). Deficiencies in tumor lymphatics can potentially increase tumor interstitial pressure and hinder the diffusion of medicines within the tumor. Nanocarriers modified by hydrophilic polymer materials serve as active targeting agents, delivering medications to specific organs or tissues (33). For example, in contrast to passive drug targeting, active targeting is the combination of active recognition between specific molecules on the surface of the nanosystem and specific molecules and proteins on the tumor site in order to obtain selective drug concentrations in tumor tissue and cells. Most active drug targeting is aimed at improving target cell identification and uptake rather than increasing total tumor accumulation (34). Targeted nano-drug preparations can be made by combining polymer nano-carriers with precise combinations of tumor cell surface receptors or antigens, allowing for the active delivery of medicines. Pharmacological nanocarriers that can remain in the bloodstream for a long period of time—such as liposomes, micelles, or polymeric nanoparticles—may be utilized to transport drugs into tumours by passive accumulation. It is common for nano drug carriers to have a long *in-vivo* half-life (35). Targeting tumor cells without damaging non-tumor cells is now possible due to improvements in targeted drug delivery. Different nanoparticles are being formulated and investigated for the efficient transport of cytotoxic drugs to the target site, improving drug distribution and bioavailability while concurrently reducing adverse effects. Immunotherapy still remains only an experimental approach despite the fact that few clinical trials have shown the ability to help patients with CRC. For successful CRC treatment, evaluation of the ongoing and finished studies is required. Researchers are working to create new carrier systems that might improve the targeting capacity of chemo- and immune-therapeutics with poor therapeutic index. Numerous preclinical investigations have shown that nanotherapy is more effective than traditional methods in treating CRC (36).

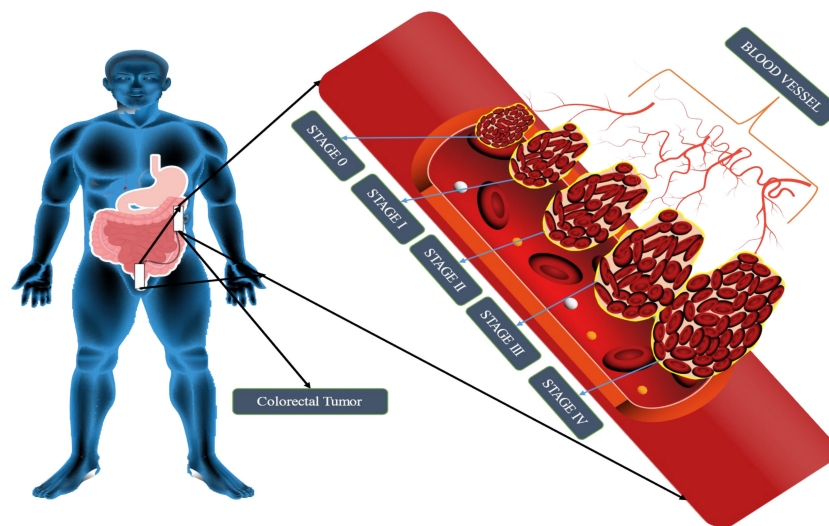


FIGURE 1

Schematic representation of CRC stages. CRC tumor growth progresses via four stages: metastasis, progression, promotion, and initiation. The liver, lung, and bone are the most typical metastatic sites. It is impossible to estimate how long each stage will take, but decades will probably be needed to develop CRC.

So that medications have a longer half-life and are more readily absorbed by tumor tissue due to their hydrophilic groups, nano-drug carriers can inhibit macrophage system affinity. The lifespan and quality of life of cancer patients, particularly in the late stages of the disease, have been dramatically diminished as a result of multidrug resistance and harm to normal cells. Some 20 to 400 nanometer-sized drug-loaded nanoparticles such as liposomes and dendrimers, as well as micelles, have improved drug delivery for CRC therapy in recent years (37). Nanoparticle-based drug delivery systems can increase medication bioavailability, reduce adverse effects, and protect healthy cells by delivering pharmaceuticals to the target spot (38). Small-molecule antitumor drugs, genes, or proteins can be transported by nanocarriers, which can avoid normal tissues while allowing the drugs to accumulate in tumor tissue, thus increasing their concentration in tumours while reducing the toxicity of the remaining body compared to the effects observed with free drugs (39). To top it all off, nanopillars provide a number of advantages over conventional pharmaceuticals, including lower renal clearance and better drug half-lives, controlled release and improved solubility. Despite the rapid development of nanomaterials, few nano agents have been successfully employed for tumor therapy at the present time (40).

Colorectal cancer stages

Staging is the process of determining whether or not cancer has migrated from the colon/rectum to other areas of the body (41). Staging is important because it helps decide the best course of action for therapy. Oncologists use the term “stage” to describe how far cancer has spread. Treatment options for colon cancer must be determined based on its stage. The TNM staging system, developed

by the Union for International Cancer Control and endorsed by the American Joint Committee on Cancer, is used to classify colon cancer. For patients diagnosed with metastatic CRC, the survival rate ranges from 90 percent to 10 percent, depending on the disease stage (42). The greater the possibility of survival, the earlier in the disease process the diagnosis is made. Cancer’s level in the body is one of the most important criteria in determining which therapy will be most effective and how successful it will be. Colorectal cancer is depicted in Figure 1. When abnormal cells form in the colonic mucosa, they have the potential to develop into malignancies (43). In stage I, cancer has spread from the mucosa of the colon wall into the submucosa and the muscularis propria of the colon. After spreading to the visceral peritoneum (IIB) and the connected organs, cancer in stage II spreads farther from the muscularis propria into the peri-colorectal tissues (IIA) (IIC) (Figure 1). Muscularis propria metastases in surrounding tissues or 1–3 regional lymph nodes or submucosa spreading with metastases in 4–6 lymph nodes and IIIB and 7 or more regional lymph nodes in stage (IIIC) (44). Stage IV cancer is further subdivided into IV A and IV B, with metastatic spread confined to a single organ such as the liver, ovary, lung, regional node, etc. (45). A 5 year survival rate of 90% for stage I CRC and 10% for stage IV CRC was found in research studies conducted over a period of five years. Physical inactivity, a diet high in processed meats, smoking, being overweight, and abusing alcohol are some of the most common risk factors and primary causes of colorectal cancer. A person having a chronic inflammatory bowel illness, type 2 diabetes, or a genetic disorder like lynch syndrome has an increased risk of CRC and a family history of the disease (46). It is possible to treat CRC in stages 0 through 1, 2, and 3, but it is rare to treat stage IV (Table 1), which can be managed depending on the illness’s rate of growth and spread (47).

TABLE 1 Different stages of cancer along with its progression and the current treatment approaches available for Colorectal Cancer.

Stages of Cancer	Progression of each stage	Current Treatment Approaches for CRC	References
Stage 0	The earliest phase of CRC, also known as carcinoma " <i>in situ</i> " or intramucosal carcinoma, denotes that the disease has not yet spread through the colon or rectum wall and is present only in the mucosa (the moist tissue lining the colon).	Local treatments: Surgical resection	(39)
Stage I	Although it has penetrated the mucosal (second or third) layer of the colon, the cancer is still present in the inner lining. But it is still not been spreaded in the surrounding lymph nodes nor any distant sites have been affected by it.	Local treatments: Surgical removal of the cancerous polyp or partial colectomy of the tumour and local lymph nodes	(40)
Stage II	The colon or rectum's outer walls have been affected by cancer, which has spreaded and connected into other surrounding tissues or organs. But it hasn't migrated to local lymph nodes or distant regions.	Local and systematic treatments: Chemotherapeutic treatment (5-FU, leucovorin, oxaliplatin, or capecitabine); surgical excision without chemotherapy	(41)
Stage III	In stage 3, colon or rectum has developed cancer, or there are tiny tumour deposits in the fat surrounding the colon or rectum. It hasn't spread to distant sites.	Local, systematic, and combined treatments: Adjuvant chemotherapy, such as FOLFOX (5-FU, leucovorin, and oxaliplatin) or CapeOx (capecitabine and oxaliplatin), & is administered after surgery. For some advanced colon cancers, neoadjuvant chemotherapy, radiation therapy, and/or chemotherapy are options for patients who are not sufficiently stable for surgery.	(42)
Stage IV	Cancer has metastasised to distant sites and has been carried through the lymph and blood systems to distant parts of the body. The lungs and liver are the organs most likely to experience metastases from colorectal cancer.	Local, systematic, and combined treatments: Radiation therapy, chemotherapy with 5-FU, LV, and irinotecan (FOLFOIRI), FOLFOX, CAPIRI (capecitabine and irinotecan), CAPOX, 5-FU with LV, irinotecan, capecitabine and Trifluridine plus Tipiracil (Lonsurf), immunotherapy with Pembrolizumab (Keytruda) or Nivolumab (Opdivo), targeted therapies	(43)

Screening methods for colorectal cancer

CRC can be detected using a variety of screening assays, each with its own set of advantages and disadvantages. There are several factors that go into determining which screening test is best for a patient or clinician, including their perceptions and preferences. The actual positive rate is the percentage of patients who get a positive result from a screening test, which is the essential quality to look for in a screening test (48). In addition to sensitivity, but less so than specificity, which is the percentage of patients without disease who have a negative result, is significant, but less so than specificity (also known as the true-negative rate). The accuracy of a test is defined by its combination of sensitivity and specificity, which are typically traded off against one another based on the clinical scenario. Sensitivity is preferred over specificity when a serious or grave consequence of failing to detect a lesion or disease state is at stake. Specificity is preferred to sensitivity when the risk of overtreatment is the greatest (49). The use of a single test with both high sensitivity and high specificity is recommended in many screening applications. False-positive results would lead to excessive worry and follow-up, whereas false-negative results would leave CRC undiscovered. High precision is therefore crucial in the search for CRC. Repeatability and precision are other important considerations for the test. Obtaining high levels of cooperation from those who require screening is essential for a good screening program; as a result, the test must be acceptable to the individual. The test should be simple to administer and use, accessible, cost-effective, and safe in order to encourage a high participation rate in

screening activities (50). CRC screening approaches, their advantages and disadvantages as well as where they are most successful in the CRC formation process, have been outlined here.

Current treatments available for colorectal cancer

Surgery, chemotherapy, and radiation are among the most common types of treatment. Research into colorectal cancer has resulted in significant changes in treatment. In the past, Surgery, chemotherapy, and radiation were among the most common treatment modalities. There has been an increase in the number of therapeutic options for both local and advanced diseases as a result of a better understanding of pathophysiology (51). Patients can get a wide range of treatments, including endoscopic and surgical excisions, downstaging preoperative radiation, and systemic therapy, as well as major surgery for local and metastatic illness. Cancer patients who receive systemic chemotherapy and multimodal treatment are more likely to be cured or live longer than those who do not receive these treatments. Adjuvant and neoadjuvant CRC treatment are the two major treatment types. Neoadjuvant therapy, on the other hand, refers to treatments that are administered prior to the major cancer treatment, such as surgery (52). Neoadjuvant therapy has the ability to eradicate early metastases, hence reducing the severity of the cancer and reducing the likelihood of surgical complications. Surgical treatment is tailored to each individual patient and tumor and attempts to maximize survival and minimize recurrence risk. At the moment, there are a wide variety

of surgical instruments and novel surgical techniques, such as minimally invasive surgery, being researched. Completely removing the tumor as well as its surrounding mesentery is a primary goal of CRC surgery (53). Patients who are unable to have this surgery due to the tumor's location or invasion of the sphincter complex may benefit most from abdominoperineal surgery. Systemic treatment for cancer, chemotherapy involves the use of chemotherapy medications (54). Chemotherapy is usually administered orally or intravenously. 5-FU, oxaliplatin, irinotecan, and capecitabine are some of the chemotherapies used to treat CRC. When it comes to CRC treatment, the first line of defense is typically chemotherapy. 5-FU is the most commonly used chemotherapeutic medication in the treatment of CRC. It has been shown that 5-FU inhibits thymidylate synthase and has an anti-CRC function because it prevents the conversion of deoxyuridine to deoxythymidine. Chemotherapy's adverse effects, which can range from nausea and vomiting to dry mouth and tongue to numb hands and feet to hair loss and reduced red blood cells, are well-known. Because of this, patient's quality of life declines and can lead to the termination of chemotherapy treatment due to intolerance. Chemotherapy-induced side effects are currently not alleviated by any single drug. As a result of the advent of immunotherapy and targeted therapy, the cure rate and quality of life for patients with CRC have increased. Some tumours have responded well to immunotherapy treatment. Invasion of surrounding tissues by tumor cells in the tumor microenvironment (TME) is possible, as is metastasis via blood and lymphatic arteries (55). Therefore, it is essential to understand the TME's immune status and investigate the distribution and activity of immune cells in order to increase the efficacy of immunotherapy in cancer. Multiple cell types in solid tumor tissues, such as malignant, innate, and adaptive immune system components including fibroblasts and endothelial cells and fibroblast-endothelial interfacial cells, contribute to the inflammatory and immunological condition of tumor tissues through cell-to-cell contact. It is possible to eradicate tumor cells from the body using the adaptive immune system and the natural immune system. As a result, tumor immunotherapy boosts the immune system's ability to fight cancer by reducing immunosuppressive elements in the tumor microenvironment. Boosting the activity of T cells is the first step. Inflammatory checkpoint inhibitors can boost T cell responsiveness. immunosuppressive checks include CTLA-4, PD-L1, OX40, and Lag3. For example, nivolumab can inhibit CTLA-4 (56).

Targeted therapy has made a big difference in the success rate of CRC patients in recent years. Precision, efficiency, and low toxicity are the hallmarks of targeted therapy. The quality of life of CRC patients increases as a result of targeted therapy. Targeted drug research is the primary focus of the development of targeted therapy. Tumorigenesis, development, survival, or anti-tumor immunity are the primary goals of targeted treatments. For anti-cancer effects, targeted medications can interfere with these molecule's functions and inhibit their signaling pathways (57). According to their method of action, CRC-targeted medicines can be categorised into three groups. For example, Cetuximab and Panitumumab inhibit tumor cell development by targeting tumor cell growth signaling pathways. Second, tumor growth-microenvironment-targeting

medications like bevacizumab and regorafenib restrict tumor cell blood supply.

Traditional Chinese medicine, on the other hand, is becoming increasingly significant in modern medicine and cancer therapy. Traditional Chinese remedies have been demonstrated to have curative effects on colorectal cancer. Colorectal cancer has been discovered to respond well to a number of natural medicines (58). In *Scutellaria baicalensis* Georgi, Baicalein is one of the naturally occurring active components. Baicalein's anti-inflammatory and anti-tumor properties are well-documented. A study found that baicalein was effective in the treatment of CRC in humans. Inhibiting colorectal cancer growth can be accomplished by baicalein's ability to modulate gene expression. HT-29 and DLD1 cell growth, migration, and invasion are all inhibited by baicalein treatment. *Hedyotis diffusa* Willd (HDW) is an effective Chinese herbal remedy for treating colorectal cancer. This is according to JIUMAO LIN's research, which states that HDW can suppress CRC by affecting the STAT3 pathway (59). HDW possesses antiangiogenic activity, which is essential for cancer growth and progression. The ability of EEHDW to prevent cancer growth has been established both *in vivo* and *in vitro*. There are multiple CRC-related signaling pathways that EEHDW inhibits and controls the expression of, among other things. The primary active ingredient in ginseng is ginsenoside, which has been shown to be effective against colorectal cancer. Many kinds of cancer, including CRC, are influenced by the epithelial-mesenchymal transition (EMT). Antiangiogenic therapy has been used successfully to treat colorectal cancer because tumor tissue contains a large number of blood vessels (60). This ginsenoside possesses anti-vascularization properties, can prevent tumor growth and metastasis and can make cancer cells more sensitive to treatment.

Nano construct preparative methods

The efficacy of many medications and therapeutically active molecules like nucleic acids and proteins can be enhanced by using nanocarriers, while the risk of harmful and side effects is reduced (61). It is possible to shield therapeutic compounds from degradation, manage their release, bypass biological barriers, and target specific locations of action with biodegradable nanoparticles (NPs) (62). By altering interactions with the biological environment, the physicochemical features of nanoparticles can influence the biodistribution and pharmacokinetics of medications. For intravenous delivery, the size of the nanoparticles is particularly important because opsonin's (plasma proteins) adsorb onto the particles, resulting in the macrophages of the RES being able to recognize and remove them from the bloodstream (63). NPs with a diameter less than 80 nm were demonstrated to be more difficult to remove from the bloodstream than larger particles, which had a higher concentration of plasma proteins on them. The spleen's ability to filter out NPs and the hepatic parenchyma's ability to trap them both depended on their size. Cancer therapy can benefit from the so-called EPR, the leaky vasculature of some solid tumours, combined with weak lymphatic drainage, may result in a selective accumulation of colloidal carriers within the target tissue,

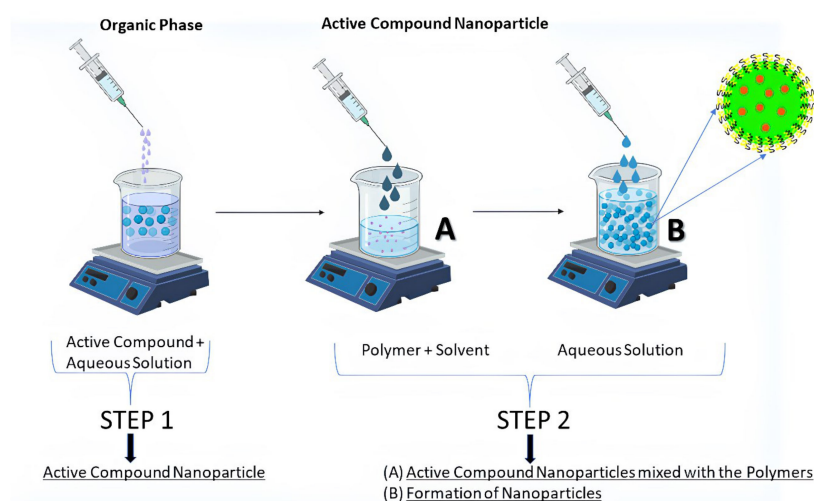


FIGURE 2
Formation of nanoparticles by the two-step nanoprecipitation method.

allowing for more effective treatment (64). Many human tumours endothelium has an effective pore size ranging from 200 nm to 600 nm, according to research. Particles must be fewer than 200 nm in diameter to benefit from the EPR effect, and much more preferable less than 100 nm. A diameter of more than 10 nm, on the other hand, usually prevents the diffusion of NPs through artery endothelium, which minimizes negative effects in healthy tissues (65). The mechanisms of NP internalization, phagocytosis, or endocytosis, are impacted by size at the cellular level as well (66). As a result, precise control of NP size and size distribution is required to provide effective and secure drug delivery. The detailed discussion of various preparative methods as described below:

Nanoprecipitation method

Fessi et al. awarded a patent in 1989 for nanoprecipitation. For hydrophobic drug compounds, it was mostly used after its invention (nanocapsule or nanosphere forms) (67). Numerous biodegradable polyesters such as PLA (Polylactide acid), PLGA (Poly (d,l-lactic co-glycolic acid)), and PCL (Poly-caprolactone) have been employed to achieve this goal, among them PLA, PLGA, and PCL. According to Fessi et al., the preparation of solvent and nonsolvent phases is necessary before the addition of one phase to the other under moderate magnetic stirring in this process. NPs can be suspended in water by evaporating organic solvents at room temperature or using a rotavapor (68). Ethanol, acetone, hexane, methylene chloride, and dioxane are the most common nanoprecipitation solvents. Water predominates in the non-solvent phase. Nonsolvent phases may also be supplemented with hydrophilic excipients. Particle size and surface morphology can be determined using TEM, SEM, or dynamic light scattering (DLS). The physical features of nanoprecipitates, such as their size, drug encapsulation effectiveness, and so on, are influenced by a wide range of parameters in nanoprecipitation. Using nanoprecipitation

(Figure 2), the most prevalent breakthroughs in the pursuit of polymer, lipid, and hybrid particles involve submicron and nanometric scales of nanoprecipitation. This technique is simple, energy-efficient, and adaptable. Nanocarrier's *In vivo* behavior is becoming better understood since industrial-scale production necessitates better control and standardization of operations. As a result, the technique and the starting materials used to make them have been improved to meet these needs. Particles with hydrophobic and hydrophilic molecular entrapment or behavior as stealth carriers can be produced using sophisticated devices with sizes less than 100 nm, and the procedure has been fine-tuned through chemical modification of polymers or careful definition of working conditions (69). Even more interesting is the invention of hybrid nanoparticles, which are able to offer substantial drug loadings, long-term drug-release patterns, and improved pharmacokinetic features. For the production of safe particles, nanoprecipitation appears to be a viable option regardless of the carrier material being used. Even when solvents with a high level of inherent toxicity are used, the positive results of safety testing show that they can be used in the pharmaceutical industry.

Pereira et al. described that PLGA-PEG NPs were generated by nanoprecipitation and loaded with paclitaxel (PCX), after which they were surface-functionalized with a monoclonal antibody targeting the carcinoembryonic antigen (CEA) of intestinal epithelial cells. Two intestinal cancer cell lines, Caco-2 clone and non-Caco-2 clone SW480, were used to evaluate the nanoparticles' physical and chemical characteristics, cytotoxicity, and ability to target. Nanoparticles with a diameter of 200 nm and close to charging neutrality were successfully produced, encasing up to 99 percent of paclitaxel. Further development of functionalized nanoparticles showed that they were non-cytotoxic to intestinal cells. Flow cytometry confirmed the capacity of functionalized nanoparticles to target Caco-2 CEA-expressing cells, unlike SW480 cells. PCX nanocarriers with CEA-targeting antibody were successfully generated as nanoparticles and interacted with CEA-expressing cells. These particles can be exploited as targeted systems for CRC

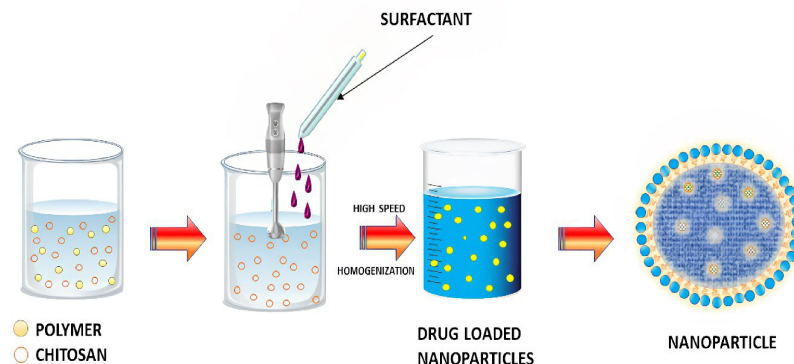


FIGURE 3
Schematic representation of ionic gelation method.

therapies because of their unique interaction (70). Ahmad et al. reported the development of amino cellulose-grafted polymeric nanoparticles containing LCS-1 for synthetic lethal targeting of checkpoint kinase 2 (CHEK2)-deficient HCT116 colon cancer cells to surpass the limitations associated with the solubility of LCS-1 (a superoxide dismutase inhibitor). To create nanoparticles containing LCS-1, amino cellulose (AC), a biocompatible and biodegradable hydrophilic polymer, was grafted onto polycaprolactone (PCL). This study utilized LCS-1-loaded PCL-AC NPs to suppress CHEK2-deficient HCT116 CRC cells using the synthetic lethal interaction between SOD1 and CHEK2. PCL-AC nanoparticles were also examined in terms of their size, cellular absorption, and cell survival after the development of protein coronas. An LCS-1-loaded NPs were analyzed for their polydispersity index (PDI), zeta potential (ZP), and morphological properties by transmission electron microscopy (TEM), scanning electron microscopy, and atomic-force microscopy. Confocal imaging showed that nanoparticles were taken up by HCT116 cells, as demonstrated by the cellular internalization. It was also shown that NPs were cytocompatibility because they did not harm hTERT and HEK-293 cells. When compared to colon cancer cells expressing CHEK2, the LCS-1-loaded PCL-AC NPs were up to 240 times more selective in their ability to kill CHEK2-deficient cells. As a result, the protein corona-coated nanoparticles of PCL-AC NPs were shown to be incubated in human and fetal bovine serum by SDS-PAGE analysis. Hydrodynamic diameter increased slightly for PCL-AC nanoparticles coated with corona, and this was validated by TEM. There was also cell uptake and no harmful effects on hTERT cells when PCL-AC NPs were coated with a coronal layer. By developing a nano formulation of LCS-1, researchers hoped to increase its ability to kill colorectal cancer cells with CHEK2 lack (71).

Ionotropic gelation method

It is one of the simplest and most cost-effective methods for ionotropic gelation in the laboratory. Nanoparticles and microparticles made of polymeric materials are being used in the

hunt for novel and better treatments (Figure 3). There are numerous advantages to these formulations due to the inclusion of biocompatible and biodegradable polymers. As a result of the technique's simplicity and mildness, the complexation of chitosan (CS) nanoparticles with two oppositely charged macromolecules has garnered considerable interest. As a result, electrostatic cross-linking, rather than chemical cross-linking, has been used to minimise probable toxicity and other negative effects on the reagents. CS can interact electrostatically with polyanion tripolyphosphate (TPP). It was after the report of Bodmeier et al. that many researchers began to investigate the possible pharmacological use of the TPP-CS complex. It is possible to obtain the cation of CS by dissolving CS in an aqueous acidic solution in the ionic gelation technique. To make a polyanionic TPP solution, add this solution dropwise while stirring continuously. It is possible to cross-link chitosan nanoparticles by reacting with the negatively charged phosphoric ions of TPP because the chitosan molecules have an abundance of the NH_3 group. Cross-linking and hardening processes may aid to maintain drug release by evaporating water from the particles throughout this period. The solution, aggregation, and opalescent suspension all occurred in making the nanoparticles (72). There is an end in sight at this point. Insulin-loaded CS nanoparticles were made by first combining insulin with TPP solution and then adding this to CS solution while stirring constantly. Both CS hydrochloride salts, with molecular weights and deacetylation levels varied, were used to create nanoparticles. CS and TPP concentrations were changed so that the CS/TPP ratio was equal to 3.6:1. A positive surface charge of between +34 and +45 mV was found on the chitosan nanoparticles produced. As a result of this strategy, insulin loading was adjusted up to 55%. Due to the gelation of protonated amino groups of CS1, the method's effectiveness was contingent on the deacetylation of CS. For example, peptide and protein formulations are shown to improve oral bioavailability in a number of ongoing studies. With the addition of nanoparticles of bioadhesive polysaccharide CS, it appears that their intestinal absorption is enhanced (73). P53 polyplex-loaded enteric-coated calcium pectinate microbeads for

oral gene delivery were developed and tested by Bhatt et al. as a potent new treatment option for CRC. In CRC, mutations in the p53 gene are a primary event and an important target for gene therapy treatment. Colon cancer cell lines were transfected with polymethacrylates-based non-viral vectors to test its ability to complex, protect, and transfect p53. At varied N/P ratios, polyplexes were formed by the complexation of cationic polymer with anionic pDNA. Ionotropic gelation was used to create p53 polyplex-loaded calcium pectinate (CP) microbeads covered with Eudragit® S100. Enteric-coated CP microbeads were shown to protect the release of p53 polyplex in the upper GIT in *in vitro* release tests with less than 10% release. Polymethacrylate carriers have been shown to effectively transfect pDNA in both *in vitro* and *in vivo* investigations in rat cell lines. Results from an *in vivo* gene expression investigation demonstrated the potential of enteric-coated calcium pectinate microbeads to transfer pDNA to the colon of rats. As a result, calcium pectinate microbeads covered with enteric-coated calcium pectinate released p53 polyplex in the colon and may be an effective alternative to CRC therapy (74). Motawi et al. created Cromolyn chitosan nanoparticles (CCSNPs) using an ionic gelation process to enhance bioavailability and tested for their anticancer properties in a dimethylhydrazine-induced model of colorectal cancer in rats. To promote colon cancer in the rats, groups were separated into seven and given dimethylhydrazine for 16 weeks; group 1 was given a normal control, group 2 cromolyn control, and group 3 CCSNPs control. Protective therapies for groups 5–7 included cromolyn solution, non-medicated NPs, and CCSNPs. Dimethylhydrazine was found to be ineffective in reducing tumor-signaling molecules and the number of abnormal crypt foci in comparison to optimal CCSNPs (size 112.4 nm, charge 39.9 mV, encapsulated 93.6% cromolyn, displayed a sustained drug release pattern over 48 h) Cromolyn solution, on the other hand, was found to have a protective impact on colon cancer cells that was enhanced by CCSNPs' ability to improve tumor pathology. Finally, in colorectal cancer tissue, CCSNPs improved tumor pathology and malignant oncogenic signaling molecules. CCSNPs, on the other hand, may offer a novel method of protecting against colorectal cancer treatment.

Additionally, the anticancer properties of cromolyn were improved when it was encapsulated in chitosan nanoparticles (75).

Solvent evaporation method

The emulsion solvent evaporation technique is a method to develop NPs and nanocapsules that is well suited for uses that need high purity and low toxicity materials, including biomedicine or electronics. An organic solvent such as chloroform, acetone or ethyl acetate is used to dissolve premade polymers such as PLA or PLGA. An emulsion of an oil and water mixture is formed by dissolving the medication in a polymer solution, which is then transferred to an aqueous phase containing a surfactant such as polyvinyl alcohol (PVAL). It is possible to speed up the evaporation of organic solvents by extending the homogenization process (76). An ultracentrifuge collects the nanoparticles at the end of the homogenization stage. The Figure 4 depicts a schematic representation of this approach. Polymer-to-organic solvent ratio, type of organic solvent, and homogenization time and speed can all be manipulated to produce the desired particle size and other characteristics. The emulsion–solvent evaporation process has been mysteriously understudied for a long time. Basically, a polymer dissolves in an excellent solvent, which is emulsified into an aqueous solution that contains a surfactant. Nucleation of the polymer occurs on the water–solvent interface due to the sluggish evaporation of the polymer–solvent. The rate of evaporation is determined by the solubility of solvent in the continuous phase; hence temperature and the type of the solvent are critical factors. Gas chromatography or NMR spectroscopy can be used to monitor the evaporation process, which is normally completed within a few hours. Particle hardening is affected by evaporation, given that the solvent in the dispersed phase is largely evaporating from a saturated continuous phase and its diffusion rate into the dispersed phase is much faster than the evaporation kinetics of the solvent. Wang and Schwendeman found that the rate-limiting phase for solvent mass transport is dependent on the solvent's characteristics in an experiment, including dichloromethane, ethyl

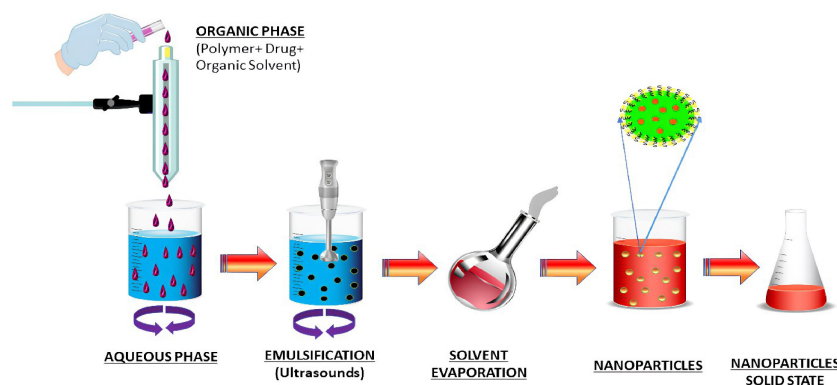


FIGURE 4

Schematic diagram of nanoparticles preparation by emulsification solvent evaporation method.

acetate, and acetonitrile as solvents. While ethyl acetate and acetonitrile were discovered to be gas-side limited, chloromethane was found to be liquid-side limited. Temperature and impeller diameter had the greatest impact on the pace at which water evaporated. Particle hardness profiles might be anticipated and determined without having to monitor the conc. of polymer in the solvent at any given moment, but rather by measuring the concentration of solvent and knowing its permeability coefficient at the liquid–air interface. The dispersions can be dialyzed to remove low molecular weight polymer and freeze-dried after the solvent has been evaporated (77). Docetaxel (Doc) and LL37 peptide polymeric nanoparticles (Doc+LL37 NPs) were coencapsulated in a thermosensitive hydrogel system by Fan et al. to create a biodegradable and injectable drug delivery system for the treatment of colorectal peritoneal cancer. Biodegradable Doc+LL37 NPs were first prepared via a solvent-evaporation approach including a water-in-oil-in-water double emulsion of PLA-Pluronic L35-PLA. This was followed by the preparation of a biodegradable and injectable thermosensitive PLA-L64-PLA hydrogel with reduced sol–gel transition temperatures near body temperatures. The Doc+LL37 NPs produced by the PLA-L35-PLA copolymer were found to be spherical using TEM. That Doc and LL37 were correctly packaged was verified using Fourier-transform infrared (FTIR). Doc was found to be encased in an amorphous X-ray diffraction pattern. HCT116 peritoneal carcinomatosis *in vivo* was greatly slowed down, and animals bearing the tumor had a longer survival time after receiving an intraperitoneal injection of Doc+LL37 NPs–hydrogel (78). The colon-specific DDS developed by Dang et al. was developed as matrix-type microspheres by solvent evaporation utilizing the ethyl cellulose (EC), cellulose acetate phthalate (CAP), and eudragit L 100-55. The drug concentration, particle size, bulk density, and angle of repose of microspheres were all measured. Drug conc. varied between 74.49% and 91.50% depending on the polymer and polymer ratio of the microcapsules, which ranged from 228 to 608 micrometer's. There was a good flow property of 1.2 g/ml mean bulk density, and a free-flow property of 40 angle of repose. Except for the microspheres containing CAP, and EC which had a rough and porous surface, all of the microspheres were spherical and nonporous. Eudragit L 100-55 microspheres combined with other polymers provided superior sustained release (78.9 and 76.6 percent after 8 hours for formulations F4 and F5, respectively) than the other microsphere formulations tested. A 1:2:1 ratio of diclofenac sodium, EC and CAP in microspheres shows the maximum drug content, good flow characteristics and surface shape, and promising drug release for colorectal cancer treatment using diclofenac sodium microspheres (79).

Salting out

Bindschaelder et al. patented the salting-out process in 1988, and it describes how to make a pseudo-latex (a colloidal dispersion) out of a water-insoluble polymer. A premade polymer dispersed in an aqueous media yields pseudo-latexes, which are colloidal systems with particles with an average size of less than one millimeter.

Pseudo-latexes can be made from a variety of polymers using the salting-out approach. In addition, low-toxicity solvents like acetone or ethanol can be used to synthesize drug-loaded PNPs, in contrast to other approaches. The first step in the salting-out process is the mechanical mixing of two phases to create an oil-in-water emulsion. The water-miscible solvent is used to dissolve a water-insoluble polymer and an active ingredient in the oil phase, while colloidal stabilizers and salting-out agents are used in the aqueous phase. Sodium bicarbonate, the salting-out agent in the water, blocks solvent diffusion. It's then diluted with enough clean water to drop the salting-out agent's concentration below a threshold, allowing the organic solvent to rapidly permeate into the water and causing interfacial turbulences and PNPs. Distillation at lower pressure removes the solvent from the PNP suspension. The salting-out agent is removed by ultracentrifugation and repeated washing processes and the leftover stabilizer. Cross-flow filtering can be used to remove the salting-out agent and the solvent (80). PNPs can be formed by salting-out in a manner similar to that postulated for the solvent displacement approach, despite the lack of research into the mechanism. An emulsion spreads violently when it is mixed with water because of the quick mutual miscibility of the solvents. Nanometric-sized solvent droplets are snatched off the interface. The surfactant ingredient quickly stabilizes these droplets, causing the polymer to aggregate into nanoparticles after complete solvent diffusion. The salting-out technique has a number of advantages over the solvent displacement method, including the ability to produce high-concentration and stable dispersions because of the inclusion of substantial amounts of polymer. When lipophilic medicines are utilized, high doses of medication can be integrated with good entrapment efficacy. Another advantage is that it may be easily scaled up to produce larger nanoparticles with the suitable selection of agitation settings (81). Allemann et al. developed aqueous polymeric nano dispersions by a reversible salting-out process. Surfactants and chlorinated solvents were avoided in the emulsion approach used to create the polymeric nanoparticles as aqueous dispersions. PVAL is a viscosity-enhancing agent and stabilizer that is added to an acetone solution of the polymer under continuous stirring in order to form the final product. A salting-out technique prevents acetone from combining with water in the saturated aqueous solution. Nanospheres are formed when water is added to an oil-in-water emulsion in a sufficient amount to allow for the complete diffusion of the acetone into the water phase. PVAL conc. And its type in the aqueous phase were also altered as well as stirring rate and internal/external phase ratio during the manufacturing process (82). Sengel et al. prepared nanoparticles by using salting-out and emulsion-evaporation steps. It was shown that PLGA and PVA molecular weight differences had an impact on the NPs' physicochemical qualities. Over the course of three months, meloxicam's stability in NPs was evaluated. Assays for cell uptake and viability were performed using the HT-29 cell line, which expresses COX-2. Size range was from 170–231 nm; the PDI was lower for NPs with a spherical form and a negative ZP. The physical stability of NPs produced with high molecular weight PLGA was demonstrated for three months at 4°C. When the polymer and the emulsifier increased in molecular weight, it also decreased meloxicam's *in vitro* release rate. It was found that

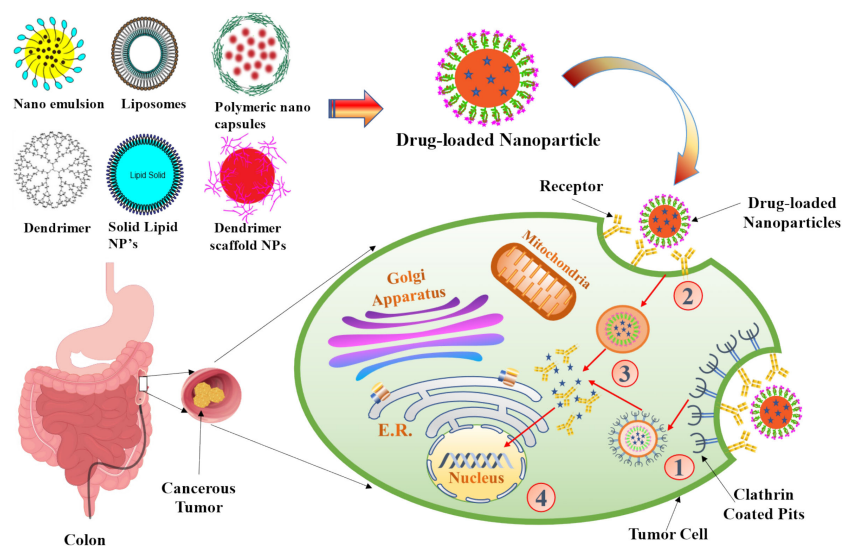


FIGURE 5

The scheme of endocytosis of the nanoparticle modified by antibodies that recognize cancer markers at the cell membrane. (1) Receptor (aptamer or antibody) on the drug-loaded nanoparticles recognize the clathrin-coated pits in the tumor cell and bind to it. (2) Phagocytosis of drug-loaded nanoparticles facilitates the transport of the carrier into the tumor cells. (3) An endocytic vesicle is formed. (4) Endosome induces the release of drug from the nanoparticles and penetrates into the nucleus. Representation of the different kinds of NPs included in this review is also shown.

meloxicam-loaded NPs were cytotoxic to HT-29 cells at 800 M. Coumarin-6-loaded NPs were highly absorbed by cancer cells. To treat colon cancer, the PLGA NPs created in this study could be an effective DDS for meloxicam (83).

Cellular mechanism of nanoparticles

Particles enter cells via the endocytosis route, that includes phagocytosis and pinocytosis, in biological systems (84). Nanoparticles with diameters of less than 200 nm are engulfed by micropinocytosis (Figure 5), which can take place in one of the following ways: with or without clathrin/caveolae (85). Phagocytosis/micropinocytosis takes in large particles. Both the pathways are distinct in their mechanisms and strictly regulated at the molecular level. The route that NPs take inside cells determines the intracellular nanoparticle transport its biological and therapeutics outcome (86). The interaction of NPs with the target cells can be essential or destructive to the organism as a whole, depending on the intended outcome as required for the particular application. NPs interact with serum and extracellular matrix (ECM) proteins as they enter the human, creating a “protein corona” surrounding them (87). Some of the NPs are recirculated back into the extracellular space via the clathrin-mediated mechanism (88). The cellular uptake of NPs (20–100 nm) is mediated by caveolin pathway, whereas the cellular uptake of submicron particles (100–350 nm) is mostly mediated by the clathrin-mediated pathway (89). Based on studies indicated, the co-localization of caveolin-1 proteins over internalised NPs discovered in the caveolae and caveosomes suggested that nanoparticle uptake could occur by caveolae-mediated endocytosis (90, 91). When chemotherapeutic drugs are delivered in nanoparticle form, their fate in the bloodstream is determined by their

physicochemical qualities, as well as the elemental compositions of those nanoparticles (92). Kou et al. have revealed a number of different mechanisms by which nanoparticles can be absorbed into cells. Nanoparticles should be made from non-toxic or biocompatible materials to avoid hazardous effects, in addition to their physicochemical features (93). Several caveolin and clathrin-independent endocytosis pathways, such as Arf-6, Rho-A (or IL2Rb-dependent pathway), flotillin, or CDC42 (CLIC/GEEC)-dependent endocytosis, exist in addition to the mechanisms mentioned above; however, the present review will not go into further detail on these pathways because they do not significantly contribute to cellular NP uptake.

Role of nanomedicine in targeted delivery for treatment of CRC

In the case of CRC, targeted therapy for nanoparticles has significantly improved the overall survival in patients with the condition. The development of checkpoint inhibitors is accelerating at an unparalleled rate due to the increasing efficacy of therapies like the anti-EGFR (epidermal growth factor receptor) agent (cetuximab) and the anti-angiogenesis agent (bevacizumab), which target multiple immunological pathways (58). Targeted delivery, which can be attained by passive or active targeting, which tries to precisely target specific cancer cells. Passive targeting uses the enhanced permeability and retention (EPR) effect, whereas active targeting involves conjugating small molecules, aptamers, peptides, and antibodies. Targeted drug delivery, as compared to free drug, aids in lowering the toxicity in normal cells, protecting drugs from deterioration, prolonging half-life, increasing loading capacity, and enhancing solubility (94, 95).

TABLE 2 Examples of different types of nanoparticle targeting ligands and their receptors along with its active agents.

Nanoparticulate Drug Delivery System	Drug (Active Agent)	Ligand	Receptor	Size Range (nm)	Sources
PEGylated hollow mesoporous ruthenium nanoparticles	[Ru(bpy) ₂ (tip)] ²⁺ , RBT	SS-Fc	Carcinoembryonic antigen	110	(93)
Hyaluronic Acid–Doxorubicin nanoparticles	Doxorubicin	Hyaluronic acid	RHAMM, CD44	175	(58)
Cyclodextrin-based host–guest complexes	Regorafenib	Mannose	Mannose receptor	100	(94)
Cationic liposomes	ESC8, anti-Hsp90 plasmid	Dexamethasone	Glucocorticoid receptor	251	(95)
Polymersomes	Doxorubicin	Transferrin	Transferrin receptor	72	(96)
Self-assembled nanoparticle	Bortezomib	Folate	Folate Receptor	196	(97)
PLGA nanoparticles	5-Fluorouracil	Wheat germ agglutinin	N-acetyl-D-glucosamine, sialic acid	156	(98)
Nanoscale metal organic framework	Talazoparib, temozolomide	Fucoidan	P-selectin	84	(99)
PAMAM dendrimers	Celastrol	EpCAM aptamer	Epithelial cell adhesion molecule	300	(91)
Human serum albumin nanoparticles	5-Fluorouracil	LRP-1 targeting peptide	Lipoprotein receptor-related protein-1	208	(100)
Lipidic core nanocapsules	Thymoquinone	Anisamide	Sigma receptors	217	(101)
Mesenchymal-stem-cell -derived exosomes	Doxorubicin	MUC1 aptamer	MUC1	50	(102)
Silica nanoparticles coated with chitosan	AntimiR-21, Doxoubicin	AS1411 aptamer	Nucleolin	87	(103)
Nanoparticles	Paclitaxel, chlorin e6	Tumor-homing peptide tLyp-1	NRP-1	107	(104)
PLGA and PEG-based polymeric nanoparticles	5-Fluorouracil	Anti-EGFR mAb	Epidermal Growth Factor Receptor	252	(92)

We included examples of published *in vitro* and/or *in vivo* nanoparticle targeting ligands and their receptors for nanomedicine applications in Table 2.

mediated by EPR is extremely heterogeneous. In order to improve the targeting capability of NPs based on EPR, it should be combined with different targeting mechanisms (103).

Passive targeting nanoparticles

The term “passive targeting” refers to nanoparticles that lack specific surface targeting ligands (96–98). Because the malignant tumor lacks functional lymphatic vessels and has a wide gap between tumor endothelial cells. The effect that makes NPs accumulate in the malignant cells is called as EPR (99, 100). In the research study, resveratrol and oxaliplatin were encapsulated into N, O-carboxymethyl chitosan NPs using emulsification crosslinking and ionic crosslinking, respectively. In comparison to the free drug, the NPs improved the solubility, stability, and EPR effect of resveratrol and oxaliplatin, leading to higher anti-CRC action in SC tumor-bearing rats (101).

The non-specific nature of the interactions between NPs and cells is indicated by passive targeting and the absorption of nanoparticles in both healthy and diseases state may be facilitated by these non-specific interactions (102). In recent years, researchers have gradually come to understand how the tumor-targeting

Active targeting nanoparticles

In active targeting, the surface of nanoparticles is modified with the targeting ligands to enable specific interaction along with the binding of these nanocarriers to cell (103). Cancer cells produce macromolecules and overexpress certain receptor types, which promote the proliferation cancer cells and its surrounding tissues through autocrine or paracrine pathways (104). In recent times, the active targeting of nanoparticulate targeted DDS for CRC has primarily utilized the receptor-ligand binding strategy, which involved many highly expressed receptors in CRC, including the EGFR, mannose receptor, CD44, epithelial cell adhesion molecule (EpCAM), nucleolin, v3 integrin receptor, folate receptor, carcinoembryonic antigen, hyaluronic acid receptor, glucocorticoid receptor, lipoprotein receptor-related protein etc (103). Ge et al. developed biological conjugates loaded with celastrol that could be captured by CRC overexpressed with EpCAM in order to decrease drug toxicity and enhance

therapeutic efficacy. The conjugates were composed of dendrimers, PEG, and the EpCAM aptamer. The findings demonstrated that when exposed to biological conjugates, SW620 will experience significant apoptosis. Moreover, the biological combination demonstrated reduced toxicity in xenograft mouse and zebrafish models (105). Another example was to deliver anti-EGFR receptor-5-fluorouracil (5-FU) in which Sankha Bhattacharya developed PLGA-PEG-coated NPs, which could enhance the pharmacodynamics and distribution of the drug *in vivo*. Through the RES, the polymeric NPs composed of PLGA and PEG can inhibit opsonic action. These nanoparticles have significant therapeutic significance due to their quick and easy production processes of solvent emulsification and evaporation (106).

Integrating cell surface receptor-specific targeting ligands to nanoparticle surfaces may improve cellular interactions. Besides specifically targeting cancer cells, active targeting approaches can also exploit the distinctive characteristics of the tumor microenvironment. One approach involves exploiting the hypoxic microenvironment within tumours for targeted therapy. Hypoxia-activated prodrugs have been developed to release cytotoxic agents specifically in response to the low oxygen levels in tumor tissues (107). Cetuximab, when combined with chemotherapy, has demonstrated improved outcomes in patients with metastatic colorectal cancer. It's worth noting that other targeted therapies, such as anti-VEGF agents (bevacizumab) and immune checkpoint inhibitors (pembrolizumab), are also being studied for colorectal cancer and utilize active targeting strategies to engage specific molecular targets in the tumor microenvironment (107).

However, precise targeting of cell populations *in vitro* and *in vivo* necessitate that the surface modifications of NPs can maintain its integrated design function. As a result of these findings, scientists now have the chance to develop nanoparticle surface patterns that can address the challenge to improve the interactions and its specific delivery between targeted cells and nanoparticles (86).

Role of nanotherapeutic in the management of CRC

One of the three most frequent malignancies in the world, colorectal cancer is typically diagnosed in the middle or late stages, and the affected population is getting younger. Intensive chemotherapy is required, especially in individuals with late-stage CRC, although it might have undesirable side effects and unpleasant reactions because of drug resistance and damage to normal cells. Various types of nanoparticles have been explored for their potential in combating drug resistance in colorectal cancer. For example, polymeric NPs like PLGA NPs have been utilized to encapsulate conventional chemotherapy drugs such as 5-FU and oxaliplatin. These nanoparticles enhance drug stability, prolong drug release, and increase drug accumulation within cancer cells, thereby overcoming mechanisms of drug resistance (108, 109). Additionally, nanoparticles have the ability to deliver innovative therapeutic agents to address drug resistance. One approach

involves loading small interfering RNA (siRNA) into nanoparticles to silence specific genes associated with drug resistance pathways. By silencing these genes, nanoparticles can sensitize cancer cells to chemotherapy and enhance their therapeutic response (110). Additionally, nanoparticles could be designed for combination therapy targeting multiple pathways involved in the immune system. For example, nanoparticles can simultaneously deliver therapeutic drugs and drug efflux pump inhibitors such as P-glycoprotein (P-gp). By inhibiting drug efflux mechanisms, nanoparticles improve intracellular antibody accumulation and overcome drug resistance (111). In conclusion, nanoparticles show the potential to resolve resistance to colon cancer by improving drug, improving drug stability and targeting cancer. Improved bioavailability and reduced adverse effects can be greatly attributed to research on targeted drug delivery, which enables the treatment of cancer without harming healthy cells (112). Small molecule medications can be carried and accumulated in tumor tissue using nanocarriers, a type of nanosystem. Nanocarriers are superior to free medications because of their excellent efficacy and low incidence of side effects. Protect the medication against degradation, limit renal clearance, boost half-life and bioavailability, and slow drug release rate with nanocarriers in addition (113). In this section, we emphasized that chemotherapeutics, targeted medicines, and natural medications are all influencing the creation of nano preparation for the treatment of CRC (Table 3).

Liposomes

A lipid vesicle with a membrane made of amphiphilic phospholipids is called a liposome, and it contains an aqueous volume. All of these compounds are made up of neutral phospholipids like lecithin or cholesterol as well as positively- or negatively-charged ones. Inert, biodegradable and biocompatible liposomes made of phospholipid molecules, which make up most of the membranes in living organisms, are produced by the RES. For the majority of phospholipids, self-assembly in water results in the formation of two or more bilayers or multilayer vesicles with an average bilayer thickness of roughly 5 nm. Liposomes can load medicinal substances selectively by encapsulating hydrophilic drugs in the aqueous core and hydrophobic drugs in the lipid bilayer throughout this process. Oral, intravenous, and rectal administration of liposomes for the treatment of CRC have all been documented in the literature. Panitumumab and cetuximab are two monoclonal antibodies that specifically target ERBB1 (EGF receptor) signaling, which plays a crucial role in the progression and development of colorectal cancer (114). Blood arteries in the vicinity of tumours are the primary target for passive targeting liposomes. Endothelial cell gaps can range from 100 to 780 nm in different cancer types, whereas in normal endothelial cells, the gap is only 5 to 10 nm wide. As a result, liposomes of a size that is acceptable in this context can extravasate into cancerous tissues. Antigens, antibodies and enzymes can all be conjugated to the surface of liposomes in order to boost their potential to target cancer cells more effectively. Proteins overexpressed in tumor cells, such as folate receptors and

TABLE 3 Detailed description of nano-vesicular based delivery system for the management of colorectal cancer.

Author (s)	Delivery system (s)	Preparative method	Drug (s)	Therapeutic Intervention	References
Bansal et al; 2016	Liposomes	Cast film method	Oxaliplatin	Folic Acid conjugated liposomes encapsulating Oxaliplatin were entrapped in alginate beads and subsequently coated with Eudragit-S-100 for efficient delivery to colon cancers. The study indicated that Eudragit coated alginate beads got into the colon of Balb/c mice between 4.20 and 4.50 h after oral administration. <i>In vivo</i> findings demonstrated that folic acid associated liposomes encapsulated in alginate beads supplied 2.82 ± 0.58 and 21.52 ± 2.76 μg L-OHP/g tissues in the colon and tumour after 12 h, showing its targeting capacity to colon and tumour.	(107)
Yang et al; 2011	Liposomes	Reverse-phase evaporation method	Oxaliplatin	An investigation was conducted on the efficacy of PEG-Oxaliplatin long circulating liposomes, to increase the therapeutic index of colorectal cancer. PEG-liposomes were able to form a stable bond with cells after only 2 hours, and the mean fluorescence intensity increased when the induction period was lengthened. Comparatively, 23.21 percent \pm 3.38 percent, respectively, of the cells were apoptotic in the presence of PEG-oxaliplatin liposomes (P-ox-L) and free oxaliplatin liposomes (ox-L). Using <i>In-Vivo</i> Imaging, fluorescence imaging showed that PEG-liposomes specifically targeted tumour tissue. Compared to free (ox-L), (P-ox-L) PEG-liposomal L-OHP reduced tumour volume by 26.08 percent \pm 12.43 percent and increased life span by 45.36 percent, respectively, after intravenous injections.	(108)
Soo et al; 2015	Liposomes	Extrusion technique		Polymeric nanoparticles and liposomes have demonstrated limited success in encapsulating resveratrol. Liposomes were used in this study to co-encapsulate both the lipophilic and hydrophilic components of the medicine by adopting a novel dual carrier strategy to build and optimise a novel drug carrier. The final formulation had a particle size of 131 nm, a polydispersity index of 0.089 nm, and a zeta potential of -2.64 mV. Nanoformulations released 100 percent of the medication in 24 hours, compared to a drug release profile of 40-60% for free resveratrol and standard liposomal formulations. It remained steady at 4°C for 14 days. Resveratrol was found to have an increased cytotoxicity profile when it was incorporated into liposomes rather than free resveratrol. The findings of the study shows that liposomal formulations containing pristine resveratrol and its cyclodextrin complex are a viable approach for improving hydrophobic chemotherapeutic drug distribution.	(109)
Chaurasia et al; 2015	Polymeric nanoparticles	Emulsification-diffusion-evaporation method	Curcumin	Curcumin bioavailability and anti-cancer activity <i>in vitro</i> and <i>in vivo</i> have been improved by the development of a novel polymeric nanoparticle. In terms of particle size and entrapment efficiency, curcumin encapsulated nanoparticles (CENPs) were found to be satisfactory. Compared to pure CUR, <i>in vitro</i> cytotoxicity experiments using 50% cell growth inhibition values showed a 19-fold reduction when CENPs were used. Oral administration of CUR as CENPs increased its oral bioavailability by 91- and 95-folds, respectively, compared to oral administration of pure CUR.	(110)
Tummala et al; 2015	Polymeric nanoparticles	Solvent evaporation emulsification method	5-Fluorouracil	The primary goal was to synthesise chitosan polymeric nanoparticles. Simulated GIT tract fluids were used for <i>in vitro</i> drug release investigations, with pH values ranging from 1.25 to 7.0. 5-FU nanoparticles with a drug:polymer ratio of 1:2 and 1:3 have shown improved particle size (149 nm and 138 nm respectively) and entrapment efficiency (48.12 ± 0.08 percent and 69.18 ± 1.89 respectively). Drug release from 5-FU after four hours is superior to that from non-enteric coated tablets, which released more than half of their medication before it reached the colon. Nanoparticles generated by this process employing a polymer with an optimum ratio can be used as a potential drug delivery mechanism for the effective delivery of the active pharmaceutical ingredient to colorectal cancers.	(111)
Yakati et al; 2022	Polymeric nanoparticles	Emulsion-solvent evaporation method	Paclitaxel	Polymeric nanoparticle delivery systems that target both cancer cells and endothelial cells should be developed, using CPKSNGVC (CPK in short) as a nanoparticle surface-bound targeting ligand for cancer cells. Nanoparticles with a diameter of 215 ± 4 nm, a zeta potential of 12 ± 3 mV, and a concentration of 16–17.5 percent w/w paclitaxel (PTX) were manufactured. Using maleimide-thiol chemistry, CPK peptide was then attached to the surface of nanoparticles (CPK-PTX-NPs). MCT1 receptor-overexpressing colorectal cancer (CRC) cells displayed MCT1 receptor-mediated cellular uptake and apoptosis-mediated cell death in CPK-PTX-NPs, but the other nontargeting nanoparticles failed to show MCT1 receptor-mediated cellular uptake. CPK-PTX-NPs were able to decrease angiogenesis in a chick embryo angiogenesis assay by targeting the specific CPK-PTX molecule. PTX-encapsulated and CPK-decorated polymeric nanoparticles, which are selective for the MCT1 receptor and encapsulated and decorated with	(112)

(Continued)

TABLE 3 Continued

Author (s)	Delivery system (s)	Preparative method	Drug (s)	Therapeutic Intervention	References
				peptides unique to the CRC, are effective carriers for antineoplastic drug delivery that result in dramatically improved therapeutic efficacy.	
Smith et al; 2020	Solid lipid nanoparticles	Hot and cold homogenization technique	5-Fluorouracil	It was possible to create the SLN-loaded 5-FU through the use of a SMART (Strategic and Unique Method to Advance and Refine the Treatment) for CRC. PEGylated lipids and a mix of surfactants were used to create the SLN. Cytotoxicity, clonogenic assays, flow cytometry, and confocal microscopy were used to investigate the cellular uptake and efficacy of 5FU-SLN in HCT-116 cancer cells. Drug effectiveness investigations on mice with subcutaneous HCT-116 cancer yielded pharmacokinetic (PK) and receptor expression data. 5FU-SLN was the most effective formulation with particle size of 263 ± 3 nm, zeta potential of 0.1 ± 0.02 and entrapment effectiveness of 81 ± 10 percent. -Fu-IC50 SLN value was lower than that of 5-FU (17.7 ± 0.03 μ M) by 2.3 times, according to the results of this study. Compared to 5-FU, 5FU-SLN considerably reduced tumour growth, and the area under the plasma concentration-time curve (AUC) of 5FU-SLN was 3.6 times greater than that of 5-FU. Comparing 5-FU-SLN treated animals to 5FU-treated mice, HER2 receptor expression was significantly reduced, but liver and kidney tissues revealed minimal damage at a dose of 20 mg/kg. When compared to 5-FU, 5FU-SLN was highly cytotoxic to HCT-116 cells and greatly reduced tumour growth in mice in the subcutaneous region. An efficient delivery system for anticancer medicines is therefore critical, as evidenced by this finding.	(113)
Serini et al; 2018	Solid lipid nanoparticles	Microemulsion technique	Resveratrol	Resveratrol esterified to stearic acid was used as a lipid matrix for the encapsulation of omega-3 PUFA in the form of solid lipid nanoparticles (SLN). Increase the efficiency of fatty acid incorporation into cells and prevent peroxidation/ degradation of these fats was our goal. The antioxidant activity of SLN derived from resveratrol was studied and defined. An increase in the amount of omega-3 PUFAs incorporated into human HT-29 CRC cells and the growth inhibitory effects they had on these cancer cells were seen when the SLN was filled with the fats.	(114)
Kamel et al; 2017	Solid lipid nanoparticles	Ultrasonication method	5-Fluorouracil + (Cinnamon/oregano)	In order to achieve a particle size of 254.77nm, a polydispersity index of 0.28, a zeta potential of +15.26, and an entrapment efficiency percent of 77.3 percent for cinnamon and 69.1 percent for oregano, the experimental model developed suggested an optimal formulation with 2% lipid and 2.3 percent surfactant and 0.4 percent chitosan as the key ingredients. Unencapsulated/encapsulated cinnamon and oregano extracts with or without 5-Fluorouracil were tested for cytotoxic activities on HCT-116 cells in phase three. To reduce side effects and allow for continued treatment, this study demonstrated the effectiveness of the 5-Fluorouracil combination proposed for treating human colon cancer at low doses.	(115)
Safwat et al; 2016	Gold nanoparticles	Citrate reduction method	5-Fluorouracil	Thioglycolic acid (TGA) and glutathione (GSH) were used to load 5-FU onto gold nanoparticles in order to increase their anticancer activity while reducing their negative effects. Researchers synthesized and evaluated GNPs in different molar ratios of 5-FU/ligand. Colorectal cancer tissue was examined using flow cytometry to determine the anticancer activity of 5-FU/GSH-GNPs. The GNPs were spherical and ranged in diameter from 9 to 17 nm. GNP stability and drug release were studied as a function of salt concentration and solution pH. For both TGA-GNPs and GSH-GNPs, maximal 5-FU loading could be achieved at molar ratios of 1:1 and 2:1. GNPs with a pluronic F127 coating was more resistant to salt. The 5-FU released from GNPs was discovered to be pH-dependent and progressive. In colorectal cancer cells, 5-FU/GSH-GNPs induced apoptosis and halted cell cycle progression. They have a two-fold stronger anticancer effect compared to free 5-FU. These data show that 5-FU's anticancer efficacy can be enhanced by GNPs.	(116)

transferrin receptors, can be targeted by these compounds with a high degree of specificity (EGFRs). Affinity interaction occurs when targeted liposomes arrive at cancer areas, allowing them to aggregate around tumor tissues (115). Shen et al. construct a bifunctional liposome by self-assembly of oxaliplatin-prodrug (Oxa (IV)) conjugated phospholipid and alkylated NLG919 (aNLG), an IDO1 inhibitor, together with other commercial lipids. An NLG919-mediated inhibition of IDO1 in the NLG/Oxa (IV), liposomes can effectively prevent the depletion of tryptophan to immunosuppressive kynurenine in cancer cells, as well as release the cytotoxic oxaliplatin into the cytosol to induce immunogenic cell death (ICD). aNLG/Oxa

(IV)-Lip, on the other hand, has been shown to have a extensive blood circulation period, allowing for highly efficient passive tumor homing. Anti-tumor efficacy of such aNLG/Oxa(IV)-Lip is enhanced in both SC and orthotopic CT26 tumours due to significantly primed anti-tumor immunity of enhanced intratumoral CD8+ T cell, cytotoxic cytokines and downregulation of immunosuppressive regulatory T cells, which are present in both tumor types. There's a lot of potential for future clinical use of this bifunctional NLG/OXA (IV)-Lip due to its good biocompatibility and strong therapeutic performance (116). Alomrani et al. prepared chitosan-coated flexible liposomes (chitosomes) containing 5-FU were developed

and characterized to use as a novel approach to target CRC cells. Using film hydration and electrostatic deposition, 5-FU-loaded flexible liposomes, as well as 5-FU-loaded chitosomes, were created. A positive surface charge ranged from 6.1 mV to 14.7 mV for chitosomes, while a negative surface charge ranged from 2.3 mV to 16.3 mV for liposomes, according to the results. Compared to 5-FU solution and liposomes, chitosomes inhibit 5-FU release an *in vitro* drug release investigation. Cytotoxicity tests on the CRC cell line HT-29 revealed that 5-FU-loaded chitosomes outperformed liposomes and the 5-FU solution in killing cancer cells over the long term. It was thus possible to successfully produce chitosomes that carry 5-FU as a nanocarrier in order to potentially harm cells of colorectal cancer (117).

Polymeric nanoparticles

Due to various characteristics, including size, surface property, and shape, the mononuclear phagocytic system (MPS) quickly opsonizes and clears standard nanoparticle formulations in circulation. These factors are mostly governed by polymer property. Recent research into the effects of polymeric nanoparticle characteristics has proven great therapeutic usefulness in the delivery of medical medicines and bioactive substances (118). EPR effect is a mechanism by which polymeric nanoparticles travel through leaky blood arteries and preferentially aggregate at tumor sites because of their small size and stealth qualities (often between 10nm and 200nm). It is possible to use natural or synthetic polymers in the manufacture of these nanoparticles. Improved medication bioavailability, control of drug release, longer circulation time and reduced non-specific toxicity can be achieved by using polymeric nanoparticles in the medical industry. By boosting the intracellular penetration of medicines into tumor cells, polymeric NPs' targeting functionality for both active and passive allows them to selectively target certain tissue regions. A regulated and targeted DDS for CRC therapy can take advantage of the biodegradable polymer nanoparticle's great capabilities (119).

Udompormmongkol et al. developed Curcumin-loaded polymeric NPs for enhanced anti-CRC applications. Curcumin was incorporated into polymeric NPs for increased anti-CRC. Chitosan and gum arabic, two naturally occurring polysaccharides, were used in the emulsification solvent diffusion process to create nanoparticles. Curcumin was found to be encapsulated in carriers with a +48 mV ZP, 136 nm size, and excellent encapsulation efficacy, according to the findings (95 percent). They rectified in their research work that curcumin NPs could withstand hydrolysis by gastric juice or tiny intestinal enzymes, and consequently, it should reach the colon substantially intact, based on an *in vitro* release study. Due to their enhanced cellular absorption, curcumin nanoparticles demonstrated stronger anti-CRC effects than free curcumin. It was so determined that curcumin was successfully encapsulated with superior anti-CRC action in chitosan-gum arabic NPs (120). Badran et al. investigated the activity of 5-FU loaded chitosan coated PLGA NPs (C-5-FU PLGA NPs) and PCL. To deliver cancer treatment, (C-5-FU PCL NPs) were used as

carriers. The synthesized NPs had a PDI of 0.30 and had a spherical shape with a particle size range of 188.1–302.2 nm. ZP changed from a negative to a positive value when nanoparticles were coated with chitosan. 5-FU's entrapment efficiency was found in the range from 32% to 51%. Initially, 5-FU was released rapidly *in vitro*, followed by a steady release profile. CRC cells (HT-29) were significantly inhibited *in vitro* by the C-5-FU PLGA NPs compared to other NPs and medication solution. These findings demonstrate that C-5-FU PLGA NPs are a promising cancer therapeutic delivery vehicle (121). Bhattacharya. S develop chitosan based polymeric NPs of Imatinib (IMT-PNPs) for CRC targeting. Ionic gelation and central composite design were used to make IMT-PNPs. There were 21 batches in which the F10 formulation has been optimized. Approximately, 208 ± 0.01 nm particle size was identified in the improved formulations, as well as a ZP of -32.56 ± 0.03 mV, an in-vitro cumulative drug release of $86.45 \pm 0.05\%$, and a drug entrapment efficacy of $68.52 \pm 0.01\%$. After intravenous delivery of fluorescent nanoparticles, epithelial colon cells display a greater concentration of fluorescent nanoparticles. Because just 0.46 percent of IMT-PNPs formulations had hemolysis as a result of intravenous administration, the formulation is considered safe. Histopathological study of the final formulations found no evidence of tissue injury, indicating that the I.V. mode of administration of the final formulation is safe. The MTT assay shows that entrapped IMT-PNPs cause greater cytotoxicity in CT26 CRC cell lines and it's this cytotoxicity is better regulated. IMT-PNPs may be a viable method for targeting colorectal cancer utilizing the intravenous route, according to the findings of this study (122).

Solid lipid nanoparticles

Solid lipid nanoparticles (SLNs) or lipospheres are a promising class of pharmaceutical nanocarriers for regulated drug delivery. Biodegradable and non-toxic lipidic components typically make up SLNs. In addition to being able to transport a range of treatments, SLNs may also carry genetic material (DNA/siRNA), vaccination antigens, and other biomacromolecules. Aqueous colloidal dispersions of solid biodegradable lipids provide the matrix of SLN. Colloid-based carriers, such as the SLN, combine the advantages and prevents the disadvantages of numerous colloidal carriers of its type, such as physical stability, protection from degradation of included labile medicines and regulated release, great tolerability. SLN formulations have been produced and comprehensively studied *in vitro* and *in vivo* for a variety of administration routes (parenteral, oral, cutaneous, ophthalmic, pulmonar, and rectal). To ensure the SLNs' quality, they must be properly and adequately characterized. Because of the small size of the particles and the dynamic nature of the delivery mechanism, characterizing SLN is extremely difficult (123). Particle size, ZP, lipid modification (polymorphism), degree of crystallinity, and coexistence of additional colloidal structures (miscelles, liposome, super cooled melts, drug nanoparticles), time scale of distribution processes, *in vitro* drug release, surface morphology, and drug content are some of the important parameters evaluated for the SLNs. They may load both hydrophilic and lipophilic medicines, which makes them unique among tiny drug molecules. From

popular and convenient modes of administration, such as oral and intravenous administration, the latter ones are quite difficult to provide. SLNs have a lovely interior core structure that can accommodate lipophilic compounds. Being small, these particles have advantages in terms of the biopharmaceutical features of nanoparticle trafficking *in vivo*, followed by drug administration and controlled release at the target site of action. Depending on how they are prepared, they are colloidal in size and can be loaded with hydrophilic and lipophilic medicines. The heated microemulsions from which SLN are made have a versatile component that can be tailored to the kind of medicine and the mode of administration (124). Rajpoot et al. develop and optimize oxaliplatin (OP) loaded SLNs. These SLNs comprise Tween 80, DSPE, Lipoid S75, tristearin, and 1,2-distearoyl-sn-glycero-3-phosphoethanolamine (DSPE). Folic acid (FA) conjugation was made possible by the use of an enhanced SLN formulation developed using the Box–Behnken design. Particle size, ZP, entrapment efficiency (EE), and the shape of the formulations were assessed for several physiological characteristics, such as XRD and DSC. OPSLNs and OPSLNFs with FA-coupled SLNs (OPSLNFs) loaded with OP showed good EE of 49.2 ± 0.38 percent and 43.5 ± 0.59 percent, respectively, and small PS of 146.2 ± 4.4 nm and 158.8 ± 5.6 nm. Results from XRD patterns and DSC analysis showed that OP was evenly distributed in SLNs in an amorphous state. Up to a six-day sustained drug release of OPSLNs and OPSLNFs formulation was demonstrated in an *in vitro* drug release investigation. As compared to OPSLNs and OP solution, OPSLNFs had the strongest anticancer activity on the cell line HT-29. The results of this study show that HT-29 cells are more sensitive to the medication encased in OPSLNFs than OPSLNs and OP solution. As a result, this unique technique may hold promise for the treatment of CRC (125). Senthil et al. evaluated the effectiveness of chitosan-coated-trans-resveratrol (RSV) and ferulic acid (FER) loaded SLNs that conjugated with folic acid (FA) (C-RSV-FER-FA-SLNs) in CRC targeting in relevant models (*in vitro*). A co-encapsulation approach of the stearic acid is used to perform the conjugation of the FAs. Even under acidic conditions, these SLNs show greater durability, demonstrating their potential for use as DDS. Physicochemical evaluations, such as FTIR, XRD, ¹HNMR and particle size, ZP and drug release, are also carried out on the optimised formulations. When compared to free RSV-FER, the C-RSV-FER-FA-SLNs efficiently involved and elevated cytotoxicity in cancer cells that resulted in apoptosis, as demonstrated by fluorescence labelling, flow cytometry and western blot analysis. Therefore, it is suggested that this C-RSV-FER-FA-SLNs may be a suitable candidate for new nanodrug formulations in cancer therapy due to its good stability under acidic circumstances (126).

Gold nanoparticles

When it comes to the ability of AuNPs to serve as an optimum drug carrier and overcome biological obstacles like macrophage clearance, their physicochemical qualities, such as their size, shape, and surface features, are critical. The interaction between membrane receptors and NPs is one of the most essential features

that governs the pace of cellular uptake (endocytosis) and hence enhances the accumulation of drug-loaded NPs at the tumor site. In order to avoid early clearance by the MPS organs, the nanoparticle size is crucial. The rate of cellular absorption and accumulation of AuNPs has been described in a number of prior investigations for different AuNP sizes. Tunability of AuNP size during chemical production might thereby enhance efficient delivery of therapeutic agents to selected cells. In addition to traditional methods, scientists are exploring new ways to produce gold NPs, called green synthesis. These systems are known for their safety, environmental friendliness and cost-effectiveness (127, 128). This process is considered non-toxic, environmentally friendly and cost-effective. Green synthesis involves the production of NPs internally and externally using sunlight, electricity and organisms such as fungi, algae and bacteria (129). This technique allows for the production of various types of gold NPs, including nanospheres, nanorods, and nanostars. Lee et al. demonstrated in 2020 that the synthesis of gold NPs heavily relies on green materials such as enzymes, bacteria, plants, and fungi. These advancements in green synthesis offer promising alternatives for the production of gold NPs (130). In a study by Rani et al., the therapeutic effects of biogenic gold nanoparticles derived from *Abutilon indicum* (AIAuNPs) were investigated in Wistar rats with 1, 2-dimethyl hydrazine (DMH)-induced CRC. The results showed a positive localization of AIAuNPs in colon tumors as assessed by ICP-OES, indicating their bioavailability. Compared with standard paclitaxel, treatment with AIAuNPs increased the level of cellular antioxidant enzymes such as catalase, SOD, GSH, GPx and decreased lipid peroxidation (LPO). In addition, AIAuNPs significantly reduce inflammatory factors (β -catenin and Tcf-4) involved in the Wnt pathway in CRC, while maintaining the expression of apoptotic caspase-9, -8 and -3 and lamin. These findings suggest that AIAuNPs have potential as therapeutic agents for CRC (131).

When nanoparticles interact with lipid bilayer cell membranes, their chemical capabilities, not their size or structure, play a major role. The surface modification of AuNPs is an essential factor in determining their usefulness in drug delivery systems. Oxidative stress and inflammation can result from the overproduction of reactive oxygen species (ROS) in the cells, and MNPs are implicated in both processes (132). ROS has been found to be the primary cause of damage to intracellular compartments such as proteins, DNA, and the cell membrane. An array of intracellular responses, including plasma membrane instability, interference with the antioxidant defense system, and cell cycle arrest, as well as genomic damage and interactions with cytoskeleton, proteins and lipids may contribute to cell death. They can harm proteins by binding with their thiol groups, which are linked to oxidation. The cytotoxicity of bio-mediated produced AuNPs was examined in a study on colorectal cancer cells HT-29 and Caco-2. When tested on HT-29 cells, the biogenic AuNPs demonstrated considerable toxicity, but no toxicity on Caco-2 cells. The analysis for apoptotic activity revealed that HT-29 cells had a 13-fold higher percentage of cells in late apoptosis/necrosis than Caco-2 cells, but the percentage of cells in early apoptosis was nearly identical in both cell lines (133). Using two thiol-containing ligands, thioglycolic acid (TGA) and

glutathione (GSH), Safwat et al. produced gold NPs to increase 5-FU anticancer activity and reduce its adverse effects. The GNPs were synthesized at various 5-FU/ligand molar ratios and tested utilizing various methods. Flow cytometry was used to examine the anticancer effectiveness of 5-FU/GSH-GNPs in colorectal cancer tissue. The GNPs had a diameter of between 9 and 17 nm and were spherical in form. The effects of salt content and solution pH on GNP stability and drug release were investigated. TGA-GNPs and GSH-GNPs were able to achieve maximum 5-FU loading at a 5-FU/ligand molar ratio of 1:1 and 2:1, respectively. The Pluronic F127 coating on GNPs increased their resistance to salt. A gradual and pH-dependent release of 5-FU from GNPs was observed. 5-FU/GSH-GNPs promoted apoptosis in colorectal cancer cells and halted cell cycle development. Compared to free 5-FU, they demonstrated a two-fold greater anticancer impact. These findings demonstrate that GNPs can improve the antitumor activity of 5-FU (134). The targeted chemo-photothermal treatment of CRC was developed by Emami et al. using doxorubicin (DOX) conjugated with anti-PD-L1 targeting gold NPs (PD-L1-AuNP-DOX). Anti-PD-L1 antibody and DOX have been linked by amide linkage to the terminal end group of lipoic acid polyethylene glycol N-hydroxysuccinimide (LA-PEG-NHS), and PD-L1-AuNP-DOX has been synthesized by attaching a short PEG chain to the surface of AuNP and joining LA-PEG-DOX and LA-PEG-PD-L1. Near-infrared (NIR) irradiation was used to characterize the PD-L1-AuNP-physicochemical DOX's properties and conduct biological research. An excellent intracellular absorption of DOX was demonstrated in CT-26 cells by the 66.0 percent apoptotic impact of PD-L1-AuNP-DOX (40.0 nm). Apoptosis and cell cycle arrest were increased by PD-L1-AuNP-DOX therapy in combination with NIR irradiation in the *in vitro* proliferation of CT-26 cells. The study shows that synergistic targeted chemo-photothermal therapy in conjunction with PD-L1-AuNP-DOX has a significant promise for treating localized CRC (135).

Dendrimers

Dendrimers are nanosized macromolecules with tree-like branches and arms originating from a central core (136). Several cationic, neutral, or anionic end groups are present on the arms. Throughout the synthesis process, branches are added to the core at successive levels known as generations. Dendritic macromolecules likely to grow linearly in diameter and adopt a globular shape as dendrimer branches increases (137). Due to their specific physicochemical properties, as well as their biodegradable backbones, dendrimers are suitable for delivering drugs and genes (138–140). Drugs and targeting moieties can be loaded into dendrimer cavities through chemical linkages, hydrogen bonds, or hydrophobic interactions. Multiple dendrimers have been investigated for cancer therapeutics, including polyamidoamine (PAMAM), polypropylene imine (PPI), poly(ethylene glycol) (PEG), Bis-MPA (2,2-bis(hydroxymethyl) propionic acid) and 5-ALA (5-aminolevulinic acid) (141). Dendrimer-DOX was studied by Mignani et al. which showed that it was 10 times less

harmful than free DOX after being exposed to C-26 CRC cells for 72 hours. When BALB/c mice with C-26 CRC tumors were given dendrimer-DOX, the tumor uptake was 9 times greater than with free DOX at 48 hours and had a half-life of 16-hour. The mice survived for two months with a single injection of dendrimer-DOX (141).

In a research conducted by Zhuo et al., different generations (0.5–5.5) of 5-FU-dendrimer conjugates were synthesized, demonstrating enhanced controlled release properties for the anticancer drug 5-FU (142). Moreover, the conjugation of DOX with PEGylated dendrimers resulted in improved circulation time, decreased drug accumulation, and reduced toxicity. When administered subcutaneously in mice with highly invasive CRC C26 cells, these dendrimer-conjugated formulations showed the ability to overcome the known resistance of these tumor cells to doxorubicin (143). Additionally, dendrimers have shown potential in preventing the initiation of metastasis by selectively binding to and cytotoxically eliminating circulating tumor cells (CTCs) (144). Due to these promising attributes, dendrimers are often referred to as “therapeutic dendrimers” and warrant further investigation and attention in the field of cancer-targeted therapy (145).

Quantum dots

Quantum dots (QDs) are tiny semiconductor nanoparticles with a diameter smaller than 10 nm. Due to their small size, they are often used as fluorescent labels in medical imaging or incorporated into nanostructure scaffolds for diagnosis and treatment purposes. QDs have been extensively studied in theoretical quantum mechanics, and their optical properties, which depend on their size and composition, make them valuable in medical imaging, especially for the gastrointestinal tract. For instance, in CRC, ODs labelled with bevacizumab, an antibody that targets VEGF, have shown promise in non-invasively tracking the overexpression of VEGF. These theranostic QDs not only possess therapeutic capabilities but also enable the visualization of antibody binding specificity (146). Additionally, a patented approach involves the use of porphyrin carbon QDs conjugated with cetuximab (C225-PCQD) for imaging and photodynamic therapy. These QDs have the ability to accumulate in CRC cells that have elevated levels of EGFR (147).

Polymeric micelles

Polymeric micelles (PMs) are self-assembled structures formed by amphiphilic block copolymers in water-based solutions. These micelles possess a hydrophobic core and a hydrophilic shell, making them suitable for encapsulating hydrophobic drugs and improving their solubility (148). PM-based carriers can be easily developed and can be optimized for drug delivery. Additionally, they can be functionalized with targeting ligands to enhance their accumulation at tumor sites, reduce side effects, and enable controlled release of drugs over an extended period (149, 150). Recent study has focused on the development of pH-responsive

copolymers for optimized delivery of anticancer drugs in colon cancer treatment. These micelles exhibit pH sensitivity and effectively target colon tissues, achieving controlled drug release rates of over 80% (151). Hence, they are regarded as “smart” nanocarriers for delivering anticancer drugs and imaging agents, with potential applications in therapeutics and diagnostics. Notably, several PM formulations loaded with drugs have entered clinical trials for cancer treatment. For instance, Genexol®-PM, a PM formulation loaded with paclitaxel (PCX), is undergoing phase IV clinical trials for CRC, and other trials aim to explore its efficacy in ovarian, lung, cervical, and pancreatic cancers. Preclinical studies on multidimensional PMs are also underway, highlighting their potential as promising platforms for drug delivery and cancer therapy, deserving further investigation and attention (152).

Mesoporous silica nanoparticles

Mesoporous silica nanoparticles (MSNs) are a class of materials composed of silica (SiO₂) that have attracted significant attention in drug delivery due to their unique porous structure, capable of accommodating large amounts of bioactive molecules. MSNs offer adjustable cavity sizes within the range of 50–300 nm, lower toxicity, easy uptake by cells, and resistance to heat and variable pH conditions (153). A hybrid system called MSN-protamine (MSN-PRM) has been developed to enable selective drug release in cancer cells, which can be activated by specific enzymes to initiate anticancer activity (154). By conjugating MSNs with hyaluronic acid, the loading capacity of doxorubicin (DOX) into the MSNs is significantly increased compared to unmodified MSNs. This improvement resulted in improved cellular uptake and cytotoxicity against human cancer cells. In addition, functionalization of MSNs with polyethyleneimine-polyethylene glycol (PEI-PEG) or PEG increased epirubicin hydrochloride (EPI) loading and improved its antitumor activity (155). Silica nanoparticles have been used in the treatment of CRC when combined with photons to selectively destroy CRC cells (156). Silica-based nanoshells encapsulate photosensitizing molecules, facilitating their uptake by tumor cells. When exposed to light, the photosensitive device releases oxygen molecules, effectively killing cancer cells (157). Clinical trials are currently investigating this technology in cancer treatment. Additionally, nanoparticles have shown promise in molecular imaging of cancer cells, enabling earlier diagnosis and targeted DDS.

Magnetic and metallic nanoparticles as photosensitizers

Metallic and magnetic nanomaterials possess distinct magnetic, optical, and photothermal properties that make them valuable in various biomedical applications. Among these materials, iron oxide stands out as a notable metallic nanomaterial with versatile uses. Its exceptional magnetic properties enable its application in imaging techniques and targeted drug delivery (158). Metallic NPs can be combined with other nanomaterials and integrated with therapies

like photothermal therapy (PTT). Iron oxide nanoparticles, specifically, exhibit excellent biodegradability within the human body, as the iron ions can be naturally adjusted. Recent research suggests that smart multifunctional magnetic nanovesicles containing the antibody-targeting peptide AP1 (MPVA AP1) hold promise as effective anticancer agents (158). These nanovesicles demonstrate remarkable selectivity and targeting towards CRC cells while ensuring minimal drug leakage without magnetic field stimulation. Additionally, nanovesicles loaded with doxorubicin release the drug rapidly, accurately, and under precise control when exposed to a high-frequency magnetic field. Consequently, smart magnetic nanovesicles like MPVA-AP1 exhibit significant potential for delivering specific doses and achieving sustained drug release in antitumor applications. Iron oxide nanoparticles also increased hyperthermia effects and prove highly beneficial in CRC diagnosis. For instance, PLGA NPs loaded with 5-FU and iron oxide induce greater DNA damage in HT-29 colon tumor cells compared to hyperthermia alone (159). Other studies reveal the controlled release of PCX and super-paramagnetic iron oxide (SPIO) from PEAL Ca micelles, with release rates influenced by pH levels. Cell culture experiments further demonstrate successful absorption of PTX-SPIO-PEALCa by CRC LoVo cells, while PCX is internalized by lysosomal cells, effectively inhibiting CRC LoVo cell growth. Thus, micelles offer substantially potential as well as greater drug release methods for CRC treatment using MRI imaging (160).

Carbon-based nanoparticles

The carbon-based nanomaterial family encompasses various members such as fullerenes, carbon nanotubes, graphene, nanodiamonds, and carbon-based quantum dots (161). These nanomaterials exhibit exceptional physical and chemical properties, including mechanical strength, electrical conductivity, thermal stability, optical characteristics, and chemical reactivity. As a result, they have attracted significant attention and are being extensively researched for a wide range of applications, particularly in biomedicine. They hold promise as carriers for therapeutic agents in disease treatment, tissue regeneration, and cell and tissue imaging. Furthermore, their anti-bacterial and anti-inflammatory activity are also being extensively investigated (162).

Carbon nanotubes (CNTs) are a widely studied type of carbon nanoparticles in the field of biomedicine. These are cylindrical structures made of extruded graphene sheets with a diameter of less than 1 µm and a nanoscale length (162). Their large surface area, needle-like structure, high thermal conductivity, and chemical stability make them suitable for various applications, including immunotherapy, diagnostics, gene therapy, and as carriers in DDS (163). Many strategies have been developed to use CNTs as anti-inflammatory agents. For example, single-walled carbon nanotubes (SWCNTs) conjugated with a synthetic polyampholyte have demonstrated enhanced anticancer effects of paclitaxel in Caco-2 and HT-29 cells compared to paclitaxel alone (164). Similarly, Eudragit®-irinotecan-loaded CNTs have shown improved efficacy in cancer treatment (165). Moreover, infrared light-activated oxaliplatin and mitomycin C-coated CNTs exhibited

higher drug delivery and localization in colon cancer cell lines (166). SWCNTs modified with TRAIL, a ligand that induces apoptosis in cancer cells, have demonstrated significantly increased cell death compared to TRAIL delivery alone in carcinoma cell lines (167).

Cyclodextrin complexes

Cyclodextrins (CDs) are cyclic oligosaccharides composed of glucose units linked by glycosidic bonds. They come in three forms: α -CD, β -CD, and γ -CD, each consisting of six, seven, or eight glucose units, respectively (168, 169). The unique structure of CDs resembles a hollow truncated cone with a hydrophobic cavity and a hydrophilic outer surface, thanks to the chair arrangement of the glucopyranose groups. This structure enables the encapsulation of hydrophobic drugs within the CD cavity, forming host-guest complexes without requiring complex chemical reactions (170, 171). Furthermore, CDs can form reversible inclusion complexes with various guest molecules, allowing for both drug loading and controlled drug release at specific sites as needed (172).

In a recent study by Bai et al., a modified γ -CD containing mannose was utilized to deliver regorafenib and effectively target colorectal cancer cells (173). The modified CD formed various types of channels that specifically targeted cancer cells, leading to cell death. The study demonstrated sustained release of the drug, resulting in increased apoptosis and a reduction in tumor supportive factors and pro-inflammatory cytokines. This research highlights the potential of CDs in targeting cancer cells, which can be further enhanced by incorporating appropriate targeting agents. Another study focused on using a polycationic β -CD complexed with camptothecin (CPT), a potent drug, to enhance its stability for the treatment of early- and late-stage colon cancers (174).

Accurately distinguishing cancerous cells from normal tissues is crucial for effective cancer diagnosis. Nanoengineering offers a promising solution by enhancing the targeting and luminescent properties of various materials, enabling their use in biomedical applications. This advancement has led to the development of bioimaging techniques that utilize nanomaterials for the identification of different types of tumors. For instance, Mortezaadeh et al. developed a targeted nanocontrast agent for magnetic resonance imaging (MRI) using gadolinium (Gd) nanoparticles coated with a β -CD-based polyester and folic acid (FA). This nanoparticulate contrasting agent enables precise localization and improved tissue discrimination, enhancing the accuracy of cancer diagnosis. The polymer coating not only provides stability to the nanoparticles in biological conditions but also prevents leakage into normal tissues. The coated spherical Gd nanoparticles, with a diameter ranging from 75 to 95 nm, demonstrated non-toxicity towards normal human breast cells (MCF-10A) in MTT assays, unlike free Gd₂O₃ (175). Although nanoscale drug delivery vehicles have made significant progress, further advancements are necessary to meet the clinical standards of

care. CDs hold great promise as versatile agents capable of fulfilling multiple roles at the nanoscale level.

Nanoimmunotherapeutics and nanovaccines

Nanoimmunotherapeutics has emerged as a promising approach for treating CRC by combining nanotechnology and immunotherapy. Zhang et al. developed NPs capable of delivering immune checkpoint inhibitors, such as anti-PD-1 or anti-CTLA-4 antibodies, directly to the tumor microenvironment. This targeted delivery enhances immune cell activation and overcomes mechanisms of immune evasion (176). Additionally, Nanoimmunotherapeutics can incorporate immune stimulants like Toll-like receptor agonists to further boost immune cell activity against tumors (177). Preclinical studies in CRC models have demonstrated the effectiveness of Nanoimmunotherapeutics, showing improved tumor regression, prolonged survival, and enhanced immune responses (177).

Nanovaccines have emerged as a promising approach for treating CRC by utilizing the immune system to target and eradicate cancer cells. These nanoscale vaccines are specifically designed to deliver tumor-specific antigens, adjuvants, and immunomodulators, thereby eliciting a potent and protective immune response against tumors. The nanovaccine uses the unique properties of nanoparticles to improve antigen presentation, activate the immune system and boost immunity against cancer (178).

A nanovaccine that comprises certain tumor antigens like carcinoembryonic antigen (CEA) or mucin 1 (MUC1) that demonstrates a response resistance to sickness and tumor progression has demonstrated promising outcomes in clinical models. Additionally, Toll-like receptor agonists or NPs containing internal components may be used in nanovaccines and nanoimmunotherapies to enhance immunity and antigen presentation (179). Although clinical studies and the development of nanovaccine and nanoimmunotherapy for CRC are still in their early phases, they have the potential to enhance the immune system's performance in CRC patients (180).

Clinical trials for nanotechnology used in CRC

Despite the fact that several nano formulations are undergoing clinical studies, there aren't many of them being utilized to treat CRC. Table 4 provides a summary of some of the nanoformulations employed for the suitable clinical studies against the CRC. In a research study, a smooth-thermosensitive liposomes containing doxorubicin called Thermodox[®] is intended for usage in combination with thermal ablation. Thermodox[®] in combination with thermal ablation was investigated for safety, viability, and effectiveness in treating liver metastases in CRC in

TABLE 4 Most recent clinical trials with nano formulations for CRC therapy.

Nanocarrier Used	Drug (Active Agent)	Applications	Clinical Trial Status	Sources
Regulatory lymphocytes (Tregs): anti-CTLA-4 ipilimumab and anti-PD-L1 atezolizuma	Cytotoxic antibodies expressed on surface of Tregs	Colorectal cancer	FDA approved	(138)
Polymeric NPs + cetuximab + somatostatin analogue	Combination of NPs Somatostatin and Cetuximab analogue	Metastatic colorectal cancer	Phase I trial	(139)
NKTR-102/IRI	Formulation for prolonged release of IRI conjugated with PEG/IRI	Metastatic CRC with KRAS-mutant	II clinical trial	(139)
PEG-PGA polymeric micelle	SN-38	Colorectal, lung, & ovarian cancers	Phase II trial	(140)
Liposome	Doxorubicin	Colon cancer with liver metastasis	Phase II trial	(141)
CPX-1 liposome	Liposomal IRI (irinotecan) hydrochloride and floxuridine	Advanced colorectal cancer	Phase II trial	(139)
Cyclodextrin nanoparticle	Camptothecin	Solid tumors, rectal cancer, renal cell carcinoma, non-small cell lung cancers	Phase I/II trial	(142)
Carbon NPs	Carbon NPs	Laparoscopic surgery of colorectal cancer	Phase I trial	(139)
TKM-080301	Lipid NPs with serine/threonine kinase inhibitor	Colorectal cancer with liver metastases and ovarian, gastric, esophageal, and breast cancer	Phase I trial	(139)
Nal-IRI	Liposomal IRI	Colorectal cancer along with advanced gastrointestinal cancers	Phase I/II trial	(139)
PEP02 liposome	Liposomal IRI hydrochloride + 5-FU and LV (leucovorin)	Metastatic colorectal cancer	Phase II trial	(139)
PEG-rhG-CSF	PEGylated recombinant human granulocyte colony stimulating factor (CSF)	Solid malignant tumors (colorectal, ovarian, lung, head, and neck cancer)	Phase IV trial	(139)
PROMITIL	PEGylated liposomal mitomycin C	Metastatic colorectal cancer	Phase I trial	(139)
Silica NPs	Fluorescent cRGDY-PEG-Cy5.5-C dots	Colorectal malignancies	Phase I-II trial	(139)
MM-398	Liposomal IRI	Advanced cancer of unresectable nature	Phase Ib trial	(139)

TABLE 5 Recent patents related to nanoformulations for the management and treatment of CRC.

Nanocarrier/ Nanoparticles	Details of patent	Molecule	Year of Patent Granted	Patent Number	Sources
Gold metallic NPs	Fluorouracil (5-FU) INCORPORATED IN Metallic NPs for connecting polynucleotide	Anticancer drug with a pyrimidine group or a purine group such as 5-FU	2014	US8673358B2	(146)
Liposome	Liposomal IRI + 5-FU/LV(leucovorin) and an EGFR inhibitor	Irinotecan(IRI)	2017	WO2017172678	(147)
PEG-modified cationic liposome	shRNA against TS(thymidylate synthase) attached to cationic modified liposome with PEG	shRNA	2014	ES2653923	(148)
Quantum points of porphyrin carbon	Quantum point of porphyrin carbon conjugated with cetuximab biocompatible	Cetuximab	2018	US20180125976A1	(144)
Glyceryl mono fatty acid ester	NPs of glyceryl monofatty acid ester, chitosan, and therapeutic agent	Antineoplastic agent	2012	US8242165B2	(149)

an open phase II investigations (NCT02181075) (181). In contrast to targeting NPs, while passive targeting NPs have already received FDA approval as cancer nanotherapeutics, active targeting NPs are still in the early phases of clinical trials (182).

Furthermore, it has been seen in clinical studies that nanoplateforms typically decrease the toxicity of drugs rather than increase their efficacy. The majority of NPs, including actively targeted nano preparations, accumulate at tumours based on EPR effect, but this effect is more persistent in animals, whereas there are variations in the EPR effect for CRC patients, which will affect the efficacy of nano preparations (183, 184).

Patents approved for nanotechnology in the treatment of CRC

A few of the clinical trial-validated nanomaterials have been trademarked for commercial use in given in Table 5. Theragnostic formulations are new approaches to CRC treatment that try to forecast the results of a specific treatment, for example, by identifying individuals who will respond to a drugs more favourably or by giving information on how a drug is acting (185). For example, Wu et al. developed porphyrin carbon QDs coupled with cetuximab (C225-PCQD), which have been patented as an imaging and photodynamic treatment strategy due to their ability to aggregate in colon cancer cells that overexpress the EGFR receptor (186). Also, a liposomal IRI formulation with 5-FU, LV, and an EGFR inhibitor has also been granted patent protection by Merrimack Pharmaceuticals for the treatment of metastatic CRC with a wild-type RAS mutation (187).

Conclusion and future perspectives

A primary goal of the center for disease control and prevention is to prevent cancer, diagnose it early, improve the health of those who have it, and decrease the financial burden of treating it. Following its tremendous success, there are some crucial elements that need further examination. In the typical bench-top technique, it has been difficult to control the nanoparticle size, resulting in batch-to-batch variance. In order to attain more atomization and large-scale capability, additional design work is needed. Nanoparticles with desired particle sizes and distributions can be manufactured continuously in a reproducible, large-scale way using this approach. Nanoparticles also tend to congregate in production and physiological settings. This physical instability can be lessened by mixing in a little amount of NaCl to the gelation media, but there are still other possibilities to consider. Innovative ionic gelation techniques may lead to nanoparticles that are stronger and more stable. Nanoparticles made from chitosan offer a promising start in this direction. In addition, further research is needed to develop stable and effective nanoparticle-based powder compositions. In the treatment of CRC, CRC-targeted nano-DDS can alter the distribution and release of drug in people by accumulating in CRC, which improves therapeutic efficacy and lowers adverse effects compared to conventional therapy

approaches. Overall, the results have demonstrated that synthesised gold NPs may be effective anti-colon cancer medications because of their distinctive optical features, which make them valuable in imaging and photothermal treatment. These nanoparticles can also be altered using specific ligands to allow for specific distribution to tumor locations. For the treatment of CRC, researchers have looked at the use of gold nanoparticles to increase the results of radiotherapy and photothermal therapy (188).

The treatment approaches of CRC may change in the future. Using nanoparticles with ligands or antibodies on their surface to deliver substances specifically to tumor cells is one such strategy. Exploiting the increased EPR effect is another strategy that takes advantage of tumours' aberrant blood arteries and impaired lymphatic drainage. This improves drug delivery by allowing nanoparticles to collect preferentially in tumor tissue. Nanomaterials can also be developed to react to certain stimuli present in the tumor microenvironment, such as pH, temperature, or enzyme activity. This enhances the efficiency of therapy by enabling regulated drug release at the tumor location. Additionally, imaging capabilities can be added to nanomaterials, enabling non-invasive monitoring of medication distribution, tumor targeting, and therapeutic response. These developments could help assist personalised medicine and enhance CRC treatment plans. Furthermore, nanomaterials can be engineered with imaging capabilities, allowing for non-invasive monitoring of drug distribution, tumor targeting, and treatment response. These advancements have the potential to support personalized medicine and optimize treatment strategies for CRC.

This review summarizes and classifies the colon-targeted NPs from the perspective of targeting power, showcasing the diversity and innovation of NPs targeting CRC in academic research. Ultimately, more preclinical and clinical testing is needed to bring gold nanoparticles to the market. There are now several clinical trials being conducted on the use of NPs in CRC. However, a number of clinical phases still need to be completed by the majority of these approaches before they can be commercialized. Toxicology, bioavailability, side effects, cost-effectiveness, and biocompatibility need to be studied further in preclinical and clinical settings. The literature that is now accessible and the research that is being done on the use of NPs in the treatment of cancer clearly suggest that treatments utilizing nanoformulations can simultaneously be used for diagnostic and therapy based on their functionalization and contents are especially promising.

Additionally, new patents for DDS based on nanotechnology are being explored. To ascertain their applicability, adverse effects, removal procedures, and therapeutic benefits, clinical studies are being conducted on them. There has been a rise in medical device and medication delivery system research as a result of the advancements in nanotechnologies. It was possible to create multipurpose platforms, like nano theranostics, using nanotechnology to create medical goods with several modes of action. As a cancer therapy, preclinical studies with nanomaterials have demonstrated their efficacy. Research into immunotoxicity testing, nanoparticle surfaces, and drug fraction encapsulation and decapsulation has shown the importance of nanotechnology in the

field of medicine in the 21st century. In biomedical research, the development of DDS with the potential to alter tissue absorption, biodistribution of drugs, and pharmacokinetics of therapeutic agents is critical. Current medical research is focused on nanoparticles. When it comes to developing new treatments for diseases, researchers have focused on using nanotechnology. Anti-degradation, as well as targeted and controlled release, are all possible with medicinal molecules combined with nanocarriers. Numerous nanocarriers for cancer treatment and diagnosis have been developed during the past 20 years as a result of rapid advancements in nanoscience, technology, and industry and cancer pathology (138). However, only few numbers of nano-drugs have been successfully produced and involved in clinical settings.

Author contributions

AJ: Investigation, conceptualization, writing original draft. SB: Validation, designing, methodology, reviewing and editing. The authors declare that the work was done, analysed, drafted by all the authors of this manuscript. All the authors had read and approved the final manuscript. All authors contributed to the article and approved the submitted version.

References

1. El Zarif T, Yibirin M, De Oliveira-Gomes D, Machaalani M, Nawfal R, Bittar G, et al. Overcoming therapy resistance in colon cancer by drug repurposing. *Cancers* (2022) 14(9):2105. doi: 10.3390/cancers14092105
2. Lang D, Ciombor KK. Diagnosis and management of rectal cancer in patients younger than 50 years: rising global incidence and unique challenges. *J Natl Compr Cancer Network* (2022) 20(10):1169–75. doi: 10.6004/jnccn.2022.7056
3. Morgan E, Arnold M, Gini A, Lorenzoni V, Cabasag C, Laversanne M, et al. Global burden of colorectal cancer in 2020 and 2040: incidence and mortality estimates from GLOBOCAN. *Gut* (2023) 72(2):338–44. doi: 10.1136/gutjnl-2022-327736
4. Yang L, Wang S, Lee JJ-K, Lee S, Lee E, Shinbrot E, et al. An enhanced genetic model of colorectal cancer progression history. *Genome Biology* (2019) 20:1–17. doi: 10.1186/s13059-019-1782-4
5. Itatani Y, Yamamoto T, Zhong C, Molinolo AA, Ruppel J, Hegde P, et al. Suppressing neutrophil-dependent angiogenesis abrogates resistance to anti-VEGF antibody in a genetic model of colorectal cancer. *Proceedings of the National Academy of Sciences* (2020) 117(35):21598–608. doi: 10.1073/pnas.2008112117
6. Lynch HT, de la Chapelle AJ. Hereditary colorectal cancer. *New England Journal of Medicine* (2003) 348(10):919–32. doi: 10.1056/NEJMra012242
7. Umar A, Boland CR, Terdiman JP, Syngal S, Chapelle A, Rüschoff J, et al. Revised Bethesda guidelines for hereditary nonpolyposis colorectal cancer (Lynch syndrome) and microsatellite instability. *Journal of the National Cancer Institute* (2004) 96(4):261–8. doi: 10.1093%2Fjnci%2F96j4034
8. Stoffel EM, Kastrinos FJ. Hepatology, familial colorectal cancer, beyond lynch syndrome. *Clinical Gastroenterology and Hepatology* (2014) 12(7):1059–68. doi: 10.1016/j.cgh.2013.08.015
9. Levin B, Lieberman DA, McFarland B, Andrews KS, Brooks D, Bond J, et al. Screening and surveillance for the early detection of colorectal cancer and adenomatous polyps, 2008: a joint guideline from the American cancer society, the US multi-society task force on colorectal cancer, and the American college of radiology. *CA: A Cancer Journal for Clinicians* (2008) 134(5):1570–95. doi: 10.1053/j.gastro.2008.02.002
10. Pino MS, Chung DC. The chromosomal instability pathway in colon cancer. *Gastroenterology* (2010) 138(6):2059–72. doi: 10.1053/j.gastro.2009.12.065
11. Weisenberger DJ, Siegmund KD, Campan M, Young J, Long TI, Faasse MA, et al. CpG island methylator phenotype underlies sporadic microsatellite instability and is tightly associated with BRAF mutation in colorectal cancer. *Nature Genetics* (2006) 38(7):787–93. doi: 10.1038/ng1834
12. Cancer Genome Atlas Network. Nature, comprehensive molecular characterization of human colon and rectal cancer. *Nature* (2012) 487(7407):330. doi: 10.1016/j.jirobp.2012.12.006
13. Brocardo M, Henderson BR. APC shuttling to the membrane, nucleus and beyond. *Trends in Cell Biology* (2008) 18(12):587–96. doi: 10.1016/j.tcb.2008.09.002
14. Herzig DO, Tsikitis V. Molecular markers for colon diagnosis, prognosis and targeted therapy. *Journal of Surgical Oncology* (2015) 111(1):96–102. doi: 10.1002/jso.23806
15. Dolatkhan R, Somi MH, Kermani IA, Ghosazadeh M, Jafarabadi MA, Farassati F, et al. Increased colorectal cancer incidence in Iran: a systematic review and meta-analysis. *BMC Public Health* (2015) 15(1):1–14. doi: 10.1186/s12889-015-2342-9
16. Erichsen R, Baron JA, Stoffel EM, Laurberg S, Sandler RS, H.T.J.O.j.o.t.A.C.o.G. Sørensen ACG. Characteristics and survival of interval and sporadic colorectal cancer patients: a nationwide population-based cohort study. *American Journal of Gastroenterology* (2013) 108(8):1332–40. doi: 10.1038/ajg.2013.175
17. Patel SG, Ahnen DJ. Hepatology, prevention of interval colorectal cancers: what every clinician needs to know. *Clinical Gastroenterology and Hepatology* (2014) 12(1):7–15. doi: 10.1016/j.cgh.2013.04.027
18. Sunkara S, Swanson G, Forsyth CB, Keshavarzian AJU. Chronic inflammation and malignancy in ulcerative colitis. *Ulcers* (2011) 2011:1–8. doi: 10.1155/2011/714046
19. Tuohy TM, Rowe KG, Mineau GP, Pimentel R, Burt RW, Samadder NJ. Risk of colorectal cancer and adenomas in the families of patients with adenomas: a population-based study in Utah. *Cancer* (2014) 120(1):35–42. doi: 10.1002/cncr.28227
20. Robertson DJ. ABC of colorectal cancer. *International Journal of Molecular Sciences* (2012) 143(3):868–9. doi: 10.1053/j.gastro.2012.07.090
21. Martinez-Useros J, Garcia-Foncillas J. Obesity and colorectal cancer: molecular features of adipose tissue. *Journal of Translational Medicine* (2016) 14(1):1–12. doi: 10.1186/s12967-016-0772-5
22. Cross AJ, Boca S, Freedman ND, Caporaso NE, Huang W-Y, Sinha R, et al. Metabolites of tobacco smoking and colorectal cancer risk. *Carcinogenesis* (2014) 35(7):1516–22. doi: 10.1093/carcin/bgu071
23. Koustaas E, Trifylli E-M, Sarantis P, Papadopoulos N, Karapedi E, Aloizos G, et al. Immunotherapy as a therapeutic strategy for gastrointestinal cancer—current treatment options and future perspectives. *Int J Mol Sci* (2022) 23(12):6664. doi: 10.3390/ijms23126664

Acknowledgments

The authors are like to acknowledge the significant contribution of Prof. Ajazuddin, Ex-Associate Dean, School of Pharmacy & Technology Management, SVKM'S NMIMS Deemed-to-be University, Shirpur, Maharashtra 425405, India, for constant motivation while developing this project.

Conflict of interest

The authors declare that the research was conducted in the absence of any commercial or financial relationships that could be construed as a potential conflict of interest.

Publisher's note

All claims expressed in this article are solely those of the authors and do not necessarily represent those of their affiliated organizations, or those of the publisher, the editors and the reviewers. Any product that may be evaluated in this article, or claim that may be made by its manufacturer, is not guaranteed or endorsed by the publisher.

24. Ebrahimi N, Afshinpour M, Fakhri SS, Kalkhoran PG, Manesh VS, Adelian S, et al. Cancer stem cells in colorectal cancer: signaling pathways involved in stemness and therapy resistance. *Crit Rev Oncology/Hematology* (2023) 103920. doi: 10.1016/j.critrevonc.2023.103920
25. Hernández-Esquivel R-A, Navarro-Tovar G, Zárate-Hernández E, Aguirre-Bañuelos P. Solid lipid nanoparticles (SLN), nanocomposite materials for biomedical and energy storage applications. *IntechOpen* (2022).
26. Rahman MM, Islam MR, Akash S, Harun-Or-Rashid M, Ray TK, Rahaman MS, et al. Recent advancements of nanoparticles application in cancer and neurodegenerative disorders: At a glance. *Biomedicine Pharmacotherapy* (2022) 153:113305. doi: 10.1016/j.biopha.2022.113305
27. Jadach B, Świątlik W, Froelich A. Sodium alginate as a pharmaceutical excipient: novel applications of a well-known polymer. *J Pharm Sci* (2022) 111(5):1250–61. doi: 10.1016/j.xphs.2021.12.024
28. Cong C, Rao C, Ma Z, Yu M, He Y, He Y, et al. “Nano-lymphatic” photocatalytic water-splitting for relieving tumor interstitial fluid pressure and achieving hydrodynamic therapy. *Materials Horizons* (2020) 7(12):3266–74. doi: 10.1039/D0MH01295E
29. Li R, Peng F, Cai J, Yang D, Zhang P. Redox dual-stimuli responsive drug delivery systems for improving tumor-targeting ability and reducing adverse side effects. *Asian J Pharm Sci* (2020) 15(3):311–25. doi: 10.1016/j.ajps.2019.06.003
30. Abumamhal-Masarweh H, Koren L, Adir O, Kaduri M, Poley M, Chen G, et al. Barriers in the tumor microenvironment to nanoparticle activity, *handbook of harnessing biomaterials in nanomedicine*. New York, USA: Jenny Stanford Publishing (2021) p. 425–61.
31. Sindhiani S, Syed AM, Ngai J, Kingston BR, Maiorino L, Rothschild J, et al. The entry of nanoparticles into solid tumours. *Nat materials* (2020) 19(5):566–75. doi: 10.1038/s41563-019-0566-2
32. Michie S, Johnston M, Carey R. *Behavior change techniques, encyclopedia of behavioral medicine*. Miami, USA: Springer (2020) p. 206–13.
33. Raj S, Khurana S, Choudhary R, Kesari KK, Kamal MA, Garg N, et al. Specific targeting cancer cells with nanoparticles and drug delivery in cancer therapy. *Semin Cancer biology Elsevier* (2021) pp:166–77. doi: 10.1016/j.semcancer.2019.11.002
34. Kashkooli FM, Soltani M, Souri M. Controlled anti-cancer drug release through advanced nano-drug delivery systems: static and dynamic targeting strategies. *J Controlled release* (2020) 327:316–49. doi: 10.1016/j.jconrel.2020.08.012
35. Fam SY, Chee CF, Yong CY, Ho KL, Mariatulqabiah AR, Tan WS. Stealth coating of nanoparticles in drug-delivery systems. *Nanomaterials* (2020) 10(4):787. doi: 10.3390/nano10040787
36. Tiwari A, Saraf S, Jain A, Panda PK, Verma A, Jain S. Research, basics to advances in nanotherapy of colorectal cancer. *Drug Delivery and Translational Research* (2020) 10(2):319–38.
37. Dahiya R, Dahiya S. *Advanced drug delivery applications of self-assembled nanostructures and polymeric nanoparticles, handbook on nanobiomaterials for therapeutics and diagnostic applications*. India: Elsevier (2021) p. 297–339.
38. Yang C, Merlin D. Can naturally occurring nanoparticle-based targeted drug delivery effectively treat inflammatory bowel disease? *Expert Opin Drug delivery* (2020) 17(1):1–4. doi: 10.1080/17425247.2020.1698543
39. Zafar S, Akhtar S, Garg N, Selvapandian A, Jain GK, Ahmad FJ. Co-Encapsulation of docetaxel and thymoquinone in mPEG-DSPE-vitamin E TPGS-lipid nanocapsules for breast cancer therapy: formulation optimization and implications on cellular and *in vivo* toxicity. *Eur J Pharmaceutics Biopharmaceutics* (2020) 148:10–26. doi: 10.1016/j.ejpb.2019.12.016
40. Li S, Xu S, Liang X, Xue Y, Mei J, Ma Y, et al. Nanotechnology: breaking the current treatment limits of lung cancer. *Advanced Healthcare Materials* (2021) 10(12):2100078. doi: 10.1002/adhm.202100078
41. Gao Z, Wang C, Cui Y, Shen Z, Jiang K, Shen D, et al. Efficacy and safety of complete mesocolic excision in patients with colon cancer: three-year results from a prospective, nonrandomized, double-blind, controlled trial. *Ann Surg* (2020) 271(3):519–26. doi: 10.1097/SLA.0000000000003012
42. Aparicio T, Henriques J, Manfredi S, Tougeron D, Bouché O, Pezet D, et al. Small bowel adenocarcinoma: results from a nationwide prospective ARCAD-NADEGE cohort study of 347 patients. *Int J Cancer* (2020) 147(4):967–77. doi: 10.1002/ijc.32860
43. Cheng WT, Kantilal HK, Davamani F. The mechanism of bacteroides fragilis toxin contributes to colon cancer formation. *Malaysian J Med sciences: MJMS* (2020) 27(4):9. doi: 10.21315/mjms2020.27.4.2
44. Reiter JG, Hung W-T, Lee I-H, Nagpal S, Giunta P, Degner S, et al. Lymph node metastases develop through a wider evolutionary bottleneck than distant metastases. *Nat Genet* (2020) 52(7):692–700. doi: 10.1038/s41588-020-0633-2
45. Onoda N, Sugitani I, Ito K-i, Suzuki A, Higashiyama T, Fukumori T, et al. Evaluation of the 8th edition TNM classification for anaplastic thyroid carcinoma. *Cancers* (2020) 12(3):552. doi: 10.3390/cancers12030552
46. Stoffel EM, Murphy CC. Epidemiology and mechanisms of the increasing incidence of colon and rectal cancers in young adults. *Gastroenterology* (2020) 158(2):341–53. doi: 10.1053/j.gastro.2019.07.055
47. Nkune NW, Kruger CA, Abrahamse H. Possible enhancement of photodynamic therapy (PDT) colorectal cancer treatment when combined with cannabidiol. *Anti-Cancer Agents Medicinal Chem (Formerly Curr Medicinal Chemistry-Anti-Cancer Agents)* (2021) 21(2):137–48. doi: 10.2174/1871520620666200415102321
48. Wikramaratna P, Paton RS, Ghafari M, Lourenco J. Estimating false-negative detection rate of SARS-CoV-2 by RT-PCR. *MedRxiv* 2020. *Eurosurveillance* (2020) 25. doi: 10.1101/2020.04.05.20053355
49. Sharib J, Esserman L, Koay EJ, Maitra A, Shen Y, Kirkwood KS, et al. Cost-effectiveness of consensus guideline based management of pancreatic cysts: the sensitivity and specificity required for guidelines to be cost-effective. *Surgery* (2020) 168(4):601–9. doi: 10.1016/j.surg.2020.04.052
50. Bowes DA, Driver EM, Halden RU. A framework for wastewater sample collection from a sewage cleanout to inform building-scale wastewater-based epidemiology studies. *Sci Total Environ* (2022) 836:155576. doi: 10.1016/j.scitotenv.2022.155576
51. van Eijk LE, Binkhorst M, Bourgonje AR, Offringa AK, Mulder DJ, Bos EM, et al. COVID-19: immunopathology, pathophysiological mechanisms, and treatment options. *J Pathol* (2021) 254(4):307–31. doi: 10.1002/path.5642
52. Kong JC, Soucisse M, Michael M, Tie J, Ngan SY, Leong T, et al. Total neoadjuvant therapy in locally advanced rectal cancer: a systematic review and metaanalysis of oncological and operative outcomes. *Ann Surg Oncol* (2021) 28(12):7476–86. doi: 10.1245/s10434-021-09837-8
53. Chen J, He B. The application value of the anatomy and treatment of inferior mesenteric artery in laparoscopic surgery for left-sided colorectal cancer. *Digital Med* (2023) 9(1):2. doi: 10.4103/digm.digm_27_22
54. Anand U, Dey A, Chandel AKS, Sanyal R, Mishra A, Pandey DK, et al. Cancer chemotherapy and beyond: current status, drug candidates, associated risks and progress in targeted therapeutics. *Genes & Diseases* (2022). doi: 10.1016/j.gendis.2022.02.007
55. Vasilaki D, Bakopoulou A, Tsouknidas A, Johnstone E, Michalakis K. Biophysical interactions between components of the tumor microenvironment promote metastasis. *Biophys Rev* (2021) 13(3):339–57. doi: 10.1007/s12551-021-00811-y
56. Suzuki S, Ogawa T, Sano R, Takahara T, Inukai D, Akira S, et al. Immune-checkpoint molecules on regulatory T-cells as a potential therapeutic target in head and neck squamous cell cancers. *Cancer Sci* (2020) 111(6):1943–57. doi: 10.1111/cas.14422
57. Wu Q, Jiang L, Li S-c, He Q-j, Yang B, Cao J. Small molecule inhibitors targeting the PD-1/PD-L1 signaling pathway. *Acta Pharmacologica Sin* (2021) 42(1):1–9. doi: 10.1038/s41401-020-0366-x
58. Xie Y-H, Chen Y-X, Fang J-Y. Comprehensive review of targeted therapy for colorectal cancer. *Signal transduction targeted Ther* (2020) 5(1):22. doi: 10.1038/s41392-020-0116-z
59. Li H, Lai Z, Yang H, Peng J, Chen Y, Lin J. Hedyotis diffusa wildd. inhibits VEGF-C-mediated lymphangiogenesis in colorectal cancer via multiple signaling pathways. *Oncol Rep* (2019) 42(3):1225–36. doi: 10.3892/or.2019.7223
60. Lugano R, Ramachandran M, Dimberg A. Tumor angiogenesis: causes, consequences, challenges and opportunities. *Cellular Mol Life Sci* (2020) 77:1745–70. doi: 10.1007/s00018-019-03351-7
61. Ramasamy T, Munusamy S, Ruttala HB, Kim JO. Smart nanocarriers for the delivery of nucleic acid-based therapeutics: a comprehensive review. *Biotechnol J* (2021) 16(2):1900408. doi: 10.1002/biot.201900408
62. Wang J, Ni Q, Wang Y, Zhang Y, He H, Gao D, et al. Nanoscale drug delivery systems for controllable drug behaviors by multi-stage barrier penetration. *J Controlled Release* (2021) 331:282–95. doi: 10.1016/j.jconrel.2020.08.045
63. Ander SE, Li FS, Carpentier KS, Morrison TE. Innate immune surveillance of the circulation: a review on the removal of circulating virions from the bloodstream. *PLoS Pathog* (2022) 18(5):e1010474. doi: 10.1371/journal.ppat.1010474
64. Rabiee N, Yarak MT, Garakani SM, Garakani SM, Ahmadi S, Lajevardi A, et al. Recent advances in porphyrin-based nanocomposites for effective targeted imaging and therapy. *Biomaterials* (2020) 232:119707. doi: 10.1016/j.biomaterials.2019.119707
65. Liang P, Ballou B, Lv X, Si W, Bruchez MP, Huang W, et al. Monotherapy and combination therapy using anti-angiogenic nanoagents to fight cancer. *Advanced Materials* (2021) 33(15):2005155. doi: 10.1002/adma.202005155
66. Manzanares D, Ceña V. Endocytosis: the nanoparticle and submicron nanocompounds gateway into the cell. *Pharmaceutics* (2020) 12(4):371. doi: 10.3390/pharmaceutics12040371
67. Malhotra N, Lee J-S, Liman RAD, Ruallo JMS, Villaflores OB, Ger T-R, et al. Potential toxicity of iron oxide magnetic nanoparticles: a review. *Molecules* (2020) 25(14):3159. doi: 10.3390/molecules25143159
68. El-Hammadi MM, Small-Howard AL, Fernández-Arévalo M, Martín-Banderas L. Development of enhanced drug delivery vehicles for three cannabis-based terpenes using poly (lactic-co-glycolic acid) based nanoparticles. *Ind Crops Products* (2021) 164:113345. doi: 10.1016/j.indcrop.2021.113345
69. Shin MG, Seo JY, Park H, Park Y-I, Ji S, Lee SS, et al. Positively charged membranes with fine-tuned nanopores for ultrafast and high-precision cation separation. *J Materials Chem A* (2021) 9(43):24355–64. doi: 10.1039/D1TA07865H
70. Carvalho M, Reis R, Oliveira JM. Dendrimer nanoparticles for colorectal cancer applications. *J Materials Chem B* (2020) 8(6):1128–38. doi: 10.1039/C9TB02289A
71. Ahmad A, Ansari MM, Verma RK, Khan R. Aminocellulose-grafted polymeric nanoparticles for selective targeting of CHEK2-deficient colorectal cancer. *ACS Appl Bio Materials* (2021) 4(6):5324–35. doi: 10.1021/acsabm.1c00437

72. Bekmukhametova A, Uddin MMN, Houang J, Malladi C, George L, Wuhrer R, et al. Fabrication and characterization of chitosan nanoparticles using the coffee-ring effect for photodynamic therapy. *Lasers Surg Med* (2022) 54(5):758–66. doi: 10.1002/lsm.23530
73. Lin C, Kuo T-C, Lin J-C, Ho Y-C, Mi F-L. Delivery of polysaccharides from ophiopogon japonicus (OJPs) using OJPs/chitosan/whey protein co-assembled nanoparticles to treat defective intestinal epithelial tight junction barrier. *Int J Biol Macromolecules* (2020) 160:558–70. doi: 10.1016/j.ijbiomac.2020.05.151
74. Bansal R, Sidhu AK. Colorectal cancer: a rapidly rising malignant disease. *Intern J Res Pub Rev* (2022) 3(11):3330–4.
75. Shao W, Pan X, Zhao Z, Cui S. Effects of process parameters on the size of low-molecular-weight chitosan nanoparticles synthesized in static mixers. *Particulate Sci Technol* (2021) 39(8):911–6. doi: 10.1080/02726351.2020.1859027
76. Khairnar SV, Pagare P, Thakre A, Nambiar AR, Junnuthula V, Abraham MC, et al. Review on the scale-up methods for the preparation of solid lipid nanoparticles. *Pharmaceutics* (2022) 14(9):1886. doi: 10.3390/pharmaceutics14091886
77. Niyom Y, Crespy D, Flood AE. Compatibility between drugs and polymer in nanoparticles produced by the miniemulsion-solvent evaporation technique. *Macromol Materials Eng* (2021) 306(7):2100102. doi: 10.1002/mame.202100102
78. Fan R, Tong A, Li X, Gao X, Mei L, Zhou L, et al. Enhanced antitumor effects by docetaxel/LL37-loaded thermosensitive hydrogel nanoparticles in peritoneal carcinomatosis of colorectal cancer. *Int J nanomedicine* (2015) 10:7291. doi: 10.2147/ijnm.S89066
79. Dang T, Cui Y, Chen Y, Meng X, Tang B, Wu J. Preparation and characterization of colon-specific microspheres of diclofenac for colorectal cancer. *Trop J Pharm Res* (2015) 14(9):1541–7. doi: 10.4314/tjpr.v14i9.1
80. Tiruwa R. A review on nanoparticles-preparation and evaluation parameters. *Indian J Pharm Biol Res* (2016) 4(2):27. doi: 10.30750/ijpbr.4.2.4
81. Patel DM, Patel NN, Patel JK. *Nanomedicine scale-up technologies: feasibility and challenges, emerging technologies for nanoparticle manufacturing*. Tampa, USA: Springer (2021) p. 511–39.
82. Allémann E, Gurny R, Doelker E. Preparation of aqueous polymeric nanodispersions by a reversible salting-out process: influence of process parameters on particle size. *Int J pharmaceutics* (1992) 87(1-3):247–53. doi: 10.1016/0378-5173(92)90249-2
83. Şengel-Türk CT, Haşçıek C, Dogan AL, Esendagli G, Guc D, Gönül N. Preparation and *in vitro* evaluation of meloxicam-loaded PLGA nanoparticles on HT-29 human colon adenocarcinoma cells. *Drug Dev Ind Pharm* (2012) 38(9):1107–16. doi: 10.3109/03639045.2011.641562
84. Moreno-Mendieta S, Guillén D, Vasquez-Martinez N, Hernandez-Pando R, Sánchez S, Rodríguez-Sanoja R. Understanding the phagocytosis of particles: the key for rational design of vaccines and therapeutics. *Pharm Res* (2022) 39(8):1823–49. doi: 10.1007/s11095-022-03301-2
85. Mohd-Zahid MH, Mohamud R, Abdullah CAC, Lim J, Alem H, Hanaffi WNW, et al. Colorectal cancer stem cells: a review of targeted drug delivery by gold nanoparticles. *RSC Adv* (2020) 10(2):973–85. doi: 10.1039/C9RA08192E
86. Donahue ND, Acar H, Wilhelm S. Concepts of nanoparticle cellular uptake. *intracellular trafficking kinetics nanomedicine* (2019) 143:68–96. doi: 10.1016/j.addr.2019.04.008
87. Marichal L, Giraudon-Colas G.L, Cousin F, Thill A, Labarre J, Boulard Y, et al. Protein-nanoparticle interactions: what are the protein-corona thickness and organization? *Langmuir* (2019) 35(33):10831–7. doi: 10.1021/acs.langmuir.9b01373
88. Mosquera J, García I, Liz-Marzán LM. Cellular uptake of nanoparticles versus small molecules: a matter of size. *Accounts Chem Res* (2018) 51(9):2305–13. doi: 10.1021/acs.accounts.8b00292
89. Gustafson HH, Holt-Casper D, Grainger DW, Ghandehari HJ. Nanoparticle uptake: the phagocytic problem. *Nanotoday* (2015) 10(4):487–510. doi: 10.1016/j.nantod.2015.06.006
90. Lee J, Twomey M, Machado C, Gomez G, Doshi M, Gesquiere AJ, et al. Caveolae-mediated endocytosis of conjugated polymer nanoparticles. *Macromolecular Bioscience* (2013) 13(7):913–20.
91. Augustine R, Hasan A, Primavera R, Wilson RJ, Thakor AS, Kevadiya B. Cellular uptake and retention of nanoparticles: insights on particle properties and interaction with cellular components. *Materialstoday Communications* (2020) 25:101692. doi: 10.1016/j.mtcomm.2020.101692
92. Mohammadinejad R, Moosavi MA, Tavakol S, Vardar D.O., Hosseini A, Rahmati M, et al. Necrotic, apoptotic and autophagic cell fates triggered by nanoparticles. *Autophagy* (2019) 15(1):4–33. doi: 10.1080/15548627.2018.1509171
93. Kou L, Bhutia YD, Yao Q, He Z, Sun J, Ganapathy V. Transporter-guided delivery of nanoparticles to improve drug permeation across cellular barriers and drug exposure to selective cell types. *Front Pharmacol* (2018) 9:27. doi: 10.3389/fphar.2018.00027
94. Ali ES, Sharker SM, Islam MT, Khan IN, Shaw S, Rahman MA, et al. *Targeting cancer cells with nanotherapeutics and nanodiagnostics: current status and future perspectives, seminars in cancer biology*. Chicago, USA: Elsevier (2021) p. 52–68.
95. Rosenblum D, Joshi N, Tao W, Karp JM, Peer DJ. Progress and challenges towards targeted delivery of cancer therapeutics. *Nature Communications* (2018) 9(1):1410. doi: 10.1038/s41467-018-03705-y
96. Shi J, Kantoff PW, Wooster R, Farokhzad O. Cancer nanomedicine: progress, challenges and opportunities. *Nature Reviews Cancer* (2017) 17(1):20–37. doi: 10.1038/nrc.2016.108
97. Wilhelm S, Tavares AJ, Chan W. Reply to “Evaluation of nanomedicines: stick to the basics” (Ontario, Canada: Nature Reviews Materials), Vol. 1. (2016). pp. 1–2.
98. Wilhelm S, Tavares AJ, Dai Q, Ohta S, Audet J, Dvorak HF, et al. Analysis of nanoparticle delivery to tumours. *Nature Reviews Materials* (2016) 1(5):1–12. doi: 10.1038/natrevmats.2016.14
99. Maeda H, Bharate G, Daruwalla J. Biopharmaceutics. *Polymeric Drugs efficient tumor-targeted Drug delivery based EPR-effect* (2009) 71(3):409–19. doi: 10.1016/j.jepb.2008.11.010
100. Maeda H, Sawa T, Konno T. Mechanism of tumor-targeted delivery of macromolecular drugs, including the EPR effect in solid tumor and clinical overview of the prototype polymeric drug SMANCS. *Journal of Controlled Release* (2001) 74(1-3):47–61. doi: 10.1016/S0168-3659(01)00309-1
101. Wang Y, Ma J, Qiu T, Tang M, Zhang X, Dong W. *In vitro* and *in vivo* combinatorial anticancer effects of oxaliplatin-and resveratrol-loaded n, O-carboxymethyl chitosan nanoparticles against colorectal cancer. *European Journal of Pharmaceutical Sciences* (2021) 163:105864. doi: 10.1016/j.ejps.2021.105864
102. Tonigold M. Pre-adsorption of antibodies enables targeting of nanocarriers despite a biomolecular corona. *Nat Nanotech* (2018) 13:862–69. doi: 10.1038/s41565-018-0171-6
103. Golombok SK, May J-N, Theek B, Appold L, Drude N, Kiessling F, et al. Tumor targeting via EPR: strategies to enhance patient responses. *Advanced Drug Delivery Reviews* (2018) 130:17–38. doi: 10.1016/j.addr.2018.07.007
104. Dabkeviciene D, Jonusiene V, Zitkute V, Zalyte E, Grigaitis P, Kirveliene V, et al. The role of interleukin-8 (CXCL8) and CXCR2 in acquired chemoresistance of human colorectal carcinoma cells HCT116. *Medical Oncology* (2015) 32:1–7. doi: 10.1007/s12032-015-0703-y
105. Ge P, Niu B, Wu Y, Xu W, Li M, Sun H, et al. Enhanced cancer therapy of celestrol *in vitro* and *in vivo* by smart dendrimers delivery with specificity and biosafety. *Chemical Engineering Journal* (2020) 383:123228. doi: 10.1016/j.cej.2019.123228
106. Bhattacharya S. Anti-EGFR-mAb and 5-fluorouracil conjugated polymeric nanoparticles for colorectal cancer. *Recent Patents on Anti-Cancer Drug Discovery* (2021) 16(1):84–100.
107. Watts ER, Walmsley SR. Inflammation and hypoxia: HIF and PHD isoform selectivity. *Trends in Molecular Medicine* (2019) 25(1):33–46. doi: 10.1016/j.molmed.2018.10.006
108. Wong KE, Ngai SC, Chan K-G, Lee L-H, Goh B-H, Chuah L-H. Curcumin nanoformulations for colorectal cancer: a review. *Frontiers in Pharmacology* (2019) 10:152. doi: 10.3389/fphar.2019.00152
109. Shao M, Chang C, Liu Z, Chen K, Zhou Y, Zheng G, et al. Polydopamine coated hollow mesoporous silica nanoparticles as pH-sensitive nanocarriers for overcoming multidrug resistance. *Colloids and Surfaces B: Biointerfaces* (2019) 183:110427. doi: 10.1016/j.colsurfb.2019.110427
110. Akbarzadeh Khiavi M, Safary A, Barar J, Ajoalabady A, Somi MH, Omid YJC, et al. Multifunctional nanomedicines for targeting epidermal growth factor receptor in colorectal cancer. *Cellular and Molecular Life Sciences* (2020) 77:997–1019.
111. Halder J, Pradhan D, Kar B, Ghosh G, Rath G. Biology, medicine, nanotherapeutics approaches to overcome p-glycoprotein-mediated multi-drug resistance in cancer. (2022) 40:102494.
112. Aminu N, Bello I, Umar NM, Tanko N, Aminu A, Audu MM. The influence of nanoparticulate drug delivery systems in drug therapy. *J Drug delivery Sci Technol* (2020) 60:101961. doi: 10.1016/j.jddst.2020.101961
113. Zhang J, Hu K, Di L, Wang P, Liu Z, Zhang J, et al. Traditional herbal medicine and nanomedicine: converging disciplines to improve therapeutic efficacy and human health. *Advanced Drug Delivery Rev* (2021) 178:113964. doi: 10.1016/j.addr.2021.113964
114. London M, Gallo E. Epidermal growth factor receptor (EGFR) involvement in epithelial-derived cancers and its current antibody-based immunotherapies. *Cell Biol Int* (2020) 44(6):1267–82. doi: 10.1002/cbin.11340
115. Zein R, Sharrouf W, Selting K. Physical properties of nanoparticles that result in improved cancer targeting. *Journal of Oncology* (2020). doi: 10.1155/2020/5194780
116. Shen F, Feng L, Zhu Y, Tao D, Xu J, Peng R, et al. Oxaliplatin-/NLG919 prodrugs-constructed liposomes for effective chemo-immunotherapy of colorectal cancer. *Biomaterials* (2020) 255:120190. doi: 10.1016/j.biomaterials.2020.120190
117. Alomrani A, Badran M, Harisa GI, Alshehry M, Alhariri M, Alshamsan A, et al. The use of chitosan-coated flexible liposomes as a remarkable carrier to enhance the antitumor efficacy of 5-fluorouracil against colorectal cancer. *Saudi Pharm J* (2019) 27(5):603–11. doi: 10.1016/j.jsps.2019.02.008
118. Zu M, Ma Y, Cannup B, Xie D, Jung Y, Zhang J, et al. Oral delivery of natural active small molecules by polymeric nanoparticles for the treatment of inflammatory bowel diseases. *Advanced Drug Delivery Rev* (2021) 176:113887. doi: 10.1016/j.addr.2021.113887
119. Idrees H, Zaidi SZJ, Sabir A, Khan RU, Zhang X, Hassan S-u. A review of biodegradable natural polymer-based nanoparticles for drug delivery applications. *Nanomaterials* (2020) 10(10):1970. doi: 10.3390/nano10101970

120. Udornpornmongkol P, Chiang B-H. Curcumin-loaded polymeric nanoparticles for enhanced anti-colorectal cancer applications. *J Biomaterials Appl* (2015) 30(5):537–46. doi: 10.1177/0885328215594479
121. Badran MM, Mady MM, Ghannam MM, Shakeel F. Preparation and characterization of polymeric nanoparticles surface modified with chitosan for target treatment of colorectal cancer. *Int J Biol macromolecules* (2017) 95:643–9. doi: 10.1016/j.jbiomac.2016.11.098
122. Bhattacharya S, Singh D, Aich J, Shete MB. Development and characterization of hyaluronic acid surface scaffolds encofenib loaded polymeric nanoparticles for colorectal cancer targeting. *Materials Today Commun* (2022) 31:103757. doi: 10.1016/j.mtcomm.2022.103757
123. Więcek AE, Jurak M, Ładniak A, Przykaza K, Szafran K. Cyclosporine CsA—the physicochemical characterization of liposomal and colloidal systems. *Colloids Interfaces* (2020) 4(4):46. doi: 10.3390/colloids4040046
124. Van NH, Vy NT, Van Toi V, Dao AH, Lee B-J. Nanostructured lipid carriers and their potential applications for versatile drug delivery via oral administration. *OpenNano* (2022) 100064. doi: 10.1016/j.onano.2022.100064
125. Rajpoot K, Jain SK. Colorectal cancer-targeted delivery of oxaliplatin via folic acid-grafted solid lipid nanoparticles: preparation, optimization, and *in vitro* evaluation. *Artif cells nanomedicine Biotechnol* (2018) 46(6):1236–47. doi: 10.1080/21691401.2017.1366338
126. Kumar CS, Thangam R, Mary SA, Kannan PR, Arun G, Madhan B. Targeted delivery and apoptosis induction of trans-resveratrol-ferulic acid loaded chitosan coated folic acid conjugate solid lipid nanoparticles in colon cancer cells. *Carbohydr polymers* (2020) 231:115682. doi: 10.1016/j.carbpol.2019.115682
127. Murthy H, Desalegn T, Kassa M, Abebe B, Assefa T. Synthesis of green copper nanoparticles using medicinal plant hagenia abyssinica (Brace) JF. *Gmel. leaf extract: Antimicrobial properties* 2020 (2020) 2020:12. doi: 10.1155/2020/3924081
128. Bhattacharya T, Soares G, Chopra H, Rahman MM, Hasan Z, Swain SS, et al. Applications of phyto-nanotechnology for the treatment of neurodegenerative disorders. *Materials* (2022) 15(3):804. doi: 10.3390/ma15030804
129. Murthy HA, Zeleke TD, Tan K, Ghotekar S, Alam MW, Balachandran R, et al. Enhanced multifunctionality of CuO nanoparticles synthesized using aqueous leaf extract of vernonia amygdalina plant. *Results in Chemistry* (2021) 3:100141. doi: 10.1016/j.rechem.2021.100141
130. Lee KX, Shameli K, Yew YP, Teow S-Y, Jahangirian H, Rafiee-Moghaddam R, et al. Recent developments in the facile bio-synthesis of gold nanoparticles (AuNPs) and their biomedical applications. *International Journal of Nanomedicine* (2020), 275–300. doi: 10.2147/IJN.S233789
131. Mata R, Nakkala JR, Sadras SR. Therapeutic role of biogenic silver and gold nanoparticles against a DMH-induced colon cancer rat model. *Biomaterials Advances* (2023) 146:213279. doi: 10.1016/j.bioadv.2023.213279
132. Liu J, Li Y, Chen S, Lin Y, Lai H, Chen B, et al. Biomedical application of reactive oxygen species-responsive nanocarriers in cancer, inflammation, and neurodegenerative diseases. *Front Chem* (2020) 8:838. doi: 10.3389/fchem.2020.00838
133. Barabadi H, Vahidi H, Damavandi Kamali K, Rashedi M, Hosseini O, Saravanan M. Emerging theranostic gold nanomaterials to combat colorectal cancer: a systematic review. *J Cluster Sci* (2020) 31(4):651–8. doi: 10.1007/s10876-019-01681-x
134. Yang Y, Zheng X, Chen L, Gong X, Yang H, Duan X, et al. Multifunctional gold nanoparticles in cancer diagnosis and treatment. *Int J nanomedicine* (2022) 17:2041–67. doi: 10.2147/IJN.S355142
135. Wang Y, Wang X, Gao T, Lou C, Wang H, Liu Y, et al. Folding of flexible protein fragments and design of nanoparticle-based artificial antibody targeting lysozyme. *J Phys Chem B* (2022) 126(27):5045–54. doi: 10.1021/acs.jpcc.2c03200
136. Din FU, Aman W, Ullah I, Qureshi OS, Mustapha O, Shafique S, et al. Effective use of nanocarriers as drug delivery systems for the treatment of selected tumors. *International Journal of Nanomedicine* (2017) 12:7291–309. doi: 10.2147/IJN.S146315
137. Krasteva N. Promising therapeutic strategies for colorectal cancer treatment based on nanomaterials. *Pharmaceutics* (2022) 14:1213. doi: 10.3390/pharmaceutics14061213
138. Cheng Z, Li M, Dey R, Chen Y. Nanomaterials for cancer therapy: current progress and perspectives. *Journal of Hematology & Oncology* (2021) 14(1):1–27. doi: 10.1186/s13045-021-01096-0
139. Huang W, Wang X, Shi C, Guo D, Xu G, Wang L, et al. Fine-tuning vitamin e-containing telodendrimers for efficient delivery of gambogic acid in colon cancer treatment. *Molecular Pharmaceutics* (2015) 12(4):1216–29. doi: 10.1021/acs.molpharmaceut.5b00051
140. L.-p. Wu M, Christensen JB, Trohopoulos PN, Moghimi S. Dendrimers in medicine: therapeutic concepts and pharmaceutical challenges. *Bioconjugate Chemistry* (2015) 26(7):1198–211.
141. Mignani S, Majoral J-P. Dendrimers as macromolecular tools to tackle from colon to brain tumor types: a concise overview. *New Journal of Chemistry* (2013) 37(11):3337–57. doi: 10.1039/c3nj00300k
142. Zhuo RX, Du B, Lu Z. *In vitro* release of 5-fluorouracil with cyclic core dendritic polymer. *Journal of Controlled Release* (1999) 57(3):249–57. doi: 10.1016/S0168-3659(98)00120-5
143. Lee CC, Gillies ER, Fox ME, Guillaudeu SJ, Fréchet JM, Dy EE, et al. A single dose of doxorubicin-functionalized bow-tie dendrimer cures mice bearing c-26 colon carcinomas. *Proceedings of the National Academy of Sciences* (2006) 103(45):16649–54. doi: 10.1073/pnas.0607705103
144. Brar B, Ranjan K, Palria A, Kumar R, Ghosh M, Sihag S, et al. Nanotechnology in colorectal cancer for precision diagnosis and therapy. *Frontiers in Nanotechnology* (2021) 3:699266. doi: 10.3389/fnano.2021.699266
145. Chauhan A. Dendrimers for drug delivery *Molecules*. (2018) 23(4):938. doi: 10.3390/molecules23040938
146. Naeimi R, Najafi R, Molaei P, Amini R, Pecic S. Nanoparticles: the future of effective diagnosis and treatment of colorectal cancer? *European Journal of Pharmacology* (2022) 936:175350. doi: 10.1016/j.ejphar.2022.175350
147. Tsakiris N, Fauvet F, Ruby S, Puisieux A, Paquot A, Muccioli GG, et al. Combined nanomedicines targeting colorectal cancer stem cells and cancer cells. *Journal of Controlled Release* (2020) 326:387–95. doi: 10.1016/j.jconrel.2020.07.025
148. Yousefpour Marzbali M, Yari Khosroushahi A. Polymeric micelles as mighty nanocarriers for cancer gene therapy: a review. *Cancer Chemotherapy and Pharmacology* (2017) 79:637–49.
149. Bhadra D, Bhadra S, Jain S, Jain N. A PEGylated dendritic nanoparticulate carrier of fluorouracil *International Journal of Pharmaceutics* (2003) 257(1–2):111–24. doi: 10.1016/S0378-5173(03)00132-7
150. Amin MC, Butt AM, Amjad MW, Kesharwani P. , *polymeric micelles for drug targeting and delivery, nanotechnology-based approaches for targeting and delivery of drugs and genes*. India: Elsevier (2017) p. 167–202.
151. Ameli H, Alizadeh N. Targeted delivery of capecitabine to colon cancer cells using nano polymeric micelles based on beta cyclodextrin. *RSC Advances* (2022) 12(8):4681–91. doi: 10.1039/D1RA07791K
152. Zhou Q, Zhang L, Yang T, Wu H. Stimuli-responsive polymeric micelles for drug delivery and cancer therapy. *International Journal of Nanomedicine* (2018) 13:2921. doi: 10.2147/IJN.S158696
153. Stang J, Haynes M, Carson P, Moghaddam M. A preclinical system prototype for focused microwave thermal therapy of the breast. *IEEE Transactions on Biomedical Engineering* (2012) 59(9):2431–8. doi: 10.1109/TBME.2012.2199492
154. Radhakrishnan K, Gupta S, Gnanadhas DP, Ramamurthy PC, Chakravorty D, Raichur A, et al. Protamine-capped mesoporous silica nanoparticles for biologically triggered drug release. *Particle & Particle Systems Characterization* (2014) 31(4):449–58. doi: 10.1002/ppsc.201300219
155. Hanafi-Bojd MY, Jaafari MR, Ramezani N, Xue M, Amin M, Shahtahmassebi N, et al. Biopharmaceutics, surface functionalized mesoporous silica nanoparticles as an effective carrier for epirubicin delivery to cancer cells *European Journal of Pharmaceutics and Biopharmaceutics* (2015) 89:248–58.
156. Bretin L, Pinon A, Bouramtane S, Ouk C, Richard L, Perrin M-L, et al. Photodynamic therapy activity of new porphyrin-ylated silica nanoparticles in human colorectal cancer. *17th International Photodynamic Association World Congress* (2019) 11(10):1474. doi: 10.1117/12.2525033
157. Espinosa A, Di Corato R, Kolosnjaj-Tabi J, Flaud P, Pellegrino T, Wilhelm C. Duality of iron oxide nanoparticles in cancer therapy: amplification of heating efficiency by magnetic hyperthermia and photothermal bimodal treatment. *ACS Nano* (2016) 10(2):2436–46. doi: 10.1021/acsnano.5b07249
158. Murali N, Rainu SK, Singh N, Betal S. Advanced materials and processes for magnetically driven micro- and nano-machines for biomedical application. *Biosensors and Bioelectronics: X* (2022) 11:100206. doi: 10.1016/j.biosx.2022.100206
159. Esmaelbeygi E, Khoei S, Khoei S, Eynali S. Role of iron oxide core of polymeric nanoparticles in the thermosensitivity of colon cancer cell line HT-29. *International Journal of Hyperthermia* (2015) 31(5):489–97. doi: 10.3109/02656736.2015.1035766
160. Feng S-T, Li J, Luo Y, Yin T, Cai H, Wang Y, et al. pH-sensitive nanomicelles for controlled and efficient drug delivery to human colorectal carcinoma LoVo cells. *PLOS ONE* (2014) 9(6):e100732. doi: 10.1371/journal.pone.0100732
161. Patel KD, Singh RK, Kim H-W. Carbon-based nanomaterials as an emerging platform for theranostics. *Materials Horizons* (2019) 6(3):434–69. doi: 10.1039/C8MH00966j
162. Maiti D, Tong X, Mou X, Yang K. Carbon-based nanomaterials for biomedical applications: a recent study. *Frontiers in Pharmacology* (2019) 9:1401. doi: 10.3389/fphar.2018.01401
163. Hampel S, Kunze D, Haase D, Krämer K, Rauschenbach M, Ritschel M, et al. Carbon nanotubes filled with a chemotherapeutic agent: a nanocarrier mediates inhibition of tumor cell growth. *Nanomedicine* (2008) 3:175–82. doi: 10.2217/17435889.3.2.175
164. Lee Y, Geckeler K. Cellular interactions of a water-soluble supramolecular polymer complex of carbon nanotubes with human epithelial colorectal adenocarcinoma cells. *Macromolecular Bioscience* (2012) 12(8):1060–7. doi: 10.1002/mabi.201200085
165. Zhou M, Peng Z, Liao S, Li P, Li S. Design of microencapsulated carbon nanotube-based microspheres and its application in colon targeted drug delivery. *Drug Delivery* (2014) 21(2):101–9. doi: 10.3109/10717544.2013.834413
166. Levi-Polyachenko NH, Merkel EJ, Jones BT, Carroll DL, Stewart JHIV. Rapid photothermal intracellular drug delivery using multiwalled carbon nanotubes. *Molecular Pharmaceutics* (2009) 6(4):1092–9. doi: 10.1021/mp800250e

167. Zakaria AB, Picaud F, Rattier T, Pudlo M, Saviot L, Chassagnon R, et al. Nanovectorization of TRAIL with single wall carbon nanotubes enhances tumor cell killing. *Nano Letters* (2015) 15(2):891–5. doi: 10.1021/nl503565t
168. Halavach TM, Savchuk ES, Bobovich AS, Dudchik NV, Tsygankow VG, Tarun EI, et al. Antimutagenic and antibacterial activity of β -cyclodextrin clathrates with extensive hydrolysates of colostrum and whey. *Biointerface Research in Applied Chemistry* (2021) 11:8626–38. doi: 10.33263/BRIAC112.86268638
169. Cid-Samamed A, Rakmai J, Mejuto JC, Simal-Gandara J, Astray GJ. Cyclodextrins inclusion complex: preparation methods, analytical techniques and food industry applications. *Food Chemistry* (2022) 384:132467. doi: 10.1016/j.foodchem.2022.132467
170. Mousazadeh H, Pilehvar-Soltanahmadi Y, Dadashpour M, Zarghami N. Cyclodextrin based natural nanostructured carbohydrate polymers as effective non-viral siRNA delivery systems for cancer gene therapy. *Journal of Controlled Release* (2021) 330:1046–70. doi: 10.1016/j.jconrel.2020.11.011
171. Kfoury M, Landy D, Fourmentin S. Characterization of cyclodextrin/volatile inclusion complexes: a review. *Molecules* (2018) 23(5):1204. doi: 10.3390/molecules23051204
172. Kost B, Brzeziński M, Socka M, Baśko M, Biela T. Biocompatible polymers combined with cyclodextrins: fascinating materials for drug delivery applications. *Molecules* (2020) 25(15):3404. doi: 10.3390/molecules25153404
173. Bai S, Zhang X, Ma X, Chen J, Chen Q, Shi X, et al. Acid-active supramolecular anticancer nanoparticles based on cyclodextrin polyrotaxanes damaging both mitochondria and nuclei of tumor cells. *Biomaterials Science* (2018) 6(12):3126–38. doi: 10.1039/C8BM01020J
174. Ünal S, Öztürk SC, Bilgiç E, Yanık H, Korkusuz P, Aktaş Y, et al. Biopharmaceutics, therapeutic efficacy and gastrointestinal biodistribution of polycationic nanoparticles for oral camptothecin delivery in early and late-stage colorectal tumor-bearing animal model. *European Journal of Pharmaceutics and Biopharmaceutics* (2021) 169:168–77. doi: 10.1016/j.ejpb.2021.10.010
175. Mortezaadeh T, Gholibegloo E, Alam NR, Dehghani S, Haghighi S, Ghanaati H, et al. Biology, medicine, gadolinium (III) oxide nanoparticles coated with folic acid-functionalized poly (β -cyclodextrin-co-pentetic acid) as a biocompatible targeted nano-contrast agent for cancer diagnostic: *in vitro* and *in vivo* studies. *Magnetic Resonance Materials in Physics, Biology and Medicine* (2019) 32:487–500. doi: 10.1007/s10334-019-00738-2
176. Golshani G, Zhang Y. Advances in immunotherapy for colorectal cancer: a review. *Therapeutic Advances in Gastroenterology* (2020) 13:1756284820917527. doi: 10.1177/1756284820917527
177. Kranz LM, Diken M, Haas H, Kreiter S, Loquai C, Reuter KC, et al. Systemic RNA delivery to dendritic cells exploits antiviral defence for cancer immunotherapy. *Nature* (2016) 534(7607):396–401. doi: 10.1038/nature18300
178. Diaz-Arévalo D, Zeng M. *Nanoparticle-based vaccines: opportunities and limitations, nanopharmaceutics*. Germany: Elsevier (2020) p. 135–50.
179. Zhao P, Xu Y, Ji W, Li L, Qiu L, Zhou S, et al. Hybrid membrane nanovaccines combined with immune checkpoint blockade to enhance cancer immunotherapy. *International Journal of Nanomedicine* (2022) 17:73–89. doi: 10.2147/IJN.S346044
180. Irvine DJ, Swartz MA, Szeto GL. Engineering synthetic vaccines using cues from natural immunity. *Nature Materials* (2013) 12(11):978–90. doi: 10.1038/nmat3775
181. Lyon PC, Griffiths LF, Lee J, Chung D, Carlisle R, Wu F, et al. Clinical trial protocol for TARDOX: a phase I study to investigate the feasibility of targeted release of lyso-thermosensitive liposomal doxorubicin (ThermoDox[®]) using focused ultrasound in patients with liver tumours. *Journal of Therapeutic Ultrasound* (2017) 5(1):1–8. doi: 10.1186/s40349-017-0104-0
182. Cheng Y-H, He C, Riviere JE, Monteiro-Riviere NA, Lin ZJ. Meta-analysis of nanoparticle delivery to tumors using a physiologically based pharmacokinetic modeling and simulation approach. *ACS Nano* (2020) 14(3):3075–95. doi: 10.1021/acsnano.9b08142
183. Bertrand N, Wu J, Xu X, Kamaly N, Farokhzad O. Cancer nanotechnology: the impact of passive and active targeting in the era of modern cancer biology. *Advanced Drug Delivery Reviews* (2014) 66:2–25. doi: 10.1016/j.addr.2013.11.009
184. Murar M, Albertazzi L, Pujals SJN. Advanced optical imaging-guided nanotheranostics towards personalized cancer drug delivery. *Nanomaterials* (2022) 12(3):399. doi: 10.3390/nano12030399
185. Praveen TK, Gangadharappa HV, Lila ASA, Moin A, Mehmood K, Krishna KL, et al. *Inflammation targeted nanomedicines: patents and applications in cancer therapy, seminars in cancer biology*. India:Elsevier (2022).
186. Xunjin Z, Wong WK, Fengshou W. Hong Kong Baptist University HKBU, 2019. *Conjugated porphyrin carbon quantum dots for targeted photodynamic therapy* (2019) U.S. Patent 10,369,221. <https://patents.google.com/patent/US10369221B2/en>
187. Bayever E, Dhindsa N, Jonathan BF, Laivins P, Moyo V, Niyikiza C. Methods for treating pancreatic cancer using combination therapies comprising liposomal irinotecan. (2016) U.S. Patent 9,492,442.
188. Kuppusamy P, Ichwan SJ, Al-Zikri PNH, Suriyah WH, Soundharrajan I, Govindan N, et al. *In vitro* anticancer activity of Au, Ag nanoparticles synthesized using Commelina nudiflora l. aqueous extract against HCT-116 colon cancer cells. *Biological Trace Element Research* (2016) 173:297–305. doi: 10.1007/s12011-016-0666-7



OPEN ACCESS

EDITED BY

Alessandro Passardi,
Scientific Institute of Romagna for the
Study and Treatment of Tumors (IRCCS),
Italy

REVIEWED BY

Michael Braun,
Christie Hospital NHS Foundation Trust,
United Kingdom
Cathy Eng,
Vanderbilt University, United States

*CORRESPONDENCE

Gudrun Piringer
✉ gudrun.piringer@hotmail.com

RECEIVED 30 May 2023

ACCEPTED 17 July 2023

PUBLISHED 09 August 2023

CITATION

Piringer G, Gruenberger T, Thaler J,
Kührer I, Kaczirek K, Längle F, Viragos-
Toth I, Amann A, Eisterer W, Függer R,
Andel J, Pichler A, Stift J, Sölkner L,
Gnant M and Öfner D (2023) LM02 trial
Perioperative treatment with panitumumab
and FOLFIRI in patients with wild-type RAS,
potentially resectable colorectal cancer
liver metastases—a phase II study.
Front. Oncol. 13:1231600.
doi: 10.3389/fonc.2023.1231600

COPYRIGHT

© 2023 Piringer, Gruenberger, Thaler,
Kührer, Kaczirek, Längle, Viragos-Toth,
Amann, Eisterer, Függer, Andel, Pichler, Stift,
Sölkner, Gnant and Öfner. This is an open-
access article distributed under the terms of
the [Creative Commons Attribution License](https://creativecommons.org/licenses/by/4.0/)
(CC BY). The use, distribution or
reproduction in other forums is permitted,
provided the original author(s) and the
copyright owner(s) are credited and that
the original publication in this journal is
cited, in accordance with accepted
academic practice. No use, distribution or
reproduction is permitted which does not
comply with these terms.

LM02 trial Perioperative treatment with panitumumab and FOLFIRI in patients with wild-type RAS, potentially resectable colorectal cancer liver metastases—a phase II study

Gudrun Piringer^{1,2*}, Thomas Gruenberger³, Josef Thaler^{1,2},
Irene Kührer⁴, Klaus Kaczirek⁴, Friedrich Längle⁵,
Istvan Viragos-Toth⁵, Arno Amann⁶, Wolfgang Eisterer⁷,
Reinhold Függer⁸, Johannes Andel⁹, Angelika Pichler¹⁰,
Judith Stift¹¹, Lidija Sölkner¹², Michael Gnant¹³
and Dietmar Öfner¹⁴ on behalf of the Austrian Breast
and Colorectal Cancer Study Group (ABCSCG)

¹Department of Internal Medicine IV, Klinikum Wels-Grieskirchen, Wels, Austria, ²Medical Faculty, Johannes Kepler University Linz, Linz, Austria, ³Department of Surgery, Clinic Favoriten, Hepato-Pancreato-Biliary Center, Health Network Vienna and Sigmund Freud University, Vienna, Austria, ⁴Division of General Surgery, Department of Surgery, Medical University of Vienna, Vienna, Austria, ⁵Department of Surgery, Landeskrankenhaus Wiener Neustadt, Wiener Neustadt, Austria, ⁶Department of Haematology and Oncology, Medical University of Innsbruck, Innsbruck, Austria, ⁷Department of Internal Medicine and Oncology, Klinikum Klagenfurt, Klagenfurt, Austria, ⁸Department of General and Visceral Surgery, Congregation Hospital, Linz, Austria, ⁹Department of Internal Medicine II, Landeskrankenhaus Steyr, Steyr, Austria, ¹⁰Department of Hematology and Oncology, Landeskrankenhaus Hochsteiermark, Leoben, Austria, ¹¹Department of Pathology, Medical University of Vienna, Vienna, Austria, ¹²Department of Statistics, Austrian Breast and Colorectal Cancer Study Group, Vienna, Austria, ¹³Comprehensive Cancer Center, Medical University of Vienna, Vienna, Austria, ¹⁴Department of Visceral-, Transplant- and Thoracic Surgery, Medical University of Innsbruck, Innsbruck, Austria

Background: Twenty percent of colorectal cancer liver metastases (CLMs) are initially resectable with a 5-year survival rate of 25%–40%. Perioperative folinic acid, 5-fluorouracil, oxaliplatin (FOLFOX) increases progression-free survival (PFS). In advanced disease, the addition of targeting therapies results in an overall survival (OS) advantage. The aim of this study was to evaluate panitumumab and FOLFIRI as perioperative therapy in resectable CLM.

Methods: Patients with previously untreated, wild-type Rat sarcoma virus (RAS), and resectable CLM were included. Preoperative four and postoperative eight cycles of panitumumab and folinic acid, 5-fluorouracil, irinotecan (FOLFIRI) were administered. Primary objectives were efficacy and safety. Secondary endpoints included PFS and OS.

Results: We enrolled 36 patients in seven centers in Austria (intention-to-treat analyses, 35 patients). There were 28 men and seven women, and the median age was 66 years. About 91.4% completed preoperative therapy and 82.9% underwent

liver resection. The R0 resection rate was 82.7%. Twenty patients started and 12 patients completed postoperative chemotherapy. The objective radiological response rate after preoperative therapy was 65.7%. About 20% and 5.7% of patients had stable disease and progressive disease, respectively. The most common grade 3 adverse events were diarrhea, rash, and leukopenia during preoperative therapy. One patient died because of sepsis, and one had a pulmonary embolism grade 4. After surgery, two patients died because of hepatic failure. Most common grade 3 adverse events during postoperative therapy were skin toxicities/rash and leukopenia/neutropenia, and the two grade 4 adverse events were stroke and intestinal obstruction. Median PFS was 13.2 months. The OS rate at 12 and 24 months were 85.6% and 73.3%, respectively.

Conclusions: Panitumumab and FOLFIRI as perioperative therapy for resectable CLM result in a radiological objective response rate in 65.7% of patients with a manageable grade 3 diarrhea rate of 14.3%. Median PFS was 13.2 months, and the 24-month OS rate was 73.3%. These data are insufficient to widen the indication of panitumumab from the unresectable setting to the setting of resectable CLM.

KEYWORDS

LM02-trial, perioperative therapy, CRLM, panitumumab-FOLFIRI, anti-EGFR-therapy

Introduction

Colorectal cancer is the second leading cause of mortality in Western countries (1, 2). Nearly half of patients will develop colorectal cancer liver metastases (CLMs) during the course of their disease, with 15%–25% of patients having CLM at the primary diagnosis and another 20% of patients will develop CLM during the first 3 years after the primary diagnosis (3, 4). About one-fifth of patients with CLM have no other sites of metastasis. Despite advances in survival with chemotherapy, surgical resection of CLM is still considered the only curative treatment option. About 20% of patients with CLM are candidates for primary resection (5) and result in a 25%–40% 5-year survival (6–9). Unfortunately, 70% of patients will develop recurrent disease after liver resection (10).

The advantages of postoperative chemotherapy after curative resection of CLM resection are uncertain. In the European Organisation for Research and Treatment of Cancer (EORTC) 40983 study, perioperative chemotherapy with FOLFOX4 and surgery were compared with surgery alone in patients with potentially resectable CLM (11). Progression-free survival (PFS) was significantly improved by 9.2% at 3 years for those who received perioperative chemotherapy. However, the trial did not demonstrate any significant benefit in overall survival (OS) (12). Similar results were shown in a meta-analysis evaluating perioperative chemotherapy for patients with resectable CLM (13). The observed benefit in PFS with perioperative FOLFOX remains one of the standard treatments for resectable CLM in many centers worldwide.

The addition of targeting therapies to chemotherapy has markedly improved outcome in metastatic colorectal cancer (mCRC) and significantly improves the objective response rate (ORR), PFS, and OS (14–20). Furthermore, combination therapies may convert unresectable to resectable liver metastases, allowing potentially curative resection.

The optimal combination of systemic drugs in the neoadjuvant setting of patients with potentially resectable CLM has not been established. Unanswered questions are the best chemotherapy combinations with or without targeted agents to induce maximum response, the length of initial treatment to verify response without liver tissue damage, and the correlation of response with potential biomarkers.

The present LM02 trial from the Austrian Breast and Colorectal Cancer Study Group (ABCSCG) investigated the use of perioperative systemic therapy with panitumumab and FOLFIRI in patients with primary resectable CLM.

Methods

Patient population

Patients with wild-type RAS mCRC with potentially histologically confirmed resectable liver metastases, at least one measurable metastatic lesion in the liver as per the Response Evaluation Criteria in Solid Tumor (RECIST) 1.1 guidelines, and without prior therapy for mCRC were eligible. CLMs were defined

as resectable when it was anticipated that the disease can be completely resected, two adjacent liver segments could be spared adequate vascular inflow and outflow and biliary drainage could be preserved, and the volume of the liver remaining after resection would be adequate (at least 20% of the total estimated liver volume). Other key eligibility criteria included: patients ≥ 18 years with Eastern Cooperative Oncology Group (ECOG) performance status 0 and 1, and adequate metabolic, hematological, renal, and hepatic functions. We excluded patients with (a) prior chemotherapy for the treatment of current mCRC including biologics; (b) extrahepatic metastatic disease; (c) prior adjuvant or neoadjuvant (chemo) therapy for the treatment of CRC ≤ 26 weeks prior to registration; (d) radiotherapy ≤ 14 days prior to registration; (e) previous malignancy other than CRC in the last 5 years except basal cell carcinoma of the skin and/or *in situ* carcinoma of the cervix; (f) active infection requiring systemic treatment; (g) any investigational agent or therapy ≤ 28 days before registration; (h) clinically significant cardiovascular disease ≤ 1 year before registration; (i) known allergy or hypersensitivity to irinotecan; 5-fluorouracil (5-FU), leucovorin, or panitumumab; (j) history of severe adverse events (AEs) to iodinated contrast agents; (k) history of interstitial pneumonitis or pulmonary fibrosis or evidence of interstitial lung disease on baseline chest computer tomography (CT) scan; (l) known positive test(s) for human immunodeficiency virus infection, hepatitis C virus, and acute or chronic active hepatitis B infection; (m) any co-morbid disease or condition that could increase the risk of toxicity; (n) any uncontrolled concurrent illness or history of any medical condition that may interfere with the interpretation of the study results; (o) major surgical procedure (requiring general anesthesia) ≤ 28 days prior registration and (p) pregnant or breastfeeding women.

Exploratory biomarker studies suggested that other activating RAS mutations also were a negative predictive biomarker for anti-epithelial growth factor receptor (EGFR) therapy. Patients with mutations beyond the known K-Rat sarcoma virus (KRAS) exon 2 mutations, in KRAS exon 3 (codons 59 and 61), exon 4 (codons 117 and 146) or NRAS exon 2 (codons 12 and 13), exon 3 (codons 59 and 61), and exon 4 (codons 117 and 146), did not respond to anti-EGFR therapy. These data were published during the running study (15, 21, 22). Therefore, the study was stopped in 2013 temporarily for an amendment. In the first phase, patients with wild-type KRAS were included, and, after the amendment, only patients with wild-type RAS mCRC were included. Microsatellite status was not evaluated because the importance of Microsatellite instability status (MSI) was not known in the recruitment period.

Medical ethics committees of all participating centers approved the trial, and all patients provided a written informed consent (EudraCT-No: 2012_000265-20). This study was sponsored by the ABCSG.

Study design

This was an open-label phase II multicenter trial to evaluate the efficacy and safety of perioperative panitumumab in combination with FOLFIRI and liver resection in patients with previously untreated, wild-type RAS, and potentially resectable CLM. The

preoperative therapy consisted of four cycles panitumumab and FOLFIRI every 14 days. Surgery was performed 4–8 weeks after the last administration of the study medication. Postoperative eight cycles of panitumumab and FOLFIRI were planned 4–6 weeks after surgery. Follow-up was done for up to 2 years after the end of postoperative chemotherapy. A uniform CT with liver protocol was done in all seven sites. PET-CT was not standard imaging. Primary endpoints were ORR and the rate of grade 3–4 diarrhea during preoperative therapy. Secondary endpoints included evaluation of resection rate, perioperative morbidity and mortality as measured by the Dindo classification (23), proportion of subjects with complete pathological response as measured by Rubbia–Brandt tumor regression grade (24), PFS, and OS. The study was a two-step design. After application of preoperative therapy to 15 patients, safety and efficacy were evaluated. If at least five patients exhibited an objective response according to RECIST 1.1 and if there were not more than three patients with grade 3–4 diarrhea during the four cycles of therapy, then additional 21 patients were included.

Treatment

Preoperative treatment

Patients were treated with four cycles panitumumab and FOLFIRI before surgery of the liver metastases. Panitumumab was administered at a dose of 6 mg/kg on day 1 of each cycle. Irinotecan of 180 mg/m² was administered followed by leucovorin 400 mg/m². Thereafter, 5-FU of 400mg/m² was given as an intravenous bolus followed by a 5-FU continuous intravenous infusion of 2,400 mg/m² over 46 h. A cycle of panitumumab and FOLFIRI was defined as 14 days. Toxicities were assessed and recorded at every visit and graded according to the common terminology criteria for AEs (National Cancer Institute common Terminology Criteria for Adverse Events (NCI CTCAE) version 4.0) (25). Panitumumab and FOLFIRI dose modification schemes were applied if patients experienced grade 2–4 toxicities. Dose modification was not required for toxicities that were considered unlikely to become serious or life-threatening (e.g., alopecia).

Surgery

After end of preoperative therapy, chest–abdomen–pelvis CT and tumor marker to access response to preoperative therapy was carried out 2–3 weeks after last administration of the study medications. Surgery was planned 4–8 weeks after end of therapy and was performed by experienced liver surgeons. Synchronous resection of liver metastases and primary tumor was allowed if liver resection was limited to <2 liver segments. Otherwise, primary tumor was resected 4–6 weeks after liver resection. In case the tumor deemed non-resectable, following therapy according to the institutional standard was recommended.

Postoperative treatment

Postoperative eight cycles of panitumumab and FOLFIRI were planned every 14 days. Therapy was started 4–6 weeks after last surgery following CT assessment and complete wound healing.

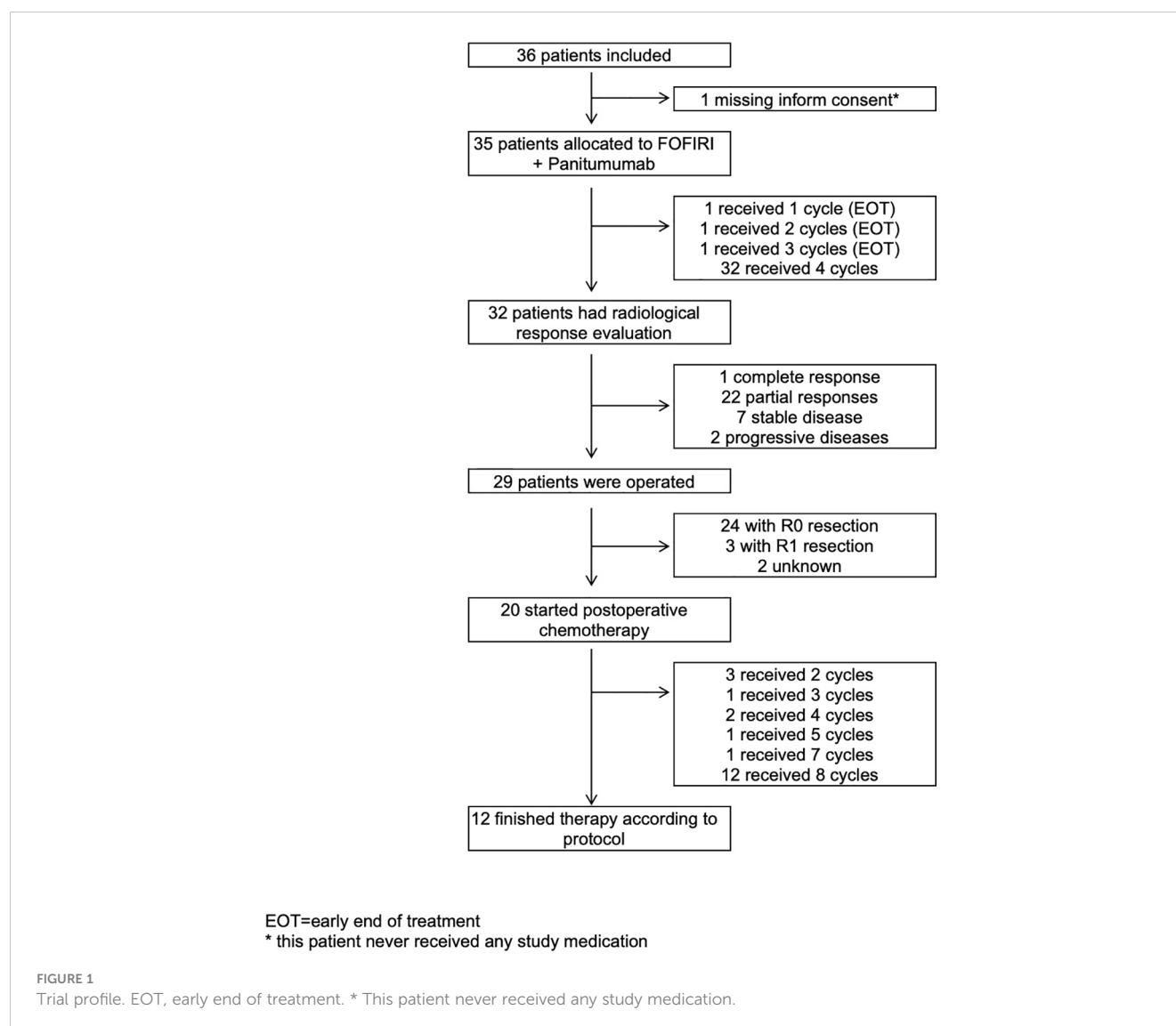
Statistical analysis

The primary endpoints ORR and safety were evaluated descriptively. ORR after four cycles of preoperative therapy was evaluated using RECIST 1.1 measured by multislice three-phase CT. To assess safety the rate of patients with grade 3–4 diarrhea during four cycles of preoperative therapy was documented. The sample size for the primary endpoints was estimated using the Bryant & Day Phase II clinical trial design. Because of the two-step design, the safety and efficacy after application of preoperative therapy to 15 patients were evaluated. If at least five patients exhibited an objective response according and if there were not more than three patients with grade 3–4 diarrhea during these four cycles, then additional 21 patients would be included. The statistical analysis was based on the “intention-to-treat” (ITT) principle, all patients enrolled were included. Patients who withdraw informed consent were considered as non-successes (without ORR and with grade 3–4 diarrhea). Patients who would not undergo surgical resection were included in the final analyses. Evaluation of secondary endpoints

included resection rate, perioperative morbidity and mortality, rate of complete pathological remission, PFS, and OS.

Results

A total of 36 patients were enrolled into the study in seven Austrian institutions from October 2012 through June 2017. ITT analyses included 35 patients (Figure 1). One patient was excluded because the informed consent was missing. Nevertheless, this patient never received any study medication due to an exclusion criterion (hepatitis C virus). Of the patients, 28 (80%) were men and seven (20%) were women. The median age was 66 years (range, 32–81). A total of 19, 6, and 10 patients had colon cancer, cancer in the rectosigmoid, and rectal cancer, respectively. Of the 35 patients, 20 (57.1%) and 15 (42.9%) developed liver metastases metachronous and synchronous at primary tumor diagnosis, respectively. Liver metastases occurred in 23 patients (65.7%) within 2 years of primary cancer diagnoses and in nine patients (25.7%) after 2



years. Most of patients had one liver metastases ($n = 13$, 37.1%), followed by two lesions in 10 patients (28.6%); three lesions in six patients (17.1%); and four, five, and six lesions each in two patients (5.7%). ECOG performance status 0 and 1 was in 29 (82.9%) and six (17.1%) patients. Fifteen (42.9%) patients had wild-type KRAS tumor, and 20 (57.1%) patients had wild-type RAS tumor. In seven (20%) patients, radiotherapy of the primary rectal tumor was done. In 25 (71.4%) and eight (22.9%) patients, primary tumors were resected before registration for the study and during study, and two (5.7%) patients had no surgery of the primary tumor. Adjuvant chemotherapy for the primary cancer was administered to seven patients (20%). [Table 1](#) shows the baseline characteristics of the patients.

Efficacy and safety were evaluated after 15 patients according to the two-step design of the trial. Objective response was found in 13 (86.7%) of the 15 patients with 12 partial remissions (PRs) and one complete response (CR). One patient had a stable disease (SD), and one patient had missing response evaluation. Grade 3 diarrhea occurred in two (13.3%) patients, and no grade 4 diarrhea was observed during the preoperative therapy. On the basis of these results, the criteria for continuing the study were met.

In the final analysis, 32 (91.4%) of the 35 patients completed the planned four cycles of preoperative therapy. One patient each had stopped preoperative therapy with panitumumab and FOLFIRI after the first, second, and third cycle. In the preoperative treatment phase, 34 (97.1%) patients suffered at least one grade 1–5 AE. Thirteen (37.1%) patients had at least one grade 3 AE, one patient (2.9%) had grade 4 AE (pulmonary embolism), and one patient (2.9%) had grade 5 AE (sepsis). Most grade 3 AEs were diarrhea in four patients (11.4%), leukopenia in three patients (8.6%), rash in three patients (8.6%), acne in two patients (5.7%), and one patient each (2.9%) had cardiac failure, pyrexia, urinary tract infection, uncontrolled hypertension, dehydration, stroke, dyspnea, and maculo-papular skin toxicity as grade 3 AEs ([Table 2](#)). Grade 3 diarrhea during preoperative therapy occurred in four patients. In one patient who discontinued treatment early due to AEs, the documentation whether he had a grade 3–4 diarrhea was missing. Therefore, the occurrence of a diarrhea grade 3–4 AE was assumed in accordance with a worst-case scenario for the main ITT analysis. Hence, diarrhea grade 3 occurred in 14.3% of patients.

Among 35 patients in the ITT population, 32 (91.4%) had a documented radiological response evaluation after preoperative therapy ([Table 3](#)). Those three patients without a documented response evaluation discontinued treatment early due to a serious AE or investigators decision and died shortly after treatment discontinuation. According to ITT rules (worst case), their objective response was evaluated as “no objective response.” Objective radiological response rate after preoperative therapy was 65.7% ($n = 23$) with one radiological complete remission (CR) (2.7%) and 22 (62.7%) PR. In 20% ($n = 7$) and 5.7% ($n = 2$) of patients, SD and progressive disease (PD) were documented, respectively. A sensitivity analysis, only in patients who finished all four cycles of preoperative therapy, resulted in an ORR of 71.9%.

Surgery of the liver metastases was done in 29 (82.9%) patients ([Table 4](#)). Surgery was done after a mean of 6.62 weeks (median, 6.14 weeks; range, 3–11.9 weeks) after last administration of

TABLE 1 Characteristics of patients at baseline.

Age (years)	
Median (range)	66 (32–81)
Sex	
Men	28 (80%)
Women	7 (20%)
WHO performance status	
0	29 (82.9%)
1	6 (17.1%)
Synchronicity of liver metastases	
Synchronous metastases	15 (42.9%)
Metachronous metastases	20 (57.1%)
Time from diagnosis of primary to diagnosis of liver metastases	
< 2 years	23 (65.7%)
> 2 years	9 (25.7%)
Number of liver metastases	
1	13 (37.1%)
2	10 (28.6%)
3	6 (17.1%)
4	2 (5.7%)
5	2 (5.7%)
6	2 (5.7%)
T category of the primary cancer	
T1	1 (2.9%)
T2	5 (14.3%)
T3	21 (60.0%)
Tx	8 (22.9%)
Lymphatic spread of the primary cancer	
N0	11 (31.4%)
N1	8 (22.9%)
N2	5 (14.3%)
Nx	11 (31.4%)
Location of primary cancer	
Colon	19 (54.3%)
Rectosigmoid	6 (17.1%)
Rectum	10 (28.6%)
Previous adjuvant chemotherapy of primary cancer	
No	28 (80%)
Yes	7 (20%)

preoperative therapy. Reasons for non-resection were early end of treatment (EOT) during preoperative phase in three patients, documented progression disease with new liver lesions in one patient, inadequate future liver remaining in one patient (despite a PR after preoperative therapy), and inoperable retrospective at baseline in one patient. R0 and R1 resection rate was 82.8% ($n = 24$) and 10.3% ($n = 3$). In one patient, the resection rate was not measurable, and, in one patient, the documentation of resection rate was missing. Types of liver resection are shown in [Table 4](#). Histological tumor response to preoperative therapy was centrally evaluated using the Rubbia–Brandt classification ([Table 5](#)) (24). From 29 patients with surgery, in four patients evaluation was not

TABLE 2 Adverse events during preoperative and postoperative therapy.

Adverse Event	Grade 3	Grade 4	Grade 5
During preoperative chemotherapy period			
Leukopenia	3 (8.6%)		
Cardiac failure	1 (2.9%)		
Diarrhoe	4 (11.4%)		
Pyrexia	1 (2.9%)		
Urinary tract infection	1 (2.9%)		
Blood pressure increased	1 (2.9%)		
Dehydration	1 (2.9%)		
Cerebrovascular stroke	1 (2.9%)		
Dyspnoe	1 (2.9%)		
Pulmonary embolism		1 (2.9%)	
Rash/Acne/Dermatitis	6 (17.1%)		
Sepsis			1 (2.9%)
During postoperative chemotherapy period			
Anaemia	1 (5%)		
Leukopenia/Neutropenia	2 (10%)		
Diarrhoea	1 (5%)		
Ileus		1 (5%)	
Anal Abscess	1 (5%)		
fungal infection	1 (5%)		
cerebrovascular stroke		1 (5%)	
Pulmonary embolism	1 (5%)		
rash/skin toxicity	4 (20%)		
deep vein thrombosis	1 (5%)		

Data in number (%) unless otherwise stated. Patients may have several complications; therefore, the number of complications does not add up to total number of patients. Common toxicity criteria (25) version 4.0 was used.

possible. There were two patients with Rubbia-Brandt tumor regression grade 1 (complete pathological response). Two patients died after surgery because of hepatic failure: one patient within 30 days after surgery and the other one 120 days after surgery (Table 4). Both patients had a hemihepatectomy right. One patient had SD, and one patient PR after preoperative therapy. The sum size of metastases was 112 and 75 mm. Surgical complications were measured by the Clavien-Dindo classification (Table 6).

Twenty (57.1%) patients started postoperative chemotherapy, of whom 12 (60%) received eight cycles. In nine patients,

postoperative therapy was not started because of AEs in the preoperative/postoperative phase in four patients (severe acneiform dermatitis in two patients and postoperative death in two patients), no response or progression in the preoperative phase in three patients, and investigators decision in two patients (one patient was non-compliant and one due to secondary carcinoma). Table 2 shows the tolerance to postoperative therapy.

Time to progression was defined as the time from registration date to the date of first observed progression including the detection of new lesions or progression of existing metastases. From 33 patients, 20 had progression and 13 had no documented progression until the end of the study. Median time without progression was 14.5 months. Twelve- and 24-month survival rates without progression were 62.4% and 34%, respectively. PFS was defined as the time from registration date to the date of first observed progression or death. From 35 patients, 26 patients had a PFS event, and nine patients had no event. First event was one secondary carcinoma, 20 patients had metastases progression as first event, and five patients died without previous progression. Median PFS was 13.2 months. Twelve- and 24-month PFS rates were 55.4% and 30.8%, respectively (Figure 2). OS was defined as the time from registration date to the date of death of any cause. Twelve- and 24- months OS rates were 85.6% and 73.3%, respectively (Figure 3). Kaplan-Meier analysis of PFS und OS by tumor side showed no statistical difference between left- and right-sided tumors (Figures 4, 5) but showed a trend toward better outcome in left-sided tumors.

Discussion

Long-term survival and cure are possible in patients with resectable CLM, leading to 5-year survival rates of 25%–40% if R0 resection is achieved (6–9). Upfront resection of resectable CLM is a therapeutic option for patients with limited CLM. In comparison to the beneficial effect of adjuvant chemotherapy in stage III CRC, the advantage of postoperative chemotherapy after curative resection of CLM is uncertain. However, only a few clinical trials were performed and the available data showed improvements in DFS but not in OS. Further studies investigated the use of perioperative chemotherapy in resectable CLM to enhance the outcome. This approach offers benefits, such as downsizing of liver metastases that enable less extensive surgery, elimination of potential micrometastases, the reduction of the risk of intrahepatic and extrahepatic recurrences, and the delineation of tumor biology. Perioperative chemotherapy with FOLFOX remains one of the standard treatments in patients with resectable CLM since presentation of the data from the EPOC study from the EORTC. In this trial, perioperative chemotherapy with FOLFOX and surgery was compared with surgery alone in CLM and demonstrated a significant better median PFS if perioperative chemotherapy was administered (11, 12). The OS showed a trend in favor of perioperative chemotherapy but was not statistically significant (median OS, 63.7 versus 55.0 months). Potential explanation was that the study was not designed or powered to detect differences in OS (17). In addition, more patients in the surgery alone group with

TABLE 3 Response to preoperative therapy according to RECIST.

Excluded from response analysis	3 (8.6%)
EOT after one cycle	1 (2.9%)
EOT after two cycles	1 (2.9%)
EOT after three cycles	1 (2.9%)
Response evaluation	32 (91.4%)
Complete response	1 (2.9%)
Partial response	22 (62.9%)
Stable disease	7 (20.0%)
Progressive disease	2 (5.7%)
Sums of largest diameters of target lesions on imaging *	
At baseline (mm)	1,770.5 mm
After preoperative therapy (mm)	1,019.5 mm
Relative reduction (%)	42.4%

*Measured in all 32 patients with imaging at baseline and with response evaluation. EOT, early end of treatment.

TABLE 4 Surgical information and postoperative complications.

Operated (number of resected liver metastases)	29 (82.9%)
1	12 (41.4%)
2	7 (24.1%)
3	1 (3.5%)
4	3 (10.3%)
5	2 (6.9%)
7	2 (6.9%)
8	1 (3.5%)
9	1 (3.5%)
Overview of type of liver resection	
Atypical resection	29 (51%)
(Bi)segmentomy	9 (16%)
Left hemihepatectomy	3 (5%)
Right hemihepatectomy	12 (21%)
Radiofrequency ablation	4 (7%)
Not operated	6 (17.1%)
EOT during preoperative phase	3 (8.6%)
Progressive disease	1 (2.9%)
Inadequate future liver remnant	1 (2.9%)
Inoperable at baseline in retrospect	1 (2.9%)
Tumor on specimen from resection	
Macroscopic	0
Only microscopic residual	3 (10.3%)
No residual tumor	24 (82.8%)
Missing	2 (6.9%)
At least one major postoperative complication	
Death during surgery	0
Postoperative death	2 (6.9%)
< 30 days after liver resection	1 (3.4%)
> 90 days after liver resection	1 (3.4%)
Suture related complication grade 3	1 (3.4%)

EOT, early end of treatment. Data in number (%) unless otherwise stated.

disease progression received palliative chemotherapy as treatment when compared with patients in the perioperative chemotherapy group who progressed. This confounding variable could clearly affect OS but not PFS.

To improve this outcome, the addition of anti-EGFR antibodies in the perioperative setting is an interesting approach, as chemotherapy in combination with anti-EGFR antibodies improved DFS and OS in advanced disease and had the potential

TABLE 6 Clavien–Dindo classification.

Clavien–Dindo classification grade	Frequency	Percent
Grade I	22	78.57
Grade II	3	10.71
Grade IIIB	1	3.57
Grade IVa	1	3.57
Grade V	1	3.57

for curative resection in previously unresectable CLM (15, 20, 26–30). First-line FOLFIRI plus panitumumab was associated with favorable efficacy in patients with wild-type RAS. In a phase II study, the median OS was 26 months. Almost a quarter of patients with previously unresectable CLM became resectable after 8 weeks of therapy. The median OS in patients with and without metastasectomies was 40 and 22 months, respectively (31). In the adjuvant setting, the addition of anti-EGFR showed no benefit (32, 33). However, the probability of circulating tumor cells in metastatic disease is increased and justified the investigation of anti-EGFR in the perioperative setting in a prospective trial.

In this LM02 study, the preoperative administration of four cycles of panitumumab and FOLFIRI in patients with primary resectable RAS wild-type CLM resulted in a radiological ORR in two-thirds of patients with a manageable grade 3 diarrhea rate of 14.3% of patients. Surgery of liver metastases was done in 82.9% of patients. Two patients died after surgery because of hepatic failure. Both patients had a major liver surgery with hemihepatectomy right. Postoperative biliary complication was the reason for death in both patients. All eight cycles of postoperative therapy could be given to 60% of all patients who started postoperative treatment. Median PFS was 13.2 months, and the 24-month OS rate was 73.3%. In the New EPOC trial, a similar approach was investigated, but, as chemotherapy backbone, FOLFOX was mainly used. In the new EPOC randomized study, perioperative chemotherapy (FOLFOX, CAPOX, or FOLFIRI) with or without cetuximab was investigated in resectable CLM (34, 35). About two-thirds of patients received chemotherapy regimen one (FOLFOX), followed by regimen two (CAPOX) in a fifth and about 10% of patients received as chemotherapy FOLFIRI with or without cetuximab. About 73% and 76% of the patients in the chemotherapy alone group (CT group) and in the chemotherapy plus cetuximab group (CTX group) completed 12 weeks of preoperative therapy, respectively. CR or PR occurred in 61% of patients receiving chemotherapy alone and in 72% of patients receiving chemotherapy plus cetuximab. About 86% of patients were operated. Most patients had a R0 resection (82% in the CT group and 79% of the CTX group). In addition, 46% and 48% of patients in the CT group and in the CTX group completed 12 weeks of postoperative therapy, respectively. Unexpectedly, median PFS and median OS were better in the CT group compared with patients who received chemotherapy plus cetuximab (median PFS, 22.2 versus 15.5 months; median OS, 81.0 versus 55.5 months). Possible explanations included interactions between cetuximab and chemotherapy backbone (FOLFOX and CAPOX), further mutations in the EGFR pathway, and upregulation of alternative signaling

TABLE 5 Rubbia–Brandt tumor regression grade.

Rubbia–Brandt tumor regression grade	Frequency	Percent
Missing (no surgery)	6	17.14
Grade 1	2	5.71
Grade 2	5	14.29
Grade 3	4	11.43
Grade 4	11	31.43
Grade 5	3	8.57
n.b. (not evaluable)	4	11.43

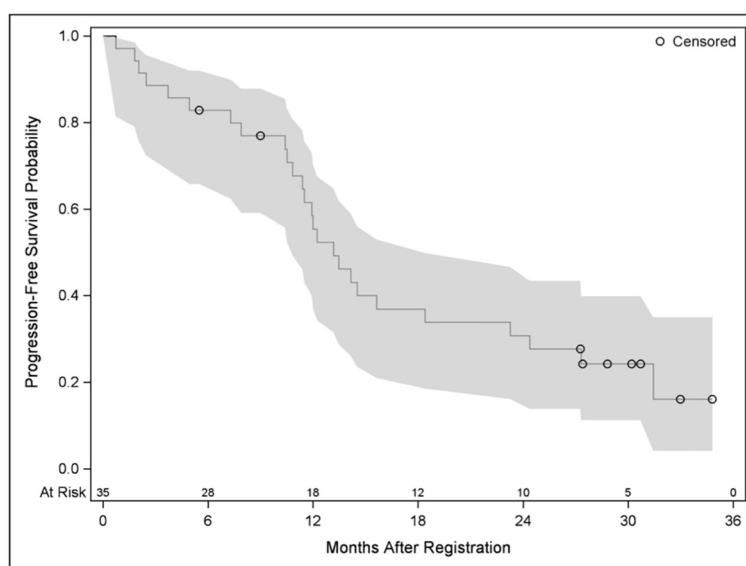


FIGURE 2
Kaplan–Meier plot for progression-free survival.

pathways in combination with surgery. It has been proposed that the interaction between oxaliplatin and cetuximab is potentially negative because cetuximab may protect against free radical damage by platinum (36). Furthermore, patients with KRAS-mutations who were treated with an EGFR inhibitor had an inferior outcome in the oxaliplatin studies (15, 18) compared with patients in the irinotecan-based studies who had a similar outcome to chemotherapy-only patients (19). Subgroup analysis of the New EPOC trial showed that cetuximab in combination with the chemotherapy FOLFOX had a detrimental effect compared with

patients receiving FOLFOX alone. However, patients receiving the chemotherapy FOLFIRI had a better PFS if cetuximab was added. However, this analysis should be interpreted cautiously due to the few patients receiving FOLFIRI as chemotherapy backbone in that study. Furthermore, in the updated analysis of the OS, the differences between the chemotherapy backbone were not confirmed.

To our knowledge, there has not been any other trial investigating preoperative panitumumab and FOLFIRI followed by liver resection and postoperative therapy with panitumumab

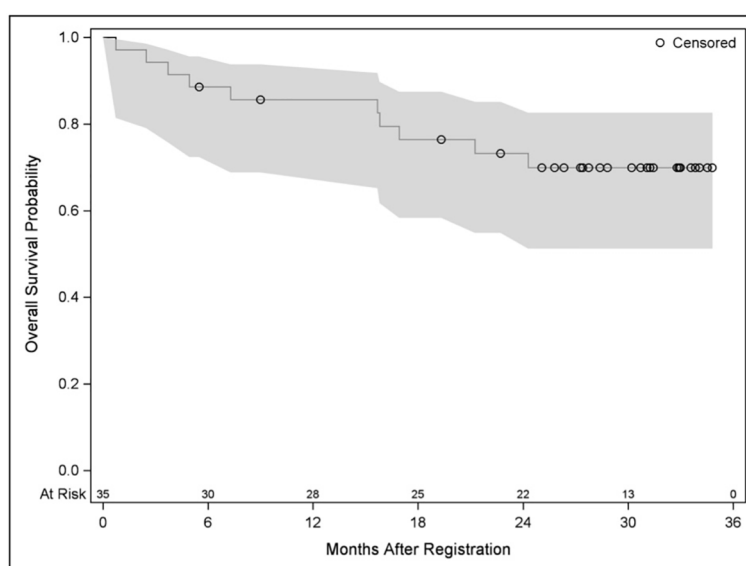


FIGURE 3
Kaplan–Meier plot for OS.

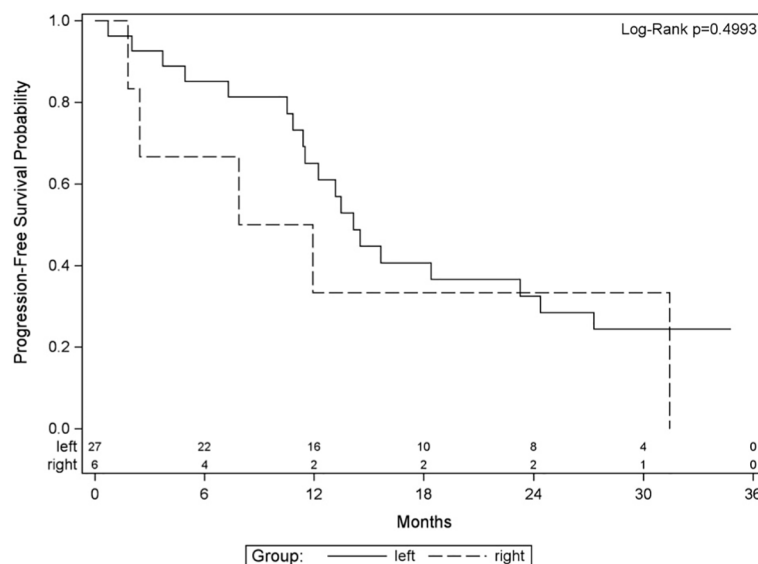


FIGURE 4
Kaplan–Meier plot for progression-free survival by tumor side.

and FOLFIRI in primary resectable CLM before. Unanswered questions in this patient population are the best chemotherapy combination with targeted agents to induce maximum response and the length of the initial treatment to verify response. The majority of available data are with oxaliplatin as chemotherapy. Treatment combination and number of preoperative cycles in the presenting LM02 trial are different from other trials that were done in the same indication. The EPOC trial administered six cycles of perioperative FOLFOX, and, in the New EPOC trial, patients received six cycles of FOLFOX/CAPOX/FOLFIRI with or without cetuximab compared with four cycles preoperative and eight cycles postoperative

panitumumab and FOLFIRI in this LM02 trial. Despite the reduced numbers of preoperative therapies, our study achieved an ORR of 65.7% compared with 43% and 72% in the EPOC and New EPOC trial. Grade 3–4 preoperative toxicities were more common in the EPOC and New EPOC trial compared with our trial. The lower toxicity rate in our trial is contributed to the reduced number of preoperative cycles. However, diarrhea grade 3 was slightly higher in the LM02 trial with 11.4% compared with 9% in the New EPOC trial and 8% in the EPOC trial. The higher diarrhea rate is attributed to irinotecan as chemotherapy backbone and is a known side effect. One patient each died in the LM02 trial

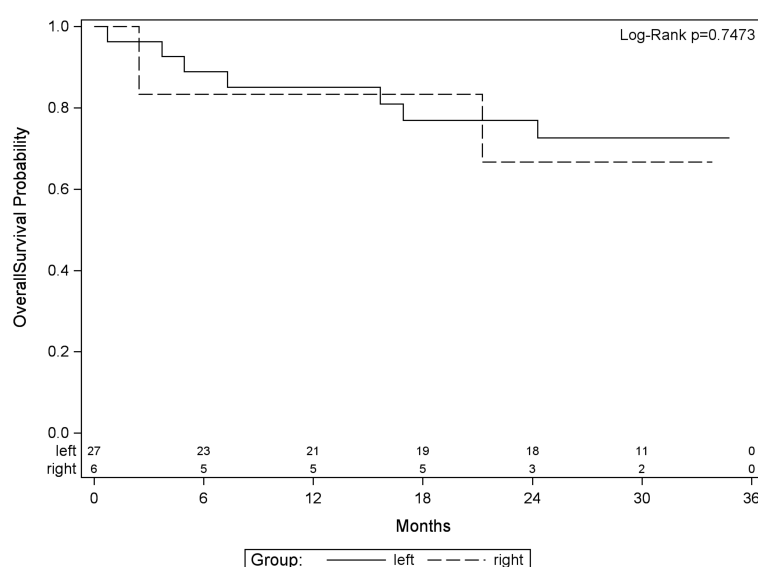


FIGURE 5
Kaplan–Meier plot for OS by tumor side.

(sepsis) and in the New EPOC trial (cardiac arrest) during the preoperative phase, whereas, in the EPOC trial, no patient died. Postoperative two patients died in the LM02 trial compared with three deaths in the EPOC trial (two in the surgery-alone group and one in the chemotherapy group) and no deaths in the New EPOC trial. Median PFS was significantly worse with the addition of cetuximab to chemotherapy in the New EPOC trial compared with chemotherapy alone (mPFS, 15.5 versus 22.2 months). In the LM02 trial, the mPFS was equally modest with 13.2 months.

Possible criticism of the LM02 trial is the small sample size of this phase II study. This combination therapy was not evaluated before as perioperative therapy in primary resectable CLMs. That is why our study group decided to plan a phase II study with a two-step design in a small sample size to evaluate efficacy and safety. At time of initiating of this study, there was only limited experience as conversion therapy of this combination in patients with primary unresectable CLMs. Furthermore, only 15 patients received this combination in the New EPOC trial. A further possible criticism is the continuation of the study despite the negative results of the New EPOC trial, which was extensively criticized for lack of adequate surgical quality control, imbalance in patients' characteristics, variations in chemotherapy backbone, and increased rate of early death without clear attribution (37). First, the LM02 study was initiated, whereas the new EPOC study was still recruiting. Data from the New EPOC trial were published in April 2014 (34). At that time, the interim analysis of the LM02 trial was performed after 15 patients. The criteria for continuation of the LM02 study were met as predefined. We were encouraged by the high ORR in the interim analysis of 86.7% compared with the new EPOC study with 70% ORR in the cetuximab + chemotherapy arm. In addition, a subgroup analysis of the New EPOC trial favored the addition of cetuximab to the chemotherapy backbone FOLFIRI. The fact that we used FOLFIRI as chemotherapy backbone, the high ORR in the interim analysis, and the subgroup analysis of the New EPOC trial favoring cetuximab + FOLFIRI justified the continuation of the LM02 study. Nevertheless, the mPFS data in the LM02 study were equally modest as compared with that in the New EPOC trial.

Conclusions

Panitumumab and FOLFIRI as perioperative therapy for resectable CLM result in a radiological ORR in 65.7% with a manageable grade 3 diarrhea rate. Median PFS was 13.2 months, and the 24-month OS rate was 73.3%. These data are insufficient to widen the indication of panitumumab from the unresectable setting to the setting of resectable CLM.

Data availability statement

The original contributions presented in the study are included in the article/supplementary material. Further inquiries can be directed to the corresponding author.

Ethics statement

The studies involving human participants were reviewed and approved by Ethik Kommission Medizinische Universität Wien. The patients/participants provided their written informed consent to participate in this study.

Author contributions

GP: Conceptualization, Investigation, writing – original draft, visualization, project administration; TG: Conceptualization, Investigation, project administration, Writing – Review and Editing; JT: Conceptualization, Review, project administration, Writing – Review and editing; IK: Investigation; KK: Investigation; FL: Investigation; AA: Investigation; WE: Investigation; RF: Investigation; JA: Investigation; AP: Investigation; JS: Investigation; LS: formal analysis; DÖ: Project administration, Investigation, Supervision, writing – Review and Editing. All authors contributed to the article and approved the submitted version.

Funding

The study was supported by Amgen, Austria GmbH. The authors declare that this study received funding from Amgen, Austria GmbH. The funder was not involved in the study design, collection, analysis, interpretation of data, the writing of this article or the decision to submit it for publication.

Conflict of interest

MG reports personal fees/travel support from Amgen, AstraZeneca, Celgene, Eli Lilly, Invecitys, Pfizer, Novartis, Puma, Nanostring, Roche, Medison, and LifeBrain; an immediate family member is employed by Sandoz.

The remaining authors declare that the research was conducted in the absence of any commercial or financial relationships that could be construed as a potential conflict of interest.

Publisher's note

All claims expressed in this article are solely those of the authors and do not necessarily represent those of their affiliated organizations, or those of the publisher, the editors and the reviewers. Any product that may be evaluated in this article, or claim that may be made by its manufacturer, is not guaranteed or endorsed by the publisher.

References

- Malvezzi M, Carioli G, Bertuccio P, Rosso T, Boffetta P, Levi F, et al. European cancer mortality predictions for the year 2016 with focus on leukaemias. *Ann Oncol* (2016) 27:725–31. doi: 10.1093/annonc/mdw022
- Siegel RL, Miller KD, Jemal A. Cancer statistics, 2017. *CA: A Cancer J Clin* (2017) 67:7–30. doi: 10.3322/caac.21387
- Midgley R, Kerr D. Colorectal cancer. *Lancet* (1999) 353:391–9. doi: 10.1016/S0140-6736(98)07127-X
- Kindler HL, Shulman KL. Metastatic colorectal cancer. *Curr Treat Options Oncol* (2001) 2:459–71. doi: 10.1007/s11864-001-0068-7
- Chong G, Cunningham D. Improving long-term outcomes for patients with liver metastases from colorectal cancer. *J Clin Oncol* (2005) 23:9063–6. doi: 10.1200/JCO.2005.04.4669
- Fong Y, Fortner J, Sun RL, Brennan MF, Blumgart LH. Clinical score for predicting recurrence after hepatic resection for metastatic colorectal cancer: analysis of 1001 consecutive cases. *Ann Surg* (1999) 230:309–21. doi: 10.1097/0000658-199909000-00004
- Choti MA, Sitzmann JV, Tiburi MF, Sumetchotimetha W, Rangsin R, Schulick RD, et al. Trends in long-term survival following liver resection for hepatic colorectal metastases. *Ann Surg* (2002) 235:759–66. doi: 10.1097/0000658-200206000-00002
- Fong Y, Cohen AM, Fortner JG, Enker WE, Turnbull AD, Coit DG, et al. Liver resection for colorectal metastases. *J Clin Oncol* (1997) 15:938–46. doi: 10.1200/JCO.1997.15.3.938
- Kanas GP, Taylor A, Primrose JN, Langeberg WJ, Kelsh MA, Mowat FS, et al. Survival after liver resection in metastatic colorectal cancer: review and meta-analysis of prognostic factors. *Clin Epidemiol* (2021) 4:283–301. doi: 10.2147/CLEP.S34285
- Zakaria S, Donohue JH, Que FG, Farnell MB, Schleck CD, Ilstrup DM, et al. Hepatic resection of colorectal metastases; value for risk scoring systems? *Ann Surg* (2007) 246:183–91. doi: 10.1097/SLA.0b013e3180603039
- Nordlinger B, Sorbye H, Glimelius B, Poston GJ, Schlag PM, Rougier P, et al. Perioperative chemotherapy with FOLFOX4 and surgery versus surgery alone for resectable liver metastases from colorectal cancer (EORTC Intergroup trial 40983): a randomised controlled trial. *Lancet* (2008) 371:1007–16. doi: 10.1016/S0140-6736(08)60455-9
- Nordlinger B, Sorbye H, Glimelius B, Poston GJ, Schlag PM, Rougier P, et al. Perioperative FOLFOX4 chemotherapy and surgery versus surgery alone for resectable liver metastases from colorectal cancer (EORTC 40983): long term results of a randomised, controlled, phase 3 trial. *Lancet Oncol* (2013) 14:1208–15. doi: 10.1016/S1470-2045(13)70447-9
- Wang ZM, Chen YY, Chen FF, Wang SY, Xiong B. Peri-operative chemotherapy for patients with resectable colorectal hepatic metastasis: a meta-analysis. *Eur J Surg* (2015) 41:1197–203. doi: 10.1016/j.ejs.2015.05.020
- Peeters M, Price TJ, Cervantes A, Sobrero AF, Ducreux M, Hotko Y, et al. Randomized phase III study of panitumumab with FOLFIRI compared with FOLFIRI alone as second line treatment in patients with metastatic colorectal cancer. *J Clin Oncol* (2010) 28:4706–13. doi: 10.1200/JCO.2009.27.6055
- Douillard JY, Oliner KS, Siena S, Tabernero J, Burkes R, Barugel M, et al. Panitumumab-FOLFOX4 treatment and RAS mutations in colorectal cancer. *N Engl J Med* (2013) 369:1023–34. doi: 10.1056/NEJMoa1305275
- Peeters M, Oliner KS, Price TJ, Cervantes A, Sobrero AF, Ducreux M, et al. Analysis of KRAS/NRAS mutations in a phase III study of panitumumab with FOLFIRI compared with FOLFIRI alone as second-line treatment for metastatic colorectal cancer. *Clin Cancer Res* (2015) 21:5469–79. doi: 10.1158/1078-0432.CCR-15-0526
- Padmanabhan C, Parikh A. Perioperative chemotherapy for resectable colorectal hepatic metastases – What does the EORTC 40983 trial update mean? *Hepatobiliary Surg Nutr* (2015) 4:80–3. doi: 10.3978/j.issn.2304-3881.2014.08.05
- Bokemeyer C, Bondarenko I, Hartmann JT, de Braud F, Schuck G, Zube A, et al. Efficacy according to biomarker status of cetuximab plus FOLFOX-4 as first-line treatment for metastatic colorectal cancer: the OPUS study. *Ann Oncol* (2011) 22:1535–46. doi: 10.1093/annonc/mdq632
- Van Cutsem E, Köhne CH, Lang I, Folprecht G, Nowacki MP, Cascinu S, et al. Cetuximab plus irinotecan, fluorouracil, and leucovorin as first-line treatment for metastatic colorectal cancer: updated analysis of overall survival according to tumor KRAS and BRAF mutation status. *J Clin Oncol* (2011) 29:2011–9. doi: 10.1200/JCO.2010.33.5091
- Douillard JY, Siena S, Cassidy J, Tabernero J, Burkes R, Barugel M, et al. Final results from PRIME: randomized phase III study of panitumumab with FOLFOX4 for first-line treatment of metastatic colorectal cancer. *Ann Oncol* (2014) 25:1346–55. doi: 10.1093/annonc/mdu141
- Schwartzberg L, Rivera F, Karthaus M, Gianpiero F, Canon JL, Hecht JR, et al. Analysis of KRAS/NRAS mutations in PEAK: a randomized phase 2 study of FOLFOX6 + panitumumab or bevacizumab as 1st line treatment for wild type KRAS (exon 2) metastatic colorectal cancer (2013). ASCO, Chicago, IL (Accessed May 31 – June 4, 2013).
- Patterson SD, Peeters M, Siena S, Van Cutsem E, Humblet Y, Van Laethem JL, et al. Comprehensive Analysis of KRAS and NRAS mutations as predictive biomarkers for single agent panitumumab response in a randomized, phase 3 metastatic colorectal cancer study (20020408) (2013). ASCO Chicago, IL (Accessed May 31 – June 4, 2013).
- Dindo D, Demartines N, Clavien PA. Classification of surgical complications. *Ann Surg* (2004) 240:205–13. doi: 10.1097/01.sla.0000133083.54934.ae
- Rubbia-Brandt L, Giostra E, Brezault C, Roth AD, Andres A, Audard V, et al. Importance of histological tumor response assessment in predicting the outcome in patients with colorectal liver metastases treated with neoadjuvant chemotherapy followed by liver surgery. *Ann Oncol* (2007) 18:299–304. doi: 10.1093/annonc/mdl386
- National Cancer Institute: Common Terminology Criteria for Adverse Events (CTCAE) version 4.0 (2009) (Accessed May 28, 2009).
- Van Cutsem E, Köhne C-H, Hitre E, Zaluski J, Chien CC, Makhson A, et al. Cetuximab and chemotherapy as initial treatment for metastatic colorectal cancer. *N Engl J Med* (2009) 360:1408–17. doi: 10.1056/NEJMoa0805019
- Bokemeyer C, Bondarenko I, Makhson A, Hartmann JT, Aparicio J, de Braud F, et al. Fluorouracil, leucovorin, and oxaliplatin with and without cetuximab in the first-line treatment of metastatic colorectal cancer. *J Clin Oncol* (2009) 27:663–71. doi: 10.1200/JCO.2008.20.8397
- Folprecht G, Gruenberger T, Bechstein WO, Raab HR, Lordick F, Hartmann JT, et al. Tumour response and secondary resectability of colorectal liver metastases following neoadjuvant chemotherapy with cetuximab: the CELIM randomised phase 2 trial. *Lancet Oncol* (2010) 11:38–47. doi: 10.1016/S1470-2045(09)70330-4
- Maughan TS, Adams RA, Smith CG, Meade AM, Seymour MT, Wilson RH, et al. Addition of cetuximab to oxaliplatin-based first-line combination chemotherapy for treatment of advanced colorectal cancer: results of the randomised phase 3 MRC COIN trial. *Lancet* (2011) 377:2103–14. doi: 10.1016/S0140-6736(11)60613-2
- Peeters M, Price TJ, Cervantes A, Sobrero AF, Ducreux M, Hotko Y, et al. Final results from a randomized phase 3 study of FOLFIRI ± panitumumab for second-line treatment of metastatic colorectal cancer. *Ann Oncol* (2014) 25:107–16. doi: 10.1093/annonc/mdt523
- Geredeli C, Yasar N. FOLFIRI plus panitumumab in the treatment of wild-type KRAS and wild-type NRAS metastatic colorectal cancer. *World J Surg Oncol* (2018) 16:67. doi: 10.1186/s12957-018-1359-9
- Alberts SR, Sargent DJ, Nair S, Mahoney MR, Mooney M, Thibodeau SN, et al. Effect of oxaliplatin, fluorouracil, and leucovorin with or without cetuximab on survival among patients with resected stage III colon cancer: a randomized trial. *JAMA* (2012) 307:1383–93. doi: 10.1001/jama.2012.385
- Taieb J, Tabernero J, Min E, Subtil F, Folprecht G, Van Laethem JL, et al. Oxaliplatin, fluorouracil, and leucovorin with or without cetuximab in patients with resected stage III colon cancer (PETACC-8): an open-label, randomised phase 3 trial. *Lancet Oncol* (2014) 15:862–73. doi: 10.1016/S1470-2045(14)70227-X
- Primrose J, Falk S, Finch-Jones M, Valle J, O'Reilly D, Siriwardena A, et al. Systemic chemotherapy with or without cetuximab in patients with resectable colorectal liver metastasis: the New EPOC randomised controlled trial. *Lancet Oncol* (2014) 15:601–11. doi: 10.1016/S1470-2045(14)70105-6
- Bridgewater JA, Pugh SA, Maishman T, Eminton Z, Mellor J, Whitehead A, et al. Systemic chemotherapy with or without cetuximab in patients with resectable colorectal liver metastasis (New EPOC): long-term results of a multicentre, randomised, controlled, phase 3 trial. *Lancet Oncol* (2020) 21:398–411. doi: 10.1016/S1470-2045(19)30798-3
- Dahan L, Sadok A, Formento JL, Seitz JF, Kovacic H. Modulation of cellular redox state underlies antagonism between oxaliplatin and cetuximab in human colorectal cancer cell lines. *Br J Pharmacol* (2009) 158:610–20. doi: 10.1111/j.1476-5381.2009.00341.x
- Nordlinger B, Poston GJ, Goldberg RM. Should the results of the new EPOC trial change practice in the management of patients with resectable metastatic colorectal cancer confined to the liver? *JCO* (2015) 33(3):241–3. doi: 10.1200/JCO.2014.58.3989



OPEN ACCESS

EDITED BY

Alessandro Passardi,
Scientific Institute of Romagna for the
Study and Treatment of Tumors
(IRCCS), Italy

REVIEWED BY

Hao Jia,
Shanghai Jiao Tong University, China
Chen Ling,
Fudan University, China

*CORRESPONDENCE

Chengcheng He
✉ cbslhy@163.com
✉ 2022683064@gzhmu.edu.cn

[†]These authors have contributed equally to
this work

RECEIVED 15 May 2023

ACCEPTED 07 August 2023

PUBLISHED 17 August 2023

CITATION

Zheng Y, Zhong G, He C and Li M (2023)
Targeted splicing therapy: new
strategies for colorectal cancer.
Front. Oncol. 13:1222932.
doi: 10.3389/fonc.2023.1222932

COPYRIGHT

© 2023 Zheng, Zhong, He and Li. This is an
open-access article distributed under the
terms of the [Creative Commons Attribution
License \(CC BY\)](https://creativecommons.org/licenses/by/4.0/). The use, distribution or
reproduction in other forums is permitted,
provided the original author(s) and the
copyright owner(s) are credited and that
the original publication in this journal is
cited, in accordance with accepted
academic practice. No use, distribution or
reproduction is permitted which does not
comply with these terms.

Targeted splicing therapy: new strategies for colorectal cancer

Yifeng Zheng[†], Guoqiang Zhong[†], Chengcheng He^{*}
and Mingsong Li

Department of Gastroenterology, The Third Affiliated Hospital of Guangzhou Medical University,
Guangzhou, Guangdong, China

RNA splicing is the process of forming mature mRNA, which is an essential phase necessary for gene expression and controls many aspects of cell proliferation, survival, and differentiation. Abnormal gene-splicing events are closely related to the development of tumors, and the generation of oncogenic isoform in splicing can promote tumor progression. As a main process of tumor-specific splicing variants, alternative splicing (AS) can promote tumor progression by increasing the production of oncogenic splicing isoforms and/or reducing the production of normal splicing isoforms. This is the focus of current research on the regulation of aberrant tumor splicing. So far, AS has been found to be associated with various aspects of tumor biology, including cell proliferation and invasion, resistance to apoptosis, and sensitivity to different chemotherapeutic drugs. This article will review the abnormal splicing events in colorectal cancer (CRC), especially the tumor-associated splicing variants arising from AS, aiming to offer an insight into CRC-targeted splicing therapy.

KEYWORDS

alternative splicing, colorectal cancer, splicing isoform, tumor-associated splicing variants, targeted splicing therapy

1 Introduction

In the past 20 years, colorectal cancer (CRC) has been one of the most life-threatening malignant tumors. According to global data released by the American Cancer Society in the Journal of Clinician's Oncology in 2023, CRC has the third-highest incidence and second-highest mortality rates of all tumors (1). For the treatment options for this disease, it is acknowledged that molecular targeted therapies can provide effective treatment solutions, especially for patients with advanced metastases. In the targeted therapy of CRC, although most drug targets (e.g. *EGFR*, *VEGF*, etc.) play an important role in the differentiation and metabolism of normal cells, drug administration claims that these drug targets cannot avoid their toxic effects on healthy tissues (2). Therefore, how we can maintain the regulatory effect of this molecule on normal cells while targeting and inhibiting them is the key to have a breakthrough in the molecular targeting therapy of CRC. In recent years, as the functions and mechanisms of splicing-related molecules in CRC have become clearer, targeted therapy using splice variants as targets has been developed, which shows a higher

tumor specificity and offers the potential for a safer and controlled CRC-targeted therapy (3). Although splice variant targeted therapy is a new type of targeted therapy, it has very limited targets for clinical application, failing to meet the drug needs of patients at different stages of CRC. Therefore, what comes first is to study the function and mechanism of splice variants in CRC to explore and screen excellent drug targets to promote targeted therapy for CRC.

1.1 RNA splicing process

The studies on pre-mRNA splicing were first reported in 1977 (4, 5). RNA splicing is the process in which DNA is transcribed to form an initial/pre-mRNA (pre-mRNA/hnRNA) and then is sheared by a spliceosome to form a mature mRNA. The spliceosome is responsible for pre-RNA splicing, which is a large molecular complex composed of five small nuclear ribonucleic acids (snRNAs) and various proteins. These five snRNAs are named U1, U2, U4, U5, and U6, each of which can be associated with specific proteins, forming five small nuclear ribonucleoprotein particles (snRNPs). These snRNPs sequentially bind to the precursor mRNA during the splicing of introns, leading to the formation of a lariat structure and bringing the upstream and downstream exons closer together. Specifically, U1 and U2 snRNAs pair with the boundary sequences at the 5' and 3' ends of the intron, followed by the addition of U4, U5, and U6 to form a complete spliceosome. What is noteworthy is that at this stage, the intron bends to form a lariat structure, and the upstream and downstream exons gradually approach each other. Finally, the spliceosome rearranges its structure, releasing U1, U4, and U5, while U2 and U6 form the

catalytic center for the trans-esterification reaction. Splicing factors (SFs) are a group of proteins that cooperate with the spliceosome to catalyze this core cellular function. And studies have shown that mutations in SFs can disrupt the expression ratios of small nuclear RNAs and impair spliceosome assembly (6). This can result in premature pathogenic termination of mRNA translation.

Alternative splicing (AS) has been regarded as one of the most important mechanisms that can maintain genomic and functional diversities since the Human Genome Project completed in 2004 (7). As a regulatory mechanism, AS affects almost all multi-exon genes in human body, in the sense that it allows multi-exon genes to produce more than one mRNA and generate multiple protein isoforms derived from the same single gene through differential sorting of exons. In this process, certain splicing patterns can cause loss or gain of key domains of proteins, leading to a lost or incomplete function, which in turn affects protein stability and changes subcellular localization. The type of AS includes intron retention, exon skipping, alternative 3' splicing, and alternative 5' splicing (Figure 1).

1.2 Alternative splicing and CRC

RNA splicing, which represents a crucial stage in gene expression, plays a pivotal role in regulating various aspects of cell proliferation, survival, and differentiation. Given this importance, abnormal changes in splicing events are closely related to the occurrence and development of tumors (3). The results of the deep mRNA sequencing of various tumor types have shown that cancer cells exhibit more complex and abnormal

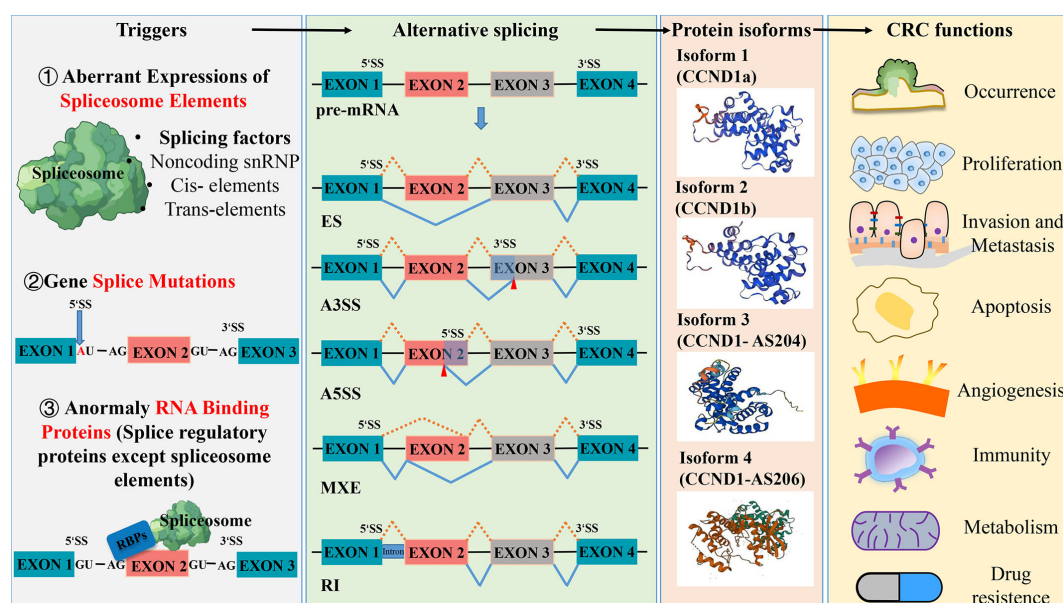


FIGURE 1

Aberrant splicing process in the occurrence and development of colorectal cancer. Abnormal spliceosome elements or gene splice mutation can trigger a variety of alternative splicing. The five common types of alternative splicing are exon skipping (ES), alternative 3' splice site (A3SS), alternative 5' splice site (A5SS), mutually exclusive exon (MXE) and retained intron (RI). These different types of alternative splicing result in the production of various protein isoforms, which can influence the function of colorectal cancer. Protein structures prediction using SWISS-MODEL (<https://swissmodel.expasy.org/>).

splicing behaviors compared to normal tissues (8), for instance, transcript ratios of cancer cells containing premature stop codons are significantly higher than the ones of normal tissues. Large-scale genome studies have discovered a series of splicing mechanisms that contribute to the development of tumors (9, 10), some of which can promote tumor growth by abnormal RNA splicing. For example, during the splicing process, abnormal changes in the copy number of splicing factors can produce more cancer-promoting splicing products (tumor-specific splicing variants) through alternative splicing (AS) and can promote the malignant growth and progression of tumor cells. Therefore, the abnormal expression of splicing factors is considered one of the direct causes of frequent and pathological splicing events in tumors (11). As the main process of tumor-specific splicing variants, AS can promote tumor progression by increasing the production of oncogenic splicing subtypes and decreasing the production of normal splicing subtypes, which is the focus of current research on the regulation of abnormal tumor splicing (12). Data from the analysis of 16 different tumors in the TCGA database show that almost all types of tumors exhibit abnormalities in intron retention, which is far more common than alterations in introns (13). In general, abnormal spliceosome elements or gene splice mutations can trigger various of AS, resulting in the production of different protein isoforms that have different functional effects on CRC (Figure 1). Capon et al. (14) were the first to discover that in CRC cell lines, c-Ki-ras (KRAS) mutates at different points within the same codon, resulting in the production of two transcript variants. So far, more than 15,000 alternative splices have been identified to be associated with various aspects of tumor biology, including cell proliferation and invasion, resistance to apoptosis, and sensitivity to different chemotherapeutic agents (15, 16).

1.3 CRC – targeted splicing therapy

Aberrant splicing is an important source that constitutes new cancer biomarkers, spliceosomes of which represent attractive drug targets for novel therapeutic agents. The research and treatment of tumor-specific splicing variants as new targets for CRC therapy have received extensive attention (7, 17, 18). Wang et al. (18) have discussed the association between various AS targets and the occurrence, progression, treatment, and prognosis of CRC. They argue that differential AS isoforms of the same gene may influence multiple biological functions in CRC, such as cell proliferation, metastasis, apoptosis, angiogenesis, immunity, and metabolism. Of the current targeted splicing therapeutic methods, oligonucleotide therapy is a relatively mature and widely used one in clinical practice, designed to alter splicing by Watson-Crick base pairing and hybridization to RNA in a sequence-specific manner. Clinical studies have shown that antisense oligonucleotides (ASO) can significantly reduce the mRNA that contributes to the survival of cancer cells. This therapy has achieved good results in correcting specific pathological splicing events in non-tumor single-gene diseases (19–21). Furthermore, small molecular compounds targeting splicing factors (e.g., RBM39) and splicing regulators have made progress in tumor treatment. Clinical studies have also

reported strategies for combining splicing modulators with traditional antitumor agents to reduce their toxicity to healthy tissues (22, 23). In CRC-targeted splicing therapy, the current work focuses on exploring tumor-specific splicing variants which are expected to be diagnostic and prognostic markers of tumors. Some promising splice isoform targets have also been reported, including VEGF165b, c-FLIPL, CCND1b, etc. Thus, this article will review the tumor-associated splicing variants arising from AS, aiming to offer an insight into CRC-targeted splicing therapy.

2 Tumor-associated splicing variants in CRC: from roles to potential therapeutic approaches

Investigating the influence of splicing variants in CRC is of paramount importance for the diagnosis and treatment of CRC. Subsequent paragraphs will elaborate on the function of splice isoforms in CRC by detailing its correlation with tumor initiation, progression, metastasis, immunity, metabolism, and drug resistance, shown in Figure 2.

2.1 Splice isoforms in the occurrence of CRC

The occurrence of cancer involves a complex process that has to do with the interaction of multiple genes and molecular pathways. Anomalies in alternative splicing have been identified as a significant contributor to the development of CRC, and studying this phenomenon has the potential to shed light on the mechanisms of tumor formation.

2.1.1 *RIP3*

Receptor-interacting protein 3 (*RIP3*) is a member of the *RIP* family that induces apoptosis (24). Based on current research, *RIP3* is known to be a crucial component of necrosomes and serves as an important mediator of inflammatory factors and infection-induced necroptosis (25). It has been implicated in promoting the occurrence and development of certain inflammatory cancer types, including pancreatic and colorectal cancers, by activating proliferation signaling pathways in cells and eliciting an immunosuppressive response within the tumor microenvironment (26).

Yang et al. reported two novel splice variants of human *RIP3*, named *RIP3β* and *RIP3γ*, which are generated by alternative splicing at the donor site of exon5 and retention of the intron between exons 5 and 6, respectively (27). Moreover, their study also revealed a significant increase in the ratio of *RIP3γ* to *RIP3* in colon and lung cancer compared to their matched normal tissues, indicating that *RIP3γ* may be the primary isoform associated with tumorigenesis (27).

Existing evidence suggests that the widely used cancer treatments multi-targeting kinase inhibitors, such as Dabrafenib, Vemurafenib, Sorafenib, Pazopanib, and Ponatinib, also exhibit anti-necroptotic activity (28). This reveals the potential of targeting *RIP3* in CRC for therapeutic interventions.


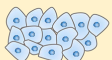
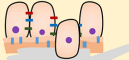





Occurrence		Proliferation	Invasion and Metastasis				
							
cAPC , BS-APC , RONAΔ160, RONAΔ155, RONAΔ170 , eIF4H-i1, RIP3γ, miniSOX9, SLC39A14-4A, SLC39A14-4B, BARD1κ, BARD1β, BARD1π BARD1δ , BARD1φ , KRAS4A, KRAS4B, CCND1b, TP53-E6, p53ψ, FIRΔE2, FIRΔE3, FIRΔE4, RAC1, RAC1b, MKNK2b, HNF4a2 , HNF4a8, BCLAF1-L, OCC-1A/B, OCC-ID		CD44v6, H2AFY1.1 , CABLE627, MAT2βV1, MAT2βV2, ΔPARK, ITGA6A, INPP4B-S, CXCR3A, ASPP2κ, UPF3A-L, RONA165E2, RONA160E2E3, TIMP1-i3 , MKNK2b, DBF4B-FL, ΔE2Smurf2 , TRA2β4, ID1a, ID1b	CD44v6, FAK0, FAK6, CCTNa, ΔE2Smurf2, CCND1b, LMNA-A, ASPP2κ, XBP1s, ZNF148FL, ZNF148ΔN , HSPA12A-ΔE2 , RONA165E2, RONA160E2E3, CCK2i4vR, TXL-2b, TXL-2c , TNIIIA2, HDM2/1338, HDM2/707, HDM2/1007, HDM2/1200, TP53-E6, p53ψ, CXCR3A, BIRC5-ΔEx3, BIRC5-3B, ZO1 E23+ , ZO1 E23-, CEACAM1-L				
		Functions of splicing variants in colorectal cancer					
Metabolism		Apoptosis				Immunity	
							
UGT1As_i1, UGT1As_i2 , PKM1, PKM2, ACSL1-v1, ACSL1-v2, ACSL1-v3, ACSL4-v1, ACSL4-v2		c-FLIPS , c-FLIPL , ZNF148FL, ZNF148ΔN, SYK(L), FOXM1b , FOXM1c , SRFA5 , PGAM5L, sFAS , MRPL33-L , WNT5A-S , WNT5A-L, BCL-X(L) , BCL-X(S)				PPARβ, PPARδ, sIL-6R, sILT3, IL-22BPi2, IL-22BPi3	
						Angiogenesis	
							
				Drug-resistance			
							
				CD44V6, ASPP2κ, c-FLIP(L), SYK(L) , SYK(S) , XBP1s, OPNc, RAC1b, PKM1/PKM2, sTIA-1, fTIA-1, LGR5FL, LGR5Δ5 , RAF1-tr , LIN28B-L			

FIGURE 2

Functions of tumor-associated splicing variants in colorectal cancer. (Black font: promoting effect; red font: inhibition effect).

2.1.2 APC

In colorectal tumors, the tumor suppressor gene *APC* (Adenomatous Polyposis Coli) is commonly found to be mutated (29). It produces various splicing isoforms associated with CRC tumorigenesis through abnormal splicing events such as exon skipping (e.g., exon 1, exons2-5, exon 7, exon 9A, exon 14, exon 10A) and intron retention (e.g., intron 11) (30). Three isoforms of the *APC* gene have been identified, namely cAPC, BS-APC, and 0.3 APC, resulting from alternative splicing of exon 1.

Previous studies have demonstrated that cAPC and BS-APC can effectively suppress the growth of colon tumor cells, while 0.3 APC lacks this effect. The loss of inhibitory function in 0.3 APC may be attributed to AS-induced changes in the conserved domain of the protein structure, which in turn impairs its ability to interact with other proteins (31). These results suggest that distinct *APC* isoforms may play different roles in the tumorigenesis of CRC.

2.1.3 EIF4H

EIF4H (Eukaryotic Translation Initiation Factor 4H) encodes a translation initiation factor that stimulates protein synthesis by promoting mRNA utilization. Previous studies have indicated that *EIF4H* selectively regulates the translation of potent growth and survival factor mRNAs, thereby playing a vital role in translational control. This function can facilitate cellular transformation and has been implicated in cancer development (32).

The *EIF4H* gene is known to generate two splice variants, isoform 1 and isoform 2 through alternative splicing of exon 5 (33). Wu et al. discovered that the expression of *EIF4H* isoform 1 increased in CRC, and its overexpression in immortalized mouse fibroblast cells induced tumor formation in nude mice. Significantly, ectopic expression of *EIF4H* isoform 1 significantly increases the level of cyclin D1, while co-transfection of *EIF4H* isoform 1 siRNA and cyclin D1 expression vector can reverse the growth of the inhibitory effect of *EIF4H* isoform 1 knockdown (34).

These findings suggest that *EIF4H* isoform 1 promotes the development of CRC through the activation of oncogenic signals and may serve as a potential therapeutic target for CRC treatment.

2.1.4 BARD1

BRCA1 Associated RING Domain 1 (*BARD1*), a binding partner of *BRCA1*, encodes a protein that interacts with the N-terminal region of *BRCA1* both *in vivo* and *in vitro* (35). Numerous studies have demonstrated that *BRCA1* plays a significant role in the onset and progression of colorectal cancer, with its mutations closely linked to CRC susceptibility (36–40). *BARD1* is necessary for the majority of *BRCA1*'s tumor suppressor functions, with *BRCA1*'s stability relying on its interaction with *BARD1* (41).

Through alternative splicing, *BARD1* can generate multiple isoforms, including *BARD1κ*, *BARD1β*, *BARD1π*, *BARD1δ*, *BARD1φ*, and others. Furthermore, the findings suggest that *BARD1* isoforms κ, β, and π are associated with the occurrence and progression of CRC tumors and may serve as specific prognostic biomarkers. Conversely, isoforms δ and φ may have an inhibitory effect (42).

Recently, studies have found that poly ADP ribose polymerase (PARP) inhibitors selectively kill *BRCA1*-deficient cells by directly suppressing the fast recruitment of the *BARD1-BRCA1* heterodimer to DNA damage sites and impairing DNA repair. In addition, *BARD1β* has been demonstrated to enhance the sensitivity of CRC cells to poly PARP-1 inhibition, suggesting that it is a promising biomarker for assessing the suitability of homologous recombination targeting with PARPi in the treatment of advanced CRC (43).

2.1.5 KRAS

The RAS (Rat Sarcoma Viral Oncogene Homolog) family is composed of small GTPases that are associated with the membrane and have critical functions in cell survival, proliferation, and differentiation (44). Central to cancer biology are the four

proteins encoded by the three mammalian *RAS* genes, namely *HRAS* (Harvey Rat Sarcoma Viral Oncogene Homolog), *NRAS* (Neuroblastoma RAS Viral Oncogene Homolog), and *KRAS* (Kirsten Rat Sarcoma Viral Oncogene Homolog) (45).

In CRC, the *KRAS* gene is the most frequently mutated *RAS* gene (46). Alternative splicing of the *KRAS* transcript produces two variants with alternative 4th exons, which are referred to as *KRAS4A* and *KRAS4B* (47). When *KRAS* is constitutively activated by the mutation in exon 2 or 3, both *KRAS4A* and *KRAS4B* exhibit oncogenic properties (48). Furthermore, the direct regulation of hexokinase 1 by *KRAS4A* implies that the metabolic weaknesses of *KRAS*-mutant tumors may be influenced, at least in part, by the expression levels of the splice variants (49).

In a co-clinical trial conducted on *RAS* mutant colorectal cancer, the combined inhibition of MEK and CDK4/6 has been shown to exhibit therapeutic efficacy in patient-derived xenografts (50). Additionally, the trial has demonstrated the safety of Binimetinib and Palbociclib in patients with metastatic colorectal cancer with *RAS* mutations, identified biomarkers associated with treatment response, and revealed mechanisms of resistance that can be targeted (50).

2.1.6 RON

The proto-oncogene receptor d'origine nantais (*RON*, *MST1R*) is a transmembrane tyrosine kinase receptor for macrophage-stimulating protein (MSP) that crucially regulates cell motility, adhesion, proliferation, apoptosis, and epithelial-to-mesenchymal transition (EMT) in various tumor biological processes.

The impact of *RON* on tumors arises from various splice variants generated by AS, including *RONΔ170*, *Δ165*, *Δ160*, *Δ155*, *Δ110*, and *Δ55* (51). *RONΔ160* is generated by skipping exons 5 and 6, while *RONΔ155* is a derivative that lacks exons 5, 6 and 11 in combination, both of which can promote cell transformation and tumor growth (52, 53). In contrast, *RONΔ170* can suppress the oncogenic activity of *RONΔ160* in CRC cells, which is generated by skipping exon 19 (54). A constitutively active isoform generated by skipping exon 11, called DeltaRON, can activate epithelial-to-mesenchymal transition and increase the motility of expressing cells (55). Merestinib is an oral kinase inhibitor with antitumor proliferative and antiangiogenic activity developed initially to target the MET kinase. However, it has also shown the activity against other receptor tyrosine kinases, such as *RON*. While the safety and tolerability profile of Merestinib has been demonstrated, further investigation is necessary to determine its efficacy in targeting *RON* in CRC patients (56).

2.1.7 CCND1

Cyclin D1 (*CCND1*) is a critical regulator of the cell cycle and is known to facilitate uncontrolled cellular proliferation, making it a key player in the development of cancer (57).

Research has shown that alterations in *CCND1* gene expression, including overexpression, underexpression, and variants, are associated with the development and poor prognosis of CRC (58–60), particularly the G870A mutation (60). This mutation is the most common splice mutation in *CCND1* (61, 62) and results in the

generation of two *CCND1* isoforms through alternative splicing: full-length *CCND1a* and divergent C-terminal *CCND1b* (63, 64). It is widely accepted that an imbalanced *CCND1a/b* ratio or high expression of *CCND1b* is closely linked to the development of cancer. Recent studies have also revealed the role of *CCND1b* in cell cycle regulation, invasion, and metastasis (65, 66).

In terms of therapeutic strategies, research has shown that correcting *CCND1* splicing through antisense oligonucleotides (ASO) and small molecule modulators can be effective in cancer therapy (67). These findings suggest that developing splicing regulatory drugs targeting *CCND1* splicing variants could be a promising new option for the treatment of CRC.

2.1.8 FIR

In colorectal cancer tissue, AS of the far-upstream element (FUSE)-binding protein (FBP)-interacting repressor (*FIR*) results in splicing variants that promote tumor development by disabling *FIR* repression, sustaining high levels of c-Myc, and opposing apoptosis (68).

Knockdown of SF3b, a subunit of SAP155 pre-mRNA-splicing factor, generates three splicing variants of *FIR*, including *FIRΔexon2*, *Δ3*, and *Δ4*. *FIRΔexon2* lacks c-myc repression activity, and both *FIRΔ3* and *Δ4* are activated in human CRC tissue. This suggests that the overexpression of *FIR* and its splicing variants in CRC lead to the feed-forward or addicted circuit c-myc transcriptional activation (69). Furthermore, the combination of *FIRΔexon2/FIR* mRNA ratios with the real-time PCR detection of *FIRΔexon2* mRNA significantly enhances the accuracy of screening for CRC, compared to conventional tumor markers CEA and CA19-9. Therefore, the mRNA expression of *FIR*, *FIRΔexon2*, *FIRΔ3*, and *FIRΔ4* represents strong biomarkers for cancer screening (70). Spliceostatin A (SSA) exhibits anti-proliferative and anti-tumor activities by inhibiting spliceosome assembly through the nonproductive recruitment of U2 snRNP of subunit SF3b. Other compounds, such as meayamycin, pladienolide B, FD-895, and H3B-8800, can also interact with the SF3b subunit, thereby inhibiting the alternative splicing of *SAP155* (71, 72).

2.1.9 RAC1

RAC1 (Ras-Related C3 Botulinum Toxin Substrate 1), a small GTPase, is involved in various numerous dynamic cellular processes such as cell proliferation, cell survival, cell-cell interactions, EMT, cell mobility, and invasion (73–75).

The *RAC1b* variant is caused by the inclusion of exon 3b, resulting in the addition of a 19-amino acid sequence that is in-frame and located directly after the switch II domain. In addition, the equilibrium between *RAC1* and *RAC1b* expression is modulated by splicing factors such as SRSF1 (76), hnRNP A1 (77), and SRp20 (78), which can promote or inhibit the inclusion of exon 3b via EGFR or Wnt signaling pathway (79). Experimental evidence indicates that *RAC1b* boosts G1/S progression and cell survival in NIH3T3 cells. Moreover, *RAC1b* may contribute to advanced stages of carcinogenesis, as it enhances Apc-dependent intestinal tumorigenesis and promotes carcinogenesis in the cecum and proximal colon during chronic inflammation (80).

Recently, highly effective and specific *RAC1* inhibitors have been discovered and developed, including GYS32661 and MBQ-167, which are currently undergoing preclinical trials for the treatment of advanced solid tumors (81). Therefore, due to its association with poor prognosis (82) and chemoresistance to oxaliplatin (83) of CRC, selectively targeting *RAC1b* and/or its interaction with molecular partners may represent a promising therapeutic approach for treating CRC.

2.1.10 Others

Abdel-Samad et al. discovered that MiniSOX9, a truncated version of *SOX9* (SRY-Box Transcription Factor 9) lacking a transactivation domain due to the retention of its second intron, acts as an inhibitor of *SOX9*, suppressing the activity of the protein kinase $C\alpha$ promoter and stimulating the classic Wnt pathway in CRC (84).

Thorsen et al. discovered that *SLC39A14*, a divalent cation transporter, undergoes the aberrant splicing in CRC tumor samples by mutually exclusive exon 4A and 4B, resulting in two splicing variants regulated by the Wnt pathway (85). Further studies found that the *SLC39A14*-exon4B transcript variant is a highly specific and sensitive cancer biomarker for colorectal tissue biopsies (86).

TP53 (Transformation-Related Protein 53) mutations are frequently observed in CRC, and its splicing mutations can generate transcript variants with different tumorigenic and prognostic properties (87). Shirole et al. found that *TP53* exon-6 truncating mutations produce the separation of the function of isoforms with pro-tumorigenic functions (88). Its function is similar to *P53 Ψ* , a transcriptionally inactive *P53* isoform, which can reprogram cells toward a metastatic-like state (89). In addition, an alternative *P2* promoter located internally in intron 4 and the retention of intron 2, as well as alternative splicing of exon 9, can also lead to various splicing variants of *TP53* and the loss of *p53* activity (90). The various *p53* proteoforms resulting from alternative splicing may aid in the early diagnosis of CRC.

Zhou et al. observed that the splicing factor *SRSF10* is involved in the post-transcriptional splicing of *Bcl-2*-associated transcription factor 1 (*BCLAF1*) and forms the L isoform, thereby promoting the development of colorectal cancer (91).

OCC-1 is considered as a differentially upregulated gene in CRC (92), which generates multiple splice variants through alternative splicing, including *OCC-1A/B*, *OCC-1C*, *OCC-1D*, and so on. The research findings indicate that the splice variants *OCC-1A/B* and *OCC-1D* of *OCC-1* can promote the occurrence of CRC by regulating the Wnt signaling pathway (93).

The nuclear receptor known as hepatocyte nuclear factor 4 α (*HNF4 α*) has been found to have tumor suppressive effects in the liver, but in colon cancer it appears to be amplified, suggesting an oncogenic role. *HNF4 α* generates two splice variants, *HNF4 α 2* (*P1*-*HNF4 α*) and *HNF4 α 8* (*P2*-*HNF4 α*), through the use of two alternative promoters (*P1* and *P2*) and two distinct 3' splice events (94). The study indicates that *HNF4 α 2* inhibits the development of colorectal cancer, while *HNF4 α 8* has the opposite effect (95).

Before colorectal cancer develops into an advanced stage, it typically remains asymptomatic. Thus, it becomes crucial to identify additional risk factors in order to determine which segment of the population should undergo further colonoscopy. Various abnormal splice variants of genes have been proven to affect the occurrence of CRC. Furthermore, some genes such as *BARD1* and *HNF4 α* have splice variants that have completely opposite effects on CRC. Therefore, it can be inferred that targeting specific splice variants may be more effective and promising in comparison to targeting disease-causing genes. Further research on the genes and splice isoforms discussed in our previous review may lead to more advancements in the prevention, early diagnosis, and treatment of CRC.

2.2 Splice isoforms in the proliferation of CRC

It is a frequent occurrence for tumor cells to exhibit abnormal splicing activity, resulting in an elevated frequency of splicing isoforms that sustain abnormal proliferation and apoptotic patterns. Alternative splicing plays a role in the processes of proliferation, differentiation, and apoptosis by regulating the alternative expression of numerous oncogenic or tumor suppressor genes, as well as splicing factors.

2.2.1 *H2AFY*

H2AFY (*MacroH2A1*) gene is a histone *H2A* variant that plays important roles in metabolic functions, transcriptional gene regulation, and DNA damage response (96).

H2AFY encodes two alternatively spliced variants, *H2AFY1.1* and *H2AFY1.2* (also known as *MacroH2A1.1* and *MacroH2A1.2*), via mutually exclusive exon splicing (97). Novikov et al. observed that the percentage of *MacroH2A1.1* relative to total *MacroH2A1* was significantly reduced in CRC samples compared to normal controls, and the level of *MacroH2A1.1* was regulated by *QKI*.

Moreover, the inhibition of proliferation mediated by *MacroH2A1.1* is attributed to the decrease in protein levels of poly(ADP-ribose) polymerase 1 (*PARP-1*) (98). Multiple lines of evidence suggest that *U2AF1* (*S34F*) can modulate alternative splicing, leading to a reduction in the *MacroH2A1.1* isoform (97, 99–101).

2.2.2 *MAT2 β*

Methionine adenosyl transferase (*MAT*) is the sole enzyme responsible for catalyzing the formation of S-adenosylmethionine, which is the primary biological methyl donor (102).

Human methionine adenosyl transferase 2 β (*MAT2 β*) encodes two splice variants, *V1* and *V2*, which differentially regulates cell growth. Of these, *V1* plays a key role in the regulation of apoptosis and its knockdown has been shown to induce apoptosis in colon cancer cell lines (103). These two variants are present in both the nucleus and cytoplasm of colon cancer cells, and the overexpression of them can increase the levels of cytoplasmic HuR (an mRNA binding protein), thereby affecting cancer cell proliferation (104).

2.2.3 ITGA6

Integrins consist of a heterodimeric pairing of an α and a β subunit. Currently, there are 18 α subunits and 8 β subunits that have been recognized, and they can combine together to create a total of 24 unique integrins (105).

During the formation of *integrin $\alpha 6$ (ITGA6)* subunit pre-messenger RNA, alternative splicing occurs to produce two distinct splice variants, namely integrins $\alpha 6A$ (ITGA6A) and integrins $\alpha 6B$ (ITGA6B) (106). These variants have different cytoplasmic domains, which contribute to their unique functions in cellular processes. Studies have suggested that the integrins $\alpha 6A$ splice variant of the integrin $\alpha 6$ subunit in CRC cells plays a pro-proliferative role and activates the Wnt/ β -catenin pathway to exert its effects (107). This pathway is recognized as the primary regulator of proliferative activity in the intestinal epithelium, both in its normal state and in CRC (108).

The study reveals that in CRC cells, the proto-oncogene MYC can control the activation of the promoter and splicing of the ITGA6 integrin gene through ESRP2 (109). This regulation promotes the production of the pro-proliferative ITGA6A variant. The pharmacological inhibition of MYC activity using the MYC inhibitor (MYCi) 10058-F4 leads to a decrease in the levels of ITGA6 and ITGA6A in CRC cells. This highlights the potential of targeted therapy against ITGA6A (109).

2.2.4 UPF3A

UPF3A, also known as up-frame shift 3A, plays a role in both the NMD pathway and GCR. Specifically, it acts as an inhibitor of the NMD pathway while simultaneously promoting GCR (110).

Human UPF3A pre-mRNA is regulated by alternative splicing, which produces two splice variants, UPF3A-L and UPF3A-S. The two variants depend on whether exon 4 is included or excluded. These splice variants can give rise to two protein isoforms, UPF3A and UPF3A-S, which have distinct functions (111). Wang et al. discovered that knockdown of UPF3A-L inhibited the proliferation of CRC cells and induced DNA damage response and cell death. Furthermore, their study also found that CHERP and SR140, both identified as U2 snRNP-associated proteins, can regulate the splicing of UPF3A pre-mRNA by binding to the enhancer elements in exon 4 of UPF3A and activating its inclusion, thereby affecting the proliferation of CRC cells (112). The target gene of UPF3A is SRSF3, which is positively correlated with the expression of UPF3A. Increasing SRSF3 could enhance the invasion and metastasis of CRC cells, resulting in a poor prognosis. Targeted inhibition of UPF3A could reduce the genetic compensation response and offer a new therapeutic approach for treating CRC (113).

2.2.5 MKNK2

Many kinase networks, such as EGFR, MAPKs, and c-Src, are involved in CRC development. MNKs, downstream of MAPKs, are protein kinases that can increase oncogenic mRNA translation by phosphorylating eIF4E, contributing to CRC pathogenesis (114).

MKNK2a and MKNK2b are two splice isoforms derived from the pre-mRNA of MKNK2 through alternative splicing (115). The

TCGA database showed that the MKNK2a/MKNK2b ratio was decreased in CRC tissues when compared to non-tumorous colon tissues (116).

Moreover, studies have found that CRC specimens exhibit decreased levels of MKNK2a and increased levels of MKNK2b, which are associated with KRAS mutations and tumor size. Their further experiments also demonstrated that elevated nuclear SRSF1 promotes MKNK2 splicing into MKNK2b rather than MKNK2a, thereby enhancing the proliferation of CRC tumors (117). SRPK inhibitors such as SRPIN340 and the PP1 α -specific inhibitor Tautomycin can efficiently disrupt SRSF1 phosphorylation, nucleus translocation, and MKNK2 alternative splicing (117). Therefore, this provides an opportunity for therapeutic intervention in CRC, such as the use of SRPK inhibitors or PP1 α allosteric activators for the treatment of malignant tumors.

2.2.6 Others

CABLES is a cell cycle regulatory protein that inhibits cdk2 activity by enhancing cdk2 tyrosine 15 phosphorylation by WEE1, ultimately leading to the inhibition of cell growth. However, research has revealed the presence of a 627bp abnormal splicing variant of CABLES in colon cancer, which leads to an increased cell growth rate in human colon cancer HT-29 cells, indicating that its role functions as a dominant negative mutant (118).

PARKIN, a tumor suppressor gene, functions as an E3 ligase and targets multiple substrates in the ubiquitin-proteasome system, inducing the degradation of cyclin E protein during the cell cycle. Its activity is modulated by growth factors. However, recent findings by Ikeuchi et al. have revealed that alternative splicing of the PARKIN gene leads to defects in the proteolysis of cyclin E, promoting colon cell proliferation and contributing to the development of colorectal cancer (119).

The 4-phosphatase Inositol polyphosphate 4-phosphatase II (INPP4B) is a regulator of the PI3K signaling pathway. The study demonstrated that a small transcript variant, INPP4B-S, generated by inserting a small exon between exon 15 and 16 and skipping exons 20-24, has been shown to promote the proliferation of colorectal cancer (120).

Flodrops et al. discovered that in CRC, tissue metalloprotease inhibitor I (TIMP1) increases proliferation and metastasis and decreases apoptosis by specifically regulating the FAK-PI3K/AKT and MAPK pathways. However, the splicing variant TIMP1-i3(+) generated by the retention of intron 3 of TIMP1 is involved in inhibiting the progression of colon cancer during the early transition from normal mucosa to colorectal adenoma, and is regulated by hnRNPA1 (121).

It is established that SMURF2 promotes the migration and invasion of cancer cells, indicating its potential oncogenic role in CRC (122). However, its splice variant Δ E2SMURF2 has been shown to control mouse intestinal tumor growth by upregulating the degradation of wild-type SMURF2 via type II TGF- β receptor and reducing the proliferation and production of pro-inflammatory cytokines (123).

The gene DBF4B produces two splicing variants, DBF4B-FL and DBF4B-S, through the inclusion or skipping of exon 6. Chen et al.

found that the upregulation of SRSF1 promotes the inclusion of exon 6 in *DBF4B*, leading to the increased expression of DBF4B-FL and promoting the occurrence and proliferation of CRC (124).

The splice variant of the human transformer 2 β (*TRA2B*) gene that contains exon 2 (*TRA2 β 4*) was found to be preferentially expressed in the nuclei of human colon cancer cells. It is possible that TRA2 β 4 could sequester Sp1 from binding to the promoters of target genes, which may promote cell growth by disrupting the gene expression program related to senescence (125). Nucleolin (126) and hnRNPA1 (127) have been shown to regulate the splicing of *TRA2 β* , which affects the levels of TRA2 β 4 and is associated with the abnormal growth of CRC cells.

The expression of the inhibitor of differentiation 1 (*ID1*) was found to be positively correlated with high tumor grade in CRC patients (128). The *ID1* gene can generate two distinct isoforms through alternative splicing, known as ID1a and ID1b. Research findings indicate that the overexpression of ID1a promotes cell proliferation, while ID1b has the opposite effect by inhibiting proliferation and maintaining an undifferentiated cancer stem cell-like phenotype, as well as inducing cell quiescence (129).

CDC14B is an important regulator of mitotic spindle assembly in eukaryotes, which can have an impact on cancer cell proliferation and mitotic spindle dynamics. Matrin3 is a splicing regulator that can suppress the inclusion of exons 13 and 14 in the *CDC14B* mRNA. Since exon 13 contains a premature termination codon (PTC), knockdown of matrin3 can increase the formation of a CDC14B-PTC variant that inhibits the proliferation of CRC cells and promotes apoptosis. Therefore, the Matrin3/CDC14B axis represents a promising target for CRC treatments (130).

Sustaining proliferation is one of the malignant characteristics of the tumor growth. This process can be further enhanced by aberrant splicing and the consequent generation of oncogenic splicing isoforms. The aforementioned splice variants have all been shown to directly or indirectly impact the proliferation of CRC. In particular, the splicing isoforms of certain genes, such as H2AFY, TIMPI, SMURF2, and ID1, have been identified to possess inhibitory proliferation properties, indicating that therapeutic approaches targeting these variants would be highly beneficial for disease control and treatment in CRC patients.

2.3 Splice isoforms in the metastasis/invasion of CRC

Overcoming invasion and metastasis are critical challenges in treating CRC. The activation of EMT during cancer metastasis and recurrence is abnormal and relies on the interactions between cancer cells and the microenvironment. Accurately identifying whether a tumor is invasive or metastatic is crucial for determining its behavior.

2.3.1 CD44

CD44, a transmembrane glycoprotein, can be alternatively spliced into multiple isoforms *via* the alternative splicing of its pre-messenger RNA (131). In the human gut epithelium, the

presence of three isoforms, namely CD44s, CD44v6, and CD44v4-10, is commonly observed (132). Studies have indicated that CD44v6 has a negative impact on the prognosis of CRC patients, as it promotes CRC colonization, invasion, and metastasis, and even increases CRC cell resistance to anti-cancer therapies (133).

The good news is that several strategies targeting CD44v6 have been developed to date. Some strategies aim to block the interaction between HA and CD44v6, such as using the soluble CD44 ectodomain, α -CD44-HABD mAb, or the small fragment of HA (sHA). Other strategies mainly target the exon v6-encoded region by developing an α -CD44v6 mAb or by synthesizing a CD44v6-specific peptide (134, 135). Ejima et al. (136) recently have developed a novel anti-CD44 mAb, C44Mab-9, which can be utilized for detecting CD44v6 in various applications, and further research needed to determine whether C44Mab-9 has antitumor activity *in vivo*.

2.3.2 CCTN

CCTN (*Cortactin*), encodes an actin-associated scaffolding protein, is overexpressed in CRC and regulates cell migration (137). The *CCTN* transcript that contains exon 11, known as CCTN isoform-a, is the most abundant among all *CCTN* transcripts. This isoform is the wild type and dominant one, containing the full functional repeats, and has the strongest abilities in binding and cross-linking filamentous actin (F-actin) and promoting cell migration (138). In contrast, CCTN isoform-b and isoform-c (which are much less abundant) lack the 6th repeat (exon 11), resulting in a reduced F-actin binding and polymerization ability and significantly decreased cell migration when compared to CCTN isoform-a (138).

Studies have shown that as a potential functional RNA-binding protein, high levels of PTBP1 lead to the inclusion of exon 11 in the *CCTN* gene, promoting the generation of CCTN isoform-a and thereby enhancing cell migration and invasion in CRC (139).

2.3.3 FAK

FAK is a type of cytoplasmic tyrosine kinase that is activated by both growth factors and integrins. Through AS of FAK pre-mRNA, specific exons (13, 14, 16, and 31) can be included independently, which in turn code for specific domains (boxes 28, 6, 7, and Pro-Trp-Arg, or PWR) that characterize FAK (140). There are different forms of FAK resulting from AS of its pre-mRNA. FAK0 is the most common form and is expressed in various tissues. FAK28 includes exon 13 and displays an increased expression with age, but its function in regulating FAK remains unknown. FAK6 and FAK7 include exons 14 and 16, respectively, and peak in expression during the final stages of embryonic development (141, 142).

The study found that FAK0 and FAK6 expressions are associated with metastatic potential in aggressive CRC cell lines HT29 and HCT116, suggesting that they could be markers of aggressiveness. FAK28 has a more specific role in tumor-microenvironment interactions. Therefore, FAK6 or FAK28 splice variants or their protein isoforms may be potential therapeutic targets for CRC primary tumors and metastasis (142).

2.3.4 TNC

Tenascin-C (TNC), encodes a matricellular protein, is abundantly expressed in both inflammatory lesions and tumor tissues (143, 144). Additionally, *TNC* contains a hidden functional site that consists of the amino acid sequence YTITIRGV, which is activated upon proteolytic cleavage (145).

Peptide TNIIIA2, a 22-mer *TNC* peptide that contains the functional sequence, has been found to strongly and persistently activate β 1-integrins (146). The active sequence of TNIIIA2 is located within the cancer-associated alternative splicing domain, fibronectin type III repeat A2 (FNIII-A2), of the *TNC* molecule (147). Therefore, it is speculated that TNIIIA2-containing *TNC* peptides/fragments may play a role in cancer pathogenesis by inducing β 1-integrin activation. OS2966 is a humanized and de-immunized monoclonal antibody that targets β 1 integrin and has been shown to have antiproliferative, anti-invasive, antivascularization, and proapoptotic functions (148). This could be beneficial in CRC cases with high *TNC* expression.

Recent studies have demonstrated that peptide TNIIIA2 directly promotes the *in vitro* invasiveness of colon cancer cells by increasing the secretion of matrix metalloproteinase (149). Moreover, *in vivo* experiments using a spontaneous metastasis model have revealed that peptide TNIIIA2 is implicated in the metastasis of colon cancer cells to the lung (150). ST2146 is a biotinylated anti-tenascin monoclonal antibody and is a promising treatment for CRC (151).

2.3.5 BIRC5 (SURVIVIN)

BIRC5 (SURVIVIN) is a member in the inhibitors of apoptosis (*IAP*) family regulating cell cycles and controlling programmed cell death (152). The human *BIRC5* gene comprises four dominant exons and two hidden exons. In addition to the wild-type *SURVIVIN*, alternative splicing of *SURVIVIN* pre-mRNA generates four different mRNAs that encode four unique proteins, namely *SURVIVIN*- Δ Ex3, *SURVIVIN*-2B, *SURVIVIN*-3B, and *SURVIVIN*-2 α (152, 153). Each splice variant has the potential to modulate survivin function by interacting with survivin during mitosis (154).

Ge et al. discovered that mRNA expression rates and levels of *SURVIVIN* and its four splice variants were increased in CRC tissues. Moreover, the expression levels of *SURVIVIN*- Δ Ex3 and *SURVIVIN*-3B were positively correlated with tumor aggressiveness (153).

Currently, several *SURVIVIN* inhibitors are undergoing clinical evaluation, and more specific and effective *SURVIVIN* inhibitors are being developed. For instance, YM155 is a small-molecule inhibitor that specifically targets and suppresses the activity of the survivin promoter. LY2181308 and SPC3042 (EZN-3042) are antisense oligonucleotides that limit survivin expression by binding to and degrading its mRNA (155). The use of survivin-2B80-88 in combination with IFA and IFN α has also been shown to result in clinical improvement and enhanced immunological responses for patients with CRC (156). However, targeted drugs against *SURVIVIN* splice variants still require further discovery and investigation (157).

2.3.6 CXCR3

The expression of C-X-C motif chemokine ligands (*CXCL*) 9, 10, and 11, along with other factors associated with EMT, is elevated at the invasive edge of CRC tissues (158). They involved in leukocyte trafficking, immune response, and cellular proliferation by binding to a common receptor, known as C-X-C motif chemokine receptor 3 (*CXCR3*) (159–161). This receptor belongs to the G protein-coupled receptor family and is expressed in CRC tissues (162).

In humans, three splice variants of *CXCR3* (*CXCR3A*, *CXCR3B*, and *CXCR3-alt*) have been discovered, and these variants play distinct roles in different types of cancer cells (163, 164). For example, gastric and renal cancer cells' invasiveness and metastasis are promoted by *CXCR3A* (165), while prostate cancer cells' invasiveness and migration are inhibited by *CXCR3B* (166). Recent studies have indicated that the *CXCL10*-induced proliferation and invasiveness of the HCT116 CRC cell line may be mediated by *CXCR3A*, not *CXCR3B* (167).

2.3.7 FOXM1

The Forkhead box m1(*FOXM1*) is known to function as a transcription factor essential for G (1)/S transition and controls proper execution of mitotic cell division (168). It is a key mediator of Wnt/ β -catenin signaling and acts by binding to β -catenin and stabilizing β -catenin in cell nuclear and enhancing transcriptional activity (169).

AS of exons 6 and 9 leads to the formation of various *FOXM1* isoforms. *FOXM1a* contains only exon 9, *FOXM1b* neither exon 6 nor 9, *FOXM1c* only exon 6 and *FOXM1d* contains both. *FOXM1* is the inactive isoforms, while *FOXM1b* and *FOXM1c* remain functional (170). Recent study has shown that *AKT1* works as an upstream kinase, regulating RBM17-mediated *FOXM1* alternative splicing and promoting the properties of cancer stem cells in CRC (171).

Rather et al. investigated the expression of *FOXM1* in 98 CRC samples and normal tissues, and found that *FOXM1* was elevated in CRC and linked to reduced disease-free survival (172). Overexpression of *FOXM1* in tumor tissues is also significantly related to metastasis in CRC through the induction of EMT (173). Another study also showed that the expression of *FOXM1* has a significant difference between CRC and adjacent noncancerous tissue samples. Silencing of *FOXM1* inhibited the proliferation, invasion, and migration of CRC cells. Furthermore, knockdown of *FOXM1* can also reduce VEGF-A levels in CRC cell lines, indicating that *FOXM1* could be a selective target for the molecularly targeted treatments of CRC (174). Additionally, SPF45/SR140/CHERP complex regulates *FOXM1* alternative splicing as well (170).

2.3.8 Others

A-type lamins, which are produced by alternative splicing of the *LMNA* gene located on chromosome 1q21.3 (175), have been shown to increase the risk of death from CRC. This is attributed to their ability to enhance invasiveness and potentially induce a more stem cell-like phenotype (176).

Pan et al. made a discovery that SRSF11 plays a pro-metastatic role in CRC by impeding the AS of *HSPA12A* (Heat Shock Protein

Family A (Hsp70) Member 12A pre-RNA). Their results highlight the novel connection between SRSF11-regulated splicing and CRC metastasis *via* *HSPA12A*, indicating that the PAK5/SRSF11/*HSPA12A* axis could serve as a promising therapeutic target and prognostic biomarker for CRC (177).

Multiple splice variants of the cholecystokinin-2 (*CCK2*)/gastrin receptor are ectopically expressed in gastrointestinal (GI) cancers. Studies have shown that one of these variants, CCK2i4svR, may enhance tumor angiogenesis through agonist-independent mechanisms, thus potentially contributing to the growth and metastasis of GI cancers (178).

TXL-2, a member of the thioredoxin (*TXN*) and nucleoside diphosphate kinase family, is a novel gene that undergoes alternative splicing to produce three distinct isoforms: *TXL-2a*, *TXL-2b*, and *TXL-2c*. Studies have demonstrated that *TXL-2b* significantly promotes cell invasion and metastasis through its interaction with the RAN and PI3K signaling pathways in CRC cells. In contrast, *TXL-2c* inhibits these processes (179).

The *HDM2* oncogene is known to negatively regulate the *P53* gene. In colorectal cancer tissues and cells, four *HDM2* splicing variants have been identified: *HDM2/1338*, *HDM2/707*, *HDM2/1007*, and *HDM2/1200*. Experimental results indicate that the expression of *HDM2* splicing variants is associated with advanced tumor stage and distant metastasis in wild-type *P53* cases, as well as poor survival of patients (180).

ZO1 is a widely recognized cytoplasmic scaffolding and tight junction protein (181), and the AS event of *ZO1* exon 23 (*ZO1 E23*) plays a crucial role in the progression of CRC. Research has shown that the deletion of *ZO1 E23* (*ZO1 E23-*) leads to a disruption in F-actin distribution, which promotes CRC cell migration and invasion (182). Conversely, the inclusion of exon 23 in *ZO1* (*ZO1 E23+*) has the opposite effect. *SRSF6* (183), *HnRNP L* (184), *RBM47* (185), and *GLTSCR1* (182) have all been shown to regulate *ZO1 E23* AS, thereby impacting the development of CRC. The β 2-adrenergic receptor agonist, indacaterol, has been identified as an inhibitor of *SRSF6*, which suppresses the AS of *ZO1* and subsequently suppresses CRC tumorigenesis (183).

Carcinoembryonic antigen-related cell adhesion molecule 1 (*CEACAM1*) is a protein that is often overexpressed in CRC and has been found to be correlated with clinical stage (186, 187). *CEACAM1* has alternatively spliced isoforms that contain either three or four Ig-like extracellular domains, and a long (*CEACAM1-L*) or a short (*CEACAM1-S*) cytoplasmic tail (188). Studies have shown that compared to *CEACAM1-S*, *CEACAM1-L* promotes the invasion and migration of CRC (189).

In addition to the aforementioned variants, two splicing variants of *RON*, *RON Δ 165E2* (190) and *RON Δ 160(E2E3)* (191), have been identified in recent years, and both have been demonstrated to enhance the growth and metastasis of CRC.

NF-Y is a heterotrimeric transcription factor composed of the DNA-binding subunit, NF-YA, and the histone-fold domain, NF-YB/NF-YC dimer. There are two splice variants of NF-YA: NF-YAs and NF-YAl. The latter results from the inclusion of exon 3 within the transactivation domain. Study has shown that high levels of NF-YAl transcription can forecast the poor overall survival in CRC patients, and tumor cells exhibiting elevated NF-YAl expression

possess greater single-cell migratory and invasive potential. Targeting the NF-YAl splice variant and increasing the NF-YAs/NF-YAl ratio may decrease the progression of metastatic CRC (192).

The dissemination of tumor cells is the most dangerous process in the development of tumors. For many years, invasion and metastasis have been challenging obstacles in the battle against cancer, causing distress for both doctors and patients. Here, we have summarized some relevant splice variants and found that different splicing isoforms of *HSPA12A*, *TXL-2*, and *ZO1* can promote or inhibit the invasion and metastasis process. Therefore, the discovery of splice variants associated with invasion and metastasis in CRC mentioned above brings new hope for effective treatment and improved prognosis in CRC.

2.4 Splice isoforms and the apoptosis in CRC

Apoptosis is a cellular process that occurs in physiological and pathological conditions, defects in apoptosis can lead to malignant transformation, tumor metastasis and drug resistance. AS of genes can impact the CRC development by affecting the apoptosis network of CRC.

2.4.1 c-FLIP

FLICE-inhibitory protein (*FLIP*) is an inhibitor that regulates apoptosis mediated by death receptors (193). The Human *FLIP* gene is approximately 48 kb in size and includes at least 14 exons, which can generate 11 different isoforms through alternative splicing (194). Cellular *FLIP* (*c-FLIP*) is predominantly expressed as two splice variants, including a long form (*c-FLIPL*) with two serial death effector domains (DEDs) in the amino-terminal followed by a caspase-like domain (CLD) in the carboxy-terminal, and a short form (*c-FLIPS*) with only two N-terminal DEDs (194). Both splice variants of *c-FLIP* can inhibit proapoptotic downstream molecules (195).

c-FLIPL has been found to be significantly higher in colorectal cancer compared with matched normal tissue, suggesting that *c-FLIPL* may contribute to *in vivo* tumor transformation (196). The apoptosis induced by silencing of one splice form may be counteracted partly by the other splice form. However, researchers also found that specific silencing of *c-FLIPL* can effectively inhibit HCT116 tumor growth and induce apoptosis as silencing both splice forms, and *c-FLIPL* overexpression can dramatically inhibit the growth-inhibitory effects of chemotherapy *in vivo* setting, suggesting that the *c-FLIPL* may be the more important regulator of CRC (195).

2.4.2 ZNF148

Zinc fingers proteins (*ZNF*) are the largest family of DNA binding proteins and can act as transcriptional factors in eukaryotes, and selectively binds to specific DNA sequences in the promoter of target genes *via* characteristic zinc finger domain (197). *ZNF148* plays a significant role in cell growth, proliferation, differentiation, apoptosis and other biological activities (198).

ZNF148 has two functionally distinct alternative splicing isoforms. *ZNF148FL* contains a complete 794 amino acids, while *ZBP-148ΔN* was generated by alternative promoter usage upstream of an alternative exon 4B, and the *ZBP-148ΔN* protein lacks the amino-terminal 129 amino acids (197, 198). Two splicing isoforms of *ZNF148* mutually antagonize with each other. Overexpression of *ZNF148FL* can decrease *ZNF148ΔN* expression, and promote the proliferation, migration, and invasion of human CRC cells through binding to the transcription factor p300 and modulating the Wnt signaling pathway. On the contrary, overexpression of *ZNF148ΔN* can reduce levels of *ZNF148FL* and inhibit the upregulation of Wnt signaling pathway by *ZNF148FL*, subsequently promote the apoptosis, and inhibits the proliferation, migration, and invasion of CRC cells (198).

2.4.3 SYK

Spleen tyrosine kinase (SYK) is a 72 kDa non-receptor tyrosine kinase that contains two tandem Src homology 2 domains at the NH2 terminus and a kinase domain at the COOH terminus (199, 200). SYK has two alternatively spliced isoforms: the full-length (SYK(L)) is predominantly found in nuclear, while the short form (SYK(S)) lacks a 69-nucleotide exon and is only expressed in the cytoplasm (199, 200). It has been shown that hnRNP-K protein regulates the splicing pattern of SYK (199).

SYK implicated in the control of apoptosis, and in the regulation of cell cycle. Deficiency of SYK (L) leads to the accumulation of cells in the G2-M phase of cell cycle, and to the emergence of cells with a >4N DNA (199). Ni et al. found that SYK (L) was downregulated in 69% of tumor tissue samples compared to the adjacent non-cancerous tissue, the expression of SYK (S) remained stable, suggesting that SYK (L) but not SYK (S) is associated with tumor suppressing activities (200). Denis et al. further demonstrated that survival of CRC cell depends on SYK(L), since silencing of SYK(L) expression affected cell viability and induced apoptosis (199, 200). C-13 is an original non-enzymatic inhibitor of SYK, which shows promising potential for the treatment of CRC and other cancer diseases (199).

2.4.4 PGAM5

PGAM5 is a member of the phosphoglycerate mutase family and has two splicing variants, including a long form (*PGAM5L*) and a short form (*PGAM5S*). Alternative splicing results in a truncation at amino acid residue 239 of the *PGAM5* protein, with the *PGAM5S* isoform contains 16 additional C-terminal hydrophobic amino acids, while the *PGAM5L* isoform containing 50 additional hydrophobic amino acids residue at the C terminus (201, 202).

Both isoforms of *PGAM5* function in the intrinsic necrosis induced by TNF- α as well as reactive oxygen species (ROS) and calcium ionophore (201, 202). Further experiment indicated that *PGAM5L* is indispensable for the execution of intrinsic apoptosis by controlling the Bax activation and Drp1 dephosphorylation and induces mitochondria fission, Bax-*PGAM5L*-Drp1 complex is a potential target for CRC treatment (201).

2.4.5 WNT5A

The canonical Wnt/ β -catenin pathway is widely recognized as being associated with the formation of CRC (203). *WNT5A* (Wnt

Family Member 5A) is an extracellular glycoprotein that activates Wnt signaling pathways, which are important in both development and tissue homeostasis (204, 205). According to a recent study, the opposing roles of *WNT5A* in cancer can be attributed to the encoding of two different splice isoforms, *WNT5A-long* (L) and *WNT5A-short* (S) (206). The *WNT5A-L* mRNA isoform can promote cell apoptosis, thereby suppressing cell proliferation and acting as a tumor suppressor in CRC cells. Conversely, the *WNT5A-S* mRNA isoform can inhibit cell apoptosis, promoting cell proliferation and playing an oncogenic role in CRC cells (207).

2.4.6 Others

It is known that *FAS* (Fas Cell Surface Death Receptor) mediates apoptosis of CRC cells (208, 209). The pre-mRNA of *FAS* undergoes alternative splicing that excludes exon 6, resulting in the production of soluble *FAS* (sFAS) protein. This protein lacks a transmembrane domain and functions to inhibit *FAS*-mediated apoptosis (210).

The *MRPL33* gene is responsible for encoding a protein found in the large subunit of the mitochondrial ribosome. The depletion of *MRPL33*'s long isoform (*MRPL33-L*) which contains exon 3, has been shown to impair proliferation and increase apoptosis in both cancer cell lines and xenograft models (211). Studies have found that *MRPL33-L* expression is elevated in human colorectal cancer tissues, and this has been correlated with the levels of hnRNP-K (211).

BCL2L1, a crucial gene in regulating apoptosis, is functionally involved in various cancer-related processes, and its protein expression has been linked to 20q gain. This suggests that the expression of *BCL2L1*, which is dependent on 20q gain, may play a role in the progression of colorectal adenoma to carcinoma. *BCL2L1* encodes two splice variants, an anti-apoptotic *BCL-X(L)* and a pro-apoptotic *BCL-X(S)* (212). ABT-737, a *BCL-2/BCL-X(L)* anti-apoptotic protein inhibitor, has successfully completed a prospective multicenter single-arm phase II study (213). This demonstrates the potential of targeting *BCL-X(L)* in CRC (colorectal cancer) therapy.

LINC00963 is an oncogenic lncRNA that is upregulated in CRC tissues. Recently, two novel variants of this gene, *LINC00963-v2* and *LINC00963-v3*, have been discovered to be downregulated in CRC tissues. *LINC00963-v2* lacks exons 2, 3, and 4, while *LINC00963-v3* lacks exons 3 and 4. Overexpression of *LINC00963-v2/-v3* in CRC cells has been found to suppress their proliferation, viability, and migration, and increase apoptosis. These effects are mainly due to attenuating the PI3K/AKT and Wnt/ β -catenin signaling pathways. Therefore, these lncRNAs could serve as potential targets for CRC therapy (214).

Cancer typically inhibits the cellular apoptosis mechanism in the body, resulting in uncontrolled tissue growth. Chemotherapy uses the association between cellular apoptosis and cancer to destabilize the tumor and cause its death. It can be observed that the above-mentioned genes and their splice variants have different effects on apoptosis in CRC. Inducing the production of more pro-apoptotic splice variants could have a certain effect on the control and treatment of CRC.

2.5 Splice isoforms and the angiogenesis in CRC

Tumor growth, dissemination and metastasis are dependent on angiogenesis. AS of angiogenesis-related genes can lead to the formation of distinct functional subtypes, while an imbalance among isoforms can impact tumor progression. It would be beneficial for the development and outcome of CRC if the regulation of splice variant proportions through targeting relevant splice variants could inhibit angiogenesis.

2.5.1 VEGF

The vascular endothelial growth factor (*VEGF*) family of proteins regulates blood flow, growth, and function in both normal and diseased states, and VEGF-A is the most significant isoform of *VEGF* responsible for regulating angiogenesis (215). Additionally, VEGF-A and its receptors have been found to be highly expressed in mCRC (215).

The *VEGF* gene resides on chromosome 6 and consists of 8 exons (216). The *VEGFxxx* family of *VEGF* is produced through differential splicing in exons 6 and 7 and the proximal splice site in exon 8, whereas the distal splice site selection 66 bp downstream of the proximal splice site in exon 8 results in *VEGFxxx*b (217). The conventional *VEGFxxx* has angiogenic properties, while the *VEGFxxx*b isoform family has antiangiogenic properties, with xxx indicating the number of amino acids in a particular isoform (217). 12 isoforms of VEGF-A have been identified (218). The increase in VEGF-Axxx isoforms and the decrease in VEGF-Axxx levels lead to an imbalance among the isoforms (215).

Bevacizumab is the first anti-angiogenetic treatment approved for clinical use in CRC patients. However, it has been reported to have a low response rate but a high rate of resistance and adverse events (219). Administering recombinant VEGF-Axxx isoforms may be a promising new therapeutic approach (220).

2.5.2 TIA-1

T-cell Intracellular Antigen-1 (*TIA-1*) is a binding protein recognizing the complex secondary structure of the 3' UTR, assisting in alternative RNA splicing, export and translational regulation that contribute to cancer formation and progression (221). *TIA-1* itself also undergo alternatively spliced in exon 6a to form two isoforms, namely flTIA-1 and sTIA-1 (222). TIA-1 can bind to VEGF-A RNA and act as a splicing and translational regulator of VEGF-A, influencing the angiogenic capability of CRC (223).

sTIA-1 had been found to be highly expressed in *KRAS* mutant colon cancers. It exerts its effects by preventing flTIA-1 from inhibiting splicing and/or translating the VEGF-A165a, a pro-angiogenic isoform of *VEGF*, to promote tumor growth and angiogenesis (222). However, flTIA-1 expression also inhibited the effect of anti-VEGF antibodies, added a layer of intricacy to the anti-angiogenic treatment.

2.5.3 CALD1

Caldesmon (CaD) is an actin-binding protein encoded by the *CALD1* gene. There are at least two high-molecular-weight isoforms

(h-CaD) and four low-molecular-weight isoforms (l-CaD) produced by alternative splicing (224, 225). The alternatively spliced variants of the l-CaD are further differentiated by inclusion (Hela l-CaD) or exclusion (WI-38 l-CaD) of exon 1 (225).

The expression of Hela l-CaD was restricted to the tumor vasculature and was not found in normal blood vessels of cancers derived from colon and other various organs and was preferentially expressed in the early stage of tumor neovascularization. This indicates that Hela l-CaD can be considered as a marker of angiogenic endothelial cells during the early stages of tumor neovascularization (225). Kim et al. found that l-CaD significantly increases in primary colon cancer and liver metastasis than in the corresponding normal tissues, while h-CaD did not differ among these groups, and colon cancer patients with high levels of l-CaD had a poor response to chemoradiotherapy (226). These data suggested that l-CaD can be used for diagnosis and prognosis, and maybe a potential target for CRC treatment.

2.5.4 VEGFR2

Vascular endothelial growth factor receptor 2 (*VEGFR2*) is the primary receptor of *VEGF*. There are two distinct forms of *VEGFR2* that are expressed: the membrane-bound *VEGFR2* (mVEGFR2) and the soluble *VEGFR2* (sVEGFR2) (227, 228).

Retention of intron 13 would lead to an in-frame early termination TAA codon, resulting in a truncated transcript variant. The protein product of this variant would lack the transmembrane and intracellular tyrosine kinase domains of *VEGFR2* (227). Tumor vascularization and tumor growth can be inhibited by both decreasing mVEGFR2 and increasing sVEGFR2 since sVEGFR2 has anti-angiogenic and anti-lymphangiogenic properties, whereas mVEGFR2 has the opposite effect (229).

Therapeutic drugs targeting *VEGFR2*, such as anti-VEGFR2 antibodies, siRNAs, and small-molecule *VEGFR2* inhibitors, have shown success in a variety of preclinical animal studies and clinical trials. Morpholino is considered a novel therapy that targets *VEGFR2* (229).

2.6 Splice isoforms and the immunity in CRC

Immune mechanism in tumor is very complex and is associated with AS. AS of genes can participate in the process of tumor immunity by affecting cytokine signaling or the function and infiltration of immune cells, which can impact tumor proliferation and migration. The discovery of immune-related splice variants associated with CRC will assist us in understanding the immune mechanisms of CRC and guide targeted and immunotherapy for CRC.

2.6.1 IL6R

Interleukin-6 receptor (*IL-6R*) plays an important role in inflammation, immune cell differentiation and cancer. IL-6 can signal in two different ways, one is classic signaling *via* the membrane-bound IL-6R, another is trans-signaling *via* soluble forms of the IL-6R (sIL-6R).

sIL-6R can be generated from different mechanism, proteolytic cleavage of membrane IL-6R by transmembrane metalloproteases, release of cytokine receptors from cells on extracellular vesicles, and the generation an alternatively spliced mRNA isoform in transcriptional mechanism without the region encoding the transmembrane domain (230, 231). IL-6 can bind to IL-6R or sIL-6R to form the IL-6/IL-6R complex which can interact with the IL-6 transducer expressed gp130, subsequently results in gp130 dimerization and phosphorylation and activates the receptor-associated kinases such as JAK1, JAK2, and Tyk2, which eventually promote the cell proliferation and tumor progression (230). Recent studies have found a correlation between increased serum levels of IL-6 and sIL-6R in patients with CRC and tumor size as well as poor prognosis in those with metastatic colorectal cancer (230, 232). For instance, the compound Evodiamine has shown potential in inhibiting intestinal inflammation and the development of CRC by suppressing IL-6 signaling (233). These findings suggest that blocking IL-6 trans-signaling could play a role in the treatment of CRC.

Therapeutic drugs targeting IL-6R are currently under development. For example, Tocilizumab, an anti-IL-6 receptor antibody, has completed phase III randomized controlled trials (234), while Olamkicept, a soluble gp130-Fc fusion protein that selectively inhibits trans-signaling of interleukin-6 (IL-6) by binding to soluble IL-6 receptor/IL-6 complex, has completed randomized clinical trials (235).

2.6.2 PPAR

Peroxisome proliferator-activated receptors (PPARs) belong to the nuclear hormone receptor family including three AS isoforms, namely PPAR α , PPAR β/δ and PPAR γ . PPAR β/δ -linked tumorigenesis was first identified in CRC and was considered as a potential drug target for CRC (236). The organization of the coding exons of PPAR β/δ corresponds to that of the genes encoding PPAR α and PPAR γ . PPAR γ 1 and γ 2 are generated by using the differential promoter and AS (237), and four different splicing isoforms of PPAR β/δ mRNAs containing one or two non-coding 5'-exons are also generated by alternative promoter (238).

PPAR can promote lipid accumulation in NK cells, inhibit of their cellular metabolism and thus inhibit their function (239). Schumann et al. found that most of PPAR β/δ target genes are upregulated in tumor-associated macrophages (TAMs) from ovarian carcinoma patients, activation of PPAR β/δ target genes by polyunsaturated fatty acids which act as potent PPAR β/δ agonists in macrophages contributes to the pro-tumorigenic polarization of ovarian carcinoma TAMs (240). Therefore, PPAR β/δ has the pro-tumorigenic functions by promoting polarization of macrophages favoring tumor progression or impairing antitumor cytotoxicity of NK cells (241). A recent study has found that blocking the PPAR pathway can promote apoptosis and inhibit the development of CRC organoids *in vitro*, indicating that the PPAR signaling pathway is involved in CRC tumorigenesis (242).

2.6.3 IL22RA2

Interleukin-22 (IL-22) is an IL-10-type cytokine involved in various pathologic processes. It is signaled through a membrane

receptor composed by the heterodimer IL-22R1/IL-10R2 and can be recognized by a secreted receptor called IL-22 binding protein (IL-22BP), which is encoded by the *IL22RA2* gene (243). Human *IL22RA2* gene can express three alternatively spliced variants including IL22RA2v1 (IL-22BPi1), IL22RA2v2 (IL-22BPi2), and IL22RA2v3 (IL-22BPi3). IL-22BPi1 was retained intracellularly because of the presence of exon 3 in its mRNA; the sequences of IL22RA2v1 and IL22RA2v2 differ only in exon 3; IL-22BPi2 consists of two fibronectin III domains, whereas IL-22BPi3 lacks the C-terminal domain except for five frameshifted residues (244).

IL-22BP is highly expressed by dendritic cells (DC) in colon under homeostatic conditions and plays a crucial role in controlling tumorigenesis and epithelial cell proliferation. Although IL-22BPi3 was more abundant in human tissues, IL-22BPi2 was more effective than IL-22BPi3 at blocking IL-22 signaling, while IL-22BPi1 was unable to antagonize IL-22 signaling because it is not secreted (244).

IL-22BP deficiency can lead to the accelerated and increased tumorigenesis in colitis-associated colon cancer model (245). However, it is also reported that CD4⁺ T cells from patient with IBD produce high levels of IL-22BP, which can block the protective actions of IL-22 during acute colitis (246, 247). A study demonstrated that the delivery of liposome-protamine-IL-22BP mRNA complex can induce tumor apoptosis, inhibit angiogenesis, and increase infiltration of immune cells, showing a promising potential for colon cancer therapy (248).

2.6.4 ILT3

Inhibitory receptor Ig-like transcript 3 (*ILT3*) is an immunoregulatory protein that belongs to the *ILT* family. Human *ILT3* is mainly expressed in dendritic cells and monocytes. It is generally viewed as having a negative regulatory function (249).

Alternatively spliced mRNA that results from the deletion of exons 5–7 of *ILT3* encodes a soluble form of the ILT3 (sILT3) protein, which lacks the ILT3 transmembrane domain, causing the release of ILT3 in the circulation (250). Both membrane-bound ILT3 and sILT3 could inhibit the proliferation of T cells, induce its anergy, and promote the differentiation of CD8⁺ T cells within the tumor microenvironment or in sentinel lymph nodes. Furthermore, patients with CRC have been found to have a significantly higher amount of sILT3, which inhibit tumor immunity in CRC (250). A study revealed that the decreased expression of ILT3 in CRC patients is associated with improved overall survivals (251). The data suggested that the expression of *ILT3* could have a significant impact on the progression of CRC and serve as a target for individualized therapy.

2.7 Splice isoforms and the metabolism reprogramming in CRC

Metabolic reprogramming is a distinguished cancer hallmark. AS can affect CRC through participating in many metabolic pathways, such as lipid metabolism and carbohydrate metabolism. Studying the genes and their splice variants associated with CRC metabolic reprogramming can aid in the development of new

treatment strategies, such as targeting these variants to interfere with the survival and proliferation of cancer cells by disrupting their metabolic pathways. This has the potential to become an important approach in future cancer therapy.

2.7.1 PKM

The Warburg effect is characterized by the preference of tumor cells for glycolysis over oxidative phosphorylation for energy production, and this metabolic shift is a crucial factor in malignant transformation. Studies have shown that this metabolic alteration results from a change in the expression of different splice variants (PKM1 and PKM2) of the glycolytic enzyme pyruvate kinase (PK) (252). The PKM1 isoform promotes oxidative metabolism, whereas PKM2 enhances aerobic glycolysis. And data suggest that the decrease in PKM1 expression may contribute to the upregulation of glycolysis and the downregulation of butyrate oxidation in CRC cells (253). Furthermore, multiple studies have suggested that PTBP1 (254), lncRNA SNHG6 (255), lncRNA HOXB-AS3 (256), Sam68 (257), MicroRNA-124 (258), lncRNA XIST/miR-137 axis (259), TRIM29 (260), and other molecules can target PKM1/PKM2 and influence their ratio, thereby impacting the growth, glycolysis, and even chemoresistance of CRC cells.

2.7.2 UGT1A

UDP-glucuronosyltransferase enzymes (UGTs) are responsible for glucuronidation pathway which is a major cellular process of conjugative metabolism (261). Girard et al. (262) found that a new exon 5b, located in between the coding exons 4 and 5, can undergo alternatively spliced with exon 5a (the classical exon 5), generating new UGT1A mRNA variants referred to as isoforms 2 or i2. UGT1A_i2 is enzymatically inactive and acts as a negative modulator of UGT1A1_i1, resulting a significant repression of UGT1A_i1-mediated drug metabolism (262, 263), and influencing cancer cell metabolism *via* complex protein network connecting other metabolic pathways (264). Studies have shown that UGT1A_i2 mRNA is downregulated in colon tumors, and the depletion of UGT1A_i2 proteins in colon tumors cell model can enforce the Warburg effect, leading to lactate accumulation and impacting migration properties (264).

2.7.3 ACSL

Long-chain acyl-CoA synthetases (ACSL) plays a crucial role in the degradation of fatty acids, the remodeling of phospholipids, and the synthesis of long acyl-CoA esters that controls a multitude of physiological processes in mammals. Five ACSL genes have been identified, namely ACSL1, ACSL3, ACSL 4, ACSL 5, and ACSL 6, with each gene having up to five different spliced variants, and most spliced variants are generated by AFE, ES, and MXE (265). Among these spliced variants, ACSL1 and ACSL4 were found to be overexpressed in CRC patients with poorer outcomes (266).

The metabolic profiles of both ACSL1 and ACSL4 isoforms were significantly different. ACSL1 was more inclined to triglyceride synthesis while ACSL4 prefers longer polyunsaturated fatty acids (PUFA) such as arachidonic acid as substrates. Furthermore,

ACSL1 exhibits a tendency towards invasive capabilities accompanied by a decrease in the basal oxygen consumption rate, whereas ACSL4 promotes the proliferation in CRC cells and is related to a more glycolytic phenotype compared to control or ACSL1 cells (266). It is reported that the combination of ACSL/SCD inhibitors can reduce the survival of CRC cells without impacting normal cells, and it is also effective in CRC cells resistant to the conventional chemotherapy. Therefore, the inhibition of ACSL/SCD axis is of great potential in cancer treatment (267).

2.8 Splice isoforms and the drug resistance in CRC

AS can not only influence therapeutic efficacy but also serve as a prognostic and predictive biomarker for CRC. Different AS isoforms may have contrasting functions in drug resistance. Targeting these isoforms is highly likely to help adjust and refine the corresponding treatment strategies, overcome cancer drug resistance, and thus improve the therapeutic efficacy of CRC.

2.8.1 ASPP2

ASPP2 is a tumor suppressor that enhances apoptosis and inhibit tumorigenesis *via* P53-dependent and P53-independent pathways (268, 269). Exon-skipping splicing of ASPP2 results in the generation of ASPP2 κ , which is a C-terminally truncated isoform that lacks the P53 binding sites. This isoform is defective in promoting stress-induced apoptosis (270). The overexpression of ASPP2 κ in tumor tissue compared to adjacent normal tissue contributes to CRC by enhancing proliferation, promoting cell migration, and conferring resistance to chemotherapy-induced apoptosis (271). It serves as a potential treatment target and acts as a prognostic and predictive biomarker for CRC.

2.8.2 OPN

Osteopontin (OPN) is an extracellular matrix protein that is overexpressed in various cancers. It promotes cancer cell proliferation, survival, metastasis, and angiogenesis. There are three main splicing isoforms of OPN: OPNa, OPNb, and OPNc. OPNa is the full-length wild-type form, while OPNb and OPNc are mutually exclusive splicing isoforms. OPNb lacks exon 5, while OPNc lacks exon 4 (272). After 5-FU treatment of colon cancer cells, the splicing isoform OPNc was found to be the most upregulated in comparison to the other two isoforms, and the secretory OPNc can stimulate cells to survive from drug-induced microenvironmental stress (273). Preventing OPN splicing could be an effective method of inhibiting tumor progression and recurrence.

2.8.3 LGR5

LGR5 can inhibit the degradation of β -catenin, resulting in the accumulation of β -catenin and its translocation into the nucleus where it regulates the expression of a wide range of target genes (274). LGR5 has been reported to be overexpressed in CRC patients and correlated with poor prognosis (275). Additionally, LGR5 has

been found to drive tumorigenesis in both the small intestine and colon (276).

LGR5 consists of 18 exons, with exons 1–17 constituting extracellular leucine-rich repeats (LRRs). There are two transcript variants of *LGR5*, one lacking exon 5 (*LGR5Δ5*) and the other lacking exon 8 (*LGR5Δ8*) (277).

LGR5FL-positive cells exhibit low proliferative activity and resistance to anti-tumor drug, while blocking *LGR5* exon 5 impairs the dormancy of *LGR5FL*-positive cells and gives the ability of proliferation, subsequently increasing the sensitivity to chemical treatments (277). The study has also demonstrated that the low level of *LGR5Δ5* expression was significantly correlated with a poor prognosis for the disease-associated survival of soft-tissue sarcoma patients (278). It appears that the *LGR5* exon 5 Ab has the potential to be a new and promising drug for CRC.

2.8.4 Others

SYK is associated with the survival of CRC cells. Although the overexpression of *SYK(S)* did not alter proliferation and metastasis, *SYK(S)* is important in the chemotherapeutic treatment of CRC. Both *SYK(L)* and *SYK(S)* can increase the sensitivity of CRC cells to 5-FU, which is significant in cancer treatment (200).

AS of *FOXM1* leads to its functional isoform and promotes 5-FU resistance by upregulating *ABCC10* through directly binding to its promoter region, silencing of *FOXM1* promoted the sensitivity of CRC cells to 5-FU by enhancing cell apoptosis (170, 279). The study has also demonstrated that *FOXM1* can potentially regulate other 5-FU targets, such as thymidylate synthase (TYMS), thymidine kinase 1 (TK-1) and thymidine phosphorylase (TYMP); inhibiting *FOXM1* leads cell cycle arrest, DNA damage, and apoptosis in CRC cell lines (280).

Alternative splicing results in the inclusion of a new exon 11 in the *RAF1* mRNA, which causes a frameshift and introduces three premature stop codons, leading to the truncation of the *RAF1* protein and the absence of its C-terminal kinase domain. The resulting splice isoform is named *RAF1-tr* (281). *RAF1-tr* can increase nuclear localization and inhibits the function of DNA damage-regulating protein. This leads to an increase in the levels of DNA damage after the exposure to bleomycin and radiation, and enhances the apoptotic response of CRC cells to double-stranded DNA damage (281).

The unfolded protein response (*UPR*) is a cellular stress response related to the endoplasmic reticulum (ER). Inositol requiring enzyme 1 (*IRE1α*) is a ER-localized proteins that constitutes one arm of the *UPR* (282). Chemotherapeutic agents trigger ER stress and activate *UPR*. Upon activation, *IRE1α* removes a 26-bp nucleotide intron from the mRNA encoding X-box binding protein (XBP) 1 to causing a frame-shift and producing an active form *XBP1s*, which controls the expression of genes involved in protein folding, ER-associated degradation, protein quality control and phospholipid synthesis (282–284). Sustained activation of the *UPR* contribute to oncogenic processes, metastasis, and tumor chemotherapy resistance (282, 285).

LIN28B has two alternative splicing isoforms which are different in 5' exons, namely the *LIN28B*-long and *LIN28B*-short isoforms.

The *LIN28B*-long isoform consists of 250 amino acids and has both cold shock domain (CSD) and zinc finger domains (ZFDs), whereas the *LIN28B*-short isoform lacks 70 amino acids in the N-terminus and deficient with a complete CSD (286, 287). The overexpression of *LIN28B*-long isoform can downregulate *LET-7* expression, which negatively regulates the RAS/ERK signaling. The *LIN28B*-short isoform does not suppress *LET-7* and acts as an antagonist against the *LIN28B*-long isoform in normal colonic epithelial homeostasis (287). Therefore, it is the *LIN28B*-long isoform rather than the *LIN28B*-short isoform that contributes to the drug resistance. Targeting the CSD of *LIN28B* may have a potential therapeutic effect in treating *LIN28B* positive CRC.

CACCLnc is a recently discovered novel lncRNA. It can promote drug resistance in CRC by specifically binding to YB1 and U2AF65, both of which are splicing factors. This binding promotes their interaction and then modulates the AS of *RAD51* mRNA, thereby promoting DNA repair and enhancing homologous recombination (288). Targeting *CACCLnc* and its associated pathway may assist in improving treatment outcomes for CRC patients with chemoresistance.

3 Conclusion and perspectives

In summary, under the influence of various factors, abnormal splicing events in genes lead to the generation of different splicing variants. Due to distinct coding information, these isoforms can encode proteins with different structural and functional characteristics, in the sense that they may impact the activity of signaling pathways, regulate the cell cycle, and affect the stability of genes, thereby exerting different functional effects on CRC. For instance, when compared to *ZNF148FL*, *ZNF148ΔN* is generated through alternative promoter usage upstream of an alternative exon 4B. Consequently, it lacks the amino-terminal 129 amino acids, part of the transcriptional activation domain of the protein. This difference leads to the mutually antagonistic effects and distinct roles in the development of CRC. Different from typical targeted therapies, targeted splicing therapy usually has higher tumor specificity due to acting on abnormal splicing events in tumors. Thus, targeted splicing therapy is expected to achieve the targeted inhibition of cancer-promoting molecules while maintaining the regulatory effect of the molecule on normal cells and reducing the impact on healthy tissues for traditional antitumor drugs cannot avoid side effects and toxicity. In other words, targeted therapies are supposed to substitute these traditional drugs. As a more effective and safer new strategy for tumor treatment, targeted splicing therapy has great potential for the development in the field of oncology treatment (e.g. CRC). Because different splicing events occur in different phenotypes of CRC, personalized targeted splicing treatments are necessary to improve outcomes and minimize adverse effects.

In this review, we summarize the current progress in targeted therapies for these splicing variants and some potential therapeutic approaches (shown in Figure 3 and Table 1). However, although numerous splicing isoforms have been identified, many of them

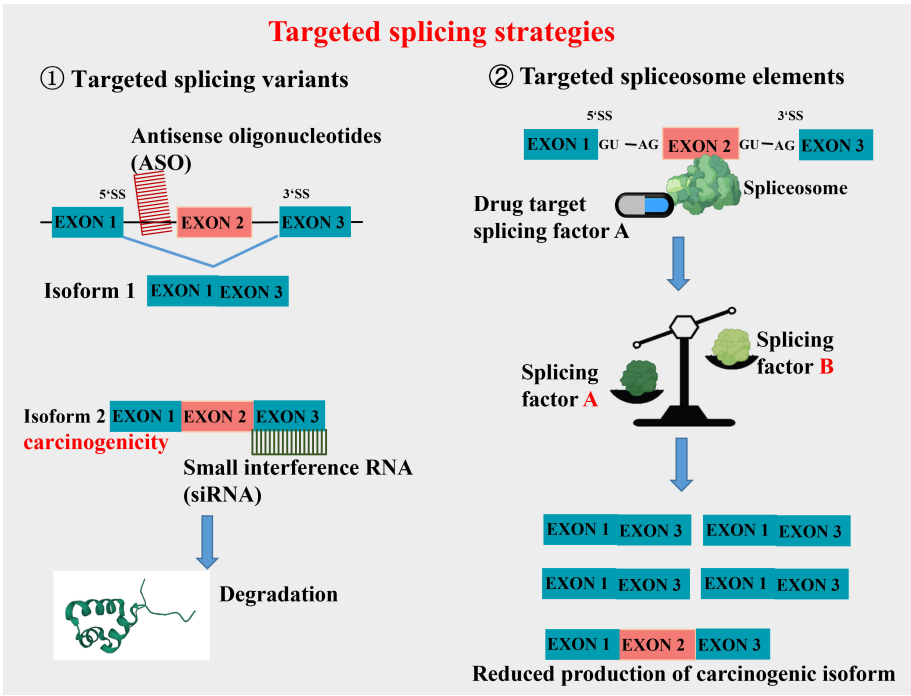


FIGURE 3
Schematic mechanisms of targeted splicing strategies. Strategies targeting splicing variants include Antisense oligonucleotides (ASO) and Small interfering RNA (siRNA). ASO can interact with specific exon or intron sequences of target mRNA and alter its splicing, thereby affecting the expression and function of the target gene. siRNA degrades targeted mRNA to inhibit the expression of the targeted gene. Drugs targeting splicing factors can affect the expression balance of splicing factors in the spliceosome, thereby reducing the production of carcinogenic isoforms.

TABLE 1 Current drugs targeted splicing in the treatment of CRC.

Drug name	Type	Target	Phase	Reference
4μ8c	Small molecules	IRE1α - XBP1s	Preclinical	(282)
Morpholino antisense oligonucleotides	ASO	CCND1a/1b	Preclinical	(67)
	siRNA	CCND1b	Preclinical	(289)
Tautomycetin	Small molecules	SRSF1 - MKNK2	Preclinical	(117)
SRPIN340	Small molecules	SRPK1/2 - MKNK2	Preclinical	
H3B-8800	Small molecules	SF3b	I	(72)
DBS1	Small molecules	SRPKs - VEGF	Preclinical	(290)
Sulfasalazine	xCT inhibitor	CD44	I	(291)
RO5429083	Antibody	CD44	I	(135)
HA oligomers	Small molecules	HA - CD44	Preclinical	
IM7 or KM201	Antibody	CD44	Preclinical	
PEP-1	Peptide	CD44	Preclinical	
shRNA or miRNA	Small molecules	CD44	Preclinical	(133)
α-CD44v6 mAb	Antibody	CD44	Preclinical	
SM08502	Small molecules	SRSF	I	(292)
OS2966	Antibody	β1-integrins	I	(148)
YM155	Small molecules	Survivin	II	(157)

(Continued)

TABLE 1 Continued

Drug name	Type	Target	Phase	Reference
LY2181308	ASO	Survivin	II	
SPC3042, EZN-3042	ASO	Survivin	I	
Survivin-2B80-88	Antigenic peptide	Survivin	I	(155)
ABT-263	Small molecules	BCL-2/BCL-X	II	(213)
Tocilizumab	Antibody	IL-6R	III	(234)
FD-895	antibiotic	SF3b	Preclinical	(71)
Spliceostatin A (SSA)	Small molecules	SF3b	Preclinical	
C-13	Small molecules	SYK	Preclinical	(199)
Merestinib	Small molecules	RON	I	(56)
Dabrafenib, Vemurafenib, Sorafenib, Pazopanib and Ponatinib	Small molecules	RIP3	III	(28)
Binimetinib and Palbociclib	Small molecules	KRAS	II	(50)
10058-F4	Small molecules	ITGA6	Preclinical	(109)
HOXB-AS3	lncRNA	PKM	Preclinical	(256)
Indacaterol	Small molecules	SRSF6 - ZO-1	Preclinical	(183)
GYS32661, MBQ-167	Small molecules	RAC1	Preclinical	(81)
Olamkicept	Fusion-protein	IL6/sIL-6R	II	(235)
Anti-VEGFR2 antibodies	Antibody	VEGFR2	Preclinical	(229)
	siRNAs	VEGFR2	Preclinical	
Sunitinib, Pazopanib	Small molecules	VEGFR2	I	
Morpholino antisense oligonucleotides	ASO	VEGFR2	Preclinical	
ST2146	Antibody	TNC	Preclinical	(151)

have not yet been ascertained whether they match appropriate target treatments. Thus, further research is needed to improve our understanding and develop effective targeted therapies. Since it is accepted that tumor-associated splice variants have promising applications in CRC diagnosis and prognosis, subsequent work should be twofold. First, we will study new tumor-associated splice variants by experimental data, especially for the study of different CRC phenotypes, which is crucial to future targeted therapeutic approaches. Second, we will extend targeted splicing therapies and explore how to manipulate splicing to make targeted CRC therapies more safely, effectively, and accurately. To conclude, this article mainly reviews abnormal splicing events and related tumor-specific splicing variants in CRC, providing insight into targeted splicing therapy in CRC.

Author contributions

YZ and GZ collected the data and wrote the manuscript. CH designed and supervised the study. ML supervised the study. All authors have read and approved the final manuscript. All authors contributed to the article and approved the submitted version.

Funding

This work was supported by the Guangdong Basic and Applied Basic Research Fund (2022A151511193), the Guangzhou Science and technology plan project (2023A04J0581).

Conflict of interest

The authors declare that the research was conducted in the absence of any commercial or financial relationships that could be construed as a potential conflict of interest.

Publisher's note

All claims expressed in this article are solely those of the authors and do not necessarily represent those of their affiliated organizations, or those of the publisher, the editors and the reviewers. Any product that may be evaluated in this article, or claim that may be made by its manufacturer, is not guaranteed or endorsed by the publisher.

References

1. Siegel RL, Miller KD, Wagle NS, Jemal A. Cancer statistics, 2023. *CA Cancer J Clin* (2023) 73(1):17–48. doi: 10.3322/caac.21763
2. Jiang L, Ping L, Yan H, Yang X, He Q, Xu Z, et al. Cardiovascular toxicity induced by anti-VEGF/VEGFR agents: a special focus on definitions, diagnoses, mechanisms and management. *Expert Opin Drug Metab Toxicol* (2020) 16(9):823–35. doi: 10.1080/17425255.2020.1787986
3. Wang E, Aifantis I. RNA splicing and cancer. *Trends Cancer* (2020) 6(8):631–44. doi: 10.1016/j.trecan.2020.04.011
4. Chow LT, Gelinus RE, Broker TR, Roberts RJ. An amazing sequence arrangement at the 5' ends of adenovirus 2 messenger RNA. *Cell* (1977) 12(1):1–8. doi: 10.1016/0092-8674(77)90180-5
5. Klessig DF. Two adenovirus mRNAs have a common 5' terminal leader sequence encoded at least 10 kb upstream from their main coding regions. *Cell* (1977) 12(1):9–21. doi: 10.1016/0092-8674(77)90181-7
6. Liu Q, Fang L, Wu C. Alternative splicing and isoforms: from mechanisms to diseases. *Genes (Basel)* (2022) 13(3):401. doi: 10.3390/genes13030401
7. Miura K, Fujibuchi W, Unno M. Splice isoforms as therapeutic targets for colorectal cancer. *Carcinogenesis* (2012) 33(12):2311–9. doi: 10.1093/carcin/bgs347
8. Chen L, Tovar-Corona JM, Urrutia AO. Increased levels of noisy splicing in cancers, but not for oncogene-derived transcripts. *Hum Mol Genet* (2011) 20(22):4422–9. doi: 10.1093/hmg/ddr370
9. Group PTC, Calabrese C, Davidson NR, Demircioglu D, Fonseca NA, He Y, et al. Genomic basis for RNA alterations in cancer. *Nature* (2020) 578(7793):129–36. doi: 10.1038/s41586-020-1970-0
10. Tian J, Wang Z, Mei S, Yang N, Yang Y, Ke J, et al. CancerSplicingQTL: a database for genome-wide identification of splicing QTLs in human cancer. *Nucleic Acids Res* (2019) 47(D1):D909–D16. doi: 10.1093/nar/gky954
11. He C, Li A, Lai Q, Ding J, Yan Q, Liu S, et al. The DDX39B/FUT3/TGFBetaR-I axis promotes tumor metastasis and EMT in colorectal cancer. *Cell Death Dis* (2021) 12(1):74. doi: 10.1038/s41419-020-03360-6
12. Bonnal SC, Lopez-Oreja I, Valcarcel J. Roles and mechanisms of alternative splicing in cancer - implications for care. *Nat Rev Clin Oncol* (2020) 17(8):457–74. doi: 10.1038/s41571-020-0350-x
13. Dvinge H, Bradley RK. Widespread intron retention diversifies most cancer transcriptomes. *Genome Med* (2015) 7(1):45. doi: 10.1186/s13073-015-0168-9
14. Capon DJ, Seeburg PH, McGrath JP, Hayflick JS, Edman U, Levinson AD, et al. Activation of Ki-ras2 gene in human colon and lung carcinomas by two different point mutations. *Nature* (1983) 304(5926):507–13. doi: 10.1038/304507a0
15. Sciarillo R, Wojtuszkiewicz A, Assaraf YG, Jansen G, Kaspers GJL, Giovannetti E, et al. The role of alternative splicing in cancer: From oncogenesis to drug resistance. *Drug Resist Update* (2020) 53:100728. doi: 10.1016/j.drug.2020.100728
16. Marima R, Francies FZ, Hull R, Molefi T, Oyomno M, Khanyile R, et al. MicroRNA and alternative mRNA splicing events in cancer drug response/resistance: potent therapeutic targets. *Biomedicine* (2021) 9(12):1818. doi: 10.3390/biomedicine9121818
17. Lee SC, Abdel-Wahab O. Therapeutic targeting of splicing in cancer. *Nat Med* (2016) 22(9):976–86. doi: 10.1038/nm.4165
18. Wang J, Wang C, Li L, Yang L, Wang S, Ning X, et al. Alternative splicing: An important regulatory mechanism in colorectal carcinoma. *Mol Carcinog* (2021) 60(4):279–93. doi: 10.1002/mc.23291
19. Kole R, Krainer AR, Altman S. RNA therapeutics: beyond RNA interference and antisense oligonucleotides. *Nat Rev Drug Discovery* (2012) 11(2):125–40. doi: 10.1038/nrd3625
20. Cirak S, Arechavala-Gomez A, Guglieri M, Feng L, Torelli S, Anthony K, et al. Exon skipping and dystrophin restoration in patients with Duchenne muscular dystrophy after systemic phosphorodiamidate morpholino oligomer treatment: an open-label, phase 2, dose-escalation study. *Lancet* (2011) 378(9791):595–605. doi: 10.1016/S0140-6736(11)60756-3
21. Zanetta C, Nizzardo M, Simone C, Monguzzi E, Bresolin N, Comi GP, et al. Molecular therapeutic strategies for spinal muscular atrophies: current and future clinical trials. *Clin Ther* (2014) 36(1):128–40. doi: 10.1016/j.clinthera.2013.11.006
22. Larrayoz M, Blakemore SJ, Dobson RC, Blunt MD, Rose-Zerilli MJ, Walewska R, et al. The SF3B1 inhibitor spliceostatin A (SSA) elicits apoptosis in chronic lymphocytic leukaemia cells through downregulation of Mcl-1. *Leukemia* (2016) 30(2):351–60. doi: 10.1038/leu.2015.286
23. Sciarillo R, Wojtuszkiewicz A, Kooi IE, Leon LG, Sonneveld E, Kuiper RP, et al. Glucocorticoid resistant pediatric acute lymphoblastic leukemia samples display altered splicing profile and vulnerability to spliceosome modulation. *Cancers (Basel)* (2020) 12(3):723. doi: 10.3390/cancers12030723
24. Sun X, Lee J, Navas T, Baldwin DT, Stewart TA, Dixit VM. RIP3, a novel apoptosis-inducing kinase. *J Biol Chem* (1999) 274(24):16871–5. doi: 10.1074/jbc.274.24.16871
25. Liu ZY, Zheng M, Li YM, Fan XY, Wang JC, Li ZC, et al. RIP3 promotes colitis-associated colorectal cancer by controlling tumor cell proliferation and CXCL1-induced immune suppression. *Theranostics* (2019) 9(12):3659–73. doi: 10.7150/thno.32126
26. Liu S, Joshi K, Denning MF, Zhang J. RIPK3 signaling and its role in the pathogenesis of cancers. *Cell Mol Life Sci* (2021) 78(23):7199–217. doi: 10.1007/s00018-021-03947-y
27. Yang Y, Hu W, Feng S, Ma J, Wu M. RIP3 beta and RIP3 gamma, two novel splice variants of receptor-interacting protein 3 (RIP3), downregulate RIP3-induced apoptosis. *Biochem Biophys Res Commun* (2005) 332(1):181–7. doi: 10.1016/j.bbrc.2005.04.114
28. Fulda S. Repurposing anticancer drugs for targeting necroptosis. *Cell Cycle* (2018) 17(7):829–32. doi: 10.1080/15384101.2018.1442626
29. Akiyama T. [The APC gene]. *Nihon Rinsho* (1996) 54(4):955–9.
30. Schwarzova L, Stekrova J, Florianova M, Novotny A, Schneiderova M, Lnenicka P, et al. Novel mutations of the APC gene and genetic consequences of splicing mutations in the Czech FAP families. *Fam Cancer* (2013) 12(1):35–42. doi: 10.1007/s10689-012-9569-8
31. Carson DJ, Santoro IM, Groden J. Isoforms of the APC tumor suppressor and their ability to inhibit cell growth and tumorigenicity. *Oncogene* (2004) 23(42):7144–8. doi: 10.1038/sj.onc.1207954
32. Vaysse C, Philippe C, Martineau Y, Quelen C, Hieblot C, Renaud C, et al. Key contribution of eIF4H-mediated translational control in tumor promotion. *Oncotarget* (2015) 6(37):39924–40. doi: 10.18632/oncotarget.5442
33. Martindale DW, Wilson MD, Wang D, Burke RD, Chen X, Duronio V, et al. Comparative genomic sequence analysis of the Williams syndrome region (LIMK1-RFC2) of human chromosome 7q11.23. *Mamm Genome* (2000) 11(10):890–8. doi: 10.1007/s003350010166
34. Wu D, Matsushita K, Matsubara H, Nomura F, Tomonaga T. An alternative splicing isoform of eukaryotic initiation factor 4H promotes tumorigenesis *in vivo* and is a potential therapeutic target for human cancer. *Int J Cancer* (2011) 128(5):1018–30. doi: 10.1002/ijc.25419
35. Wu LC, Wang ZW, Tsan JT, Spillman MA, Phung A, Xu XL, et al. Identification of a RING protein that can interact *in vivo* with the BRCA1 gene product. *Nat Genet* (1996) 14(4):430–40. doi: 10.1038/ng1296-430
36. Garcia-Patino E, Gomendio B, Lleona M, Silva JM, Garcia JM, Provencio M, et al. Loss of heterozygosity in the region including the BRCA1 gene on 17q in colon cancer. *Cancer Genet Cytogenet* (1998) 104(2):119–23. doi: 10.1016/s0165-4608(97)00460-3
37. Ford D, Easton DF, Bishop DT, Narod SA, Goldgar DE. Risks of cancer in BRCA1-mutation carriers. Breast Cancer Linkage Consortium. *Lancet* (1994) 343(8899):692–5. doi: 10.1016/s0140-6736(94)91578-4
38. Brose MS, Rebbeck TR, Calzone KA, Stopfer JE, Nathanson KL, Weber BL. Cancer risk estimates for BRCA1 mutation carriers identified in a risk evaluation program. *J Natl Cancer Inst* (2002) 94(18):1365–72. doi: 10.1093/jnci/94.18.1365
39. Lin KM, Ternent CA, Adams DR, Thorson AG, Blatchford GJ, Christensen MA, et al. Colorectal cancer in hereditary breast cancer kindreds. *Dis Colon Rectum* (1999) 42(8):1041–5. doi: 10.1007/BF02236700
40. Suchy J, Cybulski C, Gorski B, Huzarski T, Byrski T, Debnick T, et al. BRCA1 mutations and colorectal cancer in Poland. *Fam Cancer* (2010) 9(4):541–4. doi: 10.1007/s10689-010-9378-x
41. Fabbro M, Rodriguez JA, Baer R, Henderson BR. BARD1 induces BRCA1 intranuclear foci formation by increasing RING-dependent BRCA1 nuclear import and inhibiting BRCA1 nuclear export. *J Biol Chem* (2002) 277(24):21315–24. doi: 10.1074/jbc.M200769200
42. Zhang YQ, Pilyugin M, Kuester D, Leoni VP, Li L, Casula G, et al. Expression of oncogenic BARD1 isoforms affects colon cancer progression and correlates with clinical outcome. *Br J Cancer* (2012) 107(4):675–83. doi: 10.1038/bjc.2012.297
43. Cimmino F, Formicola D, Capasso M. Dualistic role of BARD1 in cancer. *Genes (Basel)* (2017) 8(12):375. doi: 10.3390/genes8120375
44. Laszlo L, Kurilla A, Takacs T, Kudlik G, Koprivanac K, Buday L, et al. Recent updates on the significance of KRAS mutations in colorectal cancer biology. *Cells* (2021) 10(3):667. doi: 10.3390/cells10030667
45. Prior IA, Lewis PD, Mattos C. A comprehensive survey of Ras mutations in cancer. *Cancer Res* (2012) 72(10):2457–67. doi: 10.1158/0008-5472.CAN-11-2612
46. Moore AR, Rosenberg SC, McCormick F, Malek S. RAS-targeted therapies: is the undruggable drugged? *Nat Rev Drug Discovery* (2020) 19(8):533–52. doi: 10.1038/s41573-020-0068-6
47. Ahearn IM, Haigis K, Bar-Sagi D, Philips MR. Regulating the regulator: post-translational modification of RAS. *Nat Rev Mol Cell Biol* (2011) 13(1):39–51. doi: 10.1038/nrm3255
48. Nuevo-Tapiolas C, Philips MR. The role of KRAS splice variants in cancer biology. *Front Cell Dev Biol* (2022) 10:1033348. doi: 10.3389/fcell.2022.1033348
49. Amendola CR, Mahaffey JP, Parker SJ, Ahearn IM, Chen WC, Zhou M, et al. KRAS4A directly regulates hexokinase 1. *Nature* (2019) 576(7787):482–6. doi: 10.1038/s41586-019-1832-9

50. Sorokin AV, Kanikarla Marie P, Bitner L, Syed M, Woods M, Manyam G, et al. Targeting RAS mutant colorectal cancer with dual inhibition of MEK and CDK4/6. *Cancer Res* (2022) 82(18):3335–44. doi: 10.1158/0008-5472.CAN-22-0198
51. Mayer S, Hirschfeld M, Jaeger M, Pies S, Iborra S, Erbes T, et al. RON alternative splicing regulation in primary ovarian cancer. *Oncol Rep* (2015) 34(1):423–30. doi: 10.3892/or.2015.3995
52. Collesi C, Santoro MM, Gaudino G, Comoglio PM. A splicing variant of the RON transcript induces constitutive tyrosine kinase activity and an invasive phenotype. *Mol Cell Biol* (1996) 16(10):5518–26. doi: 10.1128/MCB.16.10.5518
53. Zhou YQ, He C, Chen YQ, Wang D, Wang MH. Altered expression of the RON receptor tyrosine kinase in primary human colorectal adenocarcinomas: generation of different splicing RON variants and their oncogenic potential. *Oncogene* (2003) 22(2):186–97. doi: 10.1038/sj.onc.1206075
54. Wang MH, Lao WF, Wang D, Luo YL, Yao HP. Blocking tumorigenic activities of colorectal cancer cells by a splicing RON receptor variant defective in the tyrosine kinase domain. *Cancer Biol Ther* (2007) 6(7):1121–9. doi: 10.4161/cbt.6.7.4337
55. Ghigna C, Giordano S, Shen H, Benvenuto F, Castiglioni F, Comoglio PM, et al. Cell motility is controlled by SF2/ASF through alternative splicing of the Ron protooncogene. *Mol Cell* (2005) 20(6):881–90. doi: 10.1016/j.molcel.2005.10.026
56. He AR, Cohen RB, Denlinger CS, Sama A, Birnbaum A, Hwang J, et al. First-in-human phase I study of merestinib, an oral multikinase inhibitor, in patients with advanced cancer. *Oncologist* (2019) 24(9):e930–e42. doi: 10.1634/theoncologist.2018-0411
57. Montalto FI, De Amicis F. Cyclin D1 in cancer: A molecular connection for cell cycle control, adhesion and invasion in tumor and stroma. *Cells* (2020) 9(12):2648. doi: 10.3390/cells9122648
58. Yan H, Jiang F, Yang J. Association of beta-catenin, APC, SMAD3/4, tp53, and cyclin D1 genes in colorectal cancer: A systematic review and meta-analysis. *Genet Res (Camb)* (2022) 2022:5338956. doi: 10.1155/2022/5338956
59. Bahnassy AA, Zekri AR, El-Houssini S, El-Shehaby AM, Mahmoud MR, Abdallah S, et al. Cyclin A and cyclin D1 as significant prognostic markers in colorectal cancer patients. *BMC Gastroenterol* (2004) 4:22. doi: 10.1186/1471-230X-4-22
60. Yang Y, Wang F, Shi C, Zou Y, Qin H, Ma Y. Cyclin D1 G870A polymorphism contributes to colorectal cancer susceptibility: evidence from a systematic review of 22 case-control studies. *PLoS One* (2012) 7(5):e36813. doi: 10.1371/journal.pone.0036813
61. Garcia-Aguilar J, Chen Z, Smith DD, Li W, Madoff RD, Cataldo P, et al. Identification of a biomarker profile associated with resistance to neoadjuvant chemoradiation therapy in rectal cancer. *Ann Surg* (2011) 254(3):486–92. doi: 10.1097/SLA.0b013e31822b8cfa
62. El Meshawy N, El Marghany AB, Sarhan MM, Aladle DA. Cyclin D1 G870A polymorphism: relation to the risk of ALL development, prognosis impact, and methotrexate cytotoxicity. *Asian Pac J Cancer Prev* (2020) 21(10):2941–7. doi: 10.31557/APJCP.2020.21.10.2941
63. Howe D, Lynas C. The cyclin D1 alternative transcripts [a] and [b] are expressed in normal and Malignant lymphocytes and their relative levels are influenced by the polymorphism at codon 241. *Haematologica* (2001) 86(6):563–9.
64. Betticher DC, Thatcher N, Altermatt HJ, Hoban P, Ryder WD, Heighway J. Alternate splicing produces a novel cyclin D1 transcript. *Oncogene* (1995) 11(5):1005–11.
65. Wu FH, Luo LQ, Liu Y, Zhan QX, Luo C, Luo J, et al. Cyclin D1b splice variant promotes alphavbeta3-mediated adhesion and invasive migration of breast cancer cells. *Cancer Lett* (2014) 355(1):159–67. doi: 10.1016/j.canlet.2014.08.044
66. Kim CJ, Tambe Y, Mukaiyoshi KI, Sugihara H, Kawauchi A, Inoue H. Akt-dependent activation of Erk by cyclin D1b contributes to cell invasiveness and tumorigenicity. *Oncol Lett* (2016) 12(6):4850–6. doi: 10.3892/ol.2016.5286
67. Wang J, Su W, Zhang T, Zhang S, Lei H, Ma F, et al. Aberrant Cyclin D1 splicing in cancer: from molecular mechanism to therapeutic modulation. *Cell Death Dis* (2023) 14(4):244. doi: 10.1038/s41419-023-05763-7
68. Matsushita K, Tomonaga T, Shimada H, Shioya A, Higashi M, Matsubara H, et al. An essential role of alternative splicing of c-myc suppressor FUSE-binding protein-interacting repressor in carcinogenesis. *Cancer Res* (2006) 66(3):1409–17. doi: 10.1158/0008-5472.CAN-04-4459
69. Kajiwaru T, Matsushita K, Itoga S, Tamura M, Tanaka N, Tomonaga T, et al. SAP155-mediated c-myc suppressor far-upstream element-binding protein-interacting repressor splicing variants are activated in colon cancer tissues. *Cancer Sci* (2013) 104(2):149–56. doi: 10.1111/cas.12058
70. Matsushita K, Kajiwaru T, Tamura M, Satoh M, Tanaka N, Tomonaga T, et al. SAP155-mediated c-myc suppressor far-upstream element-binding protein-interacting repressor serves as a molecular switch for c-myc gene expression. *Mol Cancer Res* (2012) 10(6):787–99. doi: 10.1158/1541-7786.MCR-11-0462
71. Martinez-Montiel N, Rosas-Murrieta NH, Anaya Ruiz M, Monjaraz-Guzman E, Martinez-Contreras R. Alternative splicing as a target for cancer treatment. *Int J Mol Sci* (2018) 19(2):545. doi: 10.3390/ijms19020545
72. Steensma DP, Wermke M, Klimek VM, Greenberg PL, Font P, Komrokji RS, et al. Phase I First-in-Human Dose Escalation Study of the oral SF3B1 modulator H3B-8800 in myeloid neoplasms. *Leukemia* (2021) 35(12):3542–50. doi: 10.1038/s41375-021-01328-9
73. Svensmark JH, Brakebusch C. Rho GTPases in cancer: friend or foe? *Oncogene* (2019) 38(50):7447–56. doi: 10.1038/s41388-019-0963-7
74. Lee K, Chen QK, Lui C, Cichon MA, Radisky DC, Nelson CM. Matrix compliance regulates Rac1b localization, NADPH oxidase assembly, and epithelial-mesenchymal transition. *Mol Biol Cell* (2012) 23(20):4097–108. doi: 10.1091/mbc.E12-02-0166
75. Aljaghtmi AA, Hill NT, Cooke M, Kazanietz MG, Abba MC, Long W, et al. DeltaNp63alpha suppresses cells invasion by downregulating PKCgamma/Rac1 signaling through miR-320a. *Cell Death Dis* (2019) 10(9):680. doi: 10.1038/s41419-019-1921-6
76. Goncalves V, Henriques AF, Pereira JF, Neves Costa A, Moyer MP, Moita LF, et al. Phosphorylation of SRSF1 by SRPK1 regulates alternative splicing of tumor-related Rac1b in colorectal cells. *RNA* (2014) 20(4):474–82. doi: 10.1261/rna.041376.113
77. Wang F, Fu X, Chen P, Wu P, Fan X, Li N, et al. SPSB1-mediated HnRNP A1 ubiquitylation regulates alternative splicing and cell migration in EGF signaling. *Cell Res* (2017) 27(4):540–58. doi: 10.1038/cr.2017.7
78. Goncalves V, Matos P, Jordan P. Antagonistic SR proteins regulate alternative splicing of tumor-related Rac1b downstream of the PI3-kinase and Wnt pathways. *Hum Mol Genet* (2009) 18(19):3696–707. doi: 10.1093/hmg/ddp317
79. Gudino V, Pohl SO, Billard CV, Cammareri P, Bolado A, Aitken S, et al. RAC1B modulates intestinal tumorigenesis via modulation of WNT and EGFR signalling pathways. *Nat Commun* (2021) 12(1):2335. doi: 10.1038/s41467-021-22531-3
80. Kotelevets L, Chastre E. Rac1 signaling: from intestinal homeostasis to colorectal cancer metastasis. *Cancers (Basel)* (2020) 12(3):665. doi: 10.3390/cancers12030665
81. Bailly C, Beignet J, Loirand G, Sauzeau V. Rac1 as a therapeutic anticancer target: Promises and limitations. *Biochem Pharmacol* (2022) 203:115180. doi: 10.1016/j.bcp.2022.115180
82. Alonso-Espinaco V, Cuatrecasas M, Alonso V, Escudero P, Marmol M, Horndler C, et al. RAC1b overexpression correlates with poor prognosis in KRAS/BRAF WT metastatic colorectal cancer patients treated with first-line FOLFOX/XELOX chemotherapy. *Eur J Cancer* (2014) 50(11):1973–81. doi: 10.1016/j.ejca.2014.04.019
83. Goka ET, Chaturvedi P, Lopez DTM, Garza A, Lippman ME. RAC1b overexpression confers resistance to chemotherapy treatment in colorectal cancer. *Mol Cancer Ther* (2019) 18(5):957–68. doi: 10.1158/1535-7163.MCT-18-0955
84. Abdel-Samad R, Zalzal H, Rammah C, Giraud J, Naudin C, Dupasquier S, et al. MiniSOX9, a dominant-negative variant in colon cancer cells. *Oncogene* (2011) 30(22):2493–503. doi: 10.1038/ncr.2010.621
85. Thorsen K, Mansilla F, Schepeler T, Oster B, Rasmussen MH, Dyrskjot L, et al. Alternative splicing of SLC39A14 in colorectal cancer is regulated by the Wnt pathway. *Mol Cell Proteomics* (2011) 10(1):M110. doi: 10.1074/mcp.M110.002998
86. Sveen A, Bakken AC, Agesken TH, Lind GE, Nesbakken A, Nordgard O, et al. The exon-level biomarker SLC39A14 has organ-confined cancer-specificity in colorectal cancer. *Int J Cancer* (2012) 131(6):1479–85. doi: 10.1002/ijc.27399
87. Smeby J, Sveen A, Eilertsen IA, Danielsen SA, Hoff AM, Eide PW, et al. Transcriptional and functional consequences of TP53 splice mutations in colorectal cancer. *Oncogenesis* (2019) 8(6):35. doi: 10.1038/s41389-019-0141-3
88. Shirole NH, Pal D, Kastnerhuber ER, Senturk S, Boroda J, Pisterzi P, et al. TP53 exon-6 truncating mutations produce separation of function isoforms with pro-tumorigenic functions. *Elife* (2016) 5:e17929. doi: 10.7554/eLife.17929
89. Senturk S, Yao Z, Camiolo M, Stiles B, Rathod T, Walsh AM, et al. p53Psi is a transcriptionally inactive p53 isoform able to reprogram cells toward a metastatic-like state. *Proc Natl Acad Sci U.S.A.* (2014) 111(32):E3287–96. doi: 10.1073/pnas.1321640111
90. Montero-Calle A, Garranzo-Asensio M, Torrente-Rodriguez RM, Ruiz-Valdepenas Montiel V, Poves C, Dziakova J, et al. p53 and p63 proteoforms derived from alternative splicing possess differential seroreactivity in colorectal cancer with distinct diagnostic ability from the canonical proteins. *Cancers (Basel)* (2023) 15(7):2102. doi: 10.3390/cancers15072102
91. Zhou X, Li X, Cheng Y, Wu W, Xie Z, Xi Q, et al. BCLAF1 and its splicing regulator SRSF10 regulate the tumorigenic potential of colon cancer cells. *Nat Commun* (2014) 5:4581. doi: 10.1038/ncomms5581
92. Pibouin L, Villaudy J, Ferbus D, Muleris M, Prosperi MT, Remvikos Y, et al. Cloning of the mRNA of overexpression in colon carcinoma-1: a sequence overexpressed in a subset of colon carcinomas. *Cancer Genet Cytogenet* (2002) 133(1):55–60. doi: 10.1016/s0165-4608(01)00634-3
93. Najafi H, Soltani BM, Dokanehiifard S, Nasiri S, Mowla SJ. Alternative splicing of the OCC-1 gene generates three splice variants and a novel exonic microRNA, which regulate the Wnt signaling pathway. *RNA* (2017) 23(1):70–85. doi: 10.1261/rna.056317.116
94. Yusuf D, Butland SL, Swanson MI, Bolotin E, Ticoll A, Cheung WA, et al. The transcription factor encyclopedia. *Genome Biol* (2012) 13(3):R24. doi: 10.1186/gb-2012-13-3-r24
95. Vuong LM, Chellappa K, Dhahbi JM, Deans JR, Fang B, Bolotin E, et al. Differential effects of hepatocyte nuclear factor 4alpha isoforms on tumor growth and T-cell factor 4/AP-1 interactions in human colorectal cancer cells. *Mol Cell Biol* (2015) 35(20):3471–90. doi: 10.1128/MCB.00030-15

96. Changolkar LN, Pehrson JR. macroH2A1 histone variants are depleted on active genes but concentrated on the inactive X chromosome. *Mol Cell Biol* (2006) 26(12):4410–20. doi: 10.1128/MCB.02558-05
97. Kim SP, Srivatsan SN, Chavez M, Shirai CL, White BS, Ahmed T, et al. Mutant U2AF1-induced alternative splicing of H2afy (macroH2A1) regulates B-lymphopoiesis in mice. *Cell Rep* (2021) 36(9):109626. doi: 10.1016/j.celrep.2021.109626
98. Novikov L, Park JW, Chen H, Klerman H, Jalloh AS, Gamble MJ. QKI-mediated alternative splicing of the histone variant MacroH2A1 regulates cancer cell proliferation. *Mol Cell Biol* (2011) 31(20):4244–55. doi: 10.1128/MCB.05244-11
99. Fei DL, Zhen T, Durham B, Ferrarone J, Zhang T, Garrett L, et al. Impaired hematopoiesis and leukemia development in mice with a conditional knock-in allele of a mutant splicing factor gene U2af1. *Proc Natl Acad Sci U S A* (2018) 115(44):E10437–E46. doi: 10.1073/pnas.1812669115
100. Ilagan JO, Ramakrishnan A, Hayes B, Murphy ME, Zebari AS, Bradley P, et al. U2AF1 mutations alter splice site recognition in hematological Malignancies. *Genome Res* (2015) 25(1):14–26. doi: 10.1101/gr.181016.114
101. Yip BH, Steeples V, Repapi E, Armstrong RN, Llorian M, Roy S, et al. The U2AF1S34F mutation induces lineage-specific splicing alterations in myelodysplastic syndromes. *J Clin Invest* (2017) 127(9):3557. doi: 10.1172/JCI96202
102. Lu SC, Mato JM. S-Adenosylmethionine in cell growth, apoptosis and liver cancer. *J Gastroenterol Hepatol* (2008) 23 Suppl 1(Suppl 1):S73–7. doi: 10.1111/j.1440-1746.2007.05289.x
103. Yang H, Ara AI, Magilnick N, Xia M, Ramani K, Chen H, et al. Expression pattern, regulation, and functions of methionine adenosyltransferase 2beta splicing variants in hepatoma cells. *Gastroenterology* (2008) 134(1):281–91. doi: 10.1053/j.gastro.2007.10.027
104. Xia M, Chen Y, Wang LC, Zandi E, Yang H, Bermanian S, et al. Novel function and intracellular localization of methionine adenosyltransferase 2beta splicing variants. *J Biol Chem* (2010) 285(26):20015–21. doi: 10.1074/jbc.M109.094821
105. Margadant C, Monsuur HN, Norman JC, Sonnenberg A. Mechanisms of integrin activation and trafficking. *Curr Opin Cell Biol* (2011) 23(5):607–14. doi: 10.1016/j.cob.2011.08.005
106. Hogervorst F, Admiraal LG, Niessen C, Kuikman I, Janssen H, Daams H, et al. Biochemical characterization and tissue distribution of the A and B variants of the integrin alpha 6 subunit. *J Cell Biol* (1993) 121(1):179–91. doi: 10.1083/jcb.121.1.179
107. Groulx JF, Giroux V, Beausejour M, Boudjadi S, Basora N, Carrier JC, et al. Integrin alpha6A splice variant regulates proliferation and the Wnt/beta-catenin pathway in human colorectal cancer cells. *Carcinogenesis* (2014) 35(6):1217–27. doi: 10.1093/carcin/bgu006
108. van der Flier LG, Clevers H. Stem cells, self-renewal, and differentiation in the intestinal epithelium. *Annu Rev Physiol* (2009) 71:241–60. doi: 10.1146/annurev.physiol.010908.163145
109. Groulx JF, Boudjadi S, Beaulieu JF. MYC regulates alpha6 integrin subunit expression and splicing under its pro-proliferative ITGA6A form in colorectal cancer cells. *Cancers (Basel)* (2018) 10(2):42. doi: 10.3390/cancers10020042
110. Bao X, Huang Y, Xu W, Xiong G. Functions and clinical significance of UPF3a expression in human colorectal cancer. *Cancer Manag Res* (2020) 12:4271–81. doi: 10.2147/CMAR.S244486
111. Shum EY, Jones SH, Shao A, Chousal JN, Krause MD, Chan WK, et al. The antagonistic gene paralogs Upf3a and Upf3b govern nonsense-mediated RNA decay. *Cell* (2016) 165(2):382–95. doi: 10.1016/j.cell.2016.02.046
112. Wang Q, Wang Y, Liu Y, Zhang C, Luo Y, Guo R, et al. U2-related proteins CHERP and SR140 contribute to colorectal tumorigenesis via alternative splicing regulation. *Int J Cancer* (2019) 145(10):2728–39. doi: 10.1002/ijc.32331
113. Xu W, Ou W, Feng Y, Xu Q, Yang Y, Cui L, et al. Genetic compensation response could exist in colorectal cancer: UPF3A upregulates the oncogenic homologue gene SRSF3 expression corresponding to SRSF6 to promote colorectal cancer metastasis. *J Gastroenterol Hepatol* (2023) 38(4):634–47. doi: 10.1111/jgh.16152
114. Yang X, Zhong W, Cao R. Phosphorylation of the mRNA cap-binding protein eIF4E and cancer. *Cell Signal* (2020) 73:109689. doi: 10.1016/j.cellsig.2020.109689
115. Scheper GC, Parra JL, Wilson M, Van Kollenburg B, Vertegaal AC, Han ZG, et al. The N and C termini of the splice variants of the human mitogen-activated protein kinase-interacting kinase Mnk2 determine activity and localization. *Mol Cell Biol* (2003) 23(16):5692–705. doi: 10.1128/MCB.23.16.5692-5705.2003
116. Maimon A, Mogilevsky M, Shilo A, Golan-Gerstl R, Obiedat A, Ben-Hur V, et al. Mnk2 alternative splicing modulates the p38-MAPK pathway and impacts Ras-induced transformation. *Cell Rep* (2014) 7(2):501–13. doi: 10.1016/j.celrep.2014.03.041
117. Liu H, Gong Z, Li K, Zhang Q, Xu Z, Xu Y. SRPK1/2 and PP1alpha exert opposite functions by modulating SRSF1-guided MKNK2 alternative splicing in colon adenocarcinoma. *J Exp Clin Cancer Res* (2021) 40(1):75. doi: 10.1186/s13046-021-01877-y
118. Zhang H, Duan HO, Kirley SD, Zukerberg LR, Wu CL. Aberrant splicing of cables gene, a CDK regulator, in human cancers. *Cancer Biol Ther* (2005) 4(11):1211–5. doi: 10.4161/cbt.4.11.2085
119. Ikeuchi K, Marusawa H, Fujiwara M, Matsumoto Y, Endo Y, Watanabe T, et al. Attenuation of proteolysis-mediated cyclin E regulation by alternatively spliced Parkin in human colorectal cancers. *Int J Cancer* (2009) 125(9):2029–35. doi: 10.1002/ijc.24565
120. Croft A, Guo ST, Sherwin S, Farrelly M, Yan XG, Zhang XD, et al. Functional identification of a novel transcript variant of INPP4B in human colon and breast cancer cells. *Biochem Biophys Res Commun* (2017) 485(1):47–53. doi: 10.1016/j.bbrc.2017.02.012
121. Flodrops M, Dujardin G, Busson A, Trouve P, Ka C, Simon B, et al. TIMP1 intron 3 retention is a marker of colon cancer progression controlled by hnRNPA1. *Mol Biol Rep* (2020) 47(4):3031–40. doi: 10.1007/s11033-020-05375-w
122. Klupp F, Giese C, Halama N, Franz C, Lasitschka F, Warth A, et al. E3 ubiquitin ligase Smurf2: a prognostic factor in microsatellite stable colorectal cancer. *Cancer Manag Res* (2019) 11:1795–803. doi: 10.2147/CMAR.S178111
123. Dornhoff H, Becker C, Wirtz S, Strand D, Tenzer S, Rosfa S, et al. A variant of Smurf2 protects mice against colitis-associated colon cancer by inducing transforming growth factor beta signaling. *Gastroenterology* (2012) 142(5):1183–94.e4. doi: 10.1053/j.gastro.2012.02.005
124. Chen L, Luo C, Shen L, Liu Y, Wang Q, Zhang C, et al. SRSF1 prevents DNA damage and promotes Tumorigenesis through regulation of DBF4B pre-mRNA splicing. *Cell Rep* (2017) 21(12):3406–13. doi: 10.1016/j.celrep.2017.11.091
125. Kajita K, Kuwano Y, Satake Y, Kano S, Kurokawa K, Akaike Y, et al. Ultraconserved region-containing Transformer 2beta4 controls senescence of colon cancer cells. *Oncogenesis* (2016) 5(4):e213. doi: 10.1038/oncsis.2016.18
126. Satake Y, Kuwano Y, Nishikawa T, Fujita K, Saijo S, Itai M, et al. Nucleolin facilitates nuclear retention of an ultraconserved region containing TRA2beta4 and accelerates colon cancer cell growth. *Oncotarget* (2018) 9(42):26817–33. doi: 10.18632/oncotarget.25510
127. Nishikawa T, Kuwano Y, Takahara Y, Nishida K, Rokutan K. HnRNPA1 interacts with G-quadruplex in the TRA2B promoter and stimulates its transcription in human colon cancer cells. *Sci Rep* (2019) 9(1):10276. doi: 10.1038/s41598-019-46659-x
128. Meteoglu I, Meydan N, Erkus M. Id-1: regulator of EGFR and VEGF and potential target for colorectal cancer therapy. *J Exp Clin Cancer Res* (2008) 27(1):69. doi: 10.1186/1756-9966-27-69
129. Manrique I, Nguema P, Bleau AM, Nistal-Villan E, Lopez I, Villalba M, et al. The inhibitor of differentiation isoform Id1b, generated by alternative splicing, maintains cell quiescence and confers self-renewal and cancer stem cell-like properties. *Cancer Lett* (2015) 356(2 Pt B):899–909. doi: 10.1016/j.canlet.2014.10.035
130. Muys BR, Shrestha RL, Anastakis DG, Pongor L, Li XL, Grammatikakis I, et al. Matrin3 regulates mitotic spindle dynamics by controlling alternative splicing of CDC14B. *Cell Rep* (2023) 42(3):112260. doi: 10.1016/j.celrep.2023.112260
131. Prochazka L, Tesarik R, Turanek J. Regulation of alternative splicing of CD44 in cancer. *Cell Signal* (2014) 26(10):2234–9. doi: 10.1016/j.cellsig.2014.07.011
132. Zeilstra J, Joosten SP, van Andel H, Tolg C, Berns A, Snoek M, et al. Stem cell CD44v isoforms promote intestinal cancer formation in Apc(min) mice downstream of Wnt signaling. *Oncogene* (2014) 33(5):665–70. doi: 10.1038/onc.2012.611
133. Ma L, Dong L, Chang P. CD44v6 engages in colorectal cancer progression. *Cell Death Dis* (2019) 10(1):30. doi: 10.1038/s41419-018-1265-7
134. Orian-Rousseau V, Ponta H. Perspectives of CD44 targeting therapies. *Arch Toxicol* (2015) 89(1):3–14. doi: 10.1007/s00204-014-1424-2
135. Chen C, Zhao S, Karnad A, Freeman JW. The biology and role of CD44 in cancer progression: therapeutic implications. *J Hematol Oncol* (2018) 11(1):64. doi: 10.1186/s13045-018-0605-5
136. Ejima R, Suzuki H, Tanaka T, Asano T, Kaneko MK, Kato Y. Development of a novel anti-CD44 variant 6 monoclonal antibody C(44)Mab-9 for multiple applications against colorectal carcinomas. *Int J Mol Sci* (2023) 24(4):4007. doi: 10.3390/ijms24044007
137. Zhang LH, Tian B, Diao LR, Xiong YY, Tian SF, Zhang BH, et al. Dominant expression of 85-kDa form of cortactin in colorectal cancer. *J Cancer Res Clin Oncol* (2006) 132(2):113–20. doi: 10.1007/s00432-005-0046-8
138. van Rossum AG, de Graaf JH, Schuurin-Scholtes E, Kluijn PM, Fan YX, Zhan X, et al. Alternative splicing of the actin binding domain of human cortactin affects cell migration. *J Biol Chem* (2003) 278(46):45672–9. doi: 10.1074/jbc.M306688200
139. Wang ZN, Liu D, Yin B, Ju WY, Qiu HZ, Xiao Y, et al. High expression of PTBP1 promote invasion of colorectal cancer by alternative splicing of cortactin. *Oncotarget* (2017) 8(22):36185–202. doi: 10.18632/oncotarget.15873
140. Corsi JM, Rouer E, Girault JA, Enslin H. Organization and post-transcriptional processing of focal adhesion kinase gene. *BMC Genomics* (2006) 7:198. doi: 10.1186/1471-2164-7-198
141. Burgaya F, Toutant M, Studler JM, Costa A, Le Bert M, Gelman M, et al. Alternatively spliced focal adhesion kinase in rat brain with increased autophosphorylation activity. *J Biol Chem* (1997) 272(45):28720–5. doi: 10.1074/jbc.272.45.28720
142. Devaud C, Tilkin-Mariame AF, Vignolle-Vidoni A, Souleres P, Denadai-Souza A, Rolland C, et al. FAK alternative splice mRNA variants expression pattern in colorectal cancer. *Int J Cancer* (2019) 145(2):494–502. doi: 10.1002/ijc.32120
143. Midwood KS, Hussenet T, Langlois B, Orend G. Advances in tenascin-C biology. *Cell Mol Life Sci* (2011) 68(19):3175–99. doi: 10.1007/s00018-011-0783-6
144. Giblin SP, Midwood KS. Tenascin-C: Form versus function. *Cell Adh Migr* (2015) 9(1-2):48–82. doi: 10.4161/19336918.2014.987587
145. Saito Y, Imazeki H, Miura S, Yoshimura T, Okutsu H, Harada Y, et al. A peptide derived from tenascin-C induces beta1 integrin activation through syndecan-4. *J Biol Chem* (2007) 282(48):34929–37. doi: 10.1074/jbc.M705608200

146. Tanaka R, Seki Y, Saito Y, Kamiya S, Fujita M, Okutsu H, et al. Tenascin-C-derived peptide TNIIIA2 highly enhances cell survival and platelet-derived growth factor (PDGF)-dependent cell proliferation through potentiated and sustained activation of integrin $\alpha 5\beta 1$. *J Biol Chem* (2014) 289(25):17699–708. doi: 10.1074/jbc.M113.546622
147. Dueck M, Riedl S, Hinz U, Tandara A, Mller P, Herfarth C, et al. Detection of tenascin-C isoforms in colorectal mucosa, ulcerative colitis, carcinomas and liver metastases. *Int J Cancer* (1999) 82(4):477–83. doi: 10.1002/(sici)1097-0215(19990812)82:4<477::Aid-ijc2>3.0.Co;2-5
148. Nwagwu CD, Immidiseti AV, Bukanowska G, Vogelbaum MA, Carbonell AM. Convection-enhanced delivery of a first-in-class anti- $\beta 1$ integrin antibody for the treatment of high-grade glioma utilizing real-time imaging. *Pharmaceutics* (2020) 13(1):40. doi: 10.3390/pharmaceutics13010040
149. Suzuki H, Sasada M, Kamiya S, Ito Y, Watanabe H, Okada Y, et al. The promoting effect of the extracellular matrix peptide TNIIIA2 derived from tenascin-C in colon cancer cell infiltration. *Int J Mol Sci* (2017) 18(1):181. doi: 10.3390/ijms18010181
150. Fujita M, Ito-Fujita Y, Iyoda T, Sasada M, Okada Y, Ishibashi K, et al. Peptide TNIIIA2 Derived from Tenascin-C Contributes to Malignant Progression in Colitis-Associated Colorectal Cancer via $\beta 1$ -Integrin Activation in Fibroblasts. *Int J Mol Sci* (2019) 20(11):2752. doi: 10.3390/ijms20112752
151. De Santis R, Albertoni C, Petronzelli F, Campo S, D'Alessio V, Rosi A, et al. Low and high tenascin-expressing tumors are efficiently targeted by ST2146 monoclonal antibody. *Clin Cancer Res* (2006) 12(7 Pt 1):2191–6. doi: 10.1158/1078-0432.CCR-05-2526
152. Li F. Role of survivin and its splice variants in tumorigenesis. *Br J Cancer* (2005) 92(2):212–6. doi: 10.1038/sj.bjc.6602340
153. Ge QX, Li YY, Nie YQ, Zuo WG, Du YL. Expression of survivin and its four splice variants in colorectal cancer and its clinical significances. *Med Oncol* (2013) 30(2):535. doi: 10.1007/s12032-013-0535-6
154. Noton EA, Colnaghi R, Tate S, Starck C, Carvalho A, Ko Ferrigno P, et al. Molecular analysis of survivin isoforms: evidence that alternatively spliced variants do not play a role in mitosis. *J Biol Chem* (2006) 281(2):1286–95. doi: 10.1074/jbc.M508773200
155. Tanaka T, Kitamura H, Inoue R, Nishida S, Takahashi-Takaya A, Kawami S, et al. Potential survival benefit of anti-apoptosis protein: survivin-derived peptide vaccine with and without interferon α therapy for patients with advanced or recurrent urothelial cancer—results from phase I clinical trials. *Clin Dev Immunol* (2013) 2013:262967. doi: 10.1155/2013/262967
156. Kameshima H, Tsuruma T, Torigoe T, Takahashi A, Hirohashi Y, Tamura Y, et al. Immunogenic enhancement and clinical effect by type-I interferon of anti-apoptotic protein, survivin-derived peptide vaccine, in advanced colorectal cancer patients. *Cancer Sci* (2011) 102(6):1181–7. doi: 10.1111/j.1349-7006.2011.01918.x
157. Martinez-Garcia D, Manero-Ruperez N, Quesada R, Korrodi-Gregorio L, Soto-Cerrato V. Therapeutic strategies involving survivin inhibition in cancer. *Med Res Rev* (2019) 39(3):887–909. doi: 10.1002/med.21547
158. Kobayashi T, Masaki T, Nozaki E, Sugiyama M, Nagashima F, Furuse J, et al. Microarray analysis of gene expression at the tumor front of colon cancer. *Anticancer Res* (2015) 35(12):6577–81.
159. Datta D, Flaxenburg JA, Laxmanan S, Geehan C, Grimm M, Waaga-Gasser AM, et al. Ras-induced modulation of CXCL10 and its receptor splice variant CXCR3-B in MDA-MB-435 and MCF-7 cells: relevance for the development of human breast cancer. *Cancer Res* (2006) 66(19):9509–18. doi: 10.1158/0008-5472.CAN-05-4345
160. Bodnar RJ, Yates CC, Wells A. IP-10 blocks vascular endothelial growth factor-induced endothelial cell motility and tube formation via inhibition of calpain. *Circ Res* (2006) 98(5):e617–25. doi: 10.1161/01.RES.0000209968.66606.10
161. Groom JR, Luster AD. CXCR3 ligands: redundant, collaborative and antagonistic functions. *Immunol Cell Biol* (2011) 89(2):207–15. doi: 10.1038/icb.2010.158
162. Bai M, Chen X, Ba YI. CXCL10/CXCR3 overexpression as a biomarker of poor prognosis in patients with stage II colorectal cancer. *Mol Clin Oncol* (2016) 4(1):23–30. doi: 10.3892/mco.2015.665
163. Billottet C, Quemener C, Bikfalvi A. CXCR3, a double-edged sword in tumor progression and angiogenesis. *Biochim Biophys Acta* (2013) 1836(2):287–95. doi: 10.1016/j.bbcan.2013.08.002
164. Ehler JE, Addison CA, Burdick MD, Kunkel SL, Strieter RM. Identification and partial characterization of a variant of human CXCR3 generated by posttranscriptional exon skipping. *J Immunol* (2004) 173(10):6234–40. doi: 10.4049/jimmunol.173.10.6234
165. Yang C, Zheng W, Du W. CXCR3A contributes to the invasion and metastasis of gastric cancer cells. *Oncol Rep* (2016) 36(3):1686–92. doi: 10.3892/or.2016.4953
166. Wu Q, Dhir R, Wells A. Altered CXCR3 isoform expression regulates prostate cancer cell migration and invasion. *Mol Cancer* (2012) 11:3. doi: 10.1186/1476-4598-11-3
167. Nozaki E, Kobayashi T, Ohnishi H, Ohtsuka K, Masaki T, Watanabe T, et al. C-X-C motif receptor 3A enhances proliferation and invasiveness of colorectal cancer cells, and is mediated by C-X-C motif ligand 10. *Oncol Lett* (2020) 19(3):2495–501. doi: 10.3892/ol.2020.11326
168. Wang IC, Chen YJ, Hughes D, Petrovic V, Major ML, Park HJ, et al. Forkhead box M1 regulates the transcriptional network of genes essential for mitotic progression and genes encoding the SCF (Skp2-Cks1) ubiquitin ligase. *Mol Cell Biol* (2005) 25(24):10875–94. doi: 10.1128/MCB.25.24.10875-10894.2005
169. Zhang N, Wei P, Gong A, Chiu WT, Lee HT, Colman H, et al. FoxM1 promotes beta-catenin nuclear localization and controls Wnt target-gene expression and glioma tumorigenesis. *Cancer Cell* (2011) 20(4):427–42. doi: 10.1016/j.ccr.2011.08.016
170. Martin E, Vivori C, Rogalska M, Herrero-Vicente J, Valcarcel J. Alternative splicing regulation of cell-cycle genes by SPF45/SR140/CHERP complex controls cell proliferation. *RNA* (2021) 27(12):1557–76. doi: 10.1261/rna.078935.121
171. Fu Y, Bai C, Wang S, Chen D, Zhang P, Wei H, et al. AKT1 phosphorylates RBM17 to promote Sox2 transcription by modulating alternative splicing of FOXM1 to enhance cancer stem cell properties in colorectal cancer cells. *FASEB J* (2023) 37(1):e22707. doi: 10.1096/fj.202201255R
172. Rather TB, Parvez I, Bhat GA, Rashid G, Wani RA, Khan IY, et al. Evaluation of Forkhead BOX M1 (FOXM1) gene expression in colorectal cancer. *Clin Exp Med* (2022) 2022. doi: 10.1007/s10238-022-00929-7
173. Fei BY, He X, Ma J, Zhang M, Chai R. FoxM1 is associated with metastasis in colorectal cancer through induction of the epithelial-mesenchymal transition. *Oncol Lett* (2017) 14(6):6553–61. doi: 10.3892/ol.2017.7022
174. Zhang HG, Xu XW, Shi XP, Han BW, Li ZH, Ren WH, et al. Overexpression of forkhead box protein M1 (FOXM1) plays a critical role in colorectal cancer. *Clin Transl Oncol* (2016) 18(5):527–32. doi: 10.1007/s12094-015-1400-1
175. Lin F, Worman HJ. Structural organization of the human gene encoding nuclear lamin A and nuclear lamin C. *J Biol Chem* (1993) 268(22):16321–6.
176. Willis ND, Cox TR, Rahman-Casans SF, Smits K, Przyborski SA, van den Brandt P, et al. Lamin A/C is a risk biomarker in colorectal cancer. *PLoS One* (2008) 3(8):e2988. doi: 10.1371/journal.pone.0002988
177. Pan YJ, Huo FC, Kang MJ, Liu BW, Wu MD, Pei DS. Alternative splicing of HSPA12A pre-RNA by SRSF11 contributes to metastasis potential of colorectal cancer. *Clin Transl Med* (2022) 12(11):e1113. doi: 10.1002/ctm2.1113
178. Chao C, Goluszko E, Lee YT, Kolokoltsov AA, Davey RA, Uchida T, et al. Constitutively active CCK2 receptor splice variant increases Src-dependent HIF-1 α expression and tumor growth. *Oncogene* (2007) 26(7):1013–9. doi: 10.1038/sj.onc.1209862
179. Lu Y, Zhao X, Li K, Luo G, Nie Y, Shi Y, et al. Thioredoxin-like protein 2 is overexpressed in colon cancer and promotes cancer cell metastasis by interaction with ran. *Antioxid Redox Signal* (2013) 19(9):899–911. doi: 10.1089/ars.2012.4736
180. Yu Z, Zhang B, Cui B, Wang Y, Han P, Wang X. Identification of spliced variants of the proto-oncogene HDM2 in colorectal cancer. *Cancer* (2012) 118(4):1110–8. doi: 10.1002/cncr.26330
181. Fanning AS, Jameson BJ, Jesaitis LA, Anderson JM. The tight junction protein ZO-1 establishes a link between the transmembrane protein occludin and the actin cytoskeleton. *J Biol Chem* (1998) 273(45):29745–53. doi: 10.1074/jbc.273.45.29745
182. Han F, Yang B, Zhou M, Huang Q, Mai M, Huang Z, et al. GLTSCR1 coordinates alternative splicing and transcription elongation of ZO1 to regulate colorectal cancer progression. *J Mol Cell Biol* (2022) 14(2):mjac009. doi: 10.1093/jmcb/mjac009
183. Wan L, Yu W, Shen E, Sun W, Liu Y, Kong J, et al. SRSF6-regulated alternative splicing that promotes tumour progression offers a therapy target for colorectal cancer. *Gut* (2019) 68(1):118–29. doi: 10.1136/gutjnl-2017-314983
184. Heiner M, Hui J, Schreiner S, Hung LH, Bindereif A. HnRNP L-mediated regulation of mamMalian alternative splicing by interference with splice site recognition. *RNA Biol* (2010) 7(1):56–64. doi: 10.4161/rna.7.1.10402
185. Kim YE, Won M, Lee SG, Park C, Song CH, Kim KK. RBM47-regulated alternative splicing of TJP1 promotes actin stress fiber assembly during epithelial-to-mesenchymal transition. *Oncogene* (2019) 38(38):6521–36. doi: 10.1038/s41388-019-0892-5
186. Jantschke P, Terracciano L, Lowy A, Glatz-Krieger K, Grunert F, Mischeel B, et al. Expression of CEACAM6 in resectable colorectal cancer: a factor of independent prognostic significance. *J Clin Oncol* (2003) 21(19):3638–46. doi: 10.1200/JCO.2003.55.135
187. Kang WY, Chen WT, Wu MT, Chai CY. The expression of CD66a and possible roles in colorectal adenoma and adenocarcinoma. *Int J Colorectal Dis* (2007) 22(8):869–74. doi: 10.1007/s00384-006-0247-x
188. Barnett TR, Drake L, Pickle W 2nd. Human biliary glycoprotein gene: characterization of a family of novel alternatively spliced RNAs and their expressed proteins. *Mol Cell Biol* (1993) 13(2):1273–82. doi: 10.1128/mcb.13.2.1273-1282.1993
189. Ieda J, Yokoyama S, Tamura K, Takifuji K, Hotta T, Matsuda K, et al. Re-expression of CEACAM1 long cytoplasmic domain isoform is associated with invasion and migration of colorectal cancer. *Int J Cancer* (2011) 129(6):1351–61. doi: 10.1002/ijc.26072
190. Ling Y, Kuang Y, Chen LL, Lao WF, Zhu YR, Wang LQ, et al. A novel RON splice variant lacking exon 2 activates the PI3K/AKT pathway via PTEN phosphorylation in colorectal carcinoma cells. *Oncotarget* (2017) 8(24):39101–16. doi: 10.18632/oncotarget.16603
191. Wang D, Lao WF, Kuang YY, Geng SM, Mo LJ, He C. A novel variant of the RON receptor tyrosine kinase derived from colorectal carcinoma cells which lacks

tyrosine phosphorylation but induces cell migration. *Exp Cell Res* (2012) 318(20):2548–58. doi: 10.1016/j.yexcr.2012.08.006

192. Rigillo G, Belluti S, Campani V, Ragazzini G, Ronzio M, Misericocchi G, et al. The NF-Y splicing signature controls hybrid EMT and ECM-related pathways to promote aggressiveness of colon cancer. *Cancer Lett* (2023) 567:216262. doi: 10.1016/j.canlet.2023.216262

193. Krueger A, Baumann S, Krammer PH, Kirchhoff S. FLICE-inhibitory proteins: regulators of death receptor-mediated apoptosis. *Mol Cell Biol* (2001) 21(24):8247–54. doi: 10.1128/MCB.21.24.8247-8254.2001

194. Djerbi M, Darreh-Shori T, Zhivotovsky B, Grandien A. Characterization of the human FLICE-inhibitory protein locus and comparison of the anti-apoptotic activity of four different flip isoforms. *Scand J Immunol* (2001) 54(1-2):180–9. doi: 10.1046/j.1365-3083.2001.00941.x

195. Wilson TR, McLaughlin KM, McEwan M, Sakai H, Rogers KM, Redmond KM, et al. c-FLIP: a key regulator of colorectal cancer cell death. *Cancer Res* (2007) 67(12):5754–62. doi: 10.1158/0008-5472.CAN-06-3585

196. Ryu BK, Lee MG, Chi SG, Kim YW, Park JH. Increased expression of cFLIP(L) in colonic adenocarcinoma. *J Pathol* (2001) 194(1):15–9. doi: 10.1002/path.835

197. Law DJ, Labut EM, Adams RD, Merchant JL. An isoform of ZBP-89 predisposes the colon to colitis. *Nucleic Acids Res* (2006) 34(5):1342–50. doi: 10.1093/nar/gkl022

198. Liu Y, Huang W, Gao X, Kuang F. Regulation between two alternative splicing isoforms ZNF148(FL) and ZNF148(DeltaN), and their roles in the apoptosis and invasion of colorectal cancer. *Pathol Res Pract* (2019) 215(2):272–7. doi: 10.1016/j.prp.2018.10.036

199. Denis V, Cassagnard N, Del Rio M, Cornillot E, Bec N, Larroque C, et al. Targeting the splicing isoforms of spleen tyrosine kinase affects the viability of colorectal cancer cells. *PLoS One* (2022) 17(9):e0274390. doi: 10.1371/journal.pone.0274390

200. Ni B, Hu J, Chen D, Li L, Chen D, Wang J, et al. Alternative splicing of spleen tyrosine kinase differentially regulates colorectal cancer progression. *Oncol Lett* (2016) 12(3):1737–44. doi: 10.3892/ol.2016.4858

201. Xu W, Jing L, Wang Q, Lin CC, Chen X, Diao J, et al. Bax-PGAM5L-Drp1 complex is required for intrinsic apoptosis execution. *Oncotarget* (2015) 6(30):30017–34. doi: 10.18632/oncotarget.5013

202. Wang Z, Jiang H, Chen S, Du F, Wang X. The mitochondrial phosphatase PGAM5 functions at the convergence point of multiple necrotic death pathways. *Cell* (2012) 148(1-2):228–43. doi: 10.1016/j.cell.2011.11.030

203. Zhao H, Ming T, Tang S, Ren S, Yang H, Liu M, et al. Wnt signaling in colorectal cancer: pathogenic role and therapeutic target. *Mol Cancer* (2022) 21(1):144. doi: 10.1186/s12943-022-01616-7

204. Bueno MLP, Saad STO, Roversi FM. WNT5A in tumor development and progression: A comprehensive review. *BioMed Pharmacother* (2022) 155:113599. doi: 10.1016/j.biopha.2022.113599

205. Katula KS, Joyner-Powell NB, Hsu CC, Kuk A. Differential regulation of the mouse and human Wnt5a alternative promoters A and B. *DNA Cell Biol* (2012) 31(11):1585–97. doi: 10.1089/dna.2012.1698

206. Bauer M, Benard J, Gaasterland T, Willert K, Cappellen D. WNT5A encodes two isoforms with distinct functions in cancers. *PLoS One* (2013) 8(11):e80526. doi: 10.1371/journal.pone.0080526

207. Huang TC, Lee PT, Wu MH, Huang CC, Ko CY, Lee YC, et al. Distinct roles and differential expression levels of Wnt5a mRNA isoforms in colorectal cancer cells. *PLoS One* (2017) 12(8):e0181034. doi: 10.1371/journal.pone.0181034

208. Mo JS, Alam KJ, Kang IH, Park WC, Seo GS, Choi SC, et al. MicroRNA 196B regulates FAS-mediated apoptosis in colorectal cancer cells. *Oncotarget* (2015) 6(5):2843–55. doi: 10.18632/oncotarget.3066

209. Pryczynicz A, Guzinska-Ustymowicz K, Kemona A. Fas/FasL expression in colorectal cancer. An immunohistochemical study. *Folia Histochem Cytobiol* (2010) 48(3):425–9. doi: 10.2478/v10042-010-0058-3

210. Vilys L, Peciuliene I, Jakubauskiene E, Zinkeviciute R, Makino Y, Kanopka A. U2AF - Hypoxia-induced fas alternative splicing regulator. *Exp Cell Res* (2021) 399(1):112444. doi: 10.1016/j.yexcr.2020.112444

211. Liu L, Luo C, Luo Y, Chen L, Liu Y, Wang Y, et al. MRPL33 and its splicing regulator hnRNPK are required for mitochondria function and implicated in tumor progression. *Oncogene* (2018) 37(1):86–94. doi: 10.1038/ncr.2017.314

212. Sillars-Hardebol AH, Carvalho B, Belien JA, de Wit M, Delis-van Diemen PM, Tijssen M, et al. BCL2L1 has a functional role in colorectal cancer and its protein expression is associated with chromosome 20q gain. *J Pathol* (2012) 226(3):442–50. doi: 10.1002/path.2983

213. Joly F, Fabbro M, Follana P, Lequesne J, Medioni J, Lesoin A, et al. A phase II study of Navitoclax (ABT-263) as single agent in women heavily pretreated for recurrent epithelial ovarian cancer: The MONAVI - GINECO study. *Gynecol Oncol* (2022) 165(1):30–9. doi: 10.1016/j.ygyno.2022.01.021

214. Ghaemi Z, Mowla SJ, Soltani BM. Novel splice variants of LINC00963 suppress colorectal cancer cell proliferation via miR-10a/miR-143/miR-217/miR-512-mediated regulation of PI3K/AKT and Wnt/beta-catenin signaling pathways. *Biochim Biophys Acta Gene Regul Mech* (2023) 1866(2):194921. doi: 10.1016/j.bbagr.2023.194921

215. Canavese M, Ngo DT, Maddern GJ, Hardingham JE, Price TJ, Hauben E. Biology and therapeutic implications of VEGF-A splice isoforms and single-nucleotide polymorphisms in colorectal cancer. *Int J Cancer* (2017) 140(10):2183–91. doi: 10.1002/ijc.30567

216. Watson CJ, Webb NJ, Bottomley MJ, Brenchley PE. Identification of polymorphisms within the vascular endothelial growth factor (VEGF) gene: correlation with variation in VEGF protein production. *Cytokine* (2000) 12(8):1232–5. doi: 10.1006/cyto.2000.0692

217. Woolard J, Bevan HS, Harper SJ, Bates DO. Molecular diversity of VEGF-A as a regulator of its biological activity. *Microcirculation* (2009) 16(7):572–92. doi: 10.1080/10739680902997333

218. Des Guetz G, Uzzan B, Nicolas P, Cucherat M, Morere JF, Benamouzig R, et al. Microvessel density and VEGF expression are prognostic factors in colorectal cancer. *Meta-analysis literature. Br J Cancer* (2006) 94(12):1823–32. doi: 10.1038/sj.bjc.6603176

219. Saltz LB, Clarke S, Diaz-Rubio E, Scheithauer W, Figuer A, Wong R, et al. Bevacizumab in combination with oxaliplatin-based chemotherapy as first-line therapy in metastatic colorectal cancer: a randomized phase III study. *J Clin Oncol* (2008) 26(12):2013–9. doi: 10.1200/JCO.2007.14.9930

220. Diaz R, Pena C, Silva J, Lorenzo Y, Garcia V, Garcia JM, et al. VEGF165b and PEDF expression in human colorectal tumors: VEGF165b downregulation as a marker of poor prognosis. *Int J Cancer* (2008) 123(5):1060–7. doi: 10.1002/ijc.23619

221. Eberhardt W, Doller A, Akool el S, Pfeilschifter J. Modulation of mRNA stability as a novel therapeutic approach. *Pharmacol Ther* (2007) 114(1):56–73. doi: 10.1016/j.pharmthera.2007.01.002

222. Hamdollah Zadeh MA, Amin EM, Hoareau-Aveilla C, Domingo E, Symonds KE, Ye X, et al. Alternative splicing of TIA-1 in human colon cancer regulates VEGF isoform expression, angiogenesis, tumour growth and bevacizumab resistance. *Mol Oncol* (2015) 9(1):167–78. doi: 10.1016/j.molonc.2014.07.017

223. Suswam EA, Li YY, Mahtani H, King PH. Novel DNA-binding properties of the RNA-binding protein TIAR. *Nucleic Acids Res* (2005) 33(14):4507–18. doi: 10.1093/nar/gki763

224. Alnuaimi AR, Nair VA, Malhab LJB, Abu-Gharbieh E, Ranade AV, Pintus G, et al. Emerging role of caldesmon in cancer: A potential biomarker for colorectal cancer and other cancers. *World J Gastrointest Oncol* (2022) 14(9):1637–53. doi: 10.4251/wjgo.v14.i9.1637

225. Zheng PP, van der Weiden M, Kros JM. Differential expression of Hela-type caldesmon in tumour neovascularization: a new marker of angiogenic endothelial cells. *J Pathol* (2005) 205(3):408–14. doi: 10.1002/path.1700

226. Kim KH, Yeo SG, Kim WK, Kim DY, Yeo HY, Hong JP, et al. Up-regulated expression of l-caldesmon associated with Malignancy of colorectal cancer. *BMC Cancer* (2012) 12:601. doi: 10.1186/1471-2407-12-601

227. Albuquerque RJ, Hayashi T, Cho WG, Kleinman ME, Dridi S, Takeda A, et al. Alternatively spliced vascular endothelial growth factor receptor-2 is an essential endogenous inhibitor of lymphatic vessel growth. *Nat Med* (2009) 15(9):1023–30. doi: 10.1038/nm.2018

228. Uehara H, Cho Y, Simonis J, Cahoon J, Archer B, Luo L, et al. Dual suppression of hemangiogenesis and lymphangiogenesis by splice-shifting morpholinos targeting vascular endothelial growth factor receptor 2 (KDR). *FASEB J* (2013) 27(1):76–85. doi: 10.1096/fj.12-213835

229. Stagg BC, Uehara H, Lambert N, Rai R, Gupta I, Radmall B, et al. Morpholino-mediated isoform modulation of vascular endothelial growth factor receptor-2 (VEGFR2) reduces colon cancer Xenograft growth. *Cancers (Basel)* (2014) 6(4):2330–42. doi: 10.3390/cancers6042330

230. Turano M, Cammarota F, Duraturo F, Izzo P, De Rosa M. A potential role of IL-6/IL-6R in the development and management of colon cancer. *Membranes (Basel)* (2021) 11(5):312. doi: 10.3390/membranes11050312

231. Schumertl T, Lokau J, Rose-John S, Garbers C. Function and proteolytic generation of the soluble interleukin-6 receptor in health and disease. *Biochim Biophys Acta Mol Cell Res* (2022) 1869(1):119143. doi: 10.1016/j.bbamcr.2021.119143

232. Chung YC, Chang YF. Serum interleukin-6 levels reflect the disease status of colorectal cancer. *J Surg Oncol* (2003) 83(4):222–6. doi: 10.1002/jso.10269

233. Zhu LQ, Zhang L, Zhang J, Chang GL, Liu G, Yu DD, et al. Evodiamine inhibits high-fat diet-induced colitis-associated cancer in mice through regulating the gut microbiota. *J Integr Med* (2021) 19(1):56–65. doi: 10.1016/j.joim.2020.11.001

234. Khanna D, Lin CJF, Furst DE, Wagner B, Zucchetto M, Raghu G, et al. Long-term safety and efficacy of tocilizumab in early systemic sclerosis-interstitial lung disease: open-label extension of a phase 3 randomized controlled trial. *Am J Respir Crit Care Med* (2022) 205(6):674–84. doi: 10.1164/rccm.202103-0714OC

235. Zhang S, Chen B, Wang B, Chen H, Li Y, Cao Q, et al. Effect of induction therapy with olamkcept vs placebo on clinical response in patients with active ulcerative colitis: A randomized clinical trial. *JAMA* (2023) 329(9):725–34. doi: 10.1001/jama.2023.1084

236. You M, Yuan S, Shi J, Hou Y. PPARdelta signaling regulates colorectal cancer. *Curr Pharm Des* (2015) 21(21):2956–9. doi: 10.2174/1381612821666150514104035

237. Saha L. Role of peroxisome proliferator-activated receptors alpha and gamma in gastric ulcer: An overview of experimental evidences. *World J Gastrointest Pharmacol Ther* (2015) 6(4):120–6. doi: 10.4292/wjpt.v6.i4.120

238. Larsen LK, Amri EZ, Mandrup S, Pacot C, Kristiansen K. Genomic organization of the mouse peroxisome proliferator-activated receptor beta/delta gene: alternative promoter usage and splicing yield transcripts exhibiting differential translational efficiency. *Biochem J* (2002) 366(Pt 3):767–75. doi: 10.1042/BJ20011821
239. Michelet X, Dyck L, Hogan A, Loftus RM, Duquette D, Wei K, et al. Metabolic reprogramming of natural killer cells in obesity limits antitumor responses. *Nat Immunol* (2018) 19(12):1330–40. doi: 10.1038/s41590-018-0251-7
240. Schumann T, Adhikary T, Wortmann A, Finkernagel F, Lieber S, Schnitzer E, et al. Deregulation of PPARbeta/delta target genes in tumor-associated macrophages by fatty acid ligands in the ovarian cancer microenvironment. *Oncotarget* (2015) 6(15):13416–33. doi: 10.18632/oncotarget.3826
241. Wagner N, Wagner KD. PPAR Beta/Delta and the hallmarks of cancer. *Cells* (2020) 9(5):1133. doi: 10.3390/cells9051133
242. Wang R, Li J, Zhou X, Mao Y, Wang W, Gao S, et al. Single-cell genomic and transcriptomic landscapes of primary and metastatic colorectal cancer tumors. *Genome Med* (2022) 14(1):93. doi: 10.1186/s13073-022-01093-z
243. Gomez-Fernandez P, Urtasun A, Paton AW, Paton JC, Borrego F, Dersh D, et al. Long interleukin-22 binding protein isoform-1 is an intracellular activator of the unfolded protein response. *Front Immunol* (2018) 9:2934. doi: 10.3389/fimmu.2018.02934
244. Lim C, Hong M, Savan R. Human IL-22 binding protein isoforms act as a rheostat for IL-22 signaling. *Sci Signal* (2016) 9(447):ra95. doi: 10.1126/scisignal.aad9887
245. Huber S, Gagliani N, Zenewicz LA, Huber FJ, Bosurgi L, Hu B, et al. IL-22BP is regulated by the inflammasome and modulates tumorigenesis in the intestine. *Nature* (2012) 491(7423):259–63. doi: 10.1038/nature11535
246. Pelczar P, Witkowski M, Perez LG, Kempinski J, Hammel AG, Brockmann L, et al. A pathogenic role for T cell-derived IL-22BP in inflammatory bowel disease. *Science* (2016) 354(6310):358–62. doi: 10.1126/science.aah5903
247. Martin JC, Beriou G, Heslan M, Bossard C, Jarry A, Abidi A, et al. IL-22BP is produced by eosinophils in human gut and blocks IL-22 protective actions during colitis. *Mucosal Immunol* (2016) 9(2):539–49. doi: 10.1038/mi.2015.83
248. Zhang R, Men K, Zhang X, Huang R, Tian Y, Zhou B, et al. Delivery of a modified mRNA encoding IL-22 binding protein (IL-22BP) for colon cancer gene therapy. *J BioMed Nanotechnol* (2018) 14(7):1239–51. doi: 10.1166/jbnn.2018.2577
249. Manavalan JS, Rossi PC, Vlad G, Piazza F, Yarinina A, Cortesini R, et al. High expression of ILT3 and ILT4 is a general feature of tolerogenic dendritic cells. *Transpl Immunol* (2003) 11(3–4):245–58. doi: 10.1016/S0966-3274(03)00058-3
250. Suciu-Foca N, Feirt N, Zhang QY, Vlad G, Liu Z, Lin H, et al. Soluble Ig-like transcript 3 inhibits tumor allograft rejection in humanized SCID mice and T cell responses in cancer patients. *J Immunol* (2007) 178(11):7432–41. doi: 10.4049/jimmunol.178.11.7432
251. Liu J, Lu CX, Zhang F, Lv W, Liu C. Expression of ILT3 predicts poor prognosis and is inversely associated with infiltration of CD45RO+ T cells in patients with colorectal cancer. *Pathol Res Pract* (2018) 214(10):1621–5. doi: 10.1016/j.prp.2018.07.026
252. Blumlein K, Gruning NM, Feichtinger RG, Lehrach H, Kofler B, Ralser M. No evidence for a shift in pyruvate kinase PKM1 to PKM2 expression during tumorigenesis. *Oncotarget* (2011) 2(5):393–400. doi: 10.18632/oncotarget.278
253. Park B, Kim JY, Riffey OF, Dowker-Key P, Bruckbauer A, McLoughlin J, et al. Pyruvate kinase M1 regulates butyrate metabolism in cancerous colonocytes. *Sci Rep* (2022) 12(1):8771. doi: 10.1038/s41598-022-12827-9
254. Zhu W, Zhou BL, Rong LJ, Ye L, Xu HJ, Zhou Y, et al. Roles of PTBP1 in alternative splicing, glycolysis, and oncogenesis. *J Zhejiang Univ Sci B* (2020) 21(2):122–36. doi: 10.1631/jzus.B1900422
255. Lan Z, Yao X, Sun K, Li A, Liu S, Wang X. The Interaction Between lncRNA SNHG6 and hnRNPA1 Contributes to the Growth of Colorectal Cancer by Enhancing Aerobic Glycolysis Through the Regulation of Alternative Splicing of PKM. *Front Oncol* (2020) 10:363. doi: 10.3389/fonc.2020.00363
256. Huang JZ, Chen M, Chen D, Gao XC, Zhu S, Huang H, et al. A peptide encoded by a putative lncRNA HOXB-AS3 suppresses colon cancer growth. *Mol Cell* (2017) 68(1):171–84 e6. doi: 10.1016/j.molcel.2017.09.015
257. Zhao J, Li J, Hassan W, Xu D, Wang X, Huang Z. Sam68 promotes aerobic glycolysis in colorectal cancer by regulating PKM2 alternative splicing. *Ann Transl Med* (2020) 8(7):459. doi: 10.21037/atm.2020.03.108
258. Taniguchi K, Sugito N, Kumazaki M, Shinohara H, Yamada N, Nakagawa Y, et al. MicroRNA-124 inhibits cancer cell growth through PTB1/PKM1/PKM2 feedback cascade in colorectal cancer. *Cancer Lett* (2015) 363(1):17–27. doi: 10.1016/j.canlet.2015.03.026
259. Zheng H, Zhang M, Ke X, Deng X, Li D, Wang Q, et al. lncRNA XIST/miR-137 axis strengthens chemo-resistance and glycolysis of colorectal cancer cells by hindering transformation from PKM2 to PKM1. *Cancer biomark* (2021) 30(4):395–406. doi: 10.3233/CBM-201740
260. Han J, Zhao Z, Zhang N, Yang Y, Ma L, Feng L, et al. Transcriptional dysregulation of TRIM29 promotes colorectal cancer carcinogenesis via pyruvate kinase-mediated glucose metabolism. *Aging (Albany NY)* (2021) 13(4):5034–54. doi: 10.18632/aging.202414
261. Bellemare J, Rouleau M, Harvey M, Tetu B, Guillemette C. Alternative-splicing forms of the major phase II conjugating UGT1A gene negatively regulate glucuronidation in human carcinoma cell lines. *Pharmacogenomics J* (2010) 10(5):431–41. doi: 10.1038/tpj.2009.64
262. Girard H, Levesque E, Bellemare J, Journault K, Caillier B, Guillemette C. Genetic diversity at the UGT1 locus is amplified by a novel 3' alternative splicing mechanism leading to nine additional UGT1A proteins that act as regulators of glucuronidation activity. *Pharmacogenet Genomics* (2007) 17(12):1077–89. doi: 10.1097/FPGC.0b013e3282f1f118
263. Levesque E, Girard H, Journault K, Lepine J, Guillemette C. Regulation of the UGT1A1 bilirubin-conjugating pathway: role of a new splicing event at the UGT1A locus. *Hepatology* (2007) 45(1):128–38. doi: 10.1002/hep.21464
264. Audet-Delage Y, Rouleau M, Rouleau M, Roberge J, Miard S, Picard F, et al. Cross-talk between alternatively spliced UGT1A isoforms and colon cancer cell metabolism. *Mol Pharmacol* (2017) 91(3):167–77. doi: 10.1124/mol.116.106161
265. Soupene E, Kuypers FA. MamMalian long-chain acyl-CoA synthetases. *Exp Biol Med* (Maywood) (2008) 233(5):507–21. doi: 10.3181/0710-MR-287
266. Sanchez-Martinez R, Cruz-Gil S, Garcia-Alvarez MS, Reglero G, Ramirez de Molina A. Complementary ACSL isoforms contribute to a non-Warburg advantageous energetic status characterizing invasive colon cancer cells. *Sci Rep* (2017) 7(1):11143. doi: 10.1038/s41598-017-11612-3
267. Sanchez-Martinez R, Cruz-Gil S, Gomez de Cedron M, Alvarez-Fernandez M, Vargas T, Molina S, et al. A link between lipid metabolism and epithelial-mesenchymal transition provides a target for colon cancer therapy. *Oncotarget* (2015) 6(36):38719–36. doi: 10.18632/oncotarget.5340
268. Samuels-Lev Y, O'Connor DJ, Bergamaschi D, Trigiani G, Hsieh JK, Zhong S, et al. ASPP proteins specifically stimulate the apoptotic function of p53. *Mol Cell* (2001) 8(4):781–94. doi: 10.1016/s1097-2765(01)00367-7
269. Wang Z, Liu Y, Takahashi M, Van Hook K, Kampa-Schittenhelm KM, Sheppard BC, et al. N terminus of ASPP2 binds to Ras and enhances Ras/Raf/MEK/ERK activation to promote oncogene-induced senescence. *Proc Natl Acad Sci U.S.A.* (2013) 110(1):312–7. doi: 10.1073/pnas.1201514110
270. Schittenhelm MM, Walter B, Tsintari V, Federmann B, Bajrami Saipi M, Akmut F, et al. Alternative splicing of the tumor suppressor ASPP2 results in a stress-inducible, oncogenic isoform prevalent in acute leukemia. *EBioMedicine* (2019) 42:340–51. doi: 10.1016/j.ebiom.2019.03.028
271. Rieger I, Tsintari V, Overkamp M, Fend F, Lopez CD, Schittenhelm MM, et al. ASPP2kappa is expressed in human colorectal carcinoma and promotes chemotherapy resistance and tumorigenesis. *Front Mol Biosci* (2021) 8:727203. doi: 10.3389/fmolb.2021.727203
272. Briones-Orta MA, Avendano-Vazquez SE, Aparicio-Bautista DI, Coombes JD, Weber GF, Syn WK. Osteopontin splice variants and polymorphisms in cancer progression and prognosis. *Biochim Biophys Acta Rev Cancer* (2017) 1868(1):93–108 A. doi: 10.1016/j.bbcan.2017.02.005
273. Chang S, Huang J, Niu H, Wang J, Si Y, Bai Z, et al. Epigenetic regulation of osteopontin splicing isoform c defines its role as a microenvironmental factor to promote the survival of colon cancer cells from 5-FU treatment. *Cancer Cell Int* (2020) 20:452. doi: 10.1186/s12935-020-01541-z
274. de Lau W, Barker N, Low TY, Koo BK, Li VS, Teunissen H, et al. Lgr5 homologues associate with Wnt receptors and mediate R-spondin signalling. *Nature* (2011) 476(7360):293–7. doi: 10.1038/nature10337
275. Takahashi H, Ishii H, Nishida N, Takemasa I, Mizushima T, Ikeda M, et al. Significance of Lgr5(+)ve cancer stem cells in the colon and rectum. *Ann Surg Oncol* (2011) 18(4):1166–74. doi: 10.1245/s10434-010-1373-9
276. Barker N, Ridgway RA, van Es JH, van de Wetering M, Begthel H, van den Born M, et al. Crypt stem cells as the cells-of-origin of intestinal cancer. *Nature* (2009) 457(7229):608–11. doi: 10.1038/nature07602
277. Osawa H, Takahashi H, Nishimura J, Ohta K, Haraguchi N, Hata T, et al. Full-length LGR5-positive cells have chemoresistant characteristics in colorectal cancer. *Br J Cancer* (2016) 114(11):1251–60. doi: 10.1038/bjc.2016.112
278. Rot S, Taubert H, Bache M, Greither T, Wurl P, Eckert AW, et al. A novel splice variant of the stem cell marker LGR5/GPR49 is correlated with the risk of tumor-related death in soft-tissue sarcoma patients. *BMC Cancer* (2011) 11:429. doi: 10.1186/1471-2407-11-429
279. Xie T, Geng J, Wang Y, Wang L, Huang M, Chen J, et al. FOXM1 evokes 5-fluorouracil resistance in colorectal cancer depending on ABCG10. *Oncotarget* (2017) 8(5):8574–89. doi: 10.18632/oncotarget.14351
280. Varghese V, Magnani L, Harada-Shoji N, Mauri F, Szydlowski RM, Yao S, et al. FOXM1 modulates 5-FU resistance in colorectal cancer through regulating TYMS expression. *Sci Rep* (2019) 9(1):1505. doi: 10.1038/s41598-018-38017-0
281. Nixon BR, Sebag SC, Glennon MS, Hall EJ, Kounlavong ES, Freeman ML, et al. Nuclear localized Raf1 isoform alters DNA-dependent protein kinase activity and the DNA damage response. *FASEB J* (2019) 33(1):1138–50. doi: 10.1096/fj.201800336R
282. Gao Q, Li XX, Xu YM, Zhang JZ, Rong SD, Qin YQ, et al. IRE1alpha-targeting downregulates ABC transporters and overcomes drug resistance of colon cancer cells. *Cancer Lett* (2020) 476:67–74. doi: 10.1016/j.canlet.2020.02.007
283. Hetz C, Chevet E, Harding HP. Targeting the unfolded protein response in disease. *Nat Rev Drug Discovery* (2013) 12(9):703–19. doi: 10.1038/nrd3976

284. Calton M, Zeng H, Urano F, Till JH, Hubbard SR, Harding HP, et al. IRE1 couples endoplasmic reticulum load to secretory capacity by processing the XBP-1 mRNA. *Nature* (2002) 415(6867):92–6. doi: 10.1038/415092a
285. Xie Y, Liu C, Qin Y, Chen J, Fang J. Knockdown of IRE1a suppresses metastatic potential of colon cancer cells through inhibiting FN1-Src/FAK-GTPases signaling. *Int J Biochem Cell Biol* (2019) 114:105572. doi: 10.1016/j.biocel.2019.105572
286. Guo Y, Chen Y, Ito H, Watanabe A, Ge X, Kodama T, et al. Identification and characterization of lin-28 homolog B (LIN28B) in human hepatocellular carcinoma. *Gene* (2006) 384:51–61. doi: 10.1016/j.gene.2006.07.011
287. Mizuno R, Chatterji P, Andres S, Hamilton K, Simon L, Foley SW, et al. Differential regulation of LET-7 by LIN28B isoform-specific functions. *Mol Cancer Res* (2018) 16(3):403–16. doi: 10.1158/1541-7786.MCR-17-0514
288. Zhang X, Ma D, Xuan B, Shi D, He J, Yu M, et al. LncRNA CACClnc promotes chemoresistance of colorectal cancer by modulating alternative splicing of RAD51. *Oncogene* (2023) 42(17):1374–91. doi: 10.1038/s41388-023-02657-y
289. Kim CJ, Terado T, Tambe Y, Mukaisho KI, Sugihara H, Kawauchi A, et al. Anti-oncogenic activities of cyclin D1b siRNA on human bladder cancer cells via induction of apoptosis and suppression of cancer cell stemness and invasiveness. *Int J Oncol* (2018) 52(1):231–40. doi: 10.3892/ijo.2017.4194
290. Li Q, Zeng C, Liu H, Yung KKY, Chen C, Xie Q, et al. Protein-protein interaction inhibitor of SRPKs alters the splicing isoforms of VEGF and inhibits angiogenesis. *iScience* (2021) 24(5):102423. doi: 10.1016/j.isci.2021.102423
291. Shitara K, Doi T, Nagano O, Imamura CK, Ozeki T, Ishii Y, et al. Dose-escalation study for the targeting of CD44v(+) cancer stem cells by sulfasalazine in patients with advanced gastric cancer (EPOC1205). *Gastric Cancer* (2017) 20(2):341–9. doi: 10.1007/s10120-016-0610-8
292. Tam BY, Chiu K, Chung H, Bossard C, Nguyen JD, Creger E, et al. The CLK inhibitor SM08502 induces anti-tumor activity and reduces Wnt pathway gene expression in gastrointestinal cancer models. *Cancer Lett* (2020) 473:186–97. doi: 10.1016/j.canlet.2019.09.009

Frontiers in Oncology

Advances knowledge of carcinogenesis and tumor progression for better treatment and management

The third most-cited oncology journal, which highlights research in carcinogenesis and tumor progression, bridging the gap between basic research and applications to improve diagnosis, therapeutics and management strategies.

Discover the latest Research Topics

See more →

Frontiers

Avenue du Tribunal-Fédéral 34
1005 Lausanne, Switzerland
frontiersin.org

Contact us

+41 (0)21 510 17 00
frontiersin.org/about/contact

